ANALYTICA CHIMICA ACTA

International monthly devoted to all branches of analytical chemistry
Revue mensuelle internationale consacrée à tous les domaines de la chimie analytique
Internationale Monatsschrift für alle Gebiete der analytischen Chemie

ELSEVIER SCIENTIFIC PUBLISHING COMPANY

AMSTERDAM

Anal. Chim. Acta, Vol. 90, 1–372, May 1977

Published monthly

Complete in one issue

ANALYTICA CHIMICA ACTA

Publication Schedule for 1977

Vol. 88, No. 1	January 1977	
Vol. 88, No. 2	February 1977	(completing Vol. 88)
Vol. 89, No. 1	March 1977	
Vol. 89, No. 2	April 1977	(completing Vol. 89)
Vol. 90	May 1977	(complete in one issue)
Vol. 91, No. 1	June 1977	
Vol. 91, No. 2	July 1977	(completing Vol. 91)
Vol. 92, No. 1	August 1977	
Vol. 92, No. 2	September 1977	(completing Vol. 92)
Vol. 93	October 1977	(complete in one issue)
Vol. 94, No. 1	November 1977	
Vol. 94, No. 2	December 1977	(completing Vol. 94)

Subscription price for 1977 (Vols. 88–95): Dfl. 920.00 plus Dfl. 112.00 postage (approx. U.S.$421.22 inclusive of postage). Claims for issues not received should be made within three months of publication of the issues; if not, they cannot be honoured free of charge. Subscribers in the U.S.A. and Canada receive their copies by airmail. Additional charges for airmail to other countries are available on request. For advertising rates apply to the publishers.

Subscriptions should be sent to:
Elsevier Scientific Publishing Company, P.O. Box 211, Amsterdam, The Netherlands.

GENERAL INFORMATION

Languages

Papers will be published in English, French or German.

Detailed information

Authors should consult Vol. 73, p. 435 for detailed instructions. Reprints of this information are obtainable from Dr. Macdonald or from: Elsevier Editorial Services Ltd., Mayfield House, 256 Banbury Road, Oxford (Great Britain).

Submission of papers

Papers should be sent to:

Prof. Philip W. West,
Chemistry Department,
College of Chemistry and Physics,
Louisiana State University,
Baton Rouge,
La. 70803 (U.S.A.)

or to:

Dr. A. M. G. Macdonald,
Department of Chemistry,
The University,
P.O. Box 363
Birmingham B15 2TT (Great Britain)

Reprints

Fifty reprints will be supplied free of charge. Additional reprints (minimum 100) can be ordered at quoted prices. They must be ordered on order forms which are sent together with the proofs.

Journal of Chromatography Library

A series of books devoted to chromatographic techniques and their applications.

Although complementary to the Journal of Chromatography, each volume in the library series is an important and independent contribution in the field of chromatography. It should be stressed that the library contains no material reprinted from the journal itself.

Volume 1

CHROMATOGRAPHY OF ANTIBIOTICS

by G.H. Wagman and M J. Weinstein.

1973. ix - 238 pages.
Price: US $28.95/Dfl. 70.00.
ISBN 0-444-41106-2

At the present time thousands of antibiotics are known, yet the systematic chromatographic classification of these substances is extremely difficult.

This book has been written to aid the identification of very similar compounds by use of specific chromatographic techniques. It contains detailed data on paper and thin-layer chromatography, electrophoresis, counter-current distribution and gas chromatographic systems for over 1,200 antibiotics and their derivatives, and provides information on chromatographic media, solvents, detection methodology and mobility of the antibiotics. Complete references are given for all methods.

CONTENTS: Chromatographic classification of antibiotics. Detection of antibiotics on chromatograms. Comments on the use of this index. Abbreviations. Index - chromatography of antibiotics. Index by compound.

Volume 2

EXTRACTION CHROMATOGRAPHY

edited by T. Braun and G. Ghersini.

1975. xviii + 566 pages.
Price: US $52.95/Dfl. 130.00.
ISBN 0-444-99878-0

This volume is the result of the collective work of many specialists, each responsible for a chapter in which a definite aspect of column extraction chromatography is thoroughly presented and discussed.

Subjects presented include the basic and technical aspects of the method, the organic stationary phases and supports, the separation of elements with particular reference to radiochemical problems, the separation of lanthanides, actinides and fission products, radiotoxicological separations and the preconcentration of trace elements in various materials prior to their determination.

Author and subject indices are included.

Volume 3

LIQUID COLUMN CHROMATOGRAPHY

A survey of modern techniques and applications.

edited by Z. Deyl, K. Macek and J. Janák.

1975. xxii + 1176 pages.
Price: US $118.50/Dfl. 290.00.
ISBN 0-444-41156-9

This book provides an up-to-date account of liquid column chromatography for the specialist and non-specialist. The main attention is focussed on techniques developed or widely used during the past 10 years. Both classical and modern techniques of chromatographic separation are treated in detail, thus providing a clear reflection of the present situation in the field.

The wide selection of applications in various fields of chemistry and biochemistry, written by specialists in the area, makes this volume a necessary reference work for those involved in chromatographic investigations.

CONTENTS: Theoretical Aspects of Liquid Chromatography. Techniques of Liquid Chromatography. Practice of Liquid Chromatography. Applications. Subject index. List of compounds chromatographed.

Volume 4

DETECTORS IN GAS CHROMATOGRAPHY

by J. Ševčík.

1976. 192 pages.
Price: US $24.50/Dfl. 60.00.
ISBN 0-444-99857-8

This publication is devoted to the function and optimal working conditions of gas chromatographic detectors.

The first systematic treatment of gas chromatographic detection techniques, it

devotes special attention to so-called specific detectors and working conditions which strongly influence results (e.g. gas flow, effect of additives in gases, working temperature, detector form and dimensions). Anomalous detector responses are explained and the form and size of response for various working conditions are indicated. The problems presented are illustrated by experimental data which are summarized in numerous tables and figures.

The book should be of interest to all who use gas chromatography in research and who would like to explore the possibilities and working conditions of different detector systems.

Volume 5

INSTRUMENTAL LIQUID CHROMATOGRAPHY

A Practical Manual on High-Performance Liquid Chromatographic Methods

by N.A. Parris.

1976. x + 330 pages.
Price: US $40.95/Dfl. 100.00.
ISBN 0-444-41427-4

Available texts on liquid chromatography have tended to emphasize the developments in the theoretical understanding of the technique and methodology or to list numerous applications, complete with experimental details.

This work intends to bridge the gap between these two treatments by providing, with the minimum of theory, a practical guide to the use of technique for the development of separations. The material is based largely on practical experience and high-lights details which may have important operational value for laboratory workers. Information regarding the usefulness of available equipment and column packings is given, together with chapters devoted to the methodology of each separation method. Applications of liquid chromatography are described with reference to the potential of the technique for qualitative, quantitative and trace analysis as well as for separative applications. Numerous applications from the literature are tabulated and cross-referenced to sections concerned with the optimisation procedures of the particular methods. In addition, many of the figures have been drawn from hitherto unpublished works.

CONTENTS: Introduction and historical background. Basic principles and terminology. Chromatographic support and column. Liquid chromatographic instrumentation. Liquid chromatographic detection systems. Nature of the mobile phase. Liquid-solid (adsorption) chromatography. Liquid-liquid (partition) chromatography, Ion-exchange chromatography. Steric exclusion chromatography. Qualitative analysis. Quantitative analysis. Practical aspects of trace analysis. Practical aspects of preparative liquid chromatography. Published LC applications information. The latest trends and a glimpse into the future. Subject Index.

Volume 6

ISOTACHOPHORESIS

Theory, Instrumentation and Applications

by F.M. Everaerts, J.L. Beckers and Th.P.E.M. Verheggen.

1976. xiv + 418 pages.
Price: US $65.50/Dfl. 160.00.
ISBN 0-444-41430-4

This book is the only text currently available providing full information on the new separation technique known as Isotachophoresis. There is rapidly growing interest in this technique which will compete with other microanalytical techniques such as liquid and gas chromatography. All kinds of ionic materials can be separated using isotachophoretic equipment. Moreover, several classes of components can be analysed in quick succession as a proper rinsing of the equipment is all that is needed between separations. Each part is detailed and comprehensive.

The various chapters can be referred to more or less independently by scientists interested in fundamental aspects, by research groups intending to construct an instrument and by workers who are mainly concerned with the analytical aspects.

CONTENTS: Historical review. **Theory.** Principles of electrophoretic techniques. Concept of mobility. Mathematical model for isotachophoresis. Choice of electrolyte systems. **Instrumentation.** Detection systems. Instrumentation. **Applications.** Introduction. Practical aspects. Quantitative aspects. Separation of cationic species in aqueous solutions. Separation of anionic species in aqueous solutions. Amino acids, peptides and proteins. Separation of nucleotides in aqueous systems. Enzymatic reactions. Separations in non-aqueous systems. Counter flow of electrolyte. Appendices. Subject Index.

Volume 7

CHEMICAL DERIVATIZATION IN LIQUID CHROMATOGRAPHY

by J.F. Lawrence and R.W. Frei

1976. viii+214 pages.
Price: US $36.75/Dfl. 90.00.
ISBN 0-444-41429-0

This book is intended for all investigators concerned with the use of physical separation techniques for solving complex analytical problems. It is the first publication to provide a comprehensive account of modern derivatization in liquid chromatography with special emphasis on the practical aspects.

An introductory chapter familiarizes the reader with the basic philosophy of using chemical reactions and labelling procedures to enhance sensitivity, specificity and separation properties in liquid chromatographic techniques. The second chapter enables the practical worker to refresh his memory on some fundamental principles necessary to this work. The third deals with equipment and gives the analyst an idea of the choice of tools available to suit his needs. The final chapter helps the investigator to solve some concrete problems, to extend the concept of compounds and types of problems of immediate interest to him and to become familiar with the literature.

CONTENTS: Introduction. Background. Instrumentation. Applications. Subject Index.

Volume 8

CHROMATOGRAPHY OF STEROIDS

by E. Heftmann.

1976. xiv+204 pages.
Price: US $36.75/Dfl. 90.00.
ISBN 0-444-41441-x

The qualitative and quantitative analysis of individual steroids is of great interest to pharmacologists, physicians, biochemists, plant and animal physiologists and microbiologists.

The principal chromatographic methods of analysis applicable to steroids are: liquid column chromatography (including its recent modification, high-pressure liquid chromatography), thin-layer chromatography and gas chromatography (including the recently introduced coated capillary chromatography).

Since Neher's book "Steroid Chromatography" published by Elsevier in 1964, these applications have not been surveyed in a single volume. Here, the author takes up where Neher left off and presents a detailed description of the currently used techniques. Although some theory is included, this is mainly a laboratory handbook, arranged according to the steroids analyzed as well as according to the methods used.

CONTENTS: Introduction. Liquid column chromatography. Paper and thin-layer chromatography. Gas chromatography. Relations between structure and chromatographic mobility. Sterols. Bile acids and alcohols. Estrogens. Androstane derivatives. Pregnane derivatives. Corticosteroids. Miscellaneous steroid hormones. Vitamins D. Molting hormones. Steroid sapogenins and alkaloids. Cardenolides and bufadienolides. List of Abbreviations. References. Subject Index.

Volume 9

HPTLC - HIGH PERFORMANCE THIN-LAYER CHROMATOGRAPHY

edited by A. Zlatkis and R.E. Kaiser.

1977. 240 pages.
Price: US $44.95/Dfl. 110.00.
ISBN 0-444-41525-4.

HPTLC is the advanced technology of thin-layer chromatography and is defined as the combined action of several variables which include: an optimized coating material with a separation power superior to the best high performance liquid chromatographic separation material; a new method of feeding the mobile phase; a novel procedure for layer conditioning; a considerably improved dosage method and a competent data acquisition and processing system. Thus a complete system and procedure is discussed here. This should be understood as a stepwise improvement of an analytical method, which has been a powerful tool since the pioneering work of E. Stahl.

The results achieved, as well as the promising aspects of the new method are encouraging enough to refer to the technique as the second generation of thin-layer chromatography. The final judgement however, will be left to those who use this new methodology.

CONTENTS: Simplified theory of TLC *(R.E. Kaiser).* The separation number in linear and circular TLC *(J. Blome).* Advantages, limits and disadvantages of the ring

developing technique *(J. Blome)*. The U-chamber *(R.E. Kaiser)*. Dosage techniques in HPTLC *(R.E. Kaiser)*. High performance thin-layer chromatography: development, data and results *(H. Halpaap, J. Ripphahn)*. Consideration on the reproducibility of TLC separations *(D. Jaenchen)*. Potential and experience in quantitative HPTLC *(U.B. Hezel)*. Application of a new high-performance layer in quantitative TLC *(J. Ripphahn, H. Halpaap)*. Appendix. Index.

Volume 10

GAS CHROMATOGRAPHY OF POLYMERS

by V.G. Berezkin, V.R. Alishoyev and I.B. Nemirovskaya

1977. xiv+226 pages.
Price: US $41.95/Dfl. 103.00.
ISBN 0-444-41514-9.

At present, gas chromatography is the most widespread method for the analysis of organic compounds.

This book is devoted to the strategy of application of gas chromatography in polymer chemistry and discusses, in detail, the use of gas chromatography in research work and the polymeric compounds industry. It is the second, revised and enlarged edition of the original version published in the USSR in 1972.

The following principal applications are covered: analysis of monomers and solvents, determination of the contents of volatile substances in polymers, study of polymer formation processes, investigation into types of disintegration of high-molecular-weight compounds, polymer analysis by reaction and pyrolytic chromatography, and study of polymers and their reactivity with the aid of inverse chromatography.

This work will be of value to research institutions, industrial enterprises and senior students engaged in the fields of polymer or analytical chemistry and gas chromatography.

CONTENTS: Introduction. Basic principles of GC. GC methods for the analysis of monomers and solvents. The study of polymer formation reactions. Determination of volatile compounds in polymer systems. Study of the kinetics and mechanisms of chemical transformations of polymers at elevated temperatures. Reaction GC of polymer formation reactions. Determination Conclusion.

ELSEVIER SCIENTIFIC PUBLISHING COMPANY

ORDER FORM

Send to your bookseller or
ELSEVIER SCIENTIFIC PUBLISHING COMPANY
P.O. Box 211, Amsterdam, The Netherlands

Distributor in the U.S.A. and Canada:
ELSEVIER NORTH-HOLLAND, INC.,
52 Vanderbilt Ave., New York, N.Y. 10017

Please send me the following books _____

_____

_____

Name _____

Address _____

_____

_____

Orders from individuals must be accompanied by a remittance, following which books will be supplied postfree.

I enclose

my personal cheque	bank draft	UNESCO coupons

Date _____ Signature

The Dutch guilder price is definitive. US $ prices are subject to exchange rate fluctuations.

ANALYTICA CHIMICA ACTA
Vol. 90 (1977)

ANALYTICA CHIMICA ACTA

International monthly devoted to all branches of analytical chemistry
Revue mensuelle internationale consacrée à tous les domaines de la chimie analytique
Internationale Monatsschrift für alle Gebiete der analytischen Chemie

ELSEVIER SCIENTIFIC PUBLISHING COMPANY

AMSTERDAM

PRINTED IN THE NETHERLANDS

Analytica Chimica Acta, 90 (1977) 1—14

Review

PROBLEMS IN THE DETERMINATION OF PLUTONIUM IN BIOASSAY AND ENVIRONMENTAL ANALYSIS

J. C. VESELSKY

International Atomic Energy Agency, Laboratory Seibersdorf, A-2444 Seibersdorf (Austria)

(Received 4th October 1976)

SUMMARY

The methods available for plutonium determination in bioassay and environmental analysis are reviewed with special emphasis on urine and soil samples. The individual steps in techniques based on precipitation, solvent extraction, glass-fibre adsorption and ion exchange are discussed. The problems connected with α-counting are also considered briefly.

In the course of construction of nuclear energy plants all over the world the determination of plutonium for bioassay and environmental analysis has become of outstanding importance. In this paper, the principles and problems of suitable analytical methods are reviewed with special emphasis on urine and soil analysis; problems of sampling and sample homogeneity are excluded. Reviews of other aspects of analyses for plutonium are available [1—6]; Campbell et al. [7] have written a brief history of plutonium bioassay in the Los Alamos Scientific Laboratory.

The analytical procedures may be subdivided into the following individual steps:

1. sample decomposition, possibly connected with preconcentration of plutonium;
2. separation of the plutonium from matrix material;
3. preparation of the counting source;
4. α-spectrometric measurement of plutonium (if applicable).

DECOMPOSITION OF THE SAMPLES

The sample decomposition in urine analysis must involve liberation of plutonium from its organic bonding; the nature of "metabolized plutonium" has been discussed [8]. This can be achieved in various ways: heating of the urine with HNO_3 or HNO_3—H_2O_2 [9—13] mixtures is widely used and sometimes sulphuric acid is also added [14]. The organic substances can also be destroyed by total evaporation of the sample, followed by dry or wet ashing of the

residue; ashing temperatures are usually around 500°C. Other possibilities are "cold dry ashing" with excited oxygen or the iron(II)-catalysed H_2O_2 oxidation [15]. To save time, the total evaporation of the sample should be avoided if possible, and replaced by an acid hydrolysis of the urine followed by precipitation of the Pu on a phosphate carrier [9, 16—21], which is subsequently subjected to dry or wet ashing to remove adhering organic material. Plutonium losses may occur if this precipitation is carried out in the presence of DTPA [22, 23]. There has been some discussion about possible introduction of α-emitting contaminants into the sample with calcium phosphate carrier [10], but in this laboratory, such effects have never been observed. The dry ashing of urine (or phosphate carrier) residues at elevated temperatures always involves the formation of pyrophosphates. These must be removed by hydrolysis with or without addition of a catalyst [18, 23] because of their interference with certain analytical methods (see the section on Separation of Plutonium).

It is also possible to isolate Pu directly from nitric acid-hydrolysed urine by anion exchange [24]. A method of removing Pu from urine without pretreatment was reported by Weiss and Shipman [25]; essentially, potassium rhodizonate is added to the sample and Pu is precipitated on it with alcohol. The procedure is not very selective; Ca, Fe, Pa, Np and other elements are also precipitated so that additional separation steps are necessary [25]. Pu yields of 91.3 ± 5% were reported. The separation of protein-bound Pu by ultrafiltration [26] and its coprecipitation on barium sulphate [27], bismuth phosphate [28, 29] or iron hydroxide have also been reported [30, cf. 10, 31].

The conversion of the Pu contained in soil samples to a soluble form depends on several factors, the most important being the thermal pretreatment of the material. The purpose of the solubilization is to transform Pu to an ionogenic form connected with a complete exchange with the added tracer (^{236}Pu or ^{242}Pu in bioassay as well as environmental analysis). The addition of a suitable tracer is of great importance, because there is no possibility of achieving quantitative or even consistent plutonium recoveries by the usual processing methods. For dissolution of Pu, acid extraction and various fusion procedures are in use; the former method permits the decomposition of larger samples in a shorter time. Recently it was demonstrated by Sill that acid extraction of soil samples frequently does not result in complete exchange of native and tracer Pu. Sill extracted soil samples ashed at 700 and 1000°C, respectively, with HCl—HNO_3; with this procedure 20% (93%) of the native Pu remained in the insoluble residue, whereas the ^{236}Pu tracer appeared almost quantitatively in the solution [32]. Other samples were subjected to hydrofluoric acid treatment with similar results: in most cases equilibrium was not achieved, and about 1/3 of the plutonium remained in the residues, probably in the form of an insoluble fluoride. Attempts to decompose the residual fluorides completely with perchloric or nitric acid failed. Fuming of the sample with perchloric acid in the presence of HF seems to be dangerous, because $HClO_4$ can convert Pu to its hexavalent form and PuF_6 may be lost by volatilization (b.p. 62°C).

Butler et al. [33] ashed 5 g of soil samples at 550°C, fumed with HF followed by HCl, and fused the insoluble residue with potassium fluoride; the chemical Pu recovery of the entire procedure (see below) was given as 75 ± 6%. Adams et al. investigated the extractability of Pu from differently pretreated soils; their results show that the Pu is completely extractable with 8 M nitric acid from samples ashed at a temperature of 300°C in the presence of a tracer. An ashing temperature of 900°C reduces the recovery to 41% [34]. Pillai found three extractions of marine sediments with 8 M HNO_3 sufficient to recover Pu almost quantitatively, and good results were also obtained with HCl—HNO_3; only a few % of the Pu remained in the residue. These results were published in a recent IAEA report on the methodology of the determination of certain radionuclides in the marine environment (sea water, marine sediments etc.) [30]. Sill and Hindman [35] investigated the dependence of Pu extraction from soil samples on thermal and chemical treatment. They found that in the case of HCl—HNO_3 and HF treatments, the recovery decreased greatly with increasing ashing temperature, an addition of HF being always advantageous. Gillette et al. [36] obtained an average recovery of 93% when soil samples were leached with hot concentrated nitric acid.

Quantitative dissolution of Pu in every form, including PuO_2 (which is generated at high ashing temperatures), by acid extraction alone seems to be impossible; Sill et al. [37] recommend the application of fluoride—pyrosulphate fusions. HF—HNO_3—$HClO_4$ treatment of samples has been used by Schüttelkopf for the decomposition of plant ashes, dust filters etc. [38] and also by other authors [39—41], but it is relatively time-consuming and — because of the volatility of PuF_6 mentioned above — not free from objections. McDowell et al. [42] boiled 10-g soil samples with a mixture of concentrated HNO_3 and HF and continued boiling after the addition of HCl. HF was complexed with boric acid and the precipitate obtained with NaOH was dissolved in HNO_3, followed by extraction of the Pu with triisooctylamine (see below). Recoveries were reported to be 40—70%.

Extraction with 8 M HNO_3 was used by Inoue and Sakanoue [43, 44] partly with the aid of ultrasonic treatment; the chemical recoveries were only 3—23%. Recoveries between 30 and 99% were reported by Wong [45] for his HCl—HNO_3—H_2O_2 extraction of marine sediment samples. HNO_3—HCl was used by Chu [46, cf. 47] and gave more consistent results (78—86%); moreover, Chu found good agreement with the results obtained by carbonate fusion. McLendon [48] and deBortoli [49] extracted soil samples with 6—8 M HCl; deBortoli claimed an average recovery of 67.9 ± 32.2% calculated from the results of 13 analyses. A wet ashing process with H_2O_2, catalysed by iron(II), was used to destroy organic substances in environmental samples; the chemical recoveries were $\geqslant$ 80%.

The surest method of solubilizing the native plutonium of soil samples of unknown thermal pretreatment and chemical composition is to use a fluoride—pyrosulphate fusion technique as described by Sill and his collaborators

[27, 37]; its only disadvantage is the relatively small amount of sample which can be handled because of the need for expensive platinum dishes. A procedure which allows the determination of all α-emitters from Ra through Cf in a single sample decomposed in this way has been reported [37].

Plutonium originating from global fallout or adsorption on soil from aqueous solution is readily soluble in mineral acids. The reasons for the solubility of fallout plutonium are the small particle size and the fact that the plutonium oxide formed by a nuclear explosion, is not present as insoluble plutonium dioxide, but as an unstoichiometric product with the approximate composition Pu_2O_3 [32]. Table 1 shows the effect of various leaching and decomposition methods applied to a soil sample ashed at different temperatures.

THE SEPARATION OF PLUTONIUM FROM MATRIX MATERIALS

Several methods are available for the separation of plutonium from urine evaporation residues or carrier precipitations; they are based on precipitation, extraction, glass fibre adsorption or ion exchange.

Schwendiman and Healy [50] described a method for the isolation of plutonium from totally evaporated urine by carrier precipitation on LaF_3 from an acidic solution of the urine salts; plutonium was separated from the lanthanum by means of a TTA extraction step [cf. 1, 51]. The detection limit of the procedure was given as 0.5 d.p.m.; the standard deviation, derived from the results of analysis for 553 samples (each containing 0.57 d.p.m. ^{239}Pu), was 12%. The α-counters used initially were later replaced by a nuclear emulsion technique (detection limit <0.05 d.p.m./1.5 l). When this methodology was tested in England, an average chemical recovery of 40—60% was obtained in contrast to the 85 ± 5% claimed by the authors. The principle of this technique is still in use [30, 38, cf. 52]; Chenley et al. [53] have discussed the LaF_3 coprecipitation technique critically.

A different procedure was worked out by Smales, Brooks and others [10, 21, 54—56]. Plutonium was co-extracted along with iron as their cupferronates

TABLE 1

The extraction of plutonium from a standard soil

Ashing temp. (°C)	Chemical attack	Time (h)	%Pu in soln.
110	$HCl—HNO_3$	2.5	94
700	$HCl—HNO_3$	2.5	57
1000	$HCl—HNO_3$	2.5	17
1000	95% HNO_3, 5% HF	2.0	59
1000	HF (fuming)	1.0	54
1000	HF—8 M HNO_3 (95 + 5 or 50 + 50)	16.0	63

into chloroform; a similar process was used as early as 1944 [7]. The iron was then removed by extraction with diisopropyl ether from hydrochloric acid medium [cf. 15, 57]. Chemical recoveries were given as 80—85 ± 7%, the detection limit being 0.1 pCi/1.5 l. The nuclear emulsion technique was replaced by a silicon solid-state counter of 0.3 c.p.h. background (detection limit ca. 0.04 d.p.m.); the low background in conjunction with high energy resolution makes this instrument superior to other counting equipment [10, 58]. The historical development of the counting techniques used in Pu bioassay has been reviewed [7]. Cupferron extraction has been combined with anion exchange [40].

Adsorption and ion-exchange methods

Sanders and Leidt [11] used an anion exchanger for the separation of Pu from evaporated and wet-ashed urine, the adsorption taking place from 7—8 M nitric acid medium. Techniques of this type have been used frequently (see also ref. 59); the original method gave very fluctuating recoveries (40—80%). The authors claimed a sensitivity of 0.007 d.p.m./250 ml. The use of ion-exchange filters in urinalysis has been described [60].

Eakins and Gomm [18] introduced another separation principle: the adsorption of plutonium on a glass surface. After hydrolysis of the urine with HNO_3 and precipitation of the Pu on a calcium phosphate carrier, the carrier was ashed at 500°C and dissolved in 1 M HNO_3, and the solution was boiled to complete hydrolysis of the pyrophosphates; the Pu recovery would otherwise by very much lower, as reported after thorough investigation by Eakins and Gomm [18] and Bates et al. [23]. After reduction of plutonium to Pu^{3+} with sulphite (if Np adsorption is required the stronger reductant hydroxylamine must be used), the pH of the solution was adjusted to 5 and the liquid poured through an activated glass fibre filter; this resulted in a more or less complete adsorption of Th, Pa, U, Np, Pu, Am, and Cm. The process is impossible in the presence of large amounts of calcium and iron [61]. The recoveries of Th, Pa, Pu, Am and Cm are $\geqslant$ 80%; the method cannot be applied to the determination of Ra, Po and U. After the elution of adsorbed substances from the filter, plutonium can be purified by anion exchange [62]. The technique described is not only useful for urine analysis; Ballada et al. have applied it to the analysis of feces for Pu, Am and Cm [63], and recently the determination of Am and Cm in various tissue samples was reported [64].

The direct adsorption of plutonium from a urine digest with nitric acid on to an anion exchanger, as described by Silker [24] proved to be irreproducible [23], possibly because of incompleteness of the HNO_3—H_2O_2 wet ashing process. Plutonium was eluted by a technique introduced by Kressin and Waterbury [65]; other stripping methods have been studied [23].

The method of Kressin and Waterbury [65] has frequently formed the basis of the Pu separation by anion exchange in bioassay and environmental analysis [17, 34, 46, 48, 59, 66—69]. In principle, the Pu is adsorbed from 7—8 M nitric acid medium on an anion exchanger, which may be in the form of an

ion-exchange filter [60, 70]. The exchanger is subsequently washed with pure HNO_3 of equal concentration (to remove iron, uranium, etc.); plutonium is then eluted with dilute HCl—HF (or sometimes HNO_3—HF). Under these conditions, of all the elements of interest, only Pu, Np and Th are strongly adsorbed, although U(VI) and Pa(V) are adsorbed to a limited extent. The distribution coefficient D of Pu(IV) is about 3500 at this HNO_3 concentration. The D value for Np(IV) is ca. 2000 and that of Th ca. 300; D values of U(VI) and Pa(V) are only about 10. Iron(III), Am(III) and Cm(III) are not adsorbed at all [71]. Thorium is not retained on the exchanger in a HCl medium and can therefore be removed easily by a washing step with strong HCl [cf. 23]. An analytical method based on these principles has been used successfully in this laboratory for the determination of Pu in urine.

If a determination of ^{237}Np is required, neptunium can be eluted together with plutonium and determined α-spectrometrically. If a Pu—Np separation is necessary, Pu can be desorbed with certain reductants such as HI, NH_4I in strong HCl [9, 13, 17, 20, 23, 40, 45, 72] and others [11, 16, 73, 74], which can reduce Pu(IV) to Pu(III); the latter is not adsorbed on anion exchangers under these experimental conditions. Neptunium remains in a tetravalent form on the exchanger and can be eluted by dilute acids or complexing agents [72, 74].

The separation of plutonium by anion-exchange processes depends strongly on the stabilization of the Pu(IV) ion. This can be achieved by the addition of $NaNO_2$ to the acidic solution; the use of H_2O_2 should be avoided [75]. Without stabilization, disproportionation reactions occur, and Pu(IV) is converted to a mixture of several valencies [76], thus reducing its ability to undergo anion-exchange reactions. In the strongly acidic solutions used, there is also no danger of polymerization of Pu(IV).

For the determination of plutonium in biological and environmental samples, anion exchange from HCl medium is also used, normally followed by a second exchange step from nitric acid medium [20, 47, 77, 78]. Talvitie [77] gives a minimum detectable quantity of ^{239}Pu of 0.02 pCi.

Solvent extraction methods

Because of the rather time-consuming exchange processes, there is now an increasing tendency to extract Pu with certain tertiary amines from hydrochloric or nitric acid medium.

Butler [79] reported the extraction of various actinides with triisooctylamine (TIOA) and its applicability to urine analysis; he emphasized the similarity of the extraction behaviour of TIOA and Alamine-336, a mixture of mainly tertiary amines of some C_8—C_{10} isomers (predominantly C_8). On this basis he developed a technique [13] for the extraction of U, Np and Pu with TIOA from an 8 M hydrochloric acid solution of the evaporation residue of a single urine sample, and their selective back-extraction with 8 M HCl—NH_4I (Pu), 4 M HCl—0.02 M HF (Np) and 0.1 M HCl (U). This procedure showed some disadvantages such as the time-consuming total evaporation of the sample, the

high cost of TIOA and the improbably short extraction times. For these reasons, an extraction method for U, Np and Pu with the cheap technical product Alamine-336 from 10 M HCl was developed in this laboratory [81]; a calcium phosphate carrier precipitation step replaced the urine evaporation and the question of extraction times was re-examined. An average recovery of U, Np and Pu of 95% was achieved with negligible cross-contamination [72]; the possibility of a direct electro-deposition of Pu from the HCl-NH_4I back-extraction liquors will be discussed later.

Testa [16, 19] described an interesting variation of the Pu extraction from urine with tertiary amines by means of an extraction chromatographic technique. Urine was wet-ashed with HNO_3—H_2O_2 and the plutonium precipitated on calcium phosphate. The carrier was dissolved in 2 M HNO_3 (+ $NaNO_2$) and the solution passed through a column containing a 50% mixture of trioctylamine (TOA) and xylene on a KEL-F (polytrifluorochloroethylene) support. The Pu was eluted with sulphurous acid. The recoveries were 90.5 ± 2.3%, the detection limit being 0.1 d.p.m./l.

Other substances are also suitable for the separation of actinides from urine by extraction chromatography. Delle Site [74] used neotridecanohydroxamic acid in 0.3 M cyclohexane solution on Microthene-710 (a polyethylene preparation) to determine Np and Pu in urine, after preconcentration of the elements by calcium phosphate precipitation. Plutonium was eluted by reduction with hydroquinone, and Np with oxalic acid; the recoveries were 73.5% for Pu and 82.3% for Np. Np and Pu can be separated from uranium by tridodecylamine (TLA) on KEL-F [82]. A general review of extraction chromatographic methods in urine analysis has been published [83].

The system trioctyl phosphine oxide (TOPO)—Microthene-710 was reported for the isolation of Pu [84] and Np [85] from urine; it is also useful for Th and U determinations. Hampson and Tennant [86] have described the application of TOPO to actinide extraction from environmental samples. Uranium can be extracted by tributyl phosphate (TBP) on Microthene. The system TOPO—HDEHP—Microthene-710 has been used for the separation of certain actinides from urine [22].

Amine extraction can also be applied to the separation of plutonium from nitric acid soil digests or concentrates [39, 42—44]. Many authors [87—95] have investigated the extraction behaviour of Pu(IV) with tertiary amines from nitric acid solutions: the values of D are a function of the HNO_3 concentration in the aqueous liquid as well as the amine concentration in the organic phase. The distribution ratios for certain actinides in the extraction with 20% trioctylamine from 4 M HNO_3 are listed in Table 2.

Little work has been devoted to the extraction of plutonium from nitric acid medium with amines in the presence of large amounts of other salts. Wilson investigated the influence of U(VI) concentration on the extraction of Pu(IV) with trilaurylamine (TLA) from 1—4 M nitric acid, and found a decreasing D value with increasing uranyl concentration [90]. Srinivasan et al. [93] extracted Pu(IV) with 20% TLA in xylene; the D_{max} was

TABLE 2

Distribution ratios for some actinides in extraction with 20% TOA—xylene from 4 M HNO_3 [87]

Element	Th	Pa(V)	U(VI)	Np(IV)	Pu(III)	Pu(IV)[a]
D	10.2	1.87	2.7	175.0	0.08	850.0

[a] 2 M HNO_3.

about 300 at a nitric acid concentration of 3 M but this value was considerably lower in the presence of U(VI). Similar results were obtained by Koch et al. [94]. Data on systems containing large amounts of Ca^{2+}, Fe^{3+} etc. as in soil solutions are apparently not available [96, cf. 4].

During an investigation [97] of Pu(IV) extraction from a ca. 7 M nitric acid soil digest with 10% TLA in xylene, the value of D was only 5.3, so that under the given experimental conditions (volume ratio $V_{org}/V_{aq} = 0.2$) double extraction with 25% TLA in xylene ($D = 13.0$) was required to achieve good recovery of Pu. A bilogarithmic plot of amine concentration against D values gave a straight line with a slope of 1.0, indicating the presence of a univalent anionic plutonium nitrate complex in the organic phase. Probably complexes of the type $(R_3NH)Pu(NO_3)_5$ and/or $(R_3NH)HPu(NO_3)_6$ were extracted instead of the "normal" complex $(R_3NH)_2Pu(NO_3)_6$ known to be extracted from strong nitric acid solutions by processes of an anion exchange nature [87, 88, 90, 98—100]. Similar diagrams have also been found by other authors [101, 102]. The TLA extraction can be used for a satisfactory determination of Pu in environmental samples [97].

In some cases, Pu in environmental samples has been extracted from hydrochloric acid medium, despite the difficulties arising from the relatively high iron content of this type of sample. To avoid these troubles, deBortoli [49] complexed Fe^{3+} with EDTA at pH 0 forming a compound of anionic or neutral character; Pu remained in cationic form and was adsorbed on a cation exchanger. Plutonium was subsequently fixed on an anion exchanger from 9 M HCl and eluted with 6 M HCl—0.2 M HF. Butler et al. [33] extracted Pu from 6 M HCl soil solutions with TIOA; the element was back-extracted with 4 M HCl—0.05 M HF. Final purification was achieved by coprecipitation on LaF_3 (0.1 mg La), and the fluoride precipitate served as counting source [cf. 103]. The sensitivity of the method was 0.03 d.p.m. Instead of the commercially available lanthanum preparations, which are often contaminated with natural α-emitters, praseodymium has been recommended [1]. However, purification procedures for lanthanum have been described [47].

The isolation of plutonium by amine extraction as well as anion exchange from HCl medium offers the advantage of an immediate separation from thorium, its main disadvantage being the interference of large amounts of iron. Plutonium is adsorbed as the $PuCl_6^{2-}$ complex [81].

Other extractants are also in use for the separation of Pu from bioassay and environmental samples, e.g. HDEHP [41, 73, 104] and TBP [105]. Aarkrog

[106] and Markussen [107] purified Pu with 1-phenyl-4-benzoyl-pyrazolone-5 Butler and Hall [80] introduced the use of dibutyl *N*,*N*-diethylcarbamyl-phosphonate (DDCP) to determine actinides in biological materials [80]. The extraction of Pu with the quaternary amine Aliquat-336 after its preconcentration on barium sulphate has been reported [36, 37].

Amine extraction of plutonium can be combined with liquid scintillation counting [39, 42, 108]. The determination of Pu in biological material by gel scintillation has been described [109]. For liquid scintillation counting, the Pu is extracted from 1—5 M HNO_3 with TIOA; after back-extraction with dilute $HClO_4$, Pu is precipitated on a CeF_3 carrier, which is subsequently dissolved in HNO_3—H_3BO_3; the solution is extracted with HDEHP dissolved in the scintillator (POPOP in toluene) directly in the counting vial [39]. As reported by McDowell et al. [42], the back-extract is heated with LiCl or $LiNO_3$, the residue of molten $LiClO_4$ is brought into solution, and the Pu is extracted with HDEHP—scintillator. The extraction requires HDEHP and amines of high purity, and the latter must be essentially free of primary and secondary amines [42]. The counting efficiency is 95—100%, and the energy resolution 200—300 keV FWHM [42]. The detection limits depend on the conditions of measurement; values quoted are 0.02—1.0 d.p.m. [42] and 0.18 pCi [39]. Somewhat simplified methods have been reported [104, 110, 111]. The possibilities of α-spectrometry by liquid scintillation have been discussed [112, 115, 128].

The separation of minute amounts of Pu from rock samples by paper chromatography has been described [116].

THE PREPARATION OF COUNTING SOURCES

If α-spectrometric measurement of the plutonium is not required, the Pu solution, prepared by one of the methods described in the preceding sections, is simply evaporated in a small platinum, stainless steel or Teflon dish and counted [117]. Sometimes it is advantageous to flame the preparation before counting (removal of organic substances, conversion of Pu to PuO_2), but this process may entail plutonium losses. Teflon dishes can obviously not be subjected to such a treatment.

Sources suitable for α-spectrometric measurement of Pu, U, etc. are usually prepared by an electrodeposition technique. Many methods are known, many of them tedious and time-consuming and therefore unsuitable for routine use. The various techniques have been reviewed [69, 72, 97, 118, 119].

As a basis for a rapid, simple and reliable method, the procedure of Mitchell can be recommended [120]: quantitative electrodeposition of Pu from weak hydrochloric acid (methyl red) solution containing ammonium chloride on a platinum cathode requires only 15—20 min; stainless steel cathodes can also be used. The direct electrodeposition of plutonium from HCl solutions containing variable amounts of ammonium iodide, such as are obtained in the case of a reductive elution or back-extraction of Pu, has been proved feasible

by Irlweck and Veselsky [118, 121]. When plutonium is stripped with dilute HCl—HF as described by Kressin and Waterbury [65], the solution is evaporated to dryness, oxidized with HNO_3—H_2O_2 and finally evaporated with HCl—NH_4Cl; the ammonium chloride residue is then dissolved in water and subjected to electrolysis. Electrodepositions done in this way are rather sensitive to various contaminants such as iron [cf. 23, 122], nitric acid, etc. The pH of the electrolyte must be adjusted carefully and the cathode cleaned thoroughly. When stainless steel discs are used, the procedure with HNO_3—HF as reported by Baerring [123] can be recommended.

Plutonium is deposited as the hydroxide; even when electrolysis is done from acidic solution, a thin basic cathodic layer is formed, and this is immediately destroyed in case of a breakdown of the current supply. Therefore the electrolyte must always be made alkaline before the end of the electrolytic process to avoid dissolution of the plutonium deposit. When all other experimental parameters such as time, composition of the electrolyte, etc., are kept constant, the quantity of element deposited is directly proportional to the active diameter of the cathode and inversely proportional to the volume of the electrolyte [124]. For a given diameter of the cathode, the volume of the electrolyte should be kept as low as possible, but a lower limit is also imposed by the heating of the electrolyte during the deposition process, which may increase cathode corrosion and the redissolution of the plutonium; the cells must be cooled if necessary [36]. Instead of a pH adjustment to methyl red indicator [120], methyl violet indicator (pH $\approx$ 1) is useful; a Pu recovery of ca. 98% can be easily obtained in 20 min [97].

THE α-SPECTROMETRIC MEASUREMENT OF PLUTONIUM

When samples are processed after addition of tracer and if α-emitting contaminants such as ^{228}Th, ^{234}U, ^{238}U, etc, are expected, the plutonium preparation must be subjected to α-spectrometry. To compensate for the chemical recovery of the Pu isolation procedure, which depends on the material, especially in the case of soil samples, it is advantageous to add the tracer before the ashing process; the corresponding nuclide (in most cases, ^{242}Pu or ^{236}Pu) must be absolutely free of the isotope to be measured. The decay energies of some heavy α-emitters are listed in Table 3.

The disadvantages of ^{236}Pu as tracer were recently discussed by Kressin et al. [125]. One disadvantage arises from the relatively high α-energy of that nuclide: when the α-particles emitted suffer an energy reduction by scattering effects, additional counts may be produced in the energy region of the required Pu isotopes because of their lower α-energy. Thus the background in this part of the spectrum (and the detection limit) may be increased, and consequently the precision of low-level measurements can be reduced. Decay products of ^{236}Pu such as ^{232}U and ^{228}Th, which also emit α-radiation of relatively high energy, show the same effect. To reduce scattering effects and to improve energy resolution, the counting sources should always be as "carrier-free" as

TABLE 3

Decay energies of some heavy α-emitters

Nuclide	α-Energies (MeV)
^{228}Th (Radiothorium)	5.43 (71%), 5.34 (28%)
^{230}Th (Ionium)	4.68 (76%), 4.62 (24%)
^{234}U	4.77 (72%), 4.72 (28%)
^{238}U	4.20 (75%), 4.15 (25%)
^{231}Pa	5.06 (10%), 5.02 (32%), 5.01 (24%), 4.95 (22%), 4.73 (11%)
^{237}Np	4.78 (75%), 4.65 (12%)
^{236}Pu	5.77 (69%), 5.72 (31%)
^{238}Pu	5.50 (72%), 5.46 (28%)
^{239}Pu	5.16 (88%), 5.11 (11%)
^{242}Pu	4.90 (76%), 4.86 (24%)

possible. The tracer solution must be purified from time to time to remove interfering α-emitting decay products. Kressin et al. [125] have demonstrated this effect with a counting source as low as 20 d.p.m. ^{236}Pu on a stainless steel planchet: even under these conditions, they found a considerable increase of the ^{239}Pu background in the spectrum; therefore they recommend a maximum tracer quantity of about 10 d.p.m. ^{236}Pu.

^{242}Pu seems to be superior to ^{236}Pu; its low α-energy does not interfere with the ^{239}Pu measurement, and this is also true for the decay product ^{238}U. The only restrictions in the practical use of ^{242}Pu as the tracer in environmental plutonium analysis are isotopic purity and price.

The use of ^{238}Pu as the tracer in soil analysis [36, 116] and for the general tracer problem [126] have been discussed. The determination of plutonium in soil by mass spectrometry has been reported [127]; the development of a fission track method for the determination of fall-out plutonium in tissue samples has been described [129].

REFERENCES

1 S. A. Reynolds and T. G. Scott, Radiochem. Radioanal. Lett., 23 (1975) 269.
2 R. J. Budnitz, LBL-2039 (1973).
3 J. W. Healy, IEEE Trans. Nucl. Sci., 19 (1972) 219.
4 J. C. Veselsky, Osterr. Chem. Zeitg. H., 7—8 (1976) 2.
5 O. J. Wick (Ed.), Plutonium Handbook, Vol. 2, Gordon and Breach, 1967, p. 923.
6 J. M. Nielsen and T. M. Beasley, HW-SA-3337 (1964).
7 E. E. Campbell, M. F. Milligan, W. D. Moss and H. F. Schulte, LA-5008 (1972).
8 D. S. Popplewell, G. N. Stradling and G. J. Ham, Rad. Res., 62 (1975) 513.
9 J. D. Eakins, A. E. Lally, A. Morgan and F. J. Sandalls, AERE-AM-103 (1968).
10 F. J. Sandalls and A. Morgan, AERE-R-4391 (1964).
11 S. M. Sanders and S. C. Leidt, Health Phys., 6 (1961) 189.
12 W. R. Jacobsen, ANL-6637 (1961).
13 F. E. Butler, Health Phys., 15 (1968) 19.
14 W. J. Major, R. A. Wessman, R. Melgard and L. Leventhal, Health Phys., 10 (1964) 957.

15 H. Schieferdecker, KFK-810 (1968).
16 C. Testa, RT/Prot (67) 3 (1967).
17 E. E. Campbell and W. D. Moss, Health Phys., 11 (1965) 737.
18 J. D. Eakins and P. J. Gomm, Health Phys., 14 (1968) 461.
19 C. Testa, RT/PROT (69) 44 (1969).
20 L. C. Henley, CONF-651008 (1965).
21 M. E. D. Bains, AEEW-R292 (1963).
22 A. delle Site, G. Santori and C. Testa, CONF-730907-P1 (1974) p. 532.
23 T. H. Bates, T. H. Boyd and J. P. Clarke, BNFL-1(W) (1971).
24 W. B. Silker, Health Phys., 11 (1965) 965.
25 H. V. Weiss and W. H. Shipman, Anal. Chem., 33 (1961) 37.
26 G. N. Stradling, D. S. Popplewell and G. J. Ham, Int. J. Appl. Radiat. Isot., 25 (1974) 217.
27 C. W. Sill and R. L. Williams, Anal. Chem., 41 (1969) 1624.
28 W. A. Brobst, COO-213 (1957).
29 J. Kooi and U. Hollstein, Health Phys., 8 (1962) 41, 49.
30 Reference Methods for Marine Radioactivity Studies II. Technical Report Series No. 169, IAEA Vienna, 1975.
31 R. Lieberman and A. A. Moghissi, Health Phys., 15 (1968) 359.
32 C. W. Sill, Health Phys., 29 (1975) 619.
33 F. E. Butler, R. Lieberman, A. B. Strong and U. R. Moss, LA-4756 (1971) p. 47.
34 W. H. Adams, J. R. Buchholz, C. W. Christenson, G. L. Johnson and E. B. Fowler, LA-5661 (1974).
35 C. W. Sill and F. D. Hindman, Anal. Chem., 46 (1974) 113.
36 R. K. Gillette, M. L. Curtis, E. B. Nunn, J. O. Frye and C. T. Bishop, MLM-1901 (1972).
37 C. W. Sill, K. W. Puphal and F. D. Hindman, Anal. Chem., 46 (1974) 1725.
38 H. Schuettelkopf, Rapid Methods for Measuring Radioactivity in the Environment, Symposium Neuherberg, 5—9 July 1971, Proceedings, IAEA Vienna 1971, p. 183.
39 D. L. Bokowski, Am. Ind. Hyg. Assoc. J., June (1974) 333.
40 W. J. Major, R. A. Wessman, R. Melgard and L. Leventhal, TLW-1107 (1965).
41 G. E. Bentley, W. R. Daniels, G. W. Knobeloch, F. O. Lawrence and D. C. Hoffman, LA-4756 (1971) p. 59.
42 W. J. McDowell, D. T. Farrar and M. R. Billings, Talanta, 21 (1974) 1231.
43 Y. Inoue and M. J. Sakanoue, J. Rad. Res. 11 (1970) 98.
44 M. Sakanoue, M. Nakaura and T. Imai, Rapid Methods for Measuring Radioactivity in the Environment, Symposium Neuherberg 5—9 July 1971, Proceedings, IAEA Vienna 1971, p. 171.
45 K. M. Wong, Anal. Chim. Acta, 56 (1971) 355.
46 N. Y. Chu, Anal. Chem., 43 (1971) 449.
47 J. H. Harley (Ed.), HASL Procedures Manual, HASL-300 (1972).
48 H. R. McLendon, Health Phys., 28 (1975) 347.
49 M. C. deBortoli, Anal. Chem., 39 (1967) 375.
50 L C. Schwendiman and J. W. Healy, A/CONF-15/P/759 (1958).
51 J. C. Dalton, PG Rep., 284 (W) (1962).
52 H. Levine and A. Lamanna, Health Phys., 11 (1965) 117; R. N. Khandekar, Radiochem Radioanal. Lett., 25 (1976) 77.
53 R. B. Chenley, G. J. Hunter and T. J. Webber, AERE C/M-327 (1958).
54 A. A. Smales, C. Airey, G. N. Walton and R. O. R. Brooks, AERE C/R-533 (1950).
55 R. Brooks, AERE-AM60 (1960).
56 D. M. Kemp, AERE-R 4119 (1962).
57 J. Sommer, Kernenergie, 7 (1964) 257.
58 H. L. Butler and W. F. Splichal Jr., Health Phys., 12 (1966) 1627.
59 E. E. Campbell, M. F. Milligan, W. D. Moss, H. F. Schulte and J. F. McInroy, LA-4875 (1973).

60 F. Clanet, J. Ballada, J. Lucas and C. Gil, LA-TR-73-39 (1973).
61 L. Widua, K. Geisert and H. Schieferdecker, KFK-Ext. 23/76-1 (1976).
62 J. D. Eakins, AERE-R5637 (1967).
63 J. Ballada, L. Jeanmaire and P. Nauche, CEA-N-1667 (1973).
64 F. E. H. Crawley, Int. J. Appl. Radiat. Isot., 26 (1975) 137.
65 I. K. Kressin and G. R. Waterbury, Anal. Chem., 34 (1962) 1598.
66 W. B. Silker, BNWL-36-III, 3.37 (1965).
67 E. P. Hardy, HASL-235 (1970).
68 R. E. Rowland and J. S. Marshall, ANL-8060 Pt. III (1973).
69 N. Valentin, C. Weyers and J. Luysterborg, BLG-408 (1966); C. E. Gray (Ed.), SAND-75-0014 (1975).
70 F. Clanet, J. Ballada, J. Lucas and C. Gil, Health Phys., 23 (1972) 244.
71 F. P. Roberts, HW-59032 (1959).
72 J. C. Veselsky, Pak Chan Kirl and N. Sezginer, J. Radioanal. Chem., 21 (1974) 97.
73 F. E. Butler, Anal. Chem., 37 (1965) 340.
74 A. delle Site, J. Radioanal. Chem., 14 (1973) 45.
75 C. W. Sill, D. R. Percival and R. L. Williams, Anal. Chem., 42 (1970) 1273.
76 M. Taube, Plutonium, Verlag Chemie, Weinheim, 1974, p. 74.
77 N. A. Talvitie, Anal. Chem., 43 (1971) 1827.
78 V. F. Hodge, F. L. Hoffman, R. L. Foreman and T. R. Folsom, Anal. Chem., 46 (1974) 1334.
79 F. E. Butler, CONF-212-4 (1963).
80 F. E. Butler and R. M. Hall, Anal. Chem., 42 (1970) 1073.
81 J. C. Veselsky, M. Nedbalek and O. Suschny, Allg. Prakt. Chem., 22 (1971) 2.
82 D. Gourisse and A. Chesne, Anal. Chim. Acta, 45 (1969) 321.
83 C. Testa, Use of Extraction Chromatography in Radiotoxicology, in T. Braun and G. Ghersini (Eds.), Extraction Chromatography, Elsevier, Amsterdam (1975) p. 279.
84 C. Testa and G. Santori, G. Fis. Sanit. Prot. Radiaz., 16 (1972) 1.
85 G. Santori and C. Testa, J. Radioanal. Chem., 14 (1973) 37.
86 B. L. Hampson and D. Tennant. Analyst (London), 98 (1973) 873.
87 W. E. Keder, J. C. Sheppard and A. S. Wilson, J. Inorg. Nucl. Chem., 12 (1960) 327.
88 F. Baroncelli, G. Scibona and M. Zifferero, J. Inorg. Nucl. Chem., 24 (1962) 541.
89 W. Knoch, Z. Naturforschg., 16 (1961) 525.
90 A. S. Wilson, Proc. UN Conf. Peaceful Uses At. Energy, 2nd, Geneva, (1958) Vol. 17, p. 348.
91 G. Calleri, A. Geoffroy and J. Arroyo-Suarez, ETR-115 (1961).
92 S. V. Kumar, S. C. Kapoor and S. P. Jain, B.A.R.C.-476 (1970).
93 N. Srinivasan, M. V. Ramaniah, C. L. Rao, P. K. Khopkar, G. M. Nair and N. P. Singh, B.A.R.C.-374 (1968).
94 G. Koch, J. Schön and G. Franz, KFK-893 (1970).
95 A. Chesne, G. Koehly and A. Bathellier, Nucl. Sci. Eng., 17 (1963) 557.
96 O. J. Wick (Ed.), Plutonium Handbook Vol. 1, Gordon and Breach, New York, (1967), p. 446.
97 J. C. Veselsky, Int. J. Appl. Radiat. Isot., 27 (1976) 499.
98 J. L. Ryan and E. J. Wheelwright, Ind. Eng. Chem., 51 (1959) 60.
99 J. M. Cleveland, The Chemistry of Plutonium, Gordon and Breach, New York, 1970, p. 110.
100 M. S. Milyukova, N. I. Gusev, I. G. Sentyurin and J. S. Sklyarenko, Analytical Chemistry of Plutonium, Humphrey, Ann Arbor, 1969, p. 34.
101 R. Swarup and S. K. Patil, J. Inorg. Nucl. Chem., 38 (1976) 1203.
102 E. Lopez-Menchero and L. Gehem, Eurochem. Symp. Aq. Reprocessing Chem. Irrad. Fuels, Brussels 1963, p. 147.
103 J. Cl. Harduin and P. Montels, CEA-R-3492 (1968).
104 D. R. Atherton, COO-119-237 (1968) p. 158.

105 E. L. Geiger, Health Phys., 1 (1959) 405.
106 A. Aarkrog, Reference Methods for Marine Radioactivity Studies II, Techn. Rep. Ser. No. 169, IAEA Vienna 1975, p. 91.
107 E. K. Markussen, Rep. Riso-M-1242 (1970).
108 J. P. Ghysels, Ind. Atom. Spat., 1 (1972) 33; Atomwirtschaft, (1972) 83.
109 J. D. Eakins and A. E. Lally, AERE-R6640 (1970).
110 R. F. Keough and G. J. Powers, Anal. Chem., 42 (1970) 419.
111 T. Y. Toribara, C. Predmore and P. A. Hargrave, Talanta, 10 (1963) 209.
112 J. H. Thorngate, W. J. McDowell, P. T. Perdue and D. J. Christian, ORNL-5046 (1975).
113 W. J. McDowell and L. C. Henley, ORNL-TM-3676 (1972).
114 J. H. Thorngate, W. J. McDowell and D. J. Christian, Health Phys., 27 (1974) 123.
115 A. Lindenbaum and C. J. Lund, Rad. Res., 37 (1969) 131.
116 H. Meier, D. Bösche, G. Zeitler, W. Albrecht, W. Hecker, P. Menge, E. Unger and E. Zimmerhackl, Radiochim. Acta, 21 (1974) 110.
117 R. A. Wood, H. Nishita, M. Hamilton and S. Wakakuwa, UCLA-12-1047 (1976).
118 K. Irlweck and J. C. Veselsky, SGAE Ber. No. 2402, ST-43/75 (1975).
119 J. C. Veselsky, Radiochim. Acta, 21 (1974) 151.
120 R. F. Mitchell, Anal. Chem., 32 (1960) 326.
121 K. Irlweck and J. C. Veselsky, Int. J. Appl. Radiat. Isot., 26 (1975) 481.
122 P. O. Jackson, BNWL-715 (Pt.2) (1968) 1.
123 N.-E. Baerring, Ab. Atomenergi AE-217 (1966).
124 P. G. Hansen, J. Inorg. Nucl. Chem., 12 (1959) 30; 17 (1961) 232.
125 I. K. Kressin, W. D. Moss, E. E. Campbell and H. F. Schulte, Health Phys., 28 (1975) 41.
126 V. W. Thomas, Jr., L. J. Kirby and I. C. Nelson, BNWL-SA-5480 (1975).
127 H. A. Storms, C. C. Carlson and F. F. Hunter, CONF-740701 (1974).
128 P. T. Perdue, D. J. Christi, J. H. Thorngate, W. J. McDowell and G. N. Case, ORNL/TM-S166 (1976).
129 R. P. Larsen and R. D. Oldham, ANL-75-3 (Pt. 2) (1975) p. 142; ANL-75-60 (Pt. 2) (1975) p. 96.

Analytica Chimica Acta, 90 (1977) 15—23

ELEKTROLYTISCHE ABSCHEIDUNG IM HYDRODYNAMISCHEN SYSTEM VON ng-MENGEN EISEN, KOBALT, ZINK UND WISMUT IM GRAPHITROHR

G. VOLLAND, P. TSCHÖPEL und G. TÖLG

Laboratorium für Reinststoffe des Instituts für Werkstoffwissenschaften am Max-Planck-Institut für Metallforschung, Stuttgart und Schwäbisch Gmünd (B.R.D.)

(Eingegangen den 5. Oktober 1976)

ZUSAMMENFASSUNG

Es wird eine Elektrolysezelle beschrieben, die es erlaubt, galvanostatisch ng-Mengen von Elementen in relativ kurzer Zeit aus Lösungskonzentrationen $\leqslant$ 10 p.p.b. zu $\geqslant$ 98% abzuscheiden und von nicht abscheidbaren Matrixelementen, z.B. Be, zu trennen. Der Elektrolyt (ca. 40 ml) wird durch eine zylindrische Kathode aus Reinstgraphit (Länge 9 mm, i.ϕ 2,8 mm) mit einer PTFE-Pumpe in einem Kreislaufsystem bewegt (20—30 ml min^{-1}). Die Anode aus Pt—Ir (ϕ 1,5 mm) befindet sich zentrisch im Kathodenraum. Die Graphitrohr-Kathode kann unmittelbar zur nachweisstarken Bestimmung der abgeschiedenen Elemente z.B. durch flammenlose AAS, Emissionsspektrometrie (ICP, CMP u.a.) und Aktivierungsanalyse eingesetzt werden. Die Abscheidungsausbeuten wurden radiochemisch mit ^{59}Fe, ^{60}Co, ^{65}Zn und ^{207}Bi bestimmt und sind für ammoniumfluoridhaltige Lösungen (2—10%ig) im pH-Bereich 5—6 optimal.

SUMMARY

An electrolysis cell is described, which allows the constant-current deposition of ng amounts of elements from solutions containing less than 10 p.p.b. with yields above 98% in relative short times. Separations from elements which cannot be electrolytically deposited (e.g. Be) are possible. The electrolyte (40 ml) is cycled through a cylindrical cathode of ultrapure graphite (length 9 mm, i.d. 2.8 mm) by a PTFE-pump at 20—30 ml min^{-1}. A Pt/Ir (diam. 1.5 mm) anode is centered in the cathode space. The graphite cathode can be used directly for a sensitive determination of the deposited elements, e.g. by flameless a.a.s., o.e.s. (i.c.p., c.m.p.) and n.a.a. Radiotracers (^{59}Fe, ^{60}Co, ^{65}Zn and ^{207}Bi) were used to determine the deposition yields, which were found to be optimal in NH_4F electrolytes (2—10%) of pH 5—6.

Bei der Bestimmung sehr niedriger Elementgehalte in Reinstmetallen strebt man aus verschiedenen Gründen an, sie von den Matrix-Elementen vorher möglichst quantitativ abzutrennen. Hierfür sind für den Extrembereich nur solche Trennprinzipien — wie Verflüchtigung oder Elektrolyse — geeignet, die möglichst geringe Quellen für systematische Fehler (Kontamination, Adsorption, Desorption u.a.) aufweisen [1].

Die herkömmliche elektrolytische Abscheidung erlaubt es im allgemeinen nur, Elemente im p.p.m.-Bereich an indifferenten Metall- und Graphit-Kathoden quantitativ anzureichern. Bei Kupfer z.B. ließen sich bereits Mengen $\leqslant$ 0,1 μg/100 μl nicht mehr quantitativ in einer optimierten Mikro-

zelle abscheiden [2—5]. Für kleinere Elementmengen können die Elektrolysezeiten bis über 50 h anwachsen [6, 7] oder es werden Grenzkonzentrationen erreicht [8], die wegen des Rücklöseeffektes nicht mehr zu unterschreiten sind.

Unedlere Metalle — z.B. Fe, Co, Zn — konnten im p.p.b.-bereich an Hg-Kathoden praktisch vollständig von solchen Matrixmetallen isoliert werden, die selbst elektrolytisch nicht abscheidbar sind, z.B. Be, Al, Ti, Zr, Nb, Ta, W. Eine destillative Abtrennung des Hg von den abgeschiedenen Elementen im Vakuum bietet sich an, ist jedoch sehr aufwendig [1, 9].

Eine wesentliche Verbesserung der Abscheidung auch an Graphit und anderen Elektroden gelingt, wenn man den Massentransport im Elektrolyten, der üblicherweise durch Rühren der Lösung oder Rotation der Elektroden besorgt wird, im hydrodynamischen Fluß vornimmt [10—12] und den Abstand zwischen Anode und Kathode relativ gering hält. Der Elektrolyt wird mit Hilfe einer Pumpe in einem Kreislaufsystem durch einen zylindrischen Kathodenraum rasch bewegt. Es liegt nahe, Material und Geometrie der Röhrenkathode so zu wählen, daß die im Innern der Kathode abgeschiedenen Metalle unmittelbar durch z.B. flammenlose AAS, Emissionsspektrometrie, Neutronenaktivierungsanalyse u.a. bestimmt und die durch weitere Manipulationen bedingten Fehler möglichst klein gehalten werden.

DIE ELEKTROLYSEZELLE

Die entwickelte Durchfluß-Elektrolysezelle (Abb. 1) besteht aus einem Vorratsgefäß (1) aus PTFE (ca. 40 ml), an das sich eine Halterung (3) aus PTFE anschließt, die die Röhrchenkathode (2) aus Reinstgraphit dicht faßt. Eine über PTFE-Schläuche angeschlossene PTFE-Membran- bzw. Kreiselpumpe (5) sorgt für einen Lösungsdurchsatz zwischen 20 und 30 ml min^{-1} und pumpt die Lösung in das Vorratsgefäß zurück. Die Länge des Graphitrohrs beträgt 9 mm, der Innendurchmesser 2,8 mm und der Außendurchmesser 5 mm. Die Stromzuführung erfolgt über einen Pt-Kontakt (9), der seitlich durch eine Halterung geführt wird.

Die geometrische Kathodenfläche beträgt 0,8 cm^2, jedoch ist die reale Oberfläche wesentlich größer. Alle Angaben über die Stromdichte werden auf 0,8 cm^2 bezogen, die realen Stromdichten liegen entsprechend der Oberflächenrauhigkeit des Graphits niedriger.

Die Anode, ein Pt/Ir-Stab (90/10) (4) mit 1,5 mm Durchmesser, verläuft zentrisch in der Kathodenbohrung. Der Elektrodenabstand beträgt ca. 0,7 mm. Die Anode wird durch beide Teile der Elektrodenhalterung (8) gehalten. Durch den starken Elektrolytdurchsatz im Elektrolyseraum wird die Entwicklung von Gasblasen, die den Stromfluß unterbrechen könnten, teilweise verhindert, oder entstehende werden rasch entfernt; außerdem kann mit relativ hohen Stromdichten elektrolysiert werden. Nach Beendigung der Elektrolyse und Abpumpen der Analysenlösung bei angelegter Spannung kann die Graphitelektrode einfach und sicher aus der Anordnung herausgenommen und dem Bestimmungsverfahren zugeführt werden.

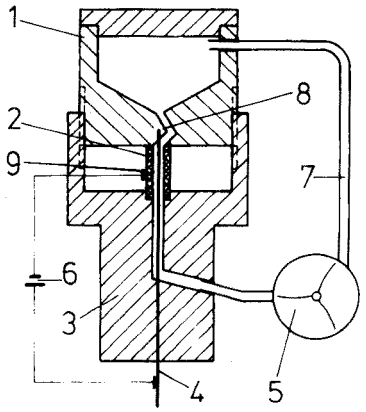

Abb. 1. Durchflußelektrolyseapparatur. 1 Vorratsgefäß (PTFE) für ca. 40 ml Elektrolytlösung; 2 Elektrolysezelle, bestehend aus einem Graphitrohr, das als Kathode geschaltet ist; Länge 9 mm, Innendurchmesser 2,8 mm, Außendurchmesser 5 mm, darin zentrisch die Pt/Ir-Anode; 3 Halterung für Kathode und Anode (PTFE) mit Bohrung für die Elektrolytlösung; 4 Pt/Ir-Anode (Durchmesser 1,5 mm); 5 Pumpe aus PTFE; 6 Stromquelle; 7 PTFE-Schläuche; 8 Führung der Anode; 9 Pt-Kontakte für Kathode.

ELEKTROLYTLÖSUNGEN

In der praktischen Anwendung des Trennverfahrens bestimmen in erster Linie die zum Lösen der Metallprobe erforderlichen Säuren die Anionenart des Elektrolyten. Da Salzsäure aus elektrochemischen Gründen ausscheidet, wurden nur solche Säuren untersucht, die wie HF, NHO_3 und H_2SO_4 extrem rein erhalten werden können [13]. Zum Neutralisieren und Einstellen der pH-Werte kam nur NH_4OH in Frage, das durch isotherme Destillation äußerst rein hergestellt werden kann. Die Abmessungen von Zelle und Pumpe legen das Volumen der Elektrolytlösung auf ca. 40 ml fest. Blindwerte wurden durch flammenlose AAS überwacht.

Bisher wurden folgende Elektrolyte untersucht: (1) 0,1 M Flußsäure; (2) 0,05 M Schwefelsäure; (3) NH_4F-Lösungen (pH-Bereich 3—10); (4) NH_4NO_3-Lösungen (pH-Bereich 4—7); (5) $(NH_4)_2SO_4$-Lösungen (pH-Bereich 4—7). Für (3)—(5) betrug die Konzentration 2, 5 und 10%.

Die abzuscheidenden Elemente wurden als Radiotracer, $^{59}Fe^{3+}$, $^{60}Co^{2+}$, $^{65}Zn^{2+}$ und $^{207}Bi^{3+}$ dosiert und die Abscheidungsraten γ-spektrometrisch (Siemens Einkanalspektrometer Typ T-A 29, Szintillationszähler mit NaJ(Tl)-Bohrlochkristall) gemessen.

Als Spannungsquelle diente ein Galvanostat "Jaissle 5000 T", an den ein erdfreies Voltmeter sowie ein mV-Schreiber zur Aufzeichnung des Spannungsverlaufs angeschlossen war. Die galvanostatische Anordnung wurde gewählt, weil durch die Geometrie der Elektrolysezelle eine Potentialmessung mit einer Referenzelektrode nicht oder nur sehr schwer möglich ist, ohne die optimierte Elektrodengeometrie entscheidend zu beeinflussen. Stattdessen

wurde der Gesamtspannungsabfall der Elektrolysezelle gemessen und als willkürliches Maß für das in der Zelle herrschende Potential betrachtet. Die Abscheidungsspannung kann durch Außenwiderstände geregelt werden. Die Stromstärke betrug für alle Untersuchungen 400 mA, entsprechend einer rechnerischen Stromdichte von ca. 50 A dm^{-2}.

ERGEBNISSE

Ausgehend von flußsauren Aufschlußlösungen, wie sie bei der Analyse von Sondermetallen im Regelfall vorliegen, sollte ein Elektrolyt gefunden werden, aus dem die Abscheidung geringster Spurenelementmengen möglich ist. Erste Versuche mit flußsauren Elektrolyten ($pH \leqslant 1$) verliefen negativ; puffert man mit NH_4OH, so zeigt sich für alle untersuchten Elemente ein optimaler pH-Bereich, der zwischen pH 4 und 8 liegt. Bei reinen NH_4OH-Elektrolyten ($pH \geqslant 10$) konnte mit der verwendeten Anordnung keine brauchbare Abscheidung erzielt werden (vgl. Abb. 2). Alkalische Elektrolyte sind für eine Reihe interessierender Matrices wie Be, Nb, Zr und W nicht geeignet, weil die Matrixelemente nicht in Lösung zu halten sind.

Für Versuche zur Optimierung wurde im Regelfall auf eine quantitative Abscheidung verzichtet und der Versuch nach einer bestimmten, konstanten Zeit abgebrochen. Aus den dabei abgeschiedenen Elementmengen kann auf die gesamte Elektrolysedauer und die Ausbeute geschlossen werden. Einzelne ausgewählte Beispiele belegen, daß ein derartiges Vorgehen berechtigt ist (vgl. Tab. 1, sowie Abb. 3—6). Als optimale Abscheidungsspannungen für die untersuchten Elemente ergaben sich im Rahmen der Versuche mit Ammoniumsalzelektrolyten im pH-Bereich zwischen 4 und 8 Spannungen zwischen 4,6 und 6,0 V.

Wie sich aus den Abbildungen 3—6 und Tabelle 1 ergibt, sind fluoridhaltige Elektrolyte für Fe und Bi optimal. Für Zn ist die Abscheidungszeit in $(NH_4)_2SO_4$-Elektrolyten etwas kürzer; bei Fe und Co ist sie stark vom Elektrolyten abhängig. Zur Abscheidung von 98% Co benötigt man bei fluoridhaltigen Elektrolyten 22 h.

Der bei der Abscheidung gebildete "Niederschlag" haftet so fest auf der Graphitoberfläuche, daß die Kathode ohne Verluste mit dreimal 2 ml bidest. Wasser und einmal 1 ml bidest. Aceton weitgehend vom Elektrolyten freigewaschen werden kann. Mit verdünnten Säuren löst sich ein großer Teil des abgeschiedenen Elementes wieder auf. Bei den Versuchen zeigt sich auch, daß die prozentuale Abscheidungsrate über einen sehr großen Konzentrationsbereich (> 6 Zehnerpotenzen) konstant ist. Tabelle 2 zeigt die Ergebnisse der Abscheidung von μg-Mengen der Elemente. K, Na, Mg, Li u.a. stören selbst bei Konzentrationen von 40 mg ml^{-1} die Abscheidung nicht. Setzt man der zu elektrolysierenden Lösung 200 mg Be^{2+} zu, sind ebenfalls keine Unterschiede in der Abscheidung zu bemerken (vgl. Abb. 3—5).

Nach den bisherigen Ergebnissen wird die hier untersuchte elektrolytische Abscheidung im wesentlichen durch 4 Faktoren beeinflußt.

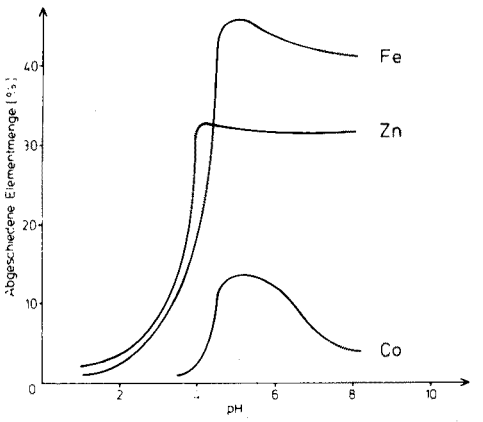

Abb. 2. Abscheidung von Fe, Co und Zn aus flußsauren und ammoniumfluoridhaltigen Lösungen in Abhängigkeit vom pH-Wert. Stromstärke: 400 mA; Spannung: Fe 5,0 V; Co 5,7 V; Zn 4,9 V; Lösungsvolumen: 40 ml; Elektrolyte 1 und 3; Konzentration der Elektrolytlösung: 5%ig; Abscheidungsdauer: 20 min; Eingesetzte Elementmenge: Fe 100 ng; Co 6 ng; Zn 150 ng.

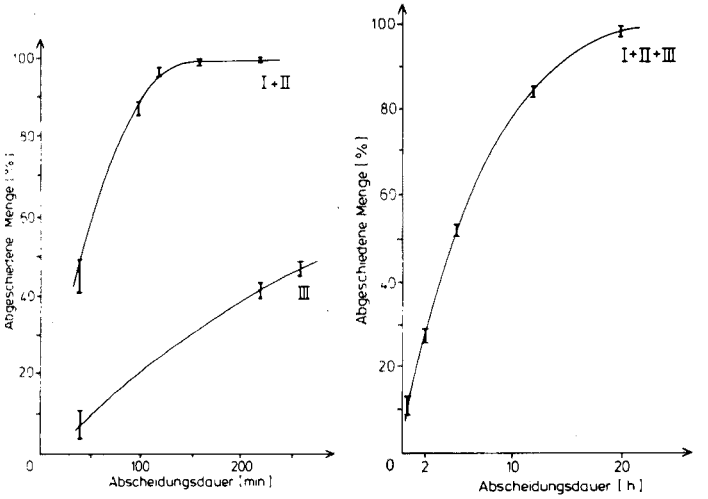

Abb. 3. Abscheidung von 100 ng ^{59}Fe in Abhängigkeit von der Elektrolysedauer. Elektrolyt: (I) 10%ige NH_4F-Lösung; (II) 10%ige NH_4F-Lösung + 200 mg Be als $BeSO_4$; (III) 2%ige $(NH_4)_2SO_4$-Lösung; pH-Wert: 4,9—5,1; Stromstärke 400 mA; Spannung: 5,0 V; Lösungsvolumen: 40 ml.

Abb. 4. Abscheidung von 6 ng ^{60}Co in Abhängigkeit von der Elektrolysedauer. Elektrolyt: (I) 5%ige NH_4F-Lösung; (II) 10%ige NH_4F-Lösung; (III) 10%ige NH_4F-Lösung + 200 mg Be als $BeSO_4$; pH-Wert: 5,0; Stromstärke: 400 mA; Spannung 5,7 V; Lösungsvolumen: 40 ml.

TABELLE 1

Abscheidung von Fe, Co, Zn und Bi in Abhängigkeit von der Art des Elektrolyten (Stromstärke 400 mA. Spannungen: Fe 5,5 V; Co 5,7 V; Zn 4,9 V; Bi 5,0 V. pH-Wert der Elektrolyte: 5,0. Elektrolytvolumen: 40 ml. Konzentration der Elektrolytlösung: 5%ig.)

Element	Elektrolyt	Abscheidungsdauer (h)	Abscheidung (%)
Fe (100 ng)	NH_4F	0,3	45,7
	NH_4F	1,3	$\geqslant$ 98
	$(NH_4)_2SO_4$	0,3	8,7
	$(NH_4)_2SO_4$	7	$\geqslant$ 98
	NH_4NO_3	22	60
Co (6 ng)	NH_4F	0,3	12,8
	NH_4F	22	$\geqslant$ 98
	$(NH_4)_2SO_4$	0,3	25,8
	$(NH_4)_2SO_4$	5	$\geqslant$ 98
	NH_4NO_3	0,3	20,4
	NH_4NO_3	8	$\geqslant$ 98
Zn (150 ng)	NH_4F	0,3	31,4
	NH_4F	3,3	$\geqslant$ 98
	$(NH_4)_2SO_4$	0,3	38,2
	$(NH_4)_2SO_4$	2	$\geqslant$ 98
	NH_4NO_3	0,3	24,6
	NH_4NO_3	5,3	$\geqslant$ 98
Bi (0,5 ng)	NH_4F	0,3	29,8
	NH_4F	2	$\geqslant$ 98

1. Sind edlere Elemente wie z.B. Cu und Ag in Konzentrationen von $\geqslant 0{,}25\ \mu g\ ml^{-1}$ im Elektrolyten vorhanden, so erhöht sich die Abscheidungszeit um das 3—4-fache (vgl. Abb. 6 und Tabelle 3).
2. Die Graphitoberfläche hat einen wesentlichen Einfluß auf die Abscheidung [14]. Zur Präkonditionierung werden die Graphitröhrchen mit 30%iger HNO_3 ausgewaschen, mit Wasser und Aceton gespült und anschließend im direkten Stromdurchfluß elektrisch bis 3000° C ausgeheizt, um sie so blindwertfrei zu erhalten.
3. Eine Reihe von Anionen wie sämtliche Halogenide (mit Ausnahme von Fluorid) in Konzentrationen von $\geqslant 50\ \mu g\ ml^{-1}$ und Borat verringern bzw. verhindern die Abscheidung. Bei Cyanidkonzentrationen von $\geqslant 1\ \mu g\ ml^{-1}$ beträgt die abgeschiedene Menge in 20 min weniger als 1%. Acetathaltige Bäder stören durch ihre Neigung zur Schaumbildung.
4. Störungen werden ebenfalls durch einige organische Verbindungen verursacht. Komplexone ($\leqslant 1\ mg\ ml^{-1}$), verringern die Abscheidungsraten auf weniger als 1% in 20 min. Eine Reihe bewährter Badzusätze der Galvanotechnik wie höhere Alkohole oder Ascorbinsäure senken die Abscheidungsrate ebenfalls. Weiter stören Methanol und Äthanol, auch wenn nur das Graphit-

TABELLE 2

Abscheidung von Co, Zn und Bi aus NH_4F-haltigen Lösungen (Elektrolyt 3) in Abhängigkeit von der Elementmenge
(Stromstärke: 400 mA. Spannungen: Co 5,7 V; Zn 4,9 V; Bi 5,0 V. pH-Wert der Elektrolytlösung: 5,0. Konzentration der Elektrolytlösung: 10%ig. Lösungsvolumen: 40 ml. Abscheidungsdauer: 20 min.)

Element	Menge (μg)	Abscheidung (%)
Zn	0,15	31,5
	10	30,7
	100	30,5
	500	31,2
Co	0,006	12,8
	0,06	12,2
	3	12,5
	30	11,9
	300	12,1
Bi	$1 \cdot 10^{-4}$	29,7
	100	29,2
	500	30,1

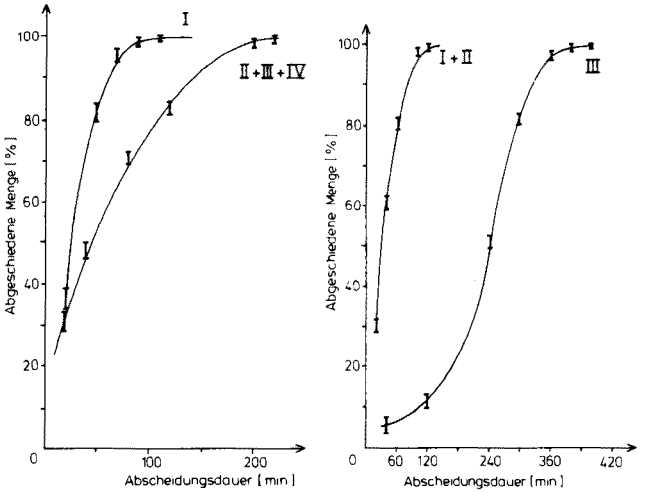

Abb. 5. Abscheidung von 150 ng ^{65}Zn in Abhängigkeit von der Elektrolysedauer. Elektrolyt: (I) 2%ige $(NH_4)_2SO_4$-Lösung; (II) 10%ige NH_4F-Lösung; (III) 10%ige NH_4F-Lösung + 100 μg Zn; (IV) 10%ige NH_4F-Lösung + 200 mg Be als $BeSO_4$; pH-Wert: 5,0; Stromstärke 400 mA; Spannung: 4,9 V; Lösungsvolumen: 40 ml.

Abb. 6. Abscheidung von 0,5 ng ^{207}Bi in Abhängigkeit von der Elektrolysedauer. Elektrolyt: (I) 10%ige NH_4F-Lösung; (II) 10%ige NH_4F-Lösung + 100 μg Bi; (III) 10%ige NH_4F-Lösung + 100 μg Cu; pH-Wert: 5,0; Stromstärke: 400 mA; Spannung 5,0 V; Lösungsvolumen: 40 ml.

TABELLE 3

Abscheidung von 0,5 ng Bi in Abhängigkeit von µg-Mengen Cu, Ag und Zn aus ammoniumfluoridhaltigen Lösungen (Elektrolyt 3)
(Stromstärke: 400 mA. Spannung: 5,0 V. pH-Wert: 5,0. Konzentration der Elektrolytlösung: 10%ige. Abscheidungsdauer: 20 min. Lösungsvolumen: 40 ml.)

Zugesetztes Element	—	Cu	Cu	Ag	Ag	Zn
Menge (µg)	—	10	100	10	100	100
Bi-Abscheidung %	29,8	27,4	5,6	13,2	4,9	28,1

röhrchen damit ausgewaschen wird, sowie viele Ketone mit Ausnahme des Acetons.

DISKUSSION

Die vorgestellte Methode zur quantitativen elektrolytischen Abscheidung im dynamischen System von ng-Mengen metallischer Spurenelemente in nicht abscheidbaren Matrices aus neutralen fluoridhaltigen Lösungen auf die Innenfläche einer zylindrischen Graphitkathode stellt ein relativ einfaches Verfahren zur Abtrennung und Anreicherung dar, wie bis jetzt bei den Elementen Fe, Zn, Co und Bi belegt werden konnte. Nach Aufschluß der Probe und Neutralisation erfolgt die Abtrennung von der Matrix und die Anreicherung auf kleiner Oberfläche in einem Schritt. Im Vergleich zur Flüssig—Flüssig-Verteilung und Mitfällung ist bei diesem System die Gefahr, durch Reagenzienzugabe und Manipulationen Blindwerte einzubringen, gering, wodurch besonders für Elemente mit hoher Allgegenwartskonzentration bessere Nachweisvermögen erzielt werden können. Der Trenn- und Anreicherungsschritt läßt sich gut in ein Verbundverfahren einfügen, mit dem diese Spurenelemente z.B. in reinstem Be, Nb und W bestimmt werden, da die Elektrolyse dem Aufschluß ohne weitere Reagenzienzugabe (mit Ausnahme von NH_4OH) folgen kann. Die in der Graphitkathode angereicherten Elementspuren, die wahrscheinlich metallisch vorliegen, lassen sich mit Wasser und Aceton ohne Verlust waschen, so daß Bestandteile der Elektrolytlösung bei späteren Operationen nicht stören können.

Mit der Versuchsanordnung ist die Trennung der abscheidbaren Elemente untereinander nicht möglich. Das sich anschließende Bestimmungsverfahren, bei dem die Graphitkathode als Probenträger direkt eingesetzt wird, sollte deshalb vorzugsweise ein Multielementverfahren sein, wie z.B. Neutronenaktivierung und OES mit Plasmaanregung (ICP oder CMP). Versuche, die Graphitkathode direkt als Ofen in der flammenlosen AAS zu verwenden, bestätigen, daß elementar vorliegende Metallspuren zu einer erheblichen Steigerung der Empfindlichkeit führen [15]. Dabei ist jedoch die obere Meßgrenze des Bestimmungsverfahrens meist schon durch die Allgegenwartskonzentration der Elemente erreicht (gilt bereits für das wenig verbreitete Bi), wodurch eine Bestimmung sehr erschwert wird. Abhilfe kann durch Wiederauflösen der metallisch abgeschiedenen Spurenelemente mit verdünnten

Säuren auf dem Graphitrohr geschaffen werden. Diese Beobachtungen unterstützen die Annahme von Fuller [16], daß die Atomisierung und damit der die Nachweisgrenze bestimmende Schritt bei der flammenlosen AAS mit Graphitrohr über den nullwertigen Zustand der Elemente abläuft.

Versuche, die beschriebene Abtrennungstechnik auf organischen Matrices anzuwenden, sind noch nicht erfolgt. Auf Grund der vorliegenden Erfahrungen kann geschlossen werden, daß eine Abscheidung von Metallspuren möglich ist, wenn organische Anteile im Aufschluß vollständig mineralisiert sind.

Wir danken der Deutschen Forschungsgemeinschaft, Bonn, die diese Arbeit durch Sachmittel unterstützte.

LITERATUR

1 G. Tölg, Talanta, 21 (1974) 327.
2 H. B. Mark Jr. und F. J. Belandi, Anal. Chem., 36 (1964) 2062.
3 H. Malissa und I. R. Marr, Mikrochim. Acta, (1971-I) 241.
4 G. Weichbrodt, Dissertation, Universität Mainz, Germany, 1970.
5 V. Z. Krasilščik, G. A. Šteinberg und A. F. Yakovleva, Zh. Anal. Khim., 26 (1971) 1897.
6 Y. Thomassen, B. V. Larsen, F. J. Langmyhr und W. Lund, Anal. Chim. Acta, 83 (1976) 103.
7 M. P. Newton und D. G. Davis, Anal. Chem., 47 (1975) 2003.
8 J. B. Dawson, D. J. Ellis, T. F. Hartley, M. E. A. Eveans und K. W. Metcalf, Analyst (London), 99 (1974) 602.
9 J. A. Page, J. A. Maxwell und R. P. Graham, Analyst (London), 87 (1962) 245.
10 H. J. S. Sand, J. Chem. Soc., 91 (1907) 373.
11 D. R. Roe, Anal. Chem., 46 (1974) 8R.
12 K. J. Vetter, Elektrochemische Kinetik, Springer Verlag, Göttingen, 1961.
13 J. W. Mitchell, Anal. Chem., 45 (1973) 492A.
14 R. Neeb, Inverse Polarographie und Voltammetrie, Verlag Chemie Weinheim/Bergstraße, 1969.
15 R. Woodriff und D. Siemer, Appl. Spectrosc., 23 (1969) 38.
16 C. W. Fuller, Analyst (London), 99 (1974) 739.

Analytica Chimica Acta, 90 (1977) 25—34

PULSED VOLTAMMETRIC STRIPPING AT THE THIN-FILM MERCURY ELECTRODE

JOHN A. TURNER, URI EISNER* and R. A. OSTERYOUNG
Department of Chemistry, Colorado State University, Ft. Collins, CO 80523 (U.S.A.)
(Received 6th October 1976)

SUMMARY

A computer-controlled data acquisition system was used to generate comparative data for thin-film anodic stripping voltammetry with staircase, differential pulse and square-wave waveforms. Each waveform was tested for its sensitivity and speed of analysis. The square-wave form is the most sensitive, whether square wave or differential pulse measurements are used. This waveform offers the advantages of fast analysis time and discrimination against charging currents.

In recent years anodic stripping voltammetry (a.s.v.) has become one of the most widely used methods for trace metal analysis at the p.p.b. level. It has been suggested as a standard method for the determination of lead in biological fluids [1] and is widely used for environmental samples [2]. A mercury electrode of some type (hanging mercury drop or thin mercury film) is normally used but for metals such as Au, Ag, Hg, solid electrodes are used [3, 4]. Recent reviews by Ellis [5] and Copeland and Skogerboe [6] have outlined the fundamentals, techniques and associated problems with a.s.v. Linear-scan voltammetry is the commonest technique employed for the dissolution step but recent studies have demonstrated the higher sensitivity achieved by fundamental a.c. [7], second harmonic a.c. [8], differential pulse [9] and staircase [10] waveforms. Linear-scan a.s.v. suffers from the disadvantage of high background because of capacitative currents, and the latter methods are designed to overcome this drawback and increase signal-to-background ratio.

Application of a.c. to a.s.v. was hampered at one time by high cost and complexity of instrumentation. The commercial availability of pulse polarographs of good dependability and reasonable price resulted in a plethora of applications of differential pulse a.s.v. as a sensitive and convenient method for trace metal analysis. With the advent and rapid development of mini and microcomputers and the sharp decrease in their price, it becomes feasible to supply voltage excitation via a digital to analog (D/A) converter to the potentiostat for the stripping step. The computer

*Present address: Israel Chemicals Ltd., P.O. Box 7164, Tel Aviv, Israel.

can sample the current and present it as a function of voltage either by print-out or plot. It is also possible to store the data for later analysis and data reduction. With a computer, a variety of different potential excitations can be applied and the various parameters governing the current can be changed easily.

In a previous paper from this laboratory [10], staircase voltammetry was investigated in detail and the utility of this approach for a.s.v. clearly demonstrated. In a logical extension of this work, a general purpose program was written, with a minicomputer system for data acquisition and control of staircase, differential pulse and square-wave experiments. Comparative data for these three methods were generated, and optimal conditions for the most sensitive determinations were established.

EXPERIMENTAL

Apparatus

The waveforms were applied and current—potential curves evaluated by a PDP-12 computer (Digital Equipment Corporation). A Hewlett-Packard x—y recorder (Model 7009 B) driven by the computer was used for hardcopy i—E curves. Princeton Applied Research models 173 and 174 were used as potentiostats and i—E converters. The model 173 was equipped with a model 179 digital coulometer. The working electrode was rotated by a Pine Instrument Rotator (Model PIR) at 1600—6400 r.p.m.

The working electrode was a mercury thin film deposited on a glassy carbon disk (area, 0.2 cm^2). The disk was press-fitted into a Teflon sleeve and polished to a mirror finish with alumina on a polishing cloth before mercury plating. The reference electrode was Ag/AgCl made from a silver wire coated with silver chloride immersed in saturated KCl in a Teflon tube, and separated from the sample solution by a porous glass plug (Corning Glass Vycor 7930). The counter electrode was a platinum spiral separated from the sample solution by a Teflon tube. The cell was made from a quartz tube (50 mm o.d., capacity 50 ml). The nitrogen bubbler was made of Teflon. The use of Teflon and quartz help to minimize trace metal adsorptive problems commonly found in stripping analysis.

Reagents

Mercury stock solution (0.01 M) was prepared by dissolving triply-distilled mercury in nitric acid. Mercury plating of the electrode was carried out in a solution $2 \cdot 10^{-4}$—$2 \cdot 10^{-3}$ M Hg^{2+}. Acetate buffer was prepared from reagent-grade acetic acid and ammonia. All solutions were diluted by distilled, deionized water.

System

The computer system is basically the same as previously reported from this laboratory [11] but has been augmented by the addition of a hardware

floating point processor and added core. The system as presently used consists of a Digital Equipment Corporation PDP-12 minicomputer, with 24 K of core, scope, x—y plotter, two 12-bit D/As, one 12-bit A/D, dual magnetic tape, disk, and floating point processor.

The addition of the added core and floating point processor facilitate the use of DEC's real-time FORTRAN IV for data acquisition and experimental control. Unlike machine language which can differ radically for different computer systems, FORTRAN IV is fairly universal and is usually familiar to incoming personnel. The "break-in" period is therefore shorter for those wanting to do experiments of their own design, and programs are easier to understand and modify.

The computer program for this work was written in FORTRAN IV and runs under OS/12. The clock and plotting subroutines used were slight modifications of those supplied by DEC. A combination A/D and D/A subroutine was written for data acquisition and output of voltages.

The program consists of a core resident mainline and a group of stored subroutines. The mainline is a series of LOGICAL IF and CALL statements. The type of wave form requested determines the subroutine called. These subroutines reside on a magnetic disk and are overlayed into core as needed. This overlay structure allows programs to be run that ordinarily would be too large to fit into the amount of core available. A flow chart for the overall system is shown in Fig. 1.

After operator input of the desired wave form and experimental parameters, the appropriate subroutine is called which generates tables of voltages and times and places them in COMMON. Figure 2 shows an example flow chart for staircase.

The times are total times, in floating point, to that time when data acquisition takes place. This allows the clock subroutine to be called only once. Data acquisition is done by reading the total time since the clock started and comparing that in an IF statement to the time at which data acquisition should take place. If it is not yet time to acquire data, then the clock is again read and compared. This cycle is repeated until the appropriate time has been reached. The combination A/D and D/A subroutine is then called and does a voltage measurement from the I to E converter and outputs the next voltage step. The data are stored and the process is repeated until the requested voltage range has been scanned. A data acquisition flow chart for staircase is shown in Fig. 3.

After data acquisition, the data are displayed on the scope. The operator then has the options of rescaling the plot, obtaining a hard copy via the x—y plotter, printing out the current—voltage values, or storing the data on the disk or magnetic tape. Program parameters can then be changed or a new wave form selected by setting the appropriate switch on the front panel of the computer.

The types of waveform that can be generated by this particular program include staircase, normal pulse (Type I or Type II measurement [12]),

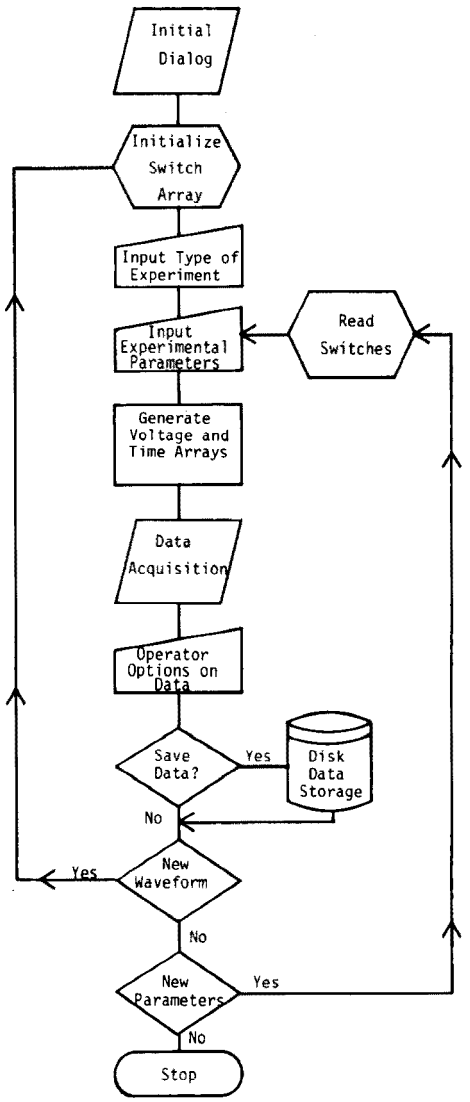

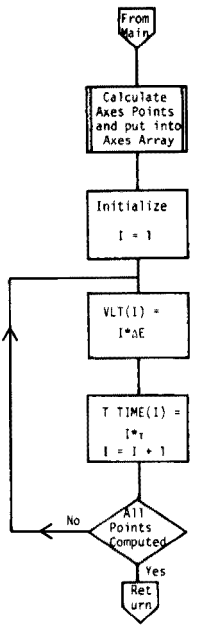

Fig. 1. (left) Flowchart for mainline data acquisition program.

Fig. 2. (right) Flowchart for calculation of arrays of D/A voltages and times—staircase waveform.

differential pulse (differential or pulse only measurement), and square-wave (forward pulse only, reverse pulse only, or the regular difference measurement) The waveforms are shown in Fig. 4. Current can be measured at the end points only, although for staircase, measurement can be made inside the step by asking for the differential pulse waveform, pulse measurement only, and inputing a pulse height equal to the step height.

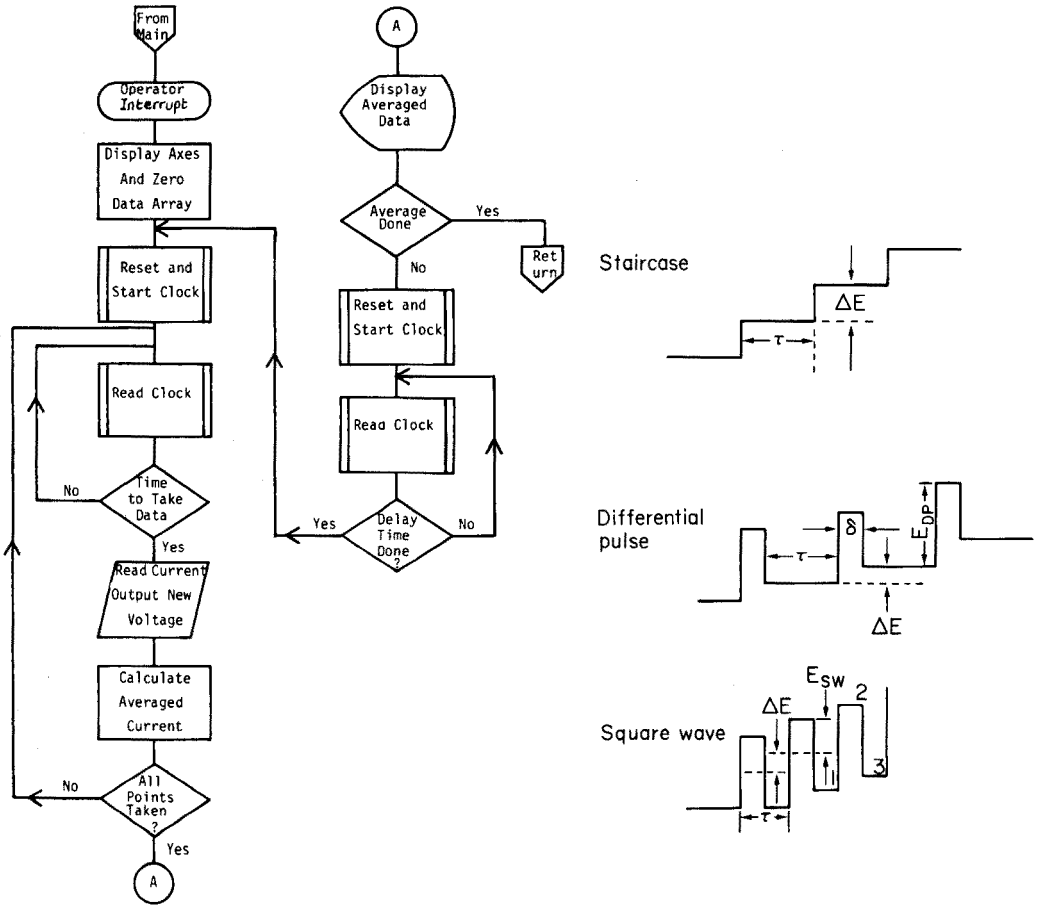

Fig. 3. Flowchart for data acquisition subroutine—staircase waveform.

Fig. 4. Waveforms generated. For staircase: ΔE = step height, τ = step time. For differential pulse: ΔE = step height, τ = delay time, δ = pulse time, E_{DP} = pulse height. For square wave: ΔE = step height, τ = cycle time (frequency^{-1}), E_{SW} = square-wave amplitude ($\frac{1}{2}p$—p). Square-wave measurement = $i_2 - i_3$. Differential pulse measurement (square waveform) = $i_2 - i_1$.

Minimum acquisition time is governed by system overhead and for this system is 3 ms with a maximum error of +0.5 ms.

RESULTS AND DISCUSSION

Staircase voltammetry

The experimental [10] and theoretical [13] aspects of a.s.v. with a staircase waveform have been investigated. The advantage of staircase over linear sweep is that it discriminates against charging current while a fast

analysis time is maintained. The parameters governing the peak current i_p are τ (the step width), ΔE (the step height), and q_m (the amount of metal plated into the electrode). For comparative purposes, we shall assume constant q_m. The peak current in staircase increases with ΔE and with $1/\tau$. The practical upper limit of ΔE is 10 mV since the peaks should be clearly defined. The lowest values for τ are governed by the response (rise time) of the system. For the present system with an electrode of 0.2 cm^2, and an acetate buffer of $2 \cdot 10^{-3}$ M, the shortest step time that could be employed was 6 ms, when the PAR 173 was used without positive feedback. A beneficial reduction in 60-cycle noise is obtained by synchronizing the step time with the line frequency (τ = 16.7 ms), thereby increasing the precision of the measurement.

Differential pulse voltammetry

A great deal of work on differential pulse anodic stripping voltammetry (d.p.a.s.v.) has been done by Copeland et al. [9, 14, 15]. They recommend the use of high amplitude pulses (100 mV) combined with short pulse duration for high sensitivity. Christie and Osteryoung [16] have pointed out the importance of the delay time in d.p.a.s.v. in that it allows some replating of analyte between stripping pulses. The analyte is therefore stripped and plated several times in a scan, so that the pulse current is enhanced. As the delay time is decreased while scan rate is kept constant (in our system maintained by decreasing the step height), the peak current decreases because of the increased frequency of pulsing and the reduced amount of material plated back during the delay time (see ref. 9, Fig. 2; ref. 16, Fig. 9). This necessitated the use of extended delay times of 0.5 s or longer which greatly increased the time of analysis.

Because of the digital nature of this differential pulse waveform, resolution can be maintained and the sweep rate increased, merely by decreasing the delay time for a constant step height. If the delay time is decreased for a constant step height, the peak current is enhanced because the scan rate is greatly increased, and because there is a significant contribution from measurement of the replating current. For pulse heights of 20 mV and greater, this replating current will be opposite in sign to the pulse current and will add to the total current in a differential measurement. Figure 5 shows the effect of decreasing the delay time on the peak current for a constant step height. It is apparent that the increase in signal obtainable by increasing the scan rate and measuring the replating current is greater than that gained from replating during an extended delay time. Further advantages are that the analysis time approaches that of staircase stripping voltammetry, and the sensitivity is enhanced. A recently published [7] modification to the PAR 174 which allows fast sweep differential pulse is not recommended because it appears that the delay time for this modification is shorter than the pulse time. This will obviously limit the sensitivity.

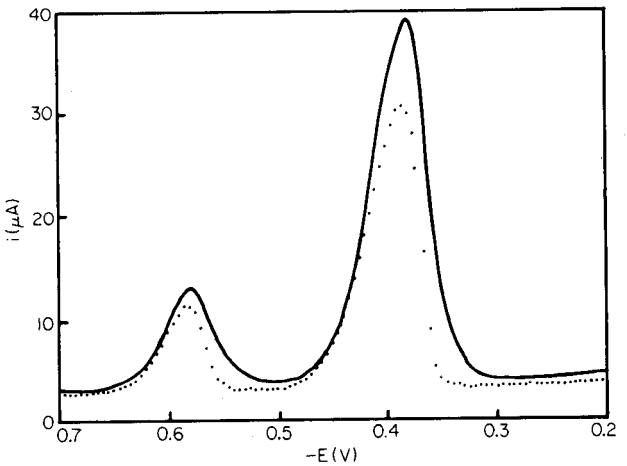

Fig. 5. Effect of scan rate on differential pulse stripping current. Lead, 10 ppb; $1 \cdot 10^{-2}$ M acetate buffer; plating time, 2 min; 6400 r.p.m.; plate, 15000 Å; δ 25 ms; E_{DP}, 60 mV; PAR 174. · · · ΔE = 5 mV, τ = 0.475 s, effective scan rate = 10 mV s^{-1}. —— ΔE = 5 mV, τ = 25 ms, effective scan rate = 100 mV s^{-1}.

As the delay time in differential pulse becomes equal to the pulse time, the waveform becomes identical to the familiar square-wave form, the only difference arising from the type of measurement being reported from each technique. Figure 4 details the differences in measurement for the two techniques when they both involve the same waveform. For any pulse technique there is a trade-off between supporting electrolyte concentration, instrument response, pulse amplitude and pulse width. Low supporting electrolyte concentrations and large pulse amplitudes can be used if care is taken to maintain proper system response. Typically, this involves increasing the pulse width and/or using a faster potentiostat. For the present PAR 173 system, supporting electrolyte concentrations in the 10^{-3} M range could be used with pulse widths as low as 6 ms and as large as 100 mV. If the PAR 174 was used, the supporting electrolyte had to be in the 10^{-2} M range and the pulse width longer than 12 ms.

Square wave voltammetry

Barker [18] mentioned the use of increasing signal-to-noise ratio in square-wave polarography by preconcentrating the trace metal into an HMDE. The square-wave frequency was 225 Hz; the square-wave amplitude was not mentioned but can be assumed to be 2—36 mV (p—p) as in Barker's usual square-wave work. Sturrock [19] has discussed the use of square wave for stripping voltammetry.

Problems with charging currents are caused by the high frequency of the square wave cycles, hence this technique has been a low amplitude one useful only in solutions of high supporting electrolyte content. Earlier work

with differential pulse voltammetry showed that square wave could be used at low supporting electrolyte concentrations if the square-wave frequency was decreased. The square-wave amplitude could then be increased to increase sensitivity.

Aside from the advantage of discrimination against charging current shown in square-wave voltammetry, there is the usual assumption that the reverse current is opposite in sign to the pulse current and therefore the total current will be enhanced. Because the system described here could be used, the individual stripping, replating and total currents were examined as a function of square wave amplitude. Figures 6 and 7 show the stripping, replating and total currents for two different amplitudes. It is obvious that at low amplitudes (Fig. 6) the signs of the two currents are the same. In a difference measurement, the total current will be lower than the stripping current alone. At higher amplitudes, the signs are opposite (Fig. 7) and the total current is greater than the individual currents. The "crossover point" seems to be about 10-mV amplitude for a 5-mV step height. Therefore, the frequency should be decreased and the amplitude increased above 20 mV to increase the sensitivity.

There is a practical limit to the increase in sensitivity that can be obtained by increasing the square-wave amplitude. By considering a double-step chronoamperometric experiment, the largest possible current difference is given by a step from in front of the wave on to the diffusion plateau and back to the front again, the reverse potential being sufficient to drive the reverse reaction at a diffusion-controlled rate. Any larger jump further into the wave and back to the front results in a broadening of the peak, but not an increase in its height. Square-wave amplitudes beyond 50 mV offer little

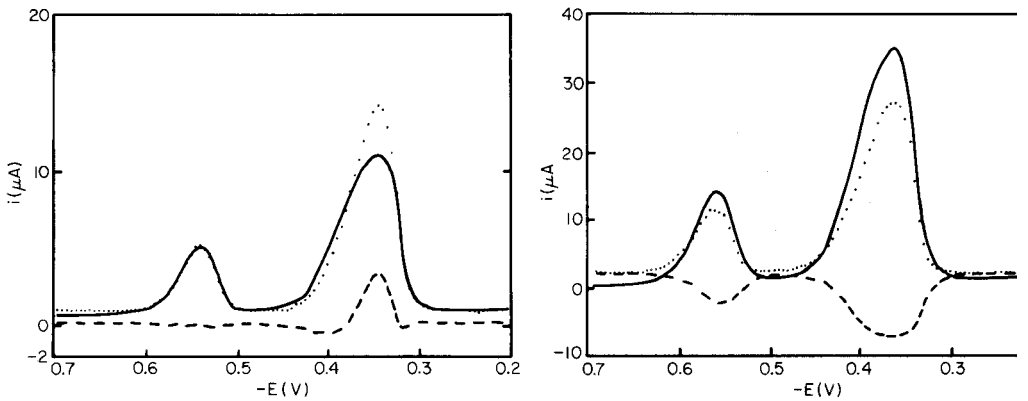

Fig. 6. Individual currents for square-wave stripping, 5 mV amplitude. Lead 10 p.p.b.; $1 \cdot 10^{-2}$ M acetate buffer; plating time, 2 min; 6400 r.p.m.; film thickness, 15000 Å: ΔE, 5 mV; τ, 33.3 ms; PAR 174. ----- Down current. ·····Up current. ——— Difference current.

Fig. 7. Individual currents for square-wave stripping; 20 mV square-wave amplitude. Conditions and legend as for Fig. 6.

gain in sensitivity (Fig. 8). The optimal conditions for square-wave stripping are a square-wave time of 16.7 ms (60 Hz), amplitude of 50 mV and a step height of 5 mV. Under these conditions, with other parameters as given in the legend to Fig. 8, the calibration graphs are linear for the range 0—10 ppb of lead, i_p being ca. 65 μA for 10 ppb of lead.

Figures 9 and 10 show the advantages of the capability of subtracting background. Figure 9 shows a trace impurity of copper superimposed on a steep background. The background is due to a chloride impurity from the reference electrode. A background scan is taken in the analyte solution by stripping the metal out at 0V, stepping back to −0.9 V without electrode rotation and immediately scanning. The background and stripping curves are stored and later subtracted point by point. The result is shown in Fig. 10. The copper peak is plainly visible and can be determined.

Figure 11 compares the three methods under the optimized conditions. It must be recognized that for this figure the square-wave and the differential pulse waveforms are virtually identical; the difference is that the base staircase is added to the forward pulse for the square-wave waveform, and subtracted from the reverse pulse for the differential pulse waveform. As expected, the square-wave currents are slightly higher than the differential pulse currents because the replating current is measured from a larger stripping pulse in the square wave used.

Conclusion

Square-wave stripping and differential pulse stripping, the latter with a short delay time, have been shown to be sensitive analytical tools for trace metal analysis. They have the advantage of a very fast analysis time and discrimination against charging currents; because of higher sensitivity, shorter plating times can be employed.

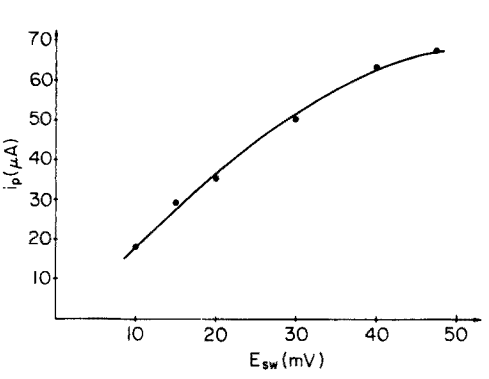

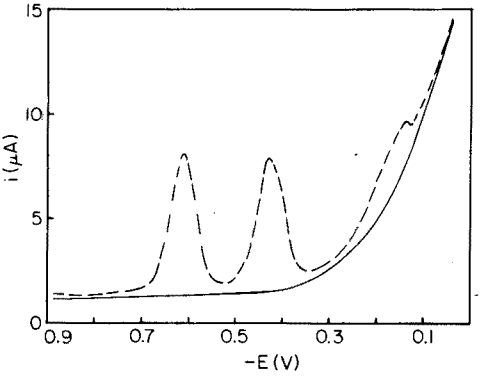

Fig. 8. Dependence of peak height on square-wave amplitude. Lead, 10 ppb; $3 \cdot 10^{-2}$ M acetate buffer; film thickness, 13000 Å; τ, 16.7 ms; plating time, 3 min; 4900 r.p.m.; PAR 173.

Fig. 9. Square-wave stripping. Lead and cadmium, 1 ppb; copper less than 0.5 ppb; $2 \cdot 10^{-3}$ M acetate buffer; E_{SW}, 50 mV; τ, 16.7 ms; plating time 3 min; 4900 r.p.m.; film thickness, 10000 Å; PAR 173. ----- Stripping peaks. —— Background.

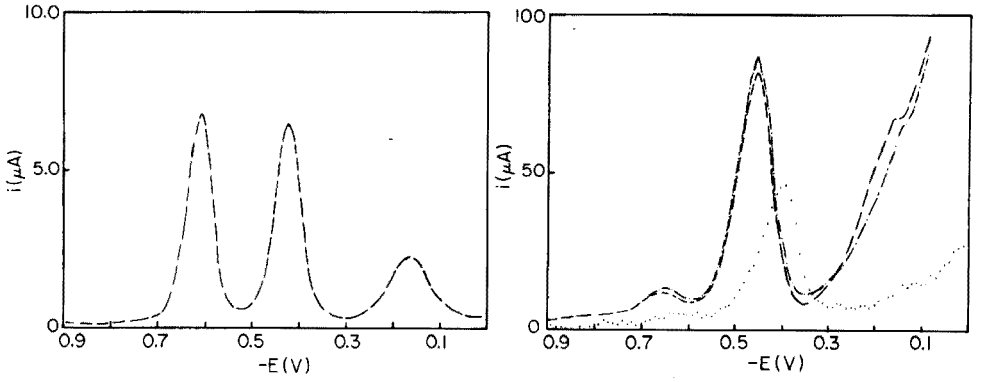

Fig. 10. Square-wave stripping, background subtracted.

Fig. 11. Comparison of the three techniques under optimum conditions for 12.5 ppb lead. 2 min plating time, 4900 r.p.m., film 15000 Å, $3 \cdot 10^{-2}$ M acetate buffer, PAR 173. · · · Staircase stripping, ΔE = 10 mV, τ = 6 ms. ---- Differential pulse stripping, ΔE = 5 mV, E_{DP} = 100 mV, τ = 8.3 ms, δ = 8.4 ms. —·—·— Square-wave stripping, ΔE = 5 mV, E_{SW} = 50 mV, τ = 16.7 ms.

This work was supported in part by the National Science Foundation under grant number CHE-7610445 and by the Office of Naval Research under Contract Number N00014-76-C-0092.

REFERENCES

1 W. R. Matson, R. M. Griffin and E. W. Zink, 1974 Pittsburgh Conference, paper #16, Cleveland, Ohio, 1974.
2 E. Ernst, H. E. Allen and K. H. Mancy, Water Res., 9 (1975) 969.
3 S. P. Perone and W. J. Kretlow, Anal. Chem., 37 (1965) 968.
4 U. Eisner and H. B. Mark, Jr., J. Electroanal. Chem. Interfacial Electrochem., 24 (1970) 345.
5 W. D. Ellis, J. Chem. Educ., 50 (1973) 131.
6 T. R. Copeland and R. K. Skogerboe, Anal. Chem., 46 (1974) 1257.
7 F. Vydra, M. Stulikova and P. Patak, J. Electroanal. Chem. Interfacial Electrochem., 40 (1972) 99.
8 M. Stulikova and F. Vydra, J. Electroanal. Chem. Interfacial Electrochem., 42 (1973) 127.
9 T. R. Copeland, J. H. Christie, R. A. Osteryoung and R. K. Skogerboe, Anal. Chem., 45 (1973) 2171.
10 U. Eisner, J. A. Turner and R. A. Osteryoung, Anal. Chem., 48 (1976) 1603.
11 H. E. Keller and R. A. Osteryoung, Anal. Chem., 43 (1971) 342.
12 J. H. Christie and R. A. Osteryoung, J. Electroanal. Chem. Interfacial Electrochem., 49 (1974) 301.
13 J. H. Christie and R. A. Osteryoung, Anal. Chem., 48 (1976) 869.
14 T. R. Copeland, Ph.D. Thesis, Colorado State University, Fort Collins, Colorado, 1973.
15 T. R. Copeland, R. A. Osteryoung and R. K. Skogerboe, Anal. Chem., 46 (1974) 2093.
16 R. A. Osteryoung and J. H. Christie, Anal. Chem., 46 (1974) 351.
17 H. Blutstein and A. M. Bond, Anal. Chem., 48 (1976) 248.
18 G. C. Barker, Report A.E.R.E. C/R (1954) 1563.
19 P. E. Sturrock and R. J. Carter, Crit. Rev. Anal. Chem., (1975) 201.

Analytica Chimica Acta, 90 (1977) 35—43

DETERMINATION OF ALKYLPHENOL- AND ALKYLALCOHOL-BASED NON-IONIC SURFACTANTS BY A DERIVATIVE CHRONOPOTENTIOMETRIC METHOD

PER HOLMQVIST

Department of Analytical Chemistry, University of Uppsala, S-75121 Uppsala-1 (Sweden)

(Received 23rd September 1976)

SUMMARY

The adsorption of surfactants at a dropping mercury electrode and at a hanging mercury drop electrode has been studied. The DME is more suitable for analytical purposes. For quantitative work the size of the indentation in the dE/dt-curve at the potential of desorption is used. A crude classification of surfactants is possible on the basis of the form of the dE/dt-curve.

The electrochemical behaviour of surface active substances is well documented [1, 2]. Electrochemical methods for determination of surfactants can be based either on their influence on selected charge-transfer reactions [3], or on more direct measurements of their effect on the electrode double layer [4, 5]. Chronopotentiometric methods have frequently been applied in the study of adsorption phenomena at electrodes [6, 7]. In cases where no charge-transfer reaction occurs the same technique is applicable, since changes in the charge distribution of the double layer also affect the shape of the chronopotentiogram. The aim of the present investigation was to study the possibility of analytical applications based on this effect.

EXPERIMENTAL

The adsorption of sixteen polyoxyethylated nonionic surfactants was investigated by a chronopotentiometric method [8]. All measurements were performed in a three-electrode cell connected to an instrument for potentiostatic or galvanostatic control [9]. Two different working electrodes were used; an ordinary polarographic capillary (Radiometer B400) and a stationary mercury electrode (Metrohm E 410). The counter electrode was a platinum wire and the reference electrode a saturated calomel electrode (SCE). The measurements with the dropping mercury electrode (DME) were synchronized by a drop-fall detector [10].

During a pre-determined quiescent period the potential of the working electrode was controlled. The mode was then switched to galvanostatic control. Simultaneously dE/dt and E were measured and displayed on an oscilloscope (Techtronix Storage Oscilloscope 645B or Nicolet Digital Oscilloscope

1090A). Thereafter the potential of the working electrode attained its initial value and the instrumentation was ready to indicate the drop-fall. Drop-time was displayed on a digital clock [11].

With the hanging mercury drop electrode (HMDE) the change from potentiostatic to galvanostatic control was done manually. Analogous measurements were performed.

Under potentiostatic conditions the potential of the working electrode was measured with a digital voltage meter with high input impedance (Schneider VN454), and directly on the screen of the oscilloscope when the current was controlled. In this investigation the current was 30.0 μA. The iR-drop in the cell can easily be compensated by the instrumentation.

The surface-active substances investigated (Table 1) were supplied by Berol Kemi AB (Stenungsund, Sweden) and used without further purification. The water content was determined by Karl Fischer titration. Stock solutions were prepared by dissolving the surfactant in absolute ethanol. The appropriate volume of a stock solution was evaporated in an empty cell and the sample dissolved in the supporting electrolyte 0.1 M KF + 0.05 M KOH. Before measurements all solutions were de-oxygenated in a stream of purified nitrogen. All measurements were performed at 25 ± 0.5°C.

RESULTS AND DISCUSSION

The polyoxyethylated substances are not oxidizable or reducible within the potential range of the mercury electrode. They are, however, adsorbed on the mercury electrode if its potential is more positive than about −1.85 V vs. SCE. For the actual compounds there is no positive desorption range within the potential limits of the electrode. If surfactants are adsorbed and a cathodic current pulse is applied over the cell, the molecules will become desorbed when the potential reaches a value in the range −1.75 V to −1.85 V. An ordinary chronopotentiogram, $E = f(t)$, for the process described is shown in Fig. 1A, and the corresponding derivative, $dE/dt = f(t)$, in Fig. 1B. To

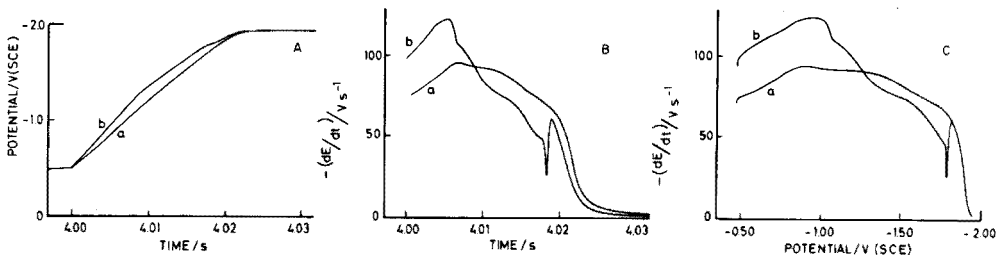

Fig. 1. Chronopotentiogram (A), derivative chronopotentiogram (B) and derivative chronopotentiogram with $dE/dt = f(E)$ (C) for (a) 0.1 M KF + 0.05 M KOH, and (b) with 12 mg l^{-1} CSA : 10 added. Starting potential −0.47 V vs. SCE.

TABLE 1

Polyoxyethylated surfactants used

Surfactant	Short form or name	Detect.-limit $\mu g\ ml^{-1}$
Nonylphenol (4 moles EO[a])	NF : 4	2
Cetyl/stearyl alcohol (4 moles EO)	CSA : 4	2
Nonylphenol (6 moles EO)	NF : 6	1
Cetyl/stearyl alcohol (6 moles EO)	CSA : 6	2
Dodecyl alcohol (10 moles EO)	DOA : 10	1
tert-Octylphenol (10 moles EO)	Triton X-100	1
Nonylphenol (10 moles EO)	NF : 10	1
Octadecyl alcohol (10 moles EO)	ODA : 10	1
Cetyl/stearyl alcohol (10 moles EO)	CSA : 10	1
Coco fatty amine (11 moles EO)	KFA : 11	2
Dinonylphenol (16 moles EO)	DNF : 16	1
Oleyl/cetyl alcohol (18 moles EO)	OCA : 18	1
Nonylphenol (30 moles EO)	NF : 30	0.8
Cetyl/stearyl alcohol (30 moles EO)	CSA : 30	0.8
Nonylphenol (50 moles EO)	NF : 50	0.5
Cetyl/stearyl alcohol (50 moles EO)	CSA : 50	0.5

[a] Ethylene oxide.

simplify the evaluation of the curves obtained for samples and the related supporting electrolyte, the time-dependent functions can be displayed against each other, i.e. $dE/dt = f(E)$ (Fig. 1C). The indentation, which occurs on desorption, can be normalized by taking the ratio of its size to the corresponding dE/dt-value of the supporting electrolyte at the same potential.

The adsorbability of the surfactants investigated is assumed to be large and the rate of adsorption fast. Under these circumstances, the adsorption equilibrium is reached slowly at low concentrations and the amount of adsorbed material at the electrode is limited by diffusion. At a stationary electrode and with semi-infinite diffusion, the following relation is valid [12]

$$\Gamma_t = 11.28 \cdot 10^{-4}\, D^{1/2}\, C\, t^{1/2}$$

Γ_t is obtained in mol cm^{-2} if D is given in $cm^2\ s^{-1}$, C in mol l^{-1}, and t in s. The amount of adsorbed material will increase initially by the square root of the adsorption time. When the bulk concentration and/or adsorption time increases, the amount of adsorbed material will be limited by the adsorption equilibrium.

The adsorption of CSA : 10 at a stationary mercury electrode was investigated at five concentrations (Fig. 2). The size of the normalized indentation is proportional to the amount of adsorbed material in cases where the value of $C \times t^{1/2}$ is a constant for a certain indentation (Fig. 3). For the actual surfactant the relation was experimentally verified up to values between 0.5 and 0.6 of the normalized indentation. For the highest concentration the

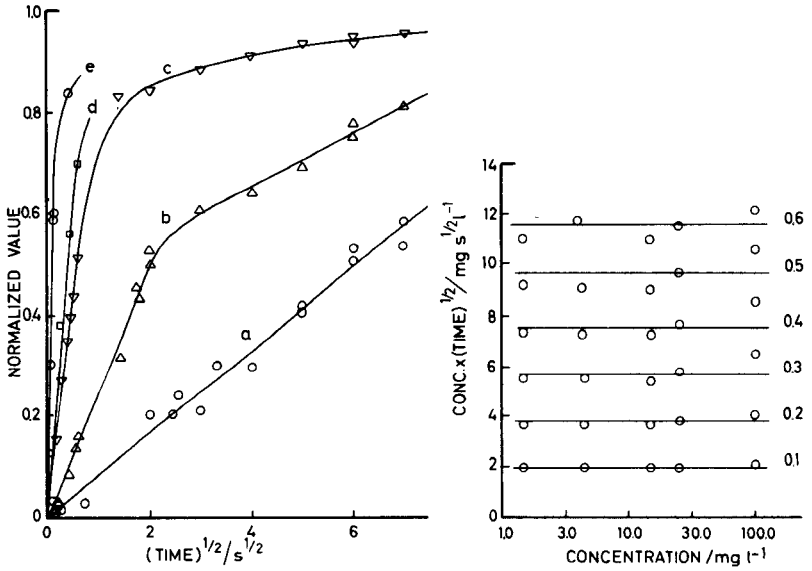

Fig. 2. Variation of the indentation of desorption with adsorption time at a HMDE for (a) 1.5, (b) 4.5, (c) 15, (d) 25, and (e) 100 mg l^{-1} of CSA : 10.

Fig. 3. Values of $C \times t^{1/2}$ obtained from Fig. 2 for different concentrations of CSA : 10. Normalized size of the indentation of desorption indicated near each line.

adsorption times required to achieve normalized values less than 0.5 are very short and less accurate.

For analogous conditions with regard to adsorbability and adsorption rate at a dropping mercury electrode, the following relationship is valid [13]

$$\Gamma_t = 7.36 \cdot 10^{-4} D^{1/2} C t^{1/2}$$

The adsorption equilibrium will, as before, limit the amount of adsorbed material when the bulk concentration and/or adsorption time increases.

The adsorption of CSA : 10 at a dropping mercury electrode was investigated under the same concentrations as for the HMDE. A certain time, dependent on concentration, is required at the beginning of each drop before any indentation of desorption is observed. Thereafter the indentation increases by the square root of the adsorption time, in a process similar to that at a stationary electrode (Fig. 4). The lack of any detectable indentation at short adsorption times may be due to a depletion of surfactants in the solution close to the electrode by adsorption on the preceding mercury drop, an effect which is equivalent to depletion of electroactive material at the DME [14]. The surface of the electrode increases very rapidly at the start of the drop growth. Consequently the concentration of adsorbed material is below the limit of detection for the method.

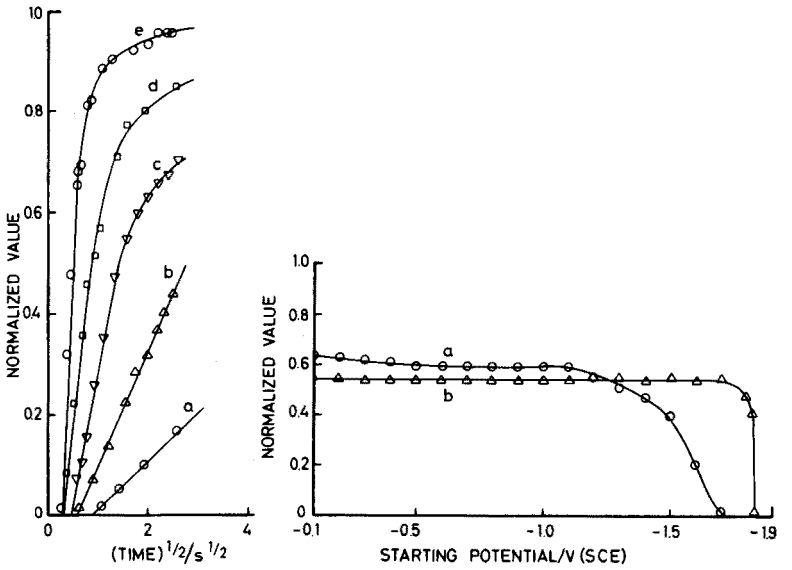

Fig. 4. Variation of the indentation of desorption with adsorption time at a DME for (a) 1.5, (b) 4.5, (c) 15, (d) 25, and (e) 100 mg l^{-1} of CSA : 10.

Fig. 5. Variation of the indentation of desorption with potential during the quiescent period for (a) 8 mg l^{-1} of Triton X-100, and (b) 10 mg l^{-1} of CSA : 10 in 0.1 M KF + 0.05 M KOH.

Because of the high surface activity of the substances investigated, considerable difficulties appeared in work with a stationary electrode of the capillary type. Because of the tendency of the solutions to creep along the inner surface of the capillary the electrical connection was easily broken. Such difficulties did not complicate the measurements with the DME. For the electrode used the drop time was adjusted to 10.80 s at the potential of the electrocapillary maximum in the supporting electrolyte. At −1.80 V vs. SCE the drop time decreased to 5.60 s. The change from potentiostatic to galvanostatic control together with adequate measurements must be completed before the fall of the drop. The longest quiescent period permissible under these circumstances at −1.80 V was 4.00 s. This quiescent period was kept constant at all potentials investigated, although longer periods would have given increased response; the constant quiescent period simplified the comparison of results.

With the current used, the potential will reach values where the molecules are desorbed 10—20 ms after the function has been changed from potentiostatic to galvanostatic control. If adsorption equilibrium is reached, the amount of adsorbed material is not increased if the adsorption time is further increased. In cases where diffusion is the limiting factor the difference in the amount of adsorbed material at 4.00 s and 4.02 s is less than 0.5%.

Thus, the size of the indentation may be used as a measure of the amount of material adsorbed during the initial 4.00 s of the life-time of a mercury drop. The change in size of the indentation of desorption with potential during the quiescent period for two of the surfactants investigated is shown in Fig. 5. It is apparent that the adsorption of surfactants of aliphatic origin is less potential-dependent than that of surfactants with aromatic groups. The aliphatic surfactants may be adsorbed at potentials close to the final desorption without any decrease in response, whereas the corresponding aromatic compounds will give diminished indentations if −1.20 V or a more negative potential is chosen during the quiescent period. This effect may be due to repulsion caused by the π-electron configuration in the hydrophobic part of the molecules. Phenol, for instance, is desorbed at about −1.10 V [1].

For the determination of surfactants, the DME was preferred because of the experimental difficulties with the HMDE mentioned above. The quiescent period was fixed at 4.00 s, and the starting potential was varied in the range −1.20 V to −1.70 V vs. SCE, where nonionic surfactants, but few other compounds, are adsorbable.

The recordings can be evaluated either by using the normalized indentation of desorption or by utilizing the normalized lowering in differential capacity at some arbitrarily chosen potential in the adsorption range. Both methods were applied in this investigation: the desorption process was recorded during a cathodic current pulse whereas the lowering in differential capacity was calculated from values obtained during an anodic pulse. The response—concentration curves obtained by the two different methods of evaluation are shown in Fig. 6.

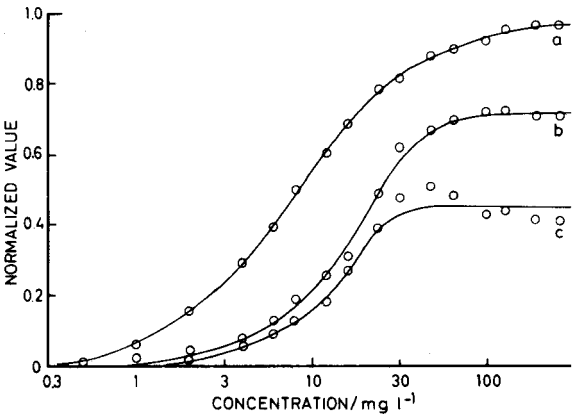

Fig. 6. Response—concentration curves for CSA : 10 by measuring (a) indentation of desorption, (b) lowering in differential capacity at −0.90 V, and (c) same at −0.40 V vs. SCE.

When normalized indentations of desorption are used for evaluation of concentrations, a somewhat lower limit of detection is achieved, compared to the differential capacity method. A larger concentration range for quantitative analysis is generally obtained if the indentation of desorption is used. For CSA : 10 the concentration range is 1—100 mg l^{-1} compared to 3—50 mg l^{-1} with the differential capacity method. The same concentration range is obtained with the indentation method for all starting potentials more positive than −1.70 V vs. SCE. The standard deviation in the steepest part of the curve is 0.017 units, resulting in a standard deviation of about 5% in the determination of concentration.

By measuring the effects during a desorption process, a more selective determination is achieved, as almost all kinds of adsorbable organic molecules have a lowering effect on the differential capacity in the vicinity of the electrocapillary maximum. Only nonionic polyoxyethylated surfactants and polyethylene glycols have been found to give indentations of desorption in the potential region of interest [15].

All surfactants investigated by this chronopotentiometric method exhibit generally similar behaviour when adsorbed at the mercury electrode. A sharp and well-defined indentation is formed at the final desorption. This common property seems to be attributable to the desorption process of the polyoxyethylated part of the molecules. Polyethylene glycols are desorbed in the same potential range [15]. However, hydrophobic compounds used in the production of the surfactants are desorbed much closer to the potential of zero charge [16]. The proportions of hydrophobic and hydrophilic parts in the molecules also support this interpretation. Surfactants with short polyoxyethylated chains must be present in a higher concentration than long chain molecules, to create indentations of equivalent size (Fig. 7).

The potential of desorption of organic molecules is in most cases dependent on the bulk concentration [1], higher concentrations giving a more negative potential of desorption. This effect was not observed for any of the surfactants investigated. dE/dt curves for different surfactants present in concentrations giving equivalent sizes of indentation of desorption are shown in Figs. 7 and 8. A small shift in the potential of the final desorption towards more negative values is observed when the polyoxyethylated part of the molecule is increased, but the effect is too small to be used for qualitative purposes.

In the potential range preceding the final desorption of the surfactants, the dE/dt values are suppressed and the shape of the curves may be used for qualitative purposes. Bulk concentrations giving indentation of desorption with a normalized value of 0.5 were found suitable for the comparison of surfactants. Those with a short polyoxyethylated chain must be present in a higher concentration than the corresponding long chain surfactants. For molecules with a short hydrophilic chain, a larger amount of hydrophobic material is present in the double layer compared with situations where molecules with a long polyoxyethylated chain are adsorbed. The reorientation

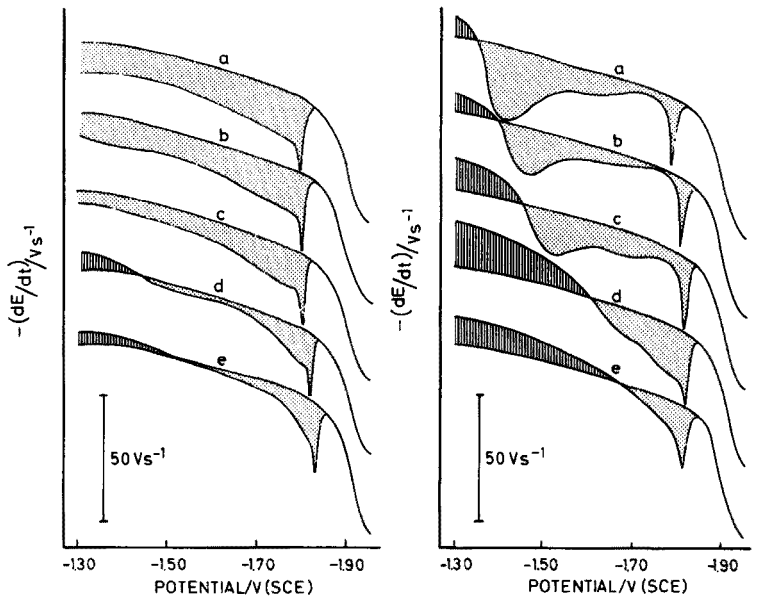

Fig. 7. Cathodic dE/dt-curves for (a) 40 mg l^{-1} of CSA : 4, (b) 30 mg l^{-1} of CSA : 6, (c) 12 mg l^{-1} of CSA : 10, (d) 5 mg l^{-1} of CSA : 30, and (e) 3 mg l^{-1} of CSA : 50 in 0.1 M KF + 0.05 M KOH.

Fig. 8. Cathodic dE/dt-curves for (a) 100 mg l^{-1} of NF : 4, (b) 5 mg l^{-1} of NF : 6, (c) 4 mg l^{-1} of NF : 10, (d) 4 mg l^{-1} of NF : 30, and (e) 4 mg l^{-1} of NF : 50 in 0.1 M KF + 0.05 M KOH.

and/or partial desorption of the hydrophobic part of the molecules will cause significant changes in the charge distribution in the double layer of the electrode. As a result a more pronounced suppression of the dE/dt curves is obtained for short-chain surfactants.

In this investigation all surfactants of aromatic origin seem to have a rounded shallow suppression region in the potential range preceding the final desorption. The suppression of the dE/dt curves for other nonionic surfactants does not show this characteristic form (Figs. 7, 8).

The useful concentration range for most of the surfactants investigated was found to be 1—200 mg l^{-1} and the relative standard deviation obtained was about 5%. A crude classification of nonionic surfactants according to the length of the hydrophilic polyoxyethylated chain may be established and the presence of surfactants containing aromatic hydrophobic parts can be distinguished by means of the chronopotentiometric method described.

REFERENCES

1 B. B. Damaskin, O. A. Petrii and V. V. Batrakov, Adsorption of Organic Compounds on Electrodes, Plenum Press, New York, 1971.
2 B. Breyer and H. H. Bauer, Alternating Current Polarography and Tensammetry, Interscience, New York, 1963.
3 E. Verdier, J. Piro and F. M. Montelongo, Talanta, 18 (1971) 1237.
4 H. Jehring, Elektrosorptionsanalyse mit der Wechselstrompolarographie, Akademie-Verlag, Berlin, 1974.
5 D. C. Grahame, J. Am. Chem. Soc., 68 (1946) 301.
6 W. Lorenz and E. O. Schmalz, Z. Elektrochem., 62 (1958) 301.
7 S. V. Tatwawadi and A. J. Bard, Anal. Chem., 36 (1964) 2.
8 P. Holmqvist, J. Electroanal. Chem. Interfacial Electrochem, 68 (1976) 31.
9 R. Danielsson, Examination Report, Institute of Technology, University of Uppsala, 1969, (in Swedish).
10 R. Danielsson, UUIP Report, Oct 1973, Institute of Chemistry, University of Uppsala.
11 R. Danielsson, UPTEC 73 61R, Oct 1973, Institute of Technology, University of Uppsala.
12 J. Crank, The Mathematics of Diffusion, 2nd edn., Clarendon Press, Oxford, 1975.
13 J. Koryta, Collect. Czech. Chem. Commun., 18 (1953) 206.
14 W. Hans, W. Henne and E. Meurer, Z. Elektrochem., 58 (1954) 836.
15 P. Holmqvist, Anal. Chim. Acta, 89 (1977) 315.
16 R. Kalvoda, Collect. Czech. Chem. Commun., 25 (1960) 3071.

Analytica Chimica Acta, 90 (1977) 45—49

A SPECIFIC ENZYME ELECTRODE FOR L-PHENYLALANINE

C. P. HSIUNG, S. S. KUAN and G. G. GUILBAULT

Department of Chemistry, University of New Orleans, New Orleans, Louisiana 70122 (U.S.A.)

(Received 13th November 1976)

SUMMARY

A specific enzyme electrode procedure is described for the rapid assay of L-phenylalanine. The enzyme L-phenylalanine ammonia lyase is used, which cleaves L-phenylalanine to ammonia. The ammonia liberated is measured with an air-gap electrode. The procedure is specific; L-tyrosine and other amino acids do not interfere, nor do Na^+ or K^+ ions. As little as $5 \cdot 10^{-5}$ M L-phenylalanine can be determined.

Some spectrophotometric [1—4] and microbiological [5] procedures have been reported for the determination of L-phenylalanine but most either lack good selectivity or require long analysis times. An enzyme electrode [6] based on catalytic generation of ammonium ion by L-amino acid oxidase was not specific since other L-amino acids are enzymatically oxidized, and since the base sensor, the NH_4^+ electrode, responds to potassium, sodium and other monovalent cations as well as to the NH_4^+ released in the enzymatic reaction. An electrode designed to determine ammonium ion in serum [7] also suffers an interference from those monovalent cations commonly present in the biological samples. Guilbault and Nagy [8] employed an antibiotic membrane electrode to improve the electrode performance by selectivity sensing the ammonium ion, but still the enzyme specificity problem [3, 6] remains, since the non-specific L-amino acid oxidase is used.

Recently, based on the pioneering work of Růžička and Hansen [9], a new type of potentiometric gas sensor, the air-gap electrode, has been developed. This new gas-sensing electrode has been used to determine both the natural content of ammonium ion in aqueous solution [9, 10] and the ammonium ion generated in the enzyme-catalyzed reactions [11—13]. The gas-permeable membrane is replaced by an air gap that separates the electrode from the sample solutions; therefore, all the common interferences resulting from direct contact of the electrode with the sample solution in a potentiometric measurement of ammonium ion are eliminated. Such an electrode provides a convenient tool for the direct, selective monitoring of substances, especially in biological samples. In this paper, a specific enzyme electrode for L-phenylalanine, based on the use of L-phenylalanine ammonia lyase (*E. C.* 4.3.1.5) and the air-gap electrode, is described. The ammonium ion, produced from L-phenylalanine (eqn. 1) in the sample solution is converted to ammonia, which is measured by the change of pH of the air-gap electrode.

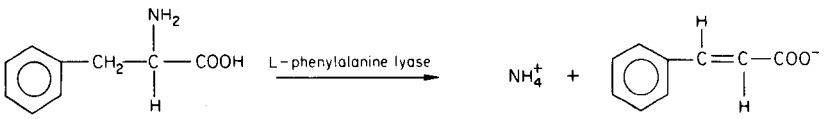

(1)

$$NH_4^+ + OH^- \rightarrow NH_3 \uparrow + H_2O \qquad (2)$$

The electrode is completely specific: there is no interference from L-tyrosine or other amino acids, nor with Na^+ or K^+ present in the biological samples. The enzyme from potato tuber [14], unlike other lyases from yeast [15], maize [16], and sweet potato [17], which does not react with L-tyrosine, was selected, purified by affinity chromatography and used in a specific method for L-phenylalanine.

EXPERIMENTAL

Apparatus

The Radiometer Type E 503610 glass electrode and the construction of the air-gap sensor used in all studies were the same as described by Hansen and Růžička [12]; a micro-chamber was used for all measurements. A digital pH meter (Corning, New York) and a strip-chart recorder (Houston Instrument Co.) were used for measuring and recording the electrode responses. A glass electrode (S-20070-10) and Radiometer pH meter (Copenhagen) were used for preparing the buffer solutions. The Radiometer flat-bottom combined glass electrode used in the air-gap system was periodically checked to ensure that a constant level of the surfactant-electrolyte filling solution was present. The calibration curve was constructed by means of a least-square analysis of the linear portion of the curve with a PDP-10 computer.

Reagents

The surfactant-electrolyte solution was $5 \cdot 10^{-3}$ M ammonium chloride saturated with wetting agent (Victawet 12, Stauffer Chemical Co., U.S.A.). The L-phenylalanine ammonia lyase was prepared by affinity chromatography [18] from several batches, which were combined to yield a final specific activity of 24.2 mU mg^{-1}. A unit is defined as one micromole of ammonium ion liberated per minute of incubation. The L-phenylalanine and L-tyrosine (Sigma Chemical Co., St. Louis, Mo.) were used for preparing standard solutions without prior purification. All the chemicals used were reagent or analytical grade. Double-distilled water was used for the sample preparation.

Procedures

To 500 μl of L-phenylalanine ammonia lyase (10^{-2} units) in 0.1 M phosphate buffer, pH 7.0, add 500 μl of the standard L-phenylalanine solutions and stir for 5—10 s with a Teflon-coated magnetic stirring bar (15 × 5 mm). Place the micro-chamber containing the reaction solution in a 30° C water

bath and incubate for 10 min. Then add 200 μl of 3.0 M sodium hydroxide solution. Immediately close the micro-chamber with the electrode body, switch on the stirrer and run at a constant speed until an equilibrium pH(pH_e) is obtained. After each run, rinse the micro-chamber with warm tap water, and dry before the next experiment. The electrolyte layer is renewed by placing the electrode on a sponge containing fresh electrolyte.

RESULTS AND DISCUSSION

Selection of optimum reaction pH

The L-phenylalanine ammonia lyase from potato tuber has an optimum pH at 8.8. In theory, it should be possible to maintain the reaction pH at this value and monitor the ammonia released by the enzyme reaction with the air-gap electrode system continuously. Only a fixed fraction of the total ammonium content in the reaction mixture can be volatilized as ammonia at pH 8.8, and quantitative conversion occurs only at a pH above 10.5 [12]. Unfortunately, the purified enzyme [18], like the enzymes obtained by other methods [14—17], has a rather low specific activity (i.e., less than 1.0 U per mg). Hence, the direct monitoring of ammonia produced from the partial conversion of ammonium ion produced in the reaction mixture at pH 8.8, the optimum pH of the enzyme, yielded poor electrode reproducibility and limited sensitivity. Hence, it was decided to perform the enzymatic reaction at a lower pH, i.e., pH 7.0, at which the ammonium ion produced during the incubation can be safely accumulated in the reaction mixture and relaesed quantitatively as ammonia upon abrupt change of pH by adding sodium hydroxide.

Calibration curve and electrode response

Figure 1 shows a calibration plot for L-phenylalanine determined with the air-gap electrode. The curve exhibits a fairly linear portion from $1.0 \cdot 10^{-4}$ M to $6 \cdot 10^{-4}$ M of L-phenylalanine concentration with a slope of 1.03 pH_e per decade and a standard deviation of 0.0195 pH_e (corresponding to a relative standard deviation of 4.67%). An L-phenylalanine concentration of 10^{-4} M could be easily detected, and the lower detection limit is $6.4 \cdot 10^{-5}$ M, which is predictable from the detection limit of the electrode sensor used. The unusually short linear range of the standard calibration curve may strongly indicate the incomplete conversion of the substrate to ammonia at substrate concentrations higher than $6 \cdot 10^{-4}$ M, after incubation for 10 min.

This can be explained either by the low activity of the enzyme or by an independence of the reaction rate on substrate at high substrate concentrations as predicted by the Michaelis—Menten equation. The total conversion mode of analysis [12] was employed as the standard procedure. The preparation of the purified enzyme with 2—3 times enhancement in specific activity by column elution is plausible [18], but an enormous decrease in total recovery was always obtained. Addition of 200 μl of 3.0 M sodium

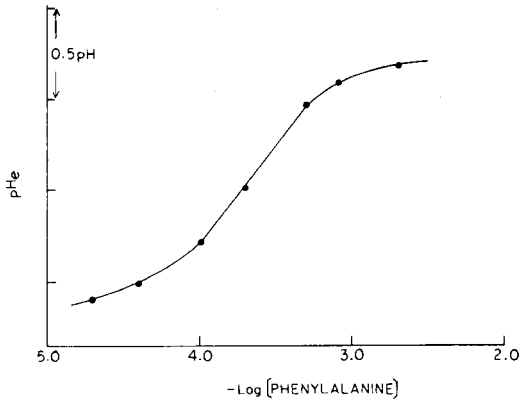

Fig. 1. Calibration curve for L-phenylalanine measurement using the air-gap electrode. Electrolyte: $5 \cdot 10^{-3}$ M ammonium chloride, $T = 30°$ C. The data were collected as the equilibrium pH values obtained after 12 minutes.

hydroxide, after pre-incubation for 10 min at 30° C, pH 7.0, raises the pH to the alkaline region required to convert the ammonium ion quantitatively to ammonia.

Interference study

The common monovalent cations present in blood, Na^+, K^+, etc., should not interfere in the assay since there is no direct contact of the electrode with the sample solutions in this system. As predicted, these ions had no effect on the response characteristics of the L-phenylalanine air-gap enzyme electrode. A $5 \cdot 10^{-4}$ M solution containing L-phenylalanine and L-tyrosine mixed in equal volumes, gave the same value of pH_e as obtained with only L-phenylalanine present, indicating no interference. Nor was any interference noted from other amino acids.

The financial assistance of the National Institutes of Health, Grant No. GM-17268, is gratefully acknowledged.

REFERENCES

1 B. N. Ladu and P. J. Michael, J. Lab. Clin. Med., 55 (1960) 491.
2 M. W. McCouman and E. Robins, J. Lab. Clin. Med., 59 (1962) 885.
3 G. G. Guilbault and J. Hieserman, Anal. Biochem., 26 (1968) 1.
4 H. V. Malmstadt and T. P. Hadjiioannou, Anal. Chem., 35 (1963) 14.
5 R. Guthrie and A. Susi, Pediatrics, 32 (1963) 238.
6 G. G. Guilbault and E. Hrabankova, Anal. Chem., 42 (1970) 1779.
7 H. F. Proelss and B. W. Wright, Clin. Chem., 19 (1973) 1162.
8 G. G. Guilbault and G. Nagy, Anal. Lett., 6 (1973) 301.
9 J. Růžička and E. H. Hansen, Anal. Chim. Acta, 69 (1974) 129.

10 J. Růžička, E. H. Hansen, P. Bisgaard and E. Reymann, Anal. Chim. Acta, 72 (1974) 215.
11 G. G. Guilbault and M. Tarp, Anal. Chim. Acta, 73 (1974) 355.
12 E. H. Hansen and J. Růžička, Anal. Chim. Acta, 72 (1974) 353.
13 C. H. Kiang, S. S. Kuan and G. G. Guilbault, Anal. Chim. Acta, 80 (1975) 209.
14 E. A. Havir and K. R. Hanson, Biochemistry, 7 (1968) 1896.
15 D. S. Hodgins, J. Biol. Chem., 246 (1971) 2977.
16 H. V. Marsh, Jr., E. A. Havir, and K. R. Hanson, Biochemistry, 7 (1968) 1915.
17 T. Minamikawa and I. Uritani, J. Biochem., 57 (1965) 678.
18 K. P. Hsiung, S. S. Kuan and G. G. Guilbault, in preparation.

Analytica Chimica Acta, 90 (1977) 51—59

APPLICATION DE L'ÉLECTRODE SÉLECTIVE AU PLOMB À LA DÉTERMINATION DE CONSTANTES D'ÉQUILIBRE

C. BIRRAUX, J-Cl. LANDRY et W. HAERDI

Département de chimie minérale et analytique, Université de Genève, Sciences II, CH-1211 Genève 4 (Suisse)

(Reçu le 4 Octobre 1976)

RÉSUMÉ

Les équilibres chimiques dans les systèmes plomb-halogènure sont étudiés par électrodes sélectives. On détermine les constantes de stabilité des complexes et les produits ioniques.

SUMMARY

Chemical equilibria in lead-halide systems are studied by means of ion-selective electrodes. The stability constants of the complexes and ionic products have been determined.

Les produits ioniques des composés peu solubles du plomb(II) ont été déterminés, il y a relativement longtemps [1], par des mesures de solubilité, ou à partir de valeurs thermodynamiques. Il est intéressant de comparer les valeurs de ces produits de solubilité à celles des produits ioniques thermodynamiques, déterminés par électrodes sélectives: les activités des ions libres sont directement introduites dans la constante.

PARTIE THÉORIQUE

On peut représenter la solubilisation d'un composé ionique peu soluble de la manière suivante

$$(M_nL_m)_s \rightleftharpoons nM^{m+} + mL^{n-} \rightleftharpoons LH_r^{(r-n)+}, \quad M_kL^{(km-ln)+}, \quad M_p(OH)_q^{(pm-q)+}$$

où $(M_nL_m)_s$ = composé peu soluble; M^{m+} = métal libre; L^{n-} = ligande libre; $M_kL^{(km-ln)+}$ = complexes solubles; $M_p(OH)_q^{(pm-q)+}$ = hydroxocomplexes; $LH_r^{(r-n)+}$ = complexes protonés du ligande.

Le produit ionique thermodynamique est défini par

$$K_i = a_{M^{m+}}^n \cdot a_{L^{n-}}^m \qquad (1)$$

où a_i est l'activité de l'ion *i*.

Les courbes théoriques de solubilité des sels de plomb en fonction de la concentration de l'anion (par exemple: Br^-, I^-) sont données dans la Fig. 1. Elles montrent que la solubilité du sel est toujours supérieure à la concentration de l'ion libre M^{m+} à cause de la présence des complexes $M_kL_e^{(km-ln)+}$, $M_p(OH)_q^{(pm-q)+}$, LH_r.

La mesure de la solubilité d'un tel composé peut s'effectuer en déterminant, par exemple, la concentration totale M' de M en solution. Toute méthode analytique le permettant convient. En connaissant le taux de complexation (C'/C) de M et de L, on calcule le produit ionique du sel. (C' = concentration totale de M ou de L; C = concentration libre de M ou de L).

$$K_i = \gamma^n(M)\,\gamma^m(L)\,C'^n(M)\cdot C'^m(L)/\alpha^n(M)\,\alpha^m(L) \qquad (2)$$

En introduisant les coefficients d'activité (γ) dans la constante, on obtient le produit de solubilité qui est une constante apparente.

$$K_s = C'^n(M)\,C'^m(L)/\alpha^n(M)\,\alpha^m(L)$$

Les électrodes sélectives permettent de déterminer les activités des ions libres en solution

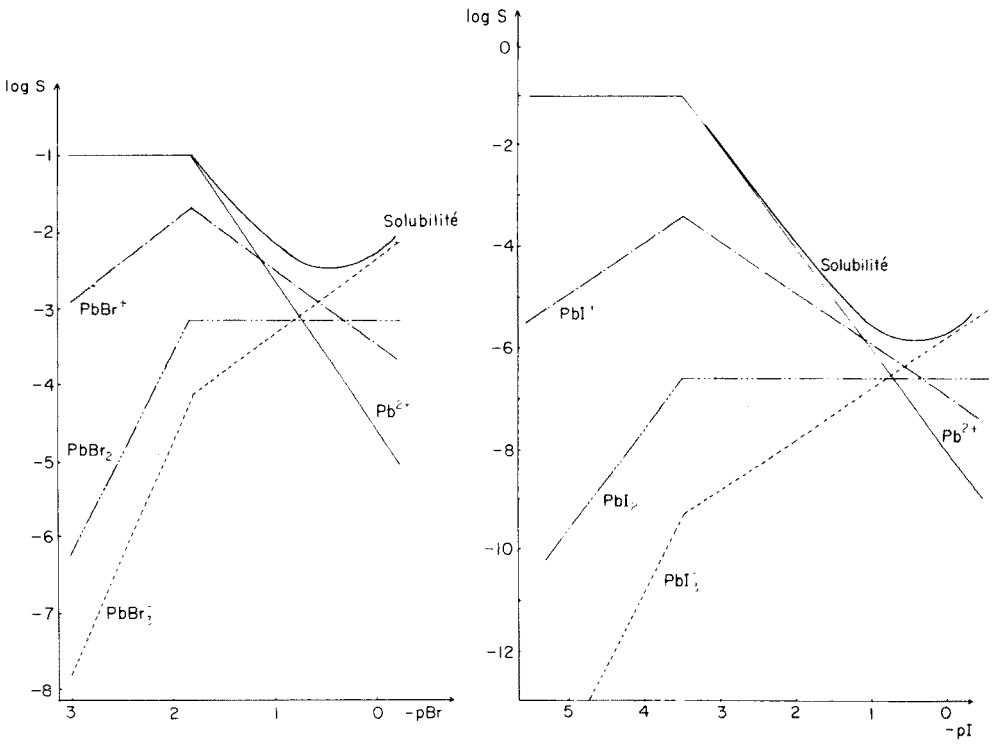

Fig. 1. Courbes donnant le log de la concentration des différentes particules en solution, en fonction de —log de la concentration de Br^- et I^- pour les systèmes Pb—Br et Pb—I (concentration initiale du plomb = 10^{-1} M).

$$E = E^0(\mathrm{M}) + \frac{s}{m} \log a(\mathrm{M}) \tag{3}$$

où $s = RT/F$; E^0 = potentiel standard de la membrane; E = potentiel mesuré; s/m = pente de la réponse de l'électrode.

En admettant que le potentiel de l'électrode n'est pas modifié par la présence d'espèces complexes du plomb, on peut introduire la valeur du produit ionique dans l'éqn. (3)

$$E = E^0(\mathrm{M}) + \frac{s(\mathrm{M})}{n \cdot m} \log K_i - \frac{s(\mathrm{M})}{n} \log a(\mathrm{L}) \tag{4}$$

Si, de plus, l'activité de L peut être mesurée à l'aide d'une seconde électrode sélective, on a

$$E(\mathrm{M}) = E^0(\mathrm{M}) + \frac{s(\mathrm{M})}{s(\mathrm{L})} E^0(\mathrm{L}) + \frac{s(\mathrm{M})}{n \cdot m} \log K_i - \frac{s(\mathrm{M})}{s(\mathrm{L})} E(\mathrm{L}) \tag{5}$$

$E(\mathrm{M})$ est proportionnel à $E(\mathrm{L})$. La valeur de l'ordonnée à l'origine permet de calculer K_i, $E^0(\mathrm{M})$, $E^0(\mathrm{L})$, $s(\mathrm{M})$ et $s(\mathrm{L})$ ayant été préalablement déterminés à l'aide d'une droite d'étalonnage.

Dans le cas où $s(\mathrm{M}) = s(\mathrm{L})$, l'expression (5) devient

$$E(\mathrm{M}) = E^0(\mathrm{M}) + E^0(\mathrm{L}) + \frac{s(\mathrm{M})}{m \cdot n} \log K_i - E(\mathrm{L}) \tag{6}$$

L'étalonnage des électrodes se fait généralement selon une échelle de concentration, à force ionique constante: $E^0(\mathrm{M})$ et $E^0(\mathrm{L})$ correspondent alors aux potentiels normaux pour une force ionique nulle. $E(\mathrm{M})$ et $E(\mathrm{L})$ sont indépendants l'un de l'autre, tant que le produit ionique n'a pas été atteint et que les complexes $\mathrm{M}_h\mathrm{L}^{(km-ln)+}$ ne sont pas formés.

Détermination de produits de solubilité par mesure de solubilité

Dans le cas où seules les concentrations de M ou de L libres peuvent être déterminées par électrode sélective, et où la stoechiométrie du sel $(\mathrm{M}_n\mathrm{L}_m)_s$ est connue, on retrouve, par le calcul, la valeur du produit de solubilité K_s.

La relation permettant de déterminer la concentration totale de la particule par la méthode des ajouts [2] s'écrit

$$(V_0 + V) \cdot \exp\left[\frac{m \cdot E}{s(\mathrm{M})}\right] \cdot \alpha(\mathrm{M}) = \exp\left[\frac{mE'_0}{s(\mathrm{M})}\right] V_0 C'(\mathrm{M}) + \exp\left[\frac{mE'_0}{s(\mathrm{M})}\right] C_a(\mathrm{M}) \cdot V \tag{7}$$

où V_0 = volume de l'aliquot; V = volume total de l'ajout; E'_0 = potentiel standard de l'électrode; C_a = concentration de la solution ajoutée; E = potentiel mesuré par électrode sélective.

Lors des ajouts de M, $\alpha(\mathrm{M})$ doit rester constant.

La relation

$$K_s = \frac{C'^n(\mathrm{M}) \cdot C'^m(\mathrm{L})}{\alpha^n(\mathrm{M}) \cdot \alpha^m(\mathrm{L})} \tag{8}$$

peut être utilisée, $\alpha(\mathrm{L})$ ayant été préalablement déterminé.

Détermination des constantes β_1 et β_2

Tant que M_nL_n n'a pas précipité, on peut écrire

$$C'(M) = C(M)\,[\alpha_{M(L)} + \alpha_{M(Y)} - 1]$$

Dès le début de la précipitation, $C'(M)$ correspond à la solubilité S du sel

$$S(M) = C(M)\,[\alpha_{M(L)} + \alpha_{M(Y)} - 1]$$

Si les constantes cumulatives des complexes hydroxylés sont connues, ou en travaillant dans des conditions telles que $\alpha_{M(Y)} = 1$, on peut écrire

$$S(M) = C(M)\left[1 + \beta_1 \frac{\gamma(M)\,\gamma(L)}{\gamma(ML)} \cdot C(L) + \beta_2 \frac{\gamma(M) \cdot \gamma(L)}{\gamma(ML_2)} \cdot C^2(L)\right] \qquad (9)$$

En définissant $\beta'_1 = \beta_1 \dfrac{\gamma(M)\,\gamma(L)}{\gamma(ML)}$ et $\beta'_2 = \beta_2 \dfrac{\gamma(M)\,\gamma(L)}{\gamma(ML_2)}$,

la mesure des concentrations du métal et du ligande libres permet de déterminer β'_1 si le terme en $\beta'_2\,C^2$ est négligeable. $S(M)/C(M)$ est alors proportionnel à $C(L)$. En utilisant deux électrodes sélectives, β'_2 est déterminé à l'aide de la relation

$$\frac{S(M) - \exp\left[\dfrac{m(E(M) - E'_0(M))}{s(M)}\right]}{\exp\left[\dfrac{m(E(M) - E'_0(M))}{s(M)} + \dfrac{n(E(L) - E'_0(L))}{s(L)}\right]} = \beta'_1 + \beta'_2 \exp\left[\frac{n(E(L) - E'_0(L))}{s(L)}\right] \qquad (10)$$

où β'_1 est l'ordonnée à l'origine et β'_2 la pente, $E'_0(M)$ et $E'_0(L)$ sont les potentiels normaux apparents des électrodes, $s(M)$ et $s(L)$ les pentes de ces électrodes.

Dans le cas où $\beta'_2 C^2(L)$ est négligeable, on obtient

$$\frac{S(M)}{\exp\left\{\dfrac{m[E(M) - E'_0(M)]}{s(M)}\right\}} - 1 = \beta'_1 \exp\left\{\frac{n[E(L) - E'_0(L)]}{s(L)}\right\} \qquad (11)$$

PARTIE EXPÉRIMENTALE

Appareillage et réactifs utilisés

Les électrodes sélectives suivantes ont été utilisées: pour le plomb, Orion No. 94.82; pour le fluorure, Beckman 39650; pour le chlorure, Philips IS 550 Cl; pour le bromure, Philips IS 550 Br; pour l'iodure, Philips IS 550 I.

Les millivoltmètres digitaux utilisés sont du type Metrohm E500, de sensibilité ±0,2 mV, les enregistreurs du type Metrohm E478, de sensibilité ±0,1 mV.

Les calculs ont été effectués sur calculatrice Hewlett-Packard HP 9100 et sur CDC 3800. Les réactifs sont p.a. Merck.

Modes opératoires

Mesure des produits de solubilité. Les composés étudiés sont précipités, filtrés, lavés et séchés, avant d'être dispersés dans KNO_3 0,1 M. Après 48 h, un aliquot de la solution surnageante est prélevé. Le plomb libre est dosé selon la méthode de Gran [2].

Mesure des produits ioniques et des constantes de stabilité. Deux électrodes sélectives sensibles à M et à L sont placées dans une solution de M, thermostatisée à 25°C. On ajoute des concentrations croissantes de L. Les potentiels de membrane sont considérés comme stables lorsqu'ils varient de moins de 0,2 mV/2 min.

RESULTATS ET DISCUSSION

Produits de solubilité de sels de plomb

Les résultats obtenus pour les produits de solubilité de différents sels (Tableau 1) sont en bonne concordance avec ceux de la littérature. Cela signifie que la méthode utilisée conjointement avec l'électrode sélective adéquate, est applicable à ces déterminations et que le taux de complexation de l'anion est calculé à partir des valeurs de la littérature, avec une approximation suffisante.

Mesure de produits ioniques et de constantes de complexes

Système Pb—F. La Fig. 2 donne les courbes $E(\mathrm{Pb}) = f(E(\mathrm{F}))$. On remarque que pour des concentrations initiales de plomb de $5 \cdot 10^{-3}$ M et 10^{-2} M, et pour des valeurs de E(F) inférieures à −100 mV et −90 mV, respectivement, la relation est linéaire. Le produit ionique vaut, dans ces conditions, $(3{,}2 \pm 0{,}1) \cdot 10^{-7}$. Pour des potentiels supérieurs à ceux mentionnés, l'interdépendance de E(Pb) et E(F) montre que le plomb est complexé par le fluorure. Les courbes obtenues en appliquant l'éqn. (11) sont données dans la Fig. 3.

Les résultats obtenus pour β_1' (Tableau 2), sont en assez bonne corrélation avec ceux obtenus par Bond et Hefter [4] qui trouvent $\beta_1' = 54 \pm 5$ (I = 0,1, T = 15°C) et par Hefter [5] qui trouve $\beta_1' = 25 \pm 1$. Ces auteurs considèrent pourtant que l'électrode sélective au plomb ne donne pas de résultats suffisamment reproductibles, et ont utilisé celle au fluorure et au plomb amalgamé.

TABLEAU 1

Mesure de produits de solubilité de différents sels de plomb

Composé étudié	Solubilité	$\alpha_{calc.}$	K_S	pK_S	pK_S littérature [1]
$PbCO_3$ [3]	$(4{,}4 \pm 0{,}8) \cdot 10^{-5}$	$10^{3{,}8}$	$(3{,}07 \pm 1{,}11) \cdot 10^{-13}$	12,51 ± 0,2	11,9—13,5
$PbCrO_4$	$(2.21 \pm 0.49) \cdot 10^{-6}$	11	$(4{,}44 \pm 1{,}96) \cdot 10^{-13}$	12,35 ± 0,19	12,5—13,7
PbC_2O_4	$(1{,}98 \pm 0{,}15) \cdot 10^{-5}$	1,05	$(3{,}7 \pm 0{,}5) \cdot 10^{-10}$	9,40 ± 0,06	9,7—10,5
$Pb(IO_3)_2$	$(3{,}74 \pm 0{,}17) \cdot 10^{-5}$	1	$(2{,}09 \pm 0{,}19) \cdot 10^{-13}$	12,68 ± 0,04	11,5—12,86
$Pb_2Fe(CN)_6$	$(7{,}92 \pm 0{,}06) \cdot 10^{-6}$	1	$(2{,}48 \pm 0{,}03) \cdot 10^{-6}$	15,6 ± 0,01	14,4—16,9

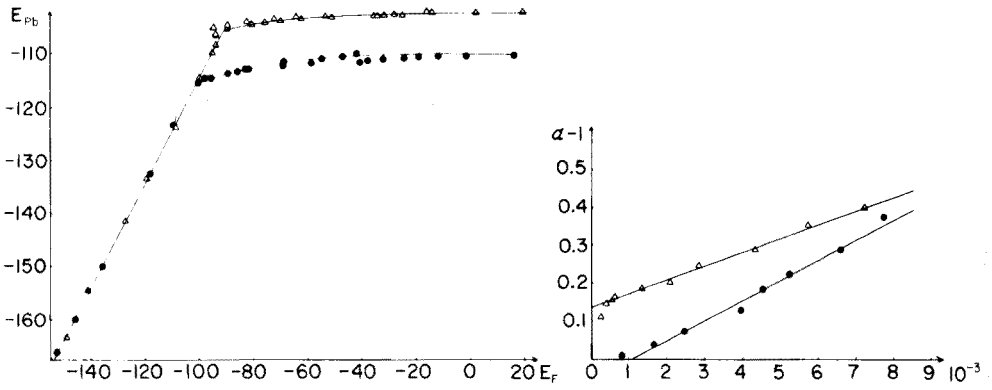

Fig. 2. Graphe du potentiel de l'électrode au plomb en fonction du potentiel de l'électrode au fluorure. (• $[Pb^{2+}] = 5 \cdot 10^{-3}$ M; △ $[Pb^{2+}] = 10^{-2}$ M).

Fig. 3. Graphe de $\alpha - 1 = f([F^-])$ relation (11) (• $[Pb^{2+}] = 5 \cdot 10^{-3}$ M; △ $[Pb^{2+}] = 10^{-2}$ M).

TABLEAU 2

Valeurs de β'_1 obtenues à partir de l'éqn. (11) pour le système Pb—halogénure (Force ionique 0,1 M KNO_3; $T = 25°C$)

Système	Concentration initiale de Pb^{2+} (M)	β'_1	Valeurs de la littérature
Pb—F	$5 \cdot 10^{-3}$	53 ± 6	25 [5]
	10^{-2}	36 ± 3	54 [4]
Pb—Cl	$6 \cdot 10^{-2}$	6,6 ± 0,6	4,6—15,8 [1]
Pb—Br	$6 \cdot 10^{-2}$	35 ± 1	
	$8 \cdot 10^{-2}$	32 ± 3	12—70 [1]
	10^{-1}	28 ± 2	
Pb—I	10^{-3}	326 ± 46	28
(I = 0,1)	10^{-2}	155 ± 51	à
Pb—I	10^{-3}	226 ± 10	200
(I = 1)	10^{-2}	257 ± 19	

Système Pb—Cl. La Fig. 4 donne les courbes $E(Pb) = f(E(Cl))$. On remarque que pour des concentrations totales de plomb de $6 \cdot 10^{-2}$ M, $8 \cdot 10^{-2}$ M et 10^{-1} M et pour des potentiels d'électrode sélective au chlorure inférieurs à 100 mV, 105 mV et 110 mV respectivement, la relation est linéaire. Le produit ionique vaut alors $(2{,}65 \pm 0{,}13) \cdot 10^{-4}$. La relation (11) ne permet de calculer qu'une valeur de β'_1. On ne peut calculer d'autres valeurs de β'_1, pour des concentrations plus élevées en plomb, la réponse de l'électrodes s'écartant, dans cette zone, par trop de la réponse nernstienne.

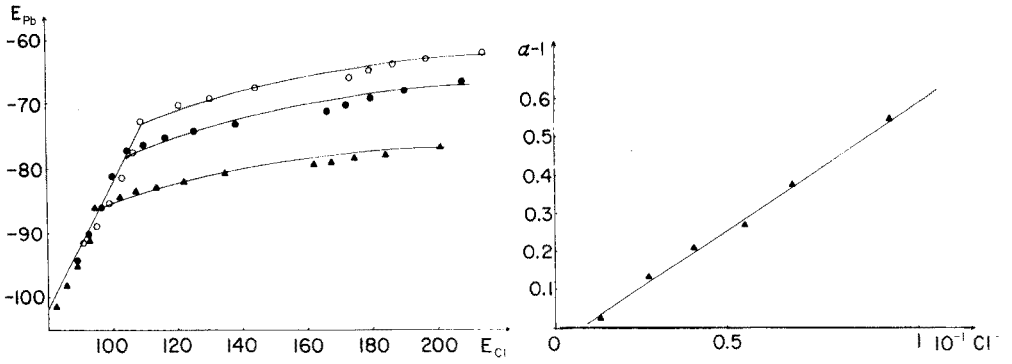

Fig. 4. Graphe du potentiel de l'électrode au plomb en fonction de celui de l'electrode au chlorure (▲ $[Pb^{2+}] = 6 \cdot 10^{-2}$ M; ● $[Pb^{2+}] = 8 \cdot 10^{-2}$ M; ○ $[Pb^{2+}] = 10^{-1}$ M; force ionique = 0,1 M KNO_3).

Fig. 5. Graphe de la relation (11), $\alpha - 1 = F([Cl^-])$, pour $[Pb^{2+}] = 6 \cdot 10^{-2}$ M.

Système Pb—Br. La Fig. 6 donne les courbes $E(Pb) = f(E(Br))$. Pour des valeurs de potentiel $E(Br)$ inférieures à —40 mV pour $6 \cdot 10^{-2}$ M en Pb^{2+}, $8 \cdot 10^{-2}$ M et 10^{-1} M en Pb^{2+}, la relation (5) est linéaire. Le produit ionique vaut $(4{,}78 \pm 0{,}33) \cdot 10^{-5}$.

La relation (11), $\alpha - 1 = f[Br^-]$, permet de calculer β_1' et d'obtenir un ensemble de valeurs très proches pour la série de concentrations étudiées. Le graphe de cette fonction est donné à la Fig. 7 et les valeurs obtenues au Tableau 2.

Système Pb—I. La Fig. 8 représente les courbes $E(Pb) = f(E(I))$, en milieu de force ionique KNO_3 0,1 M.

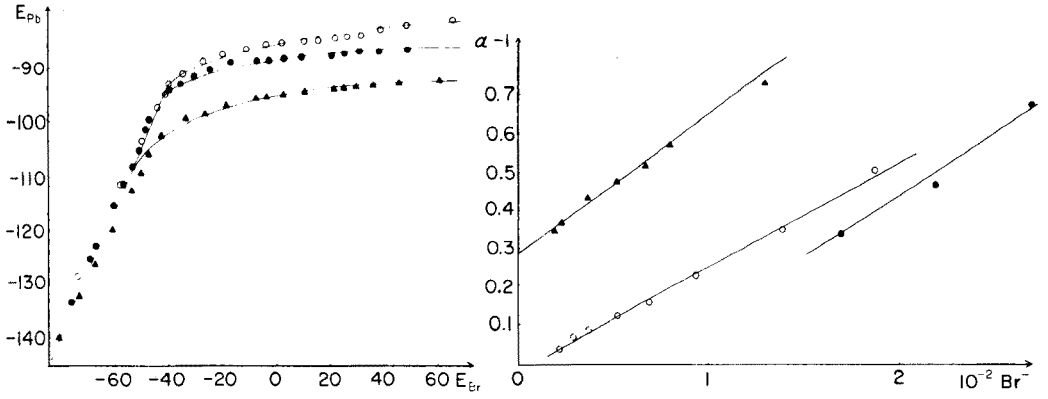

Fig. 6. Graphe du potentiel de l'électrode au plomb en fonction de celui de l'électrode au bromure (▲ $[Pb^{2+}] = 6 \cdot 10^{-2}$ M; ● $[Pb^{2+}] = 8 \cdot 10^{-2}$ M; ○ $[Pb^{2+}] = 10^{-1}$ M).

Fig. 7. Graphe de la relation (11) pour le système Pb—Br.

La Fig. 8 montre que pour des concentrations totales de plomb de 10^{-3} M, 10^{-2} M, 10^{-1} M et pour des potentiels $E(I)$ inférieurs à —170 mV, —140 mV et —120 mV, respectivement, la relation est linéaire. Le produit ionique vaut alors $(4{,}2 \pm 0{,}4) \cdot 10^{-9}$. Les valeurs de β'_1 obtenues à partir de l'éqn. (11) sont données dans le Tableau 2. Les résultats correspondants sont très dispersés.

En milieu de force ionique 1 M KNO_3, les courbes $E(Pb) = f(E(I))$, tracées à la Fig. 10, permettent de déterminer le produit ionique qui vaut $10^{-8{,}06}$.

L'équation (11) permet de calculer β'_1. Le graphe de cette relation est donné à la Fig. 11.

Les résultats obtenus pour β'_1 en milieu 1 M sont moins dispersés que pour la force ionique 0,1 M et l'erreur sur la détermination est plus faible. Cependant, toutes ces valeurs sont un peu plus élevées que celles habituellemen données dans la littérature. On peut attribuer cette imprécision au fait suivant: le domaine de concentration où l'ion iodure complexe le plomb est limité d'une part par le domaine de linéarité de l'électrode au iodure, d'autre part par la précipitation du iodure de plomb. Les variations de potentiel sont faibles, ce qui peut entraîner une erreur importante sur la détermination de β_1.

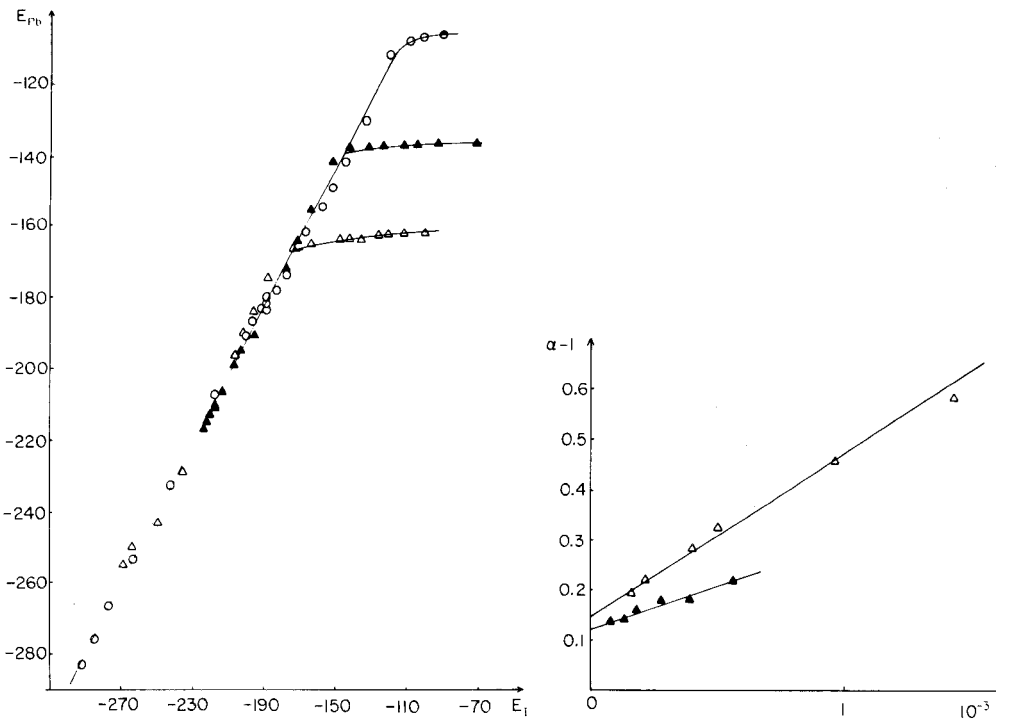

Fig. 8. Graphe du potentiel de l'électrode au plomb en fonction de celui de l'électrode au iodure, en milieu KNO_3 0,1 M. (△ $[Pb^{2+}] = 10^{-3}$ M; ▲ $[Pb^{2+}] = 10^{-2}$ M; ○ $[Pb^{2+}] = 10^{-1}$ M).

Fig. 9. Graphe de la relation (11) pour le système Pb—I en milieu 0,1 M KNO_3 (△ $[Pb^{2+}] = 10^{-3}$ M; ▲ $[Pb^{2+}] = 10^{-2}$ M).

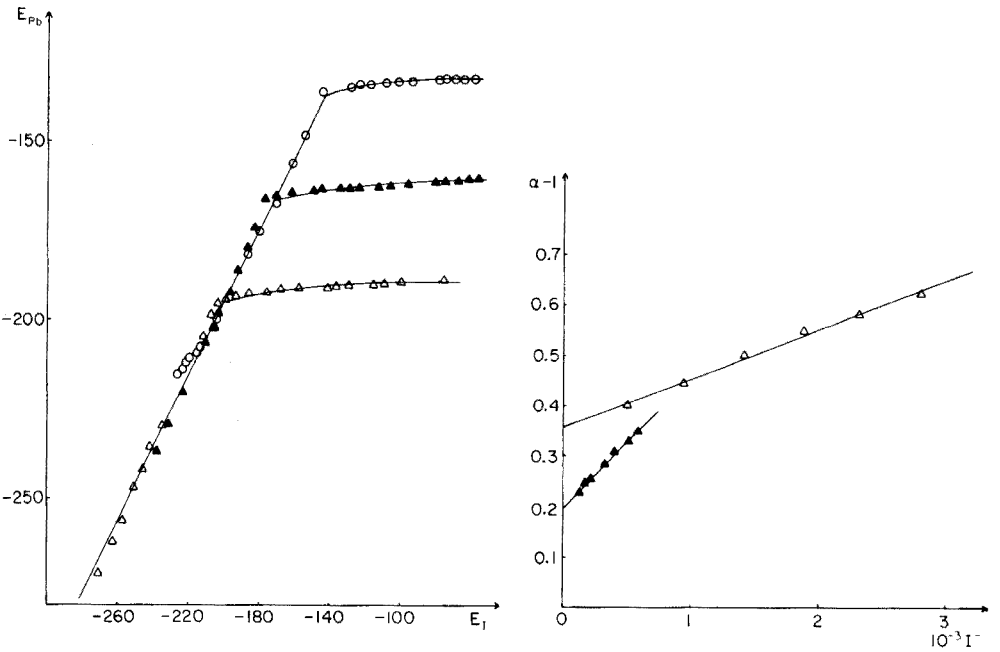

Fig. 10. Graphe du potentiel de l'électrode au plomb en fonction de celui de l'électrode au iodure, en milieu KNO_3 1 M (△ $[Pb^{2+}] = 10^{-3}$ M; ▲ $[Pb^{2+}] = 10^{-2}$ M; ○ $[Pb^{2+}] = 10^{-1}$ M).

Fig. 11. Graphe de la relation (13) en milieu KNO_3 1 M.

CONCLUSION

Les expériences effectuées permettent de dire:

(a) que les électrodes sélectives ne sont pas perturbées dans leur réponse par un milieu hétérogène et par la présence d'espèces solides de l'élément auquel elles sont sensibles;

(b) que leur sensibilité est suffisante pour pouvoir déterminer des valeurs de constantes thermodynamiques qui sont voisines de celles rencontrées dans la littérature. Toutefois, si l'approximation est bonne en ce qui concerne β'_1, il n'a pas été possible de trouver des valeurs satisfaisantes pour β'_2. On peut avancer les hypothèses que le complexe PbX_2 ne se forme pas dans nos conditions expérimentales ou que son influence est négligeable devant PbX^+.

BIBLIOGRAPHIE

1 L. G. Sillen et A. E. Martell, Stability constants, Spec. Publ. No. 17, The Chemical Society, London, 1964; No. 25. The Chemical Society, London, 1971.
2 G. Gran, Analyst (London), 77 (1952) 661.
3 N. Parthasarathy, J. Buffle, J. C. Landry, C. Birraux, J. F. Monn, M. C. Arrigo et W. Haerdi, Chimia, 27 (1973) 368.
4 M. Bond et G. Hefter, Inorg. Chem., 9 (1970) 1021.
5 G. Hefter, Electroanal. Chem. Interfacial Electrochem., 39 (1972) 345.

Analytica Chimica Acta, 90 (1977) 61—69

AN ONLINE COMPUTER METHOD FOR THE POTENTIOMETRIC TITRATION OF MIXTURES OF A STRONG AND A WEAK ACID

M. BOS

Department of Chemical Technology, Twente University of Technology, Enschede (The Netherlands)

(Received 9th November 1976)

SUMMARY

A PDP-11 online computer method for the titration of mixtures of a strong and a weak acid is described. The method is based on multiparametric curve-fitting. One of the parameters found from the calculations is the dissociation constant of the weak acid, hence the method can be applied even when this constant is unknown. Accurate results (relative error ± 1%) were obtained for weak acids with pK_a values of 0.2—10. A complete titration and calculation takes about 20 min.

Almost any mixture of a strong and a weak acid can be resolved by the use of nonaqueous titrations, but in the more frequently encountered case of aqueous samples, the water in the sample nullifies the effect of the non-aqueous solvent.

Differential potentiometric titrations of a mixture of a strong and a weak acid in aqueous solution can give rise to problems in two situations: (a) when the weak acid has a low pK_a value, normal acid—base titration methods give only the total amount of acid present; (b) when the weak acid has a very high pK_a value, it cannot be titrated, and only the strong acid can be determined.

Several authors have already developed procedures for the evaluation of poorly defined potentiometric titration curves in which the end-points cannot be located straightforwardly from the inflection points. McCallum and Midgley [1] described a method for the titration of mixtures of strong and weak acids based on linearization of the titration curve. However, the exact value of the dissociation constant of the weak acid must be known, and this precludes the use of the method when the nature of the weak acid is unknown.

Multiparametric curve-fitting seems to be a more promising technique. Its success in titrimetric analysis has been demonstrated by Meites et al. [2—5] and by Ingman et al. [6]. These authors used generalized multiparametric curve-fitting computer programs which require little extra programming effort for adaptation to various titration problems but are rather slow. Ingman et al. [6] also used generalized expressions for the titration equation. This makes their method very versatile, but very difficult to implement

online in a minicomputer because of the large program size and the length of the calculations when the dissociation constants of the titrated species are unknown.

The practical usefulness of an analytical method depends to a great extent on the time needed to produce the result. In the design of a computerized analytical method this means online data acquisition and evaluation of the result in a fraction of the time needed to complete the experiment. The latter is of prime importance when the method has to be operated in a multi-user computer environment. It has been shown [7] that the Wentworth multiparametric curve-fitting method [8] is very suitable for obtaining high calculation speeds. This paper describes how the Wentworth method can be used to provide a rapid and fully computerized titration of mixtures of a strong and a weak acid. Three parameters from the charge balance equations for the titration points are adjusted to obtain a least-squares fit: the concentration of the strong acid, the concentration of the weak acid and the dissociation constant of the weak acid.

THEORY

The symbols used are defined in Table 1.

Charge balance equation for the titration of a mixture of a strong acid HX and a weak acid HY with sodium hydroxide

The charge balance equation for each point of the titration curve is given by

$$m_{H^+} + m_{Na^+} - m_{X^-} - m_{Y^-} - m_{OH^-} = 0 \quad (1)$$

This equation can be combined with the dissociation equilibrium equations for water and the weak acid

$$K_{HY} = \frac{a_{H^+} \cdot a_{Y^-}}{a_{HY}} \quad (2)$$

TABLE 1

Glossary of symbols

HX	strong acid	C_{HX}	stoichiometric concentration of strong acid at start of titration
HY	weak acid	C_{HY}	stoichiometric concentration of weak acid at start of titration
a	activity	F_i	function relating a_{H^+} and V during the titration
K_{HY}	dissociation constant of weak acid	m	concentration
K_W	dissociation constant of water	C^0_{HX}	initial estimate of C_{HX}
f	activity coefficient	C^0_{HY}	initial estimate of C_{HY}
V	volume of NaOH added	K^0_{HY}	initial estimate of K_{HY}
V_0	volume at start of titration		
T	titer of NaOH		

and

$$K_W = a_{H^+} \cdot a_{OH^-} \tag{3}$$

to give

$$F_i = 0 = \frac{a_{H^+}}{f_{H^+}} + \frac{V \cdot T}{V + V_0} - \frac{C_{HX} V_0}{V + V_0} - \frac{C_{HY} \cdot K_{HY} \cdot V_0}{(a_{H^+} \cdot f_{Y^-} + K_{HY})(V + V_0)} - \frac{K_W}{a_{H^+} \cdot f_{OH^-}} \tag{4}$$

This equation holds for each point of the titration curve, i.e. for the complete set of a_{H^+}/V combinations.

The multiparametric curve-fitting procedure for the titration data

The experimental data set comprising the titration curve consists of n pairs of observations of a_{H^+} values versus ml of titrant, designated by

$$(a_{H^+_i}, V_i) \quad i = 1,2, \ldots, n \tag{5}$$

Equation (4) relates the two variables $a_{H^+_i}$ and V_i. This equation contains a large number of parameters, viz. f_{H^+}, V_0, T, C_{HX}, C_{HY}, K_{HY}, f_{Y^-}, K_W and f_{OH^-}. Least-squares estimates are wanted for the parameters C_{HX}, C_{HY} and K_{HY}.

The parameters K_W, T and V_0 are known previously. The activity coefficients f_{H^+}, f_{Y^-} and f_{OH^-} require some attention, because during normal titrations their values change.

If they can be treated as constants for the whole titration curve, calculations are simplified greatly. This can be accomplished by adding an excess of inert salt, which minimizes changes in the ionic strength during the titration. In this work 1 M potassium chloride was chosen, mainly because of the availability of data on activity coefficients of some compounds in its presence [9].

For 1 M potassium chloride solutions the following data for activity coefficients and dissociation constants were used [9]

$$K_W = \frac{(f_{H^+} \cdot f_{OH^-})(m_{H^+} \cdot m_{OH^-})}{a_{H_2O}} = 6.81 \cdot 10^{-15}; \quad \frac{f_{H^+} \cdot f_{OH^-}}{a_{H_2O}} = 0.600$$

Activity coefficient of hydrochloric acid [9] $f_{\pm}^2 = f_{H^+} \cdot f_{Cl^-} = 0.523$

Dissociation constant of acetic acid [10, 11]

$$K_{HAc} = \frac{(f_{H^+} \cdot f_{Ac^-})}{f_{HAc}} \frac{(m_{H^+} \cdot m_{Ac^-})}{m_{HAc}} = 1.75 \cdot 10^{-5}; \quad \frac{f_{H^+} \cdot f_{Ac^-}}{f_{HAc}} = 0.562$$

Activity coefficient $f_{\pm}$ of 1 M KCl [12] : $f_{\pm}^2 = f_{K^+} \cdot f_{Cl^-} = 0.365$.

If f_{K^+} is taken equal to f_{Cl^-} for the 1 M KCl solution then the following set of activity coefficients is consistent with the data in 1 M KCl mentioned above:

$f_{H^+} = 0.87$; $f_{OH^-} = 0.68$; $f_{Ac^-} = 0.65$; $a_{H_2O} = 0.99$; $f_{K^+} = 0.60$; $f_{Cl^-} = 0.60$.

Least-squares adjustment of the parameters C_{HX}, C_{HY} and K_{HY} can be performed by the Wentworth [8] approach if partial derivatives of the function F_i defined in eqn. (4) to these parameters and to a_{H^+} and to V are known. These partial derivatives are listed in the following equations

$$\left(\frac{\delta F_i}{\delta V}\right) = \frac{T \cdot V_0}{(V + V_0)^2} + \frac{C^0_{HY} \cdot K^0_{HY} \cdot V_0}{(a_{H^+} \cdot f_{Y^-} + K^0_{HY})(V_0 + V)^2} + \frac{C^0_{HX} \cdot V_0}{(V_0 + V)^2} \quad (6)$$

$$\left(\frac{\delta F_i}{\delta a_{H^+}}\right) = \frac{1}{f_{H^+}} + \frac{C^0_{HY} \cdot K^0_{HY} \cdot V_0 \cdot f_{Y^-}}{(V_0 + V)(a_{H^+} \cdot f_{Y^-} + K^0_{HY})^2} + \frac{K_W}{f_{OH^-} \cdot (a_{H^+})^2} \quad (7)$$

$$\left(\frac{\delta F_i}{\delta C_{HX}}\right) = -\frac{V_0}{V_0 + V} \quad (8)$$

$$\left(\frac{\delta F_i}{\delta C_{HY}}\right) = -\frac{K^0_{HY} \cdot V_0}{(a_{H^+} \cdot f_{Y^-} + K^0_{HY})(V_0 + V)} \quad (9)$$

$$\left(\frac{\delta F_i}{\delta K_{HY}}\right) = -\frac{C^0_{HY} \cdot V_0 \cdot a_{H^+} \cdot f_{Y^-}}{(a_{H^+} \cdot f_{Y^-} + K^0_{HY})^2 (V_0 + V)} \quad (10)$$

EXPERIMENTAL

Chemicals

Except where specified, all chemicals were of analytical grade. Potassium chloride, sodium acetate, acetic acid (all Merck), ammonium chloride (Brocades), *m*-cresol (Baker 'PCS' reagent), urea and tris(hydroxymethyl)-aminomethane (Fluka) were used as received.

Hydrochloric acid, sulphuric acid and sodium hydroxide solutions were prepared in 1 M potassium chloride from Merck Titrisol ampoules by adding the calculated amount of potassium chloride and diluting to the specified volume with carbon dioxide-free double-distilled water. The sodium hydroxide solution was standardized coulometrically and used to standardize the solutions of hydrochloric acid, sulphuric acid and acetic acid. The titers of the ammonium chloride, *m*-cresol, sodium acetate and tris(hydroxymethyl)-aminomethane solutions were calculated from the weight of compound added to a 1 M potassium chloride solution. The urea solution was standardized by the Kjeldahl method.

Equipment

The automatic titration system consisted of the following items: PDP-11/10 computer (Digital Equipment Corp.) with 16 K core memory, RK05 disk, and the LPS laboratory peripheral system containing a 12-bit A/D converter and Teleprint telewriter; Mettler DV11 automatic burette; Knick industrial pH-meter type DIN with Schott combined glass—calomel electrode type N

with platinum wire diaphragm; Metrohm thermostatted titration vessel; Lauda ultra thermostat, type 43/58/12. A schematic diagram of the system is given in Fig. 1.

Procedures

Calibration of the glass—calomel electrode set. Calibration of the electrode on standard NBS buffers (Electrofact) proved unsatisfactory, probably because of changes in liquid junction potential on transference to 1 M KCl solutions. To overcome this difficulty, solutions of known pa_{H^+} values were prepared in 1 M KCl, viz. 0.1 M HCl, 0.1 M acetic acid, 0.01 M acetate buffer and 0.01 M NaOH with pa_{H^+} values 1.060, 2.809, 4.573 and 12.000, respectively. These pa_{H^+} standards were used to obtain separate pa_{H^+} calibration constants for the regions $pa_{H^+} < 3$, $3 < pa_{H^+} < 8$ and $pa_{H^+} > 8$.

Titration of the samples. The sample is placed in the thermostatted (20.0 ± 0.1°C) titration vessel and 1 M KCl is added to give the starting volume required to the nearest 0.01 ml. The electrodes are allowed to equilibrate for 5 min, whereafter the titration with 0.1 M sodium hydroxide in 1 M KCl is started by the computer. The titration is carried out in a nitrogen atmosphere. Normally pa_{H^+} measurements are made at 0.100-ml intervals of titrant addition, and after each addition 10 seconds are allowed, to attain equilibrium.

Computer programs

The software for the automatic titration system was developed in four parts: (a) calibration of the glass electrode set; (b) control of the titration and recording of the titration curve; (c) the curve-fitting program; (d) a simple monitor for three real-time tasks and background facilities. The first two programs run as real-time tasks, whereas the curve-fitting program runs in the background during the recording of the next titration curve.

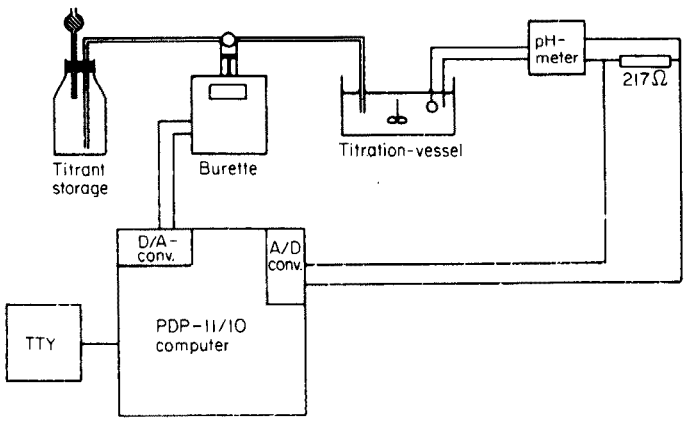

Fig. 1. Schematic diagram of automatic titration system.

(a) The calibration program for the glass electrode. From e.m.f. measurements for a set of two buffers of known pa_{H^+}, the slope and standard potential of the electrode set are calculated.

The input of the pa_{H^+} values of the two buffers is done via the teletype, and the e.m.f. readings for the two buffers are taken by the A/D converter of the LPS system connected to the pH meter. Output of the calculated calibration constants is to the teletype.

(b) The computer program for the titration. The program starts with a dialogue at the teletype in which the operator can set the various parameters that control the titration, viz. titrant addition per titration step, number of titration points, equilibration time per titration point and a sample identification. Then, alternately, pH readings are taken by the A/D converter and a pulse train is generated to activate the stepmotor of the burette to deliver the required amount of titrant. This process is stopped when the required number of titration points has been reached. The program finishes with writing the acquired data in a disk file.

(c) The curve-fitting program. The e.m.f. data acquired by program (b) are converted to pa_{H^+} vs. ml data by means of the calibration constants from program (a).

Initial estimates for the parameters required, viz. concentration of strong acid, concentration of weak acid and the dissociation constant of the weak acid are obtained as follows. The concentration of the strong acid is taken as equal to the a_{H^+}/f_{H^+} value at the start of the titration. The estimate of the total amount of acid is calculated from the volume of titrant needed to reach pH 11.0. From the estimate of the concentration of strong acid and the starting volume, the estimate for the concentration of weak acid is obtained. The pa_{H^+} value at the point where half the estimated amount of weak acid is neutralized, is then used as the estimate for the dissociation constant of the weak acid.

These initial estimates, the pa_H vs. ml data and eqns. (4)—(10) are used to calculate the coefficients of the normal equations for the corrections of the estimated parameters. These normal equations are solved by calculating the inverse matrix of the coefficients of the normal equations. Then an iterative procedure is followed to improve the calculated parameters. To obtain satisfactory convergence the final estimates are calculated by applying the calculated correction only partially. The fraction of the correction to be applied is found as described by Wentworth [8].

RESULTS AND DISCUSSION

The results of the computerized titrations and calculations for various mixtures of a strong and a weak acid in different concentration ratios are given in Table 2. The method was also applied to mixtures of an excess of hydrochloric acid and a weak base; in this case the computer output was the concentration of the free hydrochloric acid and the protonated base in the mixture. The results are presented in Table 3, where the comparison of results

TABLE 2

Computerized titrations of mixtures of a strong and a weak acid

Sample	Compound 1	Added ($\cdot 10^{-3}$ M)	Found ($\cdot 10^{-3}$ M)	Error (%)	Compound 2	Added ($\cdot 10^{-3}$ M)	Found ($\cdot 10^{-3}$ M)	Error (%)
1	HCl	4.072	4.051	−0.5	CH_3COOH	4.324	4.357	+0.7
2		8.114	8.087	−0.7		8.648	8.697	+0.6
3		4.072	4.032	−1.0		8.648	8.657	+0.1
4		2.036	2.020	−0.8		2.162	2.196	+1.5
5		2.036	2.043	+0.3		4.324	4.330	+0.1
6		4.072	4.022	−1.2		2.162	2.258	+4.4
7		2.036	2.022	−0.7		8.648	8.577	−0.8
8		8.114	8.101	−0.5		2.162	2.144	−0.8
9		10.180	10.030	−1.5		1.081	1.257	+16.3
10		1.018	1.435	+40.9		10.810	10.840	+0.3
11		2.036	2.19	+7.6		10.810	10.640	−1.6
12		10.180	10.220	+0.4		2.162	2.168	+0.3
13		10.180	10.210	+0.3		2.162	2.126	−1.7
14	H_2SO_4 (1)	5.025	5.086	+1.2	H_2SO_4 (2)	5.025	4.983	−0.8
15		2.010	2.062	+2.6		2.010	1.999	−0.5
16		1.507	1.525	+1.2		1.507	1.500	−0.5
17		1.005	1.019	+1.4		1.005	0.999	−0.6
18	(1) + HCl	14.798	14.750	−0.3	H_2SO_4 (2)	5.025	4.953	−1.4
19	(1) + HCl	11.185	11.180	−0.0		1.005	0.997	−0.8
20	(1) + HCl	10.154	10.140	−0.1		2.010	1.994	−0.8
21	(1)	5.025	5.062	+0.7		5.025	4.980	−0.9
22	HCl	3.383	3.388	+0.1	*m*-Cresol	2.938	2.976	+1.3
23		4.060	4.000	−1.5		3.525	3.514	−0.3
24	HCl	8.120	8.097	−0.3	NH_4Cl	10.290	10.280	−0.1
25		4.060	4.040	−0.5		4.116	4.133	+0.4
26		2.030	2.021	−0.4		10.290	10.260	−0.3
27		10.150	10.110	−0.4		4.116	4.170	+1.3
28		4.060	3.997	−1.5		10.290	10.350	+0.6
29		8.120	7.984	−1.7		10.290	10.360	+0.7

and the amount added for HCl were recalculated on the basis of total hydrochloric acid.

Figure 2 demonstrates that the computer method resolves mixtures even when inspection of the titration curve does not indicate that two components are present.

As can be seen from Tables 2 and 3, the method works well even for quite strong 'weak' acids like hydrogensulphate and protonated urea, and no problems arise with very weak acids such as *m*-cresol and ammonium ion. Differences in charge type of the acid do not greatly affect the accuracy of the titrations, as is shown by the results for hydrogensulphate and ammonium ion.

TABLE 3

Computerized titrations of mixtures of an excess of hydrochloric acid and a weak base

Sample	HCl added ($\cdot 10^{-3}$ M)	HCl found ($\cdot 10^{-3}$ M)	Error (%)	Compound 2	Added ($\cdot 10^{-3}$ M)	Found ($\cdot 10^{-3}$ M)	Error (%)
1	10.150	10.170	+0.2	Urea	4.000	3.982	−0.5
2	10.150	10.152	+0.0		4.000	3.985	−0.4
3	10.150	10.112	−0.4		4.000	3.987	−0.3
4	14.210	14.120	−0.6	CH_3COONa	10.000	10.060	+0.6
5	14.210	14.162	−0.3		10.000	10.040	+0.4
6	10.150	9.953	−1.9	Tris	6.000	5.914	−1.4
7	10.150	9.948	−2.0		6.000	5.952	−0.8

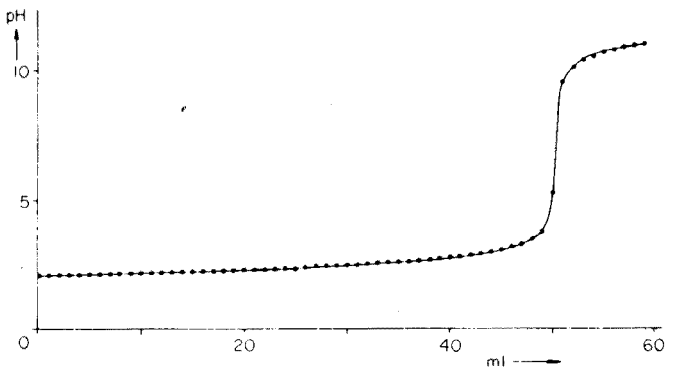

Fig. 2. Titration of a mixture of 0.5075 mmol of HCl and 0.200 mmol of urea in 50 ml of 1 M KCl with 0.100 M sodium hydroxide.

The calculations involved in a 50-point titration curve take about 4 min, which shows clearly the potentialities of the Wentworth approach in the design of computerized analytical methods for routine applications.

The activity coefficient of the acetate ion was used in all calculations for the conjugated base of the weak acid. Clearly, this is not correct, but varying this value showed that its influence was small, and it is questionable that taking this activity coefficient as a fourth parameter would improve the results significantly.

The pa_{H^+} measurements during the titration must be accurate to ± 0.02 pH unit. This implies great care in the calibration and handling of the glass electrode set and in the preparation of the pa_{H^+} standards. Separate calibration constants had to be determined for the regions $pa_{H^+} < 3$, 3—8 and > 8, in order to obtain this accuracy over the whole titration range. The sodium hydroxide titrant must be carbonate-free, otherwise poor results are obtained,

indicated by slow convergence in the calculations.

The method described for the determination of the initial estimates of the parameters C_{HX}, C_{HY} and K_{HY} does not function properly for mixtures with weak acids of $pK_a < 3$. This is because the dissociation of these acids at the start of the titration cannot be neglected. In such cases the initial estimates had to be provided manually.

The author thanks W. Tjerkstra, A. J. B. van Boxtel and A. Elling for their valuable help, Prof. Dr. Ir. E. A. M. F. Dahmen for his interest, and B. Verbeeten-v. Hettema for preparing the manuscript.

REFERENCES

1 C. McCallum and D. Midgley, Anal. Chim. Acta, 78 (1975) 171.
2 L. Meites and D. M. Barry, Talanta, 20 (1973) 1173.
3 B. H. Campbell and L. Meites, Talanta, 21 (1974) 393.
4 D. M. Barry, L. Meites and B. H. Campbell, Anal. Chim. Acta, 69 (1974) 143.
5 D. M. Barry and L. Meites, Anal. Chim. Acta, 68 (1974) 435.
6 F. Ingman, A. Johansson, S. Johansson and R. Karlsson, Anal. Chim. Acta, 64 (1973) 113.
7 M. Bos, Anal. Chim. Acta, 81 (1976) 21.
8 W. E. Wentworth, J. Chem. Educ., 42 (1965) 96.
9 H. S. Harned and B. B. Owen, The Physical Chemistry of Electrolytic Solutions, Reinhold, New York, 1964, pp. 591, 638, 752, 748.
10 H. S. Harned and R. W. Ehlers, J. Am. Chem. Soc., 55 (1933) 652.
11 H. S. Harned and F. C. Hickey, J. Am. Chem. Soc., 59 (1937) 2303.
12 H. S. Harned and M. A. Cook, J. Am. Chem. Soc., 59 (1937) 1290.

Analytica Chimica Acta, 90 (1977) 71—81

DOUBLE INDICATION IN CATALYTIC–KINETIC ANALYSIS: DETERMINATION OF IRON(III), CYANIDE AND MOLYBDENUM(VI)

HERBERT WEISZ and WOLFGANG MEINERS

Lehrstuhl für Analytische Chemie, Chemisches Laboratorium der Universität Freiburg, Freiburg i.Br. (B.R.D.)

(Received 29th November 1976)

SUMMARY

The reactions in catalytic—kinetic methods are followed simultaneously with two independent indication systems. The information delivered by the two indication methods can be used alone or in combination for the determination of the catalyst or the inhibitor. The following examples illustrate the method: the determination of iron(III) by its catalytic action on the decomposition of hydrogen peroxide (thermometric and biamperometric indication) in the range 10—100 ng Fe/6 ml; the determination of cyanide which inhibits the catalytic activity of copper on the decomposition of hydrogen peroxide (thermometric and biamperometric indication) in the range 2—60 μg CN^-/7 ml; and the determination of molybdenum based on the Landolt-type system iodide—bromate—ascorbic acid (thermometric and photometric indication) in the range 0.8—40 μg Mo/8 ml.

In catalytic methods of analysis, the concentration of the catalyst to be determined can be derived from the reaction rate of the catalyzed system. The so-called "indicator reaction" [1] is followed by observing the change in concentration of one of the reactants or products (or of any thermal phenomenon connected with the reaction). Indication methods such as photometry, biamperometry, potentiometry, thermometry, fluorimetry, etc., have been used to provide the necessary information. With this information (e.g. the slope of the graphical representation of the measured value versus time), the concentration of the catalyst can be evaluated, in most cases by extrapolation. Likewise, the optimal parameters which are necessary to provide simple kinetics and high sensitivity of the reaction can be found experimentally.

If the course of the reaction is followed simultaneously with two indication systems independent of each other, e.g. thermometry and biamperometry, it can be assumed that the precision as well as accuracy of the information, and consequently of the determination, will be improved. Moreover, the combination of two methods applied simultaneously offers additional information on the course of the reaction.

Some time ago, Beilby and Landowsky (potentiometry and photometry) [2] and Gary and Schwing (photometry and amperometry) [3] reported the

simultaneous application of two indication systems in titrimetry. Feys et al. [4] described a comparative non-simultaneous double indication in kinetic analysis (thermometry and photometry).

The double indication is obviously of special interest in cases where:
1. the two indication methods use different physical phenomena;
2. the change in the concentration of various species (reactants or products) can be followed;
3. the two indication methods reach their maxima at different times.
It is possible to evaluate the information from either of the indication methods alone. This makes error-tracking and optimization of reaction parameters much easier, because in most cases the methods respond differently to variation of the parameters. Moreover, one indication method serves always as a check on the second.

For the evaluation, the two sets of information can also be combined advantageously. For example, the measured value may involve the time which elapses until two recorder graphs intersect, the corresponding areas underneath these two crossed curves, their difference, etc. Such combinations seem to be useful for digital evaluation under automatic control.

In the sense used here, double indication means evaluation of two measured values, independently of each other and not, for example, signal data transduction of the same measured value. Basically, all possible indication methods can be combined with each other for the double indication.

In the examples described in the present paper, thermometry was always applied as one of the two indication methods; this method is instrumentally simple, nearly without inertia, and in contrast to most other methods, very flexible. Thermometric indication requires an adiabatic instrumental setup. This does not interfere with the other indication methods, as long as the reaction is always started at the same temperature. Then the influence of the change of temperature on the second indication method is reproducible and is compensated in the standardization procedure. Therefore it is not necessary to keep the temperature changes extremely small.

The methods of double indication in catalytic—kinetic determinations will be illustrated by the following examples:
1. determination of iron(III), based on the catalytic action of the iron(III)—TETA (triethylenetetramine) complex on the decomposition of hydrogen peroxide;
2. determination of cyanide, based on inhibition of the catalytic activity of the copper—tetrammine complex on the decomposition of hydrogen peroxide;
3. determination of molybdenum(VI), based on its catalytic effect on the oxidation of iodide by bromate in the Landolt-type system iodide—bromate—ascorbic acid. In the first two cases, the course of the reaction is followed by thermometry and biamperometry, whereas in the third case thermometry and spectrophotometry are used.

DETERMINATION OF IRON(III)

The iron(III)—TETA complex catalyzes the decomposition of hydrogen peroxide [5]

$$2H_2O_2 \xrightarrow{Fe/TETA} 2H_2O + O_2 + \Delta H$$

The diminution in the concentration of hydrogen peroxide can be followed biamperometrically because of its depolarizing action on the double platinum electrode. Moreover, the heat (ΔH) produced during the decomposition of hydrogen peroxide, as a physical product of the reaction, can be followed thermometrically. Both values are recorded simultaneously against time, with a two-channel recorder.

Biamperometric indication

A 10-ml PVC beaker serves as the reaction vessel. Because of the simultaneous thermometric indication, the beaker is placed in a 25-ml beaker, and the space between is filled with styropor. The beaker is covered by a suitable PVC plate with the appropriate boreholes. A double platinum micro-electrode of the conventional type for biamperometric titrations, is used at a constant potential of about 50 mV.

If variable amounts of hydrogen peroxide are present in the test solution, the electrodes are depolarized to a certain degree and an equivalent current is measured. This current is amplified and recorded on one of the channels of the recorder (Metrawatt Servogor RE 571). Curve I in Fig. 1 shows the complete recorder graph for such a biamperometric measurement. Amplification and current limiting (internal resistance of the amplifier) give Curve II from this Curve I (Fig. 1). The reaction rate, and consequently the concentration of the catalyst in the solution, is established from the time which elapses until the depolarization current falls below a preset value, because of diminution of the concentration of hydrogen peroxide. This time corresponds to the length of the horizontal part of Curve II in Fig. 1; this kind of evaluation is somewhat similar to the fixed concentration method.

Thermometric indication

During the exothermal reaction, the temperature of the solution increases. A Wheatstone bridge is used to convert the resistance of a thermistor (ITT/SEL/F23D) in the reaction vessel to an equivalent voltage, which is recorded versus time on the second channel of the recorder. The tangent of the slope of this curve (see broken lines in Fig. 2) is a measure of the rate of the reaction. Figure 2 shows clearly that the thermometric indication delivers the required value within the first 10 s of reaction time; in contrast, biamperometric indication gives the required value only near the end of the reaction.

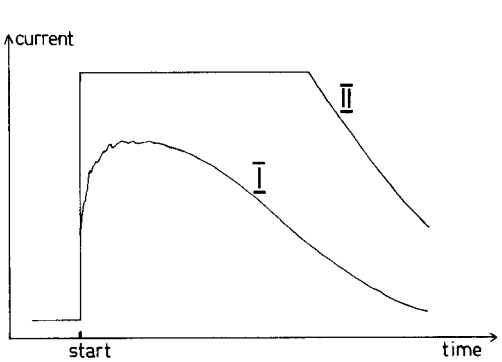

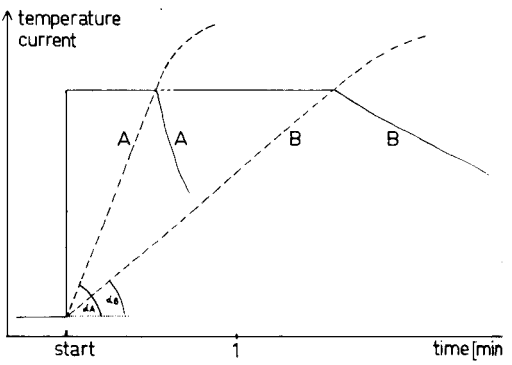

Fig. 1. Change of the depolarization current versus time. Curve II follows from I by amplification and current limiting.

Fig. 2. Change of temperature (— — — —) and depolarization current (————) versus time. (A) 80 ng Fe/6 ml, (B) 20 ng Fe/6 ml.

Procedure

For the determination of iron(III) in the range 10—100 ng/6 ml, the following reaction mixture proved to be best. Into the reaction vessel are pipetted 1 ml of aqueous 4% TETA solution, 2 ml of iron sample solution containing 10—100 ng Fe(III) (as $FeCl_3$) in 0.01 M HCl, and 2.5 ml of aqueous 1 M ammonia. The reaction is then started with 0.5 ml of hydrogen peroxide solution (20 mg H_2O_2/ml).

After each measurement the apparatus is cleaned thoroughly with 2 M hydrochloric acid and twice-distilled water. It should be noted that any change in the concentration of the ammonia has a strong influence on the biamperometric indication but very little effect on the thermometric result.

To prepare the standard graphs (Fig. 3), 10 measurements with known iron concentrations are carried out.

Table 1 gives the results for the determination of 10 samples. The values obtained by the biamperometric and the thermometric methods are given, as well as the means of the two single results.

DETERMINATION OF CYANIDE

The decomposition of hydrogen peroxide, catalyzed by the copper—tetrammine complex, is hindered by cyanide. The cyanide itself is oxidized by hydrogen peroxide; this oxidation is likewise catalyzed by copper. It is only after complete oxidation of the cyanide that the strongly exothermal decomposition of the hydrogen peroxide can start. Cyanide has already been determined in this way by using only thermometric indication to follow the reaction [6]. The time elapsed until the exothermal reaction begins, provides a measure of the cyanide concentration.

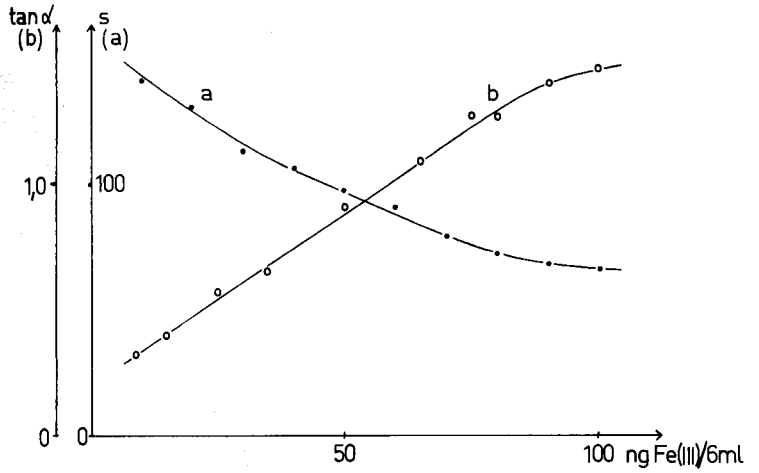

Fig. 3. Standard graphs for the determination of iron(III). (a) Thermometric indication (tan α), (b) biamperometric indication (sec).

TABLE 1

Determination of iron
(All results are given as ng Fe/6 ml)

Taken	10.0	15.0	25.0	35.0	50.0	65.0	75.0	80.0	90.0	100.0
Found thermom.	9.0	14.5	27.5	33.0	53.0	65.5	80.5	75.5	91.1	100.0
Found biamp.	8.5	19.5	25.0	36.5	43.5	67.5	76.5	86.0	95.0	110.0
Mean value	8.75	16.75	26.25	34.75	48.25	66.5	78.5	80.75	93.0	105.0

In the present paper, the reaction course is followed thermometrically and biamperometrically at the same time. The instrumental setup for both indication systems is the same as described above for the determination of iron. In this system, biamperometric indication can be applied with advantage. The constant potential (about 50 mV) applied to the double platinum micro electrode, goes to zero when the depolarizer hydrogen peroxide is present. When cyanide is also present, the depolarization, and thus the voltage decrease, is nearly inhibited. Only a very low current is measured. A possible explanation may be that the cyanide hinders the depolarization of the electrodes by the hydrogen peroxide, by covering the surface of the platinum. When all the cyanide has been oxidized, depolarization by hydrogen peroxide is no longer hindered and the current rises to a value limited by the internal resistance of the amplifier. This happens at the same time as the temperature of the reaction mixture rises because of the exothermic decomposition of

hydrogen peroxide (which is followed thermometrically, see Fig. 4). Thereafter the depolarizer hydrogen peroxide is catalytically decomposed, so that at the end of the reaction the depolarization current again reaches a minimum (Fig. 4, curve I). It was shown experimentally that the oxidation products of cyanide have no influence on the biamperometric indication.

Here, instead of using a fixed concentration of catalyst (copper), the concentration is continuously increased (15 μg Cu min^{-1}) during the reaction, starting at zero. This procedure has already been described [6]. The method certainly has some advantages for both the indication methods. First, in order to achieve reasonable reaction times (20 s—3 min), a low concentration of cyanide requires a low concentration of catalyst, whereas high concentrations of cyanide require high copper concentrations; this is achieved by continuous addition of the catalyst. Secondly, with only one fixed constant concentration of the catalyst, the standard curve (inhibition time versus the concentration of cyanide) shows a logarithmic relationship, whereas when the catalyst is added continuously, a much better linear relationship can be achieved (Fig. 5, graph a).

For the determination of the cyanide with simultaneous thermometric and biamperometric indication, the following data can be used. The time necessary for the decomposition of the cyanide is represented (a) by the horizontal part of the thermometric curve (Fig. 4, curve II), which is the time elapsed until the sudden rise in temperature, or (b) by the time elapsed until the maximum biamperometric current is reached (Fig. 4, curve I), or (c) by the time elapsed until the two curves (biamperometric and thermometric) cross each other (Fig. 4, S 1). These three possibilities lead to the same result.

Another possibility is to use the length of the horizontal part of the biamperometric curve (Fig. 4, curve I) as a measure of the cyanide concentration (Fig. 5, graph b). This length depends on the moment where the

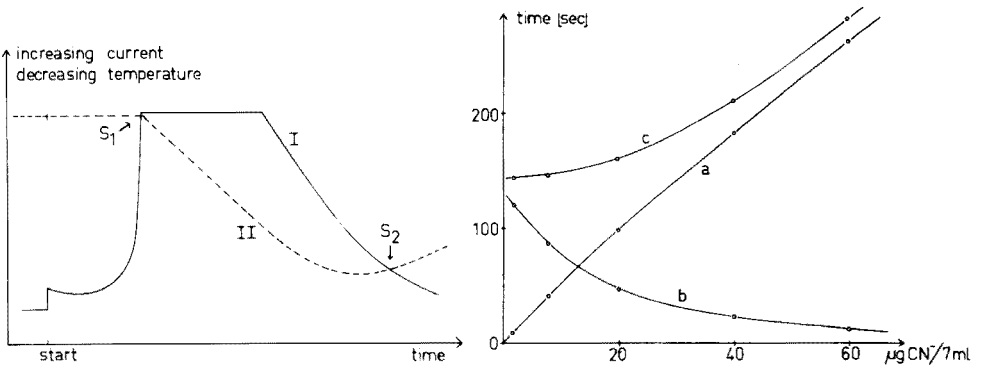

Fig. 4. Change of temperature (— — — —) and depolarization current (————) versus the reaction time (40 μg CN^-/7 ml).

Fig. 5. Standard graphs for the determination of cyanide. (a) Time for cyanide oxidation (S 1); (b) horizontal part of the biamperometric curve; (c) time to the intersection S 2.

exothermal decomposition of hydrogen peroxide begins, i.e. when the decomposition of the cyanide is complete. The higher the concentration of the cyanide, the later the decomposition of the hydrogen peroxide starts and the faster it is finished (because of the consequently higher concentration of the copper catalyst). The time between the start of the reaction and the second intersection point (Fig. 4, S 2) of the two curves also offers a possibility for evaluation of the measurement for obvious reasons (Fig. 5, graph c).

If a two-channel recorder is not available, the double indication method can still be used here. The difference between the two values (thermometric and biamperometric) is obtained by direct subtraction during the course of reaction with an operational amplifier. After amplification, the real amount of the difference is obtained by a bridge rectifier and recorded by an ordinary one-channel recorder. The two intersection points (S 1 and S 2) are represented by two distinctly formed minima (corresponding of course to zero difference). This is a general possibility for combined evaluation of the double indication method.

Procedure

For the determination of cyanide in the range of 2—60 μg CN^-/7 ml the following procedure is suitable. To 4 ml of aqueous 0.6 M ammonia solution, the cyanide sample solution (0.05—1.5 ml of KCN solution containing 40 μg CN ml^{-1}) is added and made up to 6.5 ml with twice-distilled water. Simultaneously, 0.2 ml of a solution of hydrogen peroxide (20 mg ml^{-1}) is added and the addition of the catalyst solution (100 μg Cu ml^{-1} as copper(II) acetate) from an automatic burette (Infusionsgerät Braun, Melsungen) at a speed of 0.15 ml min^{-1} is started.

The standard curves are prepared with five different standard concentrations of cyanide (see Fig. 5). Table 2 gives some results for the determination of cyanide by three different evaluation methods.

TABLE 2

Determination of cyanide
(All results are given as μg CN^-/7 ml)

Taken	2.0	5.3	8.6	14.0	20.4	30.4	42.0	48.0	56.0	60.0
Found from Δt, graph a	2.0	5.6	8.7	14.5	19.5	31.2	41.0	48.0	59.5	61.8
Found from graph b	1.8	5.0	9.0	14.3	21.9	29.6	44.1	52.5	58.1	60.5
Found from graph c	2.1	5.1	8.8	14.6	21.1	32.0	43.8	50.2	56.3	61.2

DETERMINATION OF MOLYBDENUM

For the determination of molybdenum, a well known Landolt-type system is used: molybdenum catalyzes the oxidation of iodide by bromate; the iodine formed is always instantaneously reduced by ascorbic acid. This can only happen as long as the ascorbic acid, present only in a definite substoichiometric amount, is not completely consumed. Thereafter, elemental iodine appears in the system, and can be easily indicated by photometry [7, 8].

The slower the reaction, i.e. the lower the concentration of the catalyst, the later all of the ascorbic acid will be consumed. The time which elapses until the elemental iodine appears — the induction period — is a measure of the reaction rate (and consequently of the concentration of the molybdenum). In addition, the reaction between iodide and bromate is exothermal and can also be followed thermometrically.

For the determination of the molybdenum catalyst the two indication methods are again applied simultaneously.

Photometric indication

The duration of the induction period Δt can be indicated photometrically because of the sudden increase of the absorbance (and this is recorded versus time with a two-channel recorder). Figure 6 shows the apparatus used: in front of and behind a glass cuvette (8 ml) are placed two light-sensitive elements (Photoelement, Siemens BPY 11/II). The cone of light from a low-voltage lamp is focussed by a lens on the photoelement behind the cuvette; some of the light also reaches the other photoelement in the front of the cuvette. The cuvette also contains a stirrer and a thermistor, both of which must be out of the light path. The difference of the two voltages from the photoelements is measured with the electric circuit shown in Fig. 7. Before

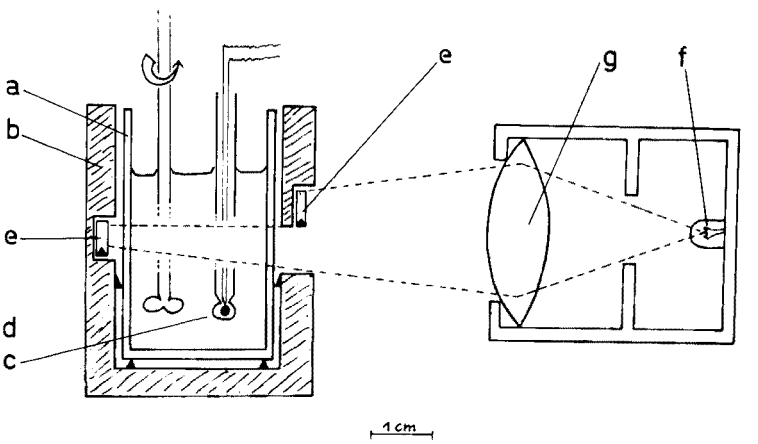

Fig. 6. Apparatus for photometric and thermometric indication. (a) Cuvette, (b) PVC insulation, (c) thermistor, (d) stirrer, (e) two photoelements, (f) low-voltage lamp, (g) lens.

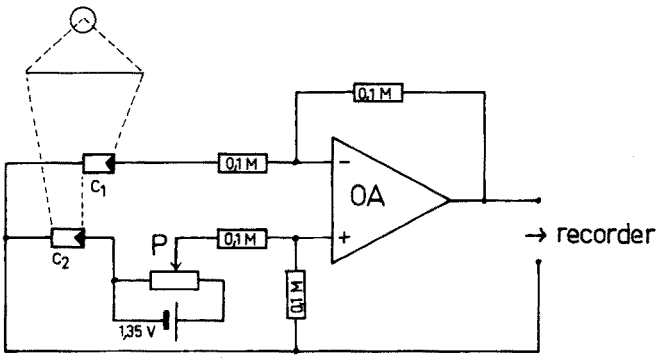

Fig. 7. Electric circuit for measuring the voltage difference of the two photoelements. OA = operational amplifier Philbrick-Nexus Q 200. $c_1 = c_2$ = Photoelements Siemens BPY 11/II.

the reaction is started, the difference of the voltages of the two photodiodes is adjusted to zero with the aid of the potentiometer P (see Fig. 7). Any change in the transmittance of the solution, e.g. the appearance of elemental iodine in the system, results in a difference of the two voltages. This difference is amplified (Fig. 7) and recorded versus time, so that its maximum range just covers the range of the recorder (Fig. 8, full lines). This unusual setup for the photometric measurement is not only very simple, but has also proved quite stable against interferences.

The standard graph is prepared by plotting the various induction times Δt for several known standard concentrations of molybdenum. This standard graph is nearly linear (Fig. 9, curves b, c).

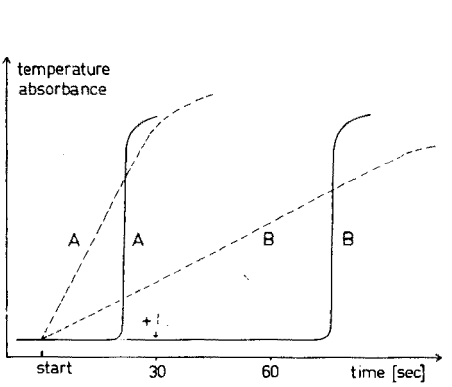

Fig. 8. Change of temperature (— — — —) and absorbance (————) versus the reaction time. (A) 20 μg Mo/8 ml, (B) 2 μg Mo/8 ml.

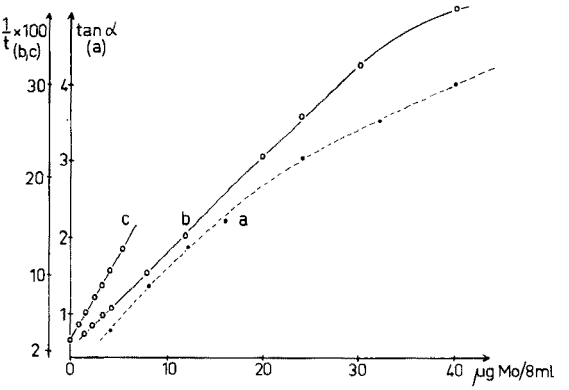

Fig. 9. Standard graphs for the determination of molybdenum. (a) Thermometric indication (tan α); (b) photometric indication (Δt); (c) photometric indication with addition of iodine.

Thermometric indication

The rise of temperature, caused by the exothermal iodide—bromate reaction is thermometrically recorded versus time with the second channel of the recorder (Fig. 8, broken lines). The thermometric indication is carried out as described above. The tan α of the slope of the recorded curve is evaluated. Gaal et al. [9] have reported a Landolt-type reaction in which the duration of the induction period has been measured thermometrically.

In the method described here, it is necessary to avoid the use of the usual citric acid buffer to avoid loss of heat; the reaction is started by the addition of sulfuric acid.

The standard graph of tan α versus molybdenum concentration is nearly linear (Fig. 9, curve a). For photometric evaluation, the standard graph is still nearly linear (see above), despite the unbuffered system. With the thermometric indication, even at the beginning of the reaction, sufficient information can be gained about the reaction rate and thus about the concentration of the catalyst. This can be utilized to cut short the induction period Δt during the measurement, if necessary. If after some seconds of reaction there is only a small change of the measured quantity (tan α), a very long induction period (more than 4 min) can be expected. In such cases, the total amount of ascorbic acid and consequently the duration of the induction period Δt is decreased by adding a definite amount of iodine. This has of course to be done logically, always at precisely the same time, e.g. 30 s after the start. This has the same consequence as if the reaction had been started with a lower concentration of ascorbic acid, and a wider range of molybdenum concentrations can be determined at reasonably short measuring times. The addition of iodine during the reaction has no influence on the kinetics of the iodide—bromate reaction.

Procedure

The following reactant mixture is prepared: 5 ml of 0.5 M $NaBrO_3$, 10 ml of 0.5 M KI, 20 ml of 0.25 M ascorbic acid and 10 ml of aqueous 0.5% starch solution are made up with distilled water to 100 ml in a measuring flask. The mixture is sufficiently stable for 7 h. For each test, 7 ml of this solution are pipetted into the reaction cuvette and 0.5 ml of sample solution or of standard solutions of molybdenum (containing 0.8—40 μg Mo as $Na_2MoO_4 \cdot 2H_2O$) for the standard graph is added. The reaction is started by adding 0.5 ml of 0.75 M sulfuric acid (Eppendorf pipette).

If the rise in the temperature at the beginning of the reaction is very low, then exactly 30 s after the start of the reaction, 1 ml of a 0.1 M iodine solution is added. This does not affect the thermometric standard graph, but two different standard graphs for the photometric method are obviously necessary, one for the higher range of molybdenum concentrations (Fig. 9, curve b) and another for the lower range (Fig. 9, curve c).

Table 3 gives some results. Not only the thermometric (tan α) and the photometric (induction period Δt) indication were evaluated for the deter-

TABLE 3

Determination of molybdenum
(All results are given as μg Mo/8 ml)

Taken	0.80	1.20	2.00	3.20	4.00	8.00	16.0	20.0	32.0	40.0
Found from Δt	0.81	1.16	2.00	3.23	3.95	7.95	16.0	20.5	32.2	40.4
Found from tan α	0.92	1.27	1.90	3.30	4.58	7.55	14.6	20.2	29.4	39.2
Found from F	0.93	1.26	1.98	3.25	4.40	7.50	14.8	20.6	29.8	39.2

mination of molybdenum, but also the area under the two recorder curves (area F). The standard curve for this third evaluation is not shown in Fig. 9, but is somewhat similar to the thermometric standard curve. The area was measured by weighing the cut out paper.

REFERENCES

1 K. B. Yatsimirskii, Kinetic Methods of Analysis, Pergamon Press, Oxford, 1966, p. 1.
2 A. L. Beilby and C. A. Landowski, J. Chem. Educ., 47 (1970) 238.
3 A. M. Gary and J. P. Schwing, Bull. Soc. Chim. France, (1972) 3654.
4 R. Feys, J. Devynck and B. Tremillon, Talanta, 22 (1975) 17.
5 J. H. Wang, J. Am. Chem. Soc., 77 (1955) 4715.
6 H. Weisz, S. Pantel and W. Meiners, Anal. Chim. Acta, 82 (1976) 145.
7 G. Svehla, Analyst (London), 94 (1969) 513.
8 J. Bognar, Mikrochim. Acta, (1968) 455.
9 F. F. Gaal, V. I. Sörös and V. J. Vajgand, Anal. Chim. Acta, 84 (1976) 127.

Analytica Chimica Acta, 90 (1977) 83—89

ACID—BASE EQUILIBRIA IN THE MIXED SOLVENT 80% DIMETHYL SULFOXIDE—20% WATER

Part I. Definition of pH Scale and Determination of pK Values of Aliphatic Monocarboxylic Acids

MILKA GEORGIEVA
Institute of Chemical Technology, Darvenitza, Sofia (Bulgaria)
GEORGI VELINOV and OMORTAG BUDEVSKY
Faculty of Pharmacy, Academy of Medicine, Ekz. Josif 15, Sofia (Bulgaria)
(Received 19th July 1976)

SUMMARY

The acid—base equilibria in the mixed solvent, 80% dimethyl sulfoxide—water, have been investigated by potentiometric measurements with a glass—silver—silver chloride electrode couple. The response of the glass electrode is quick and reproducible over the whole pH scale. The autoprotolysis constant (K_{SH}) of the mixed solvent has been determined; the value obtained, pK_{SH} = 18.40, agrees well with reported data. The pK_a values of the following aliphatic monocarboxylic acids are reported: formic, acetic, propionic, n-butyric, iso-butyric, n-valeric, iso-valeric, capric, pentadecanoic, stearic, monochloroacetic. The mixed solvent offers better titration conditions than water for the determination of these acids.

Dimethyl sulfoxide (DMSO) has recently attracted increasing interest as a medium for acid—base titration, largely because of its excellent ability to dissolve many organic and inorganic substances. Moreover, the length of the pH scale in this solvent is 33.3 units [1]. As the dielectric constant of the solvent is relatively high (45.93 [2]) and many strong acid and strong base titrants are available, it is obvious why the importance of DMSO in analytical practice has increased.

Unfortunately, the behaviour of the pure solvent in some cases restricts the full use of its favourable properties as a medium for acid—base titrations. First, nonaqueous DMSO is very hygroscopic under normal conditions (20°C), the moisture content may attain 10% [3]. Secondly, the use of the potentiometric method with a glass electrode, which is the most widely applied method in nonaqueous solvents, has some restrictions for DMSO. It has been found [4] that the response of commercial glass electrodes at high pH values in pure DMSO becomes extremely slow. Modifications improved the response, but above pH 10, stable readings required 15 min or more. Moreover, silver chloride is significantly soluble

in DMSO [5, 6]. Therefore, the commonest cell for nonaqueous solvents (glass and silver—silver chloride electrodes) is very difficult to use in pure DMSO. However, the silver—silver nitrate reference electrode, as recommended by Kolthoff and Reddy [7], is excellent in pure DMSO. The convenient glass electrode—calomel electrode cell has a slow and sometimes irreproducible response in pure DMSO and even in DMSO—water mixtures [8]. Obviously, work with pure DMSO requires special precautions, which are inconvenient for broad applications.

Accordingly, many authors have turned to studies of acid—base behaviour in DMSO—water mixtures rather than in the pure solvent. Most of the investigations have been concerned with determining autoprotolysis constants for mixtures containing varying amounts of water [9—13] or determining physico-chemical constants such as the dielectric permeability of the mixtures [2], the standard potential of the silver—silver chloride electrode [6, 13], etc.

Analysis of the available data, analogously to Baughman and Kreevoy [9], indicated that the 80% DMSO—20% water mixture has properties which make it of most interest for analytical purposes. The excellent solvating ability of DMSO itself is preserved to a considerable degree; the high dielectric permeability (ca. 65 [2]), the large pH region (18.38 [9]) and the insignificant hygroscopicity are also favourable. The acid—base properties are very different from those of water, but very suitable for acid—base titrations. Furthermore, the potential of the glass—silver—silver chloride electrode couple in 80% DMSO—water is quickly established and is highly reproducible [6, 11—13].

The present series of papers is concerned with a wide investigation of acid—base equilibria in the 80% DMSO—water mixture, to clarify the advantages and the applicability of this mixture for the nonaqueous titration of some acids and bases of different charge type.

The present paper deals with: (i) definition of pH and pOH scale in this mixed solvent, (ii) determination of the dissociation constants of some aliphatic monocarboxylic acids, and (iii) comparison of the analytical properties of the mixture to those of other solvents. The aliphatic monocarboxylic acids are of the zero charge type HA, so that conditions for their titration compared to water are worsened in various widely used nonaqueous media such as alcohols, ketones, dimethylformamide, acetonitrile etc. Since DMSO is more alkaline than water (by 1.5 pH units [4]) and the dielectric permeability of the solvent is comparatively high, titration conditions for the acids mentioned are advantageous compared to those in water.

EXPERIMENTAL

Reagents

Dimethyl sulfoxide (Fluka) was purified as described previously [13]. The 80% DMSO—water mixture was prepared by weight (± 0.01%) with redistilled water. The hydrochloric acid solution and tetraethylammonium hydroxide solutions in the mixed solvent were prepared from aqueous solutions and standardized with diphenylguanidine after mixing. Monochloroacetic, formic, acetic, propionic, n-butyric, iso-butyric, n-valeric, iso-valeric, capric, pentadecanoic and stearic acids (all reagent grade, Merck A. G.) as well as tetraethylammonium bromide (Fluka) were used without further purification.

Measurements

The potentiometric measurements were done in a thermostatted cell (25.0 ± 0.2°C) with liquid junction, consisting of a Radiometer G202B glass electrode and a silver—silver chloride reference electrode. The glass electrode was soaked in the mixed solvent for 15—20 min before use. The junction between the test and reference solutions was J-shaped. The composition of the solvent in the reference compartment was 50% DMSO—water, so as to suppress the solubility of the silver chloride. Constancy of the reference electrode potential was provided by 0.001 M potassium chloride. The test solutions were of constant ionic strength, I = 0.1 (Et_4NBr). The potential of the cell was measured with a Radelkis OP205 pH meter with an accuracy of ±0.5 mV.

RESULTS AND DISCUSSION

Determination of the autoprotolysis constant of the mixed solvent and definition of pH and pOH

The potentiometric measurements were done in a cell with liquid junction (cell I):

GE ⁞⁞ HCl(M_{HCl}), Et_4NOH(M_{Et_4NOH}), 0.1 M Et_4NBr ‖ 0.001 M KCl, AgCl | Ag

The ca. 0.01 M HCl solution was titrated with ca. 0.02 M Et_4NOH. The e.m.f. values of this cell in the acidic and in the alkaline region, respectively, are given by the equations

$$E = E_a^{0'} - k \log \{[HCl]_{tot} - [Et_4NOH]_{tot}\} = E_a^{0'} + k\, pc_H \quad (1)$$

$$E = E_b^{0'} + k \log \{[Et_4NOH]_{tot} - [HCl]_{tot}\} = E_b^{0'} - k\, pc_{OH} \quad (2)$$

where $E_a^{0'}$ and $E_b^{0'}$ are the specific constants of the cell for the acidic and alkaline region, respectively. These constants include the standard potential of the glass electrode, the potential of the reference electrode, activity factors and the liquid junction potentials — $E_{j,a}$ for the acidic region and $E_{j,b}$ for the alkaline region; k = 0.059157 V for 25°C. The autoprotolysis

constant K^c_{SH} was found in the classical way [14]

$$pK^c_{SH} = (E^{0'}_b - E^{0'}_a)/k \quad (3)$$

The equivalence points of the titrations needed for the calculations were determined by Gran plots [15]. The values of the liquid junction potentials were evaluated by the method of Biedermann and Sillén [16]. It was found that the liquid junction potential under the titration conditions (I = 0.1, and pH or pOH not lower than 2) was negligible in both the acidic and alkaline regions. The autoprotolysis constant of the mixed solvent was determined in three experiments as described above. The mean value obtained, pK^T_{SH} = 18.40 ± 0.02, is in good agreement with the reported values of 18.38 [9]. The thermodynamic value of the constant was calculated from the stoichiometric value by the enlarged Debye—Hückel equation $-\log f_\pm = 0.68\, I^{1/2}/(1 + 2.81\, I^{1/2})$.

The possibility of determining the two specific constants of the cell allows the definition of pH and pOH by means of eqns. (1) and (2), respectively. As all measurements were made at a constant ionic strength in terms of concentrations and not activity, the values defined are also in terms of concentration, i.e. pc_H and pc_{OH}.

Determination of pK_{HA} values of aliphatic monocarboxylic acids

The pK values of these acids were determined as described (alternative II) previously [17]. The potentiometric measurements were done in cell I at constant ionic strength I = 0.1 (Et_4NBr). A mixture of a 0.01 M solution of the aliphatic monocarboxylic acid (HA) and 0.01 M hydrochloric acid (HCl) was titrated with ca. 0.02 M tetraethylammonium hydroxide. When this procedure was used, then in every titration the specific constants of the cell in the acidic and alkaline regions as well as the ionic product were constant. These constants are used as a check on the accuracy of the potentiometric measurements in the galvanic cell. The titration data were then used to calculate the pK^c_{HA} values of the weak acid (HA) by means of the Henderson–Hasselbalch equation [18]

$$pK^c_{HA} = pc_H - \log \frac{[A^-] + [H_3O^+] - K^c_{SH}/[H_3O^+]}{[HA] - [H_3O^+] + K^c_{SH}/[H_3O^+]} \quad (4)$$

To check the validity of the method for the mixture in question, the pK values of monochloroacetic and acetic acids were first determined, because of the plentiful available data. The values obtained in the present work, $pK^T_{CH_3COOH}$ = 8.02 and $pK^T_{ClCH_2COOH}$ = 5.77, are in good agreement with the reported data obtained from conductometric and spectrophotometric measurements ($pK^T_{CH_3COOH}$ = 8.00 [9, 19] and $pK^T_{Cl_2CH_2COOH}$ = 5.69 [9]). Figure 1 shows some typical titration curves. The pK^T_{HA} values for all the aliphatic monocarboxylic acids examined here are given in Table 1. It can be seen that the decrease in the strength of the acids, depending on the number of carbon atoms present in the molecule, is similar to that in

TABLE 1

The pK values obtained for aliphatic monocarboxylic acids in 80% DMSO—20% water

Acid	Number of C atoms	pK^T_{HA}	$pK^T_{HA(H_2O)}$	ΔpK
Formic	1	6.46	3.75	2.71
Acetic	2	8.02	4.76	3.26
Propionic	3	8.40	4.87	3.53
n-Butyric	4	8.48	4.82	3.66
iso-Butyric	4	8.57	4.86	3.71
n-Valeric	5	8.53	4.86	3.67
iso-Valeric	5	8.57	4.78	3.79
Capric	10	8.57	—	—
Pentadecanoic	15	8.68	—	—
Stearic	18	8.73	—	—
Monochloroacetic		5.77	2.87	2.90

water, and that the change in pK_{HA} after C_4—C_5 is negligible. From column 5 it can be seen that $\Delta pK = pK^T_{HA(mixture)} - pK^T_{HA(H_2O)}$ tends to be constant (ca. 3.7), from which with some approximation the $pK^T_{HA(H_2O)}$ values of capric (C_{10}), pentadecanoic (C_{15}) and stearic (C_{18}) acids can be calculated.

If the mean value 3.5 is taken as an average by which the mixed solvent weakens the strength of acids of this charge type, HA, then it is easy to show that the proposed mixture is very suitable, and advantageous compared to water, for the titration of these acids. In fact, the length of the pH scale of the mixture is 18.40 pH units (or longer by 4.4 pH units than for water) whereas the loss from the weakening of these acids is 3.5 pK_{HA} units. Consequently, ca. 1 pH unit is gained in the lengthening of the equivalence part of the titration curve.

Figure 2 shows the theoretical titration curve for 0.01 M acetic acid in 80% DMSO—water. The curve was constructed by a graphical method [20] from equilibria data determined in the present investigation. As can be seen, there is very good coincidence between the theoretical curve (the full line) and the experimental points; the theoretical curve was constructed without taking into account the dilution effect, hence there is some deviation in the alkaline region. The data in Fig. 2 prove that the graphical method for construction of titration curves is successful in nonaqueous media. It is clear that acetic acid is better titrated in the mixture than in water, because of the lengthened equivalence part of the titration curve. Because of this advantage and the excellent solvating ability of DMSO, the 80% DMSO—water mixture is obviously very suitable for the titration of weak acids of this charge type, especially when they are sparingly soluble and too weak in water. It must be emphasized that even when solvents with basic properties are used, e.g. dimethylformamide or acetonitrile, the titration conditions for acids of this type are always worse than in aqueous medium.

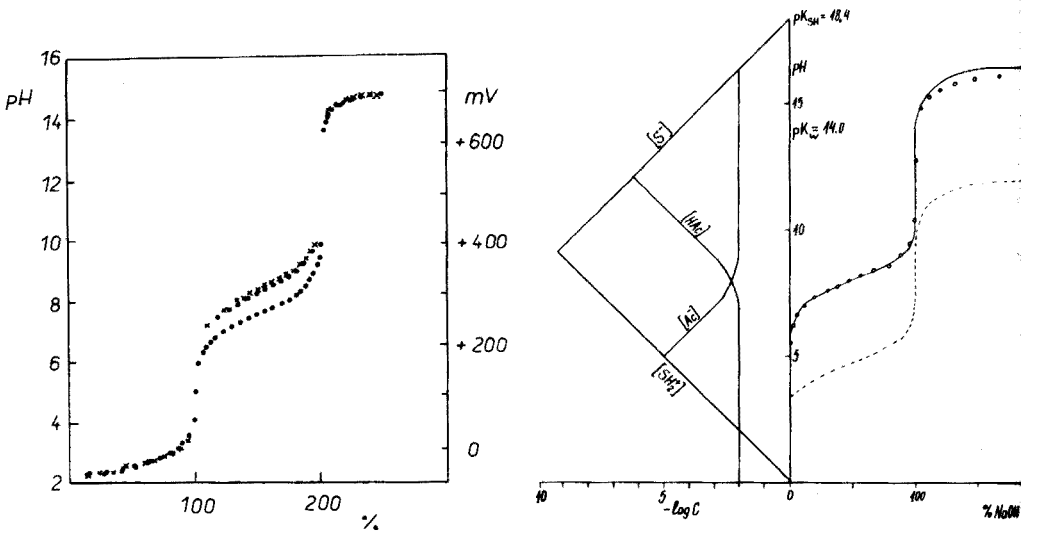

Fig. 1. Titrations of acetic, capric and pentadecanoic acids. ○ C_2. • C_{10}. × C_{15}.

Fig. 2. Theoretical curves for titrations of 0.01 M acetic acid in mixture 80% DMSO—water (———) and in water (·····). The points show the experimental data.

From the acid dissociation constants and the autoprotolysis constant obtained, the base constant of the conjugated base, i.e. charge type A^-, can be calculated easily. Calculations showed that the strength of these bases was weakened by ca. 1 pK unit compared to the values in water. Consequently, the titration conditions for such bases are improved by 5—5.5 pH units because of the extended equivalence part of the titration curve. This advantage is of minor importance, however, because many other nonaqueous solvents also improve the situation for these bases.

In conclusion, the mixture investigated — 80% DMSO—water — has considerable advantages over many nonaqueous solvents and water in the titrimetric determination of protolytes, and especially for the determination of aliphatic monocarboxylic acids which are insoluble in water.

REFERENCES

1 J. Courtot-Coupez and M. Le Démezét, Bull. Soc. Chim. Fr., (1969) 1033.
2 E. Tommila and A. Paunen, Soumen Kemistil., B 41 (1968) 172.
3 J. A. Riddick and W. B. Bunger, Techniques of Chemistry, Vol. II, Organic Solvents, Wiley-Interscience, New York, 1970.
4 C. D. Ritchie and R. E. Uschold, J. Amer. Chem. Soc., 89 (1967) 1721.
5 D. C. Luehrs, R. T. Iwamoto and J. Kleinberg, Inorg. Chem., 5 (1966) 201.
6 K. H. Khoo, J. Chem. Soc. (A), (1971) 2932.
7 I. M. Kolthoff and T. B. Reddy, Inorg. Chem., 1 (1962) 189.
8 T. B. Reddy, Ph.D. Thesis, University of Minnesota, 1960.
9 E. H. Baughman and M. M. Kreevoy, J. Phys. Chem., 18 (1974) 421.
10 J. C. Hallé, R. Gaboriaud and R. Schaal, Bull. Soc. Chim. Fr., (1969) 1851.

11 P. Fiordiponti, F. Rallo and F. Rodante, Z. Phys. Chem. Neue Folge, 88 (1974) 149.
12 E. M. Wooley, Anal. Chem., 44 (1972) 1520.
13 P. Longhi, T. Mussini and M. Veleva, Anal. Quim., 71 (1975) 1043.
14 D. Dyrssen, Sven. Kem. Tidskr., 64 (1952) 213.
15 F. J. C. Rossotti and H. Rossotti, J. Chem. Educ., 42 (1965) 377.
16 G. Biedermann and L. G. Sillén, Ark. Kem., 5 (1953) 425.
17 J. Tencheva, G. Velinov and O. Budevsky, J. Electroanal. Chem. Interfacial Electrochem., 68 (1976) 65.
18 A. Albert and E. P. Serjeant, Ionization Constants of Acids and Bases, J. Wiley, New York, 1962.
19 J. P. Morel, Bull. Soc. Chim. Fr., (1967) 1406.
20 O. Budevsky, Graphic Method for Construction of Titration Curves, in Essays on Analytical Chemistry, Ringbom's memorial volume, Pergamon Press, in press.

Analytica Chimica Acta, 90 (1977) 91—102

THE DETERMINATION OF LEAD, COPPER AND CADMIUM BY ANODIC STRIPPING VOLTAMMETRY AT A MERCURY THIN-FILM ELECTRODE

M. J. PINCHIN and J. NEWHAM

Department of Chemistry, Newcastle upon Tyne Polytechnic, Newcastle upon Tyne NE1 8ST (England)

(Received 25th October 1976)

SUMMARY

The determination of lead, copper and cadmium by anodic stripping voltammetry at a wax-impregnated graphite electrode, pre-plated with mercury, has been investigated. Electrode preparation and cell design are discussed, and the effects of mercury loading and sample pH on electrode sensitivity are described. Detection limits and precision on aqueous samples are reported. Calibration graphs are linear for lead and cadmium, but non-linear for low concentrations of copper. The depression of peak current and shift of peak potential for copper in chloride media are described and an explanation is proposed. Precision and recovery of metal additions are reported for digested samples of whole blood.

Anodic stripping voltammetry (a.s.v.) at a mercury thin-film electrode is well established for sensitive determinations of various metals, some of which, such as lead and cadmium, are of considerable medical and environmental interest. The theory and applications of the technique have been reviewed [1, 2].

The mercury film may be codeposited in situ with the analyte metal, or may be pre-formed and re-used throughout a series of determinations: despite the inherent simplicity of the latter method, most literature reports have been concerned with the in situ approach. This paper describes the use of a pre-formed film with linear voltage scanning for determinations of copper, lead and cadmium. For lead and cadmium, the reproducibility was comparable with literature values for the in situ method [3], even though less stringent timing and electrode conditioning procedures were required. In contrast, the behaviour of copper was generally less reproducible and markedly influenced by the presence of chloride ion.

EXPERIMENTAL

Apparatus

All experiments were done with a Wenking TR61 potentiostat mechanically modified to permit linear anodic scanning. Current—time curves were recorded on a Bryans 26000 A3 flat-bed recorder. To prepare the working

electrodes, graphite rods (6.15 or 4.56 mm diameter, 100—120 mm long) were impregnated under vacuum with molten ceresin wax. After cooling, the wax was removed from a suitable length of the side — leaving the tip sealed — and the exposed graphite was polished with silicon carbide and filter papers. Inactive surfaces were insulated with Teflon tape.

The working electrode, a platinum counter electrode and a silver/silver chloride reference electrode fitted into a nylon cell head, together with nitrogen inlet and outlet tubes. Both counter and reference electrodes were usually isolated in compartments containing 0.1 M sodium chloride by porous Vycor plugs (Corning glass). All potentials are quoted against the Ag/AgCl electrode (0.1 M NaCl). Sample solutions were analysed in interchangeable 90 × 19 mm glass tubes.

Reagents

Aqueous standards were prepared from the appropriate metal salts; working standards acidified to pH 2 were prepared by dilution every few days. Supporting electrolytes were purified by electrolysis over a mercury pool cathode. Acids used in micro digestions were BDH Aristar grade.

Mercury plating procedure

Introduce a volume of mercury(II) solution from a micropipette into the cell, sufficient to give the desired electrode loading (generally $8 \cdot 10^{-7}$ mol cm^{-2}), and add further reagents to give a final solution (5 ml) of pH 5.5, 0.18 M in sodium acetate and 0.1 M in sodium chloride. Plate the mercury on to the active surface of the working electrode at a potential of −1.0 V, while bubbling oxygen-free nitrogen through the solution to promote deoxygenation and stirring. At the end of the plating period scan the potential to −0.04 V to remove electroactive metals from the film; the working electrode is then ready for use.

General analytical procedure

Adjust the sample solution to a final volume of 5 ml and pH 5.5, in either 0.18 M sodium acetate or 0.18 M sodium acetate — 0.1 M sodium chloride buffer. Place the cell on the electrode assembly, turn on the nitrogen stream and apply the initial potential (−1.0 V for the determination of lead, cadmium and copper) to the working electrode for the standard plating period (15—30 min); 30 s before the end of this period redirect the nitrogen stream over the surface of the sample. Scan the potential anodically at 40 mV s^{-1} and record the current peaks. Terminate the scan when the copper peak has been recorded. Wash the electrode system with distilled water between runs.

Procedure for blood

Add 100 μl of whole blood sample to 200 μl of 61% perchloric acid in individual analytical tubes, and digest at 200°C for 1.5—2 h. Adjust the digest to a final volume of 5 ml at pH 5, containing 0.9 M sodium acetate — 0.1 M sodium chloride. Continue as for the general procedure, and run blanks and standards in buffer plus 200 μl of perchloric acid.

RESULTS AND DISCUSSION

Electrode characteristics and cell design

Preliminary studies of graphite electrodes impregnated with paraffin, carnauba or ceresin wax showed ceresin to be the most satisfactory. One ceresin electrode was used, with occasional repolishing, for more than 2000 scans over a period of 18 months.

Electrode response was dependent on mercury loading for copper and cadmium (Fig. 1). Maximum response for cadmium was found in a fairly narrow band ($6 \cdot 10^{-7}$—$1.5 \cdot 10^{-6}$ mol cm^{-2}). Below this range a marked decrease in sensitivity was observed, invariably accompanied by a chemical memory of the metal, probably because of preferential plating of cadmium on to bare graphite [3]. At high mercury loadings a less severe decrease was found, which may have the same underlying cause, the bare sites being produced in this case by coalescence of mercury droplets. This explanation would also account for the lowered response to cadmium that often followed overnight disuse. Copper showed highest response at the lowest loadings, but this was accompanied by a chemical memory and poorer reproducibility; over the whole loading range, the reproducibility was worst for copper.

When the cell was used with a large electrode (1—4 cm^2) and small sample volume (5 ml), nitrogen stirring gave good sensitivity in a reasonable time (15—30 min) for the working range 1—100 ng. Once the graphite was covered with mercury, no problems arose from adherence of gas bubbles. Peak current reproducibility was good even with 5-min deposition periods, both for turbulent

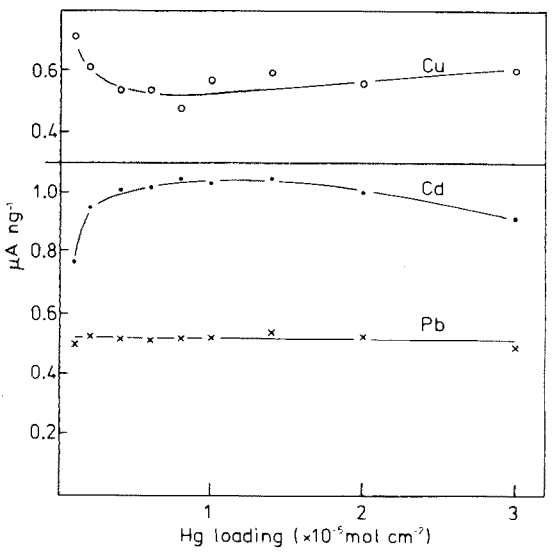

Fig. 1. Variation in electrode response to Cd, Pb and Cu with Hg loading. 3-cm^2 electrode, 15-min plate at −1.0 V, 40 mV s^{-1} scan rate, 0.18 M acetate—0.1 M NaCl pH 5.5, 5-ml sample. Data obtained on 100 ng of each metal. Each point is the mean of seven or nine runs.

flow conditions produced by directing the nitrogen stream under the tip of the electrode, and for laminar flow produced by directing the gas stream to one side of the tip.

Effect of pH

No optimum pH value for the determination of all three metals, such as that found by other workers [4], was identified. In fact, variation was small in the range 3.9—6, and a significant fall in lead and copper response occurred only above pH 6.0. Most of the determinations were done at pH 5.0—5.5 in 0.18—0.9 M sodium acetate buffer.

Precision and limit of detection

The precision obtained for successive aqueous samples with a freshly polished electrode is shown in Table 1. In general, relative standard deviations for cadmium and lead at the 100-ng level were in the range 1—3%, and for copper, 2—5%: these values compare well with published figures for lead by the in situ plating method [3]. Other precision values are given in Tables 2 and 4.

Peak heights sometimes showed a progressive rise or fall, both with repeats on successive portions of the same solution and more frequently with repeats on one sample. In the former repeat mode, repolishing the electrode corrected the tendency. Such behaviour was most commonly found with copper.

Under the best conditions of reagent purity and electrode performance, 0.1 ng of cadmium and 0.2 ng of lead (0.02 and 0.04 p.p.b. in solution) could be quantified. Copper at very low levels (20 ng) presented certain difficulties which will be referred to later.

Calibration graphs

In simultaneous determinations, cadmium and lead showed good linearity of peak height vs. ng of metal in the cell up to 400 ng for a 5-ml sample, with a 1—4 cm^2 electrode and mercury loading exceeding $5 \cdot 10^{-7}$ mol cm^{-2}. Figure 2 shows calibration graphs for the range 0—100 ng in 0.18 M sodium acetate (pH 5.5): linearity was also found for 0.18 M sodium acetate—0.1 M sodium chloride (pH 5.5), 0.1 M sodium chloride (pH 5.5), and 0.9 M sodium

TABLE 1

Reproducibility of peak current in the analysis of successive aliquots of aqueous standard (3-cm^2 electrode, $8 \cdot 10^{-7}$ mol Hg cm^{-2}, 15-min plating at −1.0 V, 40 mV s^{-1} scan rate, 0.18 M acetate—0.1 M NaCl, 5-ml sample, 100 ng of each metal.)

Metal ion	Cd	Pb	Cu
Mean peak height (μA) (n = 9)	104.73	52.04	46.93
R.s.d. (%)	0.84	1.82	1.16

acetate—0.1 M sodium chloride—perchloric acid (blood analysis matrix). In contrast, in all media, copper showed a small curved portion to the calibration line at low levels (Fig. 2) such that the regression line of peak height upon ng of metal intercepted the x-axis on the positive side of the axes origin. The value of the x-intercept varied from 5—15 ng but was generally lower in the 0.9 M acetate medium and for freshly polished electrodes. When calibration standards were run in random order, this effect could be masked by a copper memory, and an apparently linear calibration obtained. In addition, response to copper was reduced by ca. 50% in the presence of 0.1 M chloride—acetate compared to acetate buffer alone. Reduction of the chloride concentration to 0.01 M led to a severely curved calibration line; lead and cadmium remained linear (Fig. 3).

The low-level curvature of the copper calibration cannot be explained by a simple chemical memory effect. The curvature remained when post-calibration blanks and/or immediate rescanning of the potential showed that negligible oxidizable copper was left on the electrode. It was also present in acetate—chloride media, in sodium chloride alone, and when unisolated reference and counter electrodes were employed.

Cadmium and lead do not show a chloride depression. Of the three copper is by far the least soluble in mercury. For the normal electrode load used ($24 \cdot 10^{-7}$ mol in total), the amount of copper in true solution would be only 10—15 ng [5]; this certainly corresponds to the non-linear calibration region.

Effect of chloride on peak potential, peak current and peak half-width

The effect of chloride on the peak current (i_p), the peak potential (E_p) and width at half-height ($b_{\frac{1}{2}}$) for all three metals was investigated at 20°C in

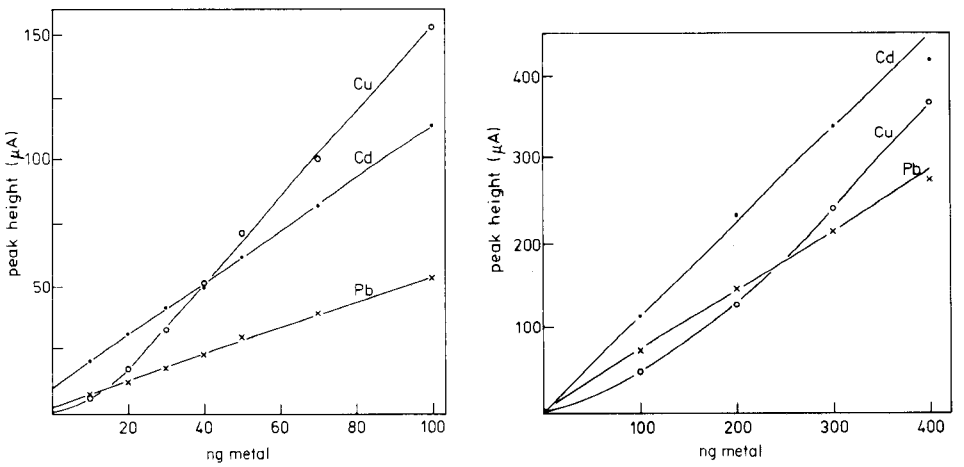

Fig. 2. Calibration lines for Cd, Pb and Cu. 0.18 M acetate pH 5.5, $8 \cdot 10^{-7}$ mol Hg cm^{-2}. Other parameters as for Fig. 1. The y-intercepts represent the blank readings.

Fig. 3. Calibration lines for Cd, Pb and Cu. 0.18 M acetate—0.01 M NaCl pH 5.5, $8 \cdot 10^{-7}$ mol Hg cm^{-2}, 30-min plate. Other parameters as for Fig. 1.

simultaneous determinations at two levels. These are designated 'low' (Table 2, a) and 'high' (Table 2, b) for convenience. The inequalities in the levels of each metal arise from the presence of measurable quantities in the acetate buffer employed. Values at each chloride concentration are from a single run and lead peak currents are corrected for addition of a small amount of metal with the purified chloride stock medium: the medium was free of measurable amounts of cadmium and copper. Experiments at each level were performed on consecutive days and with the same electrode, but with separately prepared mercury plates.

TABLE 2

Effect of chloride concentration on i_p, $b_{\frac{1}{2}}$ and E_p for cadmium, lead and copper in simultaneous determination at (a) 'low level' and (b) 'high level'
(3-cm² electrode, $8 \cdot 10^{-7}$ mol Hg cm^{-2}, 30-min plate at −1.0 V, 40 mV s^{-1} scan rate, 0.18 M acetate buffer pH 5.5, 5-ml sample.)

[Cl⁻][a]	Cd			Pb			Cu		
	i_p (μA)	E_p (mV)	$b_{\frac{1}{2}}$ (mV)	i_p (μA)	E_p (mV)	$b_{\frac{1}{2}}$ (mV)	i_p (μA)	E_p (mV)	$b_{\frac{1}{2}}$ (mV)
(a) 20.5 ng Cd, 32.0 ng Pb, 26.3 ng Cu									
0	25.0	−671	51	19.5	−514	51	55.5	−96	52
0.002	24.6	−675	52	19.4	−514	51	39.6	−112	65
0.004	25.2	−674	50	19.5	−516	50	32.1	−123	69
0.006	24.6	−676	52	19.4	−517	51	28.3	−137	69
0.01	25.0	−679	52	20.4	−517	50	30.7	−144	63
0.02	24.3	−677	51	19.7	−517	50	29.6	−168	60
0.04	24.9	−680	50	19.6	−518	49	31.7	−190	63
0.1	25.1	−692	50	19.9	−525	48	37.3	−220	61
0.2	25.1	−693	50	20.5	−525	48	36.5	−244	59
Mean	24.87			19.77					
s_r	1.21			2.12					
(b) 100.5 ng Cd, 112.0 ng Pb, 106.3 ng Cu									
0	121.1	−676	51	69.2	−514	49	239.0	−73	40
0.001	123.4	−671	50	69.7	−513	49	223.6	−78	41
0.002	123.0	−676	51	69.2	−516	50	215.8	−84	43
0.004	121.5	−675	50	70.0	−513	49	197.2	−84	44
0.006	122.9	−682	50	68.8	−521	48	169.4	−96	48
0.01	123.2	−684	50	68.9	−523	49	132.6	−107	57
0.015	121.1	−680	51	70.0	−521	49	110.6	−114	61
0.02	124.7	−679	50	69.5	−521	49	97.6	−125	59
0.04	122.7	−682	51	69.1	−519	49	89.2	−145	56
0.1	131.2	−683	50	71.1	−519	48	98.8	−178	60
0.2	125.7	−692	50	71.4	−524	48	106.6	−210	59
Mean	123.68			69.72					
s_r	2.3			1.23					

[a]Nominal concentration. Correction factor = 1.0702.

Lead and cadmium. Both i_p and $b_{\frac{1}{2}}$ were little affected by change in chloride concentration, but $b_{\frac{1}{2}}$ was higher than the value predicted by de Vries and van Dalen [6] for very small values of the film thickness (ca. 38 mV): this did not markedly affect resolution.

Peak potentials were shifted cathodically by ca. 20 mV for cadmium and ca. 10 mV for lead at the highest chloride concentrations. This may be understood from the equation [6] relating E_p to the polarographic half-wave potential ($E_{\frac{1}{2}}$)

$$n(E_p - E_{\frac{1}{2}}) = -1.43 + 29.58 \log (l^2 \nu nF R^{-1} T^{-1} D_R^{-1}) \quad (1)$$

where l = film thickness (cm), ν = scan rate (V s^{-1}), D_R = diffusion coefficient of metal in mercury (cm^2 s^{-1}), and potentials are in mV. For both metals, $E_{\frac{1}{2}}$ is shifted cathodically with increase in chloride concentration from 0.1 to 1 M [7]. If a similar shift may be supposed at the concentrations used here, then E_p must also be so shifted.

Peak potentials for cadmium and lead in acetate—0.1 M chloride, generated from eqn. (1), were −709 mV and −505 mV, respectively, which compare well with the values in Table 2. The film thickness used, $8.77 \cdot 10^{-6}$ cm, was the mean value obtained by substitution of the mean peak currents for the two metals in Table 2a into the equation [6]

$$i_p = 1.1157 \cdot 10^6 n^2 A C_m l\nu \quad (2)$$

where i_p = peak height (A), A = electrode area (cm^2), and C_m = concentration of metal in mercury (mol cm^{-3}). The plating time of 30 min allowed virtually total deposition of the metals. Values for $E_{\frac{1}{2}}$ and D_R were taken from the literature [7, 8], those for $E_{\frac{1}{2}}$ being the values in chloride alone.

Copper. In acetate buffer alone, peaks were sharp and symmetrical (Fig. 4). Both $b_{\frac{1}{2}}$ and i_p were consistent with the direct production of copper(II); with the previously calculated l value, eqn. (2) gave a value for n of 2.01. A similar procedure for the data in Table 2b gave n = 2.07.

Since eqn. (1) contains no concentration terms, the anodic shift of E_p in acetate alone for copper 'high' level compared to 'low' level (Table 2) must be explained by assuming that the activity of copper in the mercury film did not change between the two levels, i.e. the film was saturated in both cases and a solid phase was present. Under such conditions the potential of the copper amalgam electrode should be constant over a wide range of the copper : mercury ratio [9]. The shift in peak potential is then given, independently of ν and l, by

$$E_{p1} - E_{p2} = \frac{RT}{2F} \ln \frac{[Cu^{2+}]_1}{[Cu^{2+}]_2} \quad (3)$$

where subscripts 1 and 2 refer to 'high' and 'low' levels, respectively. The simple ratio of copper in the initial solutions may be used. For the above case, the calculated value of $E_{p1} - E_{p2}$ was +17.6 mV. The observed value was +23.5 mV.

In the presence of chloride, the copper peaks became asymmetrical with the steeper slope on the anodic side (Fig. 4). A distinct shoulder was often observed on the cathodic side and, more rarely, peak splitting. The width at half-height was increased, but did not reach the ca. 75 mV required for a 1e reaction. Such asymmetry and increase of $b_{\frac{1}{2}}$ are clearly visible in published voltammograms [10, 11] but have rarely elicited comment.

E_p showed a progressive cathodic shift with increasing chloride concentration and i_p dropped steadily to a minimum value but increased again at the highest chloride concentrations, particularly at the 'high' copper level (Table 2). The presence of a minimum explains the curved calibration line in 0.01 M chloride (Fig. 3). The reduction of i_p is not due to the formation of a non-labile complex in the chloride electrolyte, as the half-time for total plating is not lengthened.

The electrode equations [6] predict that i_p for a 1e reaction should be one quarter of that for an equimolar 2e reaction, and that $b_{\frac{1}{2}}$ for the former should be twice that of the latter. Since the depression reaches only ca. 50% and $b_{\frac{1}{2}}$ does not become double the value found in chloride-free media, the

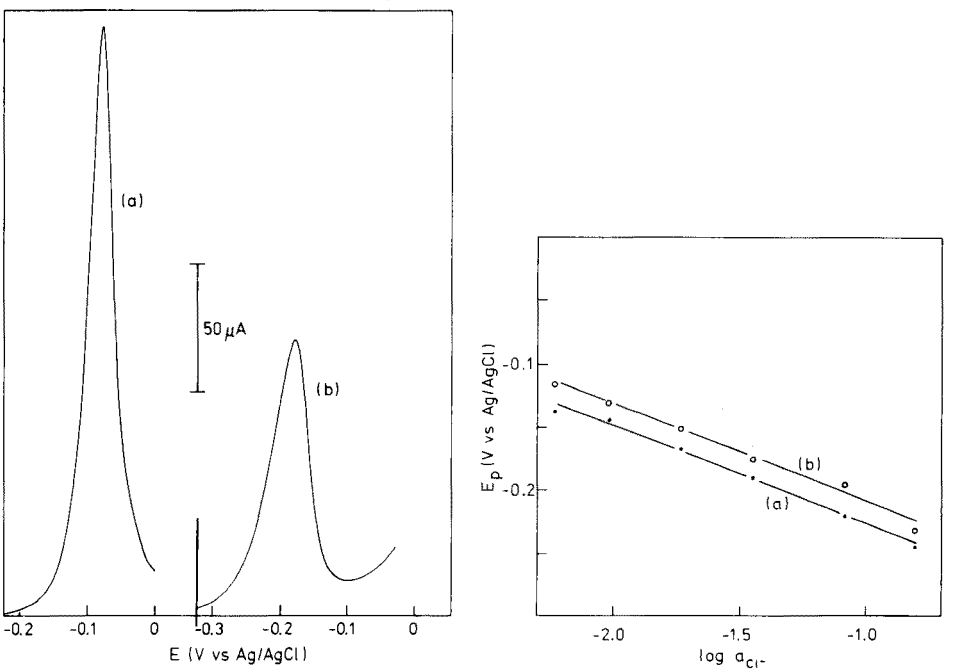

Fig. 4. Stripping waves for copper in (a) 0.18 M acetate pH 5.5 (b) 0.18 M acetate—0.1 M NaCl pH 5.5. $8 \cdot 10^{-7}$ mol Hg cm^{-2}, 30-min plate. Other parameters as for Fig. 1. Each wave represents 106.3 ng Cu.

Fig. 5. Variation of E_p for Cu with log a_{Cl}. (a) Data from Table 2a. (b) Duplicate determinati Analytical details as in Table 2. The lines drawn are the calculated regression lines.

dissolution of copper in the presence of chloride must involve two reactions which are not resolvable at the MTFE. The peak shapes suggest that these must be a 1e reaction on the cathodic side and a 2e reaction on the anodic. From the known dissolution behaviour of copper metal in chloride media of less than 1 M [12, 13], the 1e reaction must be $Cu + 2Cl^- \rightarrow CuCl_2^- + e$. In addition, some oxidation to copper(II) must occur at a similar potential. Thus n has a non-integral composite value which varies according to the extent of each reaction.

The information in Table 2a gives two ways of calculating the net number of electrons involved in the copper dissolution wave in acetate—chloride medium with ca. 26 ng of copper in the cell. At constant copper concentration in mercury and constant i_p, the amount of dichlorocuprate(I) formed must also be constant. For the information in Table 2a, the first condition applies exactly for all chloride concentrations and the second applies approximately for the six highest chloride concentrations: the variation in i_p is ±12.5% of the mean of the six over the chloride range 0.006—0.2 M. If the copper dissolution peak is treated as being solely due to formation of dichlorocuprate(I), the Nernst equation may be written

$$E_p = -4.606 \frac{RT}{nF} \log [Cl^-] + 2.303 \frac{RT}{nF} \log K + E^0 \qquad (4)$$

where K is a constant and $[Cl^-]$ may be taken as the activity in the bulk solution.

Figure 5 shows the plot of E_p vs. $\log a_{Cl^-}$ for the six points mentioned and a duplicate determination with a separately prepared plate. A correction for volume reduction during nitrogen stirring and alteration in concentration of the stock chloride solution during pre-purification was applied. Activity coefficients were obtained from the literature [14]. A slope of −0.0773 V gives n as 1.50.

In the alternative approach, the total peak current may be taken, as a first approximation, as the sum of the copper(I) and copper(II) currents. The mean i_p for the six points was substituted into eqn. (2) together with the mean value for l calculated from the cadmium and lead peaks, giving n to be 1.54. The agreement is reasonable.

At a constant chloride concentration which is high enough for the composite value of n to be also constant, the peak potential should not shift with change in copper concentration if eqn. (1) is obeyed; but a shift does occur above 20 ng of copper in the cell (Table 3). The experimental conditions allowed ca. 75% plating, and the absence of a shift between 10 and 20 ng reflects the presence of the plated copper in true solution. Above 20 ng a solid phase would appear and the potential of the amalgam electrode become constant. The peak potential would then be controlled solely by the aqueous copper concentration. The shift, as shown in Table 3, would be anodic with increasing copper concentration. The de Vries—van Dalen and Roe—Toni equations [6, 15] for E_p are not obeyed for copper when the solubility in the mercury film is exceeded, as both require the absence of a solid phase.

TABLE 3

Variation of E_p and $b_{\frac{1}{2}}$ for cadmium, lead and copper with amounts of metals added to cell, at constant chloride concentration
(3 cm^2 electrode, $8 \cdot 10^{-7}$ mol Hg cm^{-2}, 15-min plate at −1.0 V, 40 mV s^{-1} scan rate, 0.18 M acetate—0.1 M NaCl pH 5.5, 5-ml sample, 20° C, simultaneous determination of the three metals.)

Metal[a] in cell (ng)	Cd		Pb		Cu	
	E_p (mV)	$b_{\frac{1}{2}}$ (mV)	E_p (mV)	$b_{\frac{1}{2}}$ (mV)	E_p (mV)	$b_{\frac{1}{2}}$ (mV)
10	−664	51	−499	46	−221	68
20	−667	50	−503	47	−222	70
50	−663	50	−500	47	−196	64
100	−667	49	−505	47	−184	57
200	−670	50	−512	46	−175	58
300	−671	53	−511	48	−155	60
400	−664	55	−504	49	−138	60

[a] Amount added over blank. Blank reading = 0.3 ng Cd, 3.7 ng Pb, 3.0 ng Cu.

One further piece of evidence arises from the second Roe—Toni equation [15], which relates peak potential to formal potential under the condition of maintained stirring during stripping. If all factors except ν are constant, this equation becomes

$$E_p = 2.303 \frac{RT}{nF} \log \nu + k \qquad (5)$$

where k is a constant incorporating E^0 and all other terms, and potentials are in V. Thus the slope of a plot of E_p vs. log ν for a metal such as cadmium ($n = 2$) would be less than that of a similar plot for copper if n were <2 for this metal. This can be seen in a figure published by Lund and Salberg [11].

The difficulties encountered with copper did not preclude successful analyses. It was necessary to ensure that any chloride naturally present in samples was swamped to at least 0.1 M and to make regular checks on repeatability, linearity of response and chemical memory. These were best done in simultaneous determination of all three metals as copper disturbances could be present independently.

Analysis of blood

Our principal use for thin-film a.s.v. is the determination of cadmium, lead and copper in whole blood. The precision and % recovery of spiked samples were studied as follows. Aliquots of aqueous standard containing 50 ng each of cadmium, lead and copper were added to 200 µl of perchloric acid in individual cells and taken through the digestion procedure; calibration was done with separately prepared standards. Secondly, 100-µl samples of whole blood of unknown metal content were digested and analysed. Finally,

100-μl samples of the same blood spiked with 50 ng each of cadmium, lead and copper were analysed by the same procedure, against fresh standards. The results are presented in Table 4.

The best accuracy and precision were obtained with standards run in buffer and perchloric acid: subjection of aqueous standards or spiked blood to the entire digestion procedure is unnecessary. Samples run in acetate buffer alone showed highly irreproducible copper peaks; swamping of the blood chloride to at least 0.1 M was essential.

TABLE 4

Analysis of known standards and spiked blood samples for cadmium, lead and copper (3 cm^2 electrode, 8 · 10^{-7} mol Hg cm^{-2}, 15-min plate at −1.0 V, 40 mV s^{-1} scan rate, 0.9 M acetate buffer, 0.1 M NaCl, 5-ml sample.)

	Known standard (50 ng each Cd, Pb, Cu)	Unknown blood (100 μl)	Spiked blood (100 μl Unknown + 50 ng each Cd, Pb, Cu)
Cadmium			
Mean ng found[a]	49.4	1.3	51.4
s_r (%)	2.8	9.0	1.6
Mean recovery (%)	98.8	—	100.2
Lead			
Mean ng found[a]	50.4	28.5	78.1
s_r (%)	1.7	2.6	3.4
Mean recovery (%)	100.8	—	99.2
Copper			
Mean ng found[a]	49.3	127.7	172.6
s_r (%)	5.7	2.0	2.3
Mean recovery (%)	98.6	—	89.8

[a]Mean of 8 determinations.

REFERENCES

1 T. R. Copeland and R. K. Skogerboe, Anal. Chem., 46 (1974) 1257A.
2 W. D. Ellis, J. Chem. Educ., 50 (1973) A131.
3 G. E. Batley and T. M. Florence, J. Electroanal. Chem. Interfacial Electrochem., 55 (1974) 23.
4 V. H. Lewin and M. J. Rowell, Effluent Water Treat. J., 13 (1973) 273.
5 M. Hansen, Constitution of Binary Alloys, McGraw-Hill, New York, 2nd edn., 1958, p. 588.
6 W. T. de Vries and E. van Dalen, J. Electroanal. Chem. Interfacial Electrochem., 14 (1967) 315.
7 G. W. C. Milner, The Principles and Applications of Polarography and other Electroanalytical Processes, Longmans, London, 1957. pp. 204, 228.
8 A. Baranski, S. Fitak and Z. Galus, J. Electroanal. Chem. Interfacial Electrochem., 60 (1975) 175.

9 S. Ahrland and J. Rawsthorne, Acta Chem. Scand., 24 (1970) 157.
10 W. R. Matson, D. K. Roe and D. E. Carritt, Anal. Chem., 37 (1965) 1594.
11 W. Lund and M. Salberg, Anal. Chim. Acta, 76 (1975) 131.
12 T. Hurlen, Acta Chem. Scand., 15 (1961) 1231.
13 A. L. Bacarella and J. C. Griess, J. Electrochem. Soc., 120 (1973) 459.
14 R. Parsons, Handbook of Electrochemical Constants, Butterworths, London, 1959, p. 24.
15 D. K. Roe and J. E. A. Toni, Anal. Chem., 37 (1965) 1503.

Analytica Chimica Acta, 90 (1977) 103—110

CONTRIBUTION À L'ÉLECTROCHIMIE DES THIOLS ET DISULFURES PARTIE VI. POLAROGRAPHIES d.c., a.c. ET IMPULSIONNELLE DIFFÉRENTIELLE DE LA CYSTÉAMINE ET DE LA CYSTAMINE

C. A. MAIRESSE-DUCARMOIS, J. L. VANDENBALCK et G. J. PATRIARCHE

Institut de Pharmacie, Université libre de Bruxelles, Campus Plaine C.P. 205/1, Boulevard du Triomphe, B-1050 Bruxelles (Belgique)

(Reçu le 30 septembre 1976)

RÉSUMÉ

L'étude électrochimique de la cystéamine et de la cystamine est réalisée par les polarographies d.c., a.c. et p.p. Les modifications observées, lors de l'étude en fonction du pH et de la concentration, ont permis de mettre en évidence des phénomènes d'adsorption et de montrer que les vagues anodique de la cystéamine et cathodique de la cystamine répondaient aux critères d'un courant de diffusion. L'analyse logarithmique des ondes polarographiques en fonction du potentiel met en évidence deux mécanismes de réaction d'électrode. La séparation du mélange de ces deux composés est réalisable et il est encore possible de déterminer 6 mg l^{-1} de chlorhydrate de cystéamine en présence de 11 mg l^{-1} de dichlorhydrate de cystamine. En d.p.p., les limites de détection sont respectivement de $5 \cdot 10^{-7}$ M et $1 \cdot 10^{-6}$ M pour le thiol et le disulfure. D'une manière générale, le comportement polarographique du système cystamine—cystéamine ressemble en certains points à celui décrit antérieurement pour le couple cystéine—cystine.

SUMMARY

The electrochemical behaviour of the cysteamine—cystamine system was investigated by the d.c., a.c. and d.p.p. techniques, as functions of concentration and pH. Adsorption phenomena were observed, and the cysteamine anodic and the cystamine cathodic waves were found to be diffusion-controlled. Separation of these two sulfur amino acids was achieved; 6 mg l^{-1} of cysteamine HCl can be determined in the presence of 11 mg l^{-1} of cystamine dihydrochloride. Detection limits are $5 \cdot 10^{-7}$ M for cysteamine and $1 \cdot 10^{-6}$ M for cystamine; as little as 0.012 mg of the thiol and 0.23 mg of the disulfide per litre can be determined. The polarographic behaviour of the cystamine—cysteamine system resembles that described previously for the cysteine— cystine system.

Dans le cadre d'une étude électrochimique des acides aminés soufrés d'intérêts pharmaceutique et biochimique [1] nous envisageons ici le comportement polarographique de la cystéamine et de son disulfure la cystamine. Les voies de formation biochimique de la cystéamine et de la cystamine à partir de la cystéine et de la cystine ne sont pas encore bien élucidées et plusieurs mécanismes ont été proposés jusqu'ici. Novelli et al. [2] ont toutefois prouvé que la pantethéine ou la phosphopantethéine, formées au cours de la synthèse du coenzyme A, ont pour mission dans l'organisme de libérer la cystéamine. De plus, l'intérêt accordé à ce dérivé n'a

cessé de croître depuis plusieurs années à la suite de la mise en évidence de son action radioprotectrice [3—10].

Dans le présent travail, nous avons utilisé des techniques telles que la polarographie classique (d.c.) à tension sinusoïdale surimposée (a.c.) et impulsionnelle différentielle (p.p.) ainsi que la coulométrie à potentiel contrôlé afin de déterminer les caractéristiques électrochimiques de ces dérivés et d'en étudier le mécanisme réactionnel.

PARTIE EXPÉRIMENTALE

L'appareillage employé, de même que les réactifs sont identiques à ceux décrits lors de nos précédentes publications [1]. Nous avons en outre utilisé comme suppresseur de maxima une solution de Triton X100 à 0.02%.

CYSTÉAMINE

Avant d'en effectuer l'étude électrochimique, les solutions de cystéamine sont préalablement soumises à une électrolyse à potentiel contrôlé sur nappe de mercure à −1,5 V vs. ECS, opération indispensable du fait que le dérivé thiolé est très instable et s'oxyde dès sa mise en solution, Nous avons eu l'occasion de démontrer ce fait antérieurement [11].

Étude en fonction du pH

L'étude du comportement polarographique de la cystéamine est réalisée dans les mêmes milieux que ceux décrits antérieurement [1] pour une concentration en thiol de $5 \cdot 10^{-4}$ M; que l'on maintient constante tout au long des opérations (Fig. 1A). Les différentes mesures sont effectuées en cellule thermostatisée à 25,0 ± 0,1° C. Deux vagues anodiques se différencient, en polarographie conventionnelle, dans une zone de pH allant de 1,4 à 11,8. La première reste toujours bien définie, l'autre, par contre, située à des potentiels plus négatifs, apparaît faiblement aux pH acides, mais se développe nettement à partir de pH 6. Signalons toutefois que l'intensité totale de courant mesuré reste constante tout au long des opérations quelque soit le pH.

Jusqu'à pH 10,7, les potentiels de demi-palier de la première onde anodique varient linéairement avec le pH (56 mV par unité) et restent constants lorsque la valeur du pH devient supérieure à celle correspondant au pK_a de la molécule.

En ce qui concerne la deuxième vague, les valeurs de demi-palier fluctuent nettement plus: les variations de $E_{\frac{1}{2}}$ en fonction du pH, sont linéaires entre pH 1,4 et 8, présentant deux droites, une de pente égale à 65 mV jusqu'à pH 6, une autre de 30 mV entre pH 6 et 8; et au-delà de ce pH, la relation $E_{\frac{1}{2}}$—pH ne permet plus d'observer de linéarité.

Les tracés obtenus en polarographie alternative, diffèrent fortement des courbes d.c. et l'on peut observer des variations soit de l'un soit de l'autre

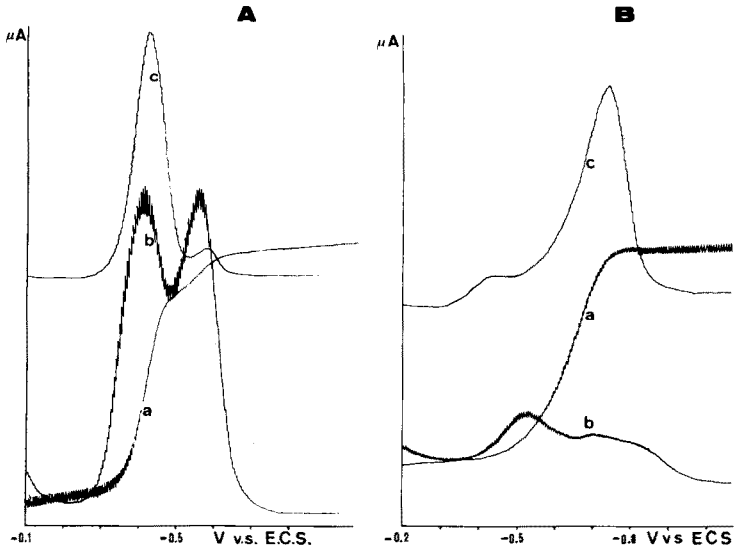

Fig. 1. A. Polarogrammes d.c. (a), a.c. (b) et p.p. (c) d'une solution $5 \cdot 10^{-4}$ M en cystéamine à pH 8. D.c. sensibilité 2,5 μA. A.c. sensibilité 2,5 μA; temps de chute de gouttes 0.9 s. P.p. sensibilité 5 μA, amplitude surimposée 20 mV; durée de l'impulsion 40 ms; temps de chute de gouttes: 2 s, retard: à l'impulsion 1 s 8; vitesse de déroulement 2 mV s^{-1}. B. Polarogrammes d.c. (a), a.c. (b) et p.p. (c) d'une solution $5 \cdot 10^{-4}$ M en cystamine à pH 8. D.c. sensibilité 2,5 μA. A.c. sensibilité 1,25 μA. P.p. sensibilité 500 nA. Les autres conditions sont identiques à celles de la Fig. 1A.

pic en fonction du pH. C'est ainsi que pour les valeurs de pH inférieures à 2, une seule réaction d'électrode se manifeste sous forme d'un pic, dont le sommet correspond au potentiel de demi-palier de la seconde onde polarographique décrite plus haut. Entre pH 2 et 4, cette dernière vague n'apparaît que sous forme d'un épaulement du pic principal. A pH 6, les deux pics se différencient très nettement et à pH plus élevé, le premier se modifie pour finalement devenir un épaulement du second.

Le comportement est encore tout autre en polarographie impulsionnelle différentielle (p.p.), où deux pics sont mesurables dès pH 4, mais l'intensité du second reste faible à toutes les valeurs du pH.

L'ensemble de ces observations se trouve consigné au Tableau 1 et la Fig. 1A illustre notamment le comportement polarographique de la cystéamine à pH 8.

Étude en fonction de la concentration

L'étude est réalisée à pH 6 où les deux vagues décrites plus haut sont bien développées. Lorsque la concentration en dépolarisant diminue, les potentiels de demi-palier se déplacent vers des tensions plus positives. La seconde vague est la plus influencée par ce déplacement et à partir de $1 \cdot 10^{-4}$ M seule l'onde anodique subsiste. En polarographie alternative, les deux pics existant pour

TABLEAU 1

Influence du pH sur le comportement polarographique de la cystéamine (Concentration $5 \cdot 10^{-4}$ M)

pH	D.c.						
	$E^1_{\frac{1}{2}}$ (V)[a]	$E^1_{\frac{3}{4}} - E^1_{\frac{1}{4}}$ (mV)	i_d (μA)	$E^2_{\frac{1}{2}}$ (V)[a]	$E^2_{\frac{3}{4}} - E^2_{\frac{1}{4}}$ (mV)	i_d (μA)	$i_{d_{total}}$ (μA)
1,4	−0,040	55	1,050	−0,172	25	0,110	1,310
1,9	−0,075	45	0,800	−0,195	35	0,120	1,030
2,9	−0,127	40	1,160	−0,250	30	0,050	1,290
4,1	−0,190	45	1,160	−0,327	50	0,080	1,285
5,7	−0,290	45	1,150	−0,445	45	0,080	1,310
6,3	−0,317	40	1,010	−0,460	30	0,130	1,260
7,7	−0,390	50	0,760	−0,500	45	0,280	1,235
8,1	−0,415	50	0,975	−0,570	45	0,145	1,250
9,1	−0,475	50	0,850	−0,650	50	0,260	1,250
11,6	−0,563	40	0,880	−0,710	35	0,200	1,250
11,8	−0,560	45	0,870	−0,700	45	0,240	1,260

pH	A.c.		P.P.			
	E_{pic_1} (V)[a]	E_{pic_2} (V)[a]	E_{pic_1} (V)[a]	i_{pic_1} μA	E_{pic_2} (V)[a]	i_{pic_2} (μA)
1,4		−0,160	−0,060	1,400	épaul −0,160	0,075
1,9		−0,175	−0,090	1,250	épaul −0,185	0,080
2,9	−0,120	−0,210 épaul	−0,130	1,870		
4,1	−0,205	−0,335	−0,195	1,750	−0,330	0,030
5,7	−0,300	−0,455	−0,285	1,750	−0,445	0,045
6,3	−0,335	−0,450	−0,325	1,610	−0,445	0,170
7,7	−0,415	−0,500	−0,400	1,000	−0,615	0,210
8,1	−0,430	−0,575	−0,432	1,315	−0,580	0,140
9,1	−0,500	−0,585	−0,480	1,290	−0,640	0,260
11,6	−0,595	−0,705	−0,570	1,410	−0,705	0,240
11,8	−0,595	−0,700	−0,565	1,370	−0,700	0,270

[a] V vs. ECS.

des concentrations allant de $5 \cdot 10^{-3}$ à $1 \cdot 10^{-3}$ M fusionnent dès que la teneur en cystéamine atteint $5 \cdot 10^{-4}$ M.

Les mesures destinées à préciser la nature des ondes polarographiques et effectuées en d.c. ont montré que pour une teneur en cystéamine allant de $8 \cdot 10^{-4}$ M à $3 \cdot 10^{-4}$ M l'intensité de la deuxième vague reste constante mais l'intensité totale de courant correspondant aux deux ondes observées est proportionnelle à cette concentration.

De plus, l'intensité de courant de la première vague anodique varie linéairement avec la racine carrée de la hauteur du réservoir de mercure, ce qui nous

permet de lui attribuer un caractère de diffusion; alors que l'intensité de la seconde vague est directement proportionnelle à la hauteur de ce même réservoir.

La courbe électrocapillaire tracée à pH 6, pour une teneur en dépolarisant de $5 \cdot 10^{-4}$ M met en évidence des phénomènes d'adsorption importants aux potentiels correspondants aux deux vagues précitées. La pente de la droite obtenue en portant les valeurs de log $(id - i)/i$ de la première vague anodique en fonction du potentiel est de 55 mV.

Dès lors, nous pouvons attribuer la première onde anodique à la formation d'un thiolate de mercure(I) et la deuxième à l'adsorption du dérivé $(RS)_2Hg$, résultant de la transformation de la forme instable RSHg [12].

CYSTAMINE

Etant donné les pics d'adsorption rencontrés lors de l'étude de ce dérivé, toutes les solutions de cystamine sont polarographiées en présence de 2,5 mg % de Triton X100.

Étude en fonction du pH

D'une manière générale, ce disulfure, réduit à l'électrode de mercure, présente un comportement beaucoup plus irréversible que le dérivé thiolé: les valeurs de $(E_{\frac{3}{4}}-E_{\frac{1}{4}})$ sont, en effet, voisines de 100 mV dans toute la zone de pH acide et neutre et ce n'est qu'à partir de pH 9 que ce caractère d'irréversibilité manifeste diminue quelque peu.

En polarographie d.c., la vague cathodique observée est précédée d'une pré-onde dont la valeur de $E_{\frac{1}{2}}$ fluctue fortement et qui se manifeste à pH 4,1 ($E_{\frac{1}{2}} = -0{,}230$ V) jusqu'à 5,7 ($E_{\frac{1}{2}} = -0{,}335$ V), disparaît et réapparaît lorsque le pH atteint une valeur de 10,5 ($E_{\frac{1}{2}} = -0{,}565$ V). A partir de pH 11, son potentiel de demi-onde reste stationnaire et vaut $-0{,}600$ V vs. ECS.

Si l'on porte en graphique les potentiels de demi-palier de la vague cathodique en fonction du pH, avant pH 7, on n'observe qu'une faible variation; par contre, le tracé s'incurve fortement vers des tensions plus négatives quand le pH croît et à partir de pH 11, se stabilise au voisinage de $-0{,}900$ V vs. ECS. (Fig. 2). Signalons toutefois que comme pour la cystéamine l'intensité totale de la vague ne se modifie pas dans toute la zone de pH.

En polarographie a.c. un pic se dessine dès pH 7,7, au potentiel correspondant à la pré-onde, bien que cette dernière n'apparaisse pas en d.c.; à partir de ce pH, son intensité est nettement supérieure à celle du deuxième pic, qui se développe lui, sous forme d'un maximum arrondi caractéristique de la réduction irréversible de ce disulfure.

En polarographie impulsionnelle différentielle (p.p.), par contre, la vague cathodique donne lieu à un pic bien formé, alors que le pic dû à la pré-onde est faible à tous les pH.

La Fig. 1B illustre le comportement polarographique de la cystamine à pH 8.

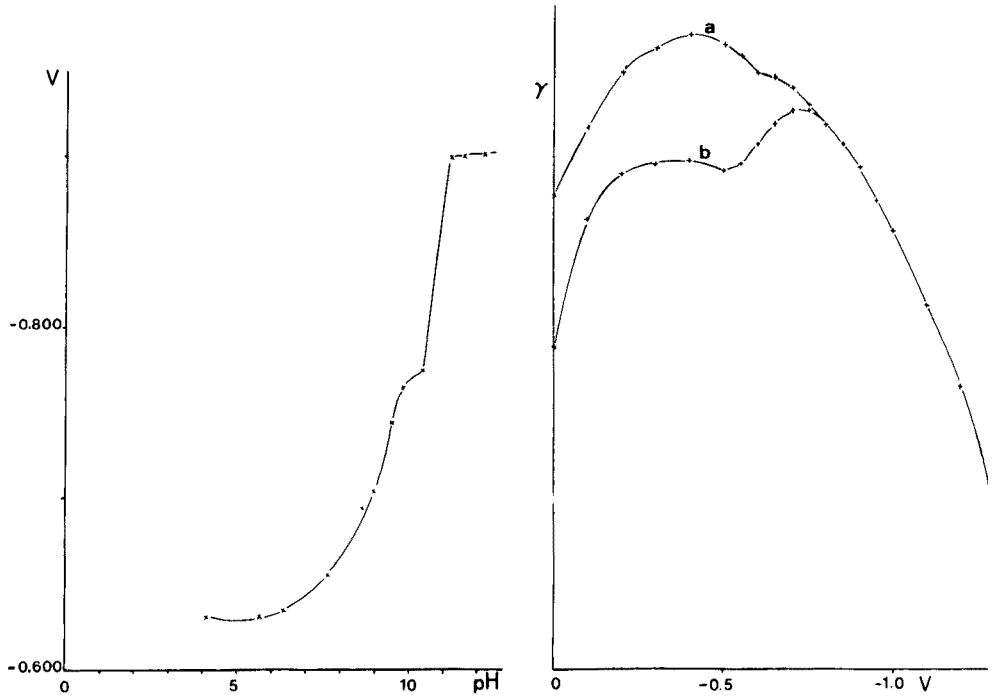

Fig. 2. Courbe $E_{\frac{1}{2}}$—pH. Solution $5 \cdot 10^{-4}$ M cystamine.

Fig. 3. Courbes électrocapillaires. (a) Electrolyte de support pH 10; (b) électrolyte de support additionné de $5 \cdot 10^{-4}$ M en cystamine.

Étude en fonction de la concentration

La teneur en dépolarisant influence fortement le potentiel de demi-onde de la vague cathodique: à pH 6,2, si la concentration varie de $1 \cdot 10^{-3}$ à $1 \cdot 10^{-5}$ M, le potentiel de demi-vague se déplace de 170 mV vers des tensions plus positives, par contre la réversibilité de la réaction ne se modifie pas.

La concentration en Triton X100 ajouté influence le caractère irréversible de la vague et modifie son potentiel de demi-palier; il y a donc lieu de contrôler minutieusement la concentration de ce suppresseur.

Une étude analogue à celle réalisée ci-dessus pour la cystéamine permet de montrer que la vague cathodique répond aux critères d'un courant de diffusior Elle correspond à la réduction du pont disulfure, mettant en jeu deux électrons, selon le processus: $RSSR + 2\,e^- + 2\,H^+ \rightleftharpoons 2\,RSH$.

La prévague observée en polarographie d.c. en milieu alcalin est une vague d'adsorption, comme l'illustre la courbe électrocapillaire tracée dans le tampon de pH 10 (Fig. 3).

ÉTUDE DE LA SÉPARATION DU MÉLANGE DES DEUX CONSTITUANTS

Si l'on en juge par les potentiels de demi-vague et de pics, la séparation à pH 8, de ces deux composés est réalisable (Fig. 4). Les vagues observées en d.c. répondant aux critères de diffusion et leur intensité variant linéairement en fonction de la concentration, nous avons pu doser une solution contenant jusqu'à 6 mg l^{-1} de chlorhydrate de cystéamine en présence de 11 mg l^{-1} de dichlorhydrate de cystamine. De plus, en d.p.p., les limites de détection atteintes sont respectivement $5 \cdot 10^{-7}$ M et $1 \cdot 10^{-6}$ M ce qui correspond à 0,012 mg l^{-1} et 0,23 mg l^{-1} en thiol et en disulfure.

Remarquons cependant que le tracé obtenu en polarographie a.c. diffère quelque peu des tracés correspondants à chaque dérivé pris séparément (Figs. 1 et 4): en effet, dans le cas du mélange, les pics de la cystéamine fusionnent en un pic élargi englobant la prévague de la cystamine, le pic obtenu en p.p. à −0,435 V vs. ECS. est lui plus symétrique lorsque les deux constituants sont présents.

En conclusion, le comportement électrochimique des dérivés soufrés étudiés dans ce travail est assez semblable à celui décrit pour le couple cystéine —cystine [1], la fonction carboxylique de la cystéine semblant procurer cependant à ce dérivé une meilleure stabilité vis-à-vis des phénomènes d'oxydation.

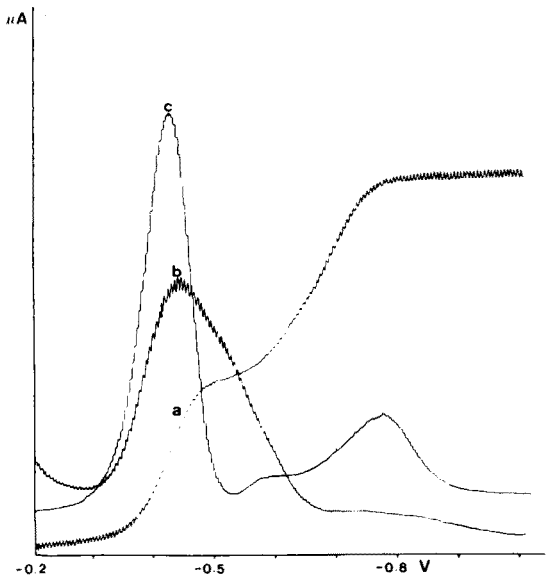

Fig. 4. Polarogrammes d.c., a.c. et p.p. d'une solution $5 \cdot 10^{-4}$ M en cystéamine et $5 \cdot 10^{-4}$ M en cystamine (pH 8). D.c.: sensibilité 2,5 μA. A.c.: sensibilité 5 μA; temps de chute de gouttes: 0,9 s. P.p. sensibilité: 2,5 μA: amplitude surimposée: 20 mV; durée de l'impulsion: 40 ms; temps de chute de gouttes: 2 s, retard à l'impulsion: 1 s 8; vitesse de déroulement: 2 mV s^{-1}.

Nos remerciements vont au Fonds National de la Recherche Scientifique (F.N.R.S.) pour l'aide précieuse qu'il apporte à l'un d'entre nous (G.J.P.).

BIBLIOGRAPHIE

1 C. A. Mairesse-Ducarmois, G. J. Patriarche et J. L. Vandenbalck, Anal. Chim. Acta, 71 (1974) 165; 76 (1975) 299; 79 (1975) 69; 84 (1976) 47; 88 (1977) 47.
2 G. D. Novelli, F. J. Schmetz Jr. et N. O. Kaplan, J. Biol. Chem., 206 (1954) 533.
3 E. Jellum et L. Eldjarn, Biochim. Biophys. Acta, 100 (1964) 144.
4 L. Revesz et H. G. Modig, Nature (London), 207 (1965) 430.
5 H. G. Modig et L. Revesz, Int. J. Radiat. Biol., 13 (1967) 469.
6 H. G. Modig, Biochem. Pharmacol., 22 (1973) 1623.
7 W. Lohmann, Prog. Biochem. Pharmacol., 1 (1965) 118.
8 W. Lohmann, A. J. Moss Jr., J. L. Sanders, B. J. Porter et D. M. Woodall, Radiat. Res., 29 (1966) 155.
9 E. D. Fults, Radiat. Res., 34 (1968) 544.
10 R. Ramanathan et U. K. Misra, Strahlentherapie, 151 (1976) 69.
11 C. A. Mairesse-Ducarmois, J. L. Vandenbalck et G. J. Patriarche, J. Pharm. Belgique, 28 (1973) 300.
12 C. A. Mairesse-Ducarmois, G. J. Patriarche et J. L. Vandenbalck, J. Pharm. Belgique, 31 (1976) 169.

Analytica Chimica Acta, 90 (1977) 111—118

ÉTUDE DE LA REDUCTION ÉLECTROCHIMIQUE DES HYDROCARBURES AROMATIQUES POLYNUCLEAIRES DANS LE DIMÉTHYLACÉTAMIDE

M. BRÉANT et J. GEORGES*

Equipe de Recherche CNRS No. 100 associée à l'INSA de Lyon, Laboratoire de Chimie Industrielle et Analytique, Bat 401, 69 621 Villeurbanne Cedex (France)

(Reçu le 13 octobre 1976)

RÉSUMÉ

Ce travail est consacré à l'étude de la réduction électrochimique de quelques hydrocarbures aromatiques polynucleaires dans le diméthylacétamide rendu anhydre par action du vitride. Nous avons déterminé les potentiels caractéristiques des différentes étapes de réduction aux électrodes de platine poli, platine platiné et à gouttes de mercure, et étudié la nature et la réversibilité des réactions. Nous avons ensuite analysé plus particulièrement la première étape de réduction en mettant en évidence la formation de radicaux anions par voie électrochimique et par résonance paramagnétique électronique.

SUMMARY

The electrochemical reduction of some aromatic polynuclear hydrocarbons has been studied in anhydrous dimethylacetamide. The half-wave potentials of the stages of reduction and the nature and the reversibility of the reactions have been studied with rotating platinum and dropping mercury electrodes. A study in greater detail of the first stage of the reduction has shown the formation of radical anions by electrochemical methods and electron spin resonance.

La réduction des hydrocarbures aromatiques non saturés met généralement en oeuvre l'addition de deux électrons et de deux protons sur une liaison π pour donner un composé dihydrogéné. Selon la structure du produit, des réactions supplémentaires peuvent intervenir pour conduire au composé tétra ou hexahydrogéné. L'ordre dans lequel intervient l'addition des électrons et du proton est variable; il est déterminé par l'activité protonique du milieu autant que par la structure du réactif. Ainsi un composé présentant en milieu aqueux ou hydroorganique une seule vague de réduction dont la hauteur correspond à la fixation de deux électrons, se réduit en milieu anhydre et aprotique en deux étapes monoélectroniques [1].

*Adresse actuelle: Laboratoire de Chimie Analytique 3, Université C. Bernard de Lyon I, 43, Bd du 11 Novembre 1918, 69 621 Villeurbanne Cedex (France).

(1) $R + e^- \leftrightarrows R^{\cdot-}$

(2) $R^{\cdot-} + e^- \leftrightarrows R^{2-}$

La première étape, généralement réversible, conduit à la formation d'un radical anion. A un potentiel suffisamment négatif, l'addition d'un deuxième électron intervient pour donner le dianion R^{2-}.

Nous nous sommes donc proposé d'étudier la réduction électrochimique de quelques hydrocarbures aromatiques dans le diméthylacétamide (DMA). Nous avons effectué la réduction successivement sur électrode de platine poli, platine platiné et mercure et nous en avons déduit la nature et la réversibilité des réactions. Ensuite, nous avons plus spécialement étudié la première étape de réduction: mise en évidence de l'espèce réduite à l'aide de la voltamétrie cyclique, de la coulométrie et de la technique de l'électrode à disque et à anneau. Enfin, nous avons caractérisé la formation des radicaux anions par résonnance paramagnétique électronique.

ÉTUDE DES ÉTAPES SUCCESSIVES DE LA RÉDUCTION — NATURE DES RÉACTIONS

L'un des critères qui permettent de juger de la nature et de la réversibilité des réactions électrochimiques consiste à vérifier que les valeurs de potentiel de réduction des hydrocarbures sont indépendantes de la nature de l'électrode Nous avons donc utilisé successivement les électrodes de platine poli, platine platiné et mercure.

Etude voltampérométrique

L'emploi de l'électrode de platine nécessite une déshydratation totale du solvant. En effet, sur platine platiné, le domaine d'électroactivité est limité par la réduction de l'eau résiduelle qui se comporte comme un acide faible. Pour une solution contenant environ $3 \cdot 10^{-2}$ mol l^{-1} d'eau, les limites par rapport à l'électrode de réference $Ag/AgCl_{sat}$, KCl_{sat} dans le DMA sont les suivantes: $LiClO_4$ 0,1 M, — 1,30 V; $NaB(C_6H_5)_4$ 0,1 M, — 1,45 V; KPF_6 0,1 M, — 1,50 V; Bu_4NI 0,1 M, — 1,75 V.

Sur platine poli, le domaine obtenu est beaucoup plus étendu mais il semble dû à une passivation de l'électrode; en présence d'eau, nous n'avons pu mettre en évidence les vagues de réduction des hydrocarbures.

Nous avons donc effectué la deshydratation complète du solvant par action du bis(méthoxy-2-éthoxy)aluminohydrure de sodium ou "vitride" [2, 3]. Les solutions ont été rendues conductrices par addition de perchlorate de lithium 0,1 M.

Etude polarographique

L'électrode à gouttes de mercure présente le double avantage de donner des courbes intensité—potentiel très reproductibles et de permettre l'observation de milieux très réducteurs sans l'emploi de vitride. L'eau résiduelle

présente dans les solutions n'est pas en quantité suffisante pour modifier l'allure des polarogrammes. L'électrolyte support utilisé est le perchlorate de lithium 0,1 M ou l'iodure de tétrabutylammonium 0,1 M pour l'étude des hydrocarbures les plus difficilement réductibles.

Résultats et discussion

Les résultats sont rassemblés dans le Tableau 1. Les valeurs des potentiels de demi-vague sont pratiquement égales avec les trois types d'électrodes. Le nombre de vagues est également le même quelle que soit l'électrode utilisée. En outre, les résultats polarographiques sont indépendants de la nature du cation (Li^+ ou Bu_4N^+) de l'électrolyte-support. Les transformées logarithmiques $E = f[\log i/(i_d - i)]$ des vagues obtenues à l'électrode de mercure sont des droites dont la pente est voisine de 60 mV/unité log. Les systèmes correspondants sont donc rapides.

Ces faits montrent que la réduction électrochimique des composés étudiés se produit, dans le diméthylacétamide, avec simple échange d'électrons. Certains hydrocarbures comme le pérylène, l'anthracène, le tétracène, le pyrène et le *p*-terphényle se réduisent en deux étapes monoélectroniques, les autres ne présentent qu'un seul échange monoélectronique dans le domaine de potentiel utilisable.

TABLEAU 1

Réduction des hydrocarbures

Hydrocarbures	$E_{\frac{1}{2}\,cat}$(V) Platine[a]	$E_{\frac{1}{2}\,cat}$(V) Mercure[a]	Pente de la transformée (mV/unité log)
Pérylène	I — 2,16	I — 2,15	59
	II — 2,83	II — 2,71	57
Anthracène	I — 2,45	I — 2,43	59
	II — 3,19	II — 2,96	61
Tétracène	I — 2,50	I — 2,49	61
	II — 3,18	II — 3,01	50
Pyrène	I — 2,57	I — 2,55	64
	—	II — 3,09	55
p-Terphényle	I — 2,83	I — 2,81	61
	—	II — 3,15	57
Phénanthrène	— 2,95	— 2,94	62
Naphtalène	— 3,05	— 3,02	64
Biphényle	— 3,10	— 3,08	61
Acénaphtène	— 3,17	— 3,16	64
Fluorène	— 3,20	— 3,18	62

[a]Valeurs rapportées au potentiel standard du couple ferrocène/ferricinium.

ÉTUDE DE LA PREMIÈRE ÉTAPE DE RÉDUCTION — MISE EN ÉVIDENCE DES RADICAUX ANIONS

Etude par voie électrochimique

Nous n'avons pu obtenir par voie électrochimique des solutions contenant à la fois l'oxydant et le réducteur, le vitride étant sans action sur les hydrocarbures. Cependant, differentes méthodes électrochimiques ont pu être utilisées pour mettre en évidence la radical anion: voltamétrie cyclique, coulométrie, emploi de l'électrode à disque et à anneau.

Voltamétrie cyclique. La formation du radical anion est caractérisée par l'apparition d'un pic anodique (Fig. 1) qui correspond à la réoxydation du produit formé à la surface de l'électrode lors du balayage aller.

Coulométrie. Dans certains cas, la coulométrie à intensité imposée, effectuée sur des solutions parfaitement deshydratées et rendues conductrices par addition de perchlorate de lithium 0,1 M, nous a permis d'obtenir, au moins pendant quelques instants des solutions contenant à la fois l'hydrocarbure et le radical anion correspondant. Le tracé des courbes intensité—potentiel effectué pendant l'électrolyse montre que le radical anion s'oxyde au même potentiel que celui correspondant à la réduction de l'hydrocarbure (Fig. 2). Les solutions de radicaux ainsi obtenues sont fortement colorées, rapidement détruites par l'entrée d'air ou d'humidité dans la cellule et de durée de vie très courte aux faibles concentrations.

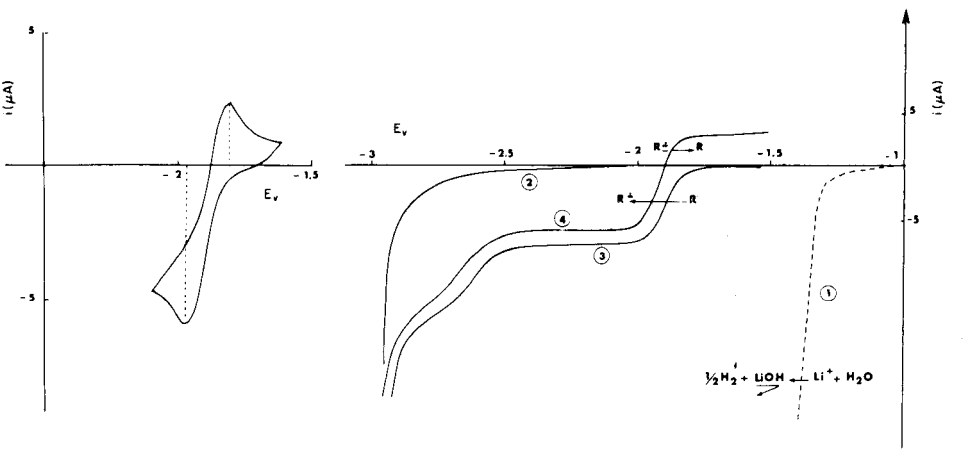

Fig. 1. Système anthracène/anthracène$^{\cdot-}$ — Voltamétrie cyclique: $V = 0{,}025$ V s^{-1}. Electrode de platine.

Fig. 2. Courbe intensité—potentiel du système anthracène/anthracène$^{\cdot-}$ à l'électrode de platine platiné en milieu $LiClO_4$ 0,1 M. 1, Réduction de l'eau en présence de $LiClO_4$. 2, Courant résiduel après élimination de l'eau par le vitride. 3, Solution d'anthracène $5 \cdot 10^{-3}$ M. 4, Solution d'anthracène partiellement réduite.

Electrode à disque et à anneau. Cette technique [4] a été ùtilisée pour suppléer à la voltamétrie cyclique dans le cas des radicaux anions les plus instables. Son avantage, par rapport aux autres techniques comme la voltamétrie cyclique réside dans le fait que c'est une méthode stationnaire: elle permet de s'affranchir du paramètre "temps", donc de détecter les espèces les plus fugaces. En effet, les radicaux anions formés par réduction électrochimique sur le disque (maintenu à un potentiel constant et suffisamment réducteur) sont entrainés par convection radiale vers l'anneau où ils peuvent être détectés par oxydation. Un exemple des courbes obtenues est donné (Fig. 3).

Résonance paramagnétique électronique

La résonance paramagnétique électronique est une excellente méthode pour mettre en évidence la formation, souvent intermédiaire, de radicaux ou d'ions radicaux lors de l'oxydation ou de la réduction chimique ou électrochimique d'hydrocarbures aromatiques [5, 6]. Tandis que l'emploi des méthodes électrochimiques nous a permis de déterminer les potentiels de demi-vague, la réversibilité des réactions et le nombre d'électrons mis en jeu, la résonance paramagnétique électronique nous a conduit à l'identification de l'espèce radicalaire formée.

Etant donnée la très faible stabilité des radicaux susceptibles de se former, nous avons adopté le dispositif présenté sous sa forme définitive par Cauquis [7] (cf. Partie expérimentale). Les spectres obtenus sont représentés (Fig. 4). L'évaluation expérimentale des constantes de couplage correspondant aux différentes classes de protons équivalents est complexe et demande des spectres hautement résolus: grand nombre de raies, chevauchements possibles dûs à de faibles différences entre les constantes de couplage. Cependant, les

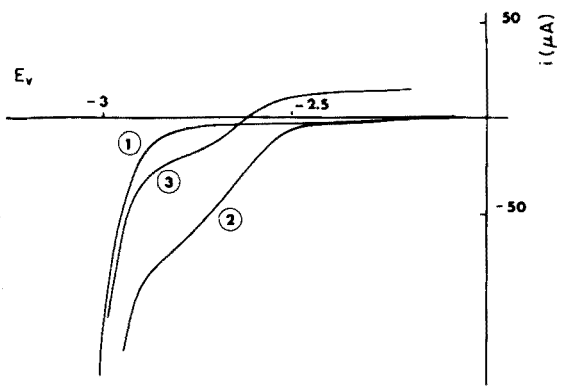

Fig. 3. Etude d'une solution de fluorène $4 \cdot 10^{-3}$ M à l'électrode à disque (D) et à anneau (A). Platine platiné. 1, Courant résiduel en milieu anhydre et $LiClO_4$ 0,1 M. $i_A = f(E_A)$. 2, Réduction du fluorène: $i_A = f(E_A)$, $E_D = -2{,}0$ V. 3, $i_A = f(E_A)$, $E_D = -2{,}8$ V.

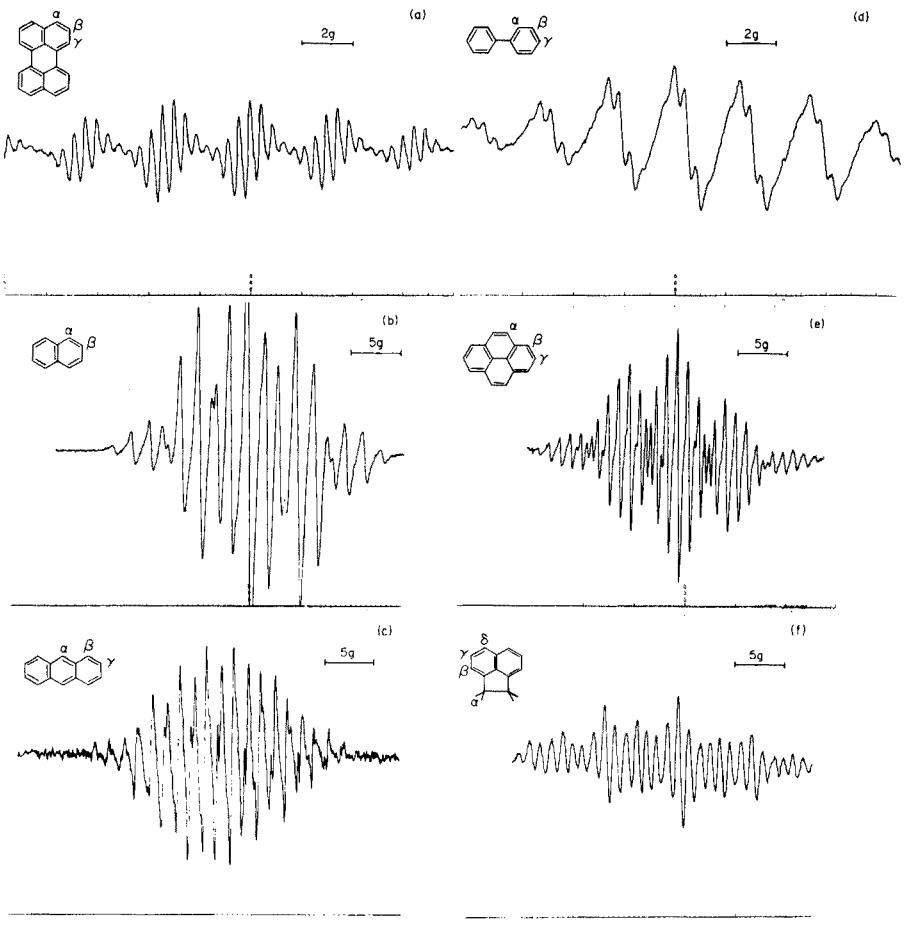

Fig. 4. Spectre de résonance paramagnétique électronique des radicaux anions (a) Pérylène. (b) Naphtalène. (c) Anthracène. (d) Biphényle. (e) Pyrène. (f) Acénaphtène.

hydrocarbures qui font l'objet de ce travail ont déjà été étudiés dans l'acide sulfurique, le tétrahydrofuranne et le diméthoxyéthane et les spectres des radicaux anions correspondants analysés [8—14]. Nous observons une bonne correspondance entre ces données et nos résultats et nous pouvons comparer les constantes de couplage (Tableau 2). Ceci nous permet de confirmer la formation de radicaux anions intermédiaires au cours de la réduction d'hydrocarbures aromatiques en solution dans le diméthylacétamide. En outre la structure de chacun des spectres étant caractéristique d'une espèce radicalaire déterminée, nous pouvons affirmer que nous avons, dans tous les cas, obtenu le radical $R^{\dot{-}}$ correspondant à l'hydrocarbure R introduit en solution. Ces résultats, ainsi que ceux que nous avons obtenus par polarographie contribuent à l'utilisation de la RPE et de l'électrochimie comme moyen d'identification et de dosage des hydrocarbures aromatiques polynucléaires dont certains sont des substances cancérigènes.

TABLEAU 2

Comparaison des constantes de couplage obtenues à partir des spectres de RPE

Hydrocarbure et couleur du radical	Réf.	a_α	a_β	a_γ	a_δ
Pérylène	8,9	3,53	0,46	3,09	
bleu intense	[a]	3,50	0,45	3,05	
Naphtalène	8	4,95	1,87		
	10	5,01	1,79		
vert	[a]	4,80	1,75		
Anthracène	8	5,41	2,76	1,53	
	9	5,56	2,74	1,57	
bleu	[a]	5,40	2,70	1,50	
Biphényle	11	2,73	0,43	5,46	
vert	[a]	2,60	0,40	5,20	
Pyrène	12	2,08	4,75	1,09	
	13	—	5,80	—	
orangé	[a]	2,00	5,75	1,00	
Acénaphtène	14	7,53	1,04	2,42	4,17
	[a]	7,35	1,00	—	4,25

[a] Valeurs obtenues dans ce travail.

PARTIE EXPÉRIMENTALE

Produits

Le diméthylacétamide (Carlo Erba) est purifié par double distillation sous pression réduite. Les électrolytes supports, le "vitride", et les hydrocarbures aromatiques sont des produits pour analyse (Carlo Erba, Merck, Prolabo ou Eastman-Kodak).

Techniques

Les mesures électrochimiques ont été éffectuées à l'aide d'appareils Solea-Tacussel. L'électrode à disque et à anneau est constituée d'un disque central de platine poli entouré d'un anneau cylindrique également en platine poli. Les deux électrodes sont isolées électriquement et, par rapport à une électrode de référence commune, leur potentiel peut varier indépendamment par branchement aux bornes d'un bipotentiostat Bipad.

Les spectres de RPE ont été tracés à l'aide d'un spectromètre Varian E-3 avec modulation de champ à 100 kHz; la puissance hyperfréquence délivrée à la cavité peut être réglée jusqu'à 200 mW. L'appareillage [7], permet de réaliser la réduction électrochimique directement dans la cavité résonnante du spectromètre et sans barbotage gazeux. La partie de la cellule où a lieu la formation des radicaux est en quartz et de forme aplatie; l'électrode génératrice, placée à l'intérieur, est une grille de platine poli. L'anode, qui est également un fil de platine est située en dehors de la cavité résonnante dans un compartiment la séparant du reste de la solution. Les solutions

d'hydrocarbures dans le diméthylacétamide sont préalablement deshydratées à l'intérieur même de la cellule.

Nous exprimons notre reconnaissance à M. G. Bodennec (Laboratoire de Chimie Organique III, Université C. Bernard de Lyon I) et à M. J. Vedrine (Institut de Recherches sur la Catalyse, Villeurbanne) pour leur collabaration à la partie de ce travail éffectuée par résonance paramagnétique électronique.

BIBLIOGRAPHIE

1 G. J. Hoijtink, J. Van Schooten, E. de Boer et W. I. Aalbersbert, Rec. Trav. Chim. Pays-Bas, 73 (1954) 355.
2 A. Caillet, Thèse, Paris, 1974.
3 M. Breant et J. Georges, C. R. Acad. Sci., 280 (1975) 457.
4 A. N. Frumkin et L. N. Nekrasov, Dokl. Akad. Nauk. SSSR, 126 (1959) 115.
5 R. N. Adams, J. Electroanal. Chem., 8 (1964) 151.
6 A. Carrington, Q. Rev. Chem. Soc., 17 (1963) 67.
7 G. Cauquis, Bull. Soc. Chim. Fr., (1968) 1618.
8 J. P. Colpa et J. R. Bolton, Mol. Phys., 6 (1963) 273.
9 A. Carrington, F. Dravnieks et M. C. R. Symons, J. Chem. Soc., (1959) 947.
10 T. R. Tuttle, R. L. Ward et S. I. Weissman, J. Chem. Phys., 25 (1956) 189.
11 A. Carrington et J. Dos Santos-Veiga, Mol. Phys., 5 (1962) 21.
12 G. J. Hoijtink, J. Townsend et S. I. Weissman, J. Chem. Phys., 34 (1961) 507.
13 E. de Boer et S. I. Weissman, J. Am. Chem. Soc., 80 (1958) 4549.
14 J. P. Colpa et E. de Boer, Mol. Phys., 7 (1963—64) 333.

Analytica Chimica Acta, 90 (1977) 119—125
Elsevier Scientific Publishing Company, Amsterdam — Printed in The Netherlands

DETERMINATION OF SUBMICROGRAM AMOUNTS OF ARSENIC AND ANTIMONY BY D.C. PLASMA ARC EMISSION SPECTROMETRY

AKIRA MIYAZAKI, AKIRA KIMURA, and YOSHIMI UMEZAKI
National Research Institute for Pollution and Resources, Ukima, Kita-ku, Tokyo (Japan)
(Received 25th October 1976)

SUMMARY

The application of a d.c. plasma arc to the determination of submicrogram amounts of arsenic and antimony is described. Arsenic or antimony hydride generated by reduction with granulated zinc or zinc powder is collected in a liquid nitrogen trap and then swept into the plasma. The effects of the argon gas flow rates, d.c. arc current, acid concentration, etc. were investigated. The limits of detection are 8 ng for arsenic and 40 ng for antimony. The standard deviations are 3.5% for 0.5 μg As and 4.5% for 0.6 μg Sb. Interference from nitric acid up to 0.3—0.5 M could be removed by adding chromium(II). The proposed method was applied to the analysis of waste water and sea water.

The application of d.c. plasma arcs to water analysis has been of interest for some years. Most of the papers published so far have been concerned with the injection of liquid samples by a conventional pneumatic nebulizer. An earlier paper dealing with the determination of mercury [1], reported that the introduction of a gaseous sample is also useful for water analysis with a d.c. plasma arc. In this paper, the approach is extended to the determination of submicrogram amounts of arsenic and antimony which are important environmental pollutants. The determination of submicrogram amounts of arsenic and antimony by emission spectrometry has been reported by Braman et al. [2], Lichte and Skogerboe [3], and Sakamoto et al. [4]; these authors used a d.c. discharge or microwave-induced plasma. The d.c. plasma arc has not been used previously for this purpose.

Arsenic and antimony were reduced with granulated zinc or zinc powder to their hydrides, which were collected in a liquid nitrogen trap [5] and then swept out into the d.c. plasma arc. The method was applied to the analysis of waste water and sea water.

EXPERIMENTAL

Apparatus

A SpectraSpan Model 101 d.c. plasma arc emission spectrometer was used with a Nippon Denshi Kagaku Model U-125M recorder and a HTV R106 photomultiplier. The hydride generation apparatus and the associated

gas flow system are shown in Fig. 1. The liquid nitrogen trap was used because hydrogen evolved with hydrides made the discharge very unstable.

The operating conditions of the d.c. plasma arc emission spectrometer are given in Table 1.

Reagents

Arsenic standard solution (1000 p.p.m.) was prepared by dissolving arsenic trioxide in sodium hydroxide (4%) and slightly acidifying with sulfuric acid (1 + 10). Antimony standard solution (1000 p.p.m.) was prepared by dissolving antimony metal (99.999%) in a little concentrated sulfuric acid and diluting with sulfuric acid (1 + 6). These standard solutions were diluted to the required concentrations just before use.

Granulated zinc (24—65 mesh) was used for reduction of arsenic because the commercially available zinc powders contained considerable amounts of arsenic. Zinc powder slurry, used for stibine generation, was prepared by mixing 100 g of zinc powder and 70 ml of water.

Chromium(II) solution was prepared by reducing a solution of chromium(III) sulfate (20%) in hydrochloric acid (0.1 M) with granulated zinc in a nitrogen atmosphere; reduction was complete in about 30 min.

All other chemicals used were of analytical-reagent grade.

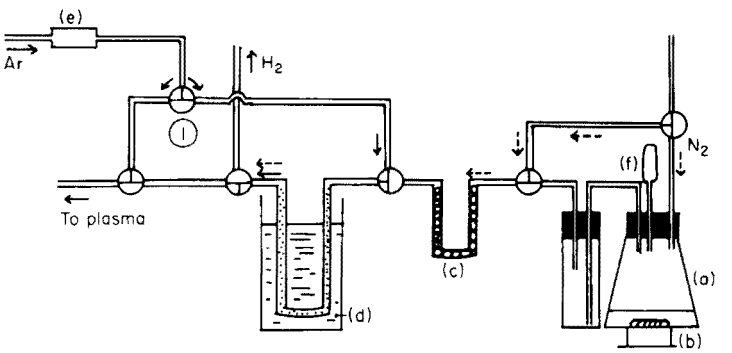

Fig. 1. Apparatus for evolution of hydrides. (a) Generating flask (50-ml Erlenmeyer). (b) Magnetic stirrer. (c) U-tube with Drierite (8 mesh) or $CaCl_2$. (d) Liquid N_2 trap. (e) Flow meter. (f) Dropping pipette.

TABLE 1

Operating conditions

Plasma current	7.5 A	Exit slit width	200 × 400 μm
Flow rate of carrier gas	7.5 units[a]	Recorder range	50 mV
Flow rate of anode gas	1.5 units	Photomultiplier	Hamamatsu TV R10
Flow rate of cathode gas	0.5 units	High voltage	800 V
Entrance slit width	400 × 600 μm	Range	× 1

[a]Scale unit = 0.47 l min^{-1}.

Determination of arsenic

Transfer 20 ml of sample solution containing 0.02—1.0 μg As to a 50-ml Erlenmeyer flask. To this solution, add 2 ml of potassium iodide solution (20%), 2 ml of tin(II) chloride solution (10%), and 8 ml of 11 M hydrochloric acid, and mix well with a Teflon-coated stirring bar. Connect the flask to the gas evolution system. Replace the atmosphere in the system with nitrogen and then cool the trap to liquid nitrogen temperature. Add 5 g of granulated zinc and collect the arsenic hydride evolved in the cold trap for 6 min. Sweep the system with nitrogen to remove residual hydrogen. With the three-way stopcocks open to the positions shown in Fig. 1, remove the U-tube from the liquid nitrogen and keep it at room temperature for 30 s. Open tap 1 fully to sweep the arsenic hydride into the arc. Record the 235.0-nm As emission line intensity.

Determination of antimony

Antimony was determined similarly to arsenic. Transfer 20 ml of sample solution containing 0.2—2.0 μg Sb to the gas evolution flask. To this solution, add 12 ml of 11 M hydrochloric acid and mix well. Cool the trap to liquid nitrogen temperature. Add 2 ml of zinc powder slurry from the dropping pipette (Fig. 1). Collect antimony hydride in the cold trap for 3 min. Remove residual hydrogen with nitrogen, and then keep the U-tube at room temperature for 60 s. Measure the 259.8-nm Sb emission line intensity.

RESULTS AND DISCUSSION

The spatial distribution of the emission intensity was investigated. The strongest emission intensity was observed at a position of 4.75 mm from the cathode and 5.0 mm from the anode. This position was used for all subsequent measurements.

Effect of gas flow rate and arc current

Gas flow rate and arc current must be optimized to achieve a satisfactory plasma stability and maximal sensitivity. Figure 2 shows the variation in the signal intensity for 0.3 μg of arsenic as a function of three gas flow rates. The cathode gas flow rate had the largest effect on the signal intensity; decreasing this flow rate enhanced the signal intensity. However, the plasma became unstable when the cathode gas flow rate was kept below 0.5 unit (1 unit = 0.47 l min^{-1}). Optimal sensitivity was achieved with anode gas, cathode gas, and carrier gas flow rates of 1.5, 0.5, and 7.5 units, respectively. Similar results were obtained for antimony.

Changes in the arc current over the range 6—8 A had no effect on the emission intensity for arsenic; for antimony, the emission intensity increased slightly as the arc current was increased from 6 to 7 A, but was essentially stable for the range 7—8 A. An arc current of 7.5 A was used in subsequent experiments.

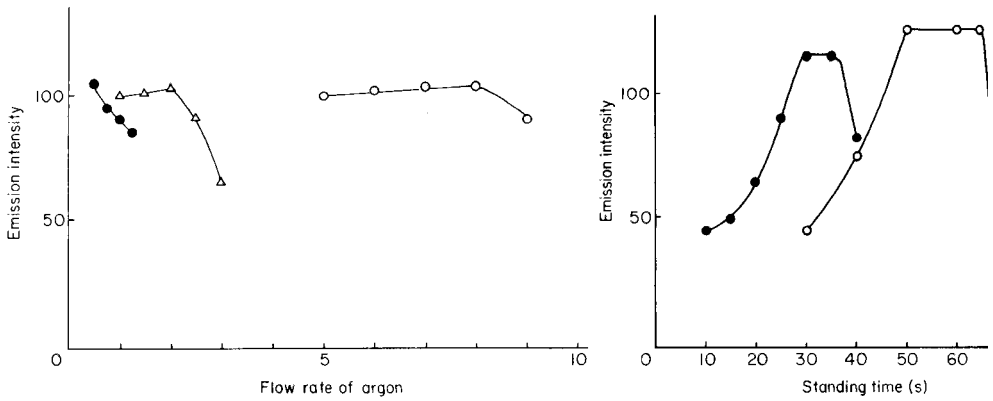

Fig. 2. Effect of argon flow rate. ○ Carrier gas. △ Anode gas. • Cathode gas.

Fig. 3. Effect of standing time of U-tube at room temperature. • 0.4 μg As. ○ 2 μg Sb.

Effect of acid concentration, reaction time and standing time

The response to arsenic was not very dependent on hydrochloric acid concentration (2—6 M). For antimony, a slight increase was observed with increasing acidity from 2 to 6 M. The final acid concentrations selected were 2 M and 4 M for arsenic and antimony, respectively.

The emission intensity increased linearly with increasing reaction time up to 5 min for arsenic (0.4 μg) and 2 min for antimony (2 μg), and became constant thereafter. Consequently, reaction times of 6 min for arsenic and 3 min for antimony were chosen.

Since the method was described by Holak [5], the liquid nitrogen trap for arsenic or antimony determination has been used by several groups of workers [4, 6—9]. In most cases, the gaseous hydrides were swept out immediately after removal of the U-tube from the liquid nitrogen trap. However, the shape and height of the recorder signal are then liable to be broad and low, because the temperature of the U-tube is too low to permit the rapid evaporation of hydrides. Keeping the U-tube for some time at room temperature made the recorder signal sharp. The stopcock (No. 1, Fig. 1) was maintained half open during the standing time to remove any remaining nitrogen in the system; nitrogen caused strong background emission. The most sensitive signal was obtained when the standing times were 30 s and 60 s for arsenic and antimony, respectively (Fig. 3). The sudden decrease of signal after 35 s for arsenic or 65 s for antimony is probably due to loss of the hydrides on standing.

Effects of diverse ions and acids

No interferences were observed in the emission process itself because only gaseous hydrides were introduced into the plasma. It was expected that interferences might result from a suppression or enhancement of hydride

generation. The results found in the interference study were similar to those reported by other authors [2, 6, 10].

For the determination of 0.5 μg As, no interference was caused by 500 μg of Na, K, Li, Mg, Ca, Sr, Ba, Al, Fe(III), Fe(II), Co, Ni, Cr(VI), Cr(III), Mn(II), Cd, Cu, Pb, Se(IV); a −30% error was caused by 500 μg of Te(IV) added as Na_2TeO_3. For the determination of 1.0 μg Sb, there was no interference from 1-mg amounts of the above-mentioned ions, except that Co(II), Ni(II), Cu(II) and Se(IV) caused negative errors of 69%, 75%, 51% and 75%, respectively. Te(IV) and As(III) in 1-mg quantities caused positive errors of 42% and 33%, respectively.

The effects of sulfuric acid and nitric acid were investigated. No interference was observed for sulfuric acid (0.5—2 M) but nitric acid interfered seriously with the formation of gaseous hydrides; as little as $5 \cdot 10^{-3}$ M nitric acid reduced the final emission intensity by 75%. Heating is effective for expelling nitric acid in the presence of sulfuric acid from the sample solution, but it is time-consuming and arsenic or antimony may be lost. An attempt was made to remove the interference from nitric acid by adding a strong reducing agent before the generation of hydrides. The oxidation potential of the reducing agent must be higher than −0.60 V for arsenic determination ($As + 3\ H^+ + 3\ e = AsH_3$; −0.60 V) and −0.51 V for antimony determination ($Sb + 3\ H^+ + 3\ e = SbH_3$; −0.51 V), otherwise arsenic or antimony will be lost.

As the reducing agent, chromium(II) was selected ($Cr^{3+} + e = Cr^{2+}$; −0.41 V); Cr^{2+} solution and urea (or hydrazine sulfate) were added to the sample containing nitric acid in a nitrogen atmosphere. The 235.0-nm As emission intensity of the mixture was compared with that of the sample in the absence of nitric acid. Results are shown in Fig. 4. For arsenic, the interference of nitric acid up to 0.3 M was eliminated by adding 4 ml of Cr^{2+} solution (20%) and 2 g of urea. When the volume of Cr^{2+} solution (20%) was raised to 8 ml,

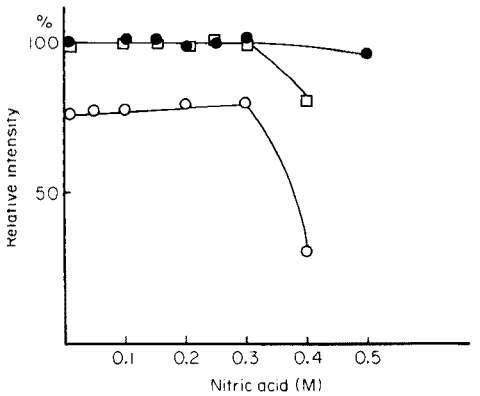

Fig. 4. Removal of interference from nitric acid with chromium(II). □ As with 4 ml of 20% Cr(II) solution and 2 g of urea. • As with 8 ml of Cr(II) solution and 2 g of urea. ○ Sb with 1 ml of Cr(II) solution and 2 g of hydrazine sulfate.

the removal of interference was successful up to 0.5 M. The addition of Cr^{2+} solution and urea for the determination of arsenic was successful in avoiding interference from 6-mg amounts of Fe(III), Cd, Cu(II), Ni(II), Co(II), Mn(II), Al, Pb, Mg and Ca; in the absence of urea, Ni and Co caused large negative interferences.

For antimony, the addition of Cr^{2+} solution caused a slight suppression of hydride generation (Fig. 4). Interference of nitric acid up to 0.3 M, however, was eliminated by adding 1 ml of Cr^{2+} solution (20%) and 2 g of hydrazine sulfate. Urea was less effective than in the case of arsenic; the reason is unknown.

Terashima [11] reported that addition of hydrazine sulfate eliminated the interference from nitric acid up to 0.1 M. Better results were obtained by the proposed method. The method would be useful for the determination of arsenic or antimony in soils and sediments, because a large amount of nitric acid is normally used in the digestion of these samples.

Calibration curves, precision and detection limits

Calibration curves were obtained at or near optimum operating conditions. The calibration curves were linear for 0.02—1.0 μg As and for 0.2—2.0 μg Sb. The standard deviations were 3.5% for 0.5 μg As and 4.5% for 0.6 μg Sb. The limits of detection were 8 ng for arsenic and 40 ng for antimony.

Applications

Table 2 shows a comparison of the results obtained for arsenic in river water, waste water, and sea water by a.a.s. and the proposed method; the results are in good agreement.

The data for recovery experiments for antimony are shown in Table 3. Satisfactory results were obtained for all types of samples.

In conclusion, the results summarized here indicate that d.c. plasma arc emission spectrometry is useful for the determination of submicrogram amounts of arsenic and antimony.

TABLE 2

Results for arsenic in water

Sample	As (p.p.m.)	
	Plasma	A.a.s.
Sea water (coastal)		
A	0.004	0.005
B	0.005	0.003
Waste water		
C	0.12	0.15
D	0.70	0.61
E	0.18	0.18
F	0.009	0.010
G	0.028	0.031

TABLE 3

Results of recovery experiments for antimony

Sample	Added (μg)	Found (μg)	Recovery (%)	Sample	Added (μg)	Found (μg)	Recovery (%)
River water				*Waste water*			
A	0	0		F	0	0.94	
	1.00	1.00	100		1.00	1.94	100
B	0	0.05		G	0	1.00	
	1.00	1.03	98		1.00	2.08	108
C	0	0		H	0	0.73	
	1.00	0.96	96		1.00	1.65	92
Mine water				I	0	0.05	
D	0	0			1.00	1.01	96
	1.00	1.03	103	*Sea water*			
E	0	0		J	0	0	
	1.00	0.98	98		1.00	0.93	93
				K	0	0	
					1.00	0.95	95

REFERENCES

1 A. Miyazaki and Y. Umezaki, Bunseki Kagaku, 24 (1975) 562.
2 R. S. Braman, L. L. Justen, and C. C. Foreback, Anal. Chem., 44 (1972) 2195.
3 F. E. Lichte and R. K. Skogerboe, Anal. Chem., 44 (1972) 1480.
4 T. Sakamoto, H. Kawaguchi, and A. Mizuike, Bunseki Kagaku, 24 (1975) 457.
5 W. Holak, Anal. Chem., 41 (1969) 1712.
6 S. Musha, Nippon Kaisui Gakkaishi, 27 (1974) 255.
7 R. M. Orheim and H. H. Bovee, Anal. Chem., 46 (1974) 921.
8 H. R. Griffin, M. B. Hocking, and D. G. Lowery, Anal. Chem., 47 (1975) 229.
9 E. J. Knudson and G. D. Christian, Anal. Lett., 6 (1973) 1039.
10 A. E. Smith, Analyst (London), 100 (1975) 300.
11 S. Terashima, Bunseki Kagaku, 23 (1974) 1331.

Analytica Chimica Acta, 90 (1977) 127—136

STATISTICAL STUDIES OF MATRIX EFFECTS ON THE DETERMINATION OF CADMIUM AND LEAD IN FERTILIZER MATERIALS AND PLANT TISSUE BY FLAMELESS ATOMIC ABSORPTION SPECTROMETRY

T. C. WOODIS, JR., G. B. HUNTER and F. J. JOHNSON

Division of Chemical Development, Tennessee Valley Authority, Muscle Shoals, Alabama 35660 (U.S.A.)

(Received 28th September 1976)

SUMMARY

The evaluation of interferences on an individual basis can give unreliable information, whereas a statistical approach shows the synergic effects of different ions and gives more reliable information with fewer determinations. Cadmium and lead in phosphate rock, wet-process phosphoric acid, and plant tissue can be determined directly after a nitric acid dissolution by carbon-rod atomization with no significant interference within the range studied. The results are in good agreement with results obtained by flame analysis when a careful control of acid concentration is maintained between samples and standards. Results on materials of low cadmium content are more reliable by carbon-rod atomization.

Environmental pollution by cadmium and lead has been discussed extensively [1—4]. One major concern is the entry of these pollutants into the food cycle through the use of fertilizers and fertilizer materials. Cadmium has been determined in fertilizer, soils, and plant tissue samples [5] by a.a.s. after concentration and elimination of matrix ions with a dithizone extraction. Cadmium in fertilizers has been determined by a.a.s. by direct aspiration of an acid solution [6]; of the several fertilizer components studied, calcium was the only significant interferent in the determination of 0.5—1.0 μg Cd ml^{-1}. Background absorption must be compensated for when calcium salts are present. Recently, flameless atomic absorption (f.a.a.s.) has been used for the determination of cadmium in soils [7] after solvent extraction with ammonium pyrrolidine dithiocarbamate, and in plant tissue [8] directly after dissolution with nitric and perchloric acids. These authors use a Perkin-Elmer HGA 2000 graphite furnace.

Several studies [9—11] have been concerned with lead contamination of soils and plants with respect to traffic volume and proximity to highways. All these studies used a.a.s. to measure lead concentration. Fletcher [12] showed a constant background absorption to be present for lead determination in plant leaves by a.a.s. at 217 nm. A hydrogen lamp continuum

source was used for correction. Kahn et al. [13] determined lead in soil and plant tissue, using a Delves microsampling cup. Blanks and standards prepared similarly to samples showed no background absorption.

Very little information is presented in any of these studies concerning matrix effects on the determination of cadmium and lead by either a.a.s. or f.a.a.s.

This study was designed to determine by statistical methods the synergic effects of matrix ions on the determination of cadmium and lead in phosphate rock, wet-process phosphoric acid, and selected plant tissue samples by f.a.a.s. The statistical technique is compared to a conventional method for studying interferences. Optimum methods of sample preparation were investigated and procedures suggested.

EXPERIMENTAL

Apparatus

A Varian-Techtron Model 63 carbon-rod atomizer coupled to an Instrumentation Laboratories Model 353 atomic absorption spectrophotometer modified for peak area integration was used with the instrumental parameters shown in Table 1.

Standard solutions

For cadmium, weigh 1 g of cadmium metal, dissolve in 20 ml of 11 M HCl, and dilute to 1 l with distilled water. For lead, weigh 1.598 g of $Pb(NO_3)_2$, dissolve in water, and dilute to 1 l. Dilute appropriate aliquots of these solutions to give a range of 0.01—0.05 μg Cd ml^{-1} and 0.05—0.2 μg Pb ml^{-1}. The final solutions are made 0.5 M in nitric acid.

TABLE 1

Instrumental parameters

Element		Voltage	Time (s)	
Atomizer settings				
Cd	Dry	6.0	10.0	
	Ash	4.5	10.0	
	Atomize	5.0	1.5	
Pb	Dry	6.0	10.0	
	Ash	4.5	10.0	
	Atomize	5.5	2.0	
Element	Wavelength (nm)	Slitwidth (μm)	Scale	Lamp current (mA)
Spectrophotometer				
Cd	228.8	160	5	4
Pb	283.3	160	1	4
Pb	217.0	320	1	4

Sample preparation

Phosphate rock and wet-process phosphoric acids. Weigh approximately 1 g of either material, transfer to a 150-ml beaker, add 20 ml of water, 3.2 ml of 16 M nitric acid, cover, and heat over low heat for 5 min. Cool and transfer to an appropriate volumetric flask so that the final concentration is 0.01—0.05 μg Cd ml^{-1} or 0.05—0.2 μg Pb ml^{-1}.

Plant tissue. Weigh 2.0 g of plant tissue into a porcelain dish and ash at 470°C for 5 h. Add 15 ml of 0.5 M HNO_3, warm to dissolve the ash, and dilute to volume in a 25-ml volumetric flask with 0.5 M HNO_3.

Procedure

With a 5-μl syringe, inject sample solutions or standards into the furnace and actuate the atomizer cycle. Record the absorbance by the peak area integration display counter. Triplicate readings of standards and unknowns are taken and averaged. Concentration is calculated from direct comparison of the unknowns to the standard solutions.

RESULTS AND DISCUSSION

In initial studies with the Model 63 graphite furnace, results were erratic for both cadmium and lead. Self-absorption occurred with cadmium at concentrations higher than 0.015 μg ml^{-1}. A larger furnace (1/4 in. o.d., 5/32 in. i.d., 3/8 in. long with 1/16 in. injection port) was constructed from surplus arc-lamp carbon rods. Results obtained with this larger furnace were more reproducible. Standard deviations for recovery of cadmium from repeated injections of standards using the small and large furnaces were 6.69 and 3.64%, respectively. Moreover, the upper limit of the standard curve could be increased from 0.015 to 0.05 μg Cd ml^{-1}. The standard deviations for recovery of lead at 283.3 nm for the small and large furnaces were even more striking, being 23.0 and 5.3%, respectively.

The effects of different acids on the determination of cadmium with both furnaces are presented in Fig. 1. The effect of $HClO_4$ is decreased significantly when the larger furnace is used. The data show that HNO_3 gives better sensitivity in both furnaces. The effect of different concentrations of HNO_3 is shown in Fig. 1B; obviously, the acidity of the samples and standards must be matched closely. Even though 0.1 M HNO_3 gave slightly greater sensitivities, 0.5 M HNO_3 was chosen because this concentration is more likely in sample digests.

The acidity in samples and standards should also be controlled carefully in the determination of lead. Comparison of HCl, HNO_3, and $HClO_4$ showed that all are suitable; HNO_3 was therefore used for all studies.

Interferences were studied by selecting seven different ions commonly found in phosphate materials to show the individual effects at three different levels on the determination of cadmium and lead. The results (Table 2) show that the only significant interference on cadmium is P_2O_5.

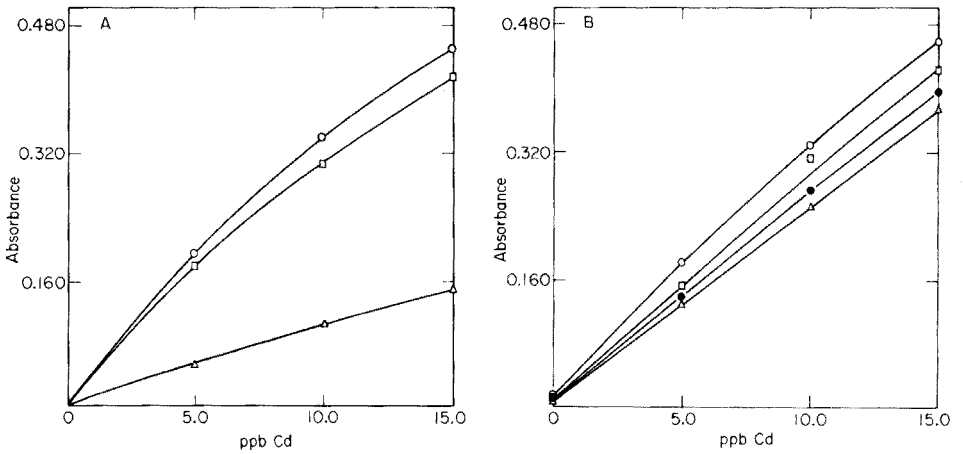

Fig. 1. Effect of various acids on determination of cadmium. (A) Small furnace. (B) Large furnace. ○ 0.1 M HNO_3. □ 0.1 M HCl. △ 0.1 M $HClO_4$. • 0.5 M HNO_3.

TABLE 2

Effects of individual ions on recovery of cadmium (0.025 μg ml^{-1}) and lead (0.1 μg ml^{-1})

Ion tested	Concn. (μg ml^{-1})	Cadmium	Concn. (μg ml^{-1})	Lead	
		Recovery (μg ml^{-1}) at 228.8 nm		Recovery (μg ml^{-1}) at	
				283.3 nm	217.0 nm
Ca	500	0.025	40	0.086	0.106
	1000	0.026	600	0.096	0.114
	2000	0.027	4000	0.105	0.100
K	250	0.026	20	0.098	0.098
	500	0.026	40	0.102	0.108
	1000	0.026	400	0.100	0.104
P_2O_5	400	0.019	400	0.116	0.104
	800	0.018	3000	0.102	0.072
	1600	0.018	6000	0.093	0.064
Mg	200	0.026	50	0.094	0.104
	400	0.026	60	0.105	0.108
	800	0.026	150	0.112	0.108
Fe	21	0.025	15	0.101	0.094
	43	0.024	100	0.112	0.098
	85	0.025	200	0.121	0.098
Al	30	0.024	30	0.098	0.095
	60	0.023	100	0.092	0.092
	120	0.024	200	0.102	0.094
Mn	6	0.026	12	0.086	0.104
	13	0.024	20	0.090	0.104
	25	0.024	200	0.112	0.104

The results for lead show that the only significant interference at 217.0 nm is P_2O_5 at the 3000—6000 $\mu g\ ml^{-1}$ level; repeated determinations of lead in standard solutions by carbon-rod atomization gave a standard deviation of ± 5.6%. Several ions gave recoveries at 283.3 nm that were more than 2 standard deviations from the true results, but only iron at the 200 $\mu g\ ml^{-1}$ level gave results more than 3 standard deviations from the true result. Many interference studies are conducted in this manner, and erroneous conclusions can be reached because the synergic effect of all matrix ions is not considered. A statistical technique proposed by Youden [14] has been used to study methods for "ruggedness" when small variations in procedural operations are introduced. A model of this technique was prepared to show the effect of matrix ions and their interactions on the determination of Cd and Pb. If seven matrix ions (Ca, K, P_2O_5, Mg, Fe, Al and Mn) are selected as variables, it is possible to have 128 combinations when the ions are studied at two levels; but with this model a subset of eight combinations can be chosen to give an elegant balance between the presence or absence of the seven ions. This model was suggested by Hinchen [15] to show the existence of effects on the property being measured.

To study these seven variables by this statistical model, synthetic samples containing a constant 0.025 μg Cd ml^{-1} were prepared that would closely represent matrix ions found in phosphate rock and plant tissue. The maximum values for phosphate rock were chosen on the basis of 0.3 g of material diluted to 100 ml. This represents the lowest level (4.4 $\mu g\ ml^{-1}$) of cadmium found in phosphate rock during this study. For cadmium in plant tissue the maximum variables were based on values obtained from a collaborative study of plant materials [16], with 2 g of material diluted to 25 ml. The low levels represent the absence of a matrix ion. The variables and results of these studies are shown in Table 3. Analysis of variance (Table 4) shows no significant interference from any of the ions at the levels studied.

Wet-process phosphoric acid was not studied because appropriate dilutions for the determination of cadmium would place the variables between or lower than those used in the phosphate rock and plant tissue studies.

Three phosphate rocks, three wet-process phosphoric acids, and three samples of ashed bean pods were analyzed by f.a.a.s.; the results are compared with a.a.s. results in Table 5. All results were in agreement, and only one sample required background correction. For the Florida phosphate rock, the a.a.s. results, without background correction, repeatedly were 8.0 $\mu g\ g^{-1}$ versus 4.4 $\mu g\ g^{-1}$ reported in Table 5. The absorbance values for cadmium in the bean pods by a.a.s. ranged from 0.014 to 0.022, while those by f.a.a.s. on the same materials ranged from 0.110 to 0.200. Considering the normal variations of absorbance values in a.a.s., results obtained by f.a.a.s. on materials low in cadmium will obviously be more reliable.

TABLE 3

Statistical test for interference on cadmium (0.25 μg ml^{-1}) in simulated solutions of phosphate rock and plant tissue

Source of variance	Concentration of indicated matrix ion (μg ml^{-1})							
Phosphate rock								
Ca	1200	1200	1200	1200	0	0	0	0
K	6	6	0	0	6	6	0	0
P_2O_5	900	0	900	0	900	0	900	0
Mg	15	15	0	0	0	0	15	15
Fe	30	0	30	0	0	30	0	30
Al	30	0	0	30	30	0	0	30
Mn	6	0	0	6	0	6	6	0
Replicate recovery (μg ml^{-1})	0.024	0.023	0.024	0.025	0.024	0.024	0.024	0.(
	0.025	0.026	0.024	0.024	0.023	0.025	0.023	0.(
	0.026	0.025	0.025	0.025	0.025	0.026	0.024	0.(
Sum of replicates	0.075	0.074	0.073	0.074	0.072	0.075	0.071	0.(
	[Average 0.024 μg Cd ml^{-1}; s^a = 0.0009631; range = 0.003]							
Plant tissue								
Ca	2000	2000	2000	2000	0	0	0	0
K	1000	1000	0	0	1000	1000	0	0
P_2O_5	1600	0	1600	0	1600	0	1600	0
Mg	800	800	0	0	0	0	800	800
Fe	85	0	85	0	0	85	0	85
Al	120	0	0	120	120	0	0	120
Mn	25	0	0	25	0	25	25	0
Replicate recovery (μg ml^{-1})	0.023	0.026	0.024	0.026	0.024	0.027	0.024	0.(
	0.024	0.027	0.026	0.026	0.026	0.027	0.026	0.(
	0.027	0.025	0.025	0.025	0.026	0.027	0.026	0.(
Sum of replicates	0.074	0.078	0.075	0.077	0.076	0.081	0.076	0.(
	[Average 0.026 μg Cd ml^{-1}; s = 0.001213; range = 0.004]							

[a] Standard deviation.

To study the effect of the seven variables on the determination of lead, synthetic samples containing a constant 0.1 μg Pb ml^{-1} were prepared that would closely represent matrix ions found in phosphate rock, wet-process acid, and plant tissue. The maximum values for phosphate rock and wet-process phosphoric acid were chosen on the basis of 1 g diluted to 100 ml. The maximum values for plant tissue were based on values obtained from a collaborative study of plant materials [16] with 1 g diluted to 50 ml. The variables and results of these interference studies are shown in Table 6. Analysis of variance (Table 7) shows no significant interference from any of the ions at the levels studied at 283.3 nm, or for wet-process phosphoric acid and plant tissue at 217.0 nm. A significant enhancement of lead in phosphate rock at 217.0 nm occurred under all conditions, and an analysis of variance was not performed.

TABLE 4

Analysis of variance for interferences on cadmium in simulated solutions of phosphate rock and plant tissue

Source of variance	Degree of freedom	Mean square ($\times 10^{-5}$)	F ratio
Phosphate rock			
Ca	1	0.2667	3.20
K	1	0.2667	3.20
P_2O_5	1	0.01667	0.20
Mg	1	0.06667	0.80
Fe	1	0.01667	0.20
Al	1	0.01667	0.20
Mn	1	0.1500	1.80
Error	16	0.083331	$F_{0.05}$ (1,16) = 4.49 $F_{0.01}$ (1,16) = 8.53
Plant tissue			
Ca	1	0.1500	1.03
K	1	0.06667	0.46
P_2O_5	1	0.6000	4.11
Mg	1	0.06667	0.46
Fe	1	0.000	0.00
Al	1	0.1500	1.03
Mn	1	0.01667	0.11
Error	16	0.14583	$F_{0.05}$ (1,16) = 4.49 $F_{0.01}$ (1,16) = 8.53

TABLE 5

Determination of cadmium by carbon-rod furnace and flame atomization

Sample	μg Cd g^{-1}	
	F.a.a.s.	A.a.s.
Florida rock	4.3	4.4[a]
North Carolina rock	39	38
Western rock	147	146
Florida acid	14	11
North Carolina acid	43	42
Western acid	120	109
Bean pods	0.12	0.17
	0.20	0.22
	0.11	0.14

[a] Background correction.

Lead was determined directly in phosphate rock and wet-process phosphoric acid by f.a.a.s. after acid dissolution, and the results (Table 8) are in excellent agreement with those obtained by dithizone concentration and back-extraction with 0.5 M HNO_3.

TABLE 6

Statistical test for interference on lead (0.1 $\mu g\ ml^{-1}$) in simulated solutions of phosphate rock, wet-process phosphoric acid and plant tissue

Source of variance	Concentration of indicated matrix ion ($\mu g\ ml^{-1}$)							
Phosphate rock								
Ca	4000	4000	4000	4000	0	0	0	0
K	20	20	0	0	20	20	0	0
P_2O_5	3000	0	3000	0	3000	0	3000	0
Mg	50	50	0	0	0	0	50	50
Fe	100	0	100	0	0	100	0	100
Al	100	0	0	100	100	0	0	100
Mn	20	0	0	20	0	20	20	0
Replicate recovery (283.3 nm)	0.111	0.105	0.094	0.107	0.095	0.097	0.098	0.1
	0.106	0.093	0.094	0.098	0.112	0.106	0.095	0.1
	0.093	0.092	0.120	0.089	0.100	0.088	0.102	0.0
Sum of replicates	0.310	0.290	0.308	0.294	0.307	0.291	0.295	0.3
[Average 0.100 μg Pb ml^{-1}; s = 0.0078; range = 0.032]								
Recovery (217.0 nm)	0.162	0.142	0.128	0.148	0.138	0.120	0.130	0.1
[Average 0.136 μg Pb ml^{-1}; s = 0.014; range = 0.042]								
Wet-process phosphoric acid								
Ca	40	40	40	40	0	0	0	0
K	40	40	0	0	40	40	0	0
P_2O_5	6000	0	6000	0	6000	0	6000	0
Mg	60	60	0	0	0	0	60	60
Fe	200	0	200	0	0	200	0	200
Al	200	0	0	200	200	0	0	200
Mn	200	0	0	200	0	200	200	0
Replicate recovery (283.3 nm)	0.097	0.091	0.091	0.114	0.114	0.092	0.093	0.1
	0.105	0.094	0.100	0.101	0.104	0.102	0.095	0.0
	0.094	0.102	0.113	0.098	0.103	0.113	0.100	0.1
Sum of replicates	0.296	0.287	0.304	0.313	0.321	0.307	0.288	0.3
[Average 0.101 μg Pb ml^{-1}; s = 0.00746; range = 0.023]								
Replicate recovery (217.0 nm)	0.095	0.100	0.107	0.113	0.099	0.097	0.101	0.1
	0.097	0.092	0.101	0.101	0.102	0.109	0.109	0.0
	0.106	0.101	0.106	0.095	0.096	0.096	0.099	0.1
Sum of replicates	0.298	0.293	0.314	0.309	0.297	0.302	0.309	0.3
[Average 0.101 μg Pb ml^{-1}; s = 0.00558; range = 0.021]								
Plant tissue								
Ca	600	600	600	600	0	0	0	0
K	400	400	0	0	400	400	0	0
P_2O_5	400	0	400	0	400	0	400	0
Mg	160	160	0	0	0	0	160	160
Fe	16	0	16	0	0	16	0	16
Al	30	0	0	30	30	0	0	30
Mn	12	0	0	12	0	12	12	0
Replicate recovery (283.3 nm)	0.094	0.091	0.094	0.100	0.103	0.106	0.109	0.0
	0.087	0.096	0.109	0.108	0.106	0.103	0.094	0.0
	0.098	0.096	0.087	0.102	0.092	0.094	0.098	0.1
Sum of replicates	0.279	0.286	0.290	0.310	0.301	0.303	0.301	0.2
[Average 0.099 μg Pb ml^{-1}; s = 0.0067; range = 0.022]								
Replicate recovery (217.0 nm)	0.102	0.111	0.098	0.094	0.100	0.093	0.107	0.1
	0.109	0.098	0.109	0.097	0.113	0.112	0.097	0.1
	0.099	0.098	0.100	0.105	0.101	0.110	0.096	0.1
Sum of replicates	0.310	0.307	0.307	0.296	0.314	0.315	0.300	0.3
[Average 0.103 μg Pb ml^{-1}; s = 0.00612; range = 0.020]								

TABLE 7

Analysis of variance for interferences on lead in simulated solutions of phosphate rock, wet-process phosphoric acid, and plant tissue

Source of variance	Degree of freedom	283.3 nm		217.0 nm	
		Mean square ($\times 10^{-4}$)	F ratio	Mean square ($\times 10^{-4}$)	F ratio
Phosphate rock					
Ca	1	0.01500	0.019	—	—
K	1	0.01667	0.0021	—	—
P_2O_5	1	0.7350	0.94	—	—
Mg	1	0.001667	0.0021	—	—
Fe	1	0.2817	0.36	—	—
Al	1	0.3750	0.48	—	—
Mn	1	0.1350	0.17	—	—
Error	16	0.78453		—	—
			$F_{0.05}$ (1,16) = 4.49 $F_{0.01}$ (1,16) = 8.53		
Wet-process phosphoric acid[a]					
Ca	1	0.02604	0.44	0.0004167	0.0011
K	1	0.03750	0.0064	0.9204	2.47
P_2O_5	1	0.02042	0.035	0.03375	0.090
Mg	1	0.1760	2.99	0.1204	0.32
Fe	1	0.002042	0.035	0.05042	0.14
Al	1	0.1170	1.99	0.03375	0.090
Mn	1	0.01204	0.20	0.03375	0.090
Error	16	0.058949		0.37331	
			$F_{0.05}$ (1,16) = 4.49 $F_{0.01}$ (1,16) = 8.53		
Plant tissues					
Ca	1	0.5704	1.14	0.3038	0.67
K	1	0.3504	0.70	0.2604	0.57
P_2O_5	1	0.2604	0.52	0.01042	0.023
Mg	1	0.7004	1.40	0.003750	0.0082
Fe	1	0.3504	0.70	0.4538	1.00
Al	1	0.02042	0.04	0.03375	0.074
Mn	1	0.1504	0.30	0.2604	0.57
Error	16	0.50202		0.45456	
			$F_{0.05}$ (1,16) = 4.49 $F_{0.01}$ (1,16) = 8.53		

[a]($\times 10^{-3}$).

A comparison of the determination of lead by f.a.a.s. and a.a.s. on phosphate rock and wet-process phosphoric acid was impossible because the dilutions necessary to fall within the limits tested made the final lead concentration too low to determine at 283.3 nm by a.a.s. However, a comparison of results for plant tissue (bean pods) was possible at 217.0 nm; the data (Table 8) are in excellent agreement.

TABLE 8

Comparison of methods for lead in different samples
(All results are given as $\mu g\ Pb\ g^{-1}$)

Sample	Direct[a]	Dithizone	Sample	F.a.a.s.	A.a.
North Carolina rock	4	4	Bean pods 7-1A	19	19
Western rock	11	12	7-1B	14	15
Florida rock	8	9	7-1C	17	19
North Carolina acid	0.4	0.5	7-7A	19	19
Western acid	2	3	7-7B	20	21
Florida acid	1	1	7-7C	18	19
			7-10A	17	18
			7-10B	7	7
			7-10C	8	9

[a]283 nm.

This investigation has shown clearly that the synergic effect of matrix ions should be considered in an interference study. In Table 2, the results for cadmium show that P_2O_5 must be lower than 400 $\mu g\ ml^{-1}$, yet 1600 $\mu g\ ml^{-1}$ of P_2O_5 was included with the other ions in the statistical model and no significant interference was noted. Likewise, for lead at 217.0 nm, none of the ions showed a significant interference on an individual basis, except for P_2O_5. Results for the statistical study in Table 6 show a significant enhancement under all conditions tested with an average positive bias of 36%. Nevertheless, the determination of cadmium and lead in fertilizer materials and plant tissue can be done by f.a.a.s. at 228.8 and 283.3 nm, respectively, with no significant interference from any of the matrix ions studied.

REFERENCES

1 P. P. Craig and E. Berlin, Environment, 13 (5) (1971) 2.
2 J. J. Dulka and T. H. Risby, Anal. Chem., 48 (1976) 640.
3 J. McCaull, Environment, 13 (7) (1971) 3.
4 H. A. Schroeder, Environment, 13 (8) (1971) 18, 29.
5 C. H. Williams, D. J. David and O. Iismaa, Commun. Soil Sci. Plant Anal., 3 (1972) 399.
6 E. Miwa and F. Yamazoe, Soil Sci. Plant Nutr., 17 (1971) 141.
7 M. J. Dudas, At. Absorpt. Newsl., 13 (1974) 109.
8 T. J. Ganje and A. L. Page, At. Absorpt. Newsl., 13 (1974) 131.
9 J. V. Lagerwerff and A. W. Specht, Environ. Sci. Technol., 4 (1970) 583.
10 H. L. Motto, R. H. Daines, D. M. Shilko and C. K. Motto, Environ. Sci. Technol., 4 (1970) 231.
11 A. L. Page and T. J. Ganje, Environ. Sci. Technol., 4 (1970) 140.
12 K. Fletcher, J. Sci. Food Agric., 22 (1971) 260.
13 H. L. Kahn, F. J. Fernandez, and S. Slavin, At. Absorpt. Newsl., 11 (1972) 42.
14 W. J. Youden, Statistical Techniques for Collaborative Tests, Association of Official Analytical Chemistry, Washington, DC, 1967.
15 J. D. Hinchen, Practical Statistics for Chemical Research, Associated Book Publishers, London, 1969, p. 62.
16 R. A. Isaac and W. C. Johnson, J. Assoc. Off. Agric. Chem., 58 (1975) 436.

Analytica Chimica Acta, 90 (1977) 137—141

EIN SCHWEFELSELEKTIVER DETEKTOR FÜR DIE FLÜSSIGKEITS-CHROMATOGRAPHIE AUF KONDUKTOMETRISCHER BASIS

H. MALISSA, J. RENDL und W. BUCHBERGER

Institut für Analytische Chemie und Mikrochemie der Technische Universität Wien, A-1060 Wien (Österreich)

(Eingegangen den 8. November 1976)

ZUSAMMENFASSUNG

Es wird ein konduktometrisches Verfahren zur Bestimmung von Schwefel in organischen Lösungmitteln beschrieben. Dabei wird die Probelösung im Sauerstoffstrom zerstäubt und das bei 1300° C entstehende SO_2 in eine Absorptionslösung geleitet, deren Leitfähigkeitszunahme registriert wird. Die Ansprechzeit liegt bei einer halben Minute und der Anwendungsbereich bei ca. 1—100 mmol S l^{-1}. Die bestehende Querempfindlichkeit auf N, P und Halogene wird diskutiert und eine Möglichkeit zur Ausschaltung der Halogen-Querempfindlichkeit angegeben.

SUMMARY

A conductometric procedure for the determination of sulfur in organic solvents is described. The sample is nebulized by a stream of oxygen and the sulfur dioxide produced by combustion at 1300° C is swept into an absorption solution, the increase in conductivity being recorded. The working range is about 1—100 mMol S l^{-1} and the response time about 30 s. Interferences of N, P and halogens are discussed. The halogen interference can be eliminated with silver wool, but the sensitivity for sulfur is then reduced.

Zu der im Rahmen einer Analyse notwendigen Auftrennung einer Probe in die einzelnen Komponenten stehen heute unter anderem die hochentwickelten chromatographischen Verfahren zur Verfügung. Demgegenüber ist die Entwicklung von — wenn möglich selektiven — Detektoren noch nicht abgeschlossen. Eine Übersicht über Detektoren für die Chromatographie wird z.B. bei Natusch und Thorpe [1] und Schomburg [2] gegeben.

Ziel dieser Arbeit war es, einen kontinuierlich arbeitenden schwefelselektiven Detektor auf konduktometrischer Basis mit möglichst raschem Ansprechverhalten zu entwickeln. Als Grundlage diente der von Bayer [3] entwickelte Analysenautomat zur Bestimmung des Gesamtschwefels in Abwässern.

DIE APPARATUR

Eine schematische Gesamtansicht der Apparatur ist in Abb. 1 wiedergegeben. Die Probe wird durch eine nach dem Prinzip einer Zweistoffdüse gefertigte Sprühdüse 1 im Sauerstoffstrom zerstäubt und in das Verbren-

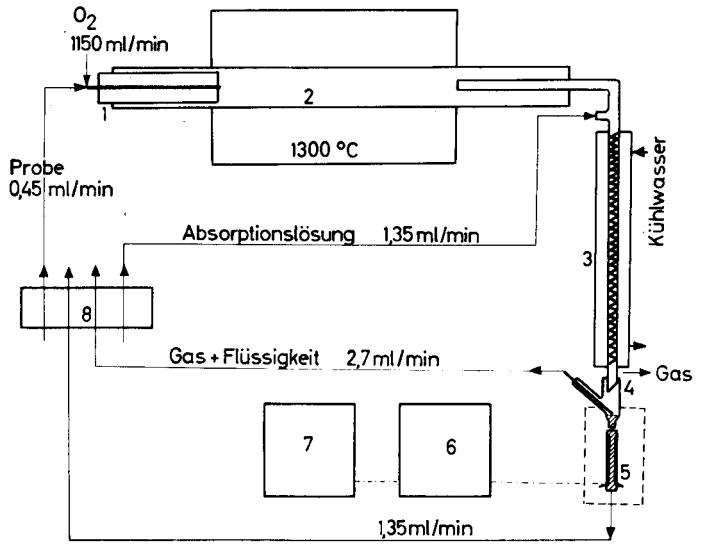

Abb. 1. Schematische Abbildung der Apparatur. 1 Einsprühdüse. 2 Verbrennungsrohr. 3 Absorptionseinheit. 4 Gas—Flüssigkeitstrenneinheit. 5 Meßzelle. 6 Leitfähigkeitsmeßgerät. 7 Kompensationsschreiber. 8 Schlauchquetschpumpe.

nungsrohr 2 aus Pythagoras eingesprüht, das mittels eines Silitstabofens auf 1300° C gehalten wird. Die bei diesem oxidativen Aufschluß entstehenden Verbrennungsgase werden durch den eingeblasenen Sauerstoff direkt aus der heißen Zone zur wassergekühlten Absorptionseinheit 3 gefördert. Diese besteht aus einem Silberrohr mit innen anliegender Silberdrahtspirale; damit soll einerseits bestmögliche Abkühlung der Verbrennungsgase und andererseits guter Stoffübergang beim Absorptionsvorgang erreicht werden. Die unmittelbar vor der Absorptionseinheit zugemischte Absorptionslösung enthält 0,5 ml 0,05 M H_2SO_4 + 0,5 ml 30%iges H_2O_2 pro Liter. In der Absorptionseinheit laufen im wesentlichen die Umwandlung des SO_2 zu H_2SO_4 und die Kondensation des Wasserdampfes ab.

Nach einer Trennung von Flüssigkeit und Gas in der Trenneinheit 4 strömt die Absorptionslösung durch die mit blanken Platinelektroden ausgestattete, thermostatisierte Meßzelle 5. Die durch die Neubildung von H_2SO_4 bedingte Konzentrationszunahme wird in einem Leitfähigkeitsmeßgerät nach Curran und Swarin [4] gemessen und mittels eines Kompensationsschreibers registriert. Innerhalb des Anwendungsbereiches der Methode (s. unten) ergab sich ein linearer Zusammenhang zwischen Schwefelgehalt der Probe und Schreiberausschlag.

Für nähere konstruktive Details der Apparatur sei auf [5] verwiesen.

Als Probe wurden zunächst in Wasser gelöste Schwefelverbindungen eingesetzt. Infolge der hohen Verdampfungswärme des Wassers kam es bei der Einsprühung allerdings zu einem Absinken der Ofentemperatur und damit zu

einer unvollständigen Umwandlung des in der Probe enthaltenen Schwefels in SO_2. Daher wurde zu brennbaren organischen Lösungsmitteln übergegangen, was insofern berechtigt erscheint, als nach einem vorausgegangenen Trennschritt die zu analysierende Substanz ohnehin häufig in organischen Lösungsmitteln gelöst vorliegt.

Testsubstanzen

Folgende Testsubstanzen wurden in Methanol als Lösungsmittel verwendet: 5-Sulfosalicylsäure Dihydrat, Alizarinsulfonsäure Natriumsalz, und Schwefelsäure.

Gemäß den aus Abb. 1 ersichtlichen Betriebsbedingungen (0,45 ml min^{-1} methanolische Probe, 1150 ml O_2 min^{-1}) ergibt sich bei der Verbrennung einer Probe mit einem Schwefelgehalt von 10^{-4} mol l^{-1} folgende Zusammensetzung der Verbrennungsgase: p_{O_2} = 0,51 atm., p_{H_2O} = 0,33 atm., p_{CO_2} = 0,16 atm., und $p_{SO_2} = 6{,}6 \cdot 10^{-7}$ atm (0,66 p.p.m.). Bei der Wahl der Verbrennungstemperatur muß das von Temperatur und Sauerstoffpartialdruck abhängige Gleichgewicht $SO_2 + \frac{1}{2}O_2 \rightleftharpoons SO_3$ berücksichtigt werden, das mit abnehmender Temperatur zugunsten der Bildung von SO_3 verschoben wird. Dagegen liegen bei 1300° C und einem Sauerstoffpartialdruck von 0,5 atm ca. 98% des Schwefels als SO_2 vor [6].

In der Absorptionskolonne, in der das aus dem Ofen kommende abgeschreckte, aber immer noch einige 100° C heiße Gas auf Kühlwassertemperatur abgekühlt und mit der Absorptionslösung in innigen Kontakt gebracht wird, sind folgende wesentliche Vorgänge zu beachten.

(a) Die Löslichkeit des SO_2 in der Absorptionslösung und die Umsetzung zu H_2SO_4. Die Löslichkeit des SO_2 in Wasser bei 15° C ist mit λ = 44 Ncm^3 g^{-1} atm^{-1}, bedeutend besser als die von CO_2. Nach thermodynamischen Gesichtspunkten liegt das Gleichgewicht für die Gesamtreaktion $SO_2 + H_2O_2 \rightleftharpoons H_2SO_4$ vollständig auf der Seite des H_2SO_4*. Der Umsatz ist aber vor allem abhängig von einem guten Stoffaustauch zwischen dem in sehr kleinen Konzentrationen vorliegenden SO_2 der Gasphase und der Reagenzlösung.

(b) Die Löslichkeit des CO_2 in der Absorptionslösung. Im Falle des CO_2 gilt für die Löslichkeit in Wasser bei 15° C λ = 0,987 Ncm^3 g^{-1} atm^{-1}. Damit ergibt sich bei p_{CO_2} = 0,16 atm. eine gelöste CO_2-Menge von 0,16 Ncm^3 ml^{-1}.

Die Gleichgewichtskonstante für die Reaktion

$$CO_2 + H_2O \rightleftharpoons H^+ + HCO_3^-$$

beträgt bei 15° C $3{,}8 \cdot 10^{-7}$. Daraus ergibt sich nach Lösung eines quadratischen Gleichungssystems, daß durch den CO_2 Einfluß der pH-Wert der verwendeten Absorptionslösung ($2{,}5 \cdot 10^{-5}$ M H_2SO_4) von 4,3 auf 3,9 absinkt.

*Die Normalpotentiale der beiden Teilreaktionen

$H_2SO_3 + H_2O \rightleftharpoons SO_4^{2-} + 4H^+$ $\quad E_0 = 0{,}14$ V

$2H_2O \rightleftharpoons H_2O_2 + 2H^+$ $\quad E_0 = 1{,}77$ V

unterscheiden sich um 1,63 V.

(c) Die Kondensation des Wasserdampfes. Diese bewirkt durch einen Auswascheffekt möglicherweise einen besseren Wirkungsgrad der Absorption. Darüber hinaus ist bei Verwendung methanolischer Lösungen und unter den gegebenen Betriebsbedingungen mit der Kondensation des Wasserdampfes eine Verdünnung der Absorptionslösung um ca. 30% verbunden.

Die unter (b) und (c) angegebenen Effekte haben jedoch bei Verwendung desselben Lösungsmittels einen konstant bleibenden Einfluß auf die Leitfähigkeit der Absorptionslösung. Diese daraus resultierende Leitfähigkeit entspricht daher der Nullinie (Bezugspunkt).

Zeitverhalten

Durch Optimierung der konstruktiven Parameter des Detektors wurde ein rasches Ansprechverhalten angestrebt. Die Totzeit beträgt 7—8 Sekunden, die 90% Zeit bei Anstieg des Schwefelgehaltes 25—30 Sekunden, bei Abfall 18—23 Sekunden.

ERFASSUNGSGRENZEN, STANDARDABWEICHUNGEN

Um eine Komponente noch sicher nachweisen zu können, muß die Signalhöhe ein bestimmtes Vielfaches k der Standardabweichung der Nullinie betragen. Der Wert k hängt von der geforderten statistischen Sicherheit ab und beträgt 2,5, wenn man eine Sicherheit von 99% zugrunde legt. Aus der Schreiberaufzeichnung einer Nullinie kann man nach Hieftje [7] die Standardabweichung als 1/5 der Schwankungsbreite annehmen. Dies erklärt sich daraus, daß die Abweichungen vom Mittelwert innerhalb eines Vertrauensbereiches von 99% nicht größer als das 2,5 fache der Standardabweichung sein werden. Da aber diese Abweichungen nach beiden Seiten gehen, kann man die Standardabweichung als 1/5 der Spitze—Spitzeabweichung leicht ermitteln.

Im vorliegenden Fall wurde als hauptsächliche Ursache für das Rauschen des Signals eine pulsierende Förderung durch die Schlauchquetschpumpe gefunden. Dadurch ist in der gegebenen Anordnung die Schwefelbestimmung in Richtung kleinerer Konzentrationen limitiert. Durch Verwendung eines geeigneteren Pumpensystems, das eine gleichmäßigere Förderung bewirkt, kann man wahrscheinlich zu geringeren Nachweisgrenzen gelangen.

Die von der Pumpe herrührenden und daher nicht zufälligen sägezahnartigen Schwankungen der Nullinie werden hier jedoch als zufälliges Rauschen bzw. Störung im Sinne von "noise" [7] behandelt. Daraus ergibt sich als Erfassungsgrenze eine Konzentration von $1{,}3 \cdot 10^{-6}$ mol S l^{-1} bzw. $4{,}2 \cdot 10^{-5}$ g S l^{-1} (entsprechend der Peakhöhe) bzw. bei einer Peakdauer von 1 Min (= zweifache 90% Zeit) eine Schwefelmenge von $6 \cdot 10^{-10}$ mol S bzw. $1{,}9 \cdot 10^{-8}$ g S (entsprechend der Peakfläche).

EICHUNG UND ANWENDUNGSBEREICH

Die Eichung des Detektors erfolgte mit Sulfosalicylsäure in Methanol und ergab einen linearen Zusammenhang zwischen Leitfähigkeit und Schwefel-

konzentration im Bereich von der Erfassungsgrenze ($1{,}3 \cdot 10^{-6}$) bis $5 \cdot 10^{-4}$ mol S l^{-1}. Diese obere Grenze kann durch Wahl einer anderen Konzentration der Absorptionslösung einerseits und durch Verkleinerung der eingesprühten Probemenge andererseits bei Bedarf zu höheren Werten verschoben werden.

QUEREMPFINDLICHKEIT

Um störende Einflüsse durch die Elemente Stickstoff, Phosphor, Chlor, Brom und Jod zu untersuchen, wurden folgende Substanzen (Testsubstanzen für die Elementaranalyse) verwendet: Harnstoff (p.A. Merck), Tribenzylphosphinoxid, 2-Chlorbenzoesäure, 4-Brombenzoesäure, 2-Jodbenzoesäure. Diese Substanzen wurden im Molverhältnis 1 : 1, Lösungen mit $5 \cdot 10^{-4}$ mol Sulfosalicylsäure/Liter Methanol zugemischt.

Die Selektivität des Detektors wurde mittels eines Verhältnisses K beurteilt, das wie folgend definiert ist

$$K = S_S/S_F$$

(S_S = Signalhöhe herrührend von Schwefel; S_F = Signalhöhe herrührend von äquimolarer Menge eines Fremdelementes.)
Die folgende Tabelle faßt die erhaltenen Ergebnisse zusammen:

$c_{Schwefel} = c_{Fremdelement} = 5 \cdot 10^{-4}$ mol l^{-1}

Fremdelement	N	P	Cl	Br	J
K	12,7	11,9	1,4	1,4	4,0

Zur Eliminierung des Störeinflusses der Halogene kann wie in der Elementaranalyse üblich Silberwolle verwendet werden. Dazu wird das Absaugrohr, durch das die Verbrennungsgase aus dem Verbrennungsrohr in die Absorptionskolonne gelangen, mit Silberwolle gefüllt. Unter diesen Bedingungen wird die Störung durch Halogene vollkommen unterdrückt allerdings sinkt dabei auch die S-Empfindlichkeit auf etwa ein Drittel.

Aus diesen Querempfindlichkeiten ergibt sich, daß der Einsatz von Lösungsmitteln, die Heteroelemente (Halogene, N, P) enthalten, nicht zulässig ist.

LITERATUR

1 D. F. S. Natusch und T. M. Thorpe, Anal. Chem., 45 (1973) 1184A.
2 G. Schomburg, Z. Anal. Chem., 277 (1975) 275.
3 E. Bayer, Dissertation am Institut für Analytische Chemie und Mikrochemie, T. H. Wien, 1973.
4 D. J. Curran und S. J. Swarin, Anal. Chem., 43 (1971) 358.
5 W. Buchberger, Diplomarbeit am Institut für Analytische Chemie und Mikrochemie, T. U. Wien, 1976.
6 J. D'Ans und E. Lax, Taschenbuch für Chemiker und Physiker, Band 1, 3. Aufl., Springer, Berlin, Heidelberg, New York, 1967.
7 G. M. Hieftje, Anal. Chem., 44 (1972) 81A.

Analytica Chimica Acta, 90 (1977) 143—150

APPLICATION OF THE THEORY OF KUBELKA AND MUNK TO DENSITOMETRY. PART II. SIMULTANEOUS REFLECTANCE AND TRANSMITTANCE DENSITOMETRY

F. A. HUF

Department of Pharmaceutical Analysis and Analytical Chemistry, Gorlaeus Laboratoria, State University, P.O. Box 75, Leiden (The Netherlands)

(Received 21st September 1976)

SUMMARY

The theory of Kubelka and Munk is evaluated for simultaneous measurement of reflectance and transmittance as a densitometric method. A relation yielding the amount of substance in a t.l.c. spot, as a function of its reflectance and transmittance, is derived. A densitometer operating according to this relation is described. To check the validity of the derived relation, measurements were made on spots of Sudan yellow developed with chloroform on silica layers. The results show a satisfactory proportionality between apparatus response and amount of substance applied.

Simultaneous measurement of reflectance and transmittance, as a densitometric method, is described by Treiber et al. [1, 2, 3] and Jork [4]. Simultaneous measurement results in a stable densitogram baseline when the densitometer is provided with a source of diffuse scattered light [5]. Measurements with a collimated light source will only give a stable baseline when the thickness of the absorbing layer is constant. The t.l.c. plates commercially available now have a much more constant layer thickness than those manufactured earlier [5]. Merck plates, type H60, are very satisfactory in this respect. In general, variations of only 5% were found, with occasional variations of up to 10%. However, even for constant layer thickness, the procedures described previously will generally not give a densitometer response proportional to the amount of substance present in the spot. When Jork's procedure [4] is followed, the densitometer response is only linear for spots with a low substance concentration, as shown in Appendix I. The linearity of the densitometer response obtained by Treiber is satisfactory but the calibration lines do not always pass through the origin [2, 3]. This deviation is probably imputable to the conversion of the relative reflectance by the Kubelka and Munk remission function, which is only applicable to media with an infinite layer thickness or, as shown in Appendix II, for media with relatively high values for the coefficients of scatter and absorbance. Additional critical notes about the procedure followed are given by Treiber [6]. The

simultaneous measurement of reflectance and transmittance as used in the above-mentioned densitometric methods is therefore subject to restrictions. This paper introduces a general procedure rather than another densitometric method.

In a previous paper [5], the theory of Kubelka and Munk was shown to be valid for transmission densitometry; the relation derived here, based on that theory, yields the substance concentration in a t.l.c. spot as a function of reflectance and transmittance values and is therefore directly suitable for densitometry. Furthermore, the relation shows a simple way of correcting the densitometer response in cases of fluctuating layer thickness. The measurement according to the derived relation also gives a stable densitogram baseline. As a consequence of a reduction in "optical noise", the detection limit is remarkably improved when compared with separate transmittance or reflectance measurements [4].

THEORY

The absorbing layer of a t.l.c. plate is a light scattering medium. The theory of Kubelka and Munk describes the light transmittance and reflection of such media; the transmittance T and reflectance R of the medium are related to the coefficients of scatter and absorbance in the following set of equations:

$$T = \frac{b}{a \sinh bSX + b \cosh bSX} \tag{1}$$

$$R = \frac{1 - R_g(a - b \operatorname{ctgh} bSX)}{(a + b \operatorname{ctgh} bSX) - R_g} \tag{2}$$

with X = thickness of the layer; S = coefficient of scatter; K = coefficient of absorption; R_g = reflectance of the supporting material; $a = S + K/S$; and $b = \sqrt{a^2 - 1}$.

When glass is the supporting material of the t.l.c. plate, R_g is usually ignored and eqn. (2) becomes:

$$R = \frac{1}{a + b \operatorname{ctgh} bSX} \tag{3}$$

From eqn. (1)

$$T^2 = \frac{b^2}{\sinh^2 bSX \, (a + b \operatorname{ctgh} bSX)^2}$$

and within

$$\operatorname{ctgh} bSX = \frac{\sqrt{1 + \sinh^2 bSX}}{\sinh^2 bSX}$$

this yields

$$T^2 = \frac{1 - a^2 + b^2\,(\text{ctgh } bSX)^2}{(a + b \text{ ctgh } bSX)^2}$$

Since $a^2 - b^2 = 1$,

$$T^2 = \frac{1 - 2a(a + b \text{ ctgh } bSX) + (a + b \text{ ctgh } bSX)^2}{(a + b \text{ ctgh } bSX)^2} \tag{4}$$

Substituting eqn. (3) in (4) yields $T^2 = R^2 - 2aR + 1$

so

$$a = \frac{R^2 + 1 - T^2}{2R}$$

and

$$\frac{K}{S} = \frac{[1 - (R - T)]\ [1 - (R + T)]}{2R}$$

or

$$KX = \frac{SX[1 - (R - T)]\ [1 - (R + T)]}{2R} \tag{5}$$

The amount of substance, m, in a t.l.c. spot is given by the surface integral of KX over the spot area [7]

$$m = \int_{\text{surface}} (KX)\, dS \tag{6}$$

Relationship (5) is therefore suitable for direct densitometric use. In contrast to eqns. (1) and (2) no hyperbolic forms appear in eqn. (5), and there is no need to invert eqn. (5) for densitometry. Inversion of eqns. (1) and (2) is quite difficult; an inversion has been published for only (1) so far [6]. Furthermore, the "optical noise" is eliminated. When the measurements are carried out with visible light the blank layer will not absorb ($KX = 0$) and the baseline equals zero because ($T + R$) = 1. A constant baseline is obtained for u.v. densitometry when the ratio K/S is calculated from T and R instead of KX. When the blank layer absorbs the incident light, the ratio K/S may be regarded as constant.

Finally, eqn. (5) shows a simple way of correcting the densitometer response when the layer thickness is not constant, because SX is directly proportional to the layer thickness. The value of SX can be obtained, for example, from

$$SX = \frac{R_0}{T_0} \tag{7}$$

where R_0 = reflectance of the blank layer in the visible part of the light spectrum, and T_0 = transmittance of the blank layer measured at the same wavelength as R_0. In the following, application of eqn. (5) is restricted to the

use of a densitometer provided with a visible light source. The indicated procedure is easily extended to densitometry with u.v. light.

EXPERIMENTAL

Apparatus

The apparatus described previously [5] was modified so that the t.l.c. plate makes a zig-zag movement with respect to two stationary detection systems (Fig. 1). Each detection system contains a circular aperture (0.25 mn an interference filter (499 nm) and a photomultiplier (RCA 6099). The photomultiplier currents are transformed to values of transmittance and reflectance by current amplifiers (Keithley). An analogue computing unit converts the values of transmittance and reflectance, T and R respectively, according to

$$D = \frac{[1 - (R - T)]\ [1 - (R + T)]}{2R} \tag{8}$$

where D is the output of the computing unit. The value of D is written by an integrating recorder (Kipp BD 12). The recorder shows continuously both the value of D and the integration value P of D over the scanned spot area. The t.l.c. spot is illuminated with a beam of collimated light at an angle of 60° to the normal on the thin layer.

Since SX is constant over the thin layer in this experiment there is no need for diffuse illumination and a simpler light source can be used than previously [5]. It is essential to illuminate the spot at 60° to obtain constant values for the effective coefficients of scatter and absorbance. With increasing light scattering the magnitude of these coefficients increases to twice those in a transparent medium.

Solutions (4 μl) containing different concentrations of Sudan yellow were

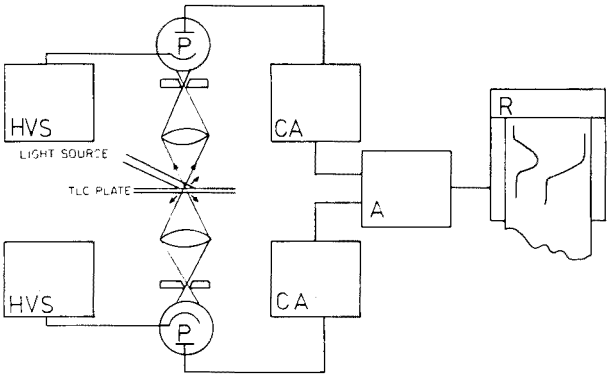

Fig. 1. HVS: High Voltage Supply (Keithley). P: Photomultiplier (RCA 6099). CA: Current amplifier (Keithley). A: Analogue computer. R: Integrating recorder (Kipp BD 12

applied to t.l.c. plates (Merck H60). On each plate, four different concentrations, giving m values from 0.10 to 0.52 μg, were used. The chromatograms were developed with chloroform over a distance of 10 cm. The spots were measured with the densitometer described above after drying for 1 h. The obtained P-values were multiplied by SX for each spot. According to eqn. (6), PSX should be equal to m. SX was calculated from the transmittance T_0 of the blank layer

$$SX = \frac{1 - T_0}{T_0} \tag{9}$$

Equation (9) follows from eqn. (1) as a limit for $KX \rightarrow 0$. The transmittance, measured at 499 nm with diffuse scattered light [5] was also used to adjust the densitometer before a spot was measured.

It would be more correct to multiply the densitometer response by SX before integration. To obtain this the analogue computing unit output D must be multiplied by SX continuously during the scanning of a spot. The SX values needed can be obtained according to eqn. (7) since T_0 and R_0 can be sampled at both sides of the spot during the zig-zag movement. A densitometer that operates in this way is under construction.

RESULTS

Table 1 shows the slopes S and the intercepts of the plots of PSX vs. m calculated by the least squares method for five densitograms. In addition, correlation coefficients and standard deviations for each line are given. The results are in good agreement with theory. There is a satisfactory proportionality between the densitometer response and the amount of Sudan yellow applied as shown by the correlation coefficients, the small values of the intercepts, and the standard deviations. The densitograms show a constant baseline signal equal to zero, even when fluctuations in the layer thickness occur. As a result the accuracy of densitometric analysis is remarkably improved, a much lower detection limit is possible, and densitometry has been simplified significantly.

The slopes S are comparable for different densitograms. It will be shown

TABLE 1

Parameters of regression lines obtained by plotting PSX vs. μg of Sudan yellow applied

Plate number	1	2	3	4	5
Slope S[a]	63.3	75.2	79.3	77.8	75.1
Intercept[a]	0.056	−0.329	−0.125	−0.087	0.165
Standard deviation (%)	2.40	1.87	1.63	0.61	1.97
Correlation coefficient	0.99971	0.99983	0.99986	0.99998	0.99980

[a]Integration units.

in a later communication that variations in S can be attributed to differences in the chromatographic conditions.

I thank Mrs. J. v. Gelder and J. H. C. Janmaat for the development of the analogue computing unit, and Miss M. A. Span for continued help.

APPENDIX 1

Simultaneous measurement of reflectance and transmittance for t.l.c. spots at low concentrations

In the procedure proposed by Jork [4, 8] the reflectance and transmittance values of the spot are added. Now the densitometer response is equal to the decrease in the sum of reflectance and transmittance

$$D = (T_0 + R_0) - (T + R) \tag{10}$$

where T_0 and R_0 are the transmittance and reflectance of the blank layer, and T and R are the transmittance and reflectance of the t.l.c. spot. The latter values are given by eqns. (1) and (3), which can be rewritten as

$$T = \frac{bSX/\sinh bSX}{KX + SX + bSX \operatorname{ctgh} bSX} \tag{11}$$

$$R = \frac{SX}{KX + SX + bSX \operatorname{ctgh} bSX} \tag{12}$$

In the visible part of the spectrum KX and bSX will be small for low substance concentration. Series expansion of the hyperbolic forms, neglecting second and higher terms of bSX, leads to

$$\frac{bSX}{\sinh bSX} = \frac{1}{1 + \frac{(bSX)^2}{3!} + \frac{(bSX)^4}{5!} + \ldots} \approx 1$$

$$bSX \operatorname{ctgh} bSX = 1 + \frac{(bSX)^2}{3} - \frac{(bSX)^4}{45} + \ldots \approx 1$$

Equations (11) and (12) then become

$$T = \frac{1}{KX + SX + 1} \quad \text{and} \quad R = \frac{SX}{KX + SX + 1}$$

respectively. For low concentration values, KX and bSX will be negligible compared with SX, and eqn. (10) becomes

$$D = \frac{KX}{SX + 1} \tag{13}$$

because $(T + R) = 1$ in the visible part of the spectrum. Therefore the decrease in $(T + R)$ is proportional to KX and from eqn. (6) a relationship suitable for densitometry is obtained.

Relation (13) shows the advantages of a constant baseline in the densitogram and the possibility of correcting the densitometer response for fluctuating layer thickness. However a restriction must be made. Relation (13) is only valid over a limited range of low concentrations.

APPENDIX II

The remission function for densitometric application

The Kubelka and Munk remission function is exactly valid only when the layer thickness of the medium is infinite. For such a medium (5) becomes

$$KX = SX \frac{(1 - R_\infty)^2}{2R_\infty} \tag{14}$$

because the transmittance T is now negligible compared with the reflectance R. The well-known remission function (14) will be shown to be suitable for thin layers when $bSX \geqslant 2$.
When $bSX \geqslant 2$, bSX ctgh $bSX = 1$
and from eqn. (3)

$$R = \frac{1 - R_g(a - b)}{(a + b) - R_g} \tag{15}$$

From eqn. (14)

$$R_\infty^2 - 2aR_\infty + 1 = 0$$

and

$$R_\infty = a - b \tag{16}$$

Because $a^2 - b^2 = 1$

$$R_\infty = \frac{1}{a + b} \tag{17}$$

Substituting eqns. (16) and (17) in (15) leads to

$$R = \frac{1 - R_g R_\infty}{1/R_\infty - R_g} \quad \text{and} \quad R = R_\infty.$$

Obviously the thickness of the layer may be regarded as infinite when $bSX \geqslant 2$. This condition is fulfilled in the visible part of the spectrum for relative high values of KX. A linear densitometer response is obtained with eqn. (14) only when the substance concentration in the t.l.c. spot is relatively high. Regression lines for m as a function of the densitometer response will not pass through the origin because eqn. (14) does not hold for low concentrations. Calculations with eqns. (3) and (14) show that the regression lines will have a negative intercept [3].

In the u.v. part of the spectrum the absorbing layer will absorb the incident light and the condition $bSX \geqslant 2$ is better met with decreasing wavelength of

the incident light [2]. Relation (14) shows the same advantages as relation (13), but relation (14) is only suitable for relatively high concentrations of substance.

REFERENCES

1 L. R. Treiber, R. Nordberg, S. Lindstedt and P. Stöllnberger, J. Chromatogr., 63 (1971) 211.
2 L. R. Treiber, J. Chromatogr., 100 (1974) 123.
3 L. R. Treiber, J. Chromatogr., 69 (1972) 399.
4 H. Jork, J. Chromatogr., 82 (1973) 85.
5 F. A. Huf, H. J. de Jong and J. B. Schute, Anal. Chim. Acta, 85 (1976) 341.
6 L. R. Treiber, J. Chromatogr., 123 (1976) 23.
7 J. B. Schute, H. J. de Jong and H. Dingjan, Ph. Weekbl., 105 (1970) 1025.
8 U. Hezel, Angew. Chem., 85 (1973) 334.

Analytica Chimica Acta, 90 (1977) 151—158
) Elsevier Scientific Publishing Company, Amsterdam — Printed in The Netherlands

CHEMICAL ANALYSIS OF MANGANESE NODULES
PART II. DETERMINATION OF URANIUM AND THORIUM AFTER ANION-EXCHANGE SEPARATION

. KORKISCH and I. STEFFAN

nstitute for Analytical Chemistry, Analysis of Nuclear Raw Materials Division, University of Vienna, Währingerstrasse 38, A-1090 Vienna (Austria)

. ARRHENIUS, M. FISK and J. FRAZER

Jniversity of California, Scripps Institution of Oceanography, Geological Research Division, La Jolla, California 92037 (U.S.A.)

Received 22nd November 1976)

SUMMARY

A method is described for the determination of uranium and thorium in manganese nodules. After dissolution of the sample in a mixture of perchloric and hydrofluoric acids, uranium is adsorbed on the strongly basic anion-exchange resin Dowex 1 (chloride form) from 6 M hydrochloric acid. The effluent is evaporated and the residue is taken up in 7 M nitric acid—0.25 M oxalic acid; thorium is then isolated quantitatively by anion-exchange on Dowex 1 (nitrate form). Thorium is eluted with 6 M hydrochloric acid and determined spectrophotometrically by the arsenazo III method. Uranium is eluted from the resin in the chloride form with 1 M hydrochloric acid and then separated from iron, molybdenum and other co-eluted elements on a column of Dowex 1 (chloride form); the medium consists of 50% (v/v) tetrahydrofuran, 40% (v/v) methyl glycol and 10% (v/v) 6 M hydrochloric acid. After removal of iron and molybdenum by washing the resin with a mixture of the same composition and with pure aqueous 6 M hydrochloric acid, the adsorbed uranium is eluted with 1 M hydrochloric acid and determined by fluorimetry. The method was used successfully for the determination of ppm-quantities of uranium and thorium in 30 samples of manganese nodules from the Pacific Ocean.

Uranium and thorium in manganese nodules have been determined by several investigators [1—9] who used a variety of analytical techniques including spectrophotometry [1—3], fluorimetry [9], and radiometry [4] as well as methods based on fission-track counting [5—7] and measurement of delayed neutrons [8].

Application of the methods in which uranium and thorium are determined by fluorimetry and spectrophotometry, respectively, requires the removal of interfering metal ions. For this purpose techniques based on ion-exchange [3, 9], solvent extraction [1] and coprecipitation [1] have been used for the isolation of either uranium [9] or thorium [1, 3].

The present paper reports a method for the determination of uranium and thorium in manganese nodule samples after isolation of these two elements by anion exchange in three different systems.

EXPERIMENTAL

Solutions and reagents

Ion-exchange resin. The strongly basic anion-exchanger Dowex 1-X8 (Bio-Rad AG1-X8; 100-200 mesh; chloride form) was used. Slurry the resin (4 g) with a few ml of 1 M hydrochloric acid and after about 30 min, pour into an ion-exchange column filled with the same acid. Subsequently pretreat the resin as mentioned in the Procedure.

Standard solutions. From aliquots of stock solutions containing 1.0 mg of UO_2(II) and 1.0 mg of Th(IV) per ml of 6 M hydrochloric acid, prepare dilute standard solutions of the elements in 6 M hydrochloric acid.

THF—MG—HCl mixture. This mixture consists of 50% (v/v) tetrahydrofuran (THF), 40% (v/v) methyl glycol (MG; monomethylether of ethylene glycol) and 10% (v/v) 6 M hydrochloric acid. The mixture can be stored for several months without loss of effectiveness.

Nitric acid—oxalic acid mixture. To 7 M nitric acid add solid oxalic acid to make the resulting solution 0.25 M in the latter acid.

Apparatus

The Teflon "bombs" (Perkin-Elmer Corporation) used for the dissolution of samples are cylindrical, thick-walled Teflon containers, of about 50-ml capacity, equipped with Teflon screwcaps.

The separations of uranium and thorium were done in ion-exchange columns of the type and dimensions described earlier [10, 11].

A Galvanek-Morrison fluorimeter, Mark V (Jarrel-Ash), and a Beckman DB-GT spectrophotometer (1-cm cells) were used.

Procedure

Dissolution of samples. The samples were dried at 110°C for two days and then kept in a desiccator until weighings were done. Transfer 200 mg of the sample to a Teflon "bomb" and add 1 ml of water, 5 ml of 72% perchloric acid and 10 ml of 40% hydrofluoric acid. Close the screw-cap tightly and heat the bomb for 48 h at 110°C in an oven. Allow to cool to room temperature, open the bomb, and transfer its contents to a platinum dish; use 20 ml of 40% hydrofluoric acid as a rinse. Evaporate the solution on a steam bath until hydrofluoric acid is removed, and then evaporate to dryness on a sand bath. Add 10 ml of perchloric acid, and evaporate to dryness on the sand bath. To the residue add another 10 ml of perchloric acid and evaporate to dryness again. Take up the residue in 10 ml of 2 M hydrobromic acid and transfer the solution to a 250-ml beaker; use 20 ml of 2 M hydrobromic acid as a rinse. Evaporate the solution to dryness on a steam-bath, take up the residue in 10 ml of concentrated hydrobromic acid and evaporate to dryness. Use another 10 ml of the same acid to repeat this evaporation step. Dissolve the residue in 10 ml of 6 M hydrochloric acid and, while evaporating on the steam-bath, add altogether 5 ml of 30% hydrogen peroxide at about equal

time intervals from the start to the end of the evaporation; use 1 ml of hydrogen peroxide for each addition. Dissolve the residue in 10 ml of 6 M hydrochloric acid and evaporate to dryness on the steam bath. Take up the residue in 6 M hydrochloric acid, allow to stand overnight, filter off any insoluble residue, rinse it with 6 M hydrochloric acid, and dilute the filtrate with the same acid to 50 ml (sample solution).

Ion-exchange separations. Pass the sample solution (see above) through an ion-exchange column (Column I) [10] containing 4 g of the anion exchanger (pretreated with 100 ml of 1 M hydrochloric acid and 50 ml of 6 M hydrochloric acid in that order) at a flow rate which corresponds to the back-pressure of the resin bed (about 0.7 ml min^{-1}). Subsequently, wash the resin bed with 50 ml of 6 M hydrochloric acid and combine this effluent with the effluent obtained when the sample solution was passed. (These combined effluents contain the thorium.) Elute uranium and co-adsorbed elements with 100 ml of 1 M hydrochloric acid and evaporate the eluate to dryness on the steam bath. Dissolve the residue in 5 ml of 6 M hydrochloric acid, and mix with 25 ml of tetrahydrofuran and 20 ml of methyl glycol; after 1 h pass the solution through an ion-exchange column (Column II) [11] containing 4 g of the anion exchanger (pretreated with 100 ml of 1 M hydrochloric acid and then with 100 ml of the THF—MG—HCl mixture) at a flow rate which corresponds to the back-pressure of the resin bed (about 0.2 ml min^{-1}). Afterwards, wash the resin bed with THF—MG—HCl mixture (100 ml) and 6 M hydrochloric acid (100 ml), and elute uranium with 100 ml of 1 M hydrochloric acid (uranium eluate).

Evaporate the combined effluents from Column I to dryness on the steam-bath. Take up the residue in 10 ml of concentrated nitric acid and evaporate on the steam-bath. Repeat this evaporation step using another 10 ml of this acid. Dissolve the final residue in 25 ml of the nitric acid—oxalic acid mixture, allow to stand overnight, filter off any insoluble residue, rinse it with nitric acid—oxalic acid solution, and dilute the filtrate with the same solution to 50 ml. Pass the solution through an ion-exchange column (Column III) [10] containing 4 g of the anion exchanger (pretreated with 100 ml of 6 M hydrochloric acid, 20 ml of water and 500 ml of 7 M nitric acid, in that order) at a flow rate corresponding to the back-pressure of the resin bed (about 0.6 ml min^{-1}). Subsequently, wash the resin bed with 150 ml of nitric acid—oxalic acid mixture and then with 50 ml of 7 M nitric acid. Elute thorium with 100 ml of 6 M hydrochloric acid (thorium eluate).

Determination of uranium. Evaporate the uranium eluate to dryness on a steam bath and carry out the fluorimetric determination of uranium as described previously [9, 11].

Determination of thorium. Evaporate the thorium eluate to dryness on a steam-bath. Dissolve the residue in 5 ml of 1 M hydrochloric acid, add 5 ml of 2% potassium permanganate solution (in case of complete decoloration add another 5 ml of permanganate solution) and evaporate to dryness on a steam bath. Take up the residue in 10 ml of concentrated hydrochloric acid,

evaporate to dryness (steam bath), dissolve the residue in 10 ml of 6 M hydrochloric acid and take to dryness again after addition of a few drops of concentrated formic acid. Repeat the evaporation with 10 ml of 6 M hydrochloric acid in the absence of formic acid, and dissolve the final residue in 5 ml of concentrated hydrochloric acid. Add 1 ml of freshly prepared and filtered 0.2% aqueous arsenazo III solution, and transfer to a 10-ml measuring flask; use water both as a rinse and to adjust the volume of the solution to 10 ml. Subsequently, measure the absorbance of the solution at 660 nm; for reference use a reagent blank solution prepared in the same way. Calculate the thorium content by comparison with a calibration curve obtained under the same experimental conditions.

Beer's law is valid up to 18 μg Th/10 ml. The absorbance for 5 μg Th/10 ml is 0.290 and the color of the Th—arsenazo III complex is stable for at least 4 h.

RESULTS AND DISCUSSION

Dissolution of samples

The dissolution method for nodule samples using Teflon "bombs" as described in the Procedure is much more efficient for dissolving thorium compounds than the dissolution procedure employed previously because thorium oxides and other compounds of this element that are present in manganese nodules may not dissolve completely when the samples are treated with hydrochloric acid only, as described in Part I of this series [9]. Furthermore, silica is removed completely by using the bomb procedure, so that practically no losses of thorium and/or uranium may occur because of incomplete dissolution.

The repeated evaporations with concentrated perchloric acid serve to transform all insoluble fluorides into soluble perchlorates.

The sample has to be transferred from the platinum dish to a beaker because the bromine which is evolved on subsequent treatment of the residue with hydrobromic acid, will damage (dissolve) the platinum. Treatment with hydrobromic acid is necessary to convert the perchlorates of the elements to chlorides and bromides. (Hydrochloric acid proved to be a much less efficient reducing agent for perchlorate). This reduction is necessary; if perchlorates were present in the sample solution (6 M hydrochloric acid), they would interfere seriously with the adsorption of uranium as the anionic chloride complex on Dowex 1 from 6 M hydrochloric acid. However, not only perchlorate but also bromide decreases the adsorption of uranium. Therefore, the residue of bromides (see Procedure) is treated with 6 M hydrochloric acid in the presence of hydrogen peroxide; the bromine formed is evaporated and the chlorides of the elements present are formed. To prevent the oxidation becoming too vigorous, the hydrogen peroxide is added portionwise during slow evaporation of the solution on the steam bath. The second evaporation with 10 ml of 6 M hydrochloric acid in absence of hydrogen

peroxide is required to destroy any peroxide present after the oxidation procedure.

Ion-exchange separations

On Column I uranium is strongly retained as the anionic chloride complex (K_d = 283) while thorium is not adsorbed from the 6 M hydrochloric acid but passes into the effluent quantitatively, together with all the other elements which do not form anionic chloride complexes under these conditions. Completely adsorbed together with the uranium are iron(III), molybdenum and zinc which are present in manganese nodules in relatively high concentrations so that they may displace the uranium from the resin during the sorption process if uranium is separated from much more than 200 mg of the original manganese nodule sample. Also retained from 6 M hydrochloric acid are cadmium, gallium, bismuth and some other trace constituents of manganese nodules; cobalt and copper are adsorbed to some extent but the bulk of these two elements passes into the effluent when, after the sorption of uranium, the resin is washed with 50 ml of 6 M hydrochloric acid. On elution of the uranium with 1 M hydrochloric acid, iron and molybdenum, as well as residual cobalt and copper are co-eluted, while zinc and the other elements are strongly retained by the resin.

Since iron, cobalt and copper interfere very seriously with the uranium determination by fluorimetry, they must be separated from the uranium. This is achieved by the second anion-exchange separation on Column II with the THF—MG—HCl system [11]. From this mixed solvent system, uranium, cobalt and copper are retained strongly by the resin while, because of the CIESE effect [11, 12], iron(III) and molybdenum pass into the effluent. Co-adsorbed cobalt and copper are removed by treatment of the resin with pure aqueous 6 M hydrochloric acid. Thus in the 1 M hydrochloric acid eluate of uranium no elements are present which might interfere with the fluorimetric uranium determination.

The repeated evaporations with concentrated nitric acid convert the chlorides contained in the evaporation residue of the combined effluents from Column I to nitrates, so that they cannot interfere with the adsorption of thorium on Dowex 1 from the 7 M nitric acid—0.25 M oxalic acid medium K_d = 189. Although adsorption of thorium as a negatively charged nitrate complex on Column III would also be quantitative in the absence of oxalic acid, this compound was found to be a very desirable ingredient because it prevented the formation of hydrated oxides of titanium and zirconium during the sorption process. In the absence of oxalic acid, titanium and zirconium tend to form insoluble compounds in 7 M nitric acid, which are difficult to filter and also frequently precipitate from the filtered solutions during the adsorption of thorium. In the latter case, not only does the insoluble material block the ion-exchange column but, since it cannot be removed with the 7 M nitric acid wash solution, titanium and zirconium are co-eluted partly when thorium is eluted with 6 M hydrochloric acid. Both titanium and zirconium

interfere strongly with the determination of thorium by the arsenazo III method. Whereas titanium causes a decrease in absorbance, zirconium reacts with arsenazo to form a complex which absorbs more strongly at 660 nm than thorium. The washing step with 7 M nitric acid which is employed after washing the resin with 150 ml of nitric acid—oxalic acid mixture, serves to remove oxalic acid as completely as possible. Consequently, the organic matter which passes into the 6 M hydrochloric acid—thorium eluate is kept to a minimum, and usually not more than 5 ml of the permanganate solution will be required for the complete destruction of the organic substances originating from a slight decomposition of the resin. Manganese dioxide, which is formed during the oxidation process, is dissolved by evaporation of the residue with concentrated hydrochloric acid; any nitrates that might still be present are destroyed with formic acid in the presence of hydrochloric acid. If these oxidation and reduction procedures are omitted, the absorbance of the solution decreases very rapidly so that reliable measurements of thorium cannot be made.

Application to manganese nodules

Table 1 gives the results obtained when the described procedure was applied. Comparison of the results for uranium in columns A, B and C shows not only that added amounts of uranium were recovered quantitatively (compare columns A and B) but also that good agreement exists between the uranium concentrations determined by the described procedure and those obtained after isolation of the uranium by the hexone—isopropanol—HCl method described earlier [9] (compare column C with columns A and B). There is also agreement between the uranium results obtained by fluorimetry and by the spectrophotometric arsenazo III method [13].

Comparison of the results of thorium determinations in columns A and B shows that, as in the case of uranium, the added amounts of thorium were recovered quantitatively.

The procedure described was used to analyse a total of 60 manganese nodule samples for uranium and thorium. The results obtained are in reasonably good agreement (i.e. fall in the same range) with those found in other nodules by other investigators (Table 2). While the uranium contents of the samples show relatively little variation (2.6—17 ppm), there is a much wider spread in the thorium concentrations (5.7—48 ppm). Uranium is much less enriched in manganese nodules than is thorium; this is due to the high stability of the uranyl carbonate complex in sea water [14]. The mechanisms of enrichment of uranium, thorium and other rarer elements in marine manganese nodules have been discussed thoroughly by Glasby [14, 15].

Geochemical interpretations of the results shown in Tables 1 and 2 will be presented at a later date.

TABLE 1

Results of determinations of uranium and thorium in manganese nodules from the Pacific Ocean
(A = Results obtained by application of the procedure. B = Same as under A but after deduction of known amounts of uranium and thorium which were added to the samples before their dissolution. The numbers in parentheses show the amounts in μg of uranium and thorium added. C = Results obtained after separation of uranium by the hexone—isopropanol—HCl method [9].)

Sample	Uranium (ppm)			Thorium (ppm)	
	A	B	C	A	B
1	3.76 3.75[a]	3.31 (5)	3.43	46.75	46.91 (50)
2	6.81	6.60 (5)	6.13	18.95	17.00 (20)
3	2.60 2.20[a]	2.60 (5)	2.45	10.96	10.35 (10)
4	9.02	8.82 (10)	8.65	26.75	28.32 (30)
5	12.74 10.00[a]	11.70 (10)	10.25	42.00	41.76 (40)
6	15.30 14.90[a]	15.10 (15)	15.02	6.67	6.33 (10)
7	5.47	5.44 (5)	5.14	28.38	26.64 (30)
8	7.16	6.79 (5)	7.08	25.77	24.48 (30)
9	17.02	16.80 (15)	16.64	10.85	11.84 (10)
10	7.63	7.17 (5)	7.43	31.13	30.16 (30)
11	4.07	4.09 (5)	3.50	14.93	14.39 (10)
12[b]	4.52 4.76[a]	4.08 (5)	3.99	21.24	20.57 (20)

[a]Determined by the spectrophotometric arsenazo (III) method [13].
[b]Manganese nodule standard GRLD 126 (Kennecott Exploration Inc., San Diego, California). In this sample thorium concentrations of 19 and 22 ppm have been measured in other laboratories.

TABLE 2

Uranium and thorium contents of Pacific Ocean nodules

Number of nodule samples analysed	Ranges found[a]		Reference
	Uranium (ppm)	Thorium (ppm)	
60	2.6—17 (F)	5.7— 48 (S)	This paper
17	5.1—14.3 (F)	—	[9]
10	3.6—13.9 (DNC)	—	[8]
8	6.0—14.0 (FTC)	—	[5]
4	5.0—7.0 (FTC; APTA)	18 — 32 (FTC; APTA)	[6]
8	—	4 — 26 (R)	[4]
6	—	5 — 84 (S)	[3]
6	—	13 — 86 (S)	[2]
4	—	24 —124 (S)	[1]

[a]The methods used are indicated in parentheses. F = fluorimetry. FTC = fission-track counting. S = spectrophotometry. APTA = α-particle track analysis. DNC = delayed neutron counting. R = radiometry.

This research was sponsored in part by the Fonds zur Förderung der wissenschaftlichen Forschung, Vienna, Austria, and the U.S. Bureau of Mines (Grant GO 264024). Samples were supplied by Lamont-Doherty Geological Observatory and the Scripps Institution of Oceanography. The generous support from these sources is gratefully acknowledged.

REFERENCES

1 E. D. Goldberg and E. Picciotto, Science, 121 (1955) 613.
2 J. Korkisch and G. E. Janauer, Anal. Chem., 33 (1961) 1930.
3 G. Arrhenius, J. Mero and J. Korkisch, Science, 144 (1964) 170.
4 W. M. Sackett, Science, 154 (1966) 646.
5 H. Yabuki, Sci. Pap. Inst. Phys. Chem. Res. Jpn., 65 (1971) 100.
6 H. Yabuki and M. Shima, Sci. Pap. Inst. Phys. Chem. Res. Jpn., 47 (1971) 27.
7 M. Shima, H. Yabuki and A. Okada, Sci. Pap. Inst. Phys. Chem. Res. Jpn., 69 (1975) 130.
8 T. Mo, A. D. Suttle and W. M. Sackett, Geochim. Cosmochim. Acta, 37 (1973) 35.
9 J. Korkisch, H. Hübner, I. Steffan, G. Arrhenius, M. Fisk, and J. Frazer, Anal. Chim. Acta, 83 (1976) 83.
10 W. Koch and J. Korkisch, Mikrochim. Acta, (1972) 687.
11 J. Korkisch and I. Steffan, Mikrochim. Acta, (1972) 837.
12 J. Korkisch, Sep. Sci., 1 (1966) 159.
13 J. Korkisch and H. Hübner, Talanta, 23 (1976) 283.
14 G. P. Glasby, Naturwissenschaften, 62 (1975) 133.
15 G. P. Glasby, Mar. Chem., 1 (1972–73) 105.

Analytica Chimica Acta, 90 (1977) 159—165

EIN HOCHSPEZIFISCHES EXTRAKTIONSKATALYMETRISCHES VERFAHREN ZUR BESTIMMUNG VON EISENSPUREN IN REINSTEN SALZEN DES KOBALTS, NICKELS UND KUPFERS

MATTHIAS OTTO und HELMUT MÜLLER

Sektion Chemie der Karl-Marx-Universität Leipzig (D.D.R.)

(Eingegangen am 3. September 1976)

ZUSAMMENFASSUNG

Die Selektivität einer Eisenbestimmung, die auf der katalytischen Wirkung von Eisen auf die Reaktion zwischen *p*-Phenetidin und Wasserstoffperoxid beruht, kann durch Kombination mit einem Trennverfahren wesentlich erhöht werden. Eisenspuren werden von der Matrix durch Extraktion mit MIBK aus 7 M LiCl-Lösung abgetrennt. Die katalytische Bestimmung des Eisens erfolgt direkt im Extrakt unter Verwendung einer Mischung aus Wasser, Äthanol und den Reagenzien der Indikatorreaktion. Spuren von Eisen können mit diesem extraktionskatalymetrischen Verfahren in Co-, Ni- und Cu-Salzen sowie in Lithiumchlorid und Magnesiumsulfat mit geringem apparativen und zeitlichen Aufwand zwischen $5 \cdot 10^{-6}$ und 10^{-3}% bei relativen Fehlern von 6—10% bestimmt werden.

SUMMARY

The selectivity of the determination of iron based on the catalytic action of iron on the oxidation of *p*-phenetidine by hydrogen peroxide, can be increased greatly by a preliminary extraction of iron with MIBK from 7 M LiCl solution. The catalytic determination of the extracted iron can be done directly in the extract by using a mixture with water, ethanol and the reagents of the indicator reaction. A simple and rapid procedure allows traces of iron ($5 \cdot 10^{-6}$—10^{-3}%) to be determined in Co, Ni and Cu salts and in LiCl and $MgSO_4$. The standard deviation is about 6—10%.

Katalytische Analysenmethoden werden seit einigen Jahren insbesondere zur Metallspurenbestimmung in steigendem Maße angewendet. Das Nachweisvermögen solcher Methoden ist vergleichbar mit anderen spurenanalytischen Verfahren, ihre Selektivität ist jedoch häufig geringer [1]. Eine Erhöhung der Selektivität kann durch Modifizierung der katalytischen Bestimmung erfolgen. Besonders selektive Verfahren sind durch Vorschalten eines Trennschrittes vor die katalytische Bestimmung ausgearbeitet worden. Sehr effektvoll ist die Kombination von Solvent-Extraktion und katalytischer Bestimmung. Die Attraktivität derartiger Verfahren leidet allerdings in vielen Fällen darunter, daß die abgetrennte Probe nicht direkt in die katalytische Reaktion eingesetzt werden kann, sondern daß eine Aufarbeitung des organischen Extraktes notwendig ist und damit die Analysenzeit erhöht und die Genauigkeit verringert wird.

Eine Aufarbeitung des Extraktes läßt sich umgehen, wenn es gelingt, das abgetrennte Metallion direkt im organischen Extrakt katalytisch zu bestimmen. Die katalytische Reaktion kann dabei in gemischt-wäßriger oder in nicht-wäßriger Phase ablaufen. Für eine direkte katalytische Bestimmung des Metallions im Extrakt schlagen wir den Begriff "Extraktionskatalymetrie" vor. Die Vorteile der neuen Arbeitstechnik sollen an Hand einer extraktionskatalymetrischen Bestimmung von Eisenspuren in verschiedenen Salzen demonstriert werden.

Als Indikatorreaktion zur Bestimmung von Eisen wurde die Oxydation von *p*-Phenetidin durch H_2O_2 mit 1,10-Phenanthrolin als Aktivator verwendet [2, 3]. Neben Eisen katalysieren u.a. auch Kobalt, Nickel und Kupfer die Reaktion, so daß eine Bestimmung von Eisen bei Überschuß dieser Elemente nicht möglich ist. Kombiniert man die katalytische Bestimmung jedoch mit einem geeigneten Extraktionsverfahren, so kann man Spuren von Eisen sogar in Salzen dieser Metalle analysieren. Durch Extraktion aus Lithiumchlorid mit Methylisobutylketon (MIBK) [4] konnte Eisen in reinsten Salzen von Kobalt, Nickel und Kupfer bei Gehalten zwischen $5 \cdot 10^{-6}$% und 10^{-3}% extraktionskatalymetrisch bestimmt werden.

EXPERIMENTELLES

Reagenzien und Apparate

Alle nicht gesondert angeführten Reagenzien waren vom Reinheitsgrad p.A. oder "reinst", MIBK der Reinheit "zur Extraktion". Es wurde bidestilliertes Wasser und 96%-iges Äthanol p.A. verwendet.

Eisenstammlösung (2,7 mg Fe(III) ml^{-1}). Für die Stammlösung wurde $FeCl_3 \cdot 6H_2O$ in 0,1 M HCl gelöst und der Gehalt komplexometrisch ermittelt. Als Arbeitslösungen dienten täglich frisch hergestellte Verdünnungen in 10^{-2} M HCl.

p-Phenetidinhydrochloridlösung ($7{,}5 \cdot 10^{-2}$ M). *p*-Phenetidin (Fluka, Schweiz) wurde fraktioniert destilliert, unter Eiskühlung in 11 M HCl eingetropft, das ausfallende Hydrochlorid mit wenig eiskaltem Wasser gewaschen, bei 50° C getrocknet und zweimal aus bidestilliertem Wasser umkristallisiert. Die entsprechenden Lösungen, die durch Einwägen hergestellt und in braunen Flaschen aufbewahrt wurden, waren über Wochen stabil.

Wasserstoffperoxidlösung (0,1 M). 30%iges H_2O_2 wurde mit Wasser verdünnt und der Gehalt volumetrisch mit Kaliumpermanganat bestimmt.

HCl der Reinheit p.A. ist isotherm destilliert [5], entsprechend verdünnt und zur Gehaltsbestimmung titriert worden. Kaliumbiphthalat p.A. wurde zweimal aus bidestilliertem Wasser umkristallisiert und mit Äthanol und Äther gewaschen. Die Lithiumchloridlösungen wurden durch Einwägen von $LiCl \cdot H_2O$ präpariert. Eisenspuren wurden nach Ansäuern der Lithiumchloridlösung mit HCl und Hinzufügen weniger Tropfen Perhydrol durch Extraktion mit MIBK entfernt.

Zur Registrierung der Extinktions-Zeit-Kurven verwendeten wir ein Spektralphotometer Spekol in Verbindung mit dem Extinktionsmeßansatz EK5 Aut und einem Kompensationsschreiber G1B1 (alle VEB Carl Zeiss Jena, D.D.R.). Der Geräteaufbau und die Arbeitsweise wurden bereits beschrieben [6].

Katalytische Bestimmung

In ein vierschenkliges Reaktionsgefäß werden in den ersten Schenkel 1 ml wäßrige *p*-Phenetidinlösung ($7{,}5 \cdot 10^{-2}$ M) und 3,5 ml äthanolische 1,10-Phenanthrolinlösung ($2{,}14 \cdot 10^{-4}$ M), in den zweiten 1 ml (0,1 M) H_2O_2, in den dritten 1 ml 0,25 M Kaliumbiphthalatlösung und 0,5 ml 0,5 M HCl sowie in den vierten Schenkel 3 ml MIBK-Extrakt gegeben. Es werden gleichzeitig vier Reaktionen angesetzt (Blindprobe und 3 Bestimmungen). Man thermostatiert die Reaktionsgefäße 10 min bei 25°C oder 40°C, und anschließend werden die Reaktionen alle 15 s durch Schütteln der Reaktionsgefäße gestartet. Nach Einfüllen der Reaktionsmischungen in 5 cm-Küvetten wird die Extinktion der Lösung bei 536 nm in einem thermostatierten Meßansatz gemessen. Die Registrierung beginnt nach ca. 3 min durch Einschalten des Papiertransportes und der Antriebswelle für den Küvettenwechsel. Der Reaktionsverlauf wurde über 10 min verfolgt. Die Auswertung erfolgte nach der Tangentenmethode [7]. Dazu mißt man die Differenz zwischen der zeitlichen Extinktionsänderung der Reaktion in Anwesenheit von Eisen ($\Delta E_{ges}/\Delta t = tg\alpha_{ges}$) und der Blindreaktion ($\Delta E_0/\Delta t = tg\alpha_0$).

Extraktionsverfahren

Lithiumchloridlösung (3,5 ml 10 M), 10 μl Perhydrol und die zu untersuchende Probe werden auf 5 ml mit Wasser aufgefüllt und mit 5 ml MIBK 1 min geschüttelt. Die organische Phase wird abgetrennt, 1 min zentrifugiert und 3 ml davon in die katalytische Reaktion eingesetzt.

ERGEBNISSE UND DISKUSSION

Auswahl des Extraktionsmittels

Für ein extraktionskatalymetrisches Verfahren können zur Abtrennung von Eisen aus Chloridlösungen Methylisobutylketon (MIBK), Diisopropyläther (DIPÄ), Butylacetat (BuOAc) oder Tributylphosphat (TBP) verwendet werden [8]. Die Extraktionsmittel beeinflussen die Fe-katalysierte Reaktion, die in einem Gemisch aus Wasser und Äthanol durchgeführt wurde, nicht oder nur unwesentlich (Tab. 1). Die Schwankungen der katalytischen Aktivität bis zu 12% bei Verwendung unterschiedlicher Solventien resultieren aus pH-Unterschieden, die sich in Gegenwart bzw. Abwesenheit der organischen Lösungsmittel ergeben. Eine Extraktion aus stark salzsauren Lösungen erwies sich als ungünstig, da zu viel Säure mit in die organische Phase übergeht und dadurch der pH-Wert der Reaktionsmischung nicht konstant gehalten werden kann. Statt Salzsäure verwendeten wir ein

TABELLE 1

Einfluß organischer Lösungsmittel auf die Fe-katalysierte Oxydation von *p*-Phenetidin durch H_2O_2 mit 1,10-Phenanthrolin als Aktivator
($7{,}5 \cdot 10^{-3}$ M *p*-Phenetidin; $7{,}5 \cdot 10^{-5}$ M 1,10-Phenanthrolin; 10^{-2} M H_2O_2; $8 \cdot 10^{-7}$ M Fe(III); $pH_{gem} = 2.5$)

Solvens	Anteil des Solvens, Vol%	Anteil von Äthanol, Vol%	Relative katalyt. Aktivität bezogen auf die Reaktion ohne Solvens (%)
MIBK	bis 30	35	112
DIPÄ	10	50	95
BuOAc	25	50	108
TBP	10	50	88

Metallchlorid, wofür Lithiumchlorid am geeignetsten ist [4]. Aus Lithiumchlorid kann Eisen(III) gut mit MIBK extrahiert werden [4]. Dabei geht kein Lithiumsalz mit in die organische Phase über, und das Extraktionssystem ist für eine nachfolgende katalytische Bestimmung des Eisens im Extrakt sehr geeignet. Als Reaktionsmischung wurde ein Gemisch aus 30 Vol% MIBK, 35 Vol% Äthanol und 35 Vol% Wasser eingesetzt.

Blindreaktion und Einfluß der Reaktionsvariablen

Für die katalytische Reaktion in gemischt-wäßriger Lösung ergaben sich relativ hohe Blindwerte, die von Verunreinigungen der Reagenzien herrührten. Bei Zusatz von ÄDTA wurde jedoch eine deutliche Verminderung der Blindreaktion beobachtet (Abb. 1). Es war dadurch möglich, eine Reinigung der Reagenzien zu umgehen, indem die Verunreinigungen durch eine geeignete Konzentration an ÄDTA maskiert wurden. Um zu vermeiden, daß durch

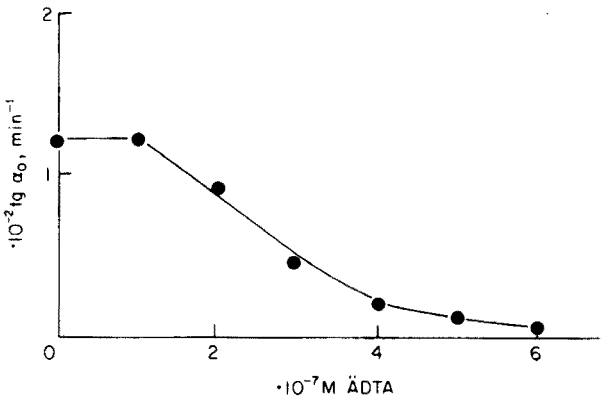

Abb. 1. Einfluß von ÄDTA auf die Blindreaktion. $7{,}5 \cdot 10^{-3}$ M *p*-Phenetidin; 10^{-2} M H_2O_2; $7{,}5 \cdot 10^{-5}$ M 1,10-Phenanthrolin; $pH_{gem} = 2{,}5$; 30 Vol% MIBK; 35 Vol% Äthanol; $t = 25°$ C.

überschüssiges ÄDTA auch Eisen aus der Probe komplexiert wird, setzten wir ÄDTA zusammen mit der Salzsäure substöchiometrisch in einer Konzentration von $3 \cdot 10^{-7}$ M zu (siehe Abb. 1).

Die Einstellung des pH-Wertes in der gemischt-wäßrigen Reaktionsmischung erfolgte unter Verwendung eines Phthalatpuffers [3]. Es wurde eine konstante Konzentration an Kaliumbiphthalat vorgelegt und der pH-Wert durch Zufügen von verdünnter Salzsäure eingestellt. Als Bezugsskala dienten die potentiometrisch (Glaselektrode | Probell KNO_3 || SCE) gemessenen pH-Werte, die in der Mischung aus Wasser, Äthanol und MIBK konditionelle Größen darstellen. Die Abhängigkeit der Reaktionsgeschwindigkeit der katalytischen Reaktion von den gemessenen pH-Werten (Abb. 2) weist als günstigsten Wert einen pH_{gem} von 2,5 aus. Bei Verwendung einer $2{,}5 \cdot 10^{-2}$ M Kaliumbiphthalatlösung entspricht dies einer HCl-Konzentration von $2{,}5 \cdot 10^{-2}$ M.

Das Oxydationsmittel H_2O_2 konnte maximal in einer Konzentration von 10^{-2} M eingesetzt werden. Eine Erhöhung der H_2O_2-Konzentration verringerte die Empfindlichkeit der Reaktion, da dabei in der gemischt-wäßrigen Reaktionsmischung die Geschwindigkeit der Blindreaktion größer und die der Reaktion in Anwesenheit von Eisen kleiner wurde. Die Konzentrationen von *p*-Phenetidin ($7{,}5 \cdot 10^{-3}$ M) und 1,10-Phenanthrolin ($7{,}5 \cdot 10^{-5}$ M) sind den Untersuchungen der Reaktion in wäßrigem Medium [3] entnommen worden.

Der Einfluß der Temperatur auf die Reaktionsgeschwindigkeit in gemischt-wäßriger Lösung ist in Abb. 3 dargestellt. Die Abhängigkeit ist der in Wasser erhaltenen vergleichbar [2].

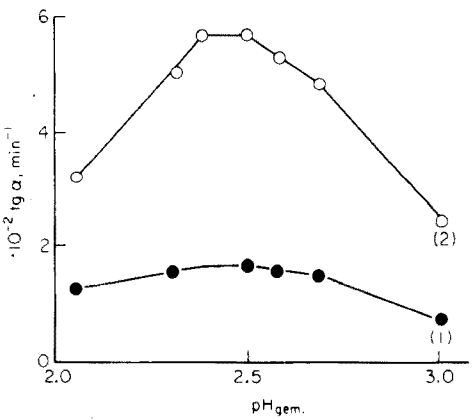

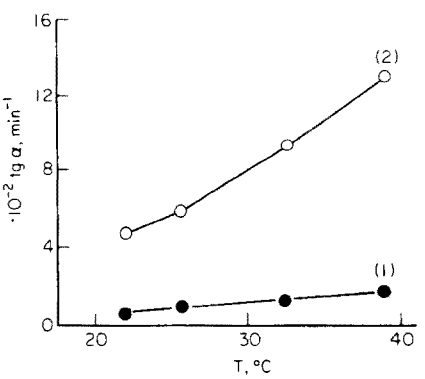

Abb. 2. Abhängigkeit der Reaktionsgeschwindigkeit vom pH-Wert. 1-Blindreaktion, 2-Reaktion mit Eisen. $7{,}5 \cdot 10^{-3}$ M *p*-Phenetidin; 10^{-2} M H_2O_2; $2{,}5 \cdot 10^{-2}$ M KHPhthalat; $7{,}5 \cdot 10^{-5}$ M 1,10-Phenanthrolin; $9 \cdot 10^{-7}$ M Fe(III); 30 Vol% MIBK; 35 Vol% Äthanol; $t = 25°$ C.

Abb. 3. Temperaturabhängigkeit der Reaktion in gemischt-wäßriger Lösung. 1-Blindreaktion, 2-Reaktion mit Eisen. $7{,}5 \cdot 10^{-3}$ M *p*-Phenetidin; 10^{-2} M H_2O_2; $7{,}5 \cdot 10^{-5}$ M 1,10-Phenanthrolin; $3 \cdot 10^{-7}$ M ÄDTA; 10^{-6} M Fe(III); 30 Vol% MIBK; 35 Vol% Äthanol; $pH_{gem} = 2{,}5$.

Eichkurven

Bei Wahl der günstigsten Reaktionsbedingungen (siehe Tab. 2) erhielten wir für eine extraktionskatalymetrische Bestimmung von Eisen bei einer Reaktionstemperatur von 25°C als Eichgerade die nachfolgende Gleichung: $tg\alpha_{ges} = 4{,}88 \cdot 10^4$ [Fe] + 0,0016, mit [Fe] in Mol l^{-1}. Bei Erhöhung der Reaktionstemperatur auf 40°C steigt die Empfindlichkeit etwa auf das Doppelte. Wir ermittelten folgende Geradengleichung: $tg\alpha_{ges} = 9{,}72 \cdot 10^4$ [Fe] + 0,0086. Der relative Fehler der Bestimmungen liegt bei einer Reaktionstemperatur von 25°C bei 6% und bei 40°C bei 10% (Tab. 2.).

Bei einem Vergleich der Ergebnisse mit den katalytischen Bestimmungen in wäßriger Phase [2, 3] kann gefolgert werden, daß durch Kombination der katalytischen Bestimmungen mit einem Trennverfahren und bei Durchführung der Reaktion in gemischt-wäßriger Lösung die Vorzüge der Methode nicht beeinflußt worden sind. Die Empfindlichkeit und die Reproduzierbarkeit des Verfahrens sind die gleichen wie bei einer katalytischen Bestimmung in wäßrigem Medium, und die Analysen sind einfach und schnell ausführbar.

Eisenspurenbestimmung in Salzen

Für die katalytischen Bestimmungen genügte in der Regel eine Reaktionstemperatur von 25°C. Die Bedingungen für das extraktionskatalymetrische Verfahren sind die gleichen wie bei der Aufstellung der Eichkurve (Tab. 2). Um sicher zu sein, daß die Eisengehalte über einen richtigen Eichfaktor

TABELLE 2

Extraktionskatalymetrische Bestimmung von Eisen in Salzen von Kobalt, Nickel und Kupfer sowie in Lithiumchlorid und Magnesiumsulfat
($7{,}5 \cdot 10^{-3}$ M *p*-Phenetidin; 10^{-2} M H_2O_2; $7{,}5 \cdot 10^{-5}$ M 1,10-Phenanthrolin; pH_{gem} = 2,5; $3 \cdot 10^{-7}$ M ÄDTA; 30 Vol% MIBK; 35 Vol% Äthanol; t = 25°C)

Salz	Einwaage g/10 ml	Zahl der Bestimm., n	Fe-Gehalt (%) $\bar{x} \pm \Delta\bar{x}$[a]	Relativ. Fehler $\Delta\bar{x} \cdot 100/\bar{x}$ (%)
$CoSO_4 \cdot 7H_2O$	0,1	6	$(2{,}20 \pm 0{,}11) \cdot 10^{-3}$	5,0
photometr.	0,1	5	$(2{,}13 \pm 0{,}13) \cdot 10^{-3}$	6,1
$Co(NO_3)_2 \cdot 6H_2O$	0,5	8	$(3{,}04 \pm 0{,}14) \cdot 10^{-4}$	4,6
$CoCl_2 \cdot 6H_2O$	0,5	11	$(1{,}63 \pm 0{,}07) \cdot 10^{-4}$	4,3
$NiSO_4 \cdot 6H_2O$[b]	3,0	10	$(2{,}28 \pm 0{,}21) \cdot 10^{-5}$	9,2
$NiCl_2 \cdot 6H_2O$[b]	0,5	10	$(1{,}95 \pm 0{,}11) \cdot 10^{-4}$	5,6
$Ni(NO_3)_2 \cdot 6H_2O$	3,5	10	$(4{,}89 \pm 100) \cdot 10^{-6}$	20,4
$CuSO_4 \cdot 5H_2O$	0,1	10	$(8{,}21 \pm 0{,}51) \cdot 10^{-4}$	6,2
$Cu(NO_3)_2 \cdot 3H_2O$	0,125	9	$(7{,}22 \pm 0{,}33) \cdot 10^{-4}$	4,6
$LiCl \cdot H_2O$	3,0	5	$(1{,}69 \pm 0{,}09) \cdot 10^{-4}$	5,3
photometr.	3,0	5	$(1{,}74 \pm 0{,}03) \cdot 10^{-4}$	1,7
$MgSO_4 \cdot 7H_2O$[b]	2,0	10	$(1{,}97 \pm 0{,}18) \cdot 10^{-5}$	9,1

[a] $\Delta\bar{x} = t(0{,}95;f) \times s_{Fe}/n^{\frac{1}{2}}$. [b] Reaktionstemperatur 40°C.

ermittelt werden, verwendeten wir die Zusatzmethode [9]. Die Ergebnisse der extraktionskatalymetrischen Bestimmung von Eisen in Salzen des Kobalts, Nickels und Kupfers sowie in Lithiumchlorid und Magnesiumsulfat sind in Tab. 2 angeführt.

Bei der Bestimmung von Eisen in Nickelnitrat und in Kupfersalzen mußte eine Nachbehandlung des Extraktes durch Waschen mit 7 M Lithiumchlorid vorgenommen werden, um mitextrahierte Matrixspuren zu entfernen. Der bei der Eisenbestimmung in Nickelnitrat resultierende relativ hohe Fehler von 20,4% ergibt sich daraus, daß bei einmaligem Waschen des Extraktes offenbar nicht alle Matrixspuren entfernt werden konnten. Für zwei Salze — Kobaltsulfat und Lithiumchlorid — wurden die Eisengehalte auch photometrisch ermittelt. Dazu ist Eisen aus der Probe mit 7 M Lithiumchlorid in MIBK extrahiert, anschließend in Wasser reextrahiert und mit 1,10-Phenanthrolin photometrisch [10] bestimmt worden. Die extraktionsphotometrisch und extraktionskatalymetrisch bestimmten Gehalte stimmten gut überein (Tab. 2).

Verglichen mit photometrischen Bestimmungsverfahren für Eisen in diesen Materialien ist das Nachweisvermögen des extraktionskatalymetrischen Verfahrens bei vergleichbarer Reproduzierbarkeit 5- bis 10-fach höher [11—14]. Das ausgearbeitete Verfahren ist hochselektiv und erfordet nur einen geringen instrumentellen und zeitlichen Aufwand.

LITERATUR

1 H. Müller und G. Werner, Z. Chem., 16 (1976) 304.
2 E. E. Kriss, Ya. S. Savichenko und K. B. Yatsimirskii, Zh. Anal. Khim., 24 (1969) 875.
3 A. Alexiev, P. R. Bontchev und D. Raykova, Mikrochim. Acta, (1974) 751.
4 W. Doll und H. Specker, Z. Anal. Chem., 161 (1958) 354.
5 I. M. Korenman, Analytische Chemie kleiner Konzentrationen, Verlag Chimiya, Moskau, 1966.
6 H. Müller, H. Schurig und G. Werner, Talanta, 21 (1974) 581.
7 K. B. Yatsimirskii, Kinetische Methoden der Analyse, 2. Auflage, Verlag Chimiya, Moskau, 1967.
8 A. Kettrup und H. Specker, Fortsch. Chem. Forsch., 10 (1968) 238.
9 G. Ehrlich und R. Gerbatsch, Z. Anal. Chem., 209 (1965) 35.
10 J. Fries, Spurenanalyse, Merck, Darmstadt, 1974.
11 E. Jackwerth, Z. Anal. Chem., 206 (1964) 335.
12 G. Uny, C. Mathien, J. P. Tardiff und Tran Van Panh, Anal. Chim. Acta, 53 (1971) 109.
13 R. P. Hair und E. J. Newman, Analyst (London), 83 (1964) 42.
14 H. Specker und W. Doll, Z. Anal. Chem., 152 (1956) 178.

Analytica Chimica Acta, 90 (1977) 167—172

UNE NOUVELLE MÉTHODE NUMÉRIQUE DE DÉTERMINATION PAR SPECTROPHOTOMÉTRIE DE CONSTANTES D'IONISATION SE CHEVAUCHANT

R. HANUS

Université libre de Bruxelles, Faculté des Sciences Appliquées, Laboratoire d'Automatique, C.P. 165, 50, avenue F-D Roosevelt, 1050 Bruxelles (Belgique)

M. HANOCQ, M. VAN DAMME et L. MOLLE

Université libre de Bruxelles, Institut de Pharmacie, Laboratoire de Chimie Analytique et de Toxicologie C.P. 205/1, Campus Plaine, Boulevard du Triomphe, 1050 Bruxelles (Belgique)

(Reçu le 13 juillet 1976)

RÉSUMÉ

Une nouvelle méthode numérique de détermination spectrophotométrique de deux constantes d'ionisation se chevauchant est proposée. Elle fait appel à la résolution d'un système de n équation à trois inconnues (l'absorbance de l'espèce monoprotonée, pK_{a_1}, pK_{a_2}) par la méthode du "complexe", beaucoup plus générale que la technique classique des moindres carrés. Un exemple d'application est donné.

SUMMARY

A new method of calculation has been developed to obtain two pK_a values from spectrophotometric data in cases when the values are so close together that the calculations usually applied for individual pK_a values are not appropriate. This technique, in which all the experimental data are used to solve for absorbance of monoprotonated species, pK_{a_1} and pK_{a_2} by a "complex" method of optimization, is more general than the classical least-squares method. An application is described.

La détermination des constantes d'ionisation d'une même substance présentant deux fonctions dont les pK_a ne sont séparés que de 1,5 à 2 unités de pK n'est pas chose aisée, les deux constantes se chevauchant. Il est nécessaire de faire appel à des techniques particulières.

Parmi celles-ci, la méthode par approximations successives [1] est longue et laborieuse. D'autres techniques ont été proposées [2, 3]. Plus récemment, Heys et al. [4] font appel à un système de n équations à 3 inconnues: en s'en référant aux deux équilibres suivants

$$A + H^+ \rightleftharpoons B \qquad K_{a_1} = [H^+]\,[A]/[B]$$

$$B + H^+ \rightleftharpoons C \qquad K_{a_2} = [H^+]\,[B]/[C]$$

la relation

$$-hD_B + (D - D_A)K_{a_1} + h^2\,(D - D_C)/K_{a_2} + hD = 0 \qquad (1)$$

est vérifiée pour un pH donné. Dans cette dernière, D_A, D_B et D_C représentent respectivement les absorbances des espèces A, B et C; D est l'absorbance correspondant à un mélange des espèces dont la composition est variable selon le pH et h est égal à 10^{-pH}.

Les trois inconnues, K_{a_1}, $1/K_{a_2}$ et D_B sont alors déterminées par résolution du système à n équations par la méthode des moindres carrés. Cette dernière fait cependant intervenir implicitement plusieurs hypothèses: (a) les seules indéterminations sur les équations portent sur leurs fermetures c'est-à-dire n'affectent que le terme indépendant; (b) ces erreurs de fermeture appartiennent à une distribution normale de moyenne nulle et d'écart type constant; (c) ces erreurs de fermeture sont incorrélées entre elles.

Or, ces hypothèses ne sont pas vérifiées pour le système considéré. En effet, les indéterminations des équations portent sur les grandeurs mesurées (qui apparaissent implicitement dans les équations) et non sur leurs fermetures. C'est pourquoi, pour résoudre ce système, nous proposons l'usage d'une fonction de coût, issue du principe du maximum de vraisemblance, nécessairement différente de celle utilisée dans la méthode des moindres carrés. Cette fonction est malheureusement non linéaire; ainsi, pour la minimiser tout en respectant les contraintes physico-chimiques et, après essais de plusieurs techniques de calcul notamment celle de Newton-Raphson, nous préconisons la méthode du complexe* [5—9]. Celle-ci offre un avantage certain: elle assure une convergence rapide de l'algorithme vers la solution la plus vraisemblable obéissant aux diverses contraintes.

La méthode originale que nous avons mise au point, et qui fait l'objet de cette étude, est donc beaucoup plus générale que la méthode classique des moindres carrés.

MÉTHODE UTILISÉE**

L'absorbance D correspondant à un mélange d'espèces, dont la composition est variable selon le pH, est explicitée à partir de l'expression (1):

$$D = \frac{D_A + 10^{(pK_{a_1} - pH)} [D_B + 10^{(pK_{a_2} - pH)} D_C]}{1 + 10^{(pK_{a_1} - pH)} [1 + 10^{(pK_{a_2} - pH)}]}$$

Le plus souvent, D_A et D_C sont connus; cependant afin de pouvoir étendre dans l'avenir la méthode proposée au cas général d'un polyélectrolyte, nous avons préféré, dans la suite de ce travail, considérer D_C comme inconnue.

---

*Les auteurs tiennent à disposition du lecteur toute documentation relative à cette méthode ainsi qu'un programme opérationnel.

**Il a été fait usage, au cours de ce travail, d'un calculateur PDP 15/20 Digital Equipment.

Hypothèses statistiques sur les mesures

(a) Chaque absorbance D_i appartient à une distribution normale de moyenne D_i° (vraie valeur de l'absorbance) et de variance σ_i^2 dont la valeur absolue n'est généralement pas connue; par contre on supposera connu le rapport des différentes variances caractérisables par un terme indépendant σ^2 et un poids connu p_i

$$\sigma_1^2/p_1 = \sigma_2^2/p_2 = \ldots\ldots\ldots = \sigma^2$$

p_i représentant la précision relative de la mesure i par rapport à toute autre.

(b) L'erreur sur la mesure d'une absorbance D_i est indépendante de l'erreur sur la mesure de toute absorbance (par exemple D_j).

(c) Les mêmes hypothèses statistiques sont faites sur les mesures de pH à l'intervention de poids connus q_i.

(d) Les erreurs sur les mesures des absorbances sont indépendantes des erreurs sur les mesures de pH.

Fonction de vraisemblance et fonction de coût

Compte tenu de ces différentes hypothèses, la fonction de vraisemblance s'exprime par la relation

$$L(D_B, D_C, pK_{a_1}, pK_{a_2}) = \frac{\exp\left\{-\frac{1}{2\sigma^2}\sum_{i=1}^{N}\left[\frac{(pH_i - pH_i^\circ)^2}{q_i} + \frac{(D_i - D_i^\circ)^2}{p_i}\right]\right\}}{(2\pi\sigma)^N \left(\prod_{i=1}^{N} p_i q_i\right)^{\frac{1}{2}}} \quad (2)$$

où N représente le nombre d'expériences.

Les valeurs D_B, D_C, pK_{a_1} et pK_{a_2} qui rendent maximum cette fonction de vraisemblance, correspondent à celles qui minimisent la fonction de coût

$$V(D_B, D_C, pK_{a_1}, pK_{a_2}) = \sum_{i=1}^{N} [(pH_i - pH_i^\circ)^2/q_i + (D_i - D_i^\circ)^2/p_i] \quad (3)$$

Au sein de l'éqn. (2), il est possible de considérer comme vraie valeur pH_i° la mesure pH_i; dans ces conditions, il y correspond un D_i° vrai donné par la relation (4), dérivée de l'expression (1)

$$D_i^\circ = \frac{D_A + 10^{(pK_{a_1} - pH_i)}[D_B + 10^{(pK_{a_2} - pH_i)} D_C]}{1 + 10^{(pK_{a_1} - pH_i)}[1 + 10^{(pK_{a_2} - pH_i)}]} \quad (4)$$

D'une manière analogue, on peut considérer $D_i = D_i^\circ$; par inversion de l'expression (4), la vraie valeur pH_i° est calculée suivant

$$pH_i^\circ = -\log \left\{ \frac{(D_B - D_i)10^{-pK_{a_2}} + [(D_B - D_i)^2 10^{-2pK_{a_2}} + 4(D_A - D_i)(D_i - D_C)10^{-(pK_{a_2} + pK_{a_1})}]}{2(D_i - D_C)} \right. \quad (5)$$

Les valeurs les plus vraisemblables de D_B°, D_C°, $pK_{a_1}^\circ$ et $pK_{a_2}^\circ$, sont celles qui rendent minimum $V(D_B, D_C, pK_{a_1}, pK_{a_2})$ où D_i° et pH_i° sont donnés par les éqns. (4) et (5), tout en respectant les contraintes

$$0 \leqslant D_C^\circ \leqslant D_B^\circ < D_A \text{ ou } 0 \geqslant D_C^\circ \geqslant D_B^\circ > D_A; pK_{a_1} > pK_{a_2}$$

(Les cas où $D_A^\circ > D_B^\circ < D_C^\circ$ n'ont pas été testés.) La solution analytique de ce problème non linéaire est ardue; aussi, préférons-nous utiliser une solution numérique basée sur une optimisation d'ordre zéro, cette dernière présentant, dans notre cas, un double avantage: la rapidité de la convergence et l'assurance d'obtenir le minimum minimorum dans le domaine admissible.

Interprétation des résultats

Correction des points de mesure. D_B°, D_C°, $pK_{a_1}^\circ$ et $pK_{a_2}^\circ$ (valeurs les plus vraisemblables) ayant été calculées par la méthode d'optimisation numérique, il est possible d'obtenir des informations quant aux corrections à apporter aux mesures D_i et pH_i, afin d'en avoir ainsi des valeurs corrigées les plus vraisemblables $D_i^1(D_i + \Delta D_i)$ et $pH_i^1(pH_i + \Delta pH_i)$ et de pouvoir les comparer aux valeurs expérimentales.

En effet, la fonction de coût pouvant être interprétée comme une somme de coûts V_i en chaque point de mesure i, on a

$$V(D_B^\circ, D_C^\circ, pK_{a_1}^\circ, pK_{a_2}^\circ) = \sum_{i=1}^{N} V_i(D_B^\circ, D_C^\circ, pK_{a_1}^\circ, pK_{a_2}^\circ),$$

le coût attaché à chaque point étant défini par la relation

$$V_i(D_B^\circ, D_C^\circ, pK_{a_1}^\circ, pK_{a_2}^\circ) = (pH_i - pH_i^\circ)^2/q_i + (D_i - D_i^\circ)^2/p_i$$

Suivant cette dernière expression, les équicoûts autour d'un point de mesure sont des ellipses de centre (D_i, pH_i) et de diamètres $(p_i)^{\frac{1}{2}}$ suivant D_i° et $(q_i)^{\frac{1}{2}}$ suivant pH_i°.

En assimilant la courbe de maximum de vraisemblance définie par l'éqn. (2) où les inconnues D_B, D_C, pK_{a_1} et pK_{a_2} sont remplacées par les valeurs les plus vraisemblables D_B°, D_C°, $pK_{a_1}^\circ$ et $pK_{a_2}^\circ$ trouvées par minimisation de l'éqn. (3), au segment de droite passant par les points de coordonnées (D_i, pH_i°) et (D_i°, pH_i) au voisinage du point de mesure de coordonnées (D_i, pH_i), on peut montrer que les corrections de ce point de mesure sont données avec une excellente approximation par

$$\Delta pH_i = (pH_i^\circ - pH_i) \Big/ \left[1 + \left(\frac{pH_i^\circ - pH_i}{D_i^\circ - D_i}\right)^2 \frac{p_i}{q_i}\right]$$

$$\Delta D_i = (D_i^\circ - D_i) \Big/ \left[1 + \left(\frac{D_i^\circ - D_i}{\mathrm{pH}_i^\circ - \mathrm{pH}_i}\right)^2 \frac{q_i}{p_i}\right]$$

Détermination des intervalles de confiance sur l'estimation des paramètres. En supposant que les estimations des paramètres D_B, D_C, pK_{a_1} et pK_{a_2} obéissent à une loi normale à L dimensions, de moyennes D_B°, D_C°, $pK_{a_1}^\circ$ et $pK_{a_2}^\circ$ et que ces paramètres sont indépendants, on peut démontrer

$$V(D_B^\circ \pm s_{D_B}, D_C^\circ, pK_{a_1}^\circ, pK_{a_2}^\circ) = V(D_B^\circ, D_C^\circ \pm s_{D_C}, pK_{a_1}^\circ, pK_{a_2}^\circ) =$$
$$V(D_B^\circ, D_C^\circ, pK_{a_1}^\circ \pm s_{pK_{a_1}}^\circ, pK_{a_2}^\circ) = \frac{L+1}{L} V(D_B^\circ, D_C^\circ, pK_{a_1}^\circ, pK_{a_2}^\circ)$$

Les L équations permettent d'estimer les écarts types sur les différents paramètres. Ces estimations portant sur une expérience de longueur finie, sont biaisées; aussi doivent-elles être corrigées par

$$s^+ = [N/(N-L)]^{\frac{1}{2}} s$$

où N représente le nombre de points expérimentaux.

RÉSULTATS ET DISCUSSION

Afin de tester la méthode mise au point, nous avons calculé à l'aide de celle-ci, et à partir des résultats expérimentaux de Albert et Serjeant [1] les valeurs des deux constantes d'ionisation de la benzidine et les avons comparées à celles obtenues par plusieurs auteurs à l'aide de différentes techniques (Tableau 1).

TABLEAU 1

Détermination spectrophotométrique des constantes d'ionisation de la benzidine: Comparaison des méthodes numériques utilisées

Ref.	Longueur d'onde (nm)	D_B	1ère fonction		2ème fonction	
			pK_{a_1}	Précision (s)	pK_{a_2}	Précision (s)
[1] (a)[a]	300	—	4,70	0,03	3,63	0,03
[1] (b)[a]	300	—	4,648	0,027	3,426	0,011
[1] + [4][b]	300	—	4,63	?	3,51	?
[4][b]	280	0,695 s = ?	4,676	0,011	3,712	0,011
Méthode du complexe[c]	300	0,490 s = 0,005	4,695	0,014	3,567	0,013

[a] Approximation successives.
[b] Méthode des moindres carrés.
[c] Les poids p_i (0,002) et q_i (0,005) nécessaires au calcul représentent respectivement les précisions classiques sur les mesures de l'absorbance et de pH.

L'analyse de l'ensemble des résultats revèle une excellente concordance entre les différentes valeurs des deux pK_a obtenues par l'une ou l'autre technique bien que Heys et al. [4] n'aient pas tenu compte des hypothèses statistiques qu'implique l'emploi de la méthode des moindres carrés. Nous montrerons au cours d'une publication ultérieure qu'il n'en va pas toujours ainsi.

Enfin, de l'examen de la Fig. 1 rassemblant les points expérimentaux [1] et ceux calculés par ordinateur (méthode du complexe), il ressort nettement que la méthode que nous proposons s'adapte parfaitement au cas envisagé.

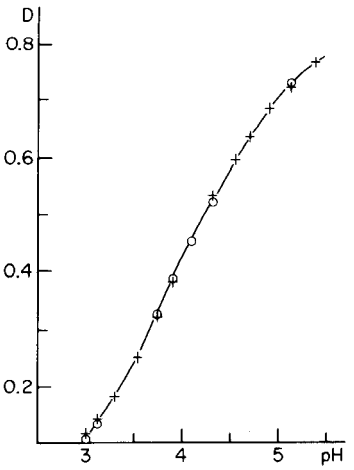

Fig. 1. Influence du pH sur l'absorbance d'une solution aqueuse $4 \cdot 10^{-5}$ M de benzidine. + Points expérimentaux; 300 nm, cellules 1 cm [1]. o Points calculés par ordinateur. (Lorsque les deux coïncident, ils ne sont notés que par le sigle + .)

Ce travail a été réalisé sous les auspices du Fonds de la Recherche Scientifique Médicale (convention no. 20-194).

BIBLIOGRAPHIE

1 A. Albert et E. P. Serjeant, (a) Ionization Constants of Acids and Bases, Methuen, London, 1962, p. 86; (b) 2e. ed., 1971.
2 B. J. Thamer et A. F. Voigt, J. Phys. Chem., 56 (1952) 225.
3 K. P. Ang, J. Phys. Chem., 62 (1958) 1109.
4 G. Heys, H. Kinns et D. D. Perrin, Analyst (London), 97 (1972) 52.
5 R. A. Barneson, N. F. Brannock, J. C. Moore et C. Morris, Chem. Eng., (1970) 132.
6 S. N. Ghani, Computer-Aided Design, (1972) 71.
7 T. Umeda et A. Ichikawa, Ind. Eng. Chem. Process. Des. Develop., 10 (1971) 229.
8 J. de Marneffe, Travail de Spécialisation, F. Sci. Appliquées, U. L. B., 1973.
9 R. Lesuisse, Travail de Spécialisation, F. Sci. Appliquées, U.L.B., 1973.

Analytica Chimica Acta, 90 (1977) 173—178

CHELATE VON β-DICARBONYLVERBINDUNGEN UND IHREN DERIVATEN

Teil L.* Die Extraktionsphotometrische Bestimmung von Zink und Wismut mit Thiodibenzoylmethan

E. UHLEMANN, R. MORGENSTERN und W. HILDEBRANDT

Sektion Chemie/Biologie, Pädagogische Hochschule "Karl Liebknecht", Potsdam, Potsdam-Sanssouci (Deutsche Demokratische Republik)

(Eingegangen den 9 November 1976)

ZUSAMMENFASSUNG

Thiodibenzoylmethan ist zur extraktionsphotometrischen Bestimmung von Zink und Wismut im Spurenmaßstab gut geeignet. Die Extraktion erfolgt im Bereich des Glykokollpuffers bei pH 12,6. Störende Metallionen können durch Diäthanolamindithiocarbamat bei der Bestimmung von Zink oder durch Cyanid im Falle des Wismuts weitgehend maskiert werden und stören dann in mehr als 100fachem Überschuß nicht mehr.

SUMMARY

Thiodibenzoylmethane is suitable for the extraction-photometric determination of traces of zinc and bismuth. The method is satisfactory in glycine-buffered solutions at pH 12.6. Interfering metal ions are masked by diethanolamine-dithiocarbamate in the determination of zinc and by cyanide in the case of bismuth; many foreign ions can be tolerated in more than 100-fold amounts.

Thiodibenzoylmethan stellt ein vielseitiges Reagens zur Bestimmung von Bunt- und Edelmetallen im Spurenmaßstab dar [1—8]. Es besitzt insbesondere die Fähigkeit, auch mit Ionen, die über abgesättigte Energieniveaus verfügen, extrahierbare farbige Komplexe bemerkenswerter Stabilität zu bilden. Allerdings treten in diesen Verbindungen keine zusätzlichen Absorptionsbanden auf, so daß die photometrischen Messungen auf der Basis von Innerligandübergängen erfolgen. Der überschüssige Ligand muß natürlich vor der Messung vollständig aus dem Extrakt entfernt werden. Dies gelingt am besten durch Reextraktion mit alkalischen Lösungen, sofern die zu bestimmenden Metallchelate unter diesen Bedingungen ausreichend stabil sind. Spezielles Interesse galt dem Verhalten der Zink- und Wismutchelate des Thiodibenzoylmethans, wobei vor allem beim Zink wegen seiner ausgeprägten Tendenz zur Bildung

*Teil XLIX, siehe [1].

von Hydroxokomplexen Störungen zu erwarten waren.

Zur extraktionsphotometrischen Analyse von Zink wird im allgemeinen das Verfahren mit Dithizon [9] vorgeschlagen. Die Störanfälligkeit der Dithizonmethoden lassen jedoch die Suche nach weiteren anwendungssicheren selektiven und empfindlichen Reagenzien gerechtfertigt erscheinen.

EXPERIMENTELLER TEIL

Thiodibenzoylmethan (Schmp. 83—84°C) wurde nach den Angaben der Literatur [10] hergestellt und in Form einer $5 \cdot 10^{-4}$ M Lösung in Cyclohexan bzw. n-Heptan verwendet.

Als Metallstandardlösungen kamen eine $2{,}5 \cdot 10^{-5}$ M Lösung von $ZnSO_4 \cdot 5\,H_2O$ bzw. $BiONO_3$ zum Einsatz. Das Wismutsalz wurde zunächst in wenig verd. Salpetersäure gelöst, mit 100 ml 0,5 M Natriumcitrat versetzt und dann auf 1 l verdünnt. Zur Bereitung der Lösungen diente ausschließlich bidestilliertes Wasser, alle Chemikalien waren von p.a. Reinheit. Die eingesetzten organischen Lösungsmittel wurden durch Destillation gereinigt. Kleine Flüssigkeitsmengen wurden mit Kolbenbüretten dosiert.

Für die photometrischen Messungen stand das Spektralkolorimeter Spekol (VEB Carl Zeiss Jena) mit Zusatzverstärker zur Verfügung. Die pH-Messungen wurden mit dem pH-Meter OP 204 mit Einstab-Glaselektrode (Fa. Radelkis Budapest) durchgeführt.

Die polarographischen Untersuchungen erfolgten mit dem Gerät OH 102 von Radelkis Budapest.

ERMITTLUNG DER EXTRAKTIONSKURVEN

Zur Aufnahme der Extraktionskurven wurde die nach der Extraktion in der wäßrigen Phase verbliebene Metallionenkonzentration polarographisch bestimmt. Dabei mußte die Variation des pH-Wertes durch gezielte Zugabe von 0,1 M NaOH, 1 M NaOH bzw. conc. Essigsäure vorgenommen werden, da die handelsüblichen Puffer infolge ihres Gehaltes an komplexbildenden und Fällungen erzeugenden Ionen die polarographische Bestimmung stören. Der sich einstellende pH-Wert konnte nach Abtrennung der organischen Phase exakt bestimmt werden. Überschüssiger Ligand, wie er in alkalischen Lösungen als Natriumsalz vorliegt, wurde vor der polarographischen Messung durch Ansäuern und anschließender Extraktion mit Benzol entfernt.

Während die Zink-Standardlösung über den gesamten pH-Bereich einsatzfähig ist, mußte die Wismutlösung durch Zusatz von Citrat gegen Hydrolyse stabilisiert werden. Der Einfluß dieses Hilfskomplexbildners fällt jedoch nicht ins Gewicht, wenn für die polarographische Wismutbestimmung ein ausreichend niedriger pH-Wert eingestellt wird.

Die Ergebnisse der polarographischen Messungen wurden bei variabler Geräteempfindlichkeit anhand von Eichgeraden ausgewertet, die unter Extraktionsbedingungen ermittelt wurden. Die maximale Geräteempfindlichkeit

betrug bei Bi^{3+} $2{,}4 \cdot 10^{-9}$ A mm^{-1} (Tast/Rapidpolarographie mit Adapter OH 991 Radelkis Budapest), bei Zn^{2+} $8 \cdot 10^{-9}$ A mm^{-1} (Normal-DC-Polarographie) entsprechend einer minimalen Konzentration von $2{,}8 \cdot 10^{-6}$ M Bi^{3+} bzw. $3{,}7 \cdot 10^{-6}$ M Zn^{2+}.

Zur Bestimmung der Extraktionskurven kamen 10^{-4} M Metallsalzlösungen in 0,1 M KCl (unter Zusatz von $4 \cdot 10^{-2}$ M Natriumcitrat bei Bi^{3+}) zur Anwendung. Die Extraktion erfolgte mit dem gleichen Volumen an 10^{-3} M benzolischer Lösung von Thiodibenzoylmethan. Nach der Phasentrennung wurde die wäßrige Phase mit 1/10 ihres Volumens an Eisessig versetzt und dann polarographiert. Die Stufenhöhe ist im pH-Bereich 2,4 bis 3,5 konstant. Die bei höheren Metallsalzkonzentrationen notwendig werdende Maximumunterdrückung konnte mit dem im Haushalt verwendeten Tensid "Fit" (VEB Fettchemie Karl-Marx-Stadt) in einer Verdünnung 1:150000 (bezogen auf die Meßlösung) wirksam erreicht werden. Die gefundene Metallsalzkonzentration wurde auf das reine Extraktionsvolumen umgerechnet.

Die erhaltenen Extraktionskurven sind in Abb. 1 dargestellt. Danach verläuft die Wismutextraktion oberhalb pH 10 quantitativ. Zink läßt sich bereits im schwach sauren Gebiet mit Thiodibenzoylmethan extrahieren, im pH-Bereich von 10—12 zeigt die Extraktionskurve jedoch ein deutliches Minimum. Wahrscheinlich liegen hier Gemischtligandkomplexe in der wäßrigen Phase vor, an deren Bildung Hydroxid- und Thiodibenzoylmethananionen beteiligt sind. Die Zunahme der Thiodibenzoylmethankonzentration mit ansteigendem pH-Wert begünstigt dann wieder die Bildung des extrahierbaren Neutralchelates. Optimale Extraktionsbedingungen wurden im Bereich des Glykokollpuffers (pH 12,6) gefunden. Zur quantitativen Extraktion ist oberhalb pH 12,6 ein 10facher Reagensüberschuß erforderlich. Die Extraktionszeit beträgt 3 min.

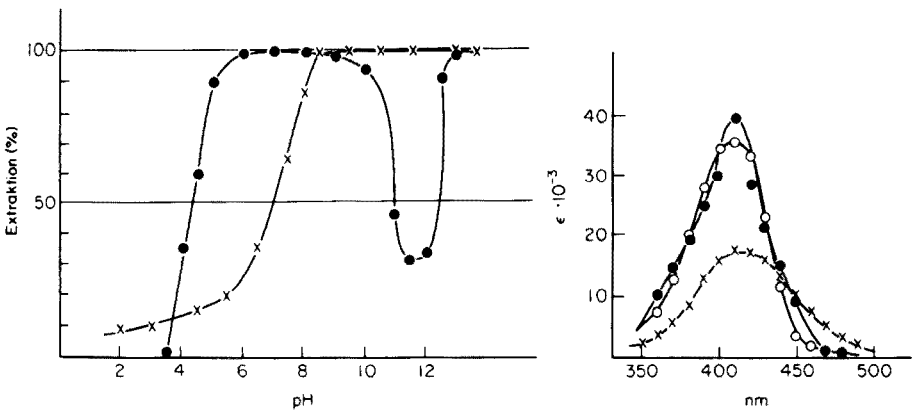

Abb. 1. pH-Abhängigkeit der Extraktion von Zink (•) und Wismut (×) mit Thiodibenzoylmethan.

Abb. 2. Absorptionsspektren der Zink- (○) und Wismutchelate (•) von Thiodibenzoylmethan sowie des freien Liganden (×).

ABSORPTIONSSPEKTREN

Die Chelate von Thiodibenzoylmethan mit Zink und Wismut sind von gelber Farbe und zeigen die gleichen Absorptionsmaxima wie der freie Ligand (Abb. 2.) Für die photometrische Auswertung sind die Maxima bei 410 nm gut geeignet. Im Bereich des Glykokollpuffers (pH 12,6) sind Bedingungen gegeben, bei denen überschüssiger Ligand eliminiert wird und die Metallbestimmung nicht mehr stört.

DURCHFÜHRUNG DER VERFAHREN

Bestimmung von Zink

Die Extraktion von Zink mit Thiodibenzoylmethan läßt sich bei Einsatz geeigneter Maskierungsmittel selektiv gestalten und ist mit geringem Arbeits- und Zeitaufwand durchführbar. Zur Maskierung von Störionen wurde eine Vielzahl von Maskierungsmitteln wie Triäthanolamin, Cyanid, Thioharnstoff, Thiosulfat, Dimercaptopropanol, Dithiocarbaminoessigsäure, Dithiocarbaminopropionsäure geprüft. Als am geeignesten hat sich Diäthanolamindithiocarbamat [11] erwiesen, welches mit vielen thiophilen Metallionen stabile wasserlösliche Komplexe bildet. Über den Fremdioneneinfluß bei Anwesenheit dieses Maskierungsmittels informiert Tabelle 1.

Der günstigste Arbeitsbereich für die Zinkbestimmung liegt zwischen 0,0025 und 0,025 µmol. Zur Testung des Verfahrens wurden jeweils 1, 2, 4, 6, 8 bzw. 10 ml der Zink-Standardlösung mit 10 ml Glykokollpuffer von pH 12,6, 1 ml 25%iger Diäthanolamindithiocarbonatlösung sowie 10 ml Reagenslösung versetzt und 2 min geschüttelt. Die organische Phase wurde abgetrennt, zentrifugiert und schließlich die Extinktion in 1 cm-Küvetten bei 410 nm gegen eine analog behandelte Blindlösung gemessen. Die statistische Auswertung erfolgte nach der von Gottschalk vorgeschlagenen Methode [12]. Über die erhaltenen Ergebnisse informiert Tabelle 2.

TABELLE 1

Einfluß von Fremdmetallen auf die photometrische Bestimmung von Zink mit Thiodibenzoylmethan bei Zusatz von Diäthanolamindithiocarbamat

Metalle	keine Störung
Alkali- und Erdalkalimetalle, B, Al, Ga, In	1 : 10 000
Bi, Pd, Cr	1 : 1 000
Ni, Fe(II)	1 : 500
Pb, Cd	1 : 200
Ag, Tl, Sn, Fe(III), Co	1 : 100
Cu, Hg	1 : 50

TABELLE 2

Kenngrößen der extraktionsphotometrischen Bestimmung von Zink und Wismut mit Thiodibenzoylmethan

	Zink	Wismut
b_u bis	0,0025	0,0025
b_o (μmol cm^{-3})	0,025	0,025
ϵ (cm^2 μmol^{-1})	36,0	39,0
$V(b_o - b_u)$Rel.%	(± 1,0 — 10,9)	(± 0,61 — 6,16)
S_K (μmol cm^{-3})	± 0,00027	± 0,00015
T (99) (μmol cm^{-3})	± 0,0007	± 0,00043
T (99.9) (μmol cm^{-3})	± 0,00103	± 0,00059

Bestimmung von Wismut

Die extraktionsphotometrische Bestimmung von Wismut mit Thiodibenzoylmethan kann bei Maskierung störender Begleitionen mit Cyanid weitgehend selektiv gestaltet und in einfacher Weise durchgeführt werden. Bei Anwesenheit von Blei ist ein Zusatz von Thiosulfat erforderlich, größere Mengen dieses Elementes dürfen jedoch nicht zugegen sein. Über den Einfluß von Fremdmetallen informiert Tabelle 3.

Zur Durchführung der Eichmessungen wurde eine vorgelegte Menge der Wismut-Standardlösung nacheinander mit 15 ml Glykokollpuffer vom pH 12,6, 1 ml 1,25 M Cyanid-bzw. 1 ml 1 M Thiosulfatlösung versetzt, danach 10 ml Reagenslösung zugegeben und 2 min geschüttelt. Nach der Phasentrennung wurde die organische Phase 2 min zentrifugiert und in 1 cm-Küvetten bei 410 nm gegen eine analog behandelte Blindlösung gemessen. Aus den

TABELLE 3

Einfluß von Fremdmetallen auf die photometrische Wismutbestimmung mit Thiodibenzoylmethan

Metall	Maskierungsmittel	keine Störung
Alkalimetalle, Mg, Ca	—	1 : 10 000
Al, Ga	—	1 : 1 000
Zn, Cd, Mn, Ag Fe, Cr	CN^-	1 : 1 000
As, Sb, Sn, In	—	1 : 500
Co, Ni, Hg	CN^-	1 : 500
Tl	—	1 : 100
Cu	CN^-	1 : 100
Pb	CN^-, $S_2O_3^{2-}$	1 : 10

Meßergebnissen folgt, daß das Lambert—Beer' sche Gesetz erfüllt ist. Einige Kenngrößen des Verfahrens sind in Tab. 2 enthalten.

LITERATUR

1 J. Hoppe und E. Uhlemann, Z. Chem., im Druck.
2 E. Uhlemann und H. Müller, Anal. Chim. Acta, 41 (1968) 311; 48 (1969) 105.
3 H. Tanaka, N. Nakanashi, J. Sugiura und A. Yokojama, Jpn. Analyst, 17 (1968) 1428.
4 E. Uhlemann, B. Schuknecht, K. D. Busse und V. Pohl, Anal. Chim. Acta, 56 (1971) 185.
5 E. Uhlemann und B. Schuknecht, Anal. Chim. Acta, 63 (1973) 236; 69 (1974) 79.
6 B. Schuknecht, G. Röbisch und E. Uhlemann, Anal. Chim. Acta, 69 (1974) 329.
7 R. R. Mulye und S. M. Khopkar, Anal. Chim. Acta, 76 (1975) 204.
8 E. Uhlemann, J. Hoppe und D. Waltz, Anal. Chim. Acta, 83 (1976) 195.
9 O. G. Koch und G. A. Koch-Dedic, Handbuch der Spurenanalyse, Bd. 2 S. 1334, Springer Verlag, Berlin, Heidelberg, New York, 1974.
10 E. Uhlemann und H. Müller, Angew. Chem., 77 (1965) 172.
11 D. M. Margerum und F. Santacana, Anal. Chem., 32 (1960) 1157.
12 G. Gottschalk, Statistik in der quantitativen chemischen Analyse, F. Enke-Verlag, Stuttgart, 1962.

Analytica Chimica Acta, 90 (1977) 179—184

THE RAPID SEPARATION AND DETERMINATION OF IRIDIUM AFTER LEAD COLLECTION AND PERCHLORIC ACID PARTING

A. DIAMANTATOS

J.C.I. Minerals Processing Research Laboratory, Knights 1413, Transvaal (South Africa)

(Received 18th October 1976)

SUMMARY

A rapid and accurate method is described for the determination of iridium in platiniferous materials. The method is based on the classical fire-assay collection of the noble metals into a lead button and the subsequent complete dissolution of lead with perchloric acid after heating at 160—180°C. Iridium remains totally unattacked by the parting acid whereas Pt, Pd, Rh and Au pass completely into the perchloric acid-lead perchlorate solution. After filtration, the residue is fused with sodium peroxide, Ru and Os are removed by boiling with perchloric acid, and iridium is finally determined photometrically or by atomic-absorption spectrometry. The proposed method shows a universal applicability and provides what is perhaps the simplest isolation procedure for iridium.

There has been considerable discussion of the efficiency of the lead collector for iridium, mainly because iridium does not alloy with lead but is spread as a suspension in the molten lead metal [1—3]. However, recent investigations by modern techniques have shown that, despite the non-uniform distribution, the iridium is collected quantitatively by the lead button after fusion. Watterson et al. [4] investigated the collection of iridium, by the classical lead fire-assay procedure, by a combined neutron-activation and radioactive-tracer technique. The lead button collected at least 99% of the iridium in the original ore; the 1% remaining in the slag could be collected by re-fusion of this slag. In a critical study, Keays and Donnelly [3] evaluated and compared the efficiency and reproducibility of the lead, tin and nickel sulphide collectors for iridium by means of radioactive tracers; the three collectors were highly efficient with recoveries of 99.1%, 90.4% and 96.9%, respectively. These results suggest that lead is perhaps the most efficient of all collectors.

For the determination of iridium collected in lead, Deville and Stas [1] used boiling dilute nitric acid to disintegrate the alloy obtained after fusion of a platinum—iridium—rhodium—palladium—iron—copper alloy with lead at a high temperature. They thus dissolved the bulk of the lead, palladium and copper, as well as a small proportion of both the platinum and the rhodium; but the iridium, ruthenium and iron remained insoluble. This early work was confirmed by Gilchrist [5, 6]. In a similar recent investi-

gation Shubochkin et al. [7] collected the noble metals in lead and parted the button with dilute nitric acid; they stated that 20% of the iridium, together with the other partially dissolved noble metals, passed into solution.

The use of nitric acid for parting the lead button therefore leads to only partial attack of the acid on the individual precious metals. These undesirable complications made it necessary to consider the use of perchloric acid for the dissolution of the lead button; under certain conditions of parting, the iridium might remain totally unattacked whereas the platinum, palladium and rhodium, which alloy with lead at high temperatures, might be completely dissolved by perchloric acid and therefore separated from the iridium by simple filtration.

This paper describes a simple method for isolating and determining iridium after lead fusion and perchloric acid parting.

EXPERIMENTAL

Apparatus and reagents

The equipment required included a fire assay fusion furnace and related equipment; an electric furnace with silicon carbide element; fireclay crucibles; cast iron conical moulds (150-ml capacity); spectrophotometer, Zeiss model PMQ II; atomic-absorption spectrophotometer, Techtron AA5; x-ray fluorescence spectrometer, Philips PW 1220; pH meter, Radiometer.

The assay lead flux (parts by weight) contained litharge 50, borax 20, soda ash 60, silica 20, flour 5—6.

Standard copper—nickel matte contained 958 p.p.m. Pt, 536 p.p.m. Pd, 93 p.p.m. Rh, 24.6 p.p.m. Ir, 205 p.p.m. Ru, 19 p.p.m. Os, 47.9 p.p.m. Au, 81 p.p.m. Ag, 28.9% Cu, 48.2% Ni, 22.4% S, 1.4% Fe, 0.45% Co, 0.06% Se, 0.02% Te, silica, etc.

Standard stock hydrochloric acid solutions of iridium, platinum, palladium, rhodium, ruthenium, osmium and gold were prepared as described previously [8].

For the tin(II) bromide solution, 12.5 g of $SnCl_2 \cdot 2H_2O$ was dissolved in 50 ml of concentrated hydrobromic acid and diluted to 100 ml with water.

Recommended procedure

Mix thoroughly 2—60 g of the sample (leach and or roast, if necessary) as required with 150—180 g of lead flux and transfer to a suitable size of fireclay crucible. Fuse at 1200°C for 1 h and then pour the molten fluid into a conical iron mould. After cooling, detach the lead button from the slag by tapping. (Re-fuse the slag if high quantities of iridium are present in the sample.) Place the button in 100 ml of a 30% (w/v) sodium hydroxide solution and boil to remove any adhering slag completely. Compress the button to produce a disc of ca. 4 mm thickness. Place the lead disc in a 1-l squat beaker; add 300 ml of perchloric acid (70%) and 30 ml of acetic acid (glacial). Cover the beaker and introduce a thermometer through the gap between its

spout and the watchglass. Heat to 180°C initially, remove the heat source for a time and then maintain the temperature at 160°C—180°C until the complete dissolution of lead is achieved. Continue heating for 20 min at ca. 150°C to ensure complete dissolution of platinum, palladium, rhodium and gold. Cool somewhat (70°C), replace the thermometer by a boiling rod, and dilute the perchlorate solution slowly with 200 ml of water while stirring. Boil the diluted solution for 5 min, and then cool. Filter the solution through a No. 540 filter paper to retain the black unattacked residue containing the iridium. Transfer the filter paper to a zirconium crucible, char, ignite, and then fuse the residue with 2—3 g of sodium peroxide. Cool, leach the melt with water in a 400-ml beaker, acidify with hydrochloric acid, and evaporate to dryness.

Dissolve the residue in water by boiling, adjust the solution to pH 2—4 with a dilute sodium hydrogen carbonate solution, and dilute to ca. 70 ml with water. Add 30 ml of glacial acetic acid and 0.2 g of ammonium acetate and bring to the boil. Remove from the hot plate and carefully add, while stirring, 10 ml of ethanolic 1% 2-mercaptobenzothiazole reagent solution [9]. Insert a boiling rod and boil the solution gently for 60 min. Cool, transfer to a 250-ml separatory funnel, and extract the precipitated yellow iridium complex with two 50-ml portions of chloroform. Evaporate the combined chloroform extracts on a steam bath while blowing air onto the surface of the solvent. To the dried residue, add 5 ml of 14 M nitric acid and 5 ml of 70% perchloric acid. Boil and fume to dryness in the presence of a little sodium chloride.

Dissolve the residue by boiling with 11 M hydrochloric acid and determine iridium by atomic-absorption spectrometry [10]. Alternatively, determine iridium spectrophotometrically [11, 12] as follows: dissolve the residue with 30 ml of concentrated hydrobromic acid by boiling for 15 min. Cool and make up to a suitable volume with concentrated hydrobromic acid, so that the resulting solution contains 4—10 μg Ir ml^{-1}. Pipette a 5-ml aliquot into a 25-ml volumetric flask, add 7 ml of 20% phosphoric acid solution and heat in a boiling water bath for 10 min. Exactly 2 min after adding 5 ml of the preheated tin(II) bromide solution, cool the flask under running water for 40 s, make up to the mark with water, and keep in darkness for 30 min. Measure the absorbance in 1-cm quartz cells at 402 nm against a reagent blank prepared in the same way.

RESULTS

The parting of the lead button with perchloric acid

A sample (25 g) of the standard platiniferous copper—nickel matte, containing 0.615 mg of iridium, was leached with 300 ml of concentrated hydrochloric acid and 100g of ammonium chloride in a 800-ml squat beaker by boiling for 1.5—2 h to dissolve the nickel, copper and iron. After dilution with hot water, the solution was filtered; the residue containing the noble

metals was roasted at 800°C and then fused with 160 g of the lead flux at 1200°C for 1 h. The 40-g lead button obtained was treated with 100 ml of 70% perchloric acid until the button had dissolved completely and effervescence of hydrogen had ceased. The dissolution process took ca. 2 h. The perchlorate solution was then boiled for 15 min. After cooling, the solution became turbid; when diluted with water, a yellowish flocculent precipitate appeared. This precipitate was filtered off. Examination by x-ray fluorescence showed an abundance of platinum, and it was therefore decided to analyze the precipitate quantitatively for the precious metals. The precipitate was dissolved in 30 ml of concentrated hydrochloric acid and a few drops of 100-vol hydrogen peroxide by boiling for 15 min and the resulting solution was analysed by atomic-absorption spectrometry [13]; 44.2% of the platinun 3.4% of the palladium, and 0.1% of the gold originally present were found to have been precipitated. Traces of rhodium were also detected. Analysis for the other platinum metals was not attempted.

The above procedure was repeated with 300 ml of perchloric acid for the parting of the lead button. This time a small yellowish precipitate was observed after dilution of the boiled perchlorate solution with water. The small precipitate was again analysed as described previously. Only 4.0% of the platinum and 0.2% of the palladium originally present were found; rhodium and gold were not detected.

In a third experiment, a lead button was dissolved with 300 ml of the perchloric acid at a temperature range of 160—170°C, but, after complete dissolution of the lead, the solution was not subsequently boiled. Instead, after cooling somewhat, the perchlorate solution was diluted to about 600 ml with water, mixed, and then boiled for 5 min. The diluted solution showed nc turbidity, and only a small black metallic residue settled at the bottom. The clear yellow perchlorate solution was filtered through an asbestos filter pad under vacuum, and the retained metallic residue was scanned by x-ray fluorescence spectrometry. The results indicated that appreciable amounts of iridium, ruthenium, and osmium were present; platinum, palladium, rhodium, and gold could not be detected. To confirm these encouraging results, the residue was chemically analysed [14] for platinum, palladium, rhodium, and gold; none of these metals was detected. This successful test was repeated with 100 ml of perchloric acid; again the same results were obtained.

In an attempt to shorten the time necessary for dissolution of the lead button, the procedure was repeated on a button which had been compressed in a hydraulic press (1 ton in^{-2}) to give a disc about 4 mm thick, in order to increase the surface area. This approach was successful; the complete parting treatment took less than 1 h.

It was also considered that the addition of some acetic acid to the perchloric acid medium used for the parting might result in a milder dissolution of the button. The observations were interesting; the sample containing acetic acid (30 ml of acetic acid in 300 ml of perchloric acid) gave a clear perchlorate solution and white perchlorate salts no longer adhered to the

sides of the beaker. The parting procedure was more gentle; for future work, the addition of acetic acid is therefore strongly recommended.

Optimum temperature range for parting

Each of five lead buttons was individually dissolved with 300 ml of 70% perchloric acid and 30 ml of glacial acetic acid, at almost constant temperatures. The temperatures used were 150°, 160°, 170°, 180° and 190°C ± 2°C, respectively. In all cases, complete dissolution of platinum, palladium, rhodium, and gold took place. However, the range 160—180°C was chosen because complete dissolution of the button takes only 1—1.5 h. At 150°C dissolution requires nearly 4 h; at higher temperature (190° C) the disintegration of the button is extremely vigorous and would not be so suitable for quantitative work of the highest accuracy.

The determination of iridium in the residue

The previously mentioned x-ray scan of the unattacked residue indicated the presence of iridium to an extent such that it appeared that all the iridium might have remained undissolved after parting of the lead button. This suspicion was easily confirmed by determining the iridium content of the metallic residue by a well established wet chemical method of analysis. The residue was fused with 2—3 g of sodium peroxide in a zirconium crucible, the melt leached with water, acidified with hydrochloric acid, and evaporated to dryness; after 10 ml of perchloric acid was added the solution was boiled and fumed to complete dryness. The residue was dissolved in 50 ml of concentrated hydrobromic acid by boiling for 15—20 min. This solution was diluted to 100 ml with concentrated hydrobromic acid in a volumetric flask. A 5-ml aliquot was added (pipette) to a 25-ml volumetric flask containing 7 ml of 20% phosphoric acid, and iridium was determined spectrophotometrically by the tin(II) chloride—hydrobromic acid method [11, 12]. The weight of iridium found (0.611 mg) represented a recovery of 99.3%.

Precision and accuracy

Ten 5-g portions of the standard copper—nickel matte were analyzed for iridium by the recommended procedure. The results showed a standard deviation of 0.007 and a relative standard deviation of 5.7%, confirming the satisfactory reproducibility of the method.

The degree of accuracy of the proposed method was evaluated as follows: five lead fluxes were spiked with synthetic noble metal solutions prepared from the standard stock solutions, containing 0.0503, 0.1006, 0.1509, 0.2012 and 0.5030 mg of iridium respectively, as well as with 0.5 mg of each of platinum, palladium, rhodium, ruthenium, osmium, and gold, and also 0.5 g of each of copper and nickel. After fusion, the lead buttons were parted and analysed for iridium, following the recommended procedure. The results obtained from all five buttons showed recoveries of iridium ranging from 97.3 to 100%.

CONCLUSION

The satisfactory recoveries of iridium again confirm the high efficiency of lead as a collector. The work described in this paper suggests that, if the disintegration of the lead button is performed under the established conditions, a quantitative separation of iridium from the other noble non-volatile metals can be easily achieved. In this respect, the use of perchloric acid as a parting acid shows a distinct advantage over nitric acid. The proposed method is, to the best knowledge of the author, the first scheme of analysis which depends on recovery of iridium directly after parting the lead collector with perchloric acid. Spectrographic or neutron-activation techniques could be applied for finishing the determination of iridium directly on the metallic unattacked residue; this would eliminate the need for the dissolution and extraction stages necessary before the use of atomic-absorption or colorimetric finishes.

The author thanks Professor A. A. Verbeek, University of Natal, for helpful discussions and suggestions.

REFERENCES

1 H. Ste-C. Deville and J. S. Stas, P.-V Seances Com. Int. Poids Més., 2 (1877) 162.
2 F. E. Beamish, Analytical Chemistry of Noble Metals, Pergamon Press, 1966.
3 R. R. Keays and T. Donnelly, paper presented at Conference on Platinum Metals, Melbourne 5—6th October, 1971.
4 J. I. Watterson, R. V. D. Robert and E. van Wyk, Nat. Inst. Met., Rep. S. Afr., Rep. No. 1048, 1970.
5 R. Gilchrist, J. Am. Chem. Soc., 45 (1923) 2820.
6 R. Gilchrist, Nat. Bur. Stand. Sci. Pap., 19 (1924) 325.
7 L. K. Shubochkin, V. N. Pichkov, A. F. Morgunov and N. I. Kolomiets, Zh. Prikl. Khim. (Leningrad), 45 (1972) 2327.
8 A. Diamantatos, Anal. Chim. Acta, 66 (1973) 147.
9 A. Diamantatos and A. A. Verbeek, Anal. Chim. Acta, 86 (1976) 169.
10 J. C. Van Loon, At. Absorpt. Newsl., 8 (1969) 6.
11 S. S. Berman and W. A. E. McBryde, Analyst (London), 81 (1956) 566.
12 G. H. Faye and W. R. Inman, Anal. Chem., 35 (1963) 985.
13 J. G. Sen Gupta, Anal. Chim. Acta, 58 (1972) 23.
14 A. Diamantatos, Anal. Chim. Acta, 67 (1973) 317.

Analytica Chimica Acta, 90 (1977) 185—191

THE SYNERGIC EXTRACTION OF URANIUM(VI) WITH SOLUTIONS OF TRIOCTYLPHOSPHINE OXIDE AND BENZOIC ACID IN CARBON TETRACHLORIDE

M. KONSTANTINOVA

Higher Institute of Chemical Technology, Sofia 1156 (Bulgaria)

(Received 24th November 1976)

SUMMARY

The synergic extraction from perchlorate media of uranium(VI) with solutions of trioctylphosphine oxide and benzoic acid in carbon tetrachloride media is studied. The concentrations of the different species of the two extractants and their distribution in the extraction systems are calculated. The values obtained together with the distribution coefficients determined for uranium are used to determine the composition of the synergic adduct and to calculate the extraction constant. The conditions for the destruction of the synergism in these systems are clarified.

Studies of the synergic extraction of uranium(VI) with a mixture of trioctylphosphine oxide (TOPO) and aromatic [1] or fatty [2] acids have established that the distribution of uranium depends on the concentration of the extractants, the strength of the organic acid, the pH of the aqueous phase, and on the diluent used. A quantitative interpretation of the synergic systems studied is complex as the extractants appear as several different species in both phases of the extraction systems. A hydrogen bond between the COOH group of the acid and the strongly polar PO group of TOPO leads the two extractants to form a complex. Furthermore, the organic acid is present as monomer and dimer anion.

A quantitative treatment of an extraction system containing TOPO and an organic acid is possible when the concentrations of the different forms of the extractants are known. These concentrations can be calculated if the dissociation, distribution, and dimerization constants of the acid, and the formation constant of the TOPO—acid complex are known.

This paper clarifies quantitatively the synergic extraction of uranium(VI) from perchlorate media with solutions of TOPO and benzoic acid in carbon tetrachloride. The distribution of uranium has been studied in a wide range of concentrations of the two extractants. By combining the results with previous data [3] for the distribution constant of the monomer of benzoic acid, its dimerization constant, and the formation constant of the TOPO—benzoic acid complex, the composition of the synergic adduct and the value of the extraction constant have been determined.

EXPERIMENTAL

Uranyl perchlorate solutions were prepared by evaporating $UO_2(NO_3)_2$ to fumes with concentrated $HClO_4$; the determination of nitrogen (Kjeldahl) showed complete transformation of $UO_2(NO_3)_2$ to $UO_2(ClO_4)_2$. The latter, dissolved in 0.01 M $HClO_4$, was used as a stock solution. The concentration of uranium was determined gravimetrically [4]. Solutions for extraction experiments were prepared by diluting suitable aliquots of the stock solution. The hydrogen ion concentration was adjusted to the desired values (pH meter) with dilute solutions of ammonia or perchloric acid. A constant ionic strength was maintained with 0.1 M $NaClO_4$.

TOPO, benzoic acid, and carbon tetrachloride were purified as described previously [1]. $UO_2(NO_3)_2$, $NaClO_4$, $HClO_4$, and NH_3 were of p.a. grade.

Solutions of TOPO and benzoic acid in carbon tetrachloride with concentrations ranging from $1 \cdot 10^{-2}$ to $8 \cdot 10^{-2}$ M and from $1.25 \cdot 10^{-3}$ to $1.6 \cdot 10^{-1}$ M, respectively, were used.

All distribution experiments were carried out at 25 ± 0.1 °C. TOPO solution (5 ml) and benzoic acid solution (5 ml) were added to 10 ml of uranyl perchlorate solution. The extraction systems were shaken for 30 min on a machine at 200 r.p.m. After centrifugation, uranium was determined spectrophotometrically in an aliquot of the aqueous phase with arsenazo III [5]. Each distribution result was obtained from at least three separate experiments.

RESULTS AND DISCUSSION

Calculation of the concentrations of the different species of the extractants

In the extraction systems studied the concentration of uranium (10^{-4} M) was negligible in comparison with the concentrations of TOPO and benzoic acid. Hence, the fractions of the extractants which interact with uranium can be neglected; the undissociated form HA and the anion A are the benzoic acid species present in the aqueous phase, whereas the monomer HA_o, the dimer H_2A_{2o}, and the complex benzoic acid—TOPO, HAB_o, are present in the organic phase. The total concentration of benzoic acid C_{HA} is given by $C_{HA} = [HA] + [A] + [HA]_o + 2[H_2A_2]_o + [HAB]_o$. The solubility of TOPO in water is negligible. TOPO is present only in the organic phase as free TOPO $[B]_o$ and as the complex $[HAB]_o$, and the total concentration of TOPO may be written as $C_B = [B]_o + [HAB]_o$. If the concentrations of different species of the extractants are expressed by the dissociation constant of the acid $K_{HA} = [H]\,[A]/[HA]$, the distribution constant of the monomer $K_d = [HA]_o/[HA]$, the dimerization constant $K_2 = [H_2A_2]_o/[HA]_o^2$, and the formation constant $K_B = [HAB]_o/[HA]_o[B]_o$ and if the expression for C_{HA} is rearranged, eqn. (1) is obtained

$$C_{HA} = \left(1 + \frac{K_{HA}}{[H^+]} + K_d + 2K_2K_d^2\,[HA] + K_BK_d\,\frac{C_B}{1 + K_BK_d\,[HA]}\right)[HA] \qquad (1)$$

The values of [HA] can be calculated from eqn. (1) for each given value of C_{HA} and C_B, since all the constants are known. When the literature value of $K_{HA} = 6.45 \cdot 10^{-5}$, and the values of $K_d = 2.7 \cdot 10^{-1}$, $K_2 = 5.0 \cdot 10^3$ and $K_B = 6.1 \cdot 10^3$ determined previously [3] were inserted, [HA] was obtained for 40 combinations of C_{HA} and C_B at $[H^+] = 10^{-3}$ M by means of an ICL 4-50 computer. From the values of [HA] obtained and the expressions for K_{HA}, K_d, K_2 and K_B, the concentrations of all other forms of TOPO and benzoic acid in both phases of the extraction systems were calculated. The results (partly given in Figs. 1, 2 and 3) show that the concentration of each species depends greatly on the ratio C_{HA}:C_B. The values of C_{HA} and C_B with which the concentrations of different species of both extractants were calculated, were not selected randomly. The extraction of uranium was studied with the same combinations of C_{HA} and C_B. The distribution coefficients of uranium obtained (Table 1) and the calculated values of [HA] and $[B]_o$ are used below for a quantitative interpretation of the system.

Determination of the composition of the synergic adduct and the extraction constant

The distribution of uranium was studied as a function of the pH of the aqueous phase in the range pH 1—3. The distribution coefficients of uranium increased with increase in pH.

The synergic extraction equilibrium may be expressed generally as follows

$$UO_2^{2+} + a\ ClO_4^- + b\ HA + m\ B_o \rightleftharpoons UO_2(ClO_4)_a\ A_b\ m\ B_o + b\ H^+$$

with the extraction constant

$$K_{ex} = \frac{[UO_2(ClO_4)_a\ A_b\ m\ B]_o\ [H^+]^b}{[UO_2^{2+}]\ [ClO_4^-]^a\ [HA]^b\ [B]_o^m} \qquad (2)$$

TABLE 1

The distribution of uranium between solutions of TOPO and benzoic acid in carbon tetrachloride and 0.1 M $NaClO_4$ ($[H^+] = 10^{-3}$ M) at different total concentrations of the acid C_{HA}, and of TOPO, C_B. The data are given as the distribution coefficients of uranium, D, at 25° C. The values used for the determinations in the text are marked with asterisks.

C_{HA}, M	C_B, M				
	$5.00 \cdot 10^{-3}$	$1.00 \cdot 10^{-2}$	$2.00 \cdot 10^{-2}$	$3.00 \cdot 10^{-2}$	$4.00 \cdot 10^{-2}$
$6.25 \cdot 10^{-4}$	0.63	2.7	11	25	—
$1.25 \cdot 10^{-3}$	1.40	6.0	32	89	161
$2.50 \cdot 10^{-3}$	1.80	10.0	64	171	200
$5.00 \cdot 10^{-3}$	—	12.0	96	214	360
$1.00 \cdot 10^{-2}$	2.40	12.9*	63	—	400
$2.00 \cdot 10^{-2}$	2.06*	7.7*	50*	171	300
$4.00 \cdot 10^{-2}$	—	—	30*	71*	150*
$8.00 \cdot 10^{-2}$	—	—	14.8*	38*	79*

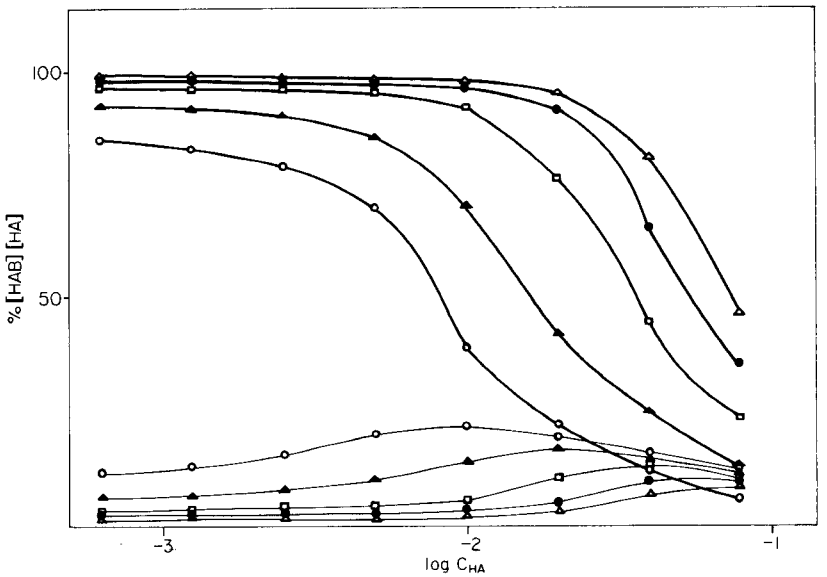

Fig. 1. The mole percentage of $[HAB]_o$ (thick lines) and [HA] (thin lines) in the two-phase system carbon tetrachloride/0.1 M $NaClO_4$ as a function of the total concentration of benzoic acid C_{HA} at different fixed concentrations of TOPO, C_B $[H^+] = 10^{-3}$ M; 25 °C. C_B in M: $5 \cdot 10^{-3}$ (○); $1 \cdot 10^{-2}$ (▲); $2 \cdot 10^{-2}$ (□); $3 \cdot 10^{-2}$ (●); $4 \cdot 10^{-2}$ (△).

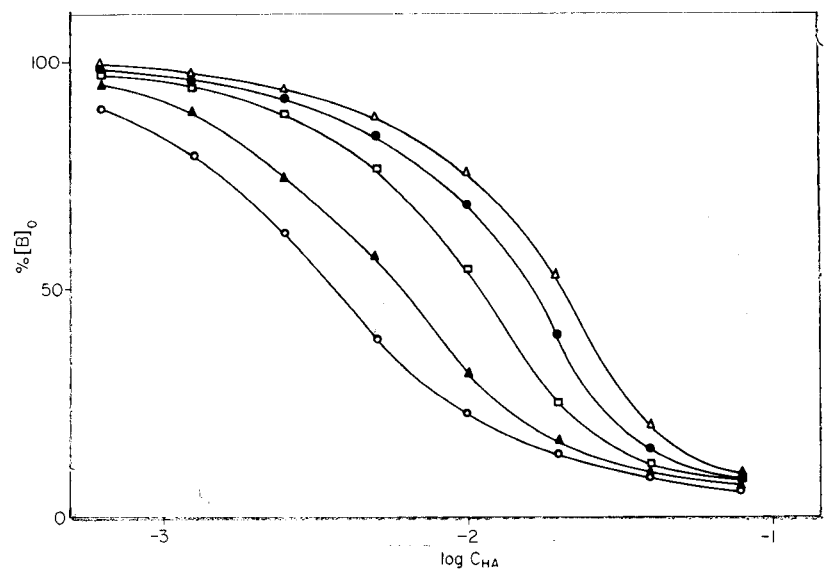

Fig. 2. The mole percentage of $[B]_o$ in the two-phase system carbon tetrachloride/0.1 M $NaClO_4$ as a function of the total concentration of benzoic acid C_{HA} at different fixed total concentrations of TOPO, C_B. Symbols as in Fig. 1 $[H^+] = 10^{-3}$ M; 25 °C.

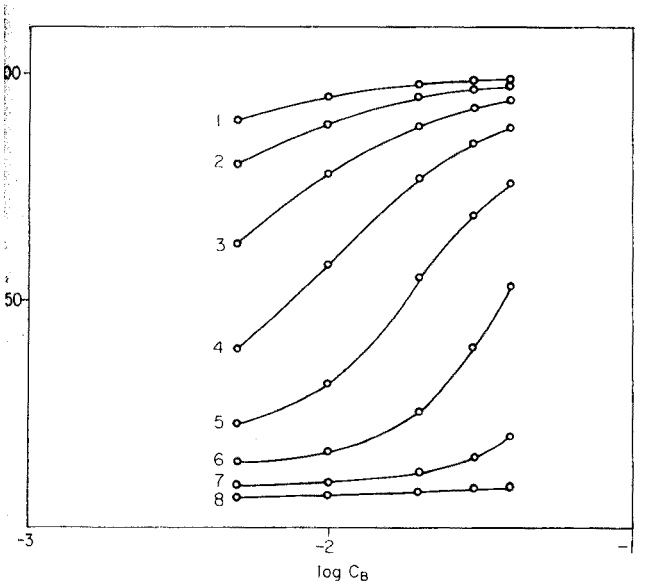

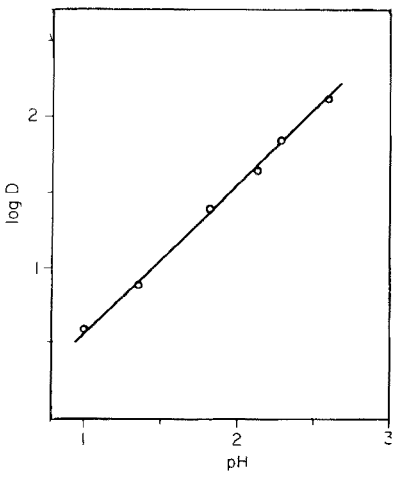

Fig. 3. The mole percentage of $[B]_o$ in the two-phase system carbon tetrachloride/ 0.1 M $NaClO_4$ as a function of the total concentration of TOPO, C_B. $[H^+] = 10^{-3}$ M; 25 °C. C_{HA} in M: Curve 1, $6.25 \cdot 10^{-4}$; curve 2, $1.25 \cdot 10^{-3}$; curve 3, $2.5 \cdot 10^{-3}$; curve 4, $5 \cdot 10^{-3}$; curve 5, $1 \cdot 10^{-2}$; curve 6, $2 \cdot 10^{-2}$; curve 7, $4 \cdot 10^{-2}$; curve 8, $8 \cdot 10^{-2}$.

Fig. 4. The distribution of uranium(VI) between carbon tetrachloride solution of TOPO and benzoic acid and 0.1 M $NaClO_4$ as a function of pH. Total concentration of TOPO, $C_B = 4 \cdot 10^{-2}$ M; total concentration of benzoic acid, $C_{HA} = 4 \cdot 10^{-2}$ M; 25 °C.

The concentration of uranium used in all experiments was such that, in the pH range studied, polymer or hydrolysis products were not formed [6]. From known data [7] for the formation of the uranyl benzoate complex, calculation showed that, under the conditions of the systems studied, the concentration of the uranyl benzoate complex in the aqueous phase is negligible in comparison with the concentration of the free uranyl ion. It is concluded that the only uranium species in the aqueous phase is UO_2^{2+}, and the distribution coefficient for uranium is:

$$D = \frac{[UO_2(ClO_4^-)_a\, A_b\, m\, B]_o}{[UO_2^{2+}]} \quad \text{or} \quad D = \frac{K_{ex}[ClO_4^-]^a\,[HA]^b\,[B]_o^m}{[H^+]^b}$$

Up to pH 3, the distribution coefficient for benzoic acid is practically constant. Hence, [HA] and $[B]_o$ for fixed C_{HA} and C_B are also constant. If $[ClO_4^-]$ is constant, as in these experiments ($[ClO_4^-] = 10^{-1}$ M), the above equation is transformed to the expression

$$\log D = \log K' + \text{pH}$$

where K' is a constant. The slope of the dependence $\log D$ vs. pH (Fig. 4) obtained from the experimental data is equal to 1; this indicates the presence

of only one benzoate ion in the extractable adduct. Therefore the second electric charge of UO_2^{2+} is neutralized with perchlorate, the other anion present in the system, and the extraction equilibrium can be expressed by

$$UO_2^{2+} + ClO_4^- + HA + m\ B_o \rightleftharpoons UO_2ClO_4\ A\ m\ B_o + H^+$$

Hence

$$\frac{D}{[HA]} = \frac{K_{ex}[ClO_4^-]}{[H^+]}[B]_o^m$$

If $[H^+]$ and $[ClO_4^-]$ are constant, this equation can be transformed to

$$\log \frac{D}{[HA]} = \log K'' + m\log [B]_o$$

The values of [HA] and $[B]_o$ calculated as described above, and the distribution coefficients of uranium obtained at $[H^+] = 10^{-3}$ (Table 1) allow $\log D/[HA]$ to be plotted vs. $\log [B]_o$. The dependence (Fig. 5) has a slope of 2; this indicates the presence of two TOPO molecules in the synergic adduct.

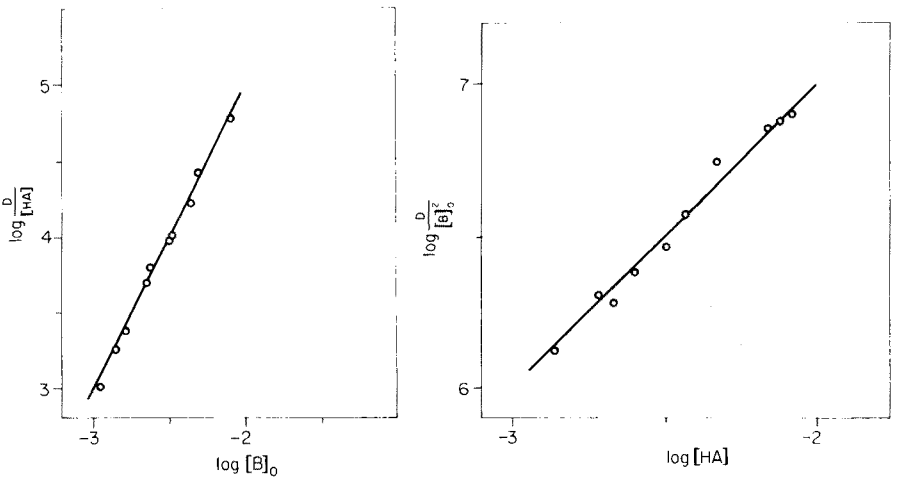

Fig. 5. The effect of increasing the concentration of free TOPO, $[B]_o$, on the extraction of uranium(VI) with carbon tetrachloride solutions of TOPO and benzoic acid from 0.1 M $NaClO_4$ (pH 3). The data are plotted as $\log D/[HA]$ vs. $\log [B]_o$. The distribution data are given in Table 1. The values of [HA] and $[B]_o$ are calculated from eqn. (1).

Fig. 6. The effect of increasing concentration of benzoic acid in the aqueous phase [HA] on the extraction of uranium(VI) with carbon tetrachloride solutions of TOPO and benzoic acid from 0.1 M $NaClO_4$ (pH 3). The data are plotted as $\log D/[B]_o^2$ vs. log [HA]. The distribution data are given in Table 1. The values for $[B]_o$ and [HA] are calculated from eqn. (1).

When the number of TOPO molecules in the adduct is known, the number of benzoate ions can be found from the data for the distribution of uranium at a constant pH. From the equation for D the following expression can be obtained

$$\log \frac{D}{[B]_o^2} = \log K''' + b \log [HA]$$

The slope of the dependence $\log D/[B]_o^2$ vs. $\log [HA]$, obtained from the calculated values of $[B]_o$ and $[HA]$ and the experimental value of D, is 1 (Fig. 6). This confirms that only one benzoate ion is present in the extractable synergic adduct.

These results show that uranium(VI) is extracted from perchlorate media by solutions of TOPO and benzoic acid in carbon tetrachloride as an adduct with the composition $UO_2ClO_4 \cdot C_6H_5COO \cdot 2(C_8H_{17})_3PO$.

The synergic extraction constant calculated from eqn. (2) with many experimental values of D is $\log K_{ex} = 7.00 \pm 0.02$.

Conclusion

The results in Table 1 show that the distribution coefficients of uranium increase with increase in TOPO concentration. The influence of benzoic acid on the distribution produces a synergic enhancement. But the dependence distribution of the uranium—benzoic acid concentration at a fixed TOPO concentration passes through a maximum. There is an optimal concentration of benzoic acid, above which the synergism is destroyed, because of an interaction between TOPO and benzoic acid. As a result the effective concentration of TOPO decreases. The concentration of the free TOPO depends to a great extent on the concentration of benzoic acid in the organic phase and on the stability of the TOPO—benzoic acid complex. The composition of the aqueous phase and the properties of the organic diluent influence the distribution of benzoic acid and its interaction with TOPO. The highest distribution coefficients of uranium are to be expected in a system in which the distribution of benzoic acid is lowest and the TOPO—benzoic acid complex is the most unstable.

REFERENCES

1 St. Mareva, N. Jordanov and M. Konstantinova, Anal. Chim. Acta, 59 (1972) 319.
2 M. Konstantinova, St. Mareva and N. Jordanov, Anal. Chim. Acta, 68 (1974) 237.
3 M. Konstantinova, St. Mareva and N. Jordanov, Anal. Chim. Acta, 90 (1977) 295.
4 V. Markov, E. Vernii, A. Vinogradov, S. Elinson, A. Kligin and I. Moiseev, Uran — Metodi ego opredelenia, Atomizdat, Moscow, 1964, p. 160.
5 S. Savvin, Arsenazo III, Atomizdat, Moscow, 1966.
6 S. Havel and L. Sommer, Chromogenic Reactions of Uranium, Folia, 1973, p. 15.
7 S. Ramamoorthy and M. Santappa, Bull. Chem. Soc. Jpn., 7 (1968) 1330.

Analytica Chimica Acta, 90 (1977) 193—200

THE DETERMINATION OF MOLYBDENUM AND TUNGSTEN IN SEA AND SURFACE WATER

H. A. v. d. SLOOT, G. D. WALS and H. A. DAS

Energieonderzoek Centrum Nederland, Westerduinweg 3, Petten-NH (The Netherlands)

(Received 30th October 1976)

SUMMARY

A simple method for the determination of molybdenum and tungsten in sea and surface water is presented. Molybdenum and tungsten are concentrated on activated charcoal by adsorption as the ammonium pyrrolidine dithiocarbamate complex; the optimal pH for adsorption is 1.3. Mo and W are then determined by thermal neutron activation, forming ^{99}Mo ($T_{1/2}$ = 66.7 h) and ^{187}W ($T_{1/2}$ = 23.8 h), respectively. The ^{99m}Tc daughter of ^{99}Mo is measured as soon as the equilibrium between ^{99m}Tc ($T_{1/2}$ = 6 h) and ^{99}Mo is established. The detection limits are 0.05 μg Mo l^{-1} and 0.05 μg W l^{-1} (or 0.001 μg W l^{-1} after a simple chemical separation).

Several methods are known for the determination of molybdenum in sea water; ion-exchange [1, 2], coprecipitation [3, 4], extraction [5, 6] and kinetic methods [7] have been used. For the determination of tungsten in sea water, fewer possibilities are available [2, 8, 9], and the methods tend to be laborious, requiring large sample volumes.

This paper reports a relatively simple method based on preconcentration of Mo and W on activated charcoal in the presence of ammonium pyrrolidine-dithiocarbamate (APDC) and a final determination of these elements by neutron activation of the charcoal adsorbers. Preconcentration at the sampling site gives small charcoal samples which can be stored easily for later analysis. For the determination of tungsten, sample volumes of 0.5—1 l are required, while 0.2 l is sufficient for the determination of molybdenum. Instrumental measurement of molybdenum by its daughter ^{99m}Tc ($T_{1/2}$ = 6 h) is performed after the equilibrium between ^{99m}Tc and ^{99}Mo ($T_{1/2}$ = 66.7 h) has been established. In the determination of tungsten in sea water a simple chemical separation is necessary to remove interfering matrix activities, e.g. ^{82}Br and ^{24}Na.

Choice of adsorption conditions

In preliminary studies of the adsorption behaviour of Mo and W on activated charcoal, the following results were obtained. The optimal pH values for adsorption of Mo and W without addition of reagents are 3.5 and 3, respectively. At the concentration levels encountered in natural

systems, the adsorption on activated charcoal is described by the Henry equation. Once adsorbed, Mo and W are only partially removed from the charcoal by washing with acid or base. Out of twelve reagents tested, only APDC and 8-hydroxyquinoline (oxine) led to a quantitative adsorption on charcoal. Since the solubility of oxine in water is low compared with that of APDC, further experiments were done with APDC.

The effects of the acidity, the concentration of APDC, the amount of charcoal, the stirring time, the salinity and the sample volume on the adsorption of molybdenum and tungsten on activated charcoal were studied to establish the optimal conditions. All experiments were done separately with ^{99}Mo and ^{187}W tracers. Instead of counting the photopeaks of ^{99}Mo, better sensitivity can be obtained with the daughter nuclide ^{99m}Tc ($T_{1/2}$ = 6 h). After a cooling time of about 60 h, the ^{99m}Tc—^{99}Mo equilibrium is established. The samples were then counted in a well-type NaI crystal connected to a single-channel analyzer. Samples containing ^{187}W were counted as soon as possible, because of the relatively short half-life of ^{187}W.

The following general conditions were used: APDC concentration, 10 mg/100 ml; amount of charcoal, 20 mg; stirring time, 20 min; sample volume of sea water, 100 ml. The above-mentioned parameters were varied one by one. Activated charcoal was added to the samples as a suspension in double-distilled water; this was kept homogeneous by continuous stirring. The "stock" suspension contained 40 g of charcoal powder per l.

Acidity. Samples (100 ml) of sea water were spiked with ^{99}Mo. The pH of the samples was adjusted to values ranging from 0.5 to 9.5, and a 500-μl aliquot of the charcoal suspension and 10 mg of APDC were added. The samples were stirred on a magnetic stirrer for 20 min. The charcoal was then separated by filtration through a membrane filter (8-μm pore), a radiochemical chimney being mounted on the suction flask. Filter and charcoal were transferred to a test tube and counted. Comparison with an aliquot of the tracer solution gave the percentage adsorption. The same procedure was applied for W, with ^{187}W as the radiotracer. The influence of acidity on the adsorption of Mo and W is shown in Fig. 1. For both elements, adsorption at pH 1.2—1.4 is adequate; a pH value of 1.3 was used in the study of other parameters.

Concentration of ammoniumpyrrolidine dithiocarbamate. The concentration of APDC was varied from 1 mg/100 ml to 50 mg/100 ml. The other parameters were kept constant at the preset values. Results are given in Fig. 2. The optimal concentration for simultaneous adsorption of both elements is 150 mg of APDC per l.

Amount of charcoal. Instead of 20 mg of charcoal as used in other experiments, the amount of charcoal was varied from 4 to 160 mg/100 ml. Results are given in Table 1.

Stirring time. Stirring times from 1—120 min were tested. The results are shown in Table 2. A period of 40—60 min was chosen for the final method.

Salinity. In the presence of APDC the salinity had no effect on the

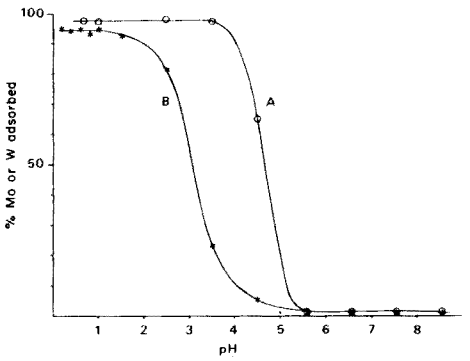

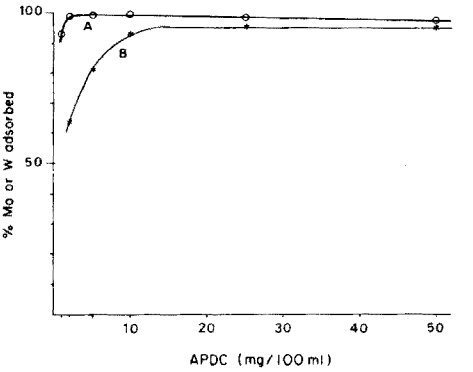

Fig. 1. The influence of pH on the adsorption of the molybdenum—APDC (curve A) and tungsten—APDC (curve B) complexes on activated charcoal.

Fig. 2. The influence of APDC-concentration on the adsorption of molybdenum (curve A) and tungsten (curve B) on activated charcoal.

TABLE 1

The influence of the amount of charcoal on the adsorption of Mo and W

Charcoal (mg/100 ml)		4	8	20	40	80	160
% Adsorbed	Mo	90.1	98.0	100.3	98.8	101.1	99.6
	W	68.6	84.6	93.3	89.4	83.4	—

TABLE 2

Influence of the stirring time on the adsorption of Mo and W

Time (min)		1	5	10	20	40	120
% Adsorbed	Mo	95.1	97.4	98.9	96.7	98.6	98.7
	W	52.7	81.7	87.8	94.5	97.2	—

adsorption of Mo and W on activated charcoal. In tap water and surface water the adsorption yield was definitely the same as in sea water.

Sample volume. For molybdenum, sample volumes ranging from 100—1000 ml were used. For tungsten, the volumes ranged from 100—800 ml. The other conditions are given in Table 3 along with the results. To obtain a higher yield for tungsten by adsorption from a larger sample volume, it is not necessary to increase the amount of charcoal pro rata. The following rule may be applied for sample volumes up to 1 l: amount of charcoal $= 20 + 0.1\ (V - 100)$ mg, where V is the volume in ml. The results obtained in this way are also shown in Table 3.

Optimal conditions for adsorption of Mo and W. On the basis of these tests, the optimal conditions for the simultaneous adsorption of Mo and W on activated charcoal are: pH 1.3; APDC concentration, 150 mg l^{-1}; amount of charcoal, $20 + 0.1\ (V - 100)$ mg (V = sample volume in ml); stirring time, 40—60 min.

TABLE 3

The influence of sample volume on the adsorption of Mo and W (pH 1.3; 20 mg of charcoal; stirring time, 20 min; APDC, 100 mg l^{-1} for Mo and 150 mg l^{-1} for W)

Sample volume (l)		0.1	0.2	0.4	0.5	0.75	0.8	1.0
% Adsorbed	Mo	99.7	99.1	—	99.5	99.0	—	98.5
	W	94.2	92.3	91.1	—	—	86.3	—
	W[a]	93.8	94.7	95.2	—	—	94.1	—

[a]Extra charcoal used, see text.

Contamination during sampling and separation of suspended matter

To minimize the contamination of water samples, sampling was done with a polyethylene bucket. The first portion was used to rinse out the bucket and then discarded. A second haul was used for analysis. Suspended matter was separated immediately after sampling. Both continuous centrifugation at 10,000 × G (flow rate 1.2 l min^{-1}) and filtration through 0.45-μm membrane filters were used. After these operations, no contamination of samples with Mo or W was noted.

Blank values of reagents

The blank values for activated charcoal, membrane filters, APDC and hydrochloric acid were determined by instrumental neutron activation analysis, by means of the reaction ^{98}Mo (n,γ) ^{99}Mo ($T_{1/2}$ = 66.7 h) β^- ^{99m}Tc ($T_{1/2}$ = 6 h), and ^{186}W (n,γ) ^{187}W ($T_{1/2}$ = 23.8 h). The 140-keV photopeak of ^{99m}Tc was counted on a Ge(Li) detector after a waiting time of 60 h. ^{187}W was counted after 24 h to allow the decay of some short-lived nuclides. The results were as follows.

Material	Blank value ($\mu g\ g^{-1}$)	
	Mo	W
Activated charcoal	0.2	Not detectable
Membrane filter (AE99)	0.015	Not detectable
APDC	0.05	0.005
Hydrochloric acid, 6 M	0.02	0.0003

Radiochemical interference

The presence of uranium in the charcoal samples may interfere with the determination of molybdenum by production of ^{99m}Tc from fission. The fraction of uranium which is adsorbed under the optimal conditions for adsorption of molybdenum and tungsten is 11 ± 1%. The contribution of ^{99m}Tc from ^{235}U fission stems from direct fission to ^{99m}Tc and from fission to ^{99}Mo, which decays to ^{99m}Tc, reaching equilibrium after approximately 60 h. Thus, when a waiting time of 60 h is used the direct production of ^{99m}Tc can be neglected.

For ^{99}Mo the fission yield is 6.1%. The abundance of ^{98}Mo is 0.24, the fission cross-section of natural uranium is 4.18 *b*, and the thermal neutron cross-section of ^{98}Mo is 0.15 *b*. This yields:

$$\frac{A(n,f)}{A(n,\gamma)} = 2.9 \frac{\text{U concentration}}{\text{Mo concentration}}$$

For sea water, which contains ca. 3.3 μg U l^{-1} and 11 μg Mo l^{-1}, the ratio amounts to 0.096 or 9.6%. Consequently, the following correction procedure was adopted. Together with the charcoal samples and molybdenum standards, a uranium standard (ca. 4 μg U) was irradiated under identical conditions. Since ^{239}U formed by a (n,γ) reaction from ^{238}U decays to ^{239}Np ($T_{1/2}$ = 2.36 d), the ^{239}Np activity can be used as a measure of the activity of ^{99m}Tc from fission of ^{235}U, provided that the isotopic composition of uranium in the sample is natural. The activity ratio of ^{239}Np to ^{99m}Tc (fission) was determined from the uranium standard. By comparison with the ^{239}Np activity of a charcoal sample, the ^{99}Mo contribution from uranium was obtained.

EXPERIMENTAL

Reagents and apparatus

All the chemicals used were of analytical-reagent grade. The activated charcoal was Type 2186 (Merck). Double-distilled nitric acid was prepared in a quartz still, and the 6 M hydrochloric acid was purified by distillation. The membrane filters were of the type Selectron AE 99 (30 mm diameter, 8-μm pores).

The apparatus included Eppendorff micropipettes with disposable tips, quartz capsules (8 mm i.d. and 3 mm i.d.) and a radiochemical chimney (Sartorius) mounted on a suction flask.

A 3 × 3-in NaI well-type crystal was connected to a single-channel analyzer for the tracer experiments. For routine work a coaxial Ge(Li) detector (Canberra) and a 1024- or 4000-channel analyzer, were used. Spectra were read out on magnetic tape.

Preparation of ^{99}Mo and ^{187}W tracer solutions

The ^{99}Mo and ^{187}W tracer solutions were prepared by irradiation of MoO_3 and Na_2WO_4 for 24 h in a thermal neutron flux of $5 \cdot 10^{13}$ n cm^{-2} s^{-1}; 2 mg of MoO_3 and 0.1 mg of Na_2WO_4 were adequate. After cooling for 1 d, the activated compounds were dissolved in concentrated ammonia. The "stock" tracer solutions of ^{99}Mo and ^{187}W were obtained by dilution to 500 ml with water.

Procedure for the concentration of Mo and W

Transfer a water sample of 500 ml obtained after filtration or centrifugation of the crude sample to a 500-ml beaker. Adjust the pH with 6 M HCl to 1.3.

Add 60 mg of charcoal as a suspension in double-distilled water, followed by 75 mg of APDC. Stir the sample on a magnetic stirrer for 40—60 min. Separate the charcoal by filtration through a membrane filter (8-μm pore) using a radiochemical chimney mounted on a suction flask. Dry the filter covered with charcoal, remove the charcoal from the filter, and transfer it to a quartz capsule (3 mm i.d.) which is sealed.

Prepare molybdenum, tungsten and uranium standards by putting 60-mg amounts of activated carbon in quartz capsules (8 mm i.d.) and moistening the charcoal with 20-μl aliquots of a molybdenum, tungsten or uranium standard solution, containing, respectively, 2.5 mg Mo ml^{-1}, 0.2 mg W ml^{-1} or 0.08 mg U ml^{-1}. After drying, seal the capsules. Clamp flux monitors on the capsules to allow corrections for differences in the integrated neutron flux.

Place the samples and standards together in an aluminium can for irradiation (ca. 15 capsules).

Irradiation and measurement

Samples and standards were irradiated for 24 h in the Poolside Isotope Facility at a thermal neutron flux of $5 \cdot 10^{13}$ n cm^{-2} s^{-1}.

After cooling for 1 d, transfer samples and standards to test tubes and count on a Ge-(Li) detector connected to a 4000-channel analyzer for ^{187}W ($T_{1/2}$ = 23.8 h). About 60 h after the end of the irradiation, start the counting of the 140-keV photopeak of ^{99m}Tc on a Ge—Li detector. The spectra were read out on magnetic tape and transferred to a computer for peak calculation and decay correction.

Taking into account possible flux corrections, calculate the original content of Mo and W in the water sample. Correct the molybdenum content for the contribution of ^{99m}Tc activity from uranium fission by means of the ^{239}Np-activity in the sample and in the uranium standard.

The specific count rate of ^{187}W at the end of the irradiation is $1.5 \cdot 10^5$ cpm/μg W for the 685-keV photopeak, and the specific count rate of ^{99}Mo at 60 h after the end of the irradiation is $2.5 \cdot 10^3$ cpm/μg Mo for the 140-keV photopeak of the ^{99m}Tc daughter of ^{99}Mo. The limits of detection are 0.02 μg Mo l^{-1} and 0.01 μg W l^{-1} based on 1-l samples. Because of matrix activities, e.g. ^{82}Br and ^{24}Na, it is not possible to determine W in sea water purely instrumentally. A chemical separation has to be applied in this case.

Chemical separation of tungsten from the charcoal matrix

The separation is based on the procedure described by Kawabuchi and Kuroda [2]. After irradiation, transfer the charcoal to a small quartz boat and add ca. 10 μg of tungstate as carrier. Carefully burn off the charcoal in a muffle furnace at 800—900°C; this takes about 3 min. No loss of either molybdenum or tungsten was observed after this treatment. Dissolve the inorganic residue in concentrated ammonia. Dilute the sample and make it

0.1 M in hydrochloric acid and 0.1 M in ammonium thiocyanate. Pass this solution through a column (3 cm × 1 cm i.d.) of Dowex 1-X8 which has been previously washed with 0.1 M HCl—0.1 M NH_4SCN; this column retains both tungstate and molybdate quantitatively. Rinse the column with the same mixture and transfer to a test tube or disk for counting on a Ge—Li detector.

The geometry factor between counting of the standard in a polythene capsule and counting of the sample as a thin layer of resin on a disk or in a test tube is determined separately with an aliquot of the ^{187}W tracer solution. The detection limit achieved in this way is 0.001 $\mu g\ W\ l^{-1}$.

RESULTS

Standard addition experiments were done by addition of known quantities of molybdenum or tungsten to 200-ml portions of double-distilled water. The results are given in Table 4.

The molybdenum concentration of tap-water samples taken at two different locations were 4.3 and 3.1 $\mu g\ Mo\ l^{-1}$, while the tungsten concentrations were 0.052 and 0.047 $\mu g\ W\ l^{-1}$.

The results of the analysis of samples of surface water are given in Table 5.

Molybdenum in sea water

Figure 3 shows the relationship between the concentration of molybdenum and the salinity for samples taken in the Scheldt estuary. Sampling was

TABLE 4

Standard addition of molybdenum and tungsten to double-distilled water

Mo added (μg)	20	10	5	0.20	0.10	
Mo found (μg)	21.1	10.2	5.23	0.19	0.10	
W added (μg)	2.00	1.00	0.50	0.20	0.10	0.05
W found (μg)	2.04	0.97	0.56	0.22	0.102	0.054

TABLE 5

Molybdenum and tungsten concentrations in surface water

Location of sampling	$\mu g\ Mo\ l^{-1}$	$\mu g\ W\ l^{-1}$
Rhine (Lobith)	1.4 ± 0.1	—
Rhine (Rotterdam)	0.8 ± 0.1	—
IJssel (Deventer)	3.8 ± 0.2	0.09 ± 0.02[a]
Noord Hollands Kanaal (Petten)	2.8 ± 0.1	0.026 ± 0.004[b]

[a] Analysed without chemical separation of tungsten after irradiation.
[b] Tungsten chemically separated from the radioactive matrix. Mean of 4 analyses.

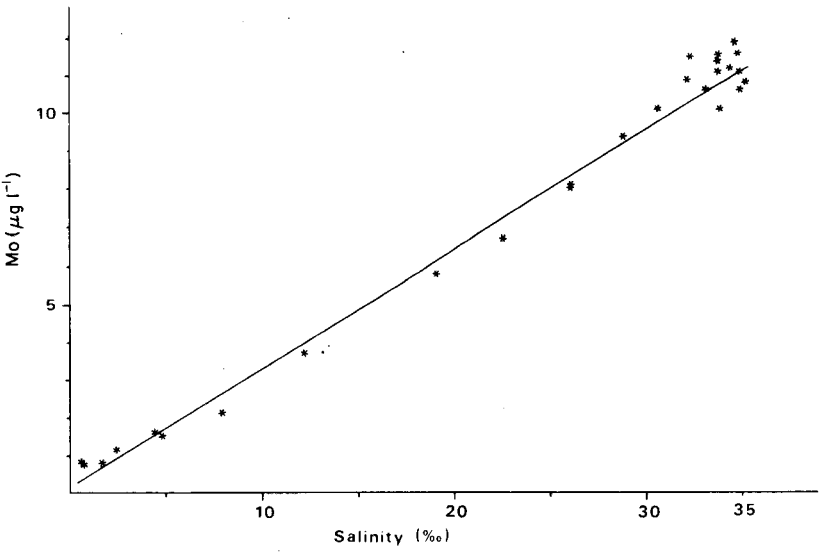

Fig. 3. The relationship between molybdenum concentration and salinity in samples taken from the Scheldt estuary.

done during a cruise of the M.S. "Aurelia" of the Netherlands Institute for Sea Research. The salinity measurements were done aboard the ship. Good agreement with the results obtained by Head and Burton [4] and by Morris [10] was found.

The ratio Mo content ($\mu g\ l^{-1}$) salinity ($^{\circ}/_{oo}$) is 0.32 ± 0.02. The average value of the Mo concentration at a considerable distance offshore was 10.7 ± 0.3 μg Mo l^{-1} (n = 3). The salinity of the sample was 35.1 $^{\circ}/_{oo}$. The tungsten concentration determined in a sample of sea water (34.9 $^{\circ}/_{oo}$) averaged 0.123 ± 0.06 μg W l^{-1} (n = 3).

The authors thank the management of the Netherlands Institute for Sea Research (Prof. Dr. J. H. Postma) and Dr. J. C. Duinker for their kind assistance. The technical assistance of A. N. M. van Yperen is gratefully acknowledged.

REFERENCES

1 J. P. Riley and D. Taylor, Anal. Chim. Acta, 41 (1968) 175.
2 K. Kawabuchi and R. Kuroda, Anal. Chim. Acta, 46 (1969) 23.
3 K. M. Chan and J. P. Riley, Anal. Chim. Acta, 36 (1966) 220.
4 P. C. Head and J. D. Burton, J. Mar. Biol. Ass. U.K., 50 (1970) 439.
5 Y. K. Chan and K. Lum-Shue-Chan, Anal. Chim. Acta, 48 (1969) 205.
6 T. Fujinaga, Y. Kusaka, M. Koyama, H. Tsuji, T. Mitsuji, S. Imai, J. Okuda, T. Takamatsu and T. Ozaki, J. Radioanal. Chem., 13 (1973) 301.
7 R. Kuroda and T. Tarui, Z. Anal. Chem., 269 (1974) 22.
8 M. Ishibashi, T. Fujinaga, T. Kuwamoto, M. Koyama and S. Sugibayashi, J. Chem. Soc. Jpn., 81 (1960) 392.
9 K. M. Chan and J. P. Riley, Anal. Chim. Acta, 39 (1967) 103.
10 A. W. Morris, Deep-Sea Res., 22 (1975) 49.

Analytica Chimica Acta, 90 (1977) 201—207

AUTOMATED DETERMINATION OF SUGAR IN MOLASSES

H. JANSHEKAR and J.-R. MOR
Institute of Microbiology, Swiss Federal Institute of Technology, Zürich (Switzerland)
(Received 29th November 1976)

SUMMARY

The importance of determining sugars in molasses is emphasized, and a short critical review of the methods available is presented. The difficulties and sources of errors in determining total sugar levels in molasses and sugar mixtures are discussed. A continuous automated procedure based on the hexacyanoferrate(III)/(II) redox reaction has been optimized by reducing the errors and interferences to a minimum. With this technique, sugar concentrations of 0—10 g l^{-1} can be determined directly.

Beet or cane molasses, the residues in the sugar industry from which no more sugar can be profitably extracted, contain most of the organic acids, minerals, nitrogenous compounds and other components remaining after the crystallization process of the sugar. As molasses also contain ca. 50% of sugars which are prevented from crystallization because of the impurities present, they have been used increasingly as substrates for microbial propagation.

One of the most important parameters in the control of microbial growth is an accurate determination of the sugar content. Although several attempts have been made to devise a sensitive and accurate determination of the sugar content in molasses, a satisfactory solution has yet to be found. Information on the sugar concentration is essential for comparing the yields obtained with theoretical values, for carbon balances, and for the calculation of substrate uptake rates.

In industrial yeast production, the analysis of molasses is generally carried out on the clarified, sterilized mash which consists, usually, of a mixture of sugars derived from beet and/or cane molasses. Most of the existing analytical methods are based on the fact that sugars have reducing properties in alkaline solution, and this has led to the exploitation of a wide variety of oxidants in assay methods.

Usually the industrial method of choice is to determine sugar, as glucose, by titration with Fehling's solution with methylene blue as indicator. The anthrone method [1] is quicker and quite sensitive, and sucrose is hydrolysed at the low pH used, but high values are given if SO_2 is present. Although the method of Luff and Schoorl [2] is quicker and more sensitive than

anthrone, and is not affected by SO_2, prior hydrolysis of sucrose is necessary. For qualitative and quantitative analysis, the Luff and Schoorl method or the anthrone method can be combined with a glucose assay (*o*-toluidine) following separation of sugars by a thin-layer chromatographic technique [3], but this method is tedious since several intermediate steps are needed.

Our first attempts to devise an operational automated assay involved a picric acid method, in which the sample was heated with HCl to hydrolyze the sucrose present, neutralized with NaOH, and mixed with an alkaline picrate solution. After incubation, the coloured product was measured at 540 nm. Although this method gave a linear response up to 1% (w/v) of sugars in solution, it proved to be unreliable at low sugar concentrations. In the search for an alternative method, more specific assays were excluded a priori because molasses contain a mixture of sugars. Furthermore, most of the methods in the literature are not suitable for automated routine analyses; they lack either specificity or precision, or do not account for interfering substances, or are too tedious. In addition to analytical imperfections, other factors of a more general nature can influence the determination of sugars. The sources of errors can be divided into four categories.

(a) Environmental factors. The reactions of sugars with analytical reagents are not simple or stoichiometric. Because the extent of oxidation is influenced by factors such as pH, temperature, and salt and oxidant concentration, the reaction conditions must be standardized completely. Although this may not be easy with manual techniques, the use of automatic systems helps to some extent to avoid some errors and so improves reproducibility [4]. The method in question should also avoid dilution steps which may introduce sources of error. If concentrated broths are to be involved, a less sensitive method may be preferable. Obviously the most acceptable method will be that which is sensitive over a relatively wide concentration range.

(b) Composition of the medium. Molasses contain coloured materials and various charged colloids in addition to sugars. The melanoidine-type nitrogen compounds and caramel compounds [5] that result from thermal decomposition of sucrose are yellow or brown and constitute up to 22% of nondialyzable matter; their molecular weights range from 10000 to 50000 daltons [6]. The colouring matter in crude molasses has reducing groups that can interfere with the accuracy of measurements based on the reducing properties of carbohydrates in alkaline solutions. Colloids, with both positive and negative charges, contribute about 85% of the colour of molasses [7] and their flocculation at various pH values interferes with colorimetric assays.

(c) Metabolic products. The metabolic breakdown of glucose produces a variety of acids, esters, aldehydes, alcohols, etc, any of which can disturb the determination of reducing sugars. For example yeast produces alcohol under anaerobic conditions through oxidative decarboxylation of pyruvate with the intermediate formation of acetaldehyde. Normally the intermediate

metabolites are present at low concentrations, particularly at the stationary growth phase. However, there may be an accumulation of these intermediates, either at the beginning of the exponential phase or under unfavourable growth conditions [8]. As acetaldehyde can be easily oxidized, trace amounts can cause considerable errors in the determination of sugars.

(d) Mixture of various sugars. Several methods are available for the calibration of the procedures used to determine the total sugar content of a mixture. A mixture of mono- and polysaccharides analogous in composition to the natural specimens, may be used to produce a calibration curve. Alternatively, an individual sugar, usually glucose, may be used for the standard curve, which is then corrected for mixtures of differing composition. In the first method, the identity of all the sugars in the sample must be known. This may be difficult since the ratios of various sugars which occur during different phases of microbial growth may change. When a glucose standard is used it is assumed that a complete hydrolysis of polysaccharides has occurred. Furthermore, the assumption that the different monosaccharides form coloured complexes of the same intensity, is seldom valid.

Taking all these points into consideration, the following method was adopted. The technique employed is the method of Hoffman [9] modified so that the interferences mentioned in the preceding section are minimized. The glucose is oxidized to gluconic acid by boiling with hexacyanoferrate(III) according to

$$C_6H_{12}O_6 + H_2O + 2[Fe(CN)_6]^{3-} \xrightarrow{95^\circ C} C_6H_{12}O_7 + 2[Fe(CN)_6]^{4-} + 2H^+$$

The yellow solution is reduced to the colourless hexacyanoferrate(II) and the decrease in intensity of the colour is measured (inverse colorimetric technique).

EXPERIMENTAL

Apparatus and reagents

The procedure was automated for a chemical flow system (AutoAnalyzer type I; Technicon Instruments Corp.). Figure 1A shows the flow diagram. The following modules were used: sampler II, proportioning pump II, two adjustable heating baths, dialyzer with standard Cuprophan membranes, N-colorimeter with 15-mm tubular flow cell and 425-nm interference filter, recorder, and voltage stabilizer. The recorder peaks were digitized by an analog/digital converter (Infotronics CRS 270) interfaced to a teletype, puncher or other data collecting system for further processing.

Potassium hexacyanoferrate(III) solution was prepared by dissolving 0.55 g of $K_3Fe(CN)_6$ in 1 l of 1 M NaOH solution. The acid solution was 1 M HCl.

To improve the flow pattern, Brij-35 (1 ml l^{-1}; polyoxyethylene lauryl ether; Merck) was added to the solutions.

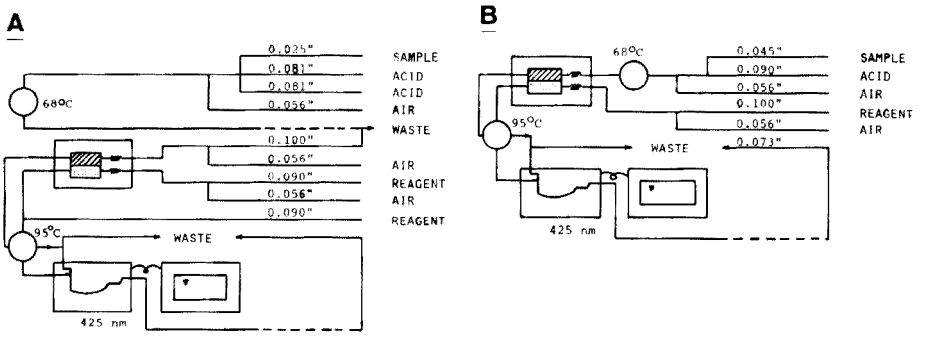

Fig. 1. Flow diagram with manifold for the automated assay of sugar in molasses. Dimensions of pump tubing shown in inches i.d. A: Flow system for sugar concentrations of 1—9 g l^{-1}. B: Optimized flow chart for sugar concentrations in the range 0—1 g l^{-1}.

Procedure

The unknown sample is hydrolyzed with 1 M HCl at 68 °C. Improper hydrolysis conditions can lead to errors in the sugar determination through sucrose destruction, caramelization, production of furfural and hydroxymethylfurfural, or incomplete hydrolysis. The brown colour formed during caramelization also absorbs in the same region as the hexacyanoferrate(III) [10]. These errors are avoided [11] by hydrolysis at 68 °C in 1 M HCl. After hydrolysis, an aliquot is dialyzed against the reagent stream (alkaline hexacyanoferrate(III) solution) which favours the reactive enediol tautomer. After incubation at 95 °C the colour disappearance is measured colorimetrically.

In the conventional AutoAnalyzer operation, the recipient stream passes through the 95 °C heater after dialysis and the donor stream goes to waste. The resulting difference in temperature causes pressure variations between the two lines, resulting in incorrect recordings. This problem was rectified by modifying the manifold of the flow system so that both streams pass through the 95 °C bath after dialysis.

RESULTS AND DISCUSSION

The flow system (Fig. 1A) was optimized for glucose concentrations of 1—9 g l^{-1}. Since a decrease in colour intensity is measured, the selectivity and precision of measurement at low sugar concentrations is poor, and the use of a recorder range expander is not recommended. Furthermore, at low sugar concentrations the relationship between colour intensity and substrate concentration deviates strongly from linearity, (Fig. 2). To determine sugars in the range 0—1.0 g l^{-1}, an alternative manifold should be employed (Fig. 1B).

Table 1 shows the percentage recovery of various sugars (xylose, arabinose, glucose, fructose, galactose, mannose, sucrose and raffinose) obtained with a glucose standard curve. A similar response was obtained with equimolar concentrations of the different sugars investigated.

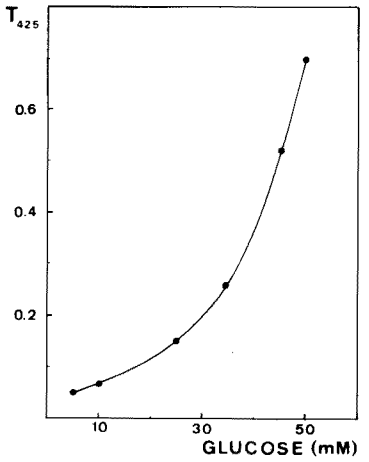

Fig. 2. Relationship between optical transmission and sugar concentration when the inverse colorimetric technique is used (T = transmission).

TABLE 1

Recovery of different sugars by the proposed method
(Percentage values calculated from a glucose calibration curve.)

	D(+)-Xylose, or D(−)-Arabinose	D(+)-Galactose	D(−)-Fructose	D(+)-Mannose	D(+)-Sucrose	Raffinose
Recovery (Average %)	96.4	96.2	101.6	102.0	101.6	56.8
S.d. (%)	0.53	1.50	1.25	1.73	0.63	2.46

The hydrolysis conditions were sufficient to hydrolyze sucrose completely but not raffinose, as indicated by the poor recovery for this sugar in Table 1. If complete hydrolysis of raffinose, starch or cellulose is achieved by increasing the time, temperature or acid concentration destruction of monosaccharides takes place. Table 2 shows the percentage carbon recovery obtained from determinations carried out with solutions containing different sugars. Again the effects of incomplete raffinose hydrolysis are evident.

This automated method overcomes most of the difficulties and sources of errors encountered with complex, natural mixtures of sugars. The poor response of raffinose, however, can lead to low results. The additions of formaldehyde (4%, w/v), glycerol (0.9%, w/v), ethanol (1%, w/v), pyruvate (0.1%, w/v), acetate (1%, w/v), benzoate (saturated) and ammonium salts (0.3%, w/v) had no detectable effects on the measurements. Acetaldehyde

TABLE 2

Carbon recovery of different sugar mixtures
A, B and C contain equimolar amounts of each sugar. In solutions D and E the amounts were not equimolar. The raffinose concentration in E was triple that in D.

	A	B	C	D	E
	glu + man + gal + fru	glu + man + gal + fru + xyl	glu + man + gal + fru + xyl + suc	glu + man + gal + fru + xyl + suc + raf	glu + man + gal + fru + xyl + suc + raf
Calcd. ($g\ C\ l^{-1}$)	2.52	2.44	2.45	2.47	2.47
Measd. ($g\ C\ l^{-1}$)	2.48	2.48	2.48	2.41	2.34
Recovery (%)	98.4	101.6	101.2	97.6	94.7

caused considerable errors at concentrations of 0.1 $g\ l^{-1}$ or less, but this problem can be overcome by heating samples for at least 20 min in a boiling water bath. Sufficient water should be added to the samples, after heating, to compensate for the loss through evaporation. Since the dialysis rate changes with aging of the membrane (a decrease of up to 0.25 $g\ l^{-1}\ h^{-1}$ can occur in the mass transfer rate) it is recommended that standards be run after every 30 samples.

Sodium hydroxide (not sodium carbonate) should be used to make the alkaline cyanoferrate solution; this prevents the formation of CO_2 which otherwise disrupts the uniform flow pattern of the liquid segments and neutralizes the hydrolysate in the dialyzer. The Cuprophan membranes of the dialyzer separate some of the colloids, especially the negatively charged ones. The other colloids do not disturb the photometer function; their flocculation time (20 min) is greater than the total residence time (14 min) of samples in the system.

The proposed method is simple; only one reagent, inexpensive and easy to prepare, is needed. The reagents are also stable against photo-oxidation. Concentration changes down to ca. 0.001% can be easily detected. The technique is rapid compared with other methods available; 40 samples per hour with a sample/wash ratio of 2:1 can be processed.

The authors are indebted to Professor Dr. A. Fiechter for his interest and help throughout this study. The work was supported by a grant from the Zentenarfonds ETH, Zürich.

REFERENCES

1 S. Bailey, Biochem. J., 68 (1958) 669.
2 S. Luff and N. Schoorl, Z. Unters. Lebensm., 57 (1929) 655.
3 V. A. de Stefanis and J. G. Ponte, J. Chromatogr., 34 (1968) 116.
4 R. D. Baillie, Can. J. Med. Tech., 38 (1976) 50.
5 I. F. Bugaenko, I. P. Slavgorodskaya and I. I. Pavlov, Pishch. Tekhnol., 6 (1972) 91.
6 F. Tsuchida, K. Hironobu and M. Komoto, Seito Gijutsu Kenkyukaishi, 22 (1970) 65.
7 H. Olbrich, Die Melasse, Inst. f. Gärungsgewerbe, Berlin, 1956, p. 58.
8 I. L. Rabotnova, L. M. Balakireva, S. A. Lirova and E. A. Andreeva, Prikl. Biokhim. Mikrobiol., 7 (1971) 416.
9 W. S. Hoffman, J. Biol. Chem., 120 (1937) 51.
10 K. W. Fuller, Automation in Analytical Chemistry, Technicon Symposia, Mediad Inc., New York, 1966.
11 W. W. Skinner (Ed.), Official and Tentative Methods of Analysis, Assoc. Off. Agric. Chem., Washington, 5th edn., 1940.

Analytica Chimica Acta, 90 (1977) 209—214

KINETIC STUDY AND ANALYTICAL APPLICATION OF THE IODATE—HYPOPHOSPHITE REACTION IN STRONGLY ACIDIC SOLUTIONS

D. P. NIKOLELIS, M. I. KARAYANNIS, E. V. KORDI and T. P. HADJIIOANNOU

Laboratory of Analytical Chemistry, University of Athens, Athens (Greece)

(Received 15th November 1976)

SUMMARY

The iodate—hypophosphite reaction in strongly acidic solutions was studied spectrophotometrically. Reaction rate constants and the activation energy of the reaction are reported. A method for determining hypophosphite on the basis of this reaction is described. Hypophosphite in the range 0.06—4 mg (10^{-3}—$6 \cdot 10^{-2}$ M) can be determined with a relative error and relative standard deviation of 2—3%.

The iodate—hypophosphite reaction takes place in two main steps [1]

$$IO_3^- + 3H_2PO_2^- \rightarrow I^- + 3H_2PO_3^- \quad (1)$$

$$IO_3^- + 5I^- + 6H^+ \rightarrow 3I_2 + 3H_2O \quad (2)$$

In the work described here, this reaction was studied in strong acidic solutions with the iodate present in large excess, so that the iodine—hypophosphite and iodine—phosphite reactions did not interfere. Also, the iodate—phosphite reaction is of minor importance. Under such conditions, the overall reaction can be described by

$$2IO_3^- + 5H_2PO_2^- + 2H^+ \rightarrow I_2 + 5H_2PO_3^- + H_2O \quad (3)$$

The rate law for the iodate—hypophosphorous acid reaction was studied by Hayward and Yost [2]. It is shown below that reaction (3) exhibits a Landolt effect [3]. The kinetics of this reaction were studied under strongly acidic conditions, and rate constants were determined. In addition, a spectrophotometric kinetic method was developed for determining hypophosphite in aqueous solutions; hypophosphite in the range 0.06—4 mg (10^{-3}—$6 \cdot 10^{-2}$ M) was determined with relative errors and relative standard deviation of 2—3%.

EXPERIMENTAL

Apparatus

A modified Heath-701 single-beam spectrophotometer and a modified Sargent Malmstadt Spectro-electrotitrator (E. H. Sargent Co., Chicago) were

used as previously reported [4, 5]. The reaction curve was recorded and its slope evaluated either manually by the glass-rod technique [6] or automatica by measuring with a double-switching system the time required for reaction (3) to proceed to a fixed extent [7]. The determination of hypophosphite was also done with a simple spectrophotometer, Spectronic 20, by measuring the final absorbance of the mixture. All absorbances were measured at 460 nm [

Reagents

All solutions were prepared with distilled water and reagent-grade substances.

Potassium iodate solution, 0.150 M. Dissolve 3.226 g of reagent in 100 ml of 2 M sulfuric acid. (For the kinetic study, this solution was prepared in various mixtures of sulfuric acid and sodium sulfate, with the ionic strength always kept constant at 2.00.) Prepare more dilute potassium iodate solutions by diluting with 2 M sulfuric acid.

Sodium hypophosphite (2.000 M). Dissolve 21.20 g of the reagent in water and dilute to 100 ml. Prepare other solutions by dilution.

Procedure

Switch on the spectrophotometer (or the Spectro-electrotitrator) and the electronics at least 30 min before the measurements are started, and calibrate the instrument for zero absorbance with the cuvette filled with water. Into the thermostated (25°C) reaction cell, pipet 4.00 ml of 0.150 M potassium iodate solution, inject 1.00 ml of sample or standard hypophosphite solution with a hypodermic syringe, close the compartment and press at once the Start button of the Universal Digital Instrument (U.D.I.). The measurement is completed automatically and the number on the U.D.I. is recorded. Press the Reset button and empty the cell with suction. Repeat the procedure for each analysis. Alternatively, record the reaction curve (absorbance vs. time). The same procedure is used with the Spectro-electrotitrator, except that the reaction cell remains open.

RESULTS AND DISCUSSION

The initial rate of formation of iodine can be expressed as

$$\frac{d[I_2]}{dt} = k\,[H_2PO_2^-]^x\,[IO_3^-]^y\,[H^+]^z \qquad (4)$$

where x, y and z are the stoichiometric coefficients for $H_2PO_2^-$, IO_3^- and H^+, respectively.

In order to study the effect of the concentration of the reactants on the reaction rate, the following two methods were applied [9].

(a) The initial rate method. For constant concentrations of iodate and hydrogen ion, eqn. (4), in relation to Beer's law, becomes

$$\frac{dA}{dt} = k_{obs}\,\epsilon\,b\,[H_2PO_2^-]^x \qquad (5)$$

where

$$k_{obs} = k\,[IO_3^-]^y [H^+]^z \tag{6}$$

Equation (5) can be written as

$$\log \left(\frac{dA}{dt}\right)_i = \log (k_{obs} \cdot \epsilon \cdot b) + x \log [H_2PO_2^-]_i \tag{7}$$

where the subscript i indicates initial rate and concentrations. The initial values of dA/dt can be determined from the slopes of the linear parts of the curves of Fig. 1. By plotting $\log(\Delta A/\Delta t)_i$ vs. $\log [H_2PO_2^-]_i$, a straight line was obtained, from the slope of which x was calculated to be 1.10. By the same technique, it was found that $y = 0.51$. When the double-switching system was used and $\log (1/t)$ vs. $\log [H_2PO_2^-]$ was plotted, the same values for x and y were obtained.

(b) Guggenheim's method. When iodate and hydrogen ions are in large excess with respect to hypophosphite ions, eqn. (4) becomes

$$\frac{d[I_2]}{dt} = k_{obs}\,[H_2PO_2^-]^x \tag{8}$$

For constant hydrogen ion concentration, eqn. (6) gives

$$\log k_{obs} = \log C + y \log [IO_3^-] \tag{9}$$

where $C = k[H^+]^z$

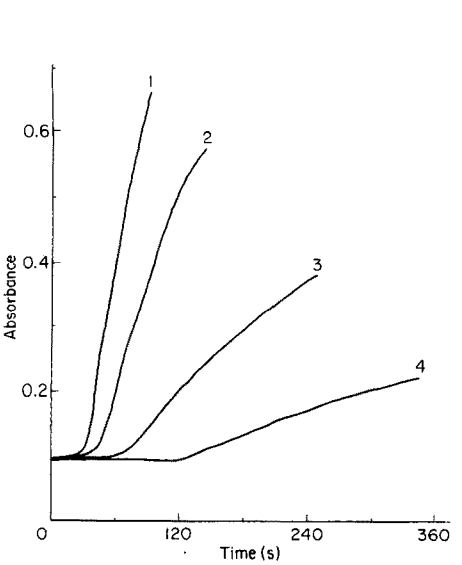

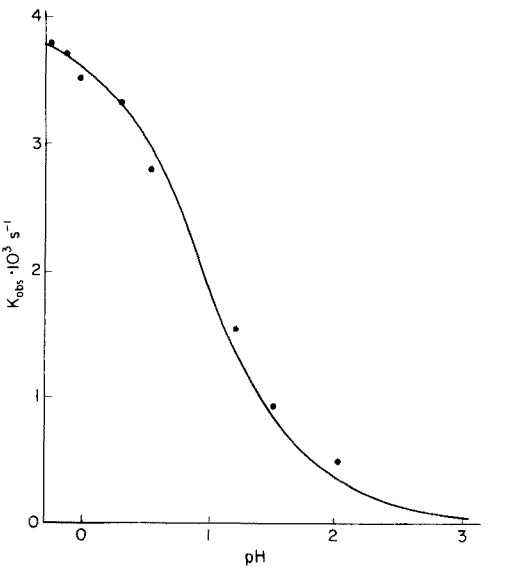

Fig. 1. Reaction curves (absorbance versus time at λ = 460 nm). The reaction mixture contained KIO_3 0.15 M in 2 M H_2SO_4, and $H_2PO_2^-$ at: (1) $6.00 \cdot 10^{-2}$ M; (2) $4.00 \cdot 10^{-2}$ M; (3) $1.50 \cdot 10^{-2}$ M; and (4) $7.50 \cdot 10^{-3}$ M.

Fig. 2. Dependence of the rate constant k_{obs} on the pH of the reaction mixture. The solid line is the theoretical curve.

By plotting $\ln [A_{t+\tau} - A_t]$ vs. time and applying Guggenheim's method, a set of values for k_{obs} at different values of $[IO_3^-]$ was obtained. By plotting $\log k_{obs}$ vs. $\log [IO_3^-]$ a straight line was obtained, from the slope of which y was calculated to be 0.49, which is in good agreement with the value of 0.51 obtained by the initial rate method. From the intercept, the rate constant k was calculated to be 0.4 ± 0.012 $M^{-\frac{1}{2}}$ min^{-1} at 19°C and ionic strength at 2.00.

Figure 2 shows the dependence of k_{obs} on pH at constant ionic strength. The S-shaped curve suggests that the main species participating is the product of a protolytic reaction, the effect of $[H^+]$ on the reaction rate being indirect Hydrogen ions control the concentration of the reacting species in the mixture. Hypophosphorous acid acts as a monoprotic acid with dissociation constant $pK_a = 1.0$ at 25°C [10]. The experimental data can be explained by the hypothesis that the active species is undissociated hypophosphorous acid. The solid line in Fig. 2 is a theoretical curve derived by multiplying the value $k_{obs} = 3.90 \cdot 10^{-3}$ s^{-1} (extrapolated value of the experimental curve) by the ratio of the concentration of the acid form to the analytical concentration of hypophosphorous acid at each pH. The experimental points of Fig. 2 do not coincide fully with the theoretical line at higher pH. Two explanations are possible: (a) the experimental value of $pK_a = 1.0$ deviates from the theoretical at higher pH values because of the effect of the high ionic strength used here; or (b) hypophosphite may react with the iodate in a similar manner to hypophosphorous acid, but with a different rate constant, thus altering the overall value of the rate constant k. Either explanation can be justified by the experimental results. Similar observations have been made with the 2,6-dichlorophenolindophenol—ascorbic acid reaction [11].

When the calculated values of x, y and z and k were substituted in eqns. (5) and (6), the molar absorptivity of iodine at 460 nm was found to be 739 mol^{-1} cm^{-1}, which is in good agreement with the reported value of 746 [8].

The effect of temperature on the reaction rate was determined by calculating k_{obs} at various temperatures in the range 17.5—30°C. From an Arrhenius plot of $\log k_{obs}$ vs. 1/T, the activation energy was calculated to be 18.3 kcal mol^{-1}.

Analytical application

The iodate—hypophosphite reaction was used for the determination of hypophosphite in aqueous solutions. Some results are shown in Table 1. The data indicate that hypophosphite in the range 0.06—4 mg (10^{-3}—$6 \cdot 10^{-2}$ M) can be determined with relative errors and relative standard deviations of 2—3%. Typical working curves are shown in Fig. 3.

The following ions did not affect the reaction rate when their concentration was 25 times that of the hypophosphite: $H_2PO_3^-$, NO_3^-, Zn^{2+}, Cd^{2+}, Ni^{2+}, Co^{2+}, Mn^{2+}, Cr(III), Al^{3+}, Mo(VI) and V(V). Higher concentrations of these ions were not tested. Table 2 summarizes the effect of interfering ions.

TABLE 1

Results for aqueous hypophosphite solutions

Method	Instrument	Range (mg)	Average relative error (%)	s_r (%) (n = 6)
Kinetic	Heath 701	0.5—4; manual	2.0	2.4 (1.3 mg)
		automatic	1.6	1.9 (1.3 mg)
Kinetic	Sargent-Malmstadt titrator	0.13—2.5; automatic	3.3	5.9 (0.65 mg)
Equilibrium	Spectronic 20[a]	0.6—2.5	3.1	2.0 (0.65 mg)

[a]When this system was used, the calibration graph was linear for the range 0—4 · 10^{-2} M hypophosphite ($A \approx 0$—1.1) but did not pass through the origin.

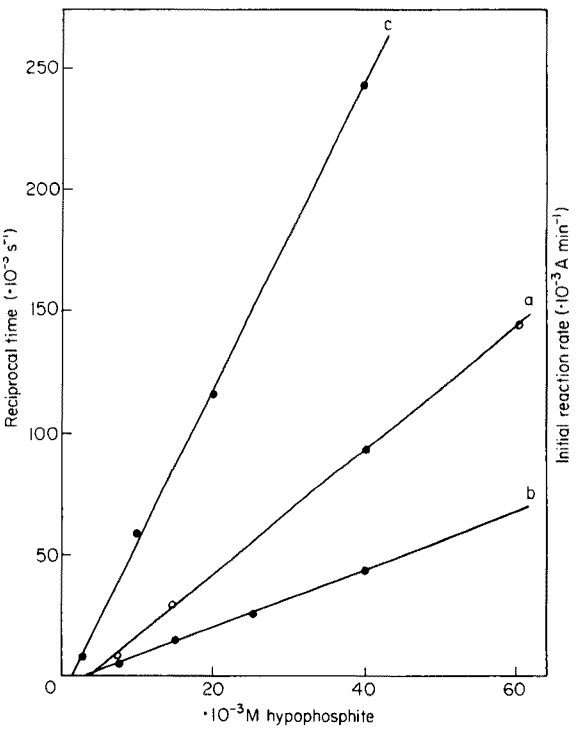

Fig. 3. Working curve for hypophosphite determination. (a) Automatically, with the Heath-701 single beam spectrophotometer. (b) Manually with the Heath-701 single beam spectrophotometer. (c) Automatically, with the Sargent-Malmstadt Spectro-electrotitrator.

Of all the ions, thiocyanate exerts the strongest inhibiting action. The possibility of determining micro amounts of thiocyanate on the basis of this inhibitory effect is being examined.

TABLE 2

Effect of various ions on the determination of hypophosphite ($1.00 \cdot 10^{-2}$ M)

Ion	Source	Ratio of added ion to hypophosphite[a]
SCN^-	KSCN	0.002
Br^-	KBr	0.02
Ce(IV)	$Ce(SO_4)_2$	0.04
Fe^{3+}	$Fe(NO_3)_3 \cdot 9H_2O$	0.1
SO_3^{2-}	Na_2SO_3	0.3
Cl^-	KCl	0.8

[a]These ions in the stated ratio caused a negative relative error of less than 5%.

REFERENCES

1 J. Bognar and S. Sarosi, Anal. Chim. Acta, 29 (1963) 406.
2 P. Hayward and D. M. Yost, J. Am. Chem. Soc., 71 (1949) 915.
3 H. Landolt, Ber., 19 (1886) 1317; 20 (1887) 745.
4 M. I. Karayannis and E. V. Kordi, Analyst (London), 100 (1975) 168.
5 T. P. Hadjiioannou and P. A. Siskos, Mikrochim. Acta, (1975) 51.
6 C. K. Patel and R. D. Patel, J. Chem. Educ., 51 (1974) 230.
7 C. Efstathiou and T. P. Hadjiioannou, Anal. Chim. Acta, 89 (1977) 55.
8 A. D. Awtrey and R. E. Connick, J. Am. Chem. Soc., 73 (1951) 1842.
9 G. M. Fleck, Chemical Reaction Mechanisms, Holt, Rinehart and Winston, New York, 1971, p. 37.
10 L. G. Sillen and A. E. Martell, Stability Constants of Metal Ion Complexes, The Chemical Society, London, 1964, p. 179.
11 M. I. Karayannis, Talanta, 23 (1976) 27.

Analytica Chimica Acta, 90 (1977) 215—221

A MODIFIED SPECTROPHOTOMETRIC METHOD FOR NITRATE IN PLANTS, SOILS AND WATER BY NITRATION OF 3,4-DIMETHYLPHENOL

R. R. ELTON-BOTT

27 Regency Drive, Thornlie, Western Australia 6108 (Australia)

(Received 5th October 1976)

SUMMARY

A spectrophotometric method suitable for rapid and precise routine analysis of plant tissue, soils and water samples with a wide range of nitrate nitrogen values is described. Ethanol replaces the acetone sometimes used as solvent for the 3,4-dimethylphenol reagent, so that spectral interference caused by acetone is eliminated. The time required for complete nitration of the reagent is reduced from 25 min to that required for mixing of reactants. Chloride ion levels of up to 6.0% in plant tissue, 1940 $\mu g\ g^{-1}$ and 970 $\mu g\ ml^{-1}$ in soil and water, respectively, do not interfere. The probable reaction mechanism of acetone interference is discussed.

There is at present a demand for rapid analytical methods that provide the sensitivity and precision required for the monitoring of nitrate ion in environmental and industrial samples. High levels of nitrogen in soils commonly account for high concentrations of NO_3^--N in plants, and toxic levels of nitrite may then be produced by micro-organism activity in the gastrointestinal tract. The possibility of formation of carcinogenic nitrosamines in processed food products containing nitrate and nitrite has been reported [1, 2]. Nitrates in potable water are possible indicators of pollution, and where they occur naturally, high levels (45—90 $\mu g\ ml^{-1}\ NO_3^-$) can cause infant methaemoglobinaemia [1, 2]. High natural nitrate levels are common in ground waters in the drier areas of Australia.

Current methods for the determination of NO_3^--N include reduction to ammonia followed by titration or colorimetry [3, 4], chemical or biochemical reduction to nitrite and its diazotization with a variety of reagents [5—7], nitration of organic reagents and determination of the nitration product [8—11], ultraviolet spectrometry [12, 13], polarography [14] and ion-selective electrode [15, 16]. The highly sensitive method [5, 6] based on copperized cadmium to reduce nitrate to nitrite and then diazotization of sulphanilamide, is precise but time-consuming.

It was considered desirable to develop a more direct method which could be applied generally to soils, plants and water, and which would meet the requirements of rapidity, precision and absence of interferences. It also had

to be suitable for samples with a wide range of NO_3^--N values. The 3,4-dimethylphenol method showed promise of meeting these criteria.

Since the method was introduced by Blom and Treschow [8], followed later by Holler and Huch [10] who showed 3,4-dimethylphenol to be the most suitable isomer, it has been applied to a very wide range of materials by many workers. The method has not been entirely free of problems. Alten et al. [17] reported that volatile components of plants distilled over and caused interference when trace amounts of nitrate were determined. Lewis [18] reported that low and erratic results were obtained when solutions containing organic matter or chlorides were analyzed. When the method was applied the distillates obtained were cloudy and samples containing known amounts of NO_3^--N gave low and variable results.

The general approach was to improve those aspects of the method which inhibited it from being a routine, versatile analytical method. Acetone, normally used by previous workers [8, 10, 18] as solvent for the reagent was suspected of participation in side reactions with xylenol. The experimental difficulties mentioned above were overcome by replacing acetone with ethanol. The present work involves several important improvements to the method: (1) nitration time is reduced from 25 min to the time taken to mix the reactants; (2) spectrally clear distillates are obtained; (3) up to 6.0% chloride in plant tissue can be tolerated; and (4) rapid and efficient distillatic is given by the Markham steam distillation apparatus.

EXPERIMENTAL

Apparatus and reagents

A Unicam SP 500 spectrophotometer with 1-cm glass cells was used. A Markham still was connected to a steam source (Buchii unit). Reagent-grade chemicals were used unless otherwise mentioned.

Ethanol was distilled before use. A 5% solution of 3,4-dimethylphenol in ethanol, and an aqueous 2% solution of sodium hydroxide were prepared. Sulphuric acid (87.5% volume or 7 + 1 concentrated sulphuric acid—water) was allowed to cool before use. Silver sulphate solution (0.065 M) made by complexing 3 g of silver sulphate in 50 ml of concentrated ammonia solutior was taken to dryness, diluted to 100 ml, and filtered.

Standard solutions

Solutions containing 0, 25, 50, and 100 $\mu g\ ml^{-1}$ were prepared by serial dilution of a 1000 $\mu g\ ml^{-1}$ NO_3^--N stock standard in distilled water.

General procedure

Plant tissue samples, oven-dried at 70°C, were milled (60-mesh). Samples (500 mg) were extracted with 10.0 ml of distilled water by shaking for 15 min. The solutions for analysis were filtered (9 cm Whatman No. 4 filter paper, nitrate-free) into 28 mm × 150 mm pyrex test tubes.

Soil samples, oven-dried at 70°C, were passed through a 2-mm screen. Samples (5.00 g) were extracted with 10.0 ml of distilled water by shaking for 15 min. The suspensions were centrifuged at 4000 r.p.m. for 2 min to remove sand and organic residue. The supernatant solutions were filtered and saved for analysis.

Aliquots (usually 1 ml) of the plant tissue extracts were pipetted into 28 mm × 150 mm test tubes, and 1 ml of reagent was added. The solution was swirled to mix. The test tube was placed in a 250-ml conical flask containing cold tap water and 7.0 ml of prepared acid was introduced slowly down the sides; the test tube was rotated during this addition. The test tube was removed from the flask, swirled to mix thoroughly, and the contents were transferred quantitatively with distilled water into the Markham still (clean and completely free from sodium hydroxide). The distillate (20—22 ml), collected in a 25-ml graduated cylinder containing 2 ml of 2% sodium hydroxide solution, was diluted to the mark with distilled water and the absorbance was measured at 430 nm. Standards containing 0—100 μg NO_3^--N in a 1-ml aliquot were treated similarly.

For soil sample extracts and water samples, 5-ml aliquots were taken and treated similarly. If chloride levels in the soil and water samples were expected to be above 1940 $\mu g\ g^{-1}$ and 970 $\mu g\ ml^{-1}$, respectively (from TSS values), 1 ml of saturated silver sulphate solution (sufficient to precipitate 4600 μg Cl^-), 1 ml of reagent and 12.0 ml of 87.5% acid were added. To standards containing 0, 5, 10, 25, 50, and 100 μg NO_3^--N in a 1-ml aliquot, 4 ml of distilled water, 1 ml of silver sulphate solution and 1 ml of reagent were added before nitration with 12.0 ml of acid.

The proposed method is suitable for plant tissue samples containing 100 μg—2200 μg NO_3^--N per g (dry weight). For soils and waters the ranges of NO_3^--N covered are 1 $\mu g\ g^{-1}$—40 $\mu g\ g^{-1}$, and 1 $\mu g\ ml^{-1}$—20 $\mu g\ ml^{-1}$, respectively. With dilution of the distillate containing a proportionate amount of sodium hydroxide solution, the upper range can be extended 8-fold (Fig. 1). Colour development is instantaneous and is stable for at least 48 h in the light or in darkness.

RESULTS AND DISCUSSION

Reaction rate

Blom and Treschow [8] noted that the time required for nitration with a given acid concentration depends on the temperature. At 30°C, the reaction was complete in 30 min. Subsequent workers [10, 17—20] allowed a similar time for complete nitration. In this method, the rate of reaction (Table 1) is greatly increased; nitration is complete immediately after mixing with acid. The observed rate increase cannot be attributed solely to the change in solvent from acetone to ethanol. When solid 3,4-dimethylphenol was used [19, 20] the same increase in nitration rate was observed.

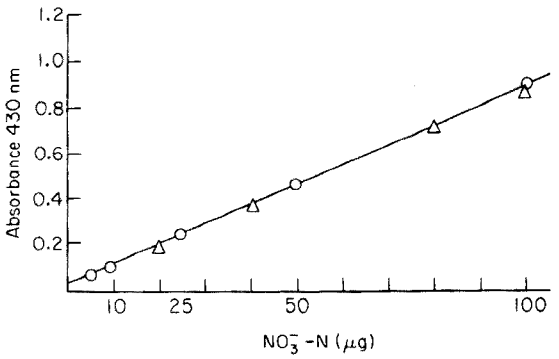

Fig. 1. Standard curve showing the linear response between absorbance and NO_3^--N. ○ Distillate contained 0—100 μg NO_3^--N in 25 ml of water. Absorbance was determined directly. △ Distillate contained 160—800 μg NO_3^--N; 25-ml distillates were diluted to 200 ml with water before absorbances were read.

Blom and Treschow [8] also reported that at 30°C, the acid concentration could be varied from 55 to 70% (by volume) without affecting the nitration. Similar observations were made here when the effect of acid concentration was investigated. The final acid concentration for this method is 62% V for plant tissue and 53% V for soil and water.

Chloride interference

Holler and Huch [10] noted that chloride and nitrite interfered. Chloride interferes when the hydrochloric acid evolved reacts with nitric acid to produce nitrosyl chloride. Nitrite interferes when the nitrous acid liberated reacts with dimethylphenol to give nitrosoxylenols which are steam-distilled, giving coloured products. Holler and Huch removed chloride interference by

TABLE 1

Effect of time on nitration of 3,4-dimethylphenol
(Absorbances of 5 replicate determinations obtained for four standard NO_3^--N solutions and a grass tissue extract (2910 μg g^{-1} NO_3^--N dry weight) containing 131 μg NO_3^--N, with distillate diluted by a factor of two)

Reaction time before distillation (min)	NO_3^--N				
	Blank	5 μg	25 μg	100 μg	Grass
	Absorbance				
Immediate	0.005	0.050	0.228	0.898	0.582
1	0.005	0.049	0.225	0.896	0.586
2	0.004	0.050	0.228	0.900	0.580
5	0.004	0.051	0.225	0.898	0.580
15	0.005	0.051	0.228	0.899	0.584
30	0.005	0.050	0.226	0.899	0.580

precipitation with silver sulphate, and the nitrous acid from nitrite was destroyed by the addition of sulphamic acid.

The effect of chloride on nitration is shown in Table 2. Interference is evident when more than 5000 μg NaCl is added per determination, but this level, equivalent to 10.0% NaCl in plant tissue, far exceeds that normally present. For 5-ml aliquots of soil extracts or water samples, interference is evident when more than 8000 μg NaCl is added. This represents allowable levels of 3200 μg NaCl g^{-1} (1940 μg Cl g^{-1}) in soils and 1600 μg NaCl ml^{-1} 970 μg Cl ml^{-1}) in water.

In Table 3, the proposed method is compared with the Devarda method 3], and the u.v. absorption method [12] used to analyse water and 1 M KCl extracts of soils. The latter method and the proposed method gave close agreement (Table 3).

Nitrate was added to extracts from grass, cape weed, and wheat tops. Recovery of NO_3^--N by the proposed method ranged from 98 to 102% (data not shown).

Acetone interference

When acetone was used as solvent for 3,4-dimethylphenol, cloudy distillates, which could not be cleared by filtration or centrifugation, were obtained. As reported by Alten et al. [17], treatment with 1 g of barium sulphate and filtration through a hard filter gave clear distillates.

It was also observed that the colour of the reaction mixtures (including blank) was red—orange when acetone was used, but grey when ethanol was used as solvent. The intensity of the red colour was increased by increasing the molar ratio of acetone to 3,4-dimethylphenol. Interference by acetone may follow the condensation between phenol and acetone to form Bisphenol A (I).

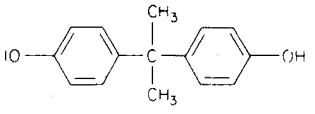

(I)

TABLE 2

Effect of chloride on nitration of 3,4-dimethylphenol
Grass tissue sample (2910 μg g^{-1} NO_3^--N dry weight) contained 1.10% Cl^-; distillate diluted by a factor of two. Soil sample (11.0 μg g^{-1} NO_3^--N dry weight) contained less than 0.01% Cl^-. Addition of Ag_2SO_4 was omitted)

NaCl added (μg)	0	500	1000	5000	8000	10000	50000
Abs. grass	0.582	0.580	0.585	0.588	0.480	0.450	0.326
Abs. soil	0.248	0.250	0.252	0.247	0.240	0.228	0.133

TABLE 3

Comparison of the 3,4-dimethylphenol, Devarda reduction, and ultraviolet absorption methods for the determination of nitrate in extracts from plant tissue, soils and water (Results are given as $\mu g\ g^{-1}$ NO_3^--N, dry weight; each is the mean duplicate determinations corrected to two significant figures.)

Sample	3,4-Dimethylphenol	Devarda reduction	U.v. spectrometry
Grass	2848[a] (65)	3023	—
Cape weed	201	190	—
Rape tops	12062	13000	—
Wheat tops	141[a] (11)	—	—
Red brown sand	4.7	—	4.8
Red brown sand	1.6	—	1.5
Red brown sand	6.9	—	6.1
Sandy loam	13	—	12
Sandy loam	11[a] (0.5)	—	10[a] (0.4)
Loamy sand	16	—	17
Bore water	1.2	—	1.3
Bore water	16[a] (0.5)	—	16[a] (0.5)
Bore water	35	—	33

[a]Mean of 7 independent, non-consecutive determinations, with standard deviation in parenthesis.

Reaction mechanism

The following reaction mechanism is suggested.

1. Protonation of acetone to yield a secondary carbonium ion

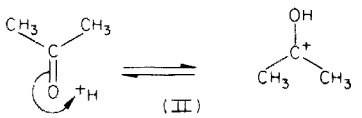

(II)

2. Electrophilic aromatic substitution by this electrophile at C6 of xylenol, to form a steam-volatile product as a result of intramolecular hydrogen bonding (the interfering species).

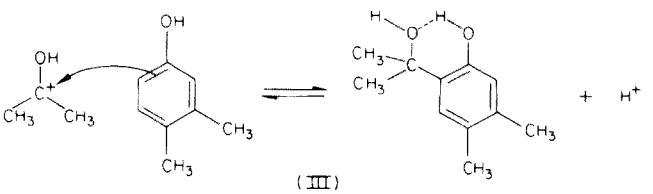

(III)

3. Further reaction may produce some dimeric product.

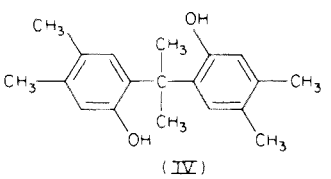

(IV)

The large reduction in chloride inhibition for the proposed method may result from the rapid rate of nitration, or the absence of interference from acetone. Adaptation of the method to an automated form appears to be feasible. The rapidity and precision of the method should also be useful for diagnosis and research applications.

The author thanks R. Taylor and members of the Agricultural Chemistry Division, Government Chemical Laboratories, for helpful suggestions; R. Schulz of the Water Division for translations; Dr. R. Alexander and Dr. R. Kagi, Western Australian Institute of Technology, for their contribution towards the proposed reaction mechanism.

REFERENCES

1 I. A. Wolff and A. E. Wasserman, Science, 177 (1972) 15.
2 National Research Council, Committee on Nitrate Accumulation, National Academy of Sciences, Washington D.C., 1972.
3 J. M. Bremner and R. R. Kenny, Anal. Chim. Acta, 32 (1956) 485.
4 J. Keay and P. M. A. Menage, Analyst (London), 95 (1970) 379.
5 E. D. Wood, F. A. J. Armstrong and F. A. Richards, J. Mar. Bio. Ass. U.K., 47 (1967) 23.
6 A. Henriksen and A. R. Selmer-Olsen, Analyst (London), 95 (1970) 514.
7 A. L. McNamarra, G. B. Meeker, P. D. Shaw and R. H. Hageman, J. Agric. Food Chem., 19 (1971) 229.
8 J. Blom and C. Treschow, Pflanzenern, Dung Bodenkunde, Berlin, 13a (1929) 159.
9 C. M. Johnson and A. Ulrich, Anal. Chem., 22 (1950) 1526.
10 A. C. Holler and R. V. Huch, Anal. Chem., 21 (1949) 1385.
11 D. A. Cataldo, M. Haroon, L. E. Schrader and V. L. Youngs, Commun. Soil Sci. Plant Anal., 6(1) (1975) 81.
12 E. Goldman and R. Jacobs, J. Am. Water Works Assoc., Feb. (1961) 187.
13 A. L. Clarke and A. C. Jennings, J. Agric. Food Chem., 13 (1965) 174.
14 G. W. Skyring, B. J. Carey and V. B. D. Skerman, Soil Sci., 91 (1961) 388.
15 D. R. Kenney, B. H. Byrnes and J. J. Genson, Analyst (London), 95 (1970) 383.
16 P. J. Milham, A. S. Awad, R. E. Paull and J. H. Bull, Analyst (London), 95 (1970) 751.
17 F. Alten, B. Wandowsky and E. Hille, Z. Pflanzenernaehrung Bodenk. 1 (1936) 340.
18 D. G. Lewis, J. Sci. Food Agric. 12 (1961) 735.
19 G. Lipp and U. Dölberg, Beitr. Tabakforsch., 2 (1964) 345.
20 E. G. Heisler, J. Siciliano, S. Krulick, W. L. Porter and J. W. White. J. Agric. Food Chem., 21 (1973) 970.

Analytica Chimica Acta, 90 (1977) 223—231

A NEW METHOD FOR DETERMINING THE COMPOSITION AND STABILITY CONSTANT OF COMPLEXES OF THE FORM A_mB_n

J. C. JIMENEZ SÁNCHEZ, J. A. MUÑOZ LEYVA and M. ROMÁN CEBA

Department of Analytical Chemistry, Faculty of Sciences, University of Extremadura, Badajoz (Spain)

(Received 13th July 1976)

SUMMARY

A new method is reported for determining the composition of complexes of the form A_mB_n; it can be used to differentiate mono- and polynuclear complexes. The method is based on that of Holme and Langmyhr. Good results were obtained for several complexes.

This paper describes a new method for determining the composition of complexes of the form A_mB_n. It can be used to differentiate mono- and polynuclear complexes, e.g. AB and A_2B_2. The method is an extension of that of Holme and Langmyhr [1].

THEORY

For the equilibrium $mA + nB \leftrightharpoons A_mB_n$ where ($m, n \geqslant 1$), according to the law of mass action

$$K = [A]^m [B]^n / [A_mB_n] \quad (1)$$

At equilibrium the concentrations of the reactants are

$$[A] = a - m[A_mB_n] \quad (2)$$

$$[B] = b - n[A_mB_n] \quad (3)$$

where a and b are the initial concentrations of A and B, respectively. According to the Beer—Lambert law

$$[A_mB_n] = E/\epsilon l \quad (4)$$

where E = absorbance, ϵ = molar absorptivity, and l = light path in cm. By combining eqns. (1), (2) and (4)

$$\left(a - m\,\frac{E}{\epsilon l}\right)^m [B]^n = K\,\frac{E}{\epsilon l} \quad (5)$$

For $m = 1$, eqn. (5) becomes identical with that developed by Asmus [2] and used by him as the basis for plotting sets of curves.

When a constant concentration of reactant A is maintained and the con-

centration of reactant B is increased, the concentration of the complex approaches an upper limit:

$$\lim_{b \to \infty} [A_m B_n] = a/m \tag{6}$$

with a corresponding upper absorption limit of E_0. Combination of eqns. (4) and (6) gives

$$\epsilon l = mE_0/a \tag{7}$$

which with eqn. (4), gives

$$[A_m B_n] = aE/mE_0 \tag{8}$$

By combining the expressions (1), (2), (3) and (8)

$$K = \frac{\left(a - \frac{E}{E_0}\right)^m \left(b - \frac{n\,E}{m\,E_0}\,a\right)^n}{a\,E/m\,E_0} \tag{9}$$

which may be rewritten as

$$\frac{1}{[B]^n} = \frac{1}{\left(b - \frac{n\,E}{m\,E_0}\,a\right)^n} = \frac{1}{K} m\,a^{m-1} \left(1 - \frac{E}{E_0}\right)^m \frac{E_0}{E} \tag{10}$$

By taking the mth root of eqn. (10)

$$\frac{1}{[B]^{n/m}} = \frac{1}{\left(b - \frac{n\,E}{m\,E_0}\,a\right)^{n/m}} = \left(\frac{1}{K} m\,a^{m-1}\right)^{1/m} \left(1 - \frac{E}{E_0}\right) \left(\frac{E_0}{E}\right)^{1/m} \tag{11}$$

From eqns. (10) and (11), two graphical methods for determining the composition of weak complexes of the form $A_m B_n$ were developed by Holme and Langmyhr [1]. Good results for $m = 1$ were obtained.

Equation (11) may be rewritten as

$$\frac{1}{[B]^{n/m}} = \left(\frac{1}{K}\,m\,a^{m-1}\right)^{\frac{1}{m}} \left(x^{\frac{1}{m}} - x^{\frac{1}{m}-1}\right) \tag{12}$$

where $E_0/E = x$. By taking the decimal logarithms of eqn. (12) and multiplyin by m/n

$$\log \frac{1}{[B]} = \frac{1}{n} \log \left(\frac{1}{K}\,m\,a^{m-1}\right) + \frac{m}{n} \log \left(x^{\frac{1}{m}} - x^{\frac{1}{m}-1}\right) \tag{13}$$

Expression (13) has the general form

$$Y = C + pX$$

i.e., it is a straight line with ordinate $\log 1/[B]$ and with an independent variable $\log \left(x^{\frac{1}{m}} - x^{\frac{1}{m}-1}\right)$. It must be remembered that the independent

variable is different for every value of m. For example, for the correct value of $m = 1$, the independent variable is $\log(x - 1)$.

If the value of m tested on the independent variable is incorrect, then curves are obtained. The curves are not influenced by the value of n, and n is calculated from the value of the slope of the straight line obtained for the correct value of m by means of eqn. (13). The values of the slopes are those obtained for whole values of n. Figure 1 shows the theoretical straight lines obtained for a correct value of $m = 1$ and different values of n. The values of x are obtained from values given for E between 0.9 and 0.1 E_0. The group of plotted straight lines corresponds to the expression

$$\log \frac{1}{[B]} = \frac{1}{n} \log \frac{1}{K} + \frac{1}{n} \log (x - 1)$$

In Fig. 1, it has been assumed that $\log 1/K = c = 0.2$ units. Figure 2 shows the theoretical straight lines for the correct value of $m = 2$; it has been assumed that $\log 2\,a/K = c' = 0.1$ units. Figure 3 presents the straight lines for the correct value of $m = 3$; in this case, $\log 3\,a^2/K = c'' = 0.3$ units has been assumed.

It should be emphasized that the straight line for a complex AB is different from the straight lines for complexes A_2B_2 and A_3B_3

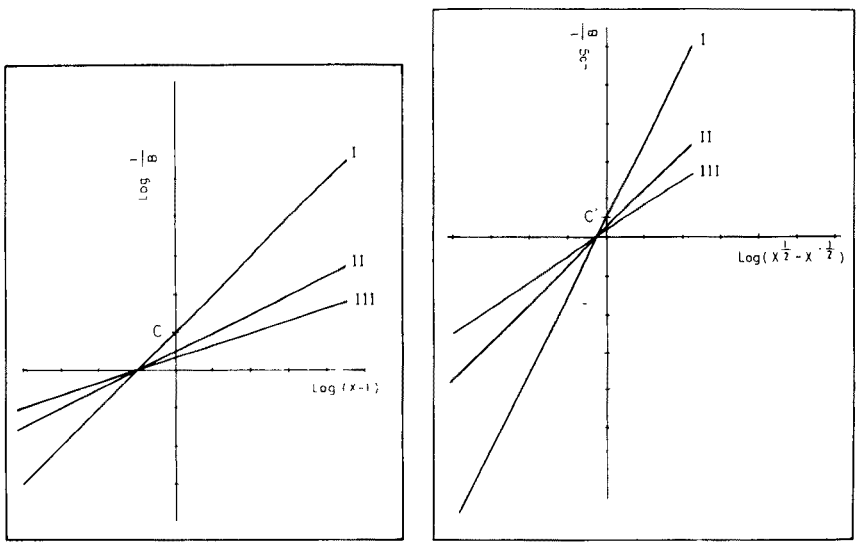

Fig. 1. Theoretical straight lines for the correct value of $m = 1$ and correct values of n (I, $n = 1$; II, $n = 2$; III, $n = 3$).

Fig. 2. Theoretical straight lines for the correct value of $m = 2$ and correct values of n (I, $n = 1$; II, $n = 2$; III, $n = 3$).

for complex AB, $\log \frac{1}{[B]} = \log \frac{1}{K} + \log (x - 1)$

for complex A_2B_2, $\log \frac{1}{[B]} = \frac{1}{2} \log \frac{2a}{K} + \log \left(x^{\frac{1}{2}} - x^{\frac{1}{2}-1} \right)$

These are different straight lines because the independent variables and ordinates of the origin differ.

When incorrect values of m are used, curved plots are obtained. Figure 4 shows the theoretical lines for a value of $m = 2$ (the correct value is $m = 1$). The values of log 1/[B] are those found theoretically for the correct value of m. In Fig. 5 are plotted the theoretical lines for the correct value of $m = 3$ and the incorrect value of $m = 1$. In these cases, and in all other cases examined (not shown here), curves are obtained; thus straight lines are obtained only when m takes its correct value, and the slope of this line will allow the value of n to be established, and with the origin-ordinate, the K value.

From the lines drawn for incorrect values of m, two criteria can be deduced for calculating the composition of the complexes.

Criterion A

This is applicable when the experimental absorbances lie between 0.9 and 0.1 E_0 (where E_0 is the maximum experimental absorbance obtained for $b \to \infty$). The E_0 value can be calculated by the Holme and Langmyhr method if it is a weak complex, or by preparing and measuring the absorbance of a

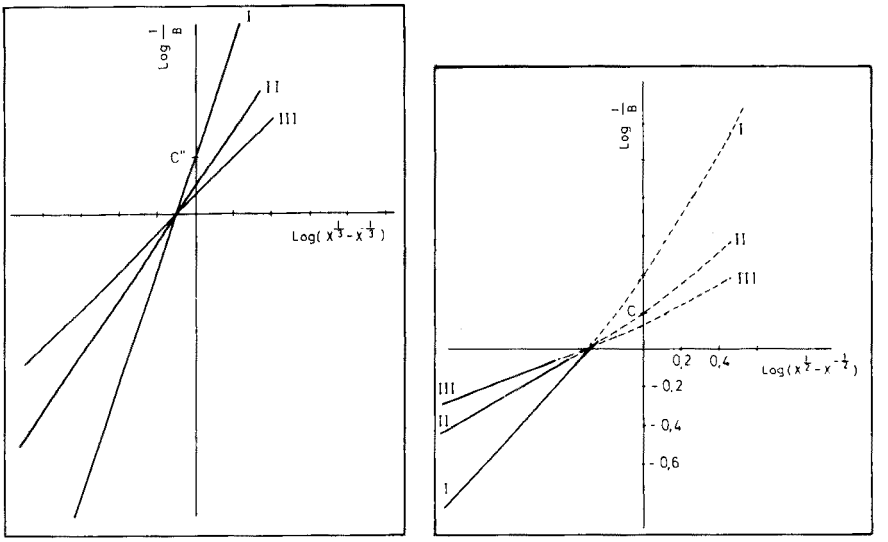

Fig. 3. Theoretical straight lines for the correct value of $m = 3$ and correct values of n (I, $n = 1$; II, $n = 2$; III, $n = 3$).

Fig. 4. Theoretical lines obtained for the incorrect value of $m = 2$ (correct value of $m = 1$) and different values of n (I, $n = 1$; II, $n = 2$; III, $n = 3$).

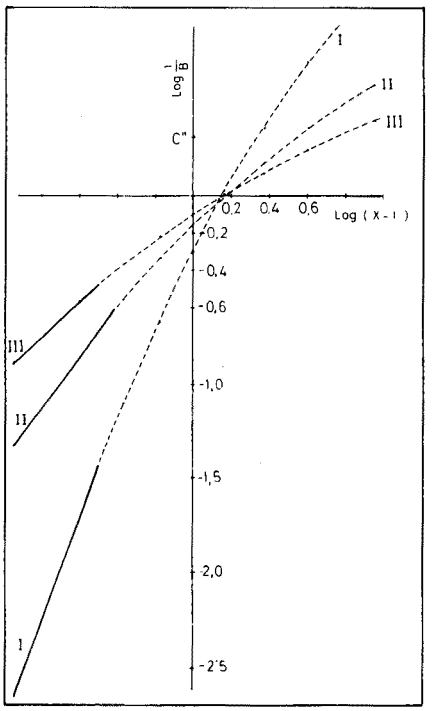

Fig. 5. Theoretical lines obtained for the incorrect value of $m = 1$ (correct value of $m = 3$) and different values of n (I, $n = 1$; II, $n = 2$; III, $n = 3$).

sample with a large excess of b, if the sample can be prepared in practice (which will be impossible if B absorbs strongly).

Criterion B

This criterion can be applied when the values of the measured absorbances lie between 0.9 and 0.8 E_0. In this case, the representation of log 1/[B] against log $\left(x^{\frac{1}{m}} - x^{\frac{1}{m}-1}\right)$ will give straight lines, but the slope obtained will indicate if it is true or a false case. The slopes of the true and false cases for values of E between 0.9 and 0.8 E_0 are given in Table 1. Table 2 shows the stoichiometries of the true complexes and other stoichiometries that can be obtained. From Table 2, it is clearly possible to distinguish easily all the stoichiometries. In many cases, false values of m lead to fractional values of n, so that the supposed stoichiometry can be rejected. In the cases underlined, when experimental errors are considered, a false case can be mistaken for a true one; but when this happens, the ratio obtained between m and n is true, unless the true stoichiometry is 1 : 3 which can be confused with 3 : 8, but this is fortunately uncommon.

Criterion B makes it easier to obtain good results than criterion A, because the ratio $b : a$ moves between limits which differ only slightly.

TABLE 1

Slopes obtained for true and false cases with the B criterion

True slope	Correct value of m	Correct value of n	Slopes obtained for incorrect values of m and different values of n	
			$m = 2$	$m = 3$
1	1	1	1.078	1.065
0.5	1	2	0.539	0.553
0.333	1	3	0.359	0.369
			$m = 1$	$m = 3$
2	2	1	1.855	2.053
1	2	2	0.927	1.026
0.666	2	3	0.618	0.684
			$m = 1$	$m = 2$
3	3	1	2.710	2.992
1.5	3	2	1.355	1.461
1	3	3	0.904	0.974

EXPERIMENTAL

Several samples were prepared in which the ion concentration is a and the reagent concentration can take higher values than 0.1 a. When samples are prepared, the absorbances are measured, and the values of log $1/[B]$ against the corresponding variable, are plotted; m and n are given appropriate test values. The origin-ordinate of the straight line obtained for true values of m and n makes it possible to calculate the equilibrium constant and, as the method is graphical, to calculate a mean of that constant.

TABLE 2

True stoichiometries and other stoichiometries that can be obtained

True stoichiometry	Stoichiometries obtained with the B criterion				
1 : 1	1 : 1	,	2 : 1.855	,	3 : 2.817
1 : 2	1 : 2	,	2 : 3.710	,	3 : 5.425
1 : 3	1 : 3	,	2 : 5.571	,	3 : 8.130
2 : 1	2 : 1	,	1 : 0.539	,	3 : 1.461
2 : 2	2 : 2	,	1 : 1.079	,	3 : 2.924
2 : 3	2 : 3	,	1 : 1.618	,	3 : 4.386
3 : 1	3 : 1	,	1 : 0.369	,	2 : 0.684
3 : 2	3 : 2	,	1 : 0.738	,	2 : 1.369
3 : 3	3 : 3	,	1 : 1.106	,	2 : 2.050

Application to the boric acid—quinalizarin system

Criteria A and B were applied to this system. In concentrated sulphuric acid media a complex with composition 1 : 1 is formed. The data obtained by Holme and Langmyhr [1] are shown in Table 3 and plotted in Fig. 6. The E_0 value is the value obtained theoretically. Figure 6 indicates different lines for several values of m and n. From criterion A it can be deduced that the stoichiometry is 1 : 1 or 2 : 2. Criterion B yields the ratios $m/n = 0.85$ for $m = 1$ and $m/n = 0.92$ for $m = 2$, i.e. the more probable stoichiometry is 2 : 2. From the slope of the straight line for $m = n = 2$ and from the a value, the value $K = 3.1 \cdot 10^{-15}$ can be deduced.

Application to the zinc(II)—1,2-cyclohexanedionebisthiosemicarbazone system

Criteria A and B can be applied to determine the stoichiometry and equilibrium constant of the complex formed in acetic acid—acetate medium between zinc(II) and the reagent mentioned [3]. The method of continuous variations indicates that $m/n = 1$. The E_0 value was determined by measuring the absorbance of a sample containing a large excess of Zn(II). The results are given in Table 3 and the plotted curves are shown in Fig. 7. Both criteria indicate that $m = n = 1$. The K value is $2.55 \cdot 10^{-5}$.

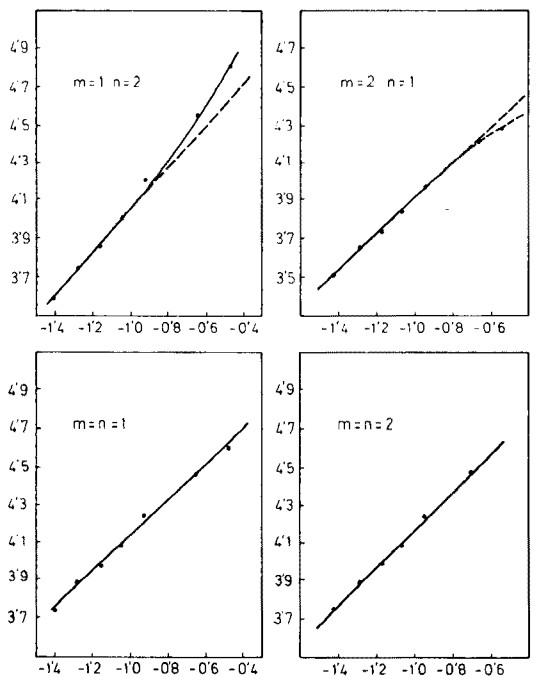

Fig. 6. Experimental lines obtained for the boric acid—quinalizarin system.

TABLE 3

Data for the three systems studied

b (mol l^{-1})	E	$\log (x^{\frac{1}{m}} - x^{\frac{1}{m-1}})$ $m = 1$	$m = 2$	$\log \frac{1}{b - \frac{nE}{mE_0} \cdot a}$		
Boric acid—quinalizarin[a]				$m/n = 1$	$m/n = 1/2$	$m/n = 2$
$6.4 \cdot 10^{-5}$	0.238	−0.48	−0.54	4.40	4.80	4.28
$8.0 \cdot 10^{-5}$	0.259	−0.65	−0.69	4.27	4.56	4.17
$1.2 \cdot 10^{-4}$	0.283	−0.92	−0.95	4.04	4.20	3.98
$1.6 \cdot 10^{-4}$	0.291	−1.05	−1.07	3.88	3.99	3.84
$2.0 \cdot 10^{-4}$	0.296	−1.15	−1.16	3.77	3.85	3.73
$2.4 \cdot 10^{-4}$	0.301	−1.27	−1.29	3.68	3.75	3.65
$3.2 \cdot 10^{-4}$	0.305	−1.40	−1.41	3.54	3.59	3.52
Zinc(II) system[b]				$m/n = 1$	$m/n = 2$	$m/n = 1/2$
$2.5 \cdot 10^{-4}$	0.285	−0.85	−0.88	3.69	3.64	3.78
$3.0 \cdot 10^{-4}$	0.290	−0.92	−0.94	3.59	3.55	3.67
$3.5 \cdot 10^{-4}$	0.296	−1.01	−1.03	3.51	3.48	3.58
$4.5 \cdot 10^{-4}$	0.304	−1.16	−1.13	3.35	3.37	3.44
$8.42 \cdot 10^{-3}$	0.325(*)					
Bismuth(III) system[c]				$m/n = 1$	$m/n = 1/3$	
$4.1 \cdot 10^{-4}$	0.409	−0.49	—	3.40	3.43	
$4.4 \cdot 10^{-4}$	0.425	−0.57	—	3.37	3.40	
$5.1 \cdot 10^{-4}$	0.471	−0.82	—	3.31	3.33	
$5.5 \cdot 10^{-4}$	0.481	−0.92	—	3.28	3.30	
$5.8 \cdot 10^{-4}$	0.490	−1.00	—	3.25	3.27	
$6.1 \cdot 10^{-4}$	0.506	−1.15	—	3.22	3.25	
$6.8 \cdot 10^{-4}$	0.509	−1.22	—	3.18	3.20	
$16.3 \cdot 10^{-4}$	0.540(*)					

[a] Quinalizarin concentration = $a = 3.2 \cdot 10^{-5}$ M. Boric acid concentration = b. E_0 (theor.) = 0.317.

[b] Reagent concentration = $a = 4.85 \cdot 10^{-5}$ M. Zn(II) concentration = b. $E_0 = 0.325$* (calculated). E measured at 415 nm.

[c] Bi(III) = $a = 1.67 \cdot 10^{-5}$ M. Reagent concentration = b. $E_0 = 0.540$* (calculated). E measured at 540 nm.

Application to the bismuth(III)—1,3-cyclohexanedionebisthiosemicarbazone monohydrochloride system

As in the preceding cases both criteria were applied to this system; the reaction occurs in acidic medium [4]. Holme and Langmyhr's method gives the value $m/n = 0.33$. The E_0 value was determined experimentally. This value, the theoretical E_0 value and other results are given in Table 3. From these results, which are plotted in Fig. 8, it can be deduced that $m = 1$ and $n = 3$ (reagent: Bi(III) = 3), and $K = 1.93 \cdot 10^{-11}$.

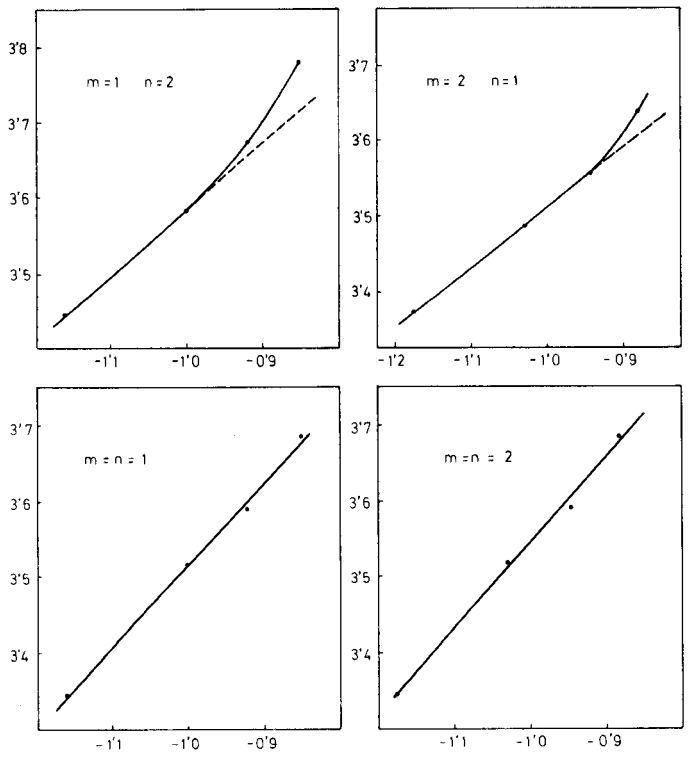

Fig. 7. Experimental lines obtained for the zinc(II)—1,2-cyclohexanedionebisthiosemicarbazone system.

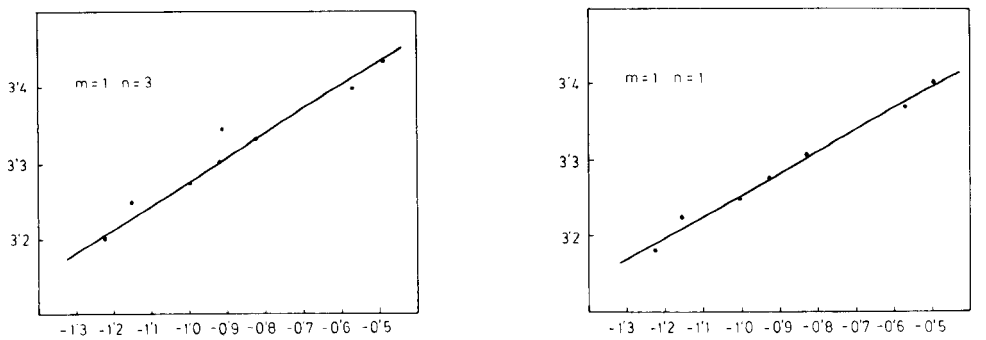

Fig. 8. Experimental lines obtained for the bismuth(III)—1,3-cyclohexanedionebisthiosemicarbazone monohydrochloride system.

REFERENCES

1 A. Holme and F. J. Langmyhr, Anal. Chim. Acta, 36 (1966) 383.
2 E. Asmus, Z. Anal. Chem., 178 (1960) 104.
3 J. A. Muñoz Leyva, J. M. Cano Pavón and F. Pino, Inf. Quim. Anal., 26 (5) (1972) 226.
4 J. J. Berzas Nevado, J. A. Muñoz Leyva and M. Roman Ceba, Talanta, 23 (1976) 257.

Analytica Chimica Acta, 90 (1977) 233—236

Short Communication

A ZINC-SENSITIVE POLYMERIC MEMBRANE ELECTRODE

LO GORTON and ULLA FIEDLER

Department of Analytical Chemistry, Chemical Center, University of Lund, S-220 07 Lund 7 (Sweden)

(Received 26th August 1976)

In the large field of newly developed ion-selective electrodes, there have been few reports about zinc-selective electrodes. Solid-state electrodes based on $ZnS—Ag_2S$ are not suitable as the precipitate is luminescent [1] and thus unstable. Electrodes based on $ZnTe—Ag_2S$ have been reported [2] but many ions interfere strongly and must be removed from the sample solution. For the determination of zinc by indirect titration, solid-state Cu-selective [3] or Ag-selective [4] electrodes have been proposed as indicator electrodes. Fogg et al. [5] have described a liquid-state electrode based on brilliant green tetrathiocyanatozincate, which has near Nernstian response to zinc(II) in the presence of excess of thiocyanate. Other zinc-sensitive electrodes based on ion-association complexes have been reported recently [6].

A suitable choice of liquid ion-exchanger for zinc(II) was suggested by the observation that zinc(II) interferes strongly with calcium-selective electrodes based on organic phosphate complexes [7, 8]. The zinc salt of di-n-octylphenylphosphoric acid was therefore prepared; this choice of acid was reinforced by the requirement for a small H^+-interference. However, this zinc complex is not so stable that the interference from Ca^{2+} ions can be neglected; in fact calcium(II) displaces zinc(II) from the complex. The use of a calcium-precipitating buffer (CPB) to prevent this interference is described here. The concept is analogous to the well-known use of the TISAB solution for determinations with the fluoride-selective electrode, when the activity of interfering ions (OH^-, Fe^{3+}, Al^{3+}) is decreased.

Experimental

Electrode system. The sensor systems investigated were based on polymeric membranes of the type described by Moody et al. [7]. The membrane composition (by weight) was 8% ligand, 62% solvent and 30% polymer. The ligand was the zinc salt of di-n-octylphenylphosphoric acid (HDOPP) [8]. The zinc salt was prepared by equilibrating 100 ml of a methanolic solution containing 0.474 g of HDOPP (1 mmol) with the stoichiometric amount (0.5 mmol) of an aqueous solution of zinc nitrate (50 ml of 0.010 M $Zn(NO_3)_2$) for about 3 h. The white precipitate obtained, $Zn(DOPP)_2$, was filtered, washed and dried.

The solvent was di-octylphenylphosphonate (DOPP-n; Specialty Organics Inc.), and the polymer was PVC (Breon 113, B.P. Chemicals, Ltd). The membranes (ca. 0.3 mm thick) were incorporated into Philips IS560 electrode bodies (N.V. Philips Gloeilampenfabriken, Eindhoven, Holland [9]).

Measuring system. All potential measurements were done with a combined amplifier/Gran plot device (constructed at this Institute) provided with a digital output and accurate to within ± 0.1 mV. For automatic titrations an Autoburette ABU 12 (Radiometer) and a Servogor recorder were used. Standard calomel electrodes (Radiometer type K 401) were used as reference electrodes.

The cell studied was: $Hg|Hg_2Cl_2|KCl(sat.)||$ sample solution | membrane ... ... $/Zn(NO_3)_2$ (0.01 M), NaCl (0.01 M) | AgCl | Ag.

The sample solutions were stirred and thermostated at 25.0 ± 0.1 °C.

Twice-distilled water (quartz still) and chemicals of the highest purity available were used for the reagents.

Calibration. All sample solutions were prepared to have a constant ionic strength (μ). For this purpose two buffers were tested: (1) acetate buffer (0.02 M HAc—0.02 M NaAc) with μ = 0.02 and pH 4.8; and (2) calcium-precipitating buffer (CPB; 0.02 M HAc—0.02 M NaAc—0.04 M NaF) with μ = 0.06 and pH 4.8. These buffers are composed so as to set the solution to a pH level where hydrogen ion interference is absent, provide a constant ionic strength background, and for the CPB, precipitate any calcium in the sample.

Calibrations were done by repeatedly adding to 50 ml of buffer solution diluted with 50 ml of water, small volumes of zinc solutions of increasing concentrations. At the constant ionic strength, the zinc(II) activity was directly proportional to the concentration of zinc ions; this formed the basis for an operational pZn scale defined by $pZn = -\log [Zn^{2+}]$.

All slopes were calculated by regression analysis on the linear part of the calibration curves. The values of slope, E^0 and pK_{ZnM} stated are mean values of measurements on at least four electrodes.

Selectivities. Selectivity coefficients were determined by the separate solution technique on aqueous 0.10 M solutions of the metal ions, from the following relationship

$$pK_{ZnM} = -\log K_{ZnM} = \frac{(E_{Zn^{2+}} - E_{M^{z+}})\,2F}{2.303 \cdot R \cdot T} - \log a_{Zn^{2+}} + \log a_{M^{z+}}^{2/z}$$

where $E_{Zn^{2+}}$ is the potential of the cell assembly for a 0.10 M Zn^{2+} solution, and $E_{M^{z+}}$ is the potential with a 0.10 M solution of the interfering cation; all other symbols have their accepted meanings.

Titrations. Potentiometric titrations were carried out automatically. Zinc solutions — 50 ml each of sample solution and buffer — were titrated with 0.20 M EDTA solution, added at a constant speed of 0.0356 or 0.141 ml min^{-1} (depending on the concentration of zinc) from the autoburette. The direct potential reading and the Gran plot were recorded.

Results and discussion

When the zinc electrode was calibrated in acetate buffer (1), a rapid response with a nearly Nernstian slope of 25.7 mV/pZn was obtained. The E^0-value of + 159 mV vs. SCE was equal to the theoretical one.

Selectivities were then determined as described above. The results (Table 1) show that Ca^{2+}-ions interfere badly. Ions like Sr^{2+} and Pb^{2+} also cause errors. It was therefore necessary to find a reagent capable of masking calcium, and preferably also lead and strontium, but not zinc. Fluoride proved to be suitable. When the zinc electrode was calibrated in CPB solutions, zinc(II) was not complexed, as shown by the calibration curve (Fig. 1). The slope was 25.7 mV/pZn and the E^0-value + 161 mV vs. SCE. The linear range was pZn 2—5; deviations at high concentrations are due to the changing ionic strength.

With the addition of CPB, calcium ions were precipitated by fluoride. From solubility data [10] the solubility product of CaF_2 was calculated to be $3.4 \cdot 10^{-11}$ (M^3). The composition of the calcium-precipitating buffer (CPB) was selected so that, after 1:1 dilution of the sample, the fluoride content would be 0.02 M; the pH was chosen so that no fluoride would be present as HF (pK = 3.1). Thus the calcium activity in the solution should be $0.8 \cdot 10^{-7}$ M. The precipitation reaction was rapid; measurements with a calcium-selective electrode showed that precipitation from a 10^{-3} M Ca^{2+} solution was complete to 99.9% within 2 min.

The activity of some other interfering ions, like Sr^{2+} and Pb^{2+}, was also decreased by the use of CPB, as they form slightly soluble fluoride salts (solubility products of $2.7 \cdot 10^{-9}$ (M^3) and $7.1 \cdot 10^{-8}$ (M^3) respectively) [10].

When zinc(II) is titrated with a complexing agent, e.g. EDTA, the pH conditions must be chosen so that the conditional stability constant for Zn—EDTA is large enough. If interfering ions (e.g. Ca^{2+}, Sr^{2+}, Pb^{2+}) are present, they are precipitated by the fluoride or even not titrated because of the low pH value. Figure 2 shows the titration curve and the Gran function curve for the titration of 100 ml of a solution containing $2.0 \cdot 10^{-4}$ M zinc(II) and $1.0 \cdot 10^{-3}$ M calcium(II) in CPB. For the evaluation of the equivalence point, the Gran plot obviously gives the more reliable result.

The life-time of this sensor is governed by the slow dissolution of the zinc salt into the aqueous sample solution. Its suitability for use in continuous automatic systems is therefore restricted. However, when the electrode was stored in a dry condition between measurements, the life-time proved to be at least three months.

TABLE 1

Selectivity coefficients, expressed as $-\log K_{ZnM} = pK_{ZnM}$

Ion	H^+	NH_4^+	Li^+	Na^+	K^+	Rb^+	Cs^+
pK	−1.7	1.3	0.1	2.0	2.7	2.4	2.6
Ion	Mg^{2+}	Ca^{2+}	Sr^{2+}	Ba^{2+}	Cu^{2+}	Cd^{2+}	Pb^{2+}
pK	0.5	−3.2	−1.6	0.4	0.6	0.0	−1.1

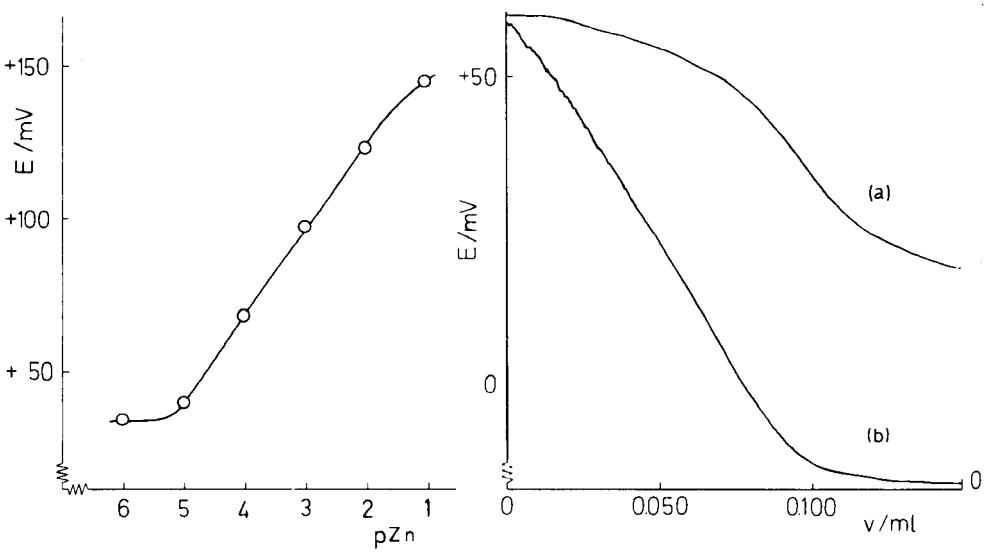

Fig. 1. Calibration curve for zinc electrode in CPB.

Fig. 2. Titration of 100 ml of $2.0 \cdot 10^{-4}$ M zinc with v ml of 0.20 M EDTA at pH 5 (CPB). (a) direct titration curve and (b) Gran function F (arbitrary scale).

REFERENCES

1 G. Hägg, Allmän och Oorganisk Kemi, AWE, Sweden, p. 217.
2 British Patent No. 1. 310.087 (1972).
3 E. H. Hansen, C. G. Lamm and J. Růžička, Anal. Chim. Acta, 59 (1972) 403.
4 A. Hulanicki, M. Trojanowicz and J. Domanska, Talanta, 20 (1973) 1117.
5 A. G. Fogg, M. Duzinkewycz and A. S. Pathan, Anal. Lett., 6 (1973) 1101.
6 R. W. Cattrall and C.-P. Pui, Anal. Chim. Acta, 87 (1976) 419.
7 G. J. Moody, R. B. Oke and J. D. R. Thomas, Analyst (London), 95 (1970) 910.
8 J. Růžička, E. H. Hansen and J. Chr. Tjell, Anal. Chim. Acta, 67 (1973) 155.
9 L. A. R. Pioda, V. Stankova and W. Simon, Anal. Lett., 2 (1969) 665.
10 Handbook of Chemistry and Physics, 53rd edn., Chemical Rubber Co., 1972.

Analytica Chimica Acta, 90 (1977) 237—240

Short Communication

UTILISATION D'UNE ÉLECTRODE SÉLECTIVE À ION CHLORURE POUR ÉTUDES CINÉTIQUES EN SOLVANT NON-AQUEUX

CLAUDE G. BEGUIN et CHRISTIANE COULOMBEAU

C.E.R.M.O., Université Scientifique et Médicale de Grenoble, B.P. 53, 38041 Grenoble (France)

(Reçu le 27 Juillet 1976)

L'étude de la réactivité des liaisons carbone—halogène nous a conduits à déterminer les vitesses de solvolyse de chlorures de benzoyle dans l'acide formique, les données de la littérature, peu nombreuses [1—3], n'étant pas toujours concordantes. La méthode de mesure consiste à utiliser une électrode sélective de l'ion chlorure fonctionnant en continu dans un solvant organique. Des mesures de vitesses de réactions en milieux aqueux à l'aide d'électrodes sélectives (à fluorure [4, 5] ou à chlorure [6]) sont déjà décrites.

Nous rapportons dans cette note les conditions d'utilisation de l'électrode sélective de l'ion chlorure en milieu acide formique et les vitesses de formolyse du chlorure de benzoyle et de cinq chlorures de benzoyle *para*-substitués.

Partie expérimentale

Produits. L'acide formique (Prolabo) est purifié [7]. Le sulfate de potassium (Prolabo) est séché à 120°C. La solution de sulfate de potassium 1 M dans l'acide formique est conservé à 0°C et à l'obscurité dans des récipients fermés hermétiquement. La quantité nécessaire à chaque expérience est prélevée à travers un septum. Le chlorure de tert-butyle et les chlorures de benzoyle (Merck—Schuchardt puriss) sont utilisés sans purification.

Appareils et mode opératoire. L'électrode sélective de l'ion chlorure est une électrode à cristal Orion 94-17 A. L'électrode de référence au sulfate de mercure(I) Tacussel est reliée à la solution étudiée par une jonction liquide d'acide formique contenant 1 M de sulfate de potassium. Les différences de potentiel sont mesurées à 1 mV près à l'aide d'un millivoltmètre Orion 701 connecté à un enregistreur Sefram modèle Servotrace.

On dispose 10 ml de la solution de sulfate de potassium 1 M dans l'acide formique dans une cellule sous azote sec, thermostatée à 15 ± 0,1°C, équipée d'un septum permettant l'introduction des chlorures à l'aide d'une seringue, des deux électrodes précédemment décrites et d'un tube desséchant. Le volume de chlorure introduit est de 50 μl, soit environ $5 \cdot 10^{-2}$ M, les concentrations exactes sont déterminées à partir de la différence de potentiel obtenue en fin de réaction.

Les concentrations en ion chlorure en fonction du temps sont obtenues par comparaison avec des étalonnages effectués soit à partir de solutions de

chlorure de potassium dans l'acide formique contenant 1 M de sulfate de potassium soit à partir de solutions de chlorure de benzoyle dans le même milieu après solvolyse complète. Pour des concentrations supérieures à 10^{-3} M les deux étalonnages concordent et sont reproductibles pendant plusieurs jours. La dissolution du substrat est lente mais la réaction étant du premier ordre on remédie à cet inconvénient en n'effectuant les mesures qu'après un temps de réaction t_0 suffisant pour que le substrat soit dissous.

Les constantes de vitesse sont calculées par la méthode des moindres carrés en utilisant la fonction $\ln(a - x)/a = f(t)$ où a est la concentration au temps t_0 et x la concentration au temps t. Bien que pour chaque traitement la corrélation entre $\ln(a - x)/a$ et t soit bonne ($r = 0{,}999$), d'un essai à l'autre on observe des déviations de la constante de vitesse (dissolution lente) aussi chaque valeur (Tableau 1) est-elle la moyenne d'au moins cinq déterminations

Resultats et discussion

Conditions pour le bon fonctionnement de l'électrode sélective en milieu acide formique. La force ionique du milieu qui doit être constante pendant toute la durée de la réaction (une variation d'environ 5% est tolérée pour des concentrations supérieures à 10^{-3} M) est fixée par du sulfate de potassium à la concentration 1 M, ce sel étant choisi en raison de sa bonne solubilité et de sa stabilité dans l'acide formique.

Le temps de réponse de l'électrode à un changement de l'activité de l'ion chlorure doit être rapide (phénomènes transitoires de l'électrode [8, 9]). Le potentiel d'électrode est atteint en quelques centaines de millisecondes pour des concentrations plus grandes que 10^{-3} M, domaine pour lequel la précision de lecture est de 1 mV. La réponse de l'électrode dans le milieu réactionnel étudié, pour des concentrations en anion chlorure supérieures à 10^{-3} M, nous apparaît comme étant le temps d'homogénéisation de la solution.

Nous avons vérifié que la réponse de l'électrode était linéaire et reproductible selon la loi de Nernst pour le domaine 10^{-3} M—1 M. Dans le milieu utilisé à 15° C, la pente de la droite $E = f(\log Cl^-)$ est de −56 mV par décade de concentration ($E_0 = -499 \pm 5$ mV); cette valeur est satisfaisante.

TABLEAU 1

Constante de vitesse de la formolyse de *p*-Z-C_6H_4COCl ($5 \cdot 10^{-2}$ M) dans l'acide formique avec K_2SO_4 1 M à 15° C

Substituant en *para*	10^4 k s^{-1}
OCH_3	184 ± 18
CH_3	48 ± 5
F	29 ± 3
H	26 ± 2
Cl	14 ± 1
CF_3	13 ± 1

Test de la méthode cinétique. Nous avons vérifié que l'électrode pouvait être un instrument de mesure pour des études cinétiques en étudiant une réaction dont la constante de vitesse est bien connue. Le substrat utilisé est le chlorure de tert-butyle [10]. Un équilibre est obtenu correspondant à un degré d'avancement de la réaction de 40%. La constante du premier ordre calculée en tenant compte de cet équilibre et de $3{,}8_5 \cdot 10^{-4} \pm 0{,}4 \cdot 10^{-4}$ s^{-1}. Cette valeur est en bon accord avec celles de Bateman et Hughes [10] pour les mêmes conditions de température et de concentration.

Le milieu réactionnel (acide anhydre contenant 1 M de sulfate de potassium) a plusieurs caractéristiques différentes de celles de l'acide pur:

(a) Changement d'acidité: cet effet peut être prévu quantitativement en utilisant les données suivantes: constante d'autoprotolyse de l'acide formique $pK_i = 6{,}2$ [7, 11], constante d'acidité de HSO_4^- $pK_A(HSO_4^-) = 4{,}3$, H_2SO_4 complétement dissocié [7]. Les concentrations ioniques (sans corrections de coefficient d'activité décrivant les interactions ioniques) sont $(HCOO^-) = (HSO_4^-) = 0{,}10$ M, $SO_4^{2-} = 0{,}89$ M et $(HCOOH_2^+) = 5{,}94 \cdot 10^{-6}$ M alors que dans l'acide pur $(HCOOH_2^+) \simeq 7{,}95 \cdot 10^{-4}$ M.

(b) Changement de nucléophilie: l'acide formique pur est faiblement nucléophile. L'introduction de sulfate de potassium est accompagnée d'une augmentation de la concentration de l'espèce formiate plus nucléophile.

(c) Possibilité d'effets de sels: les anions sulfate et hydrogénosulfate interviennent dans le milieu à fortes concentrations. Plusieurs études, dont certaines concernant des substrats mésitoyle [12, 13], montrent le rôle des effets de sels. Nous pensons cependant que cet effet n'est pas très important (forte constante diélectrique du milieu, $\epsilon = 56$ [11b]).

Comme la formolyse du chlorure de tert-butyle n'est pas catalysée par les acides et se fait par l'intermédiaire d'un carbocation, les changements des milieux tels que ceux décrits en (a), (b) et (c) ne doivent pas modifier de façon sensible la vitesse de réaction. En conséquence nous pouvons conclure à la bonne concordance entre nos valeurs et celle de Hughes et à la validité de la méthode par l'électrode sélective de l'anion chlorure.

Formolyse des chlorures de benzoyle. Les effets de milieu et de substituants seront discutés dans le cadre de l'étude de la comparaison des réactivités des liaisons carbone—halogène en série benzoyle [14]. Nous avons mesuré six constantes de vitesse pour six chlorures de benzoyle, le non-substitué et cinq *para*-substitués. Les valeurs obtenues sont consignées dans le Tableau 1. Les conditions de milieu sont celles déjà décrites.

Les auteurs sont heureux de remercier pour leurs suggestions et discussions fructueuses: MM. Bozon et Mollens (Laboratoire L.A.R.E.C. à l'Institut Polytechnique de Grenoble), Mme Badoz, MM. Herlem et Jardy de l'Ecole Nationale Supérieure de Physique et Chimie de Paris, et Mme Breant de l'I.N.S.A. à l'Université de Lyon. Nous remercions aussi le Centre National de la Recherche Scientifique (ERA n° 478 et RCP n° 279).

BIBLIOGRAPHIE

1 E. W. Cruden et R. F. Hudson, J. Chem. Soc., (1956) 501.
2 C. G. Swain, R. B. Mosely et D. E. Bown, J. Am. Chem. Soc., 77 (1955) 3731.
3 D. E. Bown, Ph.D. Thesis M.I.T., April 1953.
4 K. Srinivasan et G. A. Rechnitz, Anal. Chem., 40 (1968) 1818; 44 (1972) 300.
5 G. H. Cady et S. Misra, Inorg. Chem., 13 (1974) 837.
6 L. Boulares-Poinsignon, J. L. Adamy et F. Federlin, C. R. Acad. Sci., Ser. C, 268 (196
1894.
7 M. Bréant, C. Béguin et C. Coulombeau, Anal. Chim. Acta, 87 (1976) 201.
8 K. Toth, J. Gavaller et E. Pungor, Anal. Chim. Acta, 57 (1971) 131.
9 N. Parthasarathy, J. Buffle et D. Monnier, Anal. Chim. Acta, 68 (1974) 185.
10 L. C. Bateman et E. D. Hughes, J. Chem. Soc., (1937) 1187.
11 G. Charlot et B. Tremillon, Les Réactions Chimiques dans les Solvants et les Sels Fondus, Gauthier-Villars, Paris, 1963, (a) p. 68; (b) p. 207.
12 R. F. Hudson et G. Moss, J. Chem. Soc., (1964) 2982.
13 C. A. Bunton, J. H. Crabtree et L. Robinson, J. Am. Chem. Soc., 90 (1968) 1258.
14 C. G. Béguin, C. Coulombeau et S. Hamman, J. Chem. Res., in press.

Analytica Chimica Acta, 90 (1977) 241—244

Short Communication

NEUROPHYSIOLOGICAL APPLICATIONS OF A CALCIUM-SELECTIVE MICROELECTRODE

JEFFREY D. OWEN, H. MACK BROWN and JAMES P. PEMBERTON
Department of Physiology, University of Utah, Salt Lake City, Utah 84132 (U.S.A.)
(Received 17th May 1976)

Changes in intracellular ionized calcium have been implicated in diverse cellular functions such as cellular aggregation, muscle contraction, visual transduction and membrane permeability. Despite considerable success recently in the study of monovalent ions in cellular processes with ion-selective microelectrodes, the intracellular measurement of calcium(II) with a microelectrode has not yet been reported. This is primarily because the electrode must be able to detect very low levels of Ca^{2+} ($< 10^{-6}$ M) in the presence of relatively high amounts of K^+ (0.2 M) and Mg^{2+} (10^{-3} M). Růžička et al. [1] reported the use of the straight-chained di-[*p*-(n-octyl)phenyl] phosphoric acid (HDOPP) compound in a macro calcium-selective electrode and suggested that the use of branched chained homologs would give inferior results. Surprisingly, we found just as good results in a microelectrode with the branched chained di-[*p*-(t-octyl)phenyl] phosphoric acid compound. Jagner and Østergaard-Jensen [2] recently reported that the use of substituted HDOPP compounds did not improve the selectivity of the calcium macroelectrodes. Christoffersen and Johansen [3] have described a miniaturization of the calcium electrode tip diameter (10—20 μm) of Růžička et al., but it was too large for intracellular measurements. This communication reports the use of a Ca^{2+}-selective microelectrode with such capabilities (1-μm tip diameter) in measuring Ca^{2+} in the giant neuron of the marine mollusc, *Aplysia californica*. The design and selectivities of this microelectrode have already been described [4].

Experimental

The calcium(II) sensor. The active material was prepared by combining 0.032 g of the calcium salt of di-[*p*-(t-octyl)phenyl phosphoric] acid (t-HDOPP 0.032 g of t-HDOPP, with 0.187 g of polyvinylchloride and 0.64 g of dioctylphenylphosphonate, by dissolution in ca. 6 ml of tetrahydrofuran.

A piece of 1-mm i.d. Pyrex capillary tubing was used to prepare a 1-μm tip diameter electrode with a micropipette puller. The electrode tip was siliconized by dipping it in a 3 % (v/v) solution of tri-n-butylchlorosilane in 1-chloronaphthalene and baked in an oven for 10 min at 250° C. Next the

electrode tip was dipped into the sensor solution until the sensor filled about 100 μm of the electrode tip. The electrode was then backfilled with 0.1 M $CaCl_2$.

Measuring system. The reference electrode was a micropipette with a ca. 50-μm tip diameter filled with 3 M KCl. The electrochemical cell was AgCl/Ag| 3 M KCl||Ca^{2+} sample|membrane|0.1 M $CaCl_2$|Ag/AgCl. The Ca^{2+} electrode half-cell was connected to a varactor bridge amplifier which had an input impedance of 10^{14} ohms, and the potential difference between the electrodes was read off a digital voltmeter. The electrode techniques and neuron have been described previously [5].

Calibrating solutions. To prepare $< 10^{-6}$ M Ca^{2+} solution, which was the approximate Ca^{2+} activity of the deionized water available, calcium chelating buffers were prepared as described previously [4].

Results and discussion

Intracellular ionized calcium, Ca_i^{2+}, in the *Aplysia* giant neuron is thought to play an important role in two interesting phenomena: prolonged action potentials [6] and light-induced hyperpolarization [7]. Calcium(II) was determined by first calibrating the microelectrode in Ca^{2+} solutions, which each contained 200 mM K^+ to mimic the K^+ present in these neurons [8]. Although the electrode measured calcium ion activity, the term concentration is used because the electrodes were calibrated in essentially constant ionic strength solutions. Figure 1A shows the calibration curve for the electrode used to obtain the intracellular record shown in Fig. 1B. The top record of Fig. 1B shows the membrane potential recorded with a 3 M KCl-filled 1-μm tip diameter micropipette and the bottom record the response of the calcium selective microelectrode on impalement of the giant neutron (ca. 300 μm diameter) from the left pleural ganglion of *Aplysia* [9]. The neuron was perfused with artificial saline containing (mM): 494 NaCl, 10 KCl, 10 $CaCl_2$, 20 $MgCl_2$, 30 $MgSO_4$, 10 Tris/Tris HCl (pH 7.65). The membrane potential electrode had been in the neuron for 10 min before insertion of the Ca^{2+}-electrode; the resting potential was -38 mV. Impalement of the cell with the Ca^{2+}-electrode produced some membrane depolarization and initiated spikes from the cell. The spikes gradually subsided as the membrane potential recovered to about -35 mV; other cells recovered completely after impalement. The potential of the Ca^{2+}-elecrode, V_{Ca}, decreased gradually from the initial value outside the cell (+34 mV) to -85 mV 15 min after penetration. Upon removal of the Ca^{2+}-electrode (Fig. 1B) V_{Ca} returned quite rapidly to the same value it had in the external saline. At present we have no explanation for the difference in time course on insertion and removal of the electrode. From the steady values of V_{Ca} and E_m, Ca_i^{2+} can be determined. The difference between V_{Ca} recorded inside the cell and the membrane potential recorded with the KCl electrode yields a value of -51 mV which corresponds to $6.9 \cdot 10^{-7}$ M Ca_i^{2+} (Fig. 1). The mean Ca_i^{2+} concentration obtained in the same manner from 10 different giant cells and 10 different electrodes (8 gian

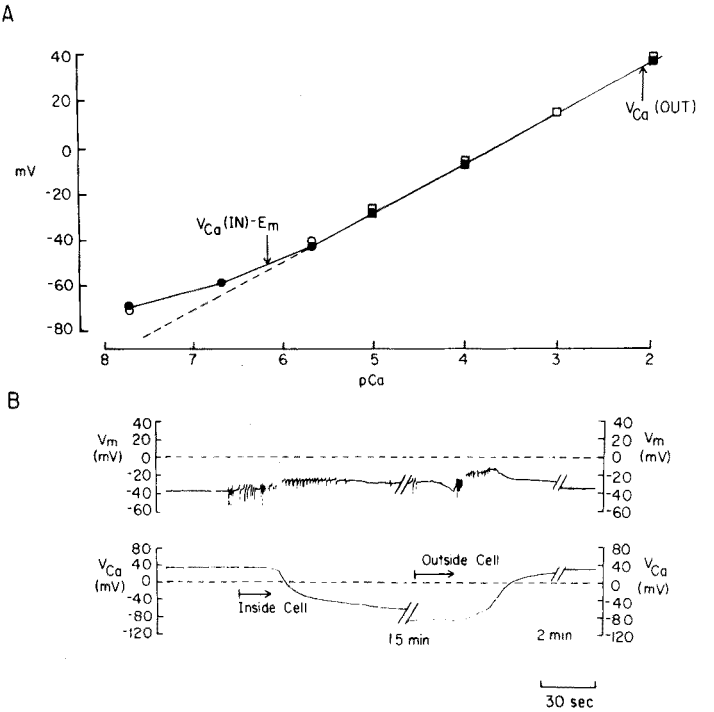

Fig. 1. A. Calibration curve for a calcium-selective microelectrode. The electrode response (mV) is plotted against the negative logarithm of the calcium concentration (pCa). The closed and open symbols denote pre- and post-experimental values (see Fig. 1B). Square symbols represent decade changes in $CaCl_2$, whereas the circles are for Ca solutions buffered with EDTA [1, 4]. All solutions also contained 0.2 M KCl and were buffered to pH 7.26. The calcium concentration inside the cell ($6.9 \cdot 10^{-7}$ M) was calculated by subtracting the membrane potential (E_m = −34 mV) from the V_{Ca} (−85 mV) obtained while the electrode was inside the cell. No theoretical significance is attached to the line drawn through the data points.

B. Membrane potential, E_m, and the potential of the calcium selective electrode, V_{Ca}, recorded within an *Aplysia* giant neuron.

cells from the abdominal ganglion and 2 giant cells in the left pleural ganglion; no difference between groups) was $7.7 \cdot 10^{-7} \pm 7.2 \cdot 10^{-7}$ M (s.d.). Assuming that the activity coefficient inside the cell is similar to that of the calibrating solutions (0.7), this Ca_i^{2+} value corresponds to an internal calcium activity of $5.4 \cdot 10^{-7}$ M. This should be considered a maximum value, because Mg^{2+} interference has not been considered. The Mg^{2+} concentration in these cells is unknown, but Mg^{2+} is known to exist in relatively large quantities (approx. 3—5 mM) in some other preparations [10]. Using the selectivity coefficients previously reported [4] for the Ca^{2+} electrode indicates that a similar Mg^{2+} concentration in *Aplysia* neurons would cause Ca_i^{2+} to be overestimated by approximately $5 \cdot 10^{-7}$ M, which is within the experimental error in determining Ca_i^{2+}.

The range of Ca_i^{2+} values in *Aplysia* giant neurons obtained with different techniques is quite broad (approx. 10^{-8}—10^{-6} M). Meech [6] estimated that Ca_i^{2+} in *Aplysia* giant neurons was about $3 \cdot 10^{-6}$ M, using the technique of pressure-injecting Ca/EGTA to produce prolonged action potentials. The light response of the giant cell is reportedly abolished and the membrane conductance is decreased at 10^{-7} M Ca^{2+}, whereas membrane conductance is increased at higher levels of Ca^{2+} injected into the neurons [11]. These Ca—EGT experiments suggest that intracellular free Ca^{2+} in *Aplysia* giant cells is in the range 10^{-6}—10^{-7} M. Stinnakre and Tauc [12] estimated that the Ca^{2+} equilibrium potential (E_{Ca}) was +165 mV from the decline of aequorin light emission at large positive membrane potentials. The Ca_i^{2+} value calculated from that E_{Ca} (ca. 10^{-8} M) is about an order of magnitude less than the value measured with the Ca^{2+}-electrode. Our estimate of E_{Ca} from the average value of Ca_i^{2+} from 10 cells would be about 120 mV. The Ca_i^{2+} value reported in Helix neurons (3—$8 \cdot 10^{-8}$ M) determined from voltage-clamp experiments in the presence and absence of Ca^{2+} [13] is in the same range reported by Stinnakre and Tauc [12]. However, the Ca_i^{2+} values measured in the present work are closer to those obtained from squid giant axon from aequorin experiments [14] and ^{45}Ca experiments [15] which were $3 \cdot 10^{-7}$ M and 0.5—$2 \cdot 10^{-7}$ M, respectively.

This work was supported in part by NIH Grant EY00762 from the National Eye Institute to H.M.B.

REFERENCES

1 J. Růžička, E. H. Hansen and J. Chr. Tjell, Anal. Chim. Acta, 67 (1973) 155.
2 D. Jagner and J. P. Østergaard-Jensen, Anal. Chim. Acta, 80 (1975) 9.
3 G. R. J. Christoffersen and E. S. Johansen, Anal. Chim. Acta, 81 (1976) 191.
4 H. M. Brown, J. P. Pemberton and J. D. Owen, Anal. Chim. Acta, 85 (1976) 261.
5 J. D. Owen, H. M. Brown and J. H. Saunders, Comp. Biochem. Physiol., 52A (1975) 175.
6 R. W. Meech, Comp. Biochem. Physiol., 48A (1974) 397.
7 H. M. Brown and A. M. Brown, Science, 178 (1972) 755; A. M. Brown and H. M. Brown, J. Gen. Physiol., 62 (1973) 239.
8 J. M. Russell and A. M. Brown, J. Gen. Physiol., 60 (1972) 519.
9 J. Kehoe, J. Physiol., 225 (1972) 115.
10 A. Scarpa and F. J. Brinley, Biophys. J., 15 (1975) 40A.
11 A. M. Brown, P. S. Baur and F. J. Tuley, Jr., Science, 188 (1975) 155.
12 J. Stinnakre and L. Tauc, Nature (London) New Biol., 242 (1973) 113.
13 R. W. Meech and N. B. Standen, J. Physiol. (London), 249 (1975) 211.
14 P. F. Baker, A. L. Hodgkin and E. B. Ridgway, J. Physiol. (London), 218 (1971) 709.
15 F. J. Brinley, S. G. Spangler and L. J. Mullins, J. Gen. Physiol., 66 (1975) 223.

nalytica Chimica Acta, 90 (1977) 245—247
Elsevier Scientific Publishing Company, Amsterdam — Printed in The Netherlands

hort Communication

'HE USE OF PERISTALTIC MINI-PUMPS IN AUTOMATIC ANALYSIS

ISE-NETTE OPHEIM and WALTER LUND*
)epartment of Chemistry, University of Oslo, Blindern, Oslo 3 (Norway)
Received 16th September 1976)

In automatic analysis of the continuous-flow type, the samples and reagents re passed through the system from the sampler tray and reservoirs to the letector unit by means of a peristaltic pump. Normally, a multichannel pump s used for this purpose, to control the flow of the samples, reagents and gas, nd also the flow to waste. However, the use of a multichannel pump has ertain disadvantages, particularly when a new method is under development. 'hus, to vary the amount of a given reagent, the diameter of the pump tubing arrying this reagent must usually be altered; when this is done the contin- ious flow is normally interrupted for all channels. Varying the speed of the ump is of little use, because this will alter the volume of the samples and eagents in the same way.

Instead of using a single multichannel pump, it may be advantageous to mploy separate mini-pumps with one or two channels each. In this case the olume of a given reagent can be adjusted simply by varying the speed of the ump controlling the flow of that reagent. The application of such a system s discussed below.

Experimental

The automatic system was of the AutoAnalyzer type, but the sampler nit and the polarographic detector were made in this laboratory; details of he system have been given elsewhere [1, 2]. Normally 2—4 separate per- staltic mini-pumps (Ismatec Mini-Micro-2) were used. Each pump had two hannels and either four or six rollers, and the fixed rotation speed was 0 r.p.m. For two of the pumps, the 500 : 20 gears were replaced by ten- tep Multur-M 120 J gearboxes (Erwin Halstrup, West Germany), so that he rotation speed of the pumps could be varied from 20 to 2 r.p.m. in ten qual steps. The mechanical gearboxes were originally driven by synchron- us motors (Philips) with 250 r.p.m. (50 Hz), giving an output rotation peed variable from 10 to 1 r.p.m; by using the 500 r.p.m. motors (AMY 8, aia AG, Murten, Switzerland) of the mini-pumps, the speed range of the earboxes was increased by a factor of 2.

*To whom communications should be addressed.

Discussion

The main advantage of using minipumps in automatic analysis is the unique flexibility offered by having completely independent pumping of each separate channel or pair of channels. When variable-speed pumps are used, the flow rate in each channel can be adjusted simply by altering the speed of that particular pump without disturbing the rest of the system in any way. Thus, in the determination of ascorbic acid in juice [3], the dilution of the samples can be adjusted by altering the speed of the pump controlling the aspiration rate of the samples, while the flow rate of the reagents is kept constant. In this way the concentration of ascorbic acid can be controlled within suitable limits before the flowing stream arrives at the detector. The volumes of reagents can be adjusted in a similar manner.

Another advantage of using mini-pumps is that the pumps can be placed near the respective modules, so that long tubings between the different parts of the system can be avoided. This may also have a favourable effect on the response time of the system, because cross-mixing of samples is minimized.

When an ordinary peristaltic pump is used to transport solutions in continuous-flow systems, the flow will pulsate slightly, as a result of the movement of the rollers along the pump tubing. The pulsation frequency depends on the rotation speed of the pump and the number of rollers. Furthermore, the flow pattern depends on the inner diameter of the pump tubing. The effect of rotation speed and diameter of pump tubing is illustrated in Fig. 1. Chlordiazepoxide solutions were analyzed in this example, and the pump in question controlled the aspiration of samples and also the exit to waste [1]. Because a polarographic detector was used, the variation in current caused by the dropping electrode is superimposed on the pulsation arising from the rotation of the pump. In curves a, b, and c, the inner diameter of the tubing is constant, and only the rotation speed is varied, whereas in curve d a smaller diameter and a higher rotation speed are used. The aspiration rate is approximately equal for curves c and d. The advantage of using a high speed and a small inner diameter of the tubing is demonstrated clearly. In practice, a maximum speed of 20 r.p.m. is recommended for the type of pumps used here. Pumps with six rollers were used, as these gave a more constant flow than the four-roller pumps.

Finally it should be mentioned that many mini-pumps can be purchased for the cost of a large multichannel pump.

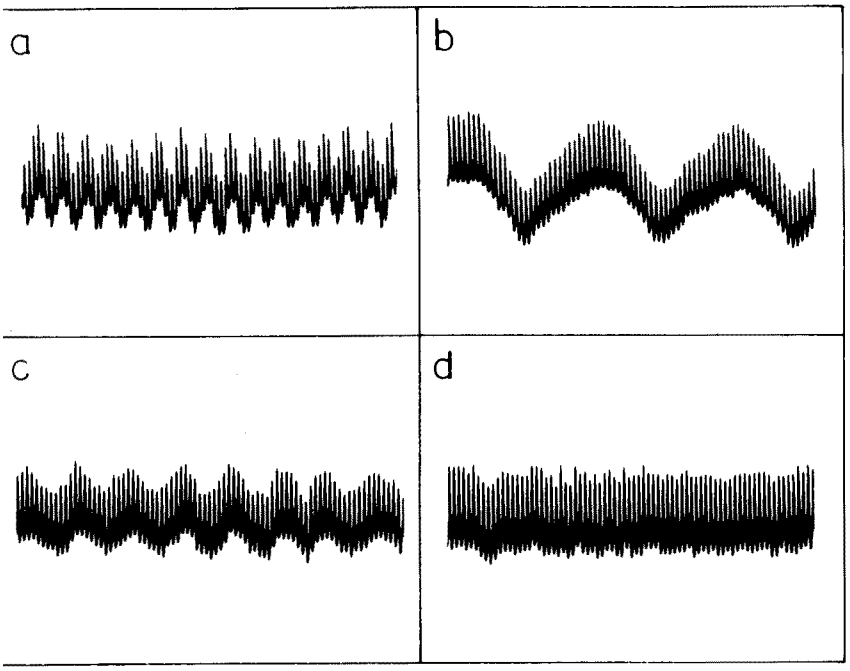

Fig. 1. Flow patterns for different values of the pump speed and inner diameter of the pump tubing.

Curve	Diameter (in.)	Rotation speed (r.p.m.)	Aspiration rate (ml min^{-1})
a	0.11	10	3.90
b	0.11	7	2.73
c	0.11	4	1.56
d	0.04	20	1.60

REFERENCES

1 W. Lund and L.-N. Opheim, Anal. Chim. Acta, 79 (1975) 35.
2 W. Lund and L.-N. Opheim, Anal. Chim. Acta, 82 (1976) 245.
3 L.-N. Opheim, Anal. Chim. Acta, in preparation.

Analytica Chimica Acta, 90 (1977) 249—252

Short Communication

POTENTIOMETRISCHE TITRATION VON SILBER MIT IONENSELEKTIVER ELEKTRODE

MANFRED GEISSLER

VEB Mansfeld Kombinat Wilhelm Pieck, Forschungsinstitut für NE-Metalle, 92-Freiberg-Sachs (D.D.R.)

(Eingegangen den 1. September 1976)

In mittel- bis hochlegierten Silber—Kupfer-Legierungen, Silberloten und ternären Legierungen mit niedrigen Silbergehalten wird das Silber im Betriebslabor noch häufig nach Volhard titriert. Daneben haben potentiometrisch indizierte Titrationsverfahren mit den Indikatorelektroden Ag/AgCl, Ag/AgBr, Ag/Hg_2SO_4 [1] und Halogenid-Maßlösungen zunehmend an Bedeutung gewonnen. Bush et al. [2] führten die potentiometrische Silberbestimmung mit der Meßkette Ag_2S/KE und Thioacetamid als Titrator ein, die Lenhardt [1] zur potentiometrischen Titration bei konstantem Strom weiterentwickelte.

Die Volhard-Titration hat den Nachteil, daß die Thiocyanat-Maßlösung auf Legierungstyp und Silbergehalt eingestellt werden muß, um positive Analysenfehler (bis + 0,4% abs, [3]) zu vermeiden. Ferner ist die visuelle Äquivalenzpunkt-Indikation durch hohe Gehalte stark farbiger Ionen (> 60% Cu, dsgl. Co und Ni) gestört. Eigene Versuche zeigten bei > 30% Cu am Äquivalenzpunkt eine Mischfarbe, die die exakte Endpunktsbestimmung erschwert.

Die genannten potentiometrischen Verfahren verlangen für eine zuverlässige Endpunktsindikation bei Routineanalysen sorgfältig präparierte Indikatorelektroden.

Diese angeführten Schwierigkeiten entfallen bei der Titration von Silber mit Thiocyanat-Maßlösung und potentiometrischer Endpunktsindikation mittels handelsüblicher ionenselektiver Silberelektrode (Ag-ISE).

Experimentelles

Elektroden und Meßgeräte. Ag/S-Sensitrode (Kombinat VEB Keramische Werke Hermsdorf, 653 Hermsdorf/Thür., DDR); gesättigte Kalomelelektrode KE 10 (Forschungsinstitut Meinsberg, DDR); Digitalvoltmeter V 530 (Meratronik, VRP; Eingangswiderstand $\geqslant 10^9\ \Omega$, Anzeigegenauigkeit 0,1 mV im Meßbereich ± 1 V); pH-Meßgerät MV 85 (VEB Präcitronic Dresden, DDR); Dosimat E 415 (Metrohm AG, Herisau, Schweiz; Anzeigegenauigkeit 0,01 ml); Potentiometerschreiber OH-814/1 (Radelkis, UVR); Registrierung der Titrationskurven: E 415, MV 85, OH-814/1.

Meßkette. Ag-ISE || Probelösung/Stromschlüssel/1 M KNO_3 || GKE.

Verfahrensgrundlagen

Zur potentiometrischen Indikation der Fällungsreaktion $Ag^+ + SCN^- \rightleftharpoons AgSCN$ eignet sich eine Ag-ISE, mit der die Ag^+-Aktivität in der Lösung gemessen wird. Aus dem Löslichkeitsprokt für AgSCN ($K_L = 10^{-12}$ [4]) ergibt sich die Ag^+-Konzentration am Äquivalenzpunkt zu 10^{-6} M ($pAg = 6$), d. h. daß die Ag-ISE bei der angegebenen Konzentration noch ein reproduzierbares Potential liefern muß. Die am Äquivalenzpunkt zu erwartende Zellspannung für die obenerwähnte Meßkette ($c_{Ag^+} = 10^{-6}$ M) errechnet sich mit Hilfe der Nernstschen Gleichung zu $E = +203$ mV.

Mit der Ag/S-Sensitrode aufgenommene Ag—pAg-Kurven für variable und konstante Ionenstärke ($I = 2$, Zusatzelektrolyt KNO_3) verliefen von pAg 1—5 linear (Nernstfaktor $F_N = 58$ mV bei 25° C) und erst oberhalb pAg = 5 wichen die Meßwerte geringfügig von der Geraden zu positiveren Potentialen ab. Für pAg = 6 wurde aus der E—pAg-Kurve die Zellspannung $E = +202{,}5$ mV bestimmt. Aus Titrationskurven von AgCu-Legierungen ergab sich für das Äquivalenzpunkt-Potential mit +203,5 bis + 204,5 mV (GKE) ein nahezu identischer Wert. Die Titrationskurve verläuft sehr steil und weist einen großen Potentialsprung (za. 200—300 mV) auf. Daraus folgt, daß bei der Titration des Silbers mit 0,02 M NH_4SCN-Maßlösung entweder die gesamte Titrationskurve registriert oder zeitsparend auf ein Äquivalenzpunkt-Potential von $E = +203 \pm 5$ mV (GKE) titriert werden kann. Bei der Bestimmung hoher Silbergehalte erweist sich auch die schnelle Umsetzung von ca. 90% des Silbers mit 0,02 M NH_4SCN und nachfolgende Titration des Restsilbers mit 0,002 M NH_4SCN als zweckmäßig.

Diskussion der Ergebnisse

In Tabelle 1 sind die Ergebnisse von Vergleichsanalysen an den Legierungen AgCu38, AgCu3,5 und LAg40Cd20 zusammengestellt, die von mehreren Beobachtern in verschiedenen Laboratorien erzielt worden sind. Sie belegen, daß das potentiometrische Analysenverfahren mit Ag-ISE zuverlässige Meßwerte liefert und durch eine kleine Standardabweichung gekennzeichnet ist. Bei der Silberbestimmung in AgCu38 ist festzustellen, daß die Einzelwerte der Volhard-Titration infolge des Kupfereinflusses viel stärker schwanken als diejenigen des potentiometrischen Verfahrens mit Ag-ISE. Durch die Mittelwertbildung beim Volhard-Verfahren ergibt sich aber ein guter Mittelwert, der gegenüber dem der potentiometrischen Titration keinen statistisch signifikanten Unterschied aufweist.

Außer auf AgCu-Legierungen und Silberlote läßt sich das potentiometrische Titrationsverfahren mit Ag-ISE auch auf PbSn-Legierungen mit hohen Blei- bzw. Zinngehalt und Silbergehalten von 0,05—4% anwenden.

Eine Deaktivierung der Ag/S-Sensitrode durch AgSCN war auch nach mehr als 100 Titrationen nicht festzustellen. Dagegen wurde bei Titrationen von Silber mit Kaliumjodid auf der Elektrodenoberfläche ein violett schimmernder Belag beobachtet. Die Sensitrode kann jedoch durch Abschleifen mit Naßschleifpapier (Körnung 600) und anschließendes Polieren mit Polierton-

TABELLE 1

Ergebnisse von Vergleichsanalysen

Probe	Ag-Gehalt n. TGL (%)	Methode[a]	Ag-Gehalt $\bar{x}$ (%)	Vert.-Ber. $\pm\Delta\bar{x}$ (%)	s (%)	Anz. Mess. N
AgCu38	61,5—62,5	Volhard	63,05	0,17	0,20	7
		Grav.	62,85	0,42	0,42	6
		Potent.	63,13	0,09	0,13	11
		Elekt.	63,25	—	—	1
AgCu3,5	96[b]	Volhard	96,26	0,20	0,25	8
		Grav.	96,17	0,15	0,15	6
		Potent.	96,19	0,06	0,09	13
LAg40Cd20	39,0—41,0	Volhard	40,02	—	—	3
		Grav.	39,90	0,18	0,18	6
		Potent.	39,78	0,18	0,35	18
		Elekt.	39,95	—	—	1

[a]Volhard; Gravimetrie als AgCl; potentiometrische Titration mit Ag-ISE; Elektrolyse.
[b]Mindestgehalt.

erde 3 und — falls nötig — Nachbehandlung mit Salpetersäure (1 + 1) bei 40° C regeneriert werden. Ausgehend von der Membranstärke wird eingeschätzt, daß die Elektrode mindestens 10—15 mal abgeschliffen werden kann.

Analysenvorschrift

Zur Bestimmung des Silbers in Silberlegierungen oder — loten werden 0,250 g des zu analysierenden Materials in 35 ml Salpetersäure (1 + 1) unter leichtem Erwärmen gelöst. Anschließend wird die Lösung bis zum feuchten Rückstand eingedampft, der nach dem Erkalten mit 10 ml Salpetersäure (d = 1,30) aufgenommen wird. Die Lösung wird in einen 250 ml-Maßkolben überführt und mit bidestilliertem Wasser bis zur Eichmarke aufgefüllt.

Für die Silbertitration werden von dieser Stammlösung 20 ml in eine geeignete Meßzelle pipettiert und mit ca. 20 ml bidestilliertem Wasser verdünnt. Dann werden die Ag/S-Sensitrode und eine gesättigte Kalomel-Referenzelektrode mit Stromschlüssel in die Meßlösung getaucht. Unter Rühren mit einem Magnetrührer wird nun mit 0,02 N Ammoniumthiocyanat-Maßlösung bis zum Äquivalenzpunkt-Potential von +203 ± 5 mV titriert.

Die Einstellung der Ammoniumthiocyanat-Maßlösung wird gegen reine Silberlösung vorgenommen. Dazu werden 0,250 g Silber (99,99%) wie oben beschrieben behandelt und entsprechende aliquote Mengen titriert.

Zur Silberbestimmung in PbSnAg-Legierungen mit > 10% Sn und 1—4% Ag werden 0,500 g Einwaage in ca. 8 ml Schwefelsäure (d = 1,83) unter Kochen gelöst. Die abgekühlte Lösung versetzt man mit 1 ml Salpetersäure (d = 1,51), überführt sie in einen 250 ml-Maßkolben und füllt mit bidestilliertem Wasser

zur Eichmarke auf. Je nach Gehalt werden aliquote Teile von 10 bzw. 25 ml mit 0,002 N Ammoniumthiocyanat-Lösung titriert.

SnPbAg-Legierungen mit 1—4% Ag werden wie PbSnAg-Legierungen gelöst und mit Niederschlag im Maßkolben mit bidestilliertem Wasser aufgefüllt und kräftig durchgeschüttelt. Nach dem Absetzen der Niederschlages wird ein aliquoter Teil der klaren Lösung zur Titration abgenommen.

Für die Bereitstellung von Ag/S-Sensitroden danke ich Herrn Dipl.-Chem. Hartmann und Herrn Dr. Grünke, Kombinat VEB Keramische Werke Hermsdorf, für sorgfältige Messungen Herrn Chem.-Ing. R. Kunze, FNE.

LITERATUR

1 K. Lenhardt, Erzmetall, 28 (1975) 172.
2 D. G. Bush, C. W. Zuehlke und A. E. Ballard, Anal. Chem., 31 (1959) 1368.
3 F. P. Treadwell, Analytische Chemie, II. Band: Quantitative Analyse, Verlag Franz Deuticke, Wien 1941, S. 612.
4 K. Rauscher, J. Voigt, I. Wilke und K.-Th. Wilke, Chemische Tabellen und Rechentafeln für die analytische Praxis, VEB Deutscher Verlag f. Grundstoffindustrie, Leipzig, 1972, S. 189.

Analytica Chimica Acta, 90 (1977) 253—256

Short Communication

COULOMETRISCHE BESTIMMUNG VON GALLIUM

P. GRÜNDLER* und P. K. AGASJAN

Chemische Fakultät der Staatlichen Lomonossow-Universität, Moskau (UdSSR)

(Eingegangen den 9. August 1976)

Für die genaue Bestimmung des Galliums in Halbleitermaterialien ist ein Verfahren hoher Präzision notwendig. Diese Voraussetzung wird von der coulometrischen Titration erfüllt. Besonders geeignet erscheint für Gallium die Komplexometrie. Da sich der Galliumkomplex nur langsam bildet, muß die Rücktitration nach Zugabe überschüssiger EDTA angewandt werden. Dafür bietet sich anodisch erzeugtes Quecksilber(II) an, das mit hoher Stromausbeute generiert werden kann.

Bekannt ist ein Verfahren zur Galliumbestimmung mit Rücktitration der EDTA durch Quecksilbernitratlösung in stark alkalischer Lösung [1]. Bei der coulometrischen Rücktitration treten im Gegensatz zur externen Reagenszugabe folgende Schwierigkeiten auf. In Abhängigkeit von der Lösungszusammensetzung tritt häufig der Fall auf, daß der EDTA-Komplex des Galliums weniger stabil ist als der des Quecksilber(II) ions.

In diesem Falle wird bei Überschreiten des Endpunktes der Rücktitration durch freie Quecksilberionen Gallium aus seinem Komplex verdrängt, so daß Fehler bei der Erkennung des Äquivalenzpunktes auftreten können. Da die Verdrängungsreaktion langsam verläuft, kann bei tropfenweiser Zugabe der Reagenslösung u.U. noch ein Endpunkt indiziert werden, während bei der kontinuierlichen und langsamen Reagenszugabe im Falle der Coulometrie die Indikation stärker beeinträchtigt wird. Wir stellten theoretisch und experimentell sicher, unter welchen Bedingungen die konditionelle Stabilitätskonstante K' des Galliumkomplexes höher ist als die des Quecksilberkomplexes, so daß eine exakte Bestimmung möglich wird.

Aus der Anwesenheit metallischen Quecksilbers in der Elektrolysezelle resultiert eine Störung der Bestimmung durch Halogenidionen, da infolge der Konproportionierung von Hg^0 und Hg^{2+} zu Hg_2^{2+} schwerlösliche Halogenide während oder am Ende der Rücktitration ausfallen können. Durch geeignete Wahl des Milieus läßt sich dieser Fehler vermeiden.

Experimentelles

Die Zelle bestand aus einem Polyäthylenbecher (400 ml) mit dicht

*Gegenwärtige Adresse: Sektion Chemie der Karl-Marx-Universität Leipzig, D.D.R.-701 Leipzig, Liebigstr. 18 (D.D.R.).

schliessendem Deckel aus Polymethacrylat, der Elektroden und Gaseinleitungsrohr trug. Das als Anode dienende Bodenquecksilber hatte eine Fläche von ca. 75 cm^2. Die Kathode des Generatorsystems (Platinnetz) befand sich im inneren zweier konzentrisch angeordneter Glasrohre mit feinem Frittenboden, die mit 2 M Natriumperchloratlösung gefüllt waren.

Zur amperometrischen Indikation des Endpunktes diente ein Platinblech von ca. 0,5 cm^2 Fläche, das gegen eine gesättigte Kalomelelktrode polarisiert wurde. Die angelegten Spannungen betrugen −30 mV bei pH 9—11, 0 mV bei pH 8, +30 mV bei pH 7, +50 mV bei pH 6 und +100 mV bei pH-Werten unter 5. Alle Generatorströme (2—20 mA) wurden über Normalwiderstände und Kompensator gemessen. Sie waren auf wenige Hundertstel Prozent konstant.

Als Grundelektrolyt diente eine 0,2 M Lösung von Ammoniumnitrat, die durch Zusatz von Natronlauge auf den jeweiligen pH-Wert gebracht wurde. Gallium-Standardlösungen wurden durch Auflösen reinsten Galliums (99,9999%) in wenig Salzsäure hergestellt. Die Lösungen wurden annähernd neutralisiert, mit einer abgewogenen Menge überschüssiger EDTA-Lösung versetzt, auf definierte Masse aufgefüllt und über Nacht stehen gelassen. Die EDTA-Lösung war vorher coulometrisch standardisiert worden.

Vor und während der Messung wurde reinstes Helium durch die Zelle geleitet. Zu Beginn wurden einige Tropfen 0,01 M EDTA-Lösung zugegeben und bis zum Beginn des Indikatorstromanstieges mit ca. 2 mA Generatorstrom vortitriert. Danach wurden definierte Mengen Gallium—EDTA-Mischung zugegeben und wiederum bis zum Auftreten des Indikatorstroms elektrolysiert. Die Zeit zwischen beiden Endpunkten diente zur Berechnung.

Ergebnisse und Diskussion

Abbildung 1 zeigt den Verlauf der konditionellen Stabilitätskonstanten von Gallium(III) und Quecksilber(II). Abbildung 2 gibt die maximale Chloridionen konzentration bei der Titration einer 0,01 M EDTA-Lösung an, d.h. die Konzentration, die am Endpunkt gerade zur Ausfällung von Kalomel führt. Zur Berechnung wurden verwendet [2—4]

$K_{Diss}(H_4Y$: pK_1—pK_4 2,07; 2,75; 6,24; 10,34

$[Hg(NH_3)_n]^{2+}$: $\lg \beta_1$—$\lg \beta_4$ 8,8; 17,5; 18,5; 19,3

$[Hg(OH)_n]^{2-n}$: $\lg \beta_1$—$\lg \beta_3$ 10,3; 21,7; 21,2

$[HgCl_n]^{2-n}$: $\lg \beta_1$—$\lg \beta_4$ 6,74; 13,22; 14,07; 15,07

$[Ga(OH)_n]^{3-n}$: $\lg \beta_1 \ldots \lg \beta_6$ 11,0; 21,7; 27,1; 34,3; 38,0; 40,3

$pK_L(Hg_2Cl_2) = 17{,}96$; $E^0(Hg/Hg^{2+}) = 0{,}854$ V; $E^0(Hg/Hg_2^{2+}) = 0{,}789$ V

In ungepufferter Lösung verdrängt Hg^{2+} das Gallium erst unterhalb pH 3 nicht mehr aus seinem Komplex (Abb. 1), jedoch stören dann geringste Chloridkonzentrationen (Abb. 2). Günstige Bedingungen für die Titration in

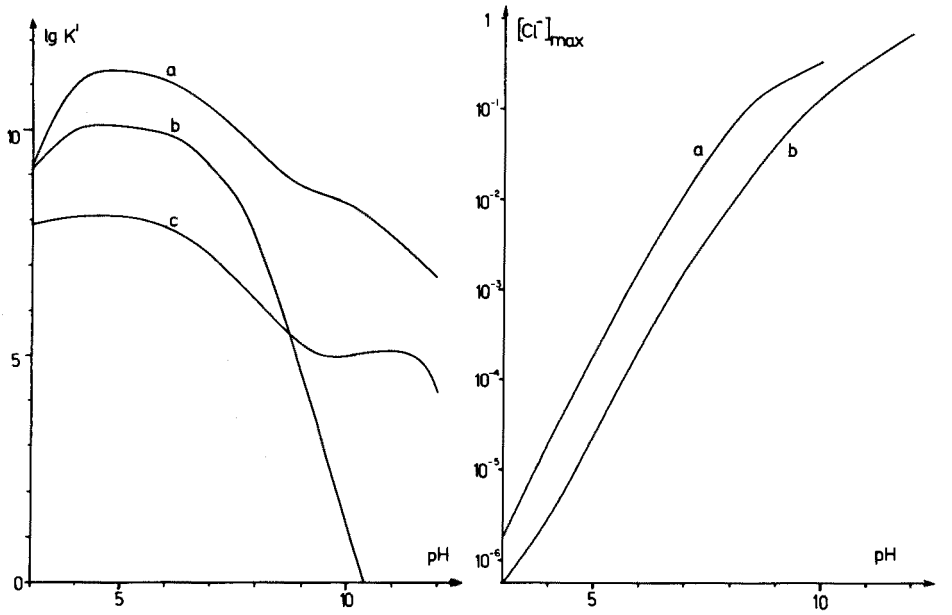

Abb. 1. Konditionelle Konstanten von Hg^{2+}- und Ga^{3+}-Komplexen mit EDTA in Anwesenheit metallischen Quecksilbers. (a) HgY^{2-} in ungepufferter Lösung. (b) GaY^{-}. (c) HgY^{2-} in Ammoniakpufferlösungen der Gesamtkonzentration $[NH_3] + [NH_4^+] = 0{,}2$ M.

Abb. 2. Maximale Chloridionenkonzentrationen bei coulometrischer Titration einer 0,01 M EDTA-Lösung mit Hg^{2+} (in Anwesenheit metallischen Quecksilbers). (a) In Ammoniakpufferlösungen der Gesamtkonzentration $[NH_3] + [NH_4^+] = 0{,}2$ M. (b) In ungepufferter Lösung.

Anwesenheit mittlerer Konzentrationen von Chlorid liegen bei pH-Wert 8 in Ammoniakpufferlösung vor.

Durch coulometrische Titration mit amperometrischer Verfolgung der Hg^{2+}-Konzentration wurde bestätigt, daß oberhalb pH 9 Gallium langsam durch Quecksilber(II) aus seinem Komplex verdrängt wird und daß die Störung durch Chloridionen unterhalb pH 7 gut mit den Angaben aus Abb. 2 übereinstimmt.

Die von uns verwendete amperometrische Indikation mit gegen ges. Kalomelelektrode negativ polarisierter Platinelektrode gab genauere Ergebnisse als alle anderen Indikationsmethoden. Am Endpunkt steigt der Strom steil infolge des Auftretens freier Quecksilber(II) ionen an. Die Indikatorelektrode wurde jeweils nach einigen Messungen durch anodische Chlorentwicklung in konz. Salzsäure regeneriert.

Nach diesem Verfahren konnten Galliummengen von 10^{-3} mol—10^{-7} mol bestimmt werden, wobei der Überschuß an EDTA etwa 10—20% betrug. Die relative Standardabweichung lag zwischen 0,09 und 0,2%. So wurde z.B. bei einer Bestimmung von 1,6036 mg Gallium ein Mittelwert von 1,6023 mg bei einem Variationskoeffizient von 0,16% erhalten.

LITERATUR

1 H. Khalifa und M. M. Khater, Z. Anal. Chem., 184 (1962) 92.
2 L. C. Sillén und A. E. Martell, Stability Constants of Metal Ion Complexes, The Chemical Society, London, 1964.
3 Ju. Ju. Lur'e, Spravočnik po analitičeskoj chimii, Chimija, Moskva, 1967.
4 A. Ringbom, Complexation in Analytical Chemistry, Interscience, New York, 1963.

Analytica Chimica Acta, 90 (1977) 257—261

Short Communication

RAPID DETERMINATIONS OF HYDRAZINE AND HYDROXYLAMINE BY POTENTIOMETRIC TITRATION WITH AN IODIDE-SELECTIVE MEMBRANE ELECTRODE

SANAE IKEDA

Faculty of Engineering, Tokushima University, Minamijôsanjima, Tokushima (Japan)

JUNKO MOTONAKA

Technical College of Tokushima University, Minamijôsanjima, Tokushima (Japan)

(Received 18th September 1976)

Hydrazine and hydroxylamine are widely used as analytical reagents and in drugs, organic syntheses, etc. Recently, Christova et al. [1] published an investigation of the determination of hydrazine, hydroxylamine, etc., by direct potentiometric measurement of the iodide activity produced by reaction of the compounds with iodine.

The present communication reports a potentiometric argentimetric titration for the determination of hydrazine and hydroxylamine with an iodide-selective membrane electrode; the method is rapid, simple and accurate, by comparison with the earlier method.

Hydrazine and hydroxylamine are treated with an iodine—methanol solution and the iodide produced is titrated potentiometrically with a silver nitrate solution. The reactions [2] involved are

$$N_2H_4 + 2I_2 \rightarrow N_2 + 4HI \quad (1)$$

$$NH_2OH + 2I_2 + H_2O \rightarrow HNO_2 + 4HI \quad (2)$$

The results obtained agree well with those obtained by Japanese Industrial Standard (JIS) methods [3, 4].

Experimental

Apparatus. An automatic potentiometric titrator (Hiranuma Sangyo Co., Ltd., RAT-11S) was used with an Orion Model 94-53 iodide-selective indicator electrode and a saturated calomel reference electrode. A Hitachi-Horiba, model M-7, pH meter was used for pH measurements.

Reagents. All reagents were of analytical-reagent grade (Wako Pure Chemical Industries, Ltd.); redistilled water was used. For experiments, the following stock solutions were diluted appropriately.

A stock solution (0.01 M) of hydrazine hydrate was standardized by the JIS K8871 method [3]. A stock solution (0.01 M) of hydroxylammonium

sulfate was standardized by the JIS K8993 method [4]. A stock iodine—methanol solution (0.1 M) was prepared by dissolving ca. 12.7 g of pure iodine in 500 ml of pure methanol, and stored in an amber bottle.

A stock silver nitrate solution (0.1 M) was standardized by amperometric titration [5].

Recommended procedure. Measure exactly 10 ml of 0.001—0.1 M hydrazine hydrate or 0.005—0.01 M hydroxylammonium sulfate into a 200-ml amber-glass titration cell and add excess of 0.01—0.1 M iodine—methanol solution. Adjust the volume to 100 ml with redistilled water. Titrate the solution potentiometrically with 0.01—0.1 M standard silver nitrate solution at room temperature. The whole procedure requires only 10 min.

Results and discussion

Effect of the amount of iodine—methanol. Hydrazine and hydroxylamine were titrated in the presence of different amounts of iodine—methanol. The analytical values for hydrazine and hydroxylamine were in good agreement with those obtained by the JIS method provided that iodine was added in excess. Large excesses did not affect the results. All subsequent titrations were carried out in the presence of 2.5 times the equivalent amount of iodine.

Effect of pH and temperature. Hydrazine and hydroxylamine were titrated in solutions of various pH values, obtained by adding sulfuric acid or sodium hydroxide. Hydrazine and hydroxylamine could be determined accurately at values in the pH range 1—5.

When a mixture of 10 ml of 0.01 M hydrazine hydrate (or 0.005 M hydroxylammonium sulfate) solution and 5 ml of 0.1 M iodine—methanol solution was diluted to 100 ml, the pH of the solution was about 2.5.

Hydrazine or hydroxylamine was titrated at temperatures of 0—70°C. Over the range 0—60°C, temperature did not affect the determinations, and for convenience all subsequent measurements were carried out at room temperature (ca. 20°C).

Effects of concomitant compounds. Solutions of hydrazine and hydroxylamine were titrated in the presence of 12 compounds; the results are shown in Table 1. As can be seen, the following compounds had little or no effect: lead nitrate, nickel nitrate, ammonium sulfate, ammonium carbonate, sodium nitrate, methanol and ethanol. Hydrazine and hydroxylamine could be determined with an error of about ±1% in the presence of any of these compounds. However, ammonium iron(II) sulfate and sodium nitrite interfered, the former being oxidized by iodine and the latter reduced by iodide. Cadmium nitrate, ammonium chloride and ammonium iron(III) sulfate did not affect the determination of hydrazine, and magnesium nitrate and potassium carbonate did not affect the determination of hydroxylamine.

Accuracy and precision. Table 2 shows the results obtained by the recommended procedure in four replicate titrations of various concentrations of hydrazine or hydroxylamine. Good results were obtained for 0.5—50 mg of hydrazine hydrate (10^{-4}—10^{-2} M) or 8—16 mg of hydroxylammonium sulfate

TABLE 1

Effect of concomitant compounds on the determinations of hydrazine and hydroxylamine

Sample	Compound added	Molar ratio (Sample: compound)	Relative error (%)
$N_2H_4 \cdot H_2O$[a]	$Pb(NO_3)_2$	1 : 25	+0.32
	$Cd(NO_3)_2$	1 : 200	+0.53
	$Ni(NO_3)_2$	1 : 200	+0.68
	$(NH_4)_2SO_4$	1 : 200	+0.41
	NH_4Cl	1 : 100	+0.26
	$(NH_4)_2CO_3$[c]	1 : 100	+0.71
	$Fe_2(SO_4)_3(NH_4)_2SO_4 \cdot 24H_2O$	1 : 200	−0.71
	$FeSO_4(NH_4)_2SO_4 \cdot 6H_2O$	1 : 1	+3.02
	$NaNO_3$	1 : 200	−0.31
	$NaNO_2$	1 : 1	−9.05
	CH_3OH	1 : 720	± 0.00
	C_2H_5OH	1 : 350	−0.16
$(NH_2OH)_2 \cdot H_2SO_4$[b]	$Pb(NO_3)_2$	1 : 1	−0.96
	$Mg(NO_3)_2$	1 : 100	−0.14
	$Ni(NO_3)_2$	1 : 100	−0.14
	$(NH_4)_2SO_4$	1 : 100	−0.81
	$(NH_4)_2CO_3$	1 : 1	−0.68
	K_2CO_3	1 : 1	−0.41
	$Fe_2(SO_4)_3(NH_4)_2SO_4 \cdot 24H_2O$	1 : 1	−1.76
	$FeSO_4(NH_4)_2SO_4 \cdot 6H_2O$	1 : 1	+6.86
	$NaNO_3$	1 : 100	−0.69
	$NaNO_2$	1 : 1	−4.46
	CH_3OH	1 : 2300	+0.71
	C_2H_5OH	1 : 3	−0.93

[a] Solution, 100 ml, of hydrazine hydrate (0.01 M, 10 ml), concomitant compound and iodine—methanol (0.1 M, 5 ml).
[b] Solution, 100 ml, of hydroxylamonium sulfate (0.005 M, 10 ml), concomitant compound and iodine—methanol (0.1 M, 5 ml).
[c] Adjusted to pH 2.5.

($5 \cdot 10^{-4}$—10^{-3} M). The relative errors and relative standard deviations were less than 0.8%. The best results with a relative error and relative standard deviation of less than 0.1% were obtained with 0.01 M hydrazine hydrate (ca. 51 mg) and 0.0005—0.001 M hydroxylammonium sulfate (ca. 8—16 mg). The analytical values were corrected for blanks at the 10^{-5}—10^{-6} M levels.

Determinations of commercial hydrazine and hydroxylamine. Commercial hydrazine and hydroxylamine were determined by the proposed method, and the results were compared with those obtained by JIS methods (Table 3).

TABLE 2

Accuracy and precision data

Sample	Concn.[a] (M)	Taken (mg)	Found (mg)	Relative error (%)	s_r (%)
$N_2H_4 \cdot H_2O$	10^{-2}	51.220	51.279[b]	+0.12[e]	0.0$_5$
	10^{-3}	5.121	5.140[b]	+0.37[e]	0.2
	10^{-4}	0.512	0.516[b]	+0.78[e]	0.6
	10^{-5}	0.051	0.053[b,d]	+3.92[e]	0.8
	10^{-6}	0.005	0.004[b,d]	−2.00[e]	5.5
$(NH_2OH)_2 \cdot H_2SO_4$	10^{-3}	15.785	15.786[c]	+0.01[f]	0.1
	$5 \cdot 10^{-4}$	7.554	7.546[c]	−0.11[f]	0.1
	10^{-4}	1.578	1.559[c]	−1.20[f]	0.3
	$5 \cdot 10^{-5}$	0.789	0.808[c]	+2.41[f]	0.2
	10^{-5}	0.151	0.148[c,d]	−0.99[f]	0.3

[a] Total volume was 100 ml.
[b] Average of 4 titrations of 100 ml of hydrazine solution with < 5 ml of 0.0001—0.1 M standard silver nitrate solution.
[c] Average of 4 titrations of 100 ml of hydroxylamine solution with < 5 ml of 0.001—0.1 M standard silver nitrate solution.
[d] A blank test was performed.
[e] Compared with value by JIS K8871-1961 method.
[f] Compared with value by JIS K8993-1961 method.

TABLE 3

Determinations of commercial hydrazine and hydroxylamine

Sample	Manufacturer	JIS method		Proposed method	
		Assay[a] (%)	s_r (%)	Assay[b] (%)	s_r (%)
$N_2H_4 \cdot H_2O$	A	91.37	0.1	91.44	0.0$_2$
	B	80.12	0.1	80.34	0.1
	C	80.08	0.1	80.14	0.1
	D	85.61	0.1	85.65	0.1
$N_2H_4 \cdot H_2SO_4$	A	99.79	0.1	99.72	0.1
	B	99.64	0.1	99.95	0.1
$(NH_2OH)_2 \cdot H_2SO_4$	A	98.69	0.2	98.22	0.1
	B	96.42	0.1	96.55	0.1
	C	98.75	0.1	98.76	0.1
	D	97.35	0.1	97.36	0.1

[a] Average of 4 determinations of ca. 0.05 g of hydrazine hydrate, ca. 0.1 g of hydrazine sulfate or ca. 0.1 g of hydroxylammonium sulfate.
[b] Average of 4 determinations of ca. 0.005 g of hydrazine hydrate, ca. 0.01 g of hydrazine sulfate or ca. 0.01 g of hydroxylammonium sulfate.

The authors are grateful to Professor Nobuyuki Tanaka (Tohoku University) for help in preparation of this manuscript.

REFERENCES

1 R. Christova, M. Ivanova and M. Novkirishka, Anal. Chim. Acta, 85 (1976) 301.
2 J. Blom, Chem. Ber., 59 (1926) 121.
3 JIS K8871-1961.
4 JIS K8993-1961.
5 I. M. Kolthoff and P. K. Kuroda, Anal. Chem., 23 (1951) 1306.

Analytica Chimica Acta, 90 (1977) 263—266

Short Communication

A VERY SIMPLE AIR-GAP ELECTRODE

JAROSŁAW FLIGIER and ZBIGNIEW GREGOROWICZ

Institute of Analytical and General Chemistry, Silesian Polytechnical University, 44-101 Gliwice, (Poland)

(Received 28th June 1976)

Potentiometric gas-sensing membrane electrodes [1, 2] are applied in the determination of free gases, e.g. CO_2, NH_3, SO_2 and NO_x, in aqueous solutions, as well as of those compounds from which these gases can be isolated selectively and quantitatively.

Recently, Růžička and Hansen [3] have improved the construction of such gas sensors by replacing the gas-permeable membrane by an air gap, which separates the electrolyte layer from the sample solution. The advantages of the air-gap electrode in comparison with a "classical" membrane probe have been well established [4—7]. Although the structure of the modified air-gap electrode [6] is simple in its concept, an even simpler device can be constructed with a conventional combined pH-electrode. In such an electrode the function of Růžička and Hansen's constructional solution is taken over by a thin gel layer covering the sensitive glass surface and connecting it with the porous pin of the calomel reference electrode. In order to determine the capacity of this simple air-gap electrode, its fundamental parameters and the responses to ammonia and carbon dioxide have been investigated.

Experimental

Apparatus. The air-gap sensor described here (Fig. 1) consists of a combined glass-calomel electrode (1; Radiometer GK 2301B) and three conical glass vessels (2), each of about 10-cm^3 capacity, with a female ground-glass joint 20/25 (3) which act as sample, electrolyte and sponge chambers. A male ground-glass joint 20/25 (4) was mounted on the electrode (1) by means of Polastil (Erg, Poland) 3 mm above the porous pin (5).

Reagents. All the solutions were prepared from analytical-grade reagents. Water with a low ammonia content was prepared by passing redistilled water through a column of cation-exchange resin (Wofatite KPS 200, H^+-form). The electrolyte solutions were: 10^{-3} M, $5 \cdot 10^{-3}$ M and 10^{-2} M sodium hydrogen carbonate and ammonium chloride, respectively. To hold the electrolyte layer on the surface of the electrode, 1% methyl cellulose (B.D.H. England) was added to the electrolyte.

Standard solutions within the range 0.20—200 mM sodium hydrogencarbonate and 0.010—1000 mM ammonium chloride were prepared. Sulphuric acid (0.1 M) and 1.0 M sodium hydroxide were used as pH regulators.

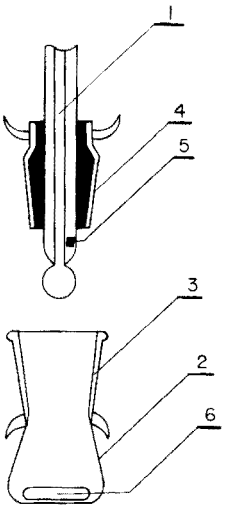

Fig. 1. The construction of the air-gap electrode (for details see text).

Measuring technique. The electrolyte layer was applied to the electrode by placing it in an electrolyte chamber, so that the level of the electrolyte was 1—2 mm above the porous pin (5) of the combined electrode (1). After 10—20 s, the electrode was moved to a sponge chamber with a cone-shaped polyurethane sponge, which just touched the surface of the electrode and soaked up the excess of electrolyte within 60 s. Then 1.0 or 2.0 ml of standard solution was pipetted into the sample chamber (2), a pH regulator solution was added to a total volume of 3.0 ml, the sample chamber was immediately closed with the electrode, and the magnetic stirrer (6) was started. The steady readings of the electrode were read off after 2—4 min with an accuracy of 0.005 pH.

Results and discussion

The choice of holding agent. In a search for a suitable material to hold a thin but stable layer of electrolyte on the electrode surface, several wetting and gelling agents were tested. The best results were obtained with methyl cellulose. The proper concentration of methyl cellulose in the electrolyte was selected by measuring the stability of the baseline as well as the response time to changes in sample concentration; a 1% solution of methyl cellulose in the electrolyte was chosen. The results of measuring the response time led to a rather unexpected conclusion: because of condensation of the methyl cellulose electrolyte the response time is shortened and when the same gel layer is used again the response time increases. As the time required for the electrode signal to return to the baseline was 7—16 min, depending on the concentration of the sample, calibration curves were set up by the surface renewal technique (about 90 s), which was faster than the surface equilibration technique.

Electrode standardization for carbon dioxide and ammonia. Calibration curves were obtained at 22°C for three concentrations of the electrolyte solutions. Each point in Fig. 2 represents the mean value of three determinations. All the calibration curves were calculated by means of a linear regression analysis in the linear part of the curves. Table 1 provides values of the regression coefficient b in the equation $pH_e = b \log [HCO_3^-$ or $NH_4^+] + c$, together with the standard deviations around these lines.

The positions of the points on the calibration curves corresponding to $5 \cdot 10^{-3}$ M electrolyte solutions were checked after about three weeks. When the same previously prepared standards and electrolytes were used it was found that the differences were about $+0.06$ pH_e. This value decreased to about $+0.03$ pH_e when the combined electrode was checked in buffer solutions.

Conclusion

The preparation of an air-gap electrode from an ordinary combined pH electrode takes only 2—3 h. Compared with the prototype of Růžička and Hansen [3], this electrode provides results of similar accuracy, though the response time is somewhat longer and the baseline is slightly less stable. Such a stability is, however, good enough for measurements by the surface renewal technique. The air-gap electrode presented here may also be used for measurements of pH; if the electrode is fitted tightly into the sample chamber, the influence of ambient gases is eliminated as well. Moreover, the simple checking of the electrode in buffer solutions makes it possible to extend the period between calibrations.

TABLE 1

Statistical evaluation of errors of the calibration curves of an air-gap electrode, applied as a carbon dioxide and ammonia electrode

Electrolyte	(M)	Regression coefficient b	s (pH)	s (%)
CO_2	10^{-3}	−0.7832	0.0148	4.3
	$5 \cdot 10^{-3}$	−0.9410	0.0125	3.0
	10^{-2}	−0.9924	0.0162	3.8
NH_3	10^{-3}	0.9477	0.0156	3.8
	$5 \cdot 10^{-3}$	0.9703	0.0144	3.4
	10^{-2}	1.0375	0.0132	2.9

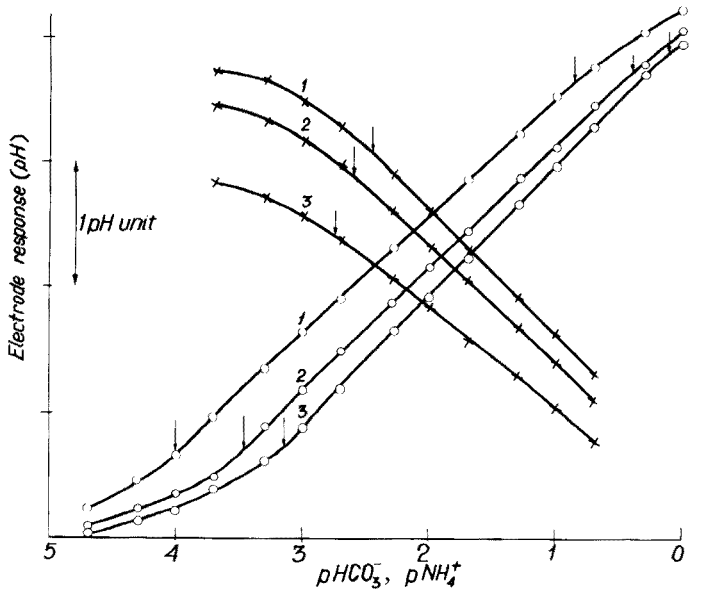

Fig. 2. Calibration curves for an air-gap electrode used as a carbon dioxide (×) and ammonia (○) electrode with various sodium hydrogencarbonate and ammonium chloride concentrations in the electrolyte. Electrolytes: (1) 10^{-3} M; (2) $5 \cdot 10^{-3}$ M; (3) 10^{-2} M solutions containing 1% methyl cellulose. The dynamic measuring range is marked on the curves by arrows.

REFERENCES

1 Orion Research, Analytical Methods Guide, Cambridge, Massachusetts, U.S.A., 6th edn., 1973.
2 Electronic Instruments Ltd., Laboratory Electrodes, Chertsey, Surrey, Dec. 1974.
3 J. Růžička and E. H. Hansen, Anal. Chim. Acta, 69 (1974) 129.
4 E. H. Hansen, H. B. Filho and J. Růžička, Anal. Chim. Acta, 71 (1974) 225.
5 J. Růžička, E. H. Hansen, P. Bisgaard and E. Reymann, Anal. Chim. Acta, 72 (1974) 215.
6 E. H. Hansen and J. Růžička, Anal. Chim. Acta, 72 (1974) 353.
7 U. Fiedler, E. H. Hansen and J. Růžička, Anal. Chim. Acta, 74 (1975) 423.

Analytica Chimica Acta, 90 (1977) 267—270

Short Communication

THE DETERMINATION OF COPPER IN ALLOYS BY ELECTROGRAPHY AND ATOMIC ABSORPTION SPECTROMETRY

J. F. ALDER, A. E. BAKER and T. S. WEST*
Chemistry Department, Imperial College, London SW7 2AY (England)
(Received 15th January 1976)

The electrographic sampling technique was first used by Glazunov [1] for the production of metallographic prints, and by Fritz [2] for the identification of the constituents of alloys. Later workers adapted the method for quantitative work involving colorimetric determination [3—5] and the ring-oven technique [6, 7], Jaluvka [8] modified the method and determined cadmium and copper in alloys colorimetrically with polarography as a reference method. Shresta and West [9] have described a rapid, semi-quantitative method for the analysis of Cu, Cr, Mn and Ni in steels by electrographic dissolution combined with carbon rod a.a.s. In the work described here, copper was dissolved electrographically from the surface of Cu, Al and Cu—Zn alloys into a moist filter paper matrix, taken up in acid, and determined by flame a.a.s.

Experimental

Instrumentation and reagents. The electrographic sampler comprises a graphite rod surrounded by a brass tube acting as the anode [9]. The electrolysis current is supplied by a constant current device with a timer. The current can be varied from 5 to 25 mA in 5 mA steps. A Varian—Techtron VA 1000 spectrometer was used in accordance with the manufacturer's instruction for the determination of copper with an air—acetylene flame. All reagents were of analytical-reagent grade. The alloys had been analysed previously by emission spectrography.

Procedure. The surface of the alloy sample is machined smooth, and cleaned with acetone or carbon tetrachloride. A filter paper disc (Whatman 40 ashless) of the same diameter as the graphite cathode of the sampler is placed on the surface and moistened with 0.1 M KNO_3 electrolyte solution (3 μl). The sampler is then placed in position and firm contact maintained with the alloy sample. The appropriate current (5 mA) is selected and the instrument switched on for a measured time. The sequence may be interrupted to replenish the electrolyte solution if the paper dries out. The

*Present address: Macaulay Institute, Craigiebuckler, Aberdeen AB9 2QJ (Scotland).

sampling is repeated for five different intervals to give a plot of weight of copper dissolved vs. time of electrolysis. Each paper disc is transferred carefully to a beaker containing 7 ml of 2 M hydrochloric acid and the contents are boiled for a few minutes to dissolve the deposited material. The solution is cooled, transferred to a 10-ml graduated flask, and made up to the mark with 2 M hydrochloric acid. The copper content of the solution is determined by a.a.s. in the usual manner with copper reference standards in 2 M hydrochloric acid. The plots of copper dissolved vs. time are constructed and the gradient of the straight line determined.

Choice of electrolyte and current. Copper, silver and lead dissolve well electrographically into nitrate electrolyte, but poorly into chloride which forms insoluble products on the metal surface [10]. This was confirmed for copper; only 62% current efficiency was obtained for pure Cu with 0.1 M ammonium chloride electrolyte, but 0.1 M potassium nitrate electrolyte gave 98% efficiency.

Current in excess of 5 mA caused greater scatter of results, probably because of thermal evaporation and some decomposition of the electrolyte. Wherever possible, a current of 5 mA was used, although protracted electrolysis times were required for the lower concentrations.

Calculation of results

From Faraday's Law, assuming that the metal dissolves as Cu^{2+}, the rate of dissolution of pure copper can be calculated to be 1.645 $\mu g\ s^{-1}$. From the straight line plot obtained experimentally, the mass of copper liberated per second can be calculated. From the ratio of this value to that obtained for a pure copper standard, the copper content of the unknown alloy can be calculated. The ratio of the mass of copper liberated experimentally per second from pure copper to that calculated for pure copper gives the current efficiency for copper, which may be valid for pure copper only, or for the particular alloy for which it is determined, because the current efficiency may depend on the nature of the alloy. Reasonable results were obtained (Table 1) by assuming the same current efficiency to hold for the alloys and the pure metal.

Discussion

This empirical approach to the electrographic analysis of copper alloys has yielded encouraging results, although the precision needs to be improved, by better control of the dissolution step before the method can be regarded as quantitative. Before extending the use of this method to other alloys it must be realised that the method will behave quantitatively only if the alloy is a solid solution presenting an equipotential surface to the transfer medium [1]. It was not known whether the alloys used were true solid solutions, but the good agreement between the experimental results and the known copper concentration suggests that they were. The assumption that the copper dissolves as Cu^{2+} appears to be valid from the experimental results, but the

TABLE 1

Analysis of copper and alloys
(Unless stated otherwise, the electrolyte was 0.1 M KNO_3, the current was 5 mA, and the solution was diluted to 10 ml for analysis.)

Sample[a]	Sampling time (s)	Rate of Cu dissolution ($\mu g\ s^{-1}$)	Cu found (%)	
Pure copper	3—10[b]	0.408	82.6	
>99.99%	3.5—20.5[c]	0.300	91.2	
	2.5—8[c]	0.312	94.8	
	3—7[c]	0.294	89.3	
	2—6.5	0.164	99.7	
	2.5—5.5	0.160	97.3	
	2—6.5	0.162	98.5	
Alloy 1	4—10[c]	0.172	52.3[d]	53.1[e]
59.3% Cu	5—11[c]	0.170	51.7[d]	52.5[e]
	5—11.5[c]	0.164	49.8[d]	50.6[e]
	6—10	0.091	55.3[d]	56.1[e]
	8—16	0.095	57.8[d]	58.8[e]
	3.5—8.5	0.094	57.1[d]	58.0[e]
	4—16	0.102	62.0[d]	63.0[e]
Alloy 2	50—155[f]	0.0015	0.90[d]	0.91[e]
1.07% Cu	75—150[f]	0.0019	1.15[d]	1.17[e]
	100—140[f]	0.0015	0.90[d]	0.91[e]
Alloy 3	3—7	0.114	69.5[d]	70.6[e]
74.7% Cu	3.5—8	0.120	83.0[d]	74.1[e]
	4—16	0.126	76.8[d]	77.7[e]
	4—16	0.124	75.4[d]	76.6[e]
	4—16	0.124	75.4[d]	76.6[e]

[a] Alloy composition (%): (1) Cu 59.3; Zn 36.03; Al 1.27; Fe 1.10; Mn 1.14. (2) Cu 1.07; Al 85.60; Si 10.34; Mg 1.15. (3) Cu 74.69; Mn 11.93; Al 8.15; Fe 3.08; Ni 1.81.
[b] Current, 15 mA. The high current dried out the paper, and changed the electrolytic conditions.
[c] Current, 10 mA (see note b).
[d] Ratio of experimental rate of Cu dissolution to theoretical rate for pure Cu (1.645 $\mu g\ s^{-1}$).
[e] Ratio of experimental rate of Cu dissolution to experimental rate for pure Cu.
[f] Solution diluted to 5 ml for a.a.s. because of inadequate sensitivity.

state in which other metals, particularly transition elements will dissolve must be determined in practice.

The authors are indebted to Mr. R. Cochrane of Stone Manganese Marine Limited, London, for the analysed alloy samples and to the Science Research Council for the award of an advanced course studentship to A.E.B.

REFERENCES

1 A. Glazunov, Chim. et Ind., 21 (1929) 425; 23 (1930) 247.
2 H. Fritz, Z. Anal. Chem., 78 (1929) 418.
3 A. Glazunov and J. Krivohlavy, J. Physik. Chem., A161 (1932) 373.
4 A. Glazunov and E. Drescher, Compt. Rend. 17me Congr. Chim. Ind., Paris, 1937, p. 572.
5 M. Garina and R. Catto, Chim. Ind. (Italy), 17 (1935) 218.
6 W. R. Nall and R. Scholey, Metallurgia, 54 (1956) 97.
7 W. I. Stephen, Mikrochim. Acta, (1956) 1540.
8 J. Jaluvka, Chem. (Prague), 10 (1958) 631; Sbornik Ved. Prac. Vysokej Skoly Techn. N. Kosiciach, 4 (1960) 53.
9 I. L. Shresta and T. S. West, Bull. Soc. Chim. Belg., 84 (1975) 549.
10 Standard Methods of Chemical Analysis, 6th edn., Vol. 3, Part A, Van Nostrand, New York, p. 500.

Analytica Chimica Acta, 90 (1977) 271—274

Short Communication

DETERMINATION OF MERCURY BY CARRIER-FREE COMBUSTION SEPARATION AND FLAMELESS ATOMIC ABSORPTION SPECTROMETRY

ERNEST S. GLADNEY and JAMES W. OWENS*

University of California, Los Alamos Scientific Laboratory, P.O. Box 1663, Los Alamos, New Mexico 87545 (U.S.A.)

(Received 1st September 1976)

Many procedures have been published for the measurement of mercury in environmental materials. The more prominent are flameless atomic absorption spectrometry [1, 2] and neutron activation analysis [3—5], both of which have largely replaced earlier colorimetric techniques [6, 7], which lack the necessary sensitivity. Several chemical separation methods have been used for isolation of mercury: ion exchange [8], various wet acid digestions, gold or silver metallic collectors, and combustion followed by a cold trap [5]. There are problems with each of these procedures in that they have generally been designed for a single matrix or around the needs of a particular analytical technique. Most of the procedures work for water, air and sometimes biological materials, but few are also applicable to geological samples. The combustion separation reported by Rook et al. [5] is one of the most sensitive, contamination-free and widely applicable techniques. This communication describes its modification for the measurement of mercury in all major sample matrices with flameless atomic absorption spectrometry as well as neutron activation as the detection system.

Experimental

Apparatus and reagents. The quartz combustion system designed by Rook et al. [5] was modified to facilitate the carrier-free separation of nanogram quantities of mercury. The neutron activation procedure requires contamination-free conditions only through the end of the irradiation, not during the post-irradiation chemical separation, and is not subject to as many contamination problems as is this carrier-free technique. Oxygen (clinical grade) is brought from a cylinder to the combustion system through rubber surgical tubing. The rubber stopper inlet connection of Rook et al. [5] proved to be a serious source of mercury contamination and was eliminated. A Vycor outer 19/38 standard taper joint was added to the upstream end of the quartz combustion tube; 1-cm (o.d.) glass tubing was attached ahead of a

*Present address: Bendix Engineering Corp., Grand Junction, Colorado.

glass inner 19/38 standard taper joint and packed with a granular silver trap, which substantially reduced mercury vapor in the inlet oxygen. The remainder of the system, including the tube furnace, was similar to that reported by Rook et al. [5].

The acid solution used to leach the mercury from the cold trap was 0.6 M nitric acid, 0.9 M sulfuric acid and 0.05% potassium permanganate. Baker Ultrex concentrated nitric and sulfuric acids and Perkin-Elmer mercury-free 5% potassium permanganate solution were used to prepare the wash solution. These concentrations were selected so that a 50-ml wash would be directly compatible with the cold-vapor atomic absorption procedure described in the instruction manual for the Perkin-Elmer Mercury Analysis System 303-0832. Mercury standards were prepared by dilution of National Bureau of Standards (NBS) Standard Reference Material (SRM) 1641 (Mercury in water — 1.49 p.p.m.) or direct use of NBS SRM 1642 (Trace mercury in water — 1.18 p.p.b.). All dilutions were made with deionized, doubly distilled water.

A Perkin-Elmer Model 306 atomic absorption spectrophotometer equipped with a deuterium background corrector and a cold-vapor mercury analysis system was used for all measurements. A Perkin-Elmer electrodeless discharge mercury lamp was the radiation source.

Procedure

In an effort to minimize sample contamination during analysis, the following measures were taken daily before sample runs. The tube furnace was heated to 800—1000°C, the quartz combustion system flamed down with a gas—oxygen torch while an oxygen flow of 100 cm^3 min^{-1} was passed through the system, and the system was baked out for 30 min with the rapid oxygen flow. After baking, the system was purged continuously with the scrubbed oxygen and opened to the air only briefly to change samples. The ceramic combustion boats were soaked in concentrated nitric and sulfuric acids (1:1) for several hours and the interior of the liquid nitrogen condensers were soaked in 50% nitric acid. The boats and condensers were rinsed with deionized, doubly distilled water and used immediately. These precautions reduced the mercury blank from the apparatus to below the detection limit.

Ecological samples were frozen in the field and were usually combusted as received. If results were required on a dry weight basis, the samples were freeze-dried before burning. Although mercury loss during lyophilization is still a subject of controversy [9, 10], we accept LaFleur's observations of limited loss [9]. Samples with high carbon content were handled differently from mineral samples. Approximately 0.5 g of tissue or vegetation was weighed into a combustion boat, the boat inserted into the quartz tube, the oxygen flow set to 50 cm^3 min^{-1}, and a freshly washed cold trap inserted downstream. The combustion was conducted as described by Rook et al. [5]. After the system had cooled, the condenser was removed and set with the

joint end into a 125-ml flask compatible with the Perkin-Elmer mercury system. The condenser was warmed to room temperature and the interior washed down with 20 × 2-ml portions of the hot acid solution followed by 5 × 2-ml portions of distilled water.

For low carbon samples (e.g. soils), the carefully controlled combustion step was eliminated and the samples were immediately baked for 10 min at 1000°C. The remainder of the procedure was the same as described above.

Chemical yield on each combustion may be determined through the use of ^{203}Hg radiotracer. Rook et al. [5] consistently observed $\geqslant$ 99% recovery when 25 mg of HgO carrier was added to the samples before combustion. Since any reasonable quantity of carrier would overwhelm the mercury in the sample, the combustion was performed carrier-free with less than 2 ng of total mercury added from a high specific activity tracer solution (20 Ci/g Hg). The wash solutions from the condensers were counted on a 3 × 3-in. NaI detector and the yield determined by comparison with the initial tracer counted in a similar volume of water.

After yield determination, the mercury content of the samples was measured by the cold vapor procedure described by Perkin-Elmer. Since the acid wash solution was designed to Perkin-Elmer specifications, initial acidification steps in the technique were omitted.

Results and discussion

The results of analyses of 1-g aliquots of NBS Bovine Liver and of 300-mg aliquots of three other NBS SRM's with certified values for mercury are shown in Table 1. These particular materials also cover the range of sample types collected for environmental studies at Los Alamos. Excellent agreement

TABLE 1

Mercury concentrations of NBS SRM's

SRM	Type	Hg concentration (p.p.b.)		
		Found	$\bar{x} \pm s$	NBS certified values
1571	Orchard Leaves	147		
		167	158 ± 10	155 ± 15[a]
		160		
1577	Bovine Liver	16		
		15	16 ± 2	16 ± 2[a]
		18		
1632	Coal	120		
		113	111 ± 10	120 ± 20
		100		
1633	Coal Fly Ash	140		
		153	141 ± 12	140 ± 10
		130		

[a]Provisional certificate.

with the certified value was obtained for all the SRM's with precisions of about ±10%. The results for the fly ash analysis particularly demonstrate the utility of this combustion procedure for the determination of mercury in silicate matrices. The detection limit estimated for the present experimental conditions is 10 ng of mercury.

The ^{203}Hg tracer studies showed the need to employ a tracer with each carrier-free combustion to obtain the greatest accuracy. For coal and fly ash, recoveries were 96 ± 2%, while the results for tissue and vegetation were more erratic. Recoveries of 70%, 95% and 109% were obtained for the Orchard Leaves while 61%, 85% and 100% were observed for the Bovine Liver. Rook et al. [5] achieved uniformly high recoveries for these biological materials when mercury carrier was used with their neutron activated samples It is thought that incompletely burned products from the biological samples interfere with the acid leaching of the mercury from the cold trap at low mercury concentrations and the carrier-free procedure described here should not be used for these materials without a tracer-based yield determination on each sample. The results for the biological SRM's show that this is an effective means for correcting for mercury loss in the condenser.

An outstanding advantage of this combustion system is the ability to analyze for mercury in almost any non-explosive matrix which is small enough to fit in the quartz tube. Such diverse matrices as single mouse organs, skulls, hides, gastrointestinal tract contents, as well as more conventional vegetation and soil samples can be successfully analyzed by this technique. Furthermore, although less sensitive than some neutron activation procedures [5], this combustion/atomic absorption system employs instruments and techniques that are more widely available than high flux reactors and involves considerably less personnel hazard from radiation exposure.

This work was performed under the auspices of the U.S. Energy Research and Development Administration.

REFERENCES

1 See, e.g., A. M. Ure, Anal. Chim. Acta, 76 (1975) 1.
2 P. E. Trujillo and E. E. Campbell, Anal. Chem., 47 (1975) 1629.
3 J. M. Rottschäfer, J. D. Jones and H. B. Mark, Environ. Sci. Technol., 5 (1971) 336.
4 J. T. Tanner, M. H. Friedman, D. N. Lincoln, L. A. Ford and M. Jaffee, Science, 177 (1972) 1102.
5 H. L. Rook, T. E. Gills and P. D. LaFleur, Anal. Chem., 44 (1972) 1114.
6 N. A. Smart and A. R. C. Hill, Analyst (London), 94 (1969) 143.
7 E. L. Kothay, Analyst (London), 94 (1969) 198.
8 S. L. Law, Science, 174 (1971) 285.
9 P. D. LaFleur, Anal. Chem., 45 (1973) 1534.
10 R. Litman, H. L. Finston and E. T. Williams, Anal. Chem., 47 (1975) 2365.

nalytica Chimica Acta, 90 (1977) 275—278
Elsevier Scientific Publishing Company, Amsterdam — Printed in The Netherlands

hort Communication

HE DETERMINATION OF CADMIUM, COPPER AND LEAD IN LUDGES BY MICROSAMPLING CUP ATOMIC ABSORPTION PECTROMETRY IN A NITROUS OXIDE—ACETYLENE FLAME

OUGLAS G. MITCHELL, WAYNE N. MILLS, ARTHUR F. WARD* and K. M. ALDOUS

ivision of Laboratories and Research, New York State Department of Health, Albany, lew York 12201 (U.S.A.)

Received 28th June 1976)

The use of a microsampling cup technique with a nitrous oxide—acetylene lame has been reported [1—3]. The technique has several important dvantages compared with other micro atomic absorption procedures such as graphite furnace atomization: (a) the cup is an efficient container for sample preparation, e.g. dry ashing and wet digestion; (b) the technique is relatively interference-free, at least for determining Ag, Cd, Cu, Pb and Zn [2]; (c) spectrometric measurement takes only about 15 s.

As a further application of this technique, the determination of Cd, Cu and Pb in sewage sludge was studied. This analytical problem was chosen so that the microsampling cup approach could be evaluated with a "difficult" matrix. Moreover, toxic metal contamination of sewage sludge is an important environmental problem, and present methods are slow and inefficient. Typically, samples are digested with various acid mixtures [4—6], followed by flame atomic absorption spectrometry. The digestion step is slow and the acids and digestion vessel are potential sources of contamination.

The method described here is simple and rapid. Sewage sludge samples are thoroughly mixed by ultrasonic treatment, diluted as necessary and pipetted into microsampling cups. Samples are dried at 105°C for 10 min and injected into a nitrous oxide—acetylene flame.

Experimental

Instrumentation and equipment. The microsampling cup system has been described [3]. Basically, molybdenum cups are injected into a position about 1 mm below the entrance hole of a silicon carbide absorption tube. A nitrous oxide—acetylene flame, burning at the 0.38 × 57 mm slot of a specially designed "safe" burner, heats the cup and absorption tube. The sample is volatilized into the tube and atomized, and an absorption signal is obtained by measuring the fraction of resonance radiation absorbed as it

*Present address: Jarrell-Ash Division, Fisher Scientific, Waltham, Massachusetts.

passes through the tube. Hot molybdenum cups are protected from aerial oxidation by withdrawing them from the flame into a sheath tube supplied with nitrogen. Measurements were carried out using either a Model AA5 (Varian-Techtron, Palo Alto, California) or a Model 151 (Instrumentation Laboratory, Lexington, Mass.) atomic absorption spectrometer. In both cases, absorption signals were displayed on a strip-chart recorder (Omniscribe, Houston Instrument, Bellaire, Texas), and peak absorbances were measured from the recorder tracing.

Eppendorf pipettes were used to measure 100-μl aliquots of sample and standard solutions.

A Model C 1000 Sonoverter (Insonator, Ultrasonic Systems Inc., Farmingdale, New York) with a 3-mm tip was used to treat the sludge samples before analysis.

Reagents. Aqueous standards were prepared daily from stock solutions (500 mg l^{-1}) of lead (as lead nitrate), cadmium (as cadmium nitrate) and copper (as copper(II) nitrate) respectively, prepared from analytical reagent-grade salts.

Sample treatment. Sludge samples collected from various sewage plants in New York State were mixed by ultrasonic treatment for 60 s at 50 W to ensure a homogeneous mixture. The mixed sludge (10 g) was diluted with deionized water as necessary (usually 1 + 99). Aliquots (100 μl) were pipetted into cups, dried at 105°C for 10 min and analyzed. The aqueous standards were in the range 0—250 μg l^{-1} for Pb and Cu, and 0—25 μg l^{-1} for Cd. These samples were also analyzed by the method of standard additions, with 0, 0.25, 0.5 and 0.75 ng added Cd and 0, 2.5, 5.0 and 12.5 ng added Pb and Cu.

Results

Detection limits (defined as the weight of analyte which can be determined in aqueous solution with a relative standard deviation of 50%), linear ranges and precision data are given in Table 1. The linear concentration ranges are for a 100-μl sample and can be readily extended a further order of magnitude by varying the sample volume from 20 to 200 μl.

TABLE 1

Detection limit, linearity and precision data

Metal	Wavelength (nm)	Spectral band-pass (nm)	Linear range μg l^{-1}	Detection limit (ng)	s_r (%)[a]
Cd	228.8	0.33	0—25	0.02	7.3
Cu	324.7	0.17	0—250	0.2	3.5
Pb	283.3	0.33	0—250	0.2	2.5

[a] Relative standard deviation for 12 replicate measurements of aqueous solutions giving a peak absorbance of ca. 0.075.

Thirteen samples were analyzed by both standardization procedures; the results are shown in Table 2. A Student "*t*" test showed no significant difference between the results obtained by the two standardization procedures:

	Equations	*t-values*
Cd	AQ = 0.934 SA + 0.3	1.99
Cu	AQ = 1.062 SA − 45	0.72
Pb	AQ = 0.958 SA + 3.5	1.03

where AQ is the predicted concentration with aqueous standards ($\mu g\ g^{-1}$ solid) and SA is the predicted concentration with standard additions.

Several samples were analyzed by conventional atomic absorption spectrometry after digestion with nitric acid. This procedure yielded an average of 17% lower results for all metals.

Discussion

The microsampling cup procedure is exceedingly rapid and yields the same results whether aqueous standards or standard additions are used for calibration. There is no evidence that total metal levels are determined, but the results are higher than those obtained by a nitric acid digestion procedure. The major application for this procedure is a rapid (and possibly semi-quantitative) method for monitoring sludge. For this purpose, it is probably not essential to obtain accurate metal levels, particularly since

TABLE 2

Comparison of results obtained by the aqueous standard (Aq.) and standard addition (S.a.) methods for Cd, Cu and Pb in sludges (Results are given as $\mu g\ g^{-1}$ of solids.)

Sample	Solids present (%)	Cadmium		Copper		Lead	
		S.a.	Aq.	S.a.	Aq.	S.a.	Aq.
1	1.01	28.2	24.9	1740	1800	150	130
2	8.09	16.8	16.4	3420	3650	240	210
3	13.8	7	7	440	410	10	10
4	1.6	14.2	12.9	840	900	110	100
5	1.20	35.8	35.2	830	760	60	60
6	1.47	8	8	1420	1270	180	170
7	0.81	<8[a]	<8	1250	1270	150	180
8	3.20	5	6	330	300	300	290
9	1.42	6	6	290	350	410	390
10	0.92	<9[a]	<9	280	270	230	230
11	0.46	15	14	870	930	130	130
12	3.26	7	6	380	390	270	260
13	4.47	9.4	8.1	490	510	260	280

[a]Minimum reportable concentrations changed slightly from sample to sample because of variations in sample dilution and day-to-day instrumental variations.

there may be large sampling errors. Simple analytical technique and speed of analysis are more important.

The authors gratefully acknowledge financial support from NIH Research Grant Number 5 R01 GM 20431-02, awarded by the Institute of General Medical Sciences, PHS/DHEW.

REFERENCES

1 D. G. Mitchell, A. F. Ward and M. Kahl, Anal. Chim. Acta, 76 (1975) 456.
2 A. F. Ward, D. G. Mitchell and K. M. Aldous, Anal. Chem., 47 (1975) 1656.
3 M. Kahl, D. G. Mitchell, G. I. Kaufman and K. M. Aldous, Anal. Chim. Acta, 87 (1976) 215.
4 H. E. Babbitt and E. R. Baumann, Sewerage and Sewage Treatment, J. Wiley, New York 1958.
5 Department of the Environment, Analysis of Raw, Potable and Waste Waters, H.M.S.O., London, 1972.
6 B. G. Oliver and H. Ayemian, Environment Canada Scientific Series 37, Further Studies on the Heavy Metal Levels in Ottawa and Rideau River Sediments; Inland Waters Directorate, Ottawa (1974).

nalytica Chimica Acta, 90 (1977) 279—282
Elsevier Scientific Publishing Company, Amsterdam — Printed in The Netherlands

hort Communication

TOMIC ABSORPTION SPECTROMETRIC DETERMINATION OF METALS N PARTICULATE MATTER IN AIR BY THE DIRECT ATOMIZATION ECHNIQUE

. THOMASSEN and R. SOLBERG
epartment of Chemistry, University of Oslo, Oslo 3 (Norway)
nd
. E. HANSSEN
orwegian Institute for Air Research, 2001 Lillestrøm (Norway)
Received 13th October 1976)

Direct atomization of metals in air particulates collected on sampling ilters has received attention [1—6]; in these methods the sample is completely vaporized and only one element per sample can be determined. Most f these methods were developed for and applied to the determination of ietals in air by a rapid low-volume sampling procedure.

A direct atomization method, described for the determination of trace lements in pulp and paper [7], is now applied to the determination of metals ı air particulates collected on paper filters.

xperimental

Apparatus. A Perkin-Elmer Model 303 atomic absorption spectrophotoıeter, with a high-frequency induction-heated graphite furnace [8], deuterım background corrector, and two-channel recorder, was used for the direct tomization of the filters. One of the channels recorded % absorption; the ther transformed the signals to absorbances and gave the integrated peak reas.

A Perkin-Elmer Model 300 atomic absorption spectrophotometer, with a IGA-72 graphite furnace, deuterium background corrector, and single-hannel recorder, was used to determine samples brought into solution. Small ample aliquots were dispensed into the graphite tube by Oxford micropipettes. erkin-Elmer hollow-cathode lamps, and an electrodeless discharge lamp for admium, were used.

Trace metals in the NBS-standard filter were determined with a Perkin-lmer 403 atomic absorption spectrophotometer by the conventional flame echnique.

Air sampling equipment. Atmospheric particulates were collected on 37-mm iameter Whatman No. 40 ash-free cellulose filter paper. The diameter of the

exposed filter area was 25 mm. The air intake was connected via a manifold to 8 filter holders made from high-density polyethylene. The filter holders were designed to give a homogeneous deposition of particles over the exposed filter area. Each filter holder was connected to a simple membrane pump (aquarium pump), calibrated with a rotameter at the start and end of the sampling period. The flow rate of the pumps was about 150 l h^{-1}.

Reagents and standard solutions. The nitric acid was reagent grade (E. Merck). The graphite furnaces were purged with argon of purity 99.9% (by volume). Deionized distilled water was used.

Primary standard solutions (1000 p.p.m.) were prepared by dissolving high-purity metals in an excess of nitric acid and diluting to 1 l. Highly diluted secondary standard solutions were prepared daily; nitric acid was added to maintain pH $\leqslant$ 2.

Analysis by leaching. The filters (No. 1, 3, 5 and 7) were cut into pieces with scissors, transferred to polyethylene centrifuge tubes and leached at 80° C with 2.0 ml of nitric acid (1 + 1). After dilution to 10 ml with water the cellulose fibers were centrifuged. Blanks were prepared by treating unexposed filters by the same procedure. Aliquots (10—50 μl) of the samples were dispensed into the graphite tube and analyzed according to the manufacturer's standard programs, against dilute metal standards containing the same amount of nitric acid.

The accuracy of the acid leaching procedure was checked by analyzing the NBS SRM 2676, "Metals on Filter Media". The NBS filter A2 (a membrane filter), was completely decomposed by the present leaching procedure. The solution was analyzed by conventional a.a.s. against metal standards containing the same amount of nitric acid.

Direct analysis. From the filters (No. 2, 4, 6 and 8), 2.5 and 5.5-mm diameter disks were cut from various parts by punchpliers. The procedure for the direct determination is described elsewhere [8]. Standard solutions were added to the filter disks by 1-μl pipettes. The standard addition curves were drawn by averaging the values from duplicate measurements of filters without and with two additions of standard solution. The analytical signals were corrected for the blank signal given by the metal content in the filters. To reduce the blank level, the filters may be leached with dilute nitric acid and washed with distilled water before use.

The operating conditions for the spectrophotometers and graphite furnaces are listed in Table 1.

Results

The very rapid atomization of lead and cadmium permitted these metals to be determined by measuring peak heights; the broader peaks of copper and manganese required integration.

The distribution of the atmospheric particulates was checked by cutting and analyzing disks from different parts of the filter. The relative standard deviation for lead (9 determinations) was 4.6% (integration) and 6.2% (peak

TABLE 1

Operating conditions

Wavelength (nm)	Time(s)/Temperature (° C)					
	HGA-72			High-frequency furnace		
	Dry	Ash	Atomize	Dry	Ash	Atomize
Cd 228.8	30/100	30/350	15/1800	60/80	60/300	15/1600
Cu 327.4	30/100	30/900	15/2600	60/80	60/300	15/1900
Mn 279.5	30/100	30/1100	15/2600	60/80	60/300	15/1900
Pb 283.3	30/100	30/550	15/2040	60/80	60/300	15/1600
Zn 213.9	Determined in the flame					

heights); the particulates were therefore satisfactorily distributed. One disk (5.5 mm) from this filter contained about 10^{-8} g Pb.

The metals on the NBS standard filter A1 were not uniformly distributed, and therefore were not suitable as standards for the direct-atomization technique.

The analytical data from the analysis of NBS filter A2 and 8 sample filters are given in Tables 2 and 3, respectively. Direct atomization in the graphite furnace gives the total content of the metals on the filters; the other method gives the amount brought into solution by leaching with nitric acid.

The detection limits for cadmium, copper, manganese, and lead in air particulates are closely related to the blank value of the filters. The detection limits with unleached Whatman No. 40 filter paper (i.e. the concentration in the exposed filters equivalent to 3 times the concentration of the blank filters) are approximately 0.05 ng m^{-3} for cadmium, 1 ng m^{-3} for copper, 2 ng m^{-3} for manganese, and 20 ng m^{-3} for lead.

The proposed direct-atomization technique permits simple and rapid determinations of cadmium, copper, manganese, and lead in particulate matter collected on filters. The accuracy is satisfactory and the precision is considerably better than that of the leaching method; no reagents are added and small samples are required. The method should be applicable to the determination of a large number of metals on one sampling filter.

TABLE 2

Analytical data for NBS filter A2 (μg metal per filter)

Element	Leaching method	Certified value
Cd	2.1	2.48 ± 0.14
Mn	8.8	10.3 ± 1.5
Pb	27	29 ± 2.6
Zn	5.2	5.10 ± 0.26

TABLE 3

Results for cadmium, copper, manganese and lead in air (The samples were collected outside the laboratory building of the Norwegian Institute for Air Research at Kjeller)

Filter no.	Sampling volume (m^3)	Cadmium (ng m^{-3})		Copper (ng m^{-3})		Manganese (ng m^{-3})		Lead (ng m^{-3})	
		A[a]	B[b]	A	B	A	B	A	B
1	7.84		1.2		11		23		360
3	7.89		1.2		8		16		380
5	8.31		0.8		8		16		320
7	7.13		1.2		12		17		380
2	7.96	1.2		10		21		380	
4	8.08	1.3		10		20		380	
6	7.36	1.4		10		19		400	
8	7.48	1.1		9		19		370	
Mean value		1.3	1.1	10	10	20	18	383	360
s		0.13	0.20	0.50	2.1	0.96	3.4	13	28
s_r		10	18	5.1	21	4.9	19	3.3	7.9

[a] Direct atomization in the furnace.
[b] Atomization of the acid extract in the furnace.

REFERENCES

1 R. Woodriff and J. F. Lech, Anal. Chem., 44 (1972) 1323.
2 J. P. Matoušek and K. G. Brodie, Anal. Chem., 45 (1973) 1606.
3 J. F. Lech, D. D. Siemer and R. Woodriff, Spectrochim. Acta, Part B, 28 (1973) 435.
4 D. Siemer, J. F. Lech and R. Woodriff, Spectrochim. Acta, Part B, 28 (1973) 469.
5 D. D. Siemer and R. Woodriff, Spectrochim. Acta, Part B, 29 (1974) 269.
6 K. G. Brodie and J. P. Matoušek, Anal. Chim. Acta, 69 (1974) 200.
7 F. J. Langmyhr, Y. Thomassen and A. Massoumi, Anal. Chim. Acta, 68 (1974) 305.
8 F. J. Langmyhr and Y. Thomassen, Z. Anal. Chem., 264 (1973) 122.

Analytica Chimica Acta, 90 (1977) 283—287

Short Communication

DETERMINATION OF ALKALI METAL IN TETRAGONAL AND HEXAGONAL TUNGSTEN BRONZES

ALTAF HUSSAIN and LARS KIHLBORG

Department of Inorganic Chemistry, Arrhenius Laboratory, University of Stockholm, S-10405 Stockholm (Sweden)

(Received 27th September 1976)

The tungsten bronzes have the general formula M_xWO_3 (where M represents a relatively electropositive metal and $0 < x < 1$) and can be divided into the perovskite tungsten bronzes, PTB, tetragonal tungsten bronzes, TTB, and hexagonal tungsten bronzes, HTB. A fourth group, intergrowth tungsten bronzes, ITB, has recently been discovered [1]. The PTB phases are formed with Li and Na, TTB with Na and K, and HTB and ITB with K, Rb and Cs, in all cases within certain limits of x. During a systematic study of the K, Rb and Cs systems the alkali content was determined conveniently by atomic absorption spectrometry. The phase analysis will be published elsewhere.

The analysis of tungsten bronzes has offered certain problems in the past. These compounds are chemically inert and cannot be dissolved without first being oxidized. Spitzin and Kaschatnoff [2] analyzed sodium tungsten bronzes after oxidation in oxygen at 550°C; Magnéli [3] found this method convenient for bronzes rich in alkali but slow for sodium TTB and described another method in which the bronzes were oxidized in a melt of ammonium peroxydisulphate. Van Duyn [4] analyzed for sodium gravimetrically after oxidizing the bronze with mercury(II) oxide and heating the product in a stream of chlorine and sulfur chloride. Raby and Banks [5] decomposed the samples with bromine trifluoride and separated all three constituents in a specially designed vacuum system. Wechter and Voigt [6] determined K, Rb and Ba in tungsten bronzes by neutron or high-energy photon activation analysis. These methods [4—6] are rather complicated and laborious. In contrast, atomic absorption spectrometry is rapid and sensitive with a small risk of interference, so that the most convenient way of oxidation and dissolution of the samples can be used.

Preparation

The tungsten bronzes were synthesized from mixtures of the appropriate amounts of tungsten trioxide (prepared by dehydration of tungstic acid, Merck, puriss.), tungsten dioxide (prepared from WO_3 by reduction with H_2/H_2O mixture) and alkali metal tungstate. Rb_2WO_4 and Cs_2WO_4 were

made from WO_3 and Rb_2CO_3 (BDH, reagent grade) or Cs_2CO_3 (Merck, reagent grade) by heating the appropriate amounts in a platinum crucible at 950°C for 5—6 h. K_2WO_4 was commercially available (BDH, reagent grade). The intimate mixtures were heated in sealed, evacuated silica tubes at 700—950°C for various periods of time. The phases formed were identified from x-ray powder patterns (Guinier-Hägg focusing camera).

The bronzes were purified from silica or unreacted material by successive treatment with boiling aqueous solutions of HF (40%) and 12 M HCl and NaOH (5%), with thorough washing with water after each step, and finally with ethanol.

Procedure

About 15 mg of finely powdered tungsten bronze was accurately weighed in a thoroughly cleaned, clear silica tube (length 7 cm, diam 4 mm) closed at one end. The tube was placed in a muffle furnace at 550—600°C for about 10 h. A known volume (1—2 ml) of 1 M NaOH was added and the tungstate was dissolved by heating for about 1 h on a water bath. The clear solutions obtained were diluted to concentrations within the optimum range (Table 1).

A Varian Techtron AA-5 atomic absorption spectrophotometer was used with an air—propane flame and the instrumental parameters given in Table 1. The photomultiplier used initially, for most potassium and rubidium analyses, was type R-213 (Hamamatsu TV Co. Ltd.). For cesium a detector with higher response in the long wavelength range (type R-466) was used.

Standard solutions made by dissolving known amounts of tungstate in 1 M NaOH (Merck, p.a.), were stored in polyethylene bottles after dilution. As a check they were standardized against solutions of the corresponding metal chloride. The observed result was always in very good agreement with the calculated composition.

Possible sources of error

The composition of the bronze may change during the purification treatment. Remeika et al. [7] found that the superconducting transition temperature is considerably higher for K— and Rb—HTB treated with hot acids than for the unetched powder. They explained this as the result of

TABLE 1

Instrumental parameters used in the analyses

Element	Wavelength (nm)	Spectral band pass (nm)	Lamp current (mA)	Optimum working range ($mg\ l^{-1}$)
K	766.5	1.0	5	0.6—1.5
Rb	780.0	0.2	15	2.0—5.0
Cs	852.1	0.4	20	15.0—35.0

reduction in the alkali concentration and mentioned that this had been confirmed by chemical and x-ray fluorescence analysis, but gave no data. To check this, one sample of each of K—HTB and K—TTB was analyzed before and after purification. The unpurified samples were examined very carefully by microscope to ensure that they did not contain extraneous material. The results (Table 2) show no significant difference in the alkali content. Electron microprobe analysis of purified and unpurified Rb—ITB previously gave the same result [1]. Our acid-alkali treatment therefore does not alter the composition significantly.

A part of the sample may volatilize during the oxidation. This was checked by careful weighing of some samples during oxidation or prolonged heat treatment. No weight loss occurred below 850°C; the temperature required for complete oxidation is at least 200°C lower.

The sodium from the hydroxide solution may influence the absorbance. Blanks with NaOH solutions of different concentrations were run with all the different lamps to investigate this possibility. Only with potassium was there an increase in absorbance with increasing NaOH concentration. This could be traced to the presence of potassium as an impurity in the sodium hydroxide used: with the highest grade NaOH (Merck, p.a., $K < 2.0 \cdot 10^{-4}\%$), no interference could be detected. Measurements were also made with a fixed concentration of the alkali to be determined and different sodium hydroxide concentrations. The results showed that the absorbance recorded is independent of the hydroxide concentration within the range 0.002—0.1 M. For K and Rb, the absorbance with no hydroxide was slightly lower than with a concentration of 0.002 M or higher. All analyses were made with a concentration above that value.

TABLE 2

Alkali metal content of a number of tungsten bronzes, M_xWO_3

Bronzes	Gross content[a] x	Mean x found[b]	n[b]	s[b]	Bronzes	Gross content[a] x	Mean x found[b]	n[b]	s[b]
K—HTB	0.20	0.197	4	0.010	Rb—HTB	0.17	0.192	3	0.006
	0.30	0.283	5	0.013		0.30	0.287	2	0.011
	0.32	0.317	4	0.010		0.32	0.302	1	—
	0.32[c]	0.308	1	—		0.36	0.321	5	0.015
	0.35	0.341	3	0.011		0.40	0.336	2	0.024
						0.60	0.313	1	—
K—TTB	0.45	0.424	3	0.009					
	0.45[c]	0.428	3	0.007	Cs—HTB	0.13	0.148	5	0.003
	0.50	0.435	2	0.006		0.30	0.276	4	0.012
	0.60	0.464	3	0.010		0.40	0.319	1	—
	0.80	0.481	2	0.013		0.60	0.344	3	0.010

[a]Gross content of alkali metal in the preparation.
[b]Mean value with standard deviation (s) and number of determinations (n).
[c]Same preparation as preceding but unpurified.

The tungsten present in the solution may interfere. The tungsten concentration was varied in K and Cs samples with fixed alkali metal content and had no measurable effect on the absorbance in the range 0—40 mg W l^{-1}.

Results

Calibration graphs prepared from measurements on solutions of tungstate in 0.003 M NaOH are shown in Fig. 1. The concentration ranges normally use are given in Table 1.

The results obtained for representative samples of different bronzes are given in Table 2. Since the samples were prepared in a closed system their compositions should generally be those of the starting mixtures. Only if the products contained phases which were wholly or partly removed in the purification process could the alkali metal content be expected to deviate significantly from the initial value.

Table 2 shows that the differences between the initial values and the results are in most cases within the standard deviation. The discrepancy for bronzes with low alkali content may be explained by the loss of unreacted WO_3 removed during the purification. The maximum alkali contents found in Rb— and Cs—HTB are x = 0.336 and 0.344, respectively. The results fit well with the theoretical upper limit x = 1/3 for HTB [8]. Rubidium and cesium do not form a TTB phase; the excess of alkali in samples with a higher initial value probably formed tungstate which was removed during purification.

In K—TTB the maximum potassium content observed was x = 0.481 although the theoretical limit for the TTB structure is x = 0.60 [9]. Magnéli found x-values as high as 0.57 but only in samples prepared differently from ours, namely by reduction of polytungstates in a stream of hydrogen.

The above method has also been used for the analysis of ITB phases and potassium polytungstates. The oxidation of ITB bronzes requires a slightly

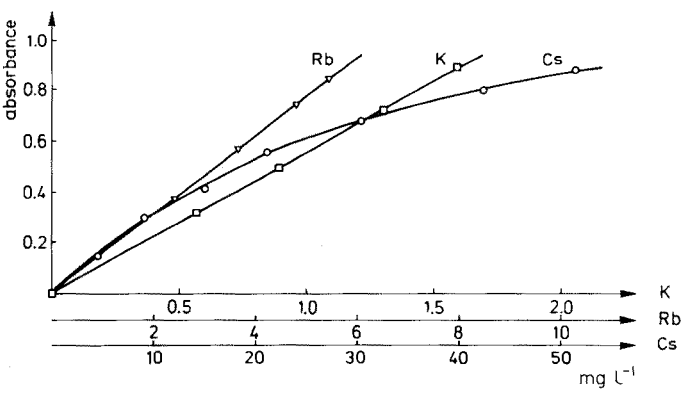

Fig. 1. Typical calibration curves.

higher temperature (650°C) to go to completion within a reasonable time, and the dissolution in hydroxide is often slower in these two cases. Apart from this there are no differences.

There should be no difficulty in applying this method to Li– and Na–tungsten bronzes (in the latter case with NaOH replaced by KOH) but these bronzes were not included in the present investigation.

This study forms a part of a research program supported by the Swedish Natural Science Research Council.

REFERENCES

1 A. Hussain and L. Kihlborg, Acta Crystallogr., Sect. A, 32 (1976) 551.
2 V. Spitzin and L. Kaschatnoff, Z. Anal. Chem., 75 (1928) 440.
3 A. Magnéli, Ark. Kemi, 1 (1949) 273.
4 D. Van Duyn, Rec. Trav. Chim. Pays-Bas, 61 (1942) 669.
5 B. A. Raby and C. V. Banks, Anal. Chem., 36 (1964) 1106.
6 M. A. Wechter and A. F. Voigt, Anal. Chem., 38 (1966) 1681.
7 J. P. Remeika, T. H. Geballe, B. T. Matthias, A. S. Cooper, G. W. Hull and E. M. Kelly, Phys. Lett. A, 24 (1967) 565.
8 A. Magnéli, Acta Chem. Scand., 7 (1953) 315.
9 A. Magnéli, Ark. Kemi, 1 (1949) 213.

Analytica Chimica Acta, 90 (1977) 289—293

Short Communication

ÉTUDE SPECTROSCOPIQUE PAR RMN PROTONIQUE DES COMPLEXES DE PHOSPHOROTRIAMIDES AVEC DES HALOGÉNOALCANES

J. P. MEILLE et J. C. MERLIN

Laboratoire de Chimie Analytique I, Université de Lyon I, U.E.R. de Chimie-Biochimie, 43 boulevard du 11 Novembre 1918, 69621 Villeurbanne (France)

(Reçu le 21 juillet 1976)

L'étude des complexes où intervient une liaison hydrogène fait souvent appel à la spectroscopie r.m.n. du proton car le signal du proton engagé dans une telle liaison est déplacé vers les champs faibles [1—4].

Un grand nombre de travaux porte sur des autoassociations telles que celles des alcools, des phénols, des amines [5—7]. Dans le cadre d'une étude des propriétés des phosphorotriamides [8—10], nous avons été amenés à comparer leur pouvoir donneur d'électrons par rapport à un accepteur-type. Il est d'usage dans ce cas d'utiliser le chloroforme dont l'autoassociation est faible. Cette autoassociation est d'autant plus négligeable que le chloroforme est plus dilué dans un solvant "inerte".

Les phosphorotriamides étudiées possèdent un des trois groupements suivants: $N_3P = O$, $N_3P = S$, N_3P. Nous utilisons, comme accepteur d'électrons, le chloroforme et quelques autres halogénoalcanes. L'évaluation des paramètres des complexes donneur—accepteur, dans un solvant, permet de comparer le pouvoir donneur d'électrons des phosphorotriamides d'une manière plus aisée que celle du déplacement chimique du proton du chloroforme à dilution infinie dans le produit pur [11].

Partie experimentale

Les phosphoramides. La tris(diméthylamino)phosphine ($[(CH_3)_2N]_3P$, (I), ou "hexamétapil") est obtenue [12] selon la réaction

$$3\,(CH_3)_2NH + PCl_3 \rightarrow [(CH_3)_2N]_3P + 3\,HCl$$

Elle est purifée par distillation sous pression réduite (E = + 36 °C sous 2 torr).

La purification du l'oxyde de tris(diméthylamino)phosphine ($[(CH_3)_2N]_3PO$, (II) ou "hexamétapol") est faite par distillation à partir du produit commercial de la Société Pierrefitte [13].

Le sulfure de tris(diméthylamino)phosphine ($[(CH_3)_2N]_3PS$ ou "thiopol") provient de l'addition du soufre sur I. Il est purifié par cristallisation fractionnée [9].

La pureté de ces produits a été controlée par chromatographie sur couches minces [9, 14], chromatographie en phase gazeuse, et par les constantes physiques. Les halogénoalcanes utilisés sont des produits Fluka "pour analyses" distillés sous azote. Les solvants "pour spectroscopie" ont été redistillés avant l'emploi. Le solvant le plus couramment utilisé a été le cyclohexane.

Les mesures du déplacement chimique sont effectuées avec un appareil Varian A60 à 60 MHz; quelques mesures ont été effectuées avec un appareil Varian HR100 à 100 MHz, dans le sulfure de carbone comme solvant. Les températures de la sonde étaient contrôlées à ± 0,2 °C. Les solutions sont préparées par pesée. Le signal du proton du chloroforme complexé est repéré par rapport à la raie du cyclohexane qui joue le rôle de référence interne. Dans les solvants autres que le cyclohexane, la référence interne est constituée d'une très faible quantité de TMS (tétraméthylsilane) ajoutée ou d'une très faible quantité de cyclohexane (de l'ordre de 1 %).

Mode de calcul des parametres des complexes a partir du deplacement chimique et domaines de validite correspondants

Dans un milieu contenant un donneur d'électrons D et un accepteur A, dans le cas où il ne se forme que le complexe 1:1 c'est à dire AD, on aura l'équilibre: $A + D \rightleftarrows AD$, auquel correspond la constante $K_{AD} = a_{AD}/a_A \cdot a_D$, a_{AD}, a_A et a_D étant respectivement, les activités à l'équilibre de AD, A et D.

Nous verrons qu'un modèle aussi simple est généralement suffisant pour la description des solutions diluées dans lesquelles le donneur est en excès par rapport à l'accepteur. Les complexes supérieurs A_2D, ... A_nD n'interviennent pratiquement pas dans ces conditions.

Les méthodes couramment utilisées pour déterminer K_{AD} par r.m.n. sont de deux types.

Les méthodes graphiques. Nous n'avons pas utilisé de méthodes du type Benesi—Hildebrand [1, 15], car elles supposent $[D_0] \gg [A_0]$, ce qui n'est pas toujours réalisable et, souvent, ne permet pas de décrire une gamme importante de fraction complexée.

Nous avons par contre utilisé la méthode de Nakano et al. [16], qui est résumée par la formule suivante

$$\frac{[D_0]}{\Delta\omega} = \frac{1}{\Delta\omega_0}([A_0] + [D_0] - [AD]) + \frac{1}{K_{AD}.\Delta\omega_0}$$

$\Delta\omega$ est la variation du déplacement chimique du chloroforme entre une solution de chloroforme pur et la même solution contenant, en plus, le donneur à la concentration $[D_0]$. $\Delta\omega_0$ correspond à la variation du déplacement chimique du chloroforme dans le cas d'une solution qui contiendrait le complexe AD à l'état pur. Cette valeur n'est évidemment pas mesurable directement.

On portera donc $[D_0]/\Delta\omega$ en fonction de $[A_0] + [D_0]$, ce qui va permettre de tracer une nouvelle droite

$$\frac{D_0}{\Delta\omega} = f([A_0] + [D_0] - [AD])$$

et ainsi de suite jusqu'à convergence des valeurs de K_{AD} et de $\Delta\omega_0$.

Les méthodes de calcul directes. Basées en particulier, sur la méthode des moindres carrés itérative [17], nous avons utilisé un programme de calcul automatique de ce type, directement dérivé de celui d'Olier [18]. Il est bon d'avoir initialement des valeurs approchées de K_{AD} et de $\Delta\omega_0$, d'où l'intérêt de la méthode de Nakano et al. [16]. (Les facteurs d'activité sont considérés comme suffisamment proches de l'unité pour que l'on puisse assimiler concentration et activité. Nous nous sommes donc maintenus en milieu assez dilué.)

Resultats et Discussion

Le tableau 1 résume nos résultats.

Le système tributylphosphate—chloroforme a été étudié à titre de comparaison. Nos résultats sont en accord avec ceux de Nishimura et al. [19] obtenus également par r.m.n., et ceux d'Olier pour les valeurs de K_{AD} obtenus par calorimétrie [18].

TABLEAU 1

Valeurs des variations de déplacement chimique du chloroforme par complexation pour les différentes systèmes etudiés

Donneur	Accepteur	Solvant	θ °C	$\Delta\omega_0$ (ppm)	K_{AD} (l mol^{-1})	$\Delta H°$ (J m
HMPT	$CHCl_3$	C_6H_{12}	39	2,01 ± 0,03	18,5 ± 2,1	16 700
			31		22,0 ± 2,0	
			25		25,8 ± 2,0	
			15		31,0 ± 2,0	
		CCl_4	39	2,06 ± 0,03	2,4 ± 0,2	
		CS_2	31	2,05 ± 0,03	6,6 ± 0,6	14 600
			0		10,5 ± 1,1	
			−25		19,9 ± 1,5	
			−40		28,1 ± 1,7	
	CH_2Cl_2	C_6H_{12}	39	1,30 ± 0,04	6.4 ± 0,8	
	$CHBr_3$	C_6H_{12}	39	2,00 ± 0,04	8,7 ± 0,7	
	$CHCl=CCl_2$	C_6H_{12}	39	2,13 ± 0,04	0,9 ± 0,1	
	$CHCl_2=CHCl_2$	C_6H_{12}	39	2,65 ± 0,03	3,4 ± 0,6	
	CHI_3	CS_2	31	0,65 ± 0,06	6,1 ± 0,8	
Thiopol	$CHCl_3$	C_6H_{12}	31	1,55 ± 0,03	1,2 ± 0,1	12 000
			25		1,35 ± 0,1	
			20		1,5 ± 0,1	
			10		1,8 ± 0,1	
			5		2,0 ± 0,1	
Hexametapil	$CHCl_3$	C_6H_{12}	39	0,92 ± 0,05	2,1 ± 0,7	
TBP	$CHCl_3$	C_6H_{12}	39	1,43 ± 0,04	3,1 ± 0,6	
	$CH_2Cl—CH_2Cl$	C_6H_{12}	39		1,8 ± 0,1	

Quant au tris(diméthylamino)phosphine et dérivés, les systèmes étudiés par d'autres auteurs concernent le HMPT et le thiopol. Les systèmes HMPT + $CHCl_3$ et thiopol + $CHCl_3$ ont été étudiés par r.m.n. [20] pour le premier, et par calorimétrie [18] pour les deux systèmes; si nos résultats sont en bon accord avec ceux d'Olier [18] il n'en est pas de même pour ceux de Gramstad et Mundheim [20].

Celui-ci utilise des concentrations en $CHCl_3$ plus élevées que les nôtres, ce qui peut expliquer ces divergences. Dans notre cas $[CHCl_3]_0$ est généralement de 10^{-2} M alors que cette concentration est proche de 10^{-1} M dans les études de Gramstad et Mundheim [20].

L'ordre de stabilité décroissante des complexes obtenus avec les halogénoalcanes étudiés et le HMPT, qui est le plus fort donneur examiné, est le suivant: $CHCl_3 > CHBr_3 > CHCl_2{-}CHCl_2 > CH_2Cl_2 > CHCl{=}CCl_2$. Il faut remarquer que, dans les domaines de concentration utilisés, il n'a pas été nécessaire d'envisager l'existence d'espèces trimoléculaires AD_2 pour rendre compte des valeurs des déplacements chimiques observés, même lorsqu'il s'agit d'halogénoalcanes tels que $CHCl_2{-}CHCl_2$ ou CH_2Cl_2 qui possèdent plusieurs protons engageables dans une liaison hydrogène. Dans ce cas, les mesures effectuées sur de tels dérivés représentent un effet moyen.

En prenant le chloroforme comme accepteur commun, l'ordre de stabilité décroissante des complexes (organophosphorés étudiés—chloroforme) est le suivant: HMPT > TBP > hexamétapil > thiopol.

La valeur de K_{AD} du complexe hexamétapil—chloroforme est très faible comparée à celle du complexe HMPT + $CHCl_3$. L'hexamétapil donne des complexes cationiques souvent beaucoup plus stables que les solvants de l'HMPT et du thiopol, en particulier avec Co^{2+}, Ag^+, etc... Un tel phénomène prouve, seulement, s'il en était besoin, que la solvatation des cations par de telles molécules polaires non protiques met en jeu des mécanismes très différents de ceux correspondants à la formation d'une liaison hydrogène.

La précision obtenue sur les valeurs de K_{AD} dépend en grande partie de l'importance de $\Delta\omega_0$. Dans le cas du thiopol et du chloroforme ou du trichloréthylène, la valeur importante de $\Delta\omega_0$ permet d'obtenir une bonne estimation de K_{AD}, pourtant très faible, car les déplacements chimiques mesurés sont assez grands. Par contre la nécessité d'obtenir une fraction importante du donneur sous forme de complexe, nous oblige à travailler à des concentrations élevées. Dans ces conditions les activités peuvent être différentes des concentrations.

L'utilisation du sulfure de carbone ou du tétrachlorure de carbone comme solvant diminue considérablement les valeurs de K_{AD}, mais pas sensiblement celles de $\Delta\omega_0$. Ceci justifie, s'il en était encore besoin, l'utilisation du cyclohexane comme milieu dispersif. Par contre, l'usage de ce solvant limite considérablement la gamme de température utilisable, inconvénient important pour la détermination de l'enthalpie ΔH_0 de complexation, obtenue à partir des valeurs de K_{AD} à différentes températures. En effet les variations de K_{AD} entre 39 °C (température maximale utilisée) et +6 °C (température minimale) ne sont pas très importantes, eu égard aux incertitudes

sur les valeurs de K_{AD}. Il découle de ce fait qu'il est difficile d'apprécier la précision obtenue sur les valeurs de $\Delta H°$. A cet égard les résultats correspondant au sulfure de carbone doivent être plus représentatifs, car la gamme de température utilisée (31 °C à −40 °C) est beaucoup plus large.

Conclusion

La r.m.n. du proton nous a permis de mesurer, avec une précision raisonnable, les constantes de formation des complexes 1:1 concernant les tris-(diméthylamino)phosphines avec un certain nombre d'halogénoalcanes.

En dehors de la calorimétrie de mélange, toujours possible, mais exigeant un appareillage de très bonne qualité pour pouvoir obtenir des résultats fiables [18], seules les méthodes spectroscopiques, surtout l'absorption dans, l'infra-rouge auraient permis une telle étude. Dans notre cas la spectroscopie i.r. était d'un emploi difficile, eu égard à la complexité des spectres des aminophosphines étudiées.

De plus $\Delta\omega_0$ étant souvent assez important, il nous a été possible avec une assez bonne précision d'atteindre des constantes de valeurs très faibles. En effet la valeur de $\Delta\omega_0$ n'est pas reliée directement à celle de ΔH_0 mais dépend de paramètres moléculaires.

L'ordre décroissant des interactions entre le HMPT et $CHCl_3$, CH_2Cl_2 et CCl_4 est identique à celui obtenu si l'on mesure le coefficient de distribution du HMPT entre deux phases, l'une constituée par l'eau, et l'autre par l'un de ces halogénoalcanes [10].

BIBLIOGRAPHIE

1 R. Foster et C. A. Fyfe, dans Progress in Nuclear Magnetic Resonance Spectroscopy, Vol. 4, édités par J. W. Emsley, J. Feeney et L. H. Sutcliffe, Ch. 1, Pergamon Press, 1969.
2 J. C. Davis et K. K. Deb, dans Advances in Magnetic Resonance, Vol. 4, J. S. Warigh (Ed.), Academic Press, New York, 1970.
3 P. Lazlo, dans Progress in Nuclear Magnetic Resonance Spectroscopy, Vol. 3, Pergamon Press, Londres, 1968.
4 R. Foster, dans Organic Charge Transfer Complexes, Academic Press, New York, 1969, pp. 104—215.
5 B. Lemanceau, C. Lussan et N. Souty, J. Chim. Phys., 1961, 148.
6 G. Mavel, Le Journal de Physique et le Radium, 21 (1960) 228.
7 W. Drinkard et D. Kivelson, J. Phys. Chem., 62 (1968) 1494.
8 J. P. Meille et J. C. Merlin, C.R. Acad. Sc. Paris, 270 (1970) 2134.
9 J. P. Meille et A. Lamotte, C.R. Acad. Sc. Paris, 272 (1971) 198.
10 J. P. Meille et H. Thozet, (à paraître).
11 G. Martin et A. Bernard, C.R. Acad. Sc. Paris, 257 (1963) 2463.
12 C. Stuebe et H. P. Lankelma, J. Am. Chem. Soc., 78 (1956) 976.
13 J. Jose, C. Michou-Saucet, P. Clechet et C. Jambon, Thermochim. Acta, 4 (1972) 123.
14 H. Naghizadeh-Nouniaz, Thèse, Lyon, 1970.
15 H. A. Benesi et J. H. Hildebrand, J. Am. Chem. Soc., 71 (1949) 2703.
16 M. Nakano, M. I. Nakano et J. Higuchi, J. Phys. Chem., 71 (1967) 3954.
17 W. E. Wentwork, W. Hirsch et E. Chen, J. Phys. Chem., 71 (1967) 218.
18 R. Olier, Thèse, Lyon, 1973.
19 S. Nishimura, C. H. Ke et N. C. Li, J. Phys. Chem., 72 (1968) 1297.
20 T. Gramstad et O. Mundheim, Spectrochim. Acta, 28A (1972) 1405.

Analytica Chimica Acta, 90 (1977) 295—299

Short Communication

THE DISTRIBUTION AND DIMERIZATION OF BENZOIC ACID. ASSOCIATION WITH TRIOCTYLPHOSPHINE OXIDE IN CARBON TETRACHLORIDE

M. KONSTANTINOVA

Higher Institute of Chemical Technology, Sofia 1156 (Bulgaria)

St. MAREVA and N. JORDANOV

Institute of General and Inorganic Chemistry, Bulgarian Academy of Sciences, Sofia 1113 (Bulgaria)

(Received 22nd July 1976)

It has been shown that uranium(VI) can be extracted with high distribution coefficients with trioctylphosphine oxide (TOPO) in the presence of aromatic [1] and fatty [2] acids. Many experimental results, including the results of an i.r. spectroscopic study, show that organic acids interact with TOPO; its strongly polar PO group acts as a hydrogen bond acceptor while the carboxyl group of the acids is the hydrogen donor. In addition, the organic acids are self-associated to a greater extent in some of the organic diluents.

A quantitative interpretation of the extraction systems containing the two extractants — TOPO and an organic acid — is possible when the concentrations of the different forms of the extractants in the two phases are known. These concentrations can be calculated if the distribution constant of the monomer form of the acid, the dimerization constant of the acid and its association constant with TOPO are known.

The purpose of this work was to determine these constants for benzoic acid, whose synergic effect on the extraction of U(VI) has been established [1]. The data for the distribution of benzoic acid between aqueous phase and carbon tetrachloride in the presence and absence of TOPO were used.

Experimental

The reagents were purified as described earlier [1, 2]. Solutions of benzoic acid (from $2.5 \cdot 10^{-4}$ M to $1.6 \cdot 10^{-1}$ M) in carbon tetrachloride were prepared; equal volumes of these solutions and of 0.1 M $NaClO_4$ acidified with $HClO_4$ to pH 3) were shaken for 1 h at 25 ± 0.1 °C. The results of a few experiments indicated that under these conditions equilibrium was reached. In another series of experiments, the distribution of the benzoic acid between 0.1 M $NaClO_4$ (pH 3) and carbon tetrachloride solutions of TOPO was studied as a function of TOPO concentration. In both cases the benzoic acid was determined photometrically in an aliquot of the aqueous phase at 273 nm.

Since absorbance depends on the concentration of hydrogen ions, before measurement, the solutions were acidified with $HClO_4$ to pH 1. The determination of the benzoic acid for the whole range of the experimental concentrations was made with two calibration curves.

Results and discussion

The experimental data (Table 1) show that the distribution of benzoic acid depends on its total concentration. The distribution coefficient increases 30 times when the benzoic acid concentration rises from $2.5 \cdot 10^{-4}$ M to $1.6 \cdot 10^{-1}$ M.

Assuming that the undissociated form HA and the anion A are the benzoic acid species in the aqueous phase, whereas the monomer HA and the dimer H_2A_2 are the forms present in the organic phase, the concentrations of the benzoic acid in the two phases are as follows

$$C = [HA] + [A]$$
$$C_o = [HA]_o + 2[H_2A_2]_o$$

The distribution coefficient D can be written as

$$D = \frac{C_o}{C} = \frac{[HA]_o + 2[H_2A_2]_o}{[HA] + [A]}$$

If K_a, K_d and K_2 are defined by $K_a = [H][A]/[HA]$; $K_d = [HA]_o/[HA]$; $K_2 = [H_2A_2]_o/[HA]_o^2$, then:

$$D = 2K_2\left(\frac{K_d}{\rho}\right)^2 C + \frac{K_d}{\rho} \qquad (1)$$

where $\rho = 1 + K_a/[H] = 1 + 6.45 \cdot 10^{-2}$ is a constant in all measurements.

Equation (1) can be solved graphically by the curve fitting method of Dyrssen and Sillén [3—5].

In Fig. 1, log D is plotted against log C. The experimental points follow the normalized curve $\log y = \log(x+1)$ very well. From the horizontal asympto and according to eqn. (1), the value of K_d is obtained. When $x \to 0$, $\log D - \log (K_d/\rho) = 0$. The point of intersection of the asymptotes of the curve gives the equation $\log 2K_2K_d/\rho = -\log C$, from which K_2 is calculated. The values of K_d and K_2 determined in this way are $\log K_d = -0.57$ and $\log K_2 = 3.70$, respectively.

TABLE 1

Distribution coefficients of benzoic acid between 0.1 M $NaClO_4$ (pH 3) and carbon tetrachloride, as a function of its total concentration at 25 ± 0.1 °C

C_{tot}, M	$1.6 \cdot 10^{-1}$	$8.0 \cdot 10^{-2}$	$4.0 \cdot 10^{-2}$	$2.0 \cdot 10^{-2}$	$1.0 \cdot 10^{-2}$	$5.0 \cdot 10^{-3}$	$2.5 \cdot 10^{-3}$
D	10.57	7.00	4.73	3.42	2.19	1.47	1.05
C_{tot}, M	$1.0 \cdot 10^{-3}$	$5.0 \cdot 10^{-4}$	$2.5 \cdot 10^{-4}$				
D	0.59	0.48	0.37				

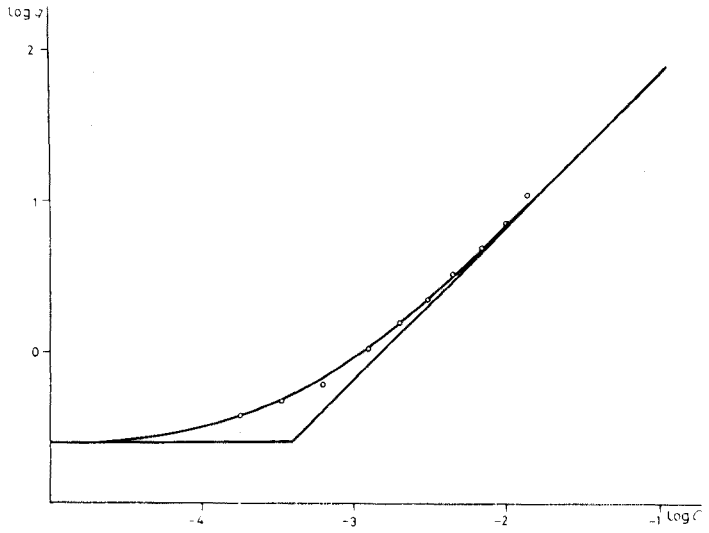

Fig. 1. Distribution of benzoic acid between carbon tetrachloride and 0.1 M $NaClO_4$ (pH 3) at 25 ± 0.1 °C as a function of the concentration of the acid in the aqueous phase. The normalized curve log y = log $(x + 1)$ is fitted to the data.

From the expression for the total concentration of the benzoic acid, $C_{tot} = C + C_o$, and from the definitions of K_a, K_d and K_2, the following equation is obtained

$$2K_2K_d^2[HA]^2 + (K_d + \rho)[HA] - C_{tot} = 0$$

where, inserting the values of the constants, [HA] can be calculated for each total concentration of the acid. Then, from the values obtained for [HA] and the expressions for K_a, K_d and K_2, the concentrations of all forms of the benzoic acid in the two phases, both aqueous and organic, can be calculated. Figure 2 shows the molar percentage of each form of the benzoic acid as a function of its total concentration.

The association constant of the benzoic acid with TOPO, which is not known from the literature, was found by studying the distribution of the acid between carbon tetrachloride and 0.1 M $NaClO_4$ (pH 3), as a function of TOPO concentration. The results (Table 2) show that the distribution coefficients of the benzoic acid rise when the concentration of TOPO increases. If the concentration of the acid is low enough for the formation of its dimeric form to be neglected, the following expression is valid: $D = ([HA]_o + [HAB]_o)/([HA] + [A])$, where $[HAB]_o$ is the concentration of the complex formed between the benzoic acid and TOPO (B symbolizes TOPO). The formation constant of this complex is: $K_B = [HAB]_o/[HA]_o[B]_o$. From the expressions for D and K_B the following equation can be derived

$$D = K_B \cdot K_d \cdot [B]_o \rho^{-1} \qquad (2)$$

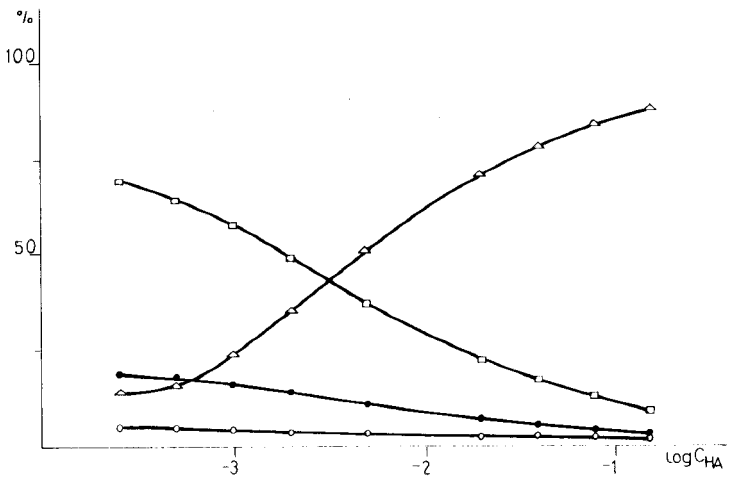

Fig. 2. The mole percentage of the different species of the benzoic acid in the two phase system — carbon tetrachloride, 0.1 M $NaClO_4$ (pH 3) at 25 ± 0.1 °C as a function of the total concentration of the acid.

Evidently, $D[B]_o^{-1}$ must be constant for each value of $[B]_o$. As the solubility of TOPO in water is negligible, and if $[HA]_o \ll [B]_o$, the total concentration of TOPO — C_B can be used instead of its equilibrium concentration $[B]_o$.

The results obtained at $5 \cdot 10^{-4}$ M benzoic acid, and the different concentrations of TOPO given in Table 2, confirm the validity of eqn. (2) and make possible the calculation of K_B. From the data in Table 2, $\log K_B = 3.78 \pm 0.01$.

Conclusions

Benzoic acid shows a pronounced tendency to dimerize in carbon tetrachloride. The value of K_2 obtained is in agreement with some of the data [6] available. From the values of K_d and K_2, the distribution coefficients of benzoic acid and the concentration of all its forms can be calculated for a wide range in total concentration of the acid.

TABLE 2

Distribution of $5 \cdot 10^{-4}$ M benzoic acid between 0.1 M $NaClO_4$ (pH 3) and carbon tetrachloride solutions of TOPO at 25 ± 0.1 °C

$C_B = [B]_o$, ($\cdot 10^{-2}$ M)	D	$\log D[B]_o^{-1}$
0.5	8.07	3.207
1.0	15.43	3.188
1.5	22.56	3.177
2.0	29.85	3.174
3.0	46.19	3.187
4.0	61.28	3.185

Benzoic acid forms a complex with TOPO in carbon tetrachloride. The interaction between TOPO and benzoic acid causes an enhancement of the distribution coefficient of the acid.

The values of the constants obtained in this work will be used for a quantitative interpretation of the synergic extraction of uranium with TOPO and benzoic acid. They can also be used successfully in any other system where the extraction is carried out with these two extractants.

REFERENCES

1 St. Mareva, N. Jordanov and M. Konstantinova, Anal. Chim. Acta, 59 (1972) 319.
2 M. Konstantinova, St. Mareva and N. Jordanov, Anal. Chim. Acta, 68 (1974) 237.
3 D. Dryssen and L. G. Sillén, Acta Chem. Scand., 7 (1953) 663.
4 D. Dyrssen, Acta. Chem. Scand., 11 (1957) 1771.
5 D. Dyrssen and Lien Djet Hay, Acta Chem. Scand., 14 (1960) 1091.
6 G. C. Pimentel and A. L. McClellan, The Hydrogen Bond, W. H. Freeman and Company, San Francisco and London, p. 370.

Analytica Chimica Acta, 90 (1977) 301—302

Short Communication

THE DETERMINATION OF SMALL AMOUNTS OF FREE LEAD OXIDE IN LEAD COMPOUNDS

H. KRUIDHOF and K. J. de VRIES

Twente University of Technology, Department of Chemical Engineering, Laboratory for Inorganic Chemistry and Materials Science, Enschede (The Netherlands)

(Received 9th August 1976)

The extraction methods [1—5] for the determination of free lead oxide in compounds containing lead oxide do not give satisfactory results when applied to powdered, annealed ceramic lead (zirconate) titanate materials; not only is the free lead oxide extracted but also lead oxide derived from the complex compounds themselves. A new method, developed to extract quantitatively only the free lead oxide, involves annealing the materials after milling, combined with an extraction step in which a weak extraction reagent is used. The measurements are conducted by a.a.s., and at least 20—40-mg samples are necessary. The error (relatively about 1.5%) is determined mainly by the atomic absorption method and not by the extraction step.

Experimental

Reagents. Prepare a 0.1 % solution of 8-hydroxyquinoline by dissolving 100 mg of 8-hydroxyquinoline in 90 ml of ethanol and 10 ml of water; then add 0.1 ml of ammonia liquor.

Procedure. Mill about 200 mg of the sample material to about 1 μm, which is well below the ceramic grain size (about 5 μm). After milling, heat the powder in a furnace for about 100 h at 500 °C in air. From the milled and annealed powder, weigh accurately about 40 mg and place in a 50-ml conical flask. Add 20.00 ml of extractant and stopper the flask, and extract ultrasonically for about 2 h. After extraction, leave the powder and extractant for about 12 h; the extraction reagent clears and the powder falls to the bottom of the flask. Carefully take a few ml of the clear solution for measurement by a.a.s., as described in detail earlier [5].

Results and discussion

To check the method, material (lead zirconate titanate) with a low percentage of free lead oxide (0.08 % by the method described above) was used. Various amounts of lead oxide were added; the mixtures were carefully ground, and then sintered to homogeneous materials at low temperature. No loss of lead oxide was found. These materials were treated

as described in the procedure. The results are shown in Table 1. Determination were performed in triplicate; the errors given in Table 1 correspond to half the difference between the extreme results. Table 1 shows that the proposed method gives satisfactory results. Obviously, only free lead oxide is extracted.

Table 2 shows that the extraction reagents described in the literature (0.02 M EDTA [2], 0.1 M HNO_3 [1] and acetic acid solutions [3, 4]) give different (and high) percentages of "free lead oxide"; these percentages also tend to increase with increasing extraction times.

It can be concluded that the method described is reliable, with an acceptable accuracy, for the materials described. It should also be applicable to such materials containing substituted aliovalent ions and to determinations of the homogeneity of such materials.

TABLE 1

Recovery of lead oxide added to a sample of lead zirconate titanate

Free lead oxide present after weighing (%)	Actual amount of lead oxide present (weighed + 0.08 %)[a] (%)	Percentage found after sintering
3.79	3.87	3.84 ± 0.03
1.97	2.05	2.03 ± 0.02
0.34	0.42	0.44 ± 0.01
4.10	4.18	4.20 ± 0.03
2.58	2.66	2.67 ± 0.03

[a] 0.08 % was the amount of free lead oxide present in the starting material.

TABLE 2

Comparison of % free lead oxide in a sample of lead zirconate titanate obtained by different methods

0.02 M EDTA [2]	0.1 M HNO_3 [1]	Various concentrations of acetic acid [3, 4]	This method
6.9	9.2	4.6—5.5	0.08

The authors wish to thank Professor A. J. Burggraaf for his stimulating interest.

REFERENCES

1 R. Gesemann and H. Neels, Hermsdorfer Tech. Mitt., 12 (1965) 339.
2 A. E. Robinson and T. A. Joyce, Trans. Br. Ceram. Soc., 61 (1962) 85.
3 Y. Matsuo and H. Sasaki, J. Am. Ceram. Soc., 48 (1965) 289.
4 G. S. Snow, J. Am. Ceram. Soc., 56 (1973) 91.
5 J. H. H. G. van Willigen, H. Kruidhof and E. A. M. F. Dahmen, Anal. Chim. Acta., 62 (1972) 279.

Analytica Chimica Acta, 90 (1977) 303—305

Short Communication

A RAPID INSTRUMENTAL METHOD FOR THE DETERMINATION OF HYDROGEN IN FLUORINE-CONTAINING INORGANIC MATERIALS

ANGELA M. BERKLEY and G. H. RISEBROW-SMITH

Division of Chemical Standards, National Physical Laboratory, Teddington, Middlesex TW11 0LW (England)

(Received 27th August, 1976)

A procedure was required for the determination of the total hydrogen content of high-fluorine ESR slags. These slags contain alumina, titania, boron and calcium fluoride from 60—100% CaF_2; the hydrogen content was expected to range from 10 p.p.m. to 1—2%. The complexity and difficulties involved in the determination of hydrogen and its compounds (water) have been reviewed [1]. Lack of suitable reference materials and the high fluorine content of the samples complicated known classical procedures [2, 3] and gave erratic and inconclusive results. The methods of Schmidt [4] did not seem to be adaptable for this range of hydrogen content. The Perkin-Elmer Elemental Analyzer Model 240 has been used [5] for highly fluorinated organic materials, hence the possibilities of using this instrument for inorganic samples containing fluorine were studied in greater detail.

The modifications to the reaction tube packing involved mainly the inclusion of a large bed of specially prepared magnesium oxide [6, 7]. Because of the nature of the slags, it was found necessary to extend the combustion time to 5 min with a furnace temperature of 950°C, and to bring the sample ladle into the high-heat zone. To reduce the risk of contamination by fluorinated gases and to ensure total oxidation of the hydrogen, an oxygen-donating flux of silver tungstate on magnesium oxide was used. A series of hydrogen determinations was run on this material; consistent results of 0.02% H_2 (200 p.p.m.) were obtained, and this is greater than that expected to be present in most of the samples. All additions of flux, therefore, had to be weighed into the sample boat, which is not the normal practice for organic analysis. The addition of roasted magnesium oxide to the weighed sample to absorb fluorinated gases was tried, but the oxide itself picked up hydrogen from the atmosphere too rapidly to produce consistent results.

The usual sample weight taken for organic materials is 1—3 mg ± 1 μg, and the sensitivity for hydrogen of the instrument is 60 ± 16 μV/μg H, giving a minimum limit of approximately 0.05% H or 0.2% H_2O. By increasing the weight of the unknown sample to 50 mg, the limit of detection can be decreased to approximately 0.002% H or 0.02% H_2O. Of course, this greater weight reduces the life of the magnesium oxide in the combustion tube if the samples contain a high percentage of fluorine.

Experimental

The Perkin-Elmer Elemental Analyzer Model 240 is used with the combustion tube packed as shown in Fig. 1. After packing the combustion tube, fit it into the furnace and connect up the sample entrance assembly, but not the connector fitting assembly. Start up the instrument normally and switch on the furnace; When the temperature has reached 900°C, maintain it at this level for 1 h to dry out the magnesium oxide. Turn the programme wheel to 2 and "purge the tube" for 5 min to remove all traces of fine dust from the MgO which would otherwise block the solenoid valves. Proceed with the usual programme at a temperature of 950°C.

A Cahn Electrobalance Model 4100 calibrated on the 20-mg and 200-mg ranges was used. The platinum boats for the increased sample weights (up to 100 mg) measured 10 mm length × 5 mm × 5 mm; these fitted into the standard sample ladle.

For the actual analyses, follow the operating sequence described in the PE 240 manual, with following modifications (1) add a known weight of approximately 10—20 mg of silver tungstate—magnesium oxide flux; (2) increase the combustion time to 5 min; (3) draw the ladle and boat into the high heat zone to ensure complete combustion; (4) maintain the combustion furnace at approximately 800°C during standby periods.

Results and discussion

In order to substantiate the efficiency of the method, various materials were analyzed, as there are few standard substances with known hydrogen contents of 0.05% or less. The results are shown in Table 1. The results for the standard materials show excellent agreement with the expected values. Those obtained for ESR Slag 281/75 were slightly higher than those obtained by the tube-furnace gravimetric method, which is a less efficient system in the presence of high amounts of fluorine.

The modified method for using a PE 240 Analyzer for inorganic materials containing high fluorine proved to be efficient and reliable. The time taken for each analysis was the programme time of the instrument — 15 min —

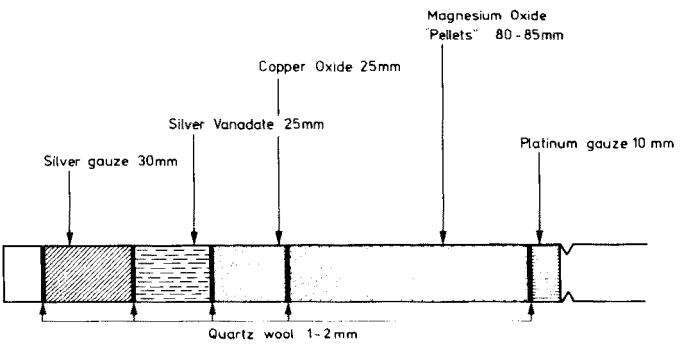

Fig. 1. Modified packing of the combustion tube.

TABLE 1

Results obtained for organic for organic and inorganic materials

	%H Expected	Sample weight (mg)	%H Found
Trifluoracetanilide (BDH M.A.S.)	3.17	2.64	2.92
		1.807	3.09
Sodium Tartrate (BDH Standard)	3.48	2.73	3.43
		2.14	3.53
ESR Slag 281/75	0.18[a]	8.79	0.22
		5.34	0.22
		45.56	0.24
		9.08	0.26
Trachyandesite (felspar)	0.09[b]	21.30	0.087
		22.12	0.090

[a] Result found by modified tube furnace/gravimetric method.
[b] Result obtained by Institute of Geological Sciences.

which is much shorter than any gravimetric method. Interference from the fluorine itself proved to be negligible and hydrogen recoveries are better than 97%.

REFERENCES

1 C. Harris, Talanta, 19 (1972) 1523.
2 A. W. Groves, Silicate Analysis, 2nd edn., Allen and Unwin, London, 1951, p. 95.
3 J. Doležal, P. Povondra and Z. Šulcek, Decomposition Techniques in Inorganic Analysis, Iliffe Books Ltd, London, 1968, pp. 185—207.
4 J. Schmidt, Arch. Eisenhüttenw., 46 (1975) 711.
5 A. M. G. Macdonald and G. G. Turton, Microchem. J., 13 (1968) 1.
6 A. D. Campbell and A. M. G. Macdonald, Anal. Chim. Acta, 26 (1962) 275.
7 R. Belcher, M. K. Bhatty, A. M. G. Macdonald, S. A. Salam and J. C. Tatlow, Anal. Chim. Acta, 27 (1962) 271.

Analytica Chimica Acta, 90 (1977) 307—309

Short Communication

THE DETERMINATION OF CADMIUM BY THE RING-OVEN TECHNIQUE

MUHAMMAD HANIF, MUHAMMAD SARWAR CHAUDHRY and TAUSEEF AHMAD QURESHI

Pakistan Council of Scientific and Industrial Research Laboratories, Lahore-16 (Pakistan)

(Received 15th September 1976)

Cadmium has been reported to be hazardous to human beings and animals in various ways [1, 2]. Thus direct, quick, precise and sensitive determinations of cadmium are valuable. The ring-oven technique, which has been used previously for the determination of cadmium [2, 3], offers good possibilities for the purpose.

Cadmium reacts with *p*-nitrobenzenediazoaminoazobenzene (Cadion 2 B) to form a coloured lake [4], and the reaction is quite sensitive [3]. In the present work, this reaction was studied by the ring-oven technique; the standard scale [3] and the segment technique [5—7] methods were evaluated.

Experimental

Cadmium stock solution. Prepare a solution containing 0.1 mg Cd^{2+} ml^{-1} by dissolving 0.057 g of $3CdSO_4 \cdot 8H_2O$ (Riedel) in 250 ml of distilled water. Prepare a working solution containing 0.02 mg Cd^{2+} ml^{-1} by exact dilution for the standard scale method. Prepare other low concentrations similarly. For the segment technique, prepare standard solutions containing 0.02, 0.04, 0.08, 0.12, 0.16 and 0.2 mg Cd^{2+} ml^{-1} (called solutions I, II, IV, VI, VIII and X, respectively) from the stock solution by exact dilutions.

Cadion solution. Prepare an ethanolic 0.02% solution which is also 0.02 M in KOH.

All reagents used were of analytical grade.

Apparatus. The ring-oven used was made in our precision workshop, from standard measurements [3]. The working temperature was 110°C.

Procedure. Place, with a micropipette, 1 drop (1.5 μl) of unknown cadmium solution on the previously marked centre of a Whatman filter paper No. 41. Wash it into the ring zone with 0.5% acetic acid; 8—10 washings suffice. Remove the paper immediately from the ring-oven and spray it first with cadion solution and after 1 min with 2 M KOH solution. Within 1 min a pinkish-red ring is obtained against a yellowish background, which is removed by washing in running water. Dry the ring between filter papers and then with hot air. The dominant ring against the light yellow background is then ready for comparison with a standard cadmium scale prepared as above by taking 1, 2, 4, 6, 8 and 10 drops of the standard working solution containing 0.02 mg Cd^{2+} ml^{-1} and getting rings numbered I, II, IV, VI, VIII and X, respectively.

For evaluation of the unknown cadmium solutions by the segment technique [5—7], use standard solutions labelled I, II, IV, VI, VIII and X, as described under *Cadmium stock solution.*

Results and discussion

Cadmium unknown solutions were analyzed by the above procedures; some results are shown in Table 1. Cadmium can be determined in microgram amounts with a maximum error of 10.0%.

The standard scale for cadmium, prepared by the above method, was checked for stability by evaluating against it standard cadmium solutions after regular intervals of time, (Table 2). The scale is stable for 3 d after which its colour deteriorates significantly.

Interferences. Interferences were studied by the method of Dharmarajan and West [2]. When the standard scale was used for evaluation of the unknown cadmium solutions, a ring (I) containing (say) 0.35 μg of the interfering ion and another ring (II) containing (say) 0.035 μg of cadmium and 0.35 μg of interfering ion were prepared. The substance was confirmed as non-interfering when ring (I) was identical to the blank ring (III) and ring (II) matched the ring of the standard scale containing 0.035 μg of cadmium.

When the segment technique was used, the interferences were checked as described earlier [8]. The following ions do not interfere even in 100-fold amounts: Na^+, K^+, Cu^{2+}, Ba^{2+}, Sr^{2+}, Al^{3+}, Ce^{4+}, Zn^{2+}, Pb^{2+}, Sn^{2+}, NH_4^+, Cr^{3+}, Fe^{3+}, Cl^-, Br^-, I^-, F^-, NO_3^-, NO_2^-, Ac^-, CO_3^{2-}, HPO_4^{2-}, BO_2^-, SO_4^{2-}, SO_3^{2-}, $S_2O_3^{2-}$, S^{2-}, $Cr_2O_7^{2-}$ and CrO_4^{2-}. A 40-fold amount of Mn^{2+} or Ni^{2+} does not interfere, while Co^{2+} interferes at more than 20-fold and Ag^+ and Hg^+ interfere even at less than 10-fold.

The selectivity and sensitivity of the method is proved from the high levels of diverse ions in whose presence cadmium can be determined.

TABLE 1

Determination of cadmium by the standard scale and segment techniques (All results are given as $\mu g\ \mu l^{-1}$.)

Standard scale		Segment technique	
Cd given	Cd found	Cd given	Cd found
0.010	0.011	0.010	0.009
0.016	0.017	0.056	0.058
0.034	0.037	0.080	0.083
0.061	0.065	0.097	0.094
0.075	0.080	0.120	0.118
0.097	0.095	0.150	0.153
0.120	0.113	0.160	0.155
0.160	0.160	0.180	0.190
0.200	0.200	0.200	0.215

TABLE 2

The stability of the standard scale
(Results are given as $\mu g\ \mu l^{-1}$)

Day	Cd given	Cd found	Day	Cd given	Cd found
0	0.012	0.011	2	0.025	0.027
	0.130	0.139		0.055	0.058
	0.200	0.215		0.180	0.195
1	0.015	0.016	3	0.013	0.014
	0.180	0.195		0.045	0.050
	0.200	0.220		0.200	0.223

Part of this work was done by M.H. in the Federal Republic of Germany as a Postdoctoral Senior Research Fellow of the Alexander Von-Humboldt Stiftung. The authors are greatly indebted to Prof. Dr. Herbert Weisz, Department of Analytical Chemistry, Freiburg University, for guidance.

REFERENCES

1 H. E. Hesketh, Understanding and Controlling Air Pollution, Ann Arbor, Michigan, 2nd edn., 1973, p. 117.
2 V. Dharmarajan and P. W. West, Anal. Chim. Acta, 57 (1971) 469.
3 H. Weisz, Microanalysis by the Ring-Oven Technique, Pergamon Press, Oxford, 2nd edn., 1970.
4 F. P. Dwyer, Aust. Chem. Inst. J. Proc., 4 (1937) 26.
5 H. Weisz, S. Pantel and I. Vereno, Mikrochim. Acta (Wien), (1976) 289.
6 H. Weisz, Proc. Soc. Anal. Chem., 11 (1974) 319.
7 H. Weisz, S. Pantel and I. Vereno, Mikrochim. Acta (Wien), (1975), 287.
8 H. Weisz and M. Hanif, Anal. Chim. Acta, 81 (1976) 179.

Analytica Chimica Acta, 90 (1977) 311—314

Short Communication

GAS CHROMATOGRAPHIC SEPARATION OF OLEFINS ON SILVER NITRATE-CONTAINING STATIONARY PHASES

D. DAUTZENBERG and H. KNÖZINGER

Institut für Physikalische Chemie, Universität München, Sophienstr. 11, 8 München 2 (West Germany)

(Received 5th October 1976)

The use of $AgNO_3$-containing stationary phases for the gas chromatographic separation of positional and *cis—trans* olefin isomers of similar boiling points is well established [1—6]. Other phases such as thallium [7], rhodium [8] and palladium salts [3] have also been applied successfully. Frequently, however, the applied liquid phases involve serious disadvantages because of their relatively high vapour pressures [9, 10], and, in the case of $AgNO_3$-containing phases, because of thermal instability [7]. They can therefore usually be operated only at around room temperature, which may in certain cases — e.g., catalytic micropulse experiments — increase the retention times of olefins with larger number of C-atoms (C_7 and higher) unfavourably. The most severe disadvantage of the commonly used liquid phases is their appreciable bleeding, even at room temperature; this restricts severely their use in connection with high-sensitivity flame-ionization detectors and on-line mass-spectrometers. In contrast, high-boiling liquid phases [11] reduce selectivity [9]. Attempts to find $AgNO_3$-containing stationary phases of high selectivity and negligible tendency to bleed, so that they can be used with flame ionization detectors and on-line mass-spectrometers above room temperature, have therefore been made.

Experimental

Materials. Gas-Chrom-R (60-80 mesh; Serva, Heidelberg, West Germany) was used as support for the stationary phases. Tetraethylene glycol TEG (≥99%; Fluka, Buchs, Switzerland) and naphthyl-1-acetonitrile NAN (ca. 97%; Ega-Chemie, Steinheim, West Germany) were used.

Methanol used as solvent for the stationary phases, and silver nitrate were both p.A. grade (Merck, Darmstadt). The columns were tested with olefins and olefin mixtures (Fluka). Their purity was ≥99% and ≥97%, respectively. All compounds were used without further purification.

TEG/$AgNO_3$, 20% on Gas-Chrom-R. TEG was saturated with silver nitrate at 43°C and dissolved in methanol. The corresponding amount of Gas-Chrom-R was added, the mixture was shaken, and methanol was

removed at 30—40°C. The packed column was conditioned at 45°C in a helium flow (40 ml min^{-1}) for 20 h before use.

NAN/$AgNO_3$, 20% on Gas-Chrom-R. NAN was saturated with silver nitrate at 75°C and dissolved in methanol. The impregnation procedure was the same as for the TEG stationary phase. The packed NAN/$AgNO_3$ column was conditioned at 60°C in a helium flow (40 ml min^{-1}) for 20 h before use.

The columns were made from teflon tubes (3 mm i.d.). The columns were packed with the aid of a vibrator: the column length was 4 m in both cases.

Procedure. A Varian Aerograph Series 1700 chromatograph with flame ionization detector was used. The column temperature was stabilized to ±0.5°C. The carrier gas was helium at a flow rate of 40 ml min^{-1} (±1%). The temperatures of the injector and detector were 120 and 100°C, respectively. A hydrogen flow rate of 40 ml min^{-1} and air flow of 400—500 ml min^{-1} were applied. Sample volumes were 0.3—0.4 μl. Analyses were repeated several times and the mean values of the retention times were determined for each compound. The mean errors of the total retention times were 3%. The interstitial time was 0.33 s.

Results and discussion

The results are summarized in Table 1 for column temperatures of 32 and 41°C. Retention time (t_r), separation factor $b = t_r/b_{1/2}$ ($b_{1/2}$ is peak width at half height measured in min) and retention index I [12, 13] are given.

Separation factors. The separation factor b generally increases with increasing molecular weight of the hydrocarbon and decreases at constant molecular weight with increasing chain branching or increasing inductive effect of the substituents towards the double bond. Branched olefins are usually more easily separated than straight chain isomers, for two reasons: (a) the lower b-values of branched olefins compared with straight chain olefins of the same number of C-atoms, are mainly the result of a drastic reduction of the retention time t_r with only a slight or no increase of $b_{1/2}$; (b) the tailing is usually less pronounced for branched olefins than for straight chain compounds.

The separation factors are generally lower for the TEG/$AgNO_3$ than for the NAN/$AgNO_3$ stationary phase (see Table 1). Terminal and internal *cis*-olefins respond particularly sensitively to a change in the liquid phase (δI values in Table 1), whereas the effect of the liquid phase is less pronounced for internal *trans*-olefins.

The separation factor usually increases with increasing temperature, the temperature coefficient being lower for the TEG/$AgNO_3$ than for the NAN/$AgNO_3$ stationary phase.

Lifetime and upper temperature limit. The stationary phases have been tested in permanent use for 2 months at 50°C without loss of efficiency; TEG/$AgNO_3$ has been used at up to 90°C for shorter periods.

TABLE 1

Retention data for saturated and unsaturated hydrocarbons on TEG/$AgNO_3$ and NAN/$AgNO_3$ (Carrier-gas, He; length of column, 4 m; i.d. 3 mm; flow 40 ml min^{-1}.)

Hydrocarbon	B.p. (°C)	TEG/$AgNO_3$-32°C			TEG/$AgNO_3$-41°C			NAN/$AgNO_3$-32°C			NAN/$AgNO_3$-41°C			δI[b]
		t_r	b[a]	I	t_r	b[a]	I	t_r	b[a]	I	t_r	b[a]	I	
n-Pentane	36	0.87	8.7	500	0.86	9.3	500	1.37	8.6	500	1.32		500	
n-Hexane	69	1.32	8.8	600	1.25	9.6	600	2.87	9.9	600	2.32	11.6	600	
n-Heptane	98.4	2.52	10.3	700	2.05	10.0	700	6.84	12.7	700	5.42	14.3	700	
Methylcyclohexane	101	3.85	9.9	757 ± 1.2%	3.00	10.0	755 ± 1.3%	10.07	11.4	743 ± 1%	7.47	12.9	744 ± 1%	11
n-Octane	125	5.27	12.9	800	4.12	11.8	800	16.8	14.7	800	11.32	16.0	800	
n-Nonane	151	12.02	15.2	900	9.07	13.0	900	42.67	17.8	900	28.22	16.8	900	
Trans-butene-2	0.9	1.09	7.3	554 ± 3%	1.11	8.2	568 ± 3.4%	1.41	8.1	504 ± 1.6%	1.23		487 ± 2.2%	81
Cis-butene-2	3.9	1.92	6.9	658 ± 0.9%	1.75	8.3	668 ± 2.2%	1.99		550 ± 1.7%	1.68		543 ± 2.1%	125
1-Butene	−6.3							1.70	6.8	529 ± 1.6%	1.44	8.0	515 ± 2.1%	
Trans-2-hexene	67.9	2.77	8.4	713 ± 1.1%	2.3	9.2	716 ± 1.2%	5.12	10.2	667 ± 1.2%	4.02	13.4	665 ± 1.3%	51
1-Hexene	63.4	5.62	9.2	808 ± 0.9%	4.42	9.4	809 ± 0.9%	7.47	10.2	710 ± 1%	5.71	12.4	707 ± 1.2%	102
Cis-2-hexene	68.9	5.45	9.4	804 ± 0.9%	4.30	10.2	805 ± 1%	8.7	11.67	727 ± 1%	6.25	12.0	719 ± 1.2%	124
Trans-2-heptene	97.9	5.37	9.4	802 ± 0.9%	4.3	10.0	805 ± 1%	11.8	9.1	760 ± 1%	9.17	13.9	771 ± 1.3%	34
1-Heptene	93.6	11.02	11.4	889 ± 1.1%	8.62	12.0	894 ± 1.2%	18.9		812 ± 0.8%	12.09	13.2	814 ± 0.8%	80
Cis-2-heptene	98.5	10.52	11.1	884 ± 1.1%	7.79	11.4	881 ± 1.1%	20.7		822 ± 0.8%	14.4	13.7	826 ± 0.8%	55
Trans-4,4-dimethyl-2-pentene	76.7	2.53	9.0	701 ± 1.1%	2.05	9.3	700	4.47	7.5	651 ± 1.2%	3.50	10.0	648 ± 1.2%	52
4,4-Dimethyl-1-pentene	72.5	3.91	8.7	760 ± 1.3%	3.1	8.9	759 ± 1.3%	5.71	7.1	679 ± 1.3%	4.3	10.2	673 ± 1.3%	86
Cis-4,4-dimethyl-2-pentene	80.4	6.37	9.1	823 ± 0.9%	4.88	9.4	821 ± 1%	10.2	8.4	745 ± 1%	7.12	11.0	737 ± 1.2%	84
2,3-Dimethyl-2-butene	73.2	3.31	8.3[c]	737 ± 1.2%	2.72	9.1[c]	741 ± 1.3%	6.87	8.6[c]	700	5.17	11.5[b]	694 ± 1.4%	47
2,3-Dimethyl-1-butene	55.6	2.97	8.3[c]	722 ± 1.2%	2.52	9.7[c]	730 ± 1.2%	4.75	7.4[c]	658 ± 1.2%	3.67	9.7[b]	654 ± 1.2%	76
3,3-Dimethylbutene	41.2	2.72	7.4[c]	710 ± 1.2%	2.27	7.8[c]	715 ± 1.2%	2.81	4.7[c]	597 ± 1.9%	2.32	7.7[b]	600	115
Cis- and *trans*-3-methyl-2-pentenes	67.7	3.02	6.6[c]	725 ± 1.2%	2.52	7.0[c]	730 ± 1.2%	5.99	6.1[c]	685 ± 1.3%				40
2-Ethyl-1-butene	64.7	5.27	9.1[c]	800	4.17	9.7[c]	802 ± 1%	8.67	8.8[c]	726 ± 1%				74
Benzene	80.0										17.68	⩾ 10	849 ± 1%	
Cyclohexene	83.0										11.76	⩾ 10	804 ± 1%	
1,3-Cyclohexadiene	80.3										22.26	⩾ 10	874 ± 1%	

[a] ±4%. [b] $\delta I = I$ (TEG) − I (NAN). [c] ±12%.

In conclusion, both stationary phases possess excellent separation properties for terminal and *cis/trans* isomeric olefins. Their upper temperature limit is higher than for the conventional liquid phases. Thus, retention times can be kept short (e.g. complete separation of 1- and *cis*- and *trans*-4,4-dimethyl-pentenes in less than 5 min at 41 °C on TEG/$AgNO_3$). Bleeding of phases is negligible, even at temperatures above 50 °C, so that the stationary phases can be used effectively in connection with a flame ionization detector and in a g.c.—m.s. system.

The financial assistance of the Deutsche Forschungsgemeinschaft and of the Fonds der Chemischen Industrie is gratefully acknowledged.

REFERENCES

1 R. A. Bernhard, Anal. Chem., 34 (1962) 1576.
2 M. H. Klouwen and R. J. ter Heide, J. Chromatogr., 7 (1962) 297.
3 M. Kraitr, R. Komers and F. Čůta, Coll. Czech. Chem. Commun., 39 (1974) 1440.
4 M. Kraitr, R. Komers and F. Čůta, J. Chromatogr., 86 (1973) 1.
5 M. Kraitr, R. Komers and F. Čůta, Anal. Chem., 46 (1974) 974.
6 J. Shabtai, J. Chromatogr., 18 (1965) 302.
7 D. V. Banthorpe, C. Gatford and B. R. Holleboul, J. Gas Chromatogr., 6 (1968) 61.
8 E. Gil-Av and V. Schurig, Anal. Chem., 43 (1971) 2030.
9 J. Herling, J. Shabtai and E. Gil-Av, J. Chromatogr., 8 (1962) 349.
10 B. Smith and R. Ohlson, Acta Chem. Scand., 16 (1962) 351.
11 A. Zlatkis, G. S. Chao and H. R. Kaufman, Anal. Chem., 36 (1964) 2354.
12 A. Wehrli and E. Kovats, Helv. Chim. Acta, 42 (1959) 2709.
13 P. Toth, E. Kugler and E. Kovats, Helv. Chim. Acta, 42 (1959) 2519.

Analytica Chimica Acta, 90 (1977) 315—318

Short Communication

A METHOD OF CONCENTRATING ANTIMONY FROM NATURAL WATERS

I. VALENTE and H. J. M. BOWEN

Chemistry Department, Reading University, Reading RG6 2AD (Gt. Britain)

(Received 27th August 1976)

The very small amounts of antimony present in natural waters makes a concentration step necessary before the element can be determined by most analytical techniques. Methods for this purpose include coprecipitation [1, 2], cocrystallization [3], freeze drying [4], solvent extraction [5] and antimony hydride generation [6—10], but these have limited applicability because of poor selectivity, the presence of interfering elements, or the extensive pretreatment necessary. Ion exchange is the only method that can be adapted easily to concentrate antimony from large volumes of water. Smith and Reynolds [11] separated antimony from hydrochloric acid solution with an anion-exchange resin; this method is not applicable to antimony in sea water. A dithiocarbamate resin synthesized by Dingman et al. [12] and used to concentrate trace metals from aqueous media at pH $\geqslant$ 2 is not selective; the recovery of antimony was not discussed. Extraction chromatography offers possibilities for the preconcentration of trace elements if a selective chelating agent for the element under study is retained on an inert support [13]; the use of a column has several advantages over liquid—liquid extraction or other types of chromatography. The main advantage over ion-exchange chromatography is that the method allows concentration from solutions such as sea water or waste water, which rapidly saturate available sites on resins. Polyurethane foams have selective adsorption properties for a number of inorganic and organic species in aqueous solution [14]. They have been used as support materials in extraction chromatography in the form of small cubes or cylinders [15—19]. Polyurethane foam treated with zinc diethyldithiocarbamate or zinc dithizonate with a plasticizer such as tributyl phosphate extracts mercury [20] and other metals [21] from solution. Diphenylthiocarbazone-treated polyurethane foams extract mercury(II) and methylmercury(II) chloride from aqueous media [22], and cobalt has been collected on 1-nitroso-2-naphthol and diethylammonium-diethyldithiocarbamate foam [23]. The extraction of gold from aqueous solutions by polyurethane foam has also been studied [24, 25].

A method of concentrating antimony from natural waters on polyurethane foams loaded with a 1% solution of 1,2-ethanedithiol in benzene, and the recovery of the adsorbed antimony with acetone, is described. Concentration

factors of 5000 can be obtained; these permit the determination of antimony in natural waters by atomic absorption spectrometry or neutron activation analysi

Experimental

Reagents and minerals. Unless otherwise specified analytical-grade chemicals were used. A sample of River Thames water collected at Caversham, was filtered through a 450-nm Millipore filter within 10 min of collection, and kept in an acid-treated polyethylene bottle. A sample of sea water, provided by the Department of Zoology, was filtered and stored similarly. The elemental concentrations involved were assumed to be within the normal ranges for natural fresh and sea water [27].

Stock solutions of radioactive ^{124}Sb(III) and (V), as well as carrier solutions were prepared as described by Alian [26]. To study the extractibility of other ions, several radiotracers in solution (^{76}As, ^{82}Br, ^{109}Cd, ^{203}Hg, ^{24}Na, ^{113}Sn and ^{65}Zn) were obtained. Lead nitrate standard solutions were prepared by diluting 1000 p.p.m. aqueous stock solution appropriately and adjusting to pH 1 with 1 M HNO_3.

The polyurethane foam used was a polyether open-cell type (Vert-Foam Company, Manchester). The chromatographic columns (15 mm diam, 12 cm long) were fitted with a separating funnel at the top. Stoppered conical flasks and mechanical shakers were used for batch experiments.

Instrumentation. Radioactive samples were counted with a well-type sodium iodide crystal and a single-channel γ-spectrometer. Lead concentrations were determined with a Shandon Southern A 3300 atomic absorption spectrophotometer fitted with an A3370 carbon rod analyzer; the backgrounds were measured with a deuterium continuum source.

Foam and column preparation. The polyurethane foam (either cubes of ca. 5 mm edge or cylindrical plugs of 55 mm length, 15 mm o.d.), were washed with 1 M HCl followed by distilled water until the washings were free from chloride ion. The foam material was dried, washed with acetone, air dried, and equilibrated with a solution (1% v/v) of ethanedithiol (B.D.H.) in benzene for 15 min to ensure complete saturation. The loaded foam was squeezed between watch glasses immediately before use to remove the excess of ethanedithiol solution. For batch experiments 0.400 g of loaded foam cubes was used.

Loaded cylindrical plugs, packed by applying gentle pressure with a glass rod, fitted snugly into the glass column and allowed gravity elution of water.

Results and discussion

Effect of shaking time on the percentage of antimony retained with foam treated with ethanedithiol. The dependence on shaking time of the percentage retention of antimony on ethanedithiol-loaded polyurethane foam was checked for distilled water, River Thames water and sea water. Aliquots (50 ml) spiked with carrier-free radioactive antimony and adjusted to pH 1 with 12 M HCl were shaken for several time intervals; the antimony not retained was determined by measuring the radioactivity of a 5-ml

sample of the aqueous solutions. The antimony retained by the foam was calculated by difference. Both oxidation states of antimony were investigated. Absorption of antimony was 50% complete in 1 min and 95% complete in 3 min and was independent of the type of water used and the oxidation state of antimony. All the subsequent work was carried out with Sb(III) solutions.

Effect of acidity on the retention of Sb(III) on foam loaded with 1,2-ethanedithiol. In batch experiments, aliquots (50 ml) of water samples containing 0.75 mg of Sb(III) were shaken for 30 min at different pH values. More than 97% was extracted from aqueous solution between pH 1—2.5. Above pH 4, the percentage extracted sharply decreased; the solutions became cloudy. The formation of a hydroxy-chloro anion or insoluble derivatives may be involved.

Isotherm for the solution of Sb(III) on foam loaded with 1,2-ethanedithiol. The isotherm obtained in batch experiments showed a linear relationship between the weight of antimony (C_f) retained by the loaded foam and its concentration (C_s) in the water samples of the form $C_f = K C_s$. For values of C_s between 10 μg l^{-1} and 0.1 g l^{-1}, K had the value 1588. The isotherm was independent of the type of water used. The experiments were carried out at pH 1 with aliquots (50 ml) of natural water samples containing different concentrations of antimony.

Retention of traces of antimony by columns of loaded foam. River water and sea water samples (1l) were prepared by taking an appropriate aliquot of radioactive antimony tracer and adding a solution of inactive antimony to give a solution containing 6μg Sb per litre; this was adjusted to pH 1. The samples were permitted to flow through the columns at 5 ml min^{-1}. The radioactivity of the eluate was compared with that of the original solutions. A plot of the amount of antimony retained per gram of foam against the mass of antimony added showed a linear relationship up to a retention of 40 μg g^{-1} of foam; above that value the foam was saturated and no more antimony was absorbed. The capacity of the columns was the same for river water and sea water.

Recovery of antimony from foam columns. Antimony can be removed quantitatively from foam columns by eluting with 10 ml of acetone at a flow rate of 1 ml min^{-1}. Both antimony and 1,2-ethanedithiol are removed simultaneously. The recovery of complexed antimony with 10 ml of acetone resulted in a 100-fold concentration of antimony for 1-l samples. Volatilization of acetone gives higher concentration factors.

Selectivity of the method. In batch experiments the extractibility of several radiotracers at pH 1 was studied to investigate possible interfering elements. Table 1 shows that, of the elements tested, only ^{76}As and ^{203}Hg were quantitatively retained. These elements do not interfere with antimony determinations by a.a.s. or i.n.a.a. The extractibility of lead was studied with solutions of lead nitrate in 0.1 M HNO_3; lead was determined by non-flame a.a.s. Under these conditions lead was not retained by the loaded foam.

Chemical form of antimony retained on loaded foam. Aqueous solutions of 50 μmol Sb (pH 1) were extracted for 1 min with various concentrations

TABLE 1

Investigation of selectivity of retention on loaded polyurethane foam

Element	Amount added to 50 ml water sample (mg)	% Extracted by foam
^{24}Na	0.14	0
^{82}Br	0.04	0
^{203}Hg	$8 \cdot 10^{-3}$	82.0
^{65}Zn	0.5	0
^{113}Sn	5	0
^{109}Cd	0.2	0
^{76}As	0.07	97.9

of 1,2-ethanedithiol in benzene. Between 10 and 50 μmol l^{-1}, the 1,2-ethanedithiol extracted equivalent amounts of antimony into the benzene layer; higher concentrations of thiol did not increase the amount of antimony extracted. For an antimony—ethanedithiol ratio of 1:1 the extractable species is probably $Sb(CH_2CH_2S_2)Cl$.

The authors thank London University Reactor Centre for irradiation facilities.

REFERENCES

1 I. Noddack and W. Noddack, Ark. Zool., 1 (1940) 32.
2 J. E. Portman and J. P. Riley, Anal. Chim. Acta, 35 (1966) 35.
3 Y. Talmi and V. E. Norvell, Anal. Chem., 47 (1975) 1510.
4 D. F. Schutz and K. K. Turekian, Geochim. Cosmochim. Acta, 29 (1965) 259.
5 C. E. Mulford, At. Absorp. Newsl., 5 (1966) 8.
6 F. J. Schmidt and J. L. Royle, Anal. Lett., 6 (1973) 17.
7 Y. Yamamoto, T. Kumamaru and Y. Hayashi, Anal. Lett., 5 (1972) 419.
8 J. C. Van Loon and E. J. Brooker, Anal. Lett., 7 (1974) 505.
9 P. D. Goulden and P. Brooksbank, Anal. Chem., 46 (1974) 1431.
10 A. E. Smith, Analyst (London), 100 (1975) 300.
11 G. W. Smith and S. A. Reynolds, Anal. Chim. Acta, 12 (1955) 151.
12 J. F. Dingman, Jr., M. Gloss, E. A. Milano and S. Siggia, Anal. Chem., 46 (1974) 774.
13 E. D. Carrit, Anal. Chem., 25 (1953) 1927.
14 H. J. M. Bowen, J. Chem. Soc. (A), (1970) 1082.
15 T. Braun and A. B. Farag, Talanta, 19 (1972) 828.
16 T. Braun and A. B. Farag, Anal. Chim. Acta, 61 (1972) 265.
17 T. Braun, E. Hsuzár and L. Bakos, Anal. Chim. Acta, 64 (1973) 77.
18 T. Braun, L. Bakos and Z. Szabó, Anal. Chim. Acta, 66 (1973) 57.
19 T. Braun and A. B. Farag, Anal. Chim. Acta, 65 (1973) 115.
20 T. Braun and A. B. Farag, Anal. Chim. Acta, 71 (1974) 133.
21 T. Braun and A. B. Farag, Anal. Chim. Acta, 69 (1974) 85.
22 A. Chow and D. Buksak, Can. J. Chem. Lett., 53 (1975) 1373.
23 T. Braun and A. B. Farag, Anal. Chim. Acta, 76 (1975) 107.
24 S. Sukiman, Radiochem. Radioanal. Lett., 18 (1974) 129.
25 P. Schiller and G. B. Cook, Anal. Chim. Acta, 54 (1971) 364.
26 A. Alian and W. Samad, Talanta, 14 (1967) 659.
27 J. P. Riley and R. Chester, Introduction to Marine Chemistry, Academic Press, 1971, pp. 64, 65.

Analytica Chimica Acta, 90 (1977) 319—322

Short Communication

SPECTROPHOTOMETRIC DETERMINATION OF TRACES OF ANIONIC SURFACTANTS WITH METHYLENE BLUE DERIVATIVES

KYOJI TÔEI and HIDEYO FUJII

Department of Chemistry, Faculty of Science, Okayama University, Tsushima-naka 3-1-1, Okayama-shi 700 (Japan)

(Received 12th August 1976)

Anionic surfactants, alkylbenzenesulfonate (ABS) and alkylsulfate (LAS), can react with methylene blue to form ion-associates extractable into chloroform. By measuring the absorbance in chloroform, the concentration of ABS or LAS can be determined. In this procedure, however, the surfactant is not extracted completely; the extraction must be repeated and the extract washed with acidic methylene blue solution to remove impurities [1].

It would be very convenient if the ion-associate could be extracted completely into an organic solvent in one stage and if the final washing of the extract could be omitted. An attempt was therefore made to synthesize a new reagent by replacing the methyl group in methylene blue by a long-chain alkyl group. Such a compound would have cationic surfactant character, with a positive charge and surface activity, and could combine strongly with ABS or LAS to form a stable ion-pair.

Experimental

Synthesis of methylene blue derivatives. The reaction for the preparation is shown below [2]. When *N,N*-diethylaminoaniline, *N,N*-dibutylaminoaniline or *N*-methyl-*N*-octylaminoaniline was used in place of *N,N*-dimethylamino-aniline, the higher analogues were obtained. As the aliphatic chain-length increased, tarry masses were produced and the yield decreased abruptly.

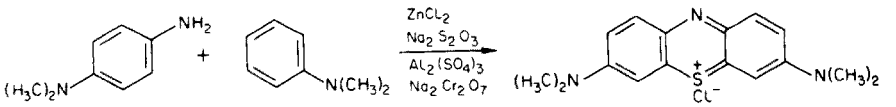

For convenience, the names of the derivatives are abbreviated: [3,7-bis-(N,N-dimethylamino)phenazathionium chloride] to methylene blue; [3-(N,N-diethylamino)-7-(N,N-dimethylamino)-phenazathionium chloride] to EB; [3-(N,N-dibutylamino)-7-(N,N-dimethylamino)phenazathionium chloride] to BB; and [3-(N-octyl-N-methyl)amino-7-(N,N-dimethylamino)-phenazathionium chloride] to OB.

The methylene blue derivatives are dark-red or dark-green crystals with a metallic luster; their elemental analyses are shown in Table 1.

Anionic surfactants. The anionic surfactants used were sodium laurylbenzenesulfonate (ABS), sodium laurylsulfate (LAS) and sodium di-(2-ethylhexyl)-sulfosuccinate (DESS; 96.3%, certificated by the Japan Oil Chemists' Society). The latter is used widely as a standard substance for the determination of anionic surfactants in Japan.

Apparatus. The absorbance was measured with a Shimazu spectrophotometer QV-50 with 1-cm glass cells. A Hitachi spectrophotometer EPS-3T was used for the absorption spectrum. The pH was measured with a Hitachi-Horiba F5ss meter and an Iwaki shaker KM was used in extractions.

Extractability of methylene blue derivatives

The methylene blue derivatives dissolve in water to form blue-colored solutions. The molar absorptivities (l mol^{-1} cm^{-1}) at the maximum wavelengths are $6.5 \cdot 10^4$ at 664 nm (MB), $5.9 \cdot 10^4$ at 666 nm (EB), $6.0 \cdot 10^4$ at 668 nm (BB) and $6.3 \cdot 10^4$ at 667 nm (OB). As the molecular weight of the derivatives increased, the compounds tended to become less soluble in water, e.g. the concentration of a saturated solution of BB was about 10^{-3} M.

Preferably, the methylene blue derivatives should be readily soluble in water, but should not be extracted into organic solvents immiscible with water unless they form ion-pairs with anionic surfactants. To find such a solvent, the following experiment was carried out.

In a test tube, 3 ml of 10^{-5} M reagent solution and 2 ml of 10^{-5} M anionic surfactant solution were mixed; 2 ml of an extractant was added and the tube was shaken vigorously. The coloration of the solvent was observed after the phases separated completely. A blank was prepared by the same procedure, 2 ml of water being added in place of the surfactant solution, and the colors were compared.

Twenty-two organic solvents were examined. As the molecular weight of the reagents increased, the reagent tended to be extracted into the organic solvent. Generally, as the dielectric constant of the solvent became larger, the reagent tended to be extracted, e.g. nitrobenzene (dielectric constant, 35) extracted all the derivatives. The solvents useful for ion-pairs of BB or OB

TABLE 1

Elemental analysis of methylene blue derivatives

Derivative	Molecular formula	C (%)		H (%)		N (%)	
		Found	Calcd.	Found	Calcd.	Found	Calcd
EB	$C_{18}H_{22}N_3SCl\frac{1}{2}ZnCl_2H_2O$	44.03	43.05	4.71	4.82	7.48	8.37
BB	$C_{22}H_{30}N_3SCl\frac{1}{2}ZnCl_2H_2O$	53.85	53.91	6.40	6.58	8.86	8.57
OB	$C_{23}H_{32}N_3SCl\frac{1}{2}ZnCl_2\frac{1}{2}H_2O$	55.83	55.79	6.89	6.72	8.62	8.49

with a surfactant were carbon tetrachloride, diethyl ether, benzene, toluene, xylene, cyclohexane, iso-amyl acetate and iso-propylbenzene. The ion-pair tended to be extracted at higher pH. Because OB reacts with a surfactant to form a precipitate at pH 8—10, and tends to be extracted into organic solvents, BB is the preferable reagent for anionic surfactants. Toluene was used for solvent extraction; the blank value is smaller than for other solvents, and the color extracted is relatively stable.

Absorption spectrum of BB in aqueous solution and extraction with toluene

The absorption spectrum of BB in aqueous solution is shown in Fig. 1. The effects of pH and the coexistence of the anionic surfactant on the spectrum were examined as follows. In a 25-ml measuring flask, 2.5 ml of 10^{-4} M BB solution, 5 ml of a buffer solution and 1 ml of 10^{-4} M anionic surfactant were added, and the mixture was diluted to the mark with distilled water. The absorption spectrum did not change over the range pH 4—11 with or without the presence of ABS and LAS. The wavelength of maximum absorption was 668 nm.

The extraction of the BB-anionic surfactant ion-associate by toluene was examined. In a 25-ml glass-stoppered glass tube, 2 ml of BB solution, 0.5 ml of an anionic surfactant and 2.5 ml of a buffer solution were mixed and 5 ml of toluene was added. The tube was shaken mechanically and left for a time. After the two phases had separated completely, the absorbance in toluene at 660 nm was measured. The absorbance became constant after shaking for 15 min. At higher pH values the absorbance increased. At about pH 10 the absorbance became constant; the blank was relatively small. The absorbance in toluene decreased gradually and became almost constant on standing for 3 h after mechanical shaking for 30 min. The effect of an excess of reagent was examined; the addition of 10—20 times molar excess of BB gave a constant absorbance.

These experiments led to the following procedure. In a 25-ml glass-stoppered glass tube, 2 ml of $5 \cdot 10^{-4}$ M BB solution, 0.5 ml of 10^{-4} M anionic surfactant and 2.5 ml of a buffer solution (pH 10; 10.7 g of ammonium chloride, 48 ml of ammonia liquor and 952 ml of water) were mixed and extracted with 5 ml of toluene by shaking for 30 min. After 3 h, the absorption spectrum in toluene was determined. The result is shown in Fig. 1.

Calibration curves and recommended procedure

To determine traces of anionic surfactants in water samples the following procedure was used.

In a 150-ml separatory funnel, place 85 ml of a water sample, 5 ml of $5 \cdot 10^{-4}$ M BB solution, and 10 ml of buffer solution (pH 10). Add 10 ml or 5 ml of toluene by pipette. Shake the funnel for 30 min mechanically, and allow to stand for 3 h. Measure the absorbance at 660 nm in the toluene layer.

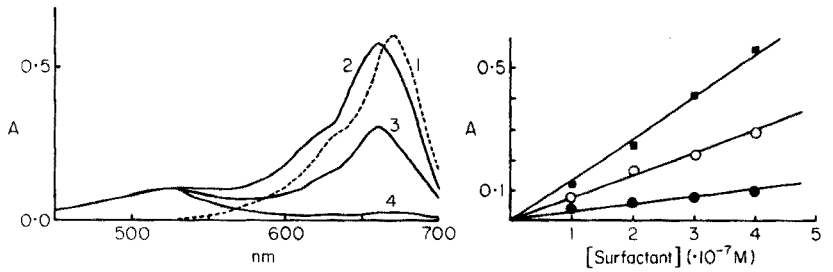

Fig. 1. Absorption spectra of BB in aqueous solution and the BB—AS and BB—ABS complexes in toluene. (1) 10^{-5} M BB in aqueous solution. (2) BB—AS complex in toluene. (3) BB—ABS complex in toluene. (4) Blank for BB in toluene.

Fig. 2. Calibration curves. The absorbance at 660 nm for 5 ml of toluene extract is plotted against the molar concentration of surfactant in 100 ml of solution.

When 10 ml of toluene were used, linear calibration plots were found for the range 0—$1.6 \cdot 10^{-6}$ M surfactant. The calibration curves shown in Fig. 2 were obtained when 5 ml of toluene were used. The order of the apparent molar absorptivities is DESS > LAS > ABS.

Comparison of this method with the methylene blue—chloroform extraction method

In the JIS method [1], the methylene blue solution must previously be washed thoroughly with chloroform to remove colored matter soluble in chloroform, and the methylene blue—surfactant complex extract must be washed with acidic methylene blue solution which has been similarly pretreated. The extraction procedure is repeated and the chloroform extracts are combined. The absorbance at 650 nm in chloroform is then measured.

In the proposed method, pre-extraction of the reagent is eliminated, only one extraction is required, and sensitivity is increased because only 5 ml of toluene is needed for the extraction.

The authors thank the Ministry of Education of Japan for a Scientific Research Grant.

REFERENCES

1 Japanese Industrial Standard Method (JIS) K-0102-1974.
2 Gatterman-Wieland, Die Praxis des organischen Chemikers, Walter de Gruyter, Berlin, 1961, p. 277.

Analytica Chimica Acta, 90 (1977) 323—327

Short Communication

POTASSIUM *O,O*-DI-[4-(1-PHENYL-3-METHYL-4-BENZYLIDENE-PYRAZOLONE-5)] DITHIOPHOSPHATE AS AN ANALYTICAL REAGENT

A. I. BUSEV
Moscow State University, Moscow (U.S.S.R.)
A. K. PANOVA
High Institute of Chemical Technology, Sofia (Bulgaria)
(Received 12th August 1976)

Compounds containing a thiol or thione group are important analytical reagents, often of high sensitivity and selectivity. Their analytical properties may be considerably altered by substituent effects and by changes in molecular structure and reaction conditions. The reagents containing sulphur and phosphorus are particularly promising in this respect.

Dithiophosphates [1] show higher selectivity than H_2S and many other sulphur-containing organic reagents. Several metal ions that form sulphides and dithiocarbamates, namely V(III), Mn(II), Fe(II), Co(II), Zn(II), Ge(IV), Sn(IV), W(III) and Ga(III), are not precipitated with diethyldithiophosphates. A useful analytical property of the dithiophosphates is their high stability in acidic media. Diethyldithiophosphates, except for the dithiophosphates of Cd(II), Fe(III), In(III) and Tl(I), are practically insoluble in concentrated acids.

The derivatives of dithiophosphoric acid are promising for the separation of elements by solvent extraction [2, 3]. The sulphur-containing organophosphorus compounds are more selective extractive reagents than those containing a phosphoryl group. The increase in the hydrocarbon chain-length in dithiophosphoric acid derivatives affects the extractive power of the dithiophosphoric acid extensively. The distribution coefficient increases with the number of carbon atoms; the number of elements that can be extracted is also increased [4].

Of the dithiophosphoric acid derivatives studied, the diethyl and diphenyl derivatives have found the widest analytical application [1, 2, 5]. Other derivatives have also been studied to assess the effect of alkyl and aryl groups on the analytical behaviour of the acid [4—8].

The analytical properties of the heterocyclic derivative of dithiophosphoric acid, prepared on the basis of the OH-tautomeric form of 1-phenyl-3-methyl-4-benzoyl-pyrazolone-5, are described here.

Experimental

The dipyrazolonedithiophosphoric acid ($p_2$dtp) was prepared [9] as follows

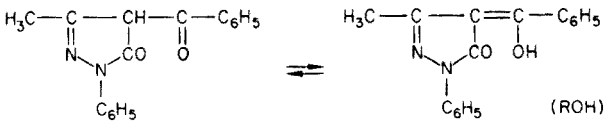

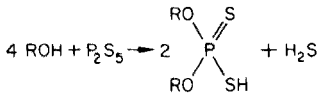

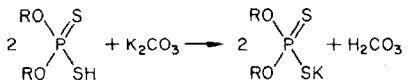

The reactivity of this reagent was studied qualitatively with Ag(I), Pb(II), Hg(I), Hg(II), Cu(II), Cd(II), Bi(III), Sb(III), Sn(II), Ni(II), Co(II), Zn(II), Cr(III), Al(III), Fe(III), Ti(IV), In(III), Ga(III), Sc(II), Pd(II), Ru(II), Au(III) and Te(IV). The interaction of $p_2$dtp with these metal ions is accompanied by the precipitation of coloured, easily coagulated, precipitates that are soluble in polar and apolar organic solvents.

Results and discussion

Unlike the alkyl and aryl dtp derivatives, $p_2$dtp exhibits a dualistic (ambidentate) reactivity. The presence of a carbonylic group allows protonation in comparatively strong acid solutions; a positively charged bulky organic cation is formed, capable of interacting with the negatively charged anionic complexes of the metals, thus forming ion associates. At pH 1 for example, Bi(III) interacts with $p_2$dtp, forming a yellow amorphous precipitate soluble in polar and apolar organic solvents. If $p_2$dtp is added to a solution that contains BiI_4^- (in 2 M $HClO_4$), an orange-red precipitate soluble in polar organic solvents is obtained. The ambidentate reactivity of the reagent widens its application to analytical problems.

The protolytic constant of the reagent was determined in view of other studies [9]. The value obtained (pK = 3.95) supports the conclusion [10] that the dtp acid is intermediate in strength between sulphuric and acetic acids). Compared with the alkyl and aryl dtp derivatives, however, $p_2$dtp is a weaker acid [1]. The increase in electronic density at the sulphur atom of the SH-group is one of the major factors favouring the formation of more stable complexes with metal ions.

The dtp derivatives are suitable reagents for extraction-spectrophotometric determinations [1, 3]. The methods for the determination of Cu(II) [12, 13] Pd(II) [14, 15] and Bi(III) [16] are characterized by high sensitivity and selectivity. The alkyl and aryl dtp derivatives form coloured complexes only

with elements that possess chromophoric properties. Spectrophotometric determination of the colourless dtp complexes in the visible region can be carried out indirectly by the exchange reaction of Cu(II) and the corresponding dtp [14]. Coloured complexes with elements that show no chromophoric properties are given by $p_2$dtp. This makes the reagent more useful for spectrophotometric determinations; the complexes are more stable over periods of time than the aryl and alkyl dtp derivatives. This finding has provided a basis of studying the complexation reactions of $p_2$dtp with Pd(II), Cu(II), Bi(III), Mo(VI) and Mo(V) in more detail for quantitative analytical purposes.

Most of the methods proposed for the spectrophotometric determination of Pd(II) have not found wide application because of insufficient selectivity, the necessity to observe conditions rigourously, and complexity of operation.

P_2dtp interacts with Pd(II) under a wide range of experimental conditions. The sequence and manner of reagent addition and the reaction duration before extraction have no effect on the final result. Palladium(II) is quantitatively extracted in a single stage for 2 min with a 4—5-fold excess of $p_2$dtp over a wide concentration range (1—6 M) of $HClO_4$.

The spectrum of the chloroform extract of the complex displays an absorption maximum at 415 nm, stable overnight. The absorbance of the reagent at this wavelength is negligible (Fig. 1). The determination of Pd(II) with $p_2$dtp is possible in the presence of considerable amounts of Ni, Co, Cr, Fe, Al, Bi, Pb, Cd, As, Sb and Sn.

The data on the interaction of Pd(II) with $p_2$dtp have shown that under the influence of the new substituent (1-phenyl-3-methyl-4-benzoyl-pyrazolone-5), the analytical properties of the dtp acid are considerably improved. The longer chain of conjugated double bonds causes a bathochromic shift from 295 nm (Pd—Et_2dtp and Pd—Ph_2dtp) to 415 nm for Pd—$p_2$dtp. The period of stability of the solvent extracts increases from 90 min for Pd—Ph_2dtp to 24 h for Pd—$p_2$dtp. The efficiency of a single extraction is also increased. The selectivity of the reagent, particularly with respect to Pb, Bi and Fe, is considerably increased (Table 1).

Detailed studies have shown that Cu(II) forms a much more stable complex with $p_2$dtp than with Et_2dtp. The apparent stability constant of Cu(p_2-dtp)$_2$, determined in ethanol—water (1 : 1), is $\log \beta = 17.26$. The stability constant of the complex Cu(Et_2dtp)$_2$, under similar conditions, is $\log \beta = 9.88$ [17].

Quantitative extraction of Cu(II) with $p_2$dtp was obtained in a single stage with a ten-fold excess of the reagent in the pH 2—2 M HCl (H_2SO_4, $HClO_4$) range. Extraction equilibrium was attained in 2 min, and the absorbance of the solutions was constant for 24 h.

On the basis of these results, a comparatively simple and sensitive method for an extraction—spectrophotometric determination of Cu(II) with $p_2$dtp was developed. The determination is possible in the presence of considerable amounts of Pb, Cd, As, Sb, Cr, Mn, Al, and Zn. The method was applied to

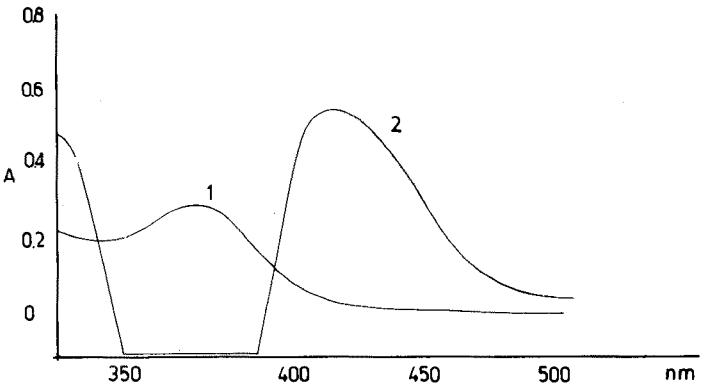

Fig. 1. Absorption spectra. (1) $4 \cdot 10^{-5}$ M K—$p_2$dtp, 2 M $HClO_4$. (2) $4 \cdot 10^{-5}$ M Pd(II), $4 \cdot 10^{-4}$ M K—$p_2$dtp, 2 M $HClO_4$; reference solution, $4 \cdot 10^{-4}$ M K—$p_2$dtp in $CHCl_3$, b = 1 cm.

TABLE 1

Comparative data on the extraction—spectrophotometric determination of Pd(II) with various dtp acid derivatives

	Pd—Et_2dtp	Pd—Ph_2dtp	Pd—$p_2$dtp
λ_{max} (nm)	295	295	415
$\epsilon_{\lambda max}$	$3.1 \cdot 10^4$	$3.35 \cdot 10^4$	$1.75 \cdot 10^4$
(solvent)	(CCl_4)	(CCl_4)	($CHCl_3$)
Acid concn. in aq. phase	1 M HCl	0.3 M HCl	5 M $HClO_4$ (HCl)
Extract stability with time	—	1.5 h	24 h
Selectivity with respect to Pb, Bi, Fe			
Pd : Pb	1 : 1	1 : 1	1 : 1000
Pd : Bi	1 : 1	1 : 1	1 : 100
Pd : Fe	1 : 1	1 : 1	1 : 1000

the determination of small amounts of copper in aluminium; the mean of 6 determinations was 0.907 ± 0.006% (theoretical 0.890%).

The dtp group is an analytical functional group for molybdenum [18], which can be detected in the presence of V, W, U, Zr, Ti, Cr, Mn, and many other elements [19]. The determination of molybdenum with dtp has not been realized previously because the complexes are not stable on standing. Obviously the reduction of molybdenum(VI), as a result of which ill-defined complexes are obtained, is involved.

Studies have shown that $p_2$dtp does not reduce molybdenum(VI) under a wide range of experimental conditions (Mo(VI) concentration, excess of $p_2$dtp, pH, temperature, and time). Thus the determination of molybdenum is possible [20].

REFERENCES

1 A. I. Busev and M. I. Ivanyutin, Tr. Kom. Anal. Khim., Akad. Nauk, S.S.R., 11 (1960) 172.
2 T. H. Handley, Talanta, 12 (1965) 893.
3 H. Bode and W. Arnswald, Z. Anal. Chem., 185 (1962) 179.
4 T. H. Handley and J. Dean, Anal. Chem., 34 (1962) 1312.
5 H. Bode and W. Arnswald, Z. Anal. Chem., 193 (1963) 415.
6 A. I. Busev and M. I. Ivanyutin, Zh. Anal. Khim., 13 (1958) 312.
7 T. H. Handley, R. Zucal and J. Dean, Anal. Chem., 35 (1963) 1163.
8 R. Zucal, J. Dean and T. Handley, Anal. Chem., 35 (1963) 988.
9 A. I. Busev, A. K. Panova and A. N. Shishkov, C. R. Acad. Sci., 27 (1974) 811.
10 C. V. Smalheer and T. W. Mastin, J. Inst. Pet., London, 42 (1956) 337.
11 M. P. Kabachnik and T. A. Mastryukova, Zh. Obshch. Khim., 31 (1961) 140.
12 A. I. Busev and M. I. Ivanyutin, Vestn. Mosk. Univ., Ser. Mat., Fiz. Khim., 51 (1957) 157.
13 A. I. Busev and A. N. Shishkov, Zh. Anal. Khim., 23 (1968) 181.
14 A. I. Busev and M. I. Ivanyutin, Zh. Anal. Khim., 13 (1958) 18.
15 A. I. Busev and A. N. Shishkov, Zh. Anal. Khim., 23 (1968) 1675.
16 M. I. Ivanyutin and A. I. Busev, Nauchn. Dokl. Vyssh. Shk., Khim. Khim. Tekhnol., 1 (1958) 73.
17 K. Burger, E. Papp-Mozual, H. Vasarhelyi-Nagy and L. Korecr, Acta Chim. Sci. Hung., 64 (1970) 323.
18 I. S. Mustafin and L. A. Molot, Organicheskie reactivi, izd. Saratovskogo universiteta, 1967, p. 10.
19 A. I. Busev, Dokl. Akad. Nauk S.S.S.R., 66 (1949) 1093.
20 A. I. Busev and A. K. Panova, C. R. Acad. Sci., 29 (1976) 225.

Analytica Chimica Acta, 90 (1977) 329—334

Short Communication

CATALYTIC TITRATION OF MERCURY(II), IODIDE AND THIOACETAMIDE

T. P. HADJIIOANNOU and E. A. PIPERAKI

University of Athens, Laboratory of Analytical Chemistry, Athens (Greece)

(Received 26th August 1976)

The application of catalyzed reactions for the indication of end-points in titrimetric analysis has increased in recent years [1—12]. Catalytic titrations are ideal for the determination of inhibitors; for example, microgram amounts of mercury(II) can be determined by means of their inhibitory effect on the iodide-catalyzed Ce(IV)—As(III) reaction [1, 2, 4, 7, 8, 10—12]; automation of such titrations has already been described [4]. The present communication reports a modification which provides greater sensitivity; titrations are performed either automatically by using a second derivative technique or semi-automatically by recording the potentiometric or spectrophotometric titration curves. It is also shown that sulfur-containing compounds, such as thioacetamide and thiourea, can be determined indirectly, after alkaline hydrolysis, by adding a known amount of standard mercury(II) solution and back-titrating with standard iodide solution. The back-titration technique is also used for the indirect determination of iodide.

The semi-automatic procedure can be used even with very dilute samples, down to the 10^{-7} M level for mercury(II) and iodide, and 10^{-6} M for thioacetamide, and is simple, accurate and precise. Micro amounts of Hg(II) in the range 0.15—2000 μg, of iodide in the range 0.1—1200 μg, of thioacetamide in the range 0.1—50 μg, and of thiourea in the range 7—50 μg can be determined with relative errors of about 1%.

Experimental

Apparatus. The titration system previously described was used [8, 13]. All titrations were performed at room temperature in a 50-ml beaker.

Reagents. All reagents were prepared in twice-distilled deionized water from reagent-grade materials.

Cerium(IV) and As(III) solutions were prepared as previously reported [8]. An aqueous 0.1 M thioacetamide solution was required. For the murexide indicator, a saturated aqueous solution was prepared fresh daily.

Dilute standard mercury(II) and iodide solutions were prepared from stock 0.00500 M mercury(II) chloride and 0.0600 M potassium iodide solutions daily. The very dilute solutions ($< 10^{-6}$ M) were prepared just before measurements, to avoid losses [14].

Preparation of equipment. Fill the burette with the appropriate standard iodide solution, depending on the mercury(II) concentration of the sample. For automatic potentiometric titrations turn the span switch to the position 200 mV, and for semi-automatic potentiometric titrations to the positions 500, 200, 100 and 100 or 50 mV for the ranges $5 \cdot 10^{-6}$—$5 \cdot 10^{-4}$, $5 \cdot 10^{-7}$—$5 \cdot 10^{-6}$, $2.5 \cdot 10^{-7}$—$5 \cdot 10^{-7}$ and $4 \cdot 10^{-8}$—$2.5 \cdot 10^{-7}$ M mercury(II), respectively. In all cases, turn the lower pH index switch to the appropriate position to bring the pen on scale. For spectrophotometric titrations work as previously reported [8] but turn the span switch to the position 250 mV.

Semi-automatic titration of mercury(II). Pipette into a 50-ml beaker a 20.00-ml aliquot of the sample, 5.00 ml of 1 M sulfuric acid, 1.00 ml of the arsenic(III) solution and 1.00 ml of the cerium(IV) solution. Lock the burette "ON" and start the stirrer. After the pen has stabilized (5—30 s), turn the function switch to "Record" to obtain the titration curve. For the best accuracy, calibrate the recorder for each titration, using the burette reading.

Automatic titration of mercury(II). Proceed as for the semi-automatic potentiometric titration, but at the beginning turn the function switch to "Measure" and start the titration by pushing the "automatic" button. Automatic termination occurs at the end-point.

Semi-automatic titration of iodide. Pipette into a 50-ml beaker a 10.00-ml aliquot of the sample and a known amount of standard mercury(II) solution; dilute to 20 ml and continue as in the semi-automatic titration of mercury(II) from the point of sulfuric acid addition. To estimate the amount of standard mercury(II) solution to be added, add a drop of murexide indicator to the sample, and then slowly add the standard mercury(II) solution until the color changes from violet to yellowish; then add 2.0 ml in excess. An iodide-selective electrode can also be used.

Semi-automatic titration of thioacetamide. Mix a 10.00-ml aliquot of the sample with 2.00 ml of 0.001 M NaOH and heat the mixture for a few minutes at 60—70° C to hydrolyze the thioacetamide. Cool the solution and continue as in the semi-automatic determination of iodide from the point of mercury(II) addition.

RESULTS AND DISCUSSION

Ions which react with iodide to form precipitates or strong complexes, e.g. Ag(I), Pd, Au(III), etc., and strong oxidants which could oxidize iodide must be absent.

The indicator reaction can be followed either with a platinum electrode which responds rapidly to changes in concentrations of the Ce(IV)—As(III) mixture or spectrophotometrically by monitoring the decrease in absorbance at 390 nm caused by the reduction of Ce(IV). During the titration iodide reacts with the inhibitor (Hg II) and the signal remains almost constant (it may change very slowly because of the uncatalyzed reaction) until the equivalence point is reached; at that point a small excess of titrant results in

large changes in the rate of the indicator reaction and therefore in sharp changes in the signal level which can be easily detected. Recorded curves for the semi-automatic titration of mercury(II) with iodide are shown in Fig. 1. The end-point was obtained by extrapolating the linear segments of the titration curve.

Working curves are obtained by plotting the end-point volumes against the amount of mercury(II). They were made to read molar concentrations or micrograms of mercury(II) in the titrated sample (20 ml). Three standard mercury(II) solutions suffice for each working curve. These plots are linear for all the concentration ranges tested. For reproducibility, it is essential to maintain all working conditions constant. The mercury(II) concentration can also be found by the proportional method [8].

Results for aqueous mercury(II) solutions of known concentrations are shown in Table 1. In the proportional method, the unknown and the control had the same mercury(II) concentration. The results indicate that micro amounts of mercury(II) in the range 0.15—2000 μg in a total volume of 27 ml can be determined semi-automatically with relative errors of less than 1% and relative standard deviations of about 0.6%. The semi-automatic method provided the best accuracy but took longer than the automatic method. Accuracy and precision were about the same for the potentiometric and spectrophotometric methods. The highly sensitive and accurate method may be adapted to many specific cases, e.g., mercury(II) in fish, sea water etc.

Results for aqueous iodide solutions of known concentrations are given in Table 2. Iodide is calculated by subtracting the excess of mercury(II) back-titrated from the known amount of mercury(II) added to the iodide sample. With the proportional method either a separate iodide standard was used for each iodide sample or a common iodide standard was used for samples covering a decade of concentrations. The first approach gave more accurate results (about 1% vs. 2% for the second approach) but took longer. Accuracy

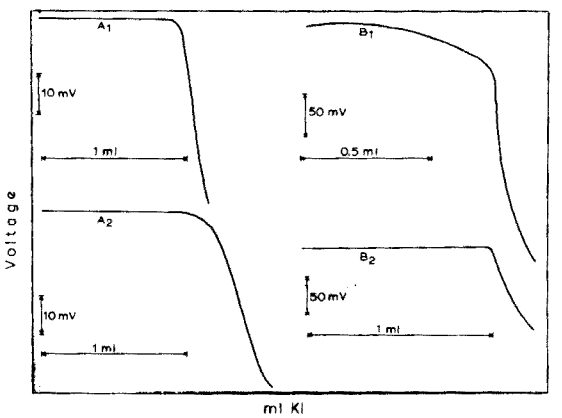

Fig. 1. Recorded curves for the semi-automatic spectrophotometric (A) and potentiometric (B) titration of mercury(II) with iodide. A_1 and B_1: 20 ml of $1.2 \cdot 10^{-4}$ M Hg(II) titrated with $6 \cdot 10^{-3}$ M KI. A_2 and B_2: 20 ml of $1.2 \cdot 10^{-5}$ M Hg(II) titrated with $6 \cdot 10^{-4}$ M KI.

TABLE 1

Catalytic titration of mercury(II) with potassium iodide

KI titrant (M)	Hg(II) range taken (μg)	% Error		s_r (%)
		Working curve	Proportional method	
Automatic potentiometric method (n = 5)				
$6 \cdot 10^{-6}$	0.5—2	1.8	3.0	6.6 (0.5)[a]
$6 \cdot 10^{-5}$	3—20	1.1	1.5	2.6 (3)
$6 \cdot 10^{-4}$	30—200	2.2	0.3	0.5(30)
	Av.	1.7	1.6	3.2
Semi-automatic potentiometric method (n = 5)				
$3 \cdot 10^{-6}$	0.15—1	3.4	0.6	0.6 (0.25)
$6 \cdot 10^{-6}$	0.3—2	1.3	1.3	0.5 (0.5)
$6 \cdot 10^{-5}$	3—20	1.4	1.3	0.5 (5)
$6 \cdot 10^{-4}$	30—200	0.1	0.4	0.2 (50)
$6 \cdot 10^{-3}$	300—2000	0.3	0.3	0.5 (500)
	Av.	1.3	0.8	0.5
Semi-automatic spectrophotometric method (n = 4—9)				
$3 \cdot 10^{-6}$	0.15—0.5	—	0.2	0.9 (0.15)
$6 \cdot 10^{-6}$	0.5—2	0.6	0.5	0.8 (0.5)
$6 \cdot 10^{-5}$	3—20	1.5	1.0	0.5 (5)
$6 \cdot 10^{-4}$	30—200	0.6	0.4	0.5 (50)
$6 \cdot 10^{-3}$	300—2000	0.1	1.0	0.7 (500)
	Av.	0.7	0.6	0.7

[a]The numbers in brackets are μg Hg.

and precision were about the same for the potentiometric and spectrophotometric methods. The results indicate that micro amounts of iodide on the range 0.1—1200 μg in a total volume of 27 ml can be determined with a precision of about 1%.

Thioacetamide is a widely used reagent in both qualitative and quantitative analysis, being determined titrimetrically [15—17]. Thioacetamide hydrolyzes forming sulfide ions, and since mercury(II) forms a very insoluble sulfide ($K_{so} = 10^{-54}$) thioacetamide can be determined by indirect catalytic titration of the sulfide ions produced during its hydrolysis. Hydrolysis in alkaline medium is faster than in acidic solutions [18, 19]. Results for aqueous thioacetamide solution of known concentrations are given in Table 3. Accuracy was better when dilute thioacetamide solutions (10^{-7}—$7 \cdot 10^{-5}$ M) were prepared by dilution from hydrolyzed concentrated thioacetamide solutions (10^{-2} M) than when dilute thioacetamide solutions (10^{-6}—$4 \cdot 10^{-5}$ M were hydrolyzed and subsequently titrated. The results indicate that micro amounts of thioacetamide in the range 0.1—50 μg in a total volume of 27 ml can be determined with an accuracy and precision of 1—2 %.

TABLE 2

Indirect semi-automatic titration of potassium iodide

KI titrant (M)	Iodide taken (μg) range	% Error		s_r (%) (n = 5, 6)
		Separate standard	Common standard	
Potentiometric method				
$6 \cdot 10^{-6}$	0.13—1	1.2	3.0	1.7 (0.38)[a]
$2 \cdot 10^{-5}$	1.3—9	0.7	1.3	0.3 (3.8)
$2 \cdot 10^{-4}$	13—90	0.4	2.7	0.4 (38)
$2 \cdot 10^{-3}$	130—1140	1.5	1.2	1.0 (380)
	Av.	1.0	2.0	0.8
Spectrophotometric method				
$6 \cdot 10^{-6}$	0.13—1	3.1	4.1	1.2 (0.25)
$2 \cdot 10^{-5}$	1.3—9	0.6	0.7	
$2 \cdot 10^{-4}$	13—90	0.7	1.5	0.6 (25)
$2 \cdot 10^{-3}$	130—1140	0.5	1.4	0.6 (254)
	Av.	1.2	1.9	0.8

[a] The numbers in brackets are μg I^-.

TABLE 3

Indirect semi-automatic potentiometric titration of thioacetamide

KI titrant (M)	Thioacetamide taken (μg) range	% Error		s_r (%) (n = 5)
		Working curve	Proportional method	
$3 \cdot 10^{-5}$	0.1—0.5		0.7[a]	1.8 (0.3)[a]
$6 \cdot 10^{-5}$	0.7—5.3		0.6[a]	0.5[a] (3)
	1.5—3	4.2[b]	1.8[b]	1.3[b] (2.3)
$6 \cdot 10^{-4}$	7.5—53		0.5[a]	0.6[a] (30)
	7.5—53	1.9[b]	2.4[b]	1.5[b] (23)

[a] Titration of thioacetamide solutions prepared by dilution from hydrolyzed 0.01 M thioacetamide solutions. The numbers in brackets are μg TAA.
[b] Titration of hydrolyzed dilute (10^{-6}—$4 \cdot 10^{-5}$ M) thioacetamide solutions.

In a similar way, thiourea was determined in dilute solutions (10^{-6}—10^{-5} M) prepared by dilution from hydrolyzed 0.01 M thiourea solution with relative errors of about 1%. Titration of hydrolyzed dilute (10^{-6}—10^{-5} M) thiourea solutions gave erratic results, because of incomplete hydrolysis.

REFERENCES

1 K. B. Yatsimirskii, Kinetic Methods of Analysis, Pergamon Press, Oxford, 1966.
2 H. Weisz and D. Klockow, Z. Anal. Chem., 232 (1967) 321.
3 H. Weisz, T. Kiss and D. Klockow, Z. Anal. Chem., 247 (1969) 248.
4 H. Weisz, S. Pantel and H. Ludwig, Z. Anal. Chem., 262 (1972) 269.
5 H. Weisz and S. Pantel, Anal. Chim. Acta, 62 (1972) 361.
6 T. Kiss, Z. Anal. Chem., 252 (1970) 12.
7 K. C. Burton and H. M. N. H. Irving, Anal. Chim. Acta, 52 (1970) 441.
8 T. P. Hadjiioannou, E. A. Piperaki and D. S. Papastathopoulos, Anal. Chim. Acta, 68 (1974) 447.
9 T. P. Hadjiioannou, M. A. Koupparis and C. E. Efstathiou, Anal. Chim. Acta, 88 (1977) 281.
10 T. P. Hadjiioannou and M. M. Timotheou, Mikrochim. Acta, in press.
11 T. P. Hadjiioannou, Rev. Anal. Chem., 3 (1976) 82.
12 H. A. Mottola, CRC Crit. Rev. Anal. Chem., 4 (1975) 229.
13 T. P. Hadjiioannou and D. S. Papastathopoulos, Talanta, 17 (1970) 399.
14 R. V. Coyne and J. A. Collins, Anal. Chem., 44 (1972) 1093.
15 T. J. Jacob and C. C. R. Nair, Talanta, 13 (1966) 154.
16 R. J. Thibert and M. Sarwar, Microchem. J., 14 (1969) 271.
17 M. K. Papay, K. Toth, V. Izvekov and E. Pungor, Anal. Chim. Acta, 64 (1973) 409.
18 A. W. Butler, D. G. Peters and E. H. Swift, Anal. Chem., 30 (1958) 1379.
19 E. H. Swift and F. C. Anson, Advances in Analytical Chemistry and Instrumentation, Vol. 1, Interscience, New York, 1960.

Analytica Chimica Acta, 90 (1977) 335—338

Short Communication

THE THIO-AZOMETHINE-FERROINE GROUP AS A NEW FUNCTIONAL GROUP FOR IRON(II): DETERMINATION OF IRON WITH 2-ACETYL-PYRIDINE-4-PHENYL-3-THIOSEMICARBAZONE

M. T. MARTINEZ AGUILAR, J. M. CANO PAVON and F. PINO

Department of Analytical Chemistry, Faculty of Sciences, University of Seville (Spain)

(Received 7th September 1976)

In recent years, diverse thio and phenylthiosemicarbazones have been proposed as spectrophotometric reagents for iron(II), e.g. picolinaldehyde thiosemicarbazone [1], 3-hydroxy-picolinaldehyde thiosemicarbazone [2], bipyridylglyoxal dithiosemicarbazone [3], picolinaldehyde phenylthiosemicarbazone [4], 1,2-cyclohexanedione dithiosemicarbazone [5], and picolinaldehyde selenosemicarbazone [6]. The green complexes formed with iron(II) show similar absorption maxima between 600 and 650 nm. With iron(III), yellow complexes are formed in all cases.

Various other new reagents with this functional group for iron(II) are possible. The use of 2-acetylpyridine-4-phenyl-3-thiosemicarbazone (APPT) as a spectrophotometric reagent for iron(II) and (III) is described below. The results obtained with APPT and other similar reagents are compared and the characteristics of this functional grouping are discussed.

Experimental

Apparatus and reagents. Unicam SP 8000 and SP 600s-2 spectrophotometers and a Coleman 55 (digital) spectrophotometer, equipped with 1.0-cm glass or quartz cells, as well as a digital pH meter (Philips PW 9408) with glass-calomel electrodes, were used.

2-Acetylpyridine-4-phenyl-3-thiosemicarbazone (0.1% w/v) was used in dimethylformamide solution. This solution was stable for 1 week.

All solvents and reagents were of analytical grade.

Synthesis of the reagent. Dissolve 1.45 g of 2-acetylpyridine in 25 ml of ethanol and add to 2.0 g of 4-phenyl-3-thiosemicarbazide dissolved in 75 ml of hot ethanol. Reflux for 2 h, and then cool to room temperature. Filter off the yellow crystals and recrystallize twice from ethanol (yield 43%, m.p. 187—189°C). Analytical results: 62.0% C, 5.3% H, 21.0% N, 11.9% S; calculated for $C_{14}H_{14}N_4S$: 62.2% C, 5.2% H, 20.7% N, 11.8% S.

Procedure for determination as iron(II). To the aqueous iron(II) or (III) solution (20—90 μg) in a separating funnel, add 2 ml of the APPT solution, 0.05 g of ascorbic acid and 2 ml of buffer solution, and dilute to 10 ml with

distilled water. Extract with 10 ml of benzene, by shaking vigorously for 2 min, allow the phases to separate, and transfer the organic phase to a 25-ml flask containing anhydrous sodium sulphate. Measure the absorbance of the green extract at 650 nm, against water, 15 min after extraction ($\epsilon = 6.8 \cdot 10^3$ l mol^{-1} cm^{-1}).

Beer's law holds for 2—9 p.p.m. of iron(II); the optimum concentration range is 3—7 p.p.m., the relative error (P = 0.05) being ± 0.48%. Interferences are Co(II), Cu(II), Ni(II), Zn(II), Pd(II), Hg(II) and EDTA (< 5 p.p.m.); Ag(I) Pb(II), and Cd(II) (> 25 p.p.m.); Pt(IV), Au(III) and Cr(III) (> 50 p.p.m.).

Procedure for determination as iron(III). To the iron(III) solution (10—100 μg) in a 50-ml volumetric flask, add 15 ml of the APPT solution, and adjust the pH to 5.0—6.0 with an acetate buffer solution. Dilute with distilled water, and measure the absorbance at 395 nm, against a reagent blank ($\epsilon = 2.4 \cdot 10^4$ l mol^{-1} cm^{-1}).

Beer's law holds for 0.2—2 p.p.m. of iron(III); the optimum concentration range is 0.6—1.8 p.p.m., the relative error (P = 0.05) being ± 0.52%. Interferences are Ag(I), Pb(II), Hg(II), Cu(II), Cd(II), Bi(III), Pd(II), Sb(III), Sn(II) Pt(IV), Au(III), V(V), Mn(II), Ni(II), Co(II), and Zn(II) (< 5 p.p.m.); Mo(VI) and Ce(IV) (> 10 p.p.m.); W(VI) and Zr(IV) (> 50 p.p.m.).

Results and discussion

APPT is sparingly soluble in water, moderately soluble in ethanol (1.11 g l^{-1}), amyl alcohol (0.82 g l^{-1}) and carbon tetrachloride (1.18 g l^{-1}), and very soluble in chloroform (9.84 g l^{-1}), nitrobenzene (10.01 g l^{-1}) and dimethylformamide (> 47.26 g l^{-1}), at room temperature. Acid dissociation constants of the reagent (average pK values) were found to be 4.13 (pyridinium-N), and 11.03 (—SH group) at 25 °C and ionic strength 0.1.

The most sensitive reactions of APPT were shown for Fe(II) and (III), Co(II), Ni and Cu(II), which formed intensely coloured solutions under favourable conditions. Maximal absorption bands appeared between 380 and 450 nm (yellow), except for iron(II) (green).

Reaction of iron(II) and iron(III) with APPT. Iron(II) forms a green complex (λ_{max}, 610 nm) with APPT at certain pH values, and iron(III) forms a yellow complex (λ_{max} 390 nm) with a high absorptivity (Fig. 1). The green complex is formed immediately in homogeneous solutions, but is oxidized in a few minutes by atmospheric oxygen to the yellow iron(III) complex. Ascorbic acid (0.15 g in a sample of 50 ml) prevents the oxidation, although the absorption of the solutions decreases, because of precipitation of the complex. However, this complex can be extracted into benzene, in which the absorbance remains constant for at least 3 h; there is a bathochromic shift from 610 to 650 nm.

The optimum pH range for the formation of the green complex is 5.6—9.8 in a homogeneous medium, and 4.9—11.0 in the benzene phase; for the yellow iron(III) complex, the range is 3.4—7.8. In all cases, outside these pH ranges the absorbances decrease swiftly.

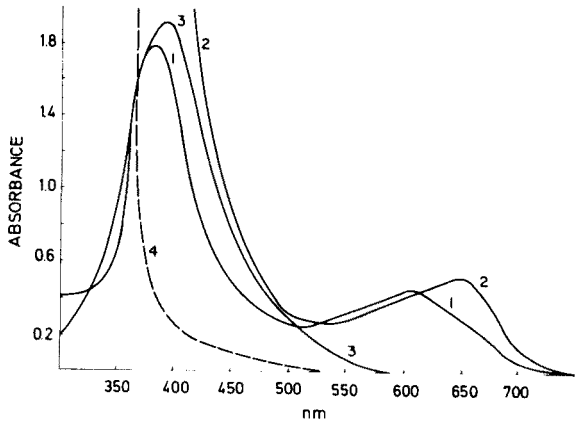

Fig. 1. Absorption spectra of solutions of iron—APPT complexes (5 p.p.m. in each case). (1) Fe(II)—APPT in homogeneous medium (pH 6.0). (2) Fe(II)—APPT extracted into benzene. (3) Fe(III)—APPT in homogeneous medium (pH 5.0). (4) Reagent alone.

The metal—ligand stoicheiometric ratios obtained by the continuous variations methods are 1 : 2 in both cases.

Comparison with other thiosemicarbazones and phenylthiosemicarbazones with the same selective group

The grouping —N=C—C=N—N=C(—S)— (thio-azomethine-ferroine group) may be considered as a new functional group for iron(II); the wavelength of maximum absorption is more favourable (600—650 nm) than with the classical ferroine group. This group is contained in thio- and phenylthio-semicarbazones of picolinaldehyde, and related aldehydes and ketones, as well as in the *vic*-dithiosemicarbazones. The maximum wavelengths and molar absorptivities are compared in Table 1. The molar ratios for these complexes are 1 : 2 metal ion-reagent in all cases, except for bipyridylglyoxal dithiosemicarbazone (1 : 1) [3] because it contains basically two molecules of picolinaldehyde thiosemicarbazone. These complexes are neutral, and are not retained by cation- or anion-exchange resins, whereas the iron(III) complexes are retained by a cationic resin. The structure of the green iron(II) complexes is probably

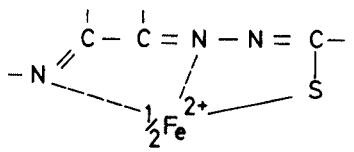

Picolinaldehyde selenosemicarbazone [6] shows a similar behaviour; but when the S atom is replaced by oxygen (picolinaldehyde semicarbazone [7]) the green iron(II) complex is not formed.

TABLE 1

Comparison of iron(II) complexes

Reagent	λ_{max}(nm)	ϵ (l mol^{-1} cm^{-1})	Medium
Picolinaldehyde thiosemicarbazone	610	5800	Water—ethanol 4 : 1
3-Hydroxypicolinaldehyde thiosemicarbazone	600	7500	Water—ethanol 4 : 1
Picolinaldehyde phenylthiosemicarbazone	625	6400	Water—DMF 3 : 2
Bipyridylglyoxal dithiosemicarbazone	610	7140	Water—ethanol 3.5 : 1.5.
1,2-Cyclohexanedione dithiosemicarbazone	640	4700	Water—DMF 9 : 1.
Picolinaldehyde selenosemicarbazone	615	6900	Water—ethanol 4 : 1.
APPT	650	6800	Benzene

The yellow iron(III) complexes of these compounds have absorption maxima between 360 and 400 nm, and molar absorptivities between $1.4 \cdot 10^4$ and $3.56 \cdot 10^4$ l mol^{-1} cm^{-1}.

The thio-azomethine-ferroine group is not specific, since octahedral complexes are formed with other metal ions, especially Ni(II) and Co(II), but these complexes are yellow. The wavelength of maximum absorption of the iron(II) complexes allows the determination of iron in the presence of diverse metal ions. The rate of atmospheric oxidation of the green complexes decreas appreciably in alkaline medium in all cases. Addition of ascorbic acid prevents the oxidation; hydroxylamine and hydrazine sulphate cannot be used because of the C=N exchange reaction.

The green iron(II) complexes are not very soluble in aqueous ethanol or aqueous dimethylformamide, so that extraction into organic solvents with small dielectric constants is often necessary. The complexes of phenylthiosemicarbazones are soluble in benzene, whereas the thiosemicarbazone complexes are insoluble in benzene, but soluble in chloroform.

The different compounds tested for the behaviour of this functional group with iron(II) show small variations in selectivity and sensitivity; phenylthiosemicarbazones give small increases in molar absorptivity, and a slight bathochromic shift.

APPT shows a sensitivity similar to that of the other thiosemicarbazones, but the methyl group decreases the selectivity. Nevertheless, determinations of iron(II) and (III) are feasible.

REFERENCES

1 J. M. Cano Pavón, D. P. Bendito and F. Pino, An. Quim., 167 (1971) 299.
2 J. M. Cano Pavón, A. Lavado and F. Pino, Mikrochim. Acta, in press.
3 J. L. López Bahamonde, D. P. Bendito and F. Pino, Talanta, 20 (1973) 694.
4 J. L. Gómez Ariza and J. M. Cano Pavón, unpublished results.
5 J. A. Muñoz Leyva, J. M. Cano Pavón and F. Pino, Inf. Quim. Anal., 28 (1974) 90.
6 J. M. Cano Pavón and F. Pino, Talanta, 19 (1972) 1659.
7 M. P. Martínez, D. P. Bendito and F. Pino, An. Quim., 69 (1973) 747.

Analytica Chimica Acta, 90 (1977) 339—341

Short Communication

THE FLUORIMETRIC DETERMINATION OF BORON BY MEANS OF THE BORIC ACID—MORIN—OXALIC ACID COMPLEX IN ANHYDROUS ACETIC ACID MEDIUM

WŁODZIMIERZ TKACZ and LEON PSZONICKI

Institute of Nuclear Research, 03 195-Warsaw-91 (Poland)

(Received 18th July 1976)

The structure and properties of the fluorescent binary and ternary complexes of boric acid with morin or quercetin and oxalic acid in anhydrous acetic acid medium have been reported recently [1]. The very good detection limit for boron (0.1 ng ml^{-1}) and the reproducibility of the fluorimetric measurements with the ternary morin complex indicated that these ternary compounds could be applied to fluorimetric determination of nanogram amounts of boron. Moreover, the simple procedure and high efficiency of the complex formation suggested that this method should be more effective than the methods based on formation of similar compounds in aqueous solutions [2, 3]. The main problem with the proposed method is the transfer of boron from the sample to an anhydrous acetic acid solution. The most effective separation of boron from interfering species involves distillation of trimethyl borate followed by its absorption and hydrolysis in alkaline solution. This solution can be evaporated to dryness and the residue dissolved in anhydrous acetic acid. However, this solution cannot be used directly for the fluorimetric determination because of the quenching effects of alkali metals. It was found that the alkali metals can be removed from samples containing nanogram amounts of boron with an ion-exchange resin, if the distilled trimethyl borate is absorbed in as little sodium carbonate solution as possible [3, 4]. The yield of this distillation procedure is at least 90%, which is acceptable for such a low concentration level.

Experimental

Apparatus. A Spekker photometer H-760 was used with a special fluorimetric photomultiplier attachment [5]; a scintillation counter with integrator was also used. The silica columns (8 mm i.d.) were fitted with stopcocks. Silica glassware was used throughout.

Reagents. Boric acid and morin stock solutions, as well as the oxalic acid and anhydrous acetic acid, were prepared as described previously [1]. Solutions (0.05 M) of alkali metals were prepared by dissolving the requisite amounts of the acetate salts in anhydrous acetic acid. The Dowex 50W-X8 ion exchanger was used in the acidic form (200-275 mesh). Methanol was purified by distillation over mannitol and potassium hydroxide. The tracer ^{24}Na was obtained as sodium acetate in anhydrous acetic acid. The fluorescence

standard was a $1 \cdot 10^{-6}$ M solution of 3-aminophthalimide in 0.05 M sulfuric acid.

Distilled water was prepared by double-stage distillation in silica apparatus of glass-distilled water. All chemicals used were reagent grade.

Preparation of the column. Place a 5-cm bed of resin in the column and treat with 20 ml of 4 M hydrochloric acid. Then wash the resin with water until the pH of the eluate is constant. Immediately before the separation, pass two 25-ml portions of anhydrous acetic acid through the resin.

Procedure. Dissolve the sample, containing 0.005—0.2 μg of boron, in 5 ml of 5 M sulfuric acid, transfer to a small silica distillation flask, add 10 ml of methanol, and heat slowly while bubbling simultaneously the methanol vapour through the sample solution. Absorb the distillate emerging from a drawn-out tube, in 3ml of 0.05 M sodium carbonate cooled in an ice bath until the final volume is about 15 ml. Evaporate the solution slowly to dryness on an air bath and dissolve the residue in 1 ml of anhydrous acetic acid. Transfer this solution to the column, rinse the dish with two 1-ml portions of anhydrous acetic acid, add the washings to the column, and add 2 ml of acetic acid directly to the column. The flow rate is 0.5 ml min^{-1}. Collect 5 ml of the eluate in a 25-ml volumetric flask. For very small amounts of boron in the range 0.005—0.05 μg, use a 10-ml flask. To the eluate, add 1 ml of solution containing 500 mg of morin followed by 10 mg of dry powdered oxalic acid. Stopper the flask, leave at room temperature for 20 min, and dilute to the mark with anhydrous acetic acid. Measure the fluorescence with 3-aminophthalimide as standard. Prepare a blank in the same manner. Calculate the results as the average value of three determinations.

Results and discussion

The fluorescence of the boric acid—morin—oxalic acid complex is strongly quenched by alkali metals (Table 1). Similar results were obtained when the alkali metals were added to solutions containing the complex already formed. This is probably caused by reaction of the alkali metals with the 4′-carbonyl group of morin and the formation of compounds of the phenolate type. This reaction eliminates from the complex molecule the conjugated double bonds that provide the fluorescence emission. The situation is analogous to the sodium quenching of the boron—curcumin complex [6].

Sodium as well as other alkali metals can be separated from boron and removed from anhydrous acetic acid solution with the ion-exchanger Dowex 50W-X8. Sodium ions are completely adsorbed whilst the boron passes through in the first few ml of eluate and is recovered quantitatively from the sample being separated. The separation of sodium was checked with radioactive tracer ^{24}Na. The proposed procedure allowed the separation of up to 10 mg of sodium; larger amounts were not investigated but it seems, on the basis of column volume and capacity, that five-fold quantities should be separated. A disadvantage of the method is that the ion exchanger can be used only once. After regeneration with hydrochloric acid, the boron is partially adsorbed by the resin.

TABLE 1

The quenching effect of alkali metals (0.1 mmol) on the fluorescence intensity for 8 ng ml^{-1} of boron

Species	F.i.	Quenching %	Species	F.i.	Quenching %
—	1270	0	K	305	76.0
Li	280	78.0	Cs	300	76.4
Na	320	74.8	NH_4^+	100	92.0

When fresh resin was used, total recovery of boron was obtained. The results of boron recovery from fresh and repeatedly regenerated resin are presented in Table 2; the losses observed with regenerated resin are probably caused by deterioration of the resin structure in anhydrous acetic acid. The recovery of boron from the column separation process (without the distillation step) was established by comparison of the fluorescence intensity of the separated sample, with the fluorescence intensity of corresponding amounts of boron in pure solution.

The proposed method gives a linear response of fluorescence intensities for the range 0.2—8 ng B ml^{-1} in the solution measured. The limit of detection is on the level of the standard sample without sodium [1] and is 0.1 ng B ml^{-1} in the solution measured. The relative standard deviation calculated from ten determinations of boron at the 8 ng ml^{-1} level is 3%.

TABLE 2

The recovery of boron with regenerated resin

No. of regenerations	0	1	2	3
Recovery (%)	100.0	80.3	68.9	63.0

REFERENCES

1 L. Pszonicki and W. Tkacz, Anal. Chim. Acta, 87 (1976) 177.
2 A. Murata and F. Yamauchi, J. Chem. Soc. Jpn., Pure Chem. Soc., 79 (1958) 231.
3 J. Dabrowski and L. Pszonicki, Chem. Anal. (Warsaw), 16 (1971) 51.
4 G. S. Spicer and J. D. H. Strickland, Anal. Chim. Acta, 18 (1958) 523.
5 L. Pszonicki, Chem. Anal. (Warsaw), 12 (1967) 431.
6 D. W. Dyrssen, J. P. Nowikow and L. R. Uppström, Anal. Chim. Acta, 60 (1972) 139.

Analytica Chimica Acta, 90 (1977) 343—347

Short Communication

A SOLVENT EXTRACTION METHOD FOR THE SPECTROPHOTOMETRIC DETERMINATION OF SULPHATE

W. W. FLYNN

AAEC Research Establishment, Private Mail Bag, Sutherland, N.S.W. 2232 (Australia)

(Received 4th November 1976)

For many years the determination of sulphate has depended on precipitation of barium sulphate from hydrochloric acid solution. This method is subject to many sources of error, both positive and negative, e.g. co-precipitation, occlusion, and interference by the formation of heavy metal sulphates. A typical gravimetric analysis takes ca. 4 h to complete; the accuracy is questionable when amounts of sulphate lower than 10 mg are determined. Essentially the same method is used in the turbidimetric procedure of Thomas and Cotton [1] which lowers the minimum detectable concentration of sulphate to about 1.0 mg l^{-1} for water analysis. The absorbance of the barium sulphate suspension is measured and the sulphate ion determined from a standard curve. Many similar procedures have been suggested, but the method calls for considerable skill on the part of the analyst; coloured samples and those containing suspended material are particularly prone to interference effects.

Bertolacini and Barney [2] proposed a spectrophotometric determination of sulphate based on the reaction of solid barium chloranilate with sulphate to give barium sulphate and chloranilate. The colour development of the chloranilate depends on the removal of interfering cations by ion exchange.

The spectrophotometric method developed in this laboratory, based on the extraction of sulphate ion with methyltricaprylammonium chloride (Aliquat 336), requires no precipitation. The sulphate is stripped from the extractant with hydrochloric acid and the solution is evaporated to dryness on a water bath; the sulphuric acid so obtained is then determined by measuring the hydrogen ion concentration with cresol red indicator. The method is rapid and accurate; only a minimum of preparation is necessary before extraction. Sulphate can be determined in the presence of many foreign ions to a minimum detectable limit of 0.5 mg.

Experimental

Apparatus. A Unicam SP 600 spectrophotometer was used with 1-cm cells.

Sulphuric acid standard solution (4.80 mg sulphate ml^{-1}). Dilute a standardized concentrated volumetric solution with demineralized water to obtain a 0.05 M solution.

Aliquat 336 extraction solution, 20%. Dilute 200 ml of Aliquat 336 (General Mills Inc., Kankakee, Illinois) to 1.0 l with cyclohexane containing 5% (w/v) of phenol.

Cresol red indicator solution, 0.05%. Weigh accurately 0.25 g of cresol red into a 250-ml beaker, add 125 ml of methanol and stir until dissolved. Transfer to a 500-ml volumetric flask and dilute to volume with demineralized water.

Procedure. Take a sample aliquot containing less than 10 mg of sulphate and ensure that the pH is in the range 2—6. Adjust the pH by adding sodium hydroxide or hydrochloric acid to a maximum of 2.5 mmol or, preferably, by diluting with demineralized water to a maximum of 800 ml. Where solutions contain large quantities of hydrochloric or nitric acid, evaporation of the solution to about 5 ml on a hot plate, followed by evaporation to dryness on a water bath, will minimize interference. Transfer the solution to a 500-ml separating funnel, add 100 ml of Aliquat 336 solution, then adjust the total volume of solution with demineralized water until the level is within about 2 ml of the maximum funnel volume. Shake gently for 2 min, allow to settle, and discard the aqueous phase. Wash the organic phase with 25 ml of 0.01 M hydrochloric acid by shaking gently for 1 min, allow to settle, and discard the wash solution. Add 25 ml of 3 M HCl solution, shake gently for 2 min, allow to settle, and transfer the hydrochloric acid strip solution to a 100-ml separating funnel. Repeat the sulphate strip with another 25 ml of 3 M HCl, and then discard the organic phase. Wash the combined strip solution with 25 ml of di-isopropyl ether and, after phase separation, run the aqueous solution into a 100-ml beaker, discarding the ether.

Place the beaker on a water bath until the ether has evaporated; then transfer to a hot plate to reduce the volume to about 5 ml. Evaporate the remaining solution to residual H_2SO_4 on a water bath, and leave for 30 min to ensure that all the hydrochloric acid has evaporated. Quantitatively transfer the sulphate to a 50-ml volumetric flask with demineralized water. Add 10 ml of cresol red indicator solution and dilute to volume. Read the absorbance at 520 nm in 1-cm cells against a blank solution of demineralized water with the same amount of indicator. Obtain the sulphate concentration from a curve previously prepared from standard sulphuric acid solutions.

Discussion

This method was developed from earlier investigations of an extraction procedure for the determination of sulphur-35 in reactor effluent. Separation of the sulphate from the hydrochloric acid strip solution is based on the different boiling points of sulphuric and hydrochloric acids. Experiments showed no loss of a standard sulphuric acid solution, containing 30 mg of sulphate, on a water bath for 24 h at 80—90° C. Hydrochloric acid solutions were evaporated at the same temperature; 15 min after reaching dryness there was no evidence of HCl.

The hydrogen ion concentration was determined colorimetrically with a pH indicator. Cresol red was suitable for the detection of the low concentrations of hydrogen ion associated with sulphate in milligram quantities; 10 ml of 0.05% cresol red solution in 50-ml volume gave a molar absorptivity of 305 in the range 0—10 mg of sulphate against a blank of demineralized water with the same amount of indicator. The absorptivity depends on the amount of indicator used; solutions containing 50—100 mg of sulphate can be accurately determined with 2.0 ml of 0.05% cresol red. Maximum absorbance was obtained at 520 nm and was stable for at least 1 h; only a 4% drop was observed in 24 h. No change in absorbance was found in the range 20—30° C.

Of the many solvents tried as diluents for Aliquat 336, cyclohexane gave the phase separation needed for good recovery. The technique for obtaining efficient phase contact was important in achieving fast separation of the aqueous and solvent layers. Vigorous mixing resulted in the formation of a light emulsion which was slow to separate; gentle contact of the two phases gave recoveries of the order of 90—95% with one extraction. The addition of 5 g of phenol per 100 ml of cyclohexane improved the separation and increased the extraction efficiency to give quantitative recovery in the range 0—100 mg of sulphate from as much as 1.0 l of aqueous solution with 100 ml of extractant. The most satisfactory extraction technique was to fill the separating funnel close to capacity to prevent vigorous mixing.

An investigation of the extraction of sulphate as a function of pH showed quantitative recovery in the pH range 2—6. Poor phase separation at higher pH led to low recovery. Most drinking water and river water samples required no pH adjustment but, because the extraction conditions are favourable, dilution can be used for any necessary adjustment of pH. Samples with high acidity can be evaporated to dryness on a water bath. With samples containing large quantities of foreign ions, extraction with 100 ml of Aliquat 336 solution is recommended provided that the amounts are below those listed in Table 1.

When different aliquots of cresol red indicator solution are used, a series of standard curves must be prepared to obtain maximum accuracy. Small aliquots of sample reduce the possibility of interference; thus for the determination of sulphate, the smallest possible sample size is preferred. The blank values observed were 0.2—0.4 mg of sulphate on extraction from 400 ml of demineralized water with 100 ml of extractant, when 5.0 ml of indicator solution was used. The accuracy of the method based on the extraction of 15.0 mg of sulphate was ±1—2% with 5.0 ml of indicator solution, with a precision of 3—4%. Minimum detectable sulphate was 0.5 mg; the time taken for analysis was 2—3 h.

If sulphate must be determined in the presence of sulphite ion, the addition of ascorbic acid prevents oxidation to sulphate. No appreciable extraction of sulphite was observed from a solution containing 100 mg of ascorbic acid to which 25 mg of sulphite ion was added as solid sodium sulphite.

TABLE 1

Effect of various ions on recovery of 50 mg of sulphate from 400 ml of water with 100 ml of extractant and 2.0 ml of indicator

Ion	Amount (mg)	Added as	Recovery (%)
Al^{3+}	25	$AlCl_3$	97
As^{3+}	25	As_2O_3	103
Ba^{2+}	5	$BaCl_2$	100
Bi^{3+}	5	$Bi(NO_3)_3$	96[a]
BO_3^{3-}	50	H_3BO_3	105
Br^-	200	KBr	105
Ca^{2+}	50	$CaCl_2$	102
Cl^-	200	NaCl	99
ClO_4^-	200	$HClO_4$	102
CO_3^{2-}	200	Na_2CO_3	97
Co^{2+}	50	$Co(NO_3)_2$	102
Cr^{2+}	50	$CrCl_2$	96
Cu^{2+}	50	$Cu(NO_3)_2$	103
F^-	100	NH_4F	97
Fe^{3+}	50	$FeCl_3$	95
Hg^{2+}	50	$HgCl_2$	100
I^-	100	KI	96
Mn^{2+}	50	$MnCl_2$	107
Nb^{5+}	25	NbF_5	103
NH_4^+	100	NH_4Cl	101
Ni^{2+}	50	$Ni(NO_3)_2$	105
NO_3^-	200	KNO_3	97
Pb^{2+}	25	$Pb(NO_3)_2$	106
PO_4^{3-}	50	KH_2PO_4	105
Se^{4+}	5	SeO_2	99
Si^{4+}	10	SiO_2	101
Sn^{2+}	50	$SnCl_2$	96
Te^{4+}	100	K_2TeO_3	102
Th^{4+}	10	$Th(NO_3)_4$	104
U^{6+}	25	$UO_2(NO_3)_2$	103
Y^{3+}	10	$Y(NO_3)_3$	99
Zn^{2+}	50	$ZnCl_2$	98
Zr^{4+}	10	$Zr(NO_3)_4$	100
Acetate	200	$NaC_2H_3O_2$	99
Ascorbic acid	100	Ascorbic acid	100
Citrate	100	Citric acid	105
EDTA	50	di-Na salt	97

[a] Bi is extracted and follows sulphate through the system. In this case, the bismuth residue was filtered off before addition of indicator.

The analysis of several samples of river water by three different methods showed good agreement (Table 2).

TABLE 2

Comparison of sulphate content of river water samples found by three different methods

Sample Number	Main Constituents (mg l^{-1})								SO_4^{2-} (mg l^{-1})		
	Cu	Mn	Ca	Cl^-	K	Al	Mg	Na	Turb.[a]	Grav.[b]	Spec.[c]
1	1.5	0.35	21	438					77	70	70
2	0.03	1.5	38	9.6					284	270	310
3[d]	0.96	0.22	29	2.8					17.7	14	14
4	0.19	1.6	43	7.1					201	182	190
5	19	13	44	9.7	1.9	37	330	12	1810	1828	1810
6	13	6.6	64	6.0	1.1	5.8	160	10	860	864	850
7[e]	2.1	2.5	40	6.6	1.0	0.08	36	6.0	440	403	380
8	16	8.4	80	12	1.8	18.3	190	11	1140	1134	1130

[a]Turbidimetric method (analyses by P. Pakalns).
[b]Gravimetric method.
[c]Spectrophotometric—extraction method; 10-ml aliquot taken for analysis of all samples except No. 3 (100 ml).
[d]2.0 ml of 16 M HNO_3 added to 500 ml of sample when collected.
[e]2.0 ml of 16 M HNO_3 added to 250 ml of sample when collected.

REFERENCES

1 J. F. Thomas and J. E. Cotton, Water and Sewage Works, 101 (1954) 462.
2 R. J. Bertolacini and J. E. Barney, Anal. Chem., 29 (1957) 281.

Analytica Chimica Acta, 90 (1977) 349—354

Short Communication

ANALYTISCHE UNTERSUCHUNGEN AN MALONSÄURESALZEN

Ch. JAUKER und R. PIETSCH

Institut für anorganische und analytische Chemie, Universität Graz (Österreich)

(Eingegangen den 26 August 1976)

Wie das Studium der Literatur zeigt, ist Malonsäure befähigt, die verschiedenartigsten Salze zu bilden. Sowohl einfache von der Form MX [1], (M = zweiwertiges Metallion, X = Malonatanion) als auch komplexe Anionen und Kationen von der Form $[MX_2]^{2-}$ [2] bzw. $[M(III)(HX)]^{2+}$, $[M(III)(HX)_2]^{+}$ sowie neutrale, lösliche, undissoziierte der Form (MX) [3]. Die Art der entstehenden Spezies hängt von M^{n+} und dem Medium in dem präpariert wird, ab (pH-Wert, Konzentration, etc.).

In der vorliegenden Arbeit sollte untersucht werden, unter welchen Bedingungen einfache und substituierte Malonsäuren analytisch verwendbar sind und wie weit durch Einführung von Substituenten die analytischen Eigenschaften, besonders die Löslichkeit der entstehenden Verbindungen, differenziert werden können. Zunächst wurde der Fällungsbeginn einer Anzahl von Metallionen mit verschiedenen Malonsäuren untersucht. In die Untersuchungen einbezogen wurden die Metallionen der Alkali-, Erdalkalimetalle sowie Fe^{3+}, Cu^{2+}, Zn^{2+}, Pb^{2+}, Al^{3+}, Ni^{2+}, Mn^{2+}, Cr^{3+}, Cd^{2+}, Bi^{3+}, VO_2^{+}, Mo(VI), V(V), W(VI), Th(IV), TiO^{2+}, Ce^{4+}, Ce^{3+}, ZrO^{2+}, Ag^{+}, Tl^{+}, Pd^{2+}, Pt^{4+}, Au^{3+}, Cr(VI), Ga^{3+}, In^{3+}, Hg^{2+}, La^{3+}, Sn^{2+}, Sb(V), Nb(V) und die Säuren Malon- (Mal), Methylmalon- (Me), Dimethylmalon- (Dime), Diäthylmalon- (Diä), Dipropylmalon- (Diprop), Dibutylmalon- (Dibut), Isopropylmalon- (Isoprop), Phenylmalon-, Benzylmalon-, Dichlormalon-, *p*-Methoxybenzoylmalonsäure sowie Tartron- und Mesoxalsäure. Die Lösungen waren an Metallion $3 \cdot 10^{-2}$ M, an Malonsäure $1{,}5 \cdot 10^{-1}$ M. In der Hitze wurde der pH-Wert mit NaOH-Lösung bis zum Fällungsbeginn erhöht und mit der Glaselektrode gemessen.

Durch Vergleich mit den Fällungs-pH-Werten der Hydroxidfällung läßt sich bereits abschätzen, in welchen Fällen eine höhere Affinität der Malonationen den Metallionen gegenüber vorlag. Eine Auswahl der erhaltenen Fällungseigenschaften zeigt Tabelle 1. Die Zahlen geben den pH-Wert bei Fällungsbeginn an.

Weiters wurde die Fällbarkeit der angeführten Metallionen in Gegenwart von Weinsäure untersucht. Hiebei zeigten lediglich die Ionen Pb^{2+}, BiO^{+}, UO_2^{2+}, Ce^{4+}, Ce^{3+}, La^{3+} eine Reaktion. Bei Diprop noch zusätzlich Hg^{2+}. Wie zu erwarten, zeigte sich bei der Messung der Löslichkeitsprodukte (L_p), daß unter diesen Metallen diejenigen mit den kleinsten L_p waren. Tabelle 2 zeigt die Fällungs-pH-Werte für Metallionen mit Malonsäuren in Gegenwart von Weinsäure.

TABELLE 1

Fällungsbeginne (pH-Werte) der Metallionen mit Malonsäuren

M	pH-F					
	OH^-	Mal	Me	Dime	Diä	Diprop
Fe^{3+}	3,5	2,5	6,5	2,2	1,3	1,0
Cu^{2+}	5,5	8,1	8,7	6,1	8,2	3,0
Zn^{2+}	6,9	7,7	8,0	7,8	7,6	5,6
Pb^{2+}	6,5	3,1	7,5	—	2,8	1,8
Al^{3+}	6,3	5,1	7,4	—	7,6	7,9
Ni^{2+}	7,5	9,0	8,6	8,2	8,2	6,3
Mn^{2+}	8,0	9,1	9,1	9,5	9,5	7,7
Co^{2+}	7,2	8,5	8,5	8,6	8,1	5,8
Cd^{2+}	8,0	9,2	8,5	8,9	7,6	4,2
Ca^{2+}	—	12,2	13	—	11	8,4
Bi^{3+}	2,2	1,2	1,7	1,5	1,2	1,3
UO_2^{2+}	5,0	7,8	7,8	7,5	1	1,5
Th^{4+}	3,5	2,1	2,2	0,7	1	1,2
Ti^{4+}	1,5	1,5	1	1,0	1,0	0,9
Ce^{4+}	5,5	2,6	1	2,3	1	0,6
Zr^{4+}	2,5	1	1	1,6	1,4	1,5
Ag^+	5,5	1,0	(6,7)	8	—	2,0
Ga^{3+}	6,0	6,3	5,5	3,9	4,8	2,8
Hg^{2+}	1	1	1	1,9	1	1
In^{3+}	3,5	5,8	5,4	3,1	1,4	1,4
La^{3+}	8,5	3,5	4,3	4,3	3,9	3,0
Ce^{3+}	5,5	4,7	7,6	8,0	4,9	2,7

M	pH-F					
	Dibut	Isoprop	Phenyl	Benzyl	Dichlor	*p*-Methoxy benzyl
Fe^{3+}	1	1	6,6	1	1,5	2,0
Cu^{2+}	2,4	9,1	8,0	5,2	6,1	11,5
Zn^{2+}	6,3	6,5	7,3	7,8	6,7	9,2
Pb^{2+}	2,7	3,0	3,2	2,4	5,7	2,0
Al^{3+}	5,1	4,0	7,3	5,0	4,4	—
Ni^{2+}	6,0	8,9	8,2	8,3	7,8	10,8
Mn^{2+}	7,5	9,5	9,1	9,5	7,8	9,9
Co^{2+}	5,6	8,4	8,2	8,0	7,7	9,1
Cd^{2+}	4,4	6,6	8,1	3,1	6,8	3,9
Ca^{2+}	7,6	3,9	6,4	4,8	10,5	3,5
Bi^{3+}	1	1	1,0	1	1,5	1,5
UO_2^{2+}	1	8,1	7,5	1,9	6,7	8,0
Th^{4+}	1	1,7	1,6	1	2,4	2,1
Ti^{4+}	1	1	0,5	1	1,1	1,5
Ce^{4+}	1	1	1,6	2,5	1,9	1,0
Zr^{4+}	1	1,4	1,5	1,7	1	2,1
Ag^+	6,4	—	1	2,3	—	5,6
Ga^{3+}	1,0	5,7	5,0	3,2	7,6	4,7
Hg^{2+}	1	1	0,7	1	—	2,2
In^{3+}	1,4	2,3	3,2	1,	3,3	2,3
La^{3+}	2,9	2,8	3,5	1,5	6,0	2,9
Ce^{3+}	4,1	2,9	2,9	2,8	5,2	3,1

TABELLE 2

Fällungsbeginne (pH-Werte) für M^{n+} mit Malonsäuren in Gegenwart von Weinsäure

M^{n+}	Diprop	Dibut
Pb^{2+}	3,0	2,9
BiO^{+}	1,5	1
VO_2^{2+}	1	1
Ce^{4+}/Ce^{3+}	3,5	2,1
La^{3+}	2,2	2,2
Hg^{2+}	1	—

Unter den in Tabelle 1 angeführten Fällungen wurden folgende Metalle und Säuren einer näheren Untersuchung unterzogen: Pb^{2+}, Ni^{2+}, Cu^{2+}, Cd^{2+}, Zn^{2+}, Hg^{2+}, In^{3+}, Ga^{3+}, und Mal, Me, Dime, Diä, Diprop, Dibut. Aus Tabelle 1 ist zu folgern, daß, je niedriger der Fällungs-pH-Wert für eine Säure mit einem Metall ist, umso kleiner auch das L_p dieses Metallmalonates sein soll.

Um bei den im Detail näher untersuchten Metallen exakt den pH-Wert bei Fällungsbeginn und -ende zu kennen, wurden Fällungskurven auf turbidimetrischem Wege aufgenommen.

Darstellung der Metallmalonate

Die Malonsäuren wurden in wässriger Lösung $3 \cdot 10^{-2}$ M in der Siedehitze vorgelegt und das Metallion meist als Nitrat im Molverhältnis Malonsäure: Metall = 5 : 1 in gelöster Form zugegeben. Der pH-Wert wurde entsprechend den aus den Fällungskurven gewonnenen Werten eingestellt. Die Gesamtkonzentration entsprach der der Vorversuche. Das Molverhältnis reicht zur Bildung von Verbindungen auch in hohem Verhältnis aus. Die Fällungen wurden abgesaugt, kurz mit Wasser gewaschen und im Vakuumexsikkator bis zur Gewichtskonstanz getrocknet. Die so gewonnenen Präparate wurden auf Metall, Wasser, C und H analysiert. Die Metallanalysen wurden nach thermischer Zersetzung des Präparates durch Titration mit ÄDTA ausgeführt, Wasser durch thermogravimetrische Analyse (TG), C und H durch Mikroanalyse. IR-Spektren wurden aufgenommen und die erwarteten Banden für CH_2, COO^-—, sowie fallweise für H_2O gefunden. Die TG zeigte vielfach neben dem Kristallwasser auch Zersetzung des Malonates zum Metalloxid an. Die Abgabe des Kristallwassers erfolgte etwa zwischen 80 und 120° C, die Zersetzung begann bei ca. 200 und endete bei ca. 400° C. Indium-Diä zeigte thermische Stabilität bis 300° C und eine sehr scharfe Zersetzung zwischen 300 und 350° C. Auch die anderen In- und Ga-Malonate zeigten erst ab ca. 260° C Zersetzung.

Tabelle 3 zeigt eine Übersicht über die untersuchten Malonate. Die Ni- und Cu-Malonate zeigten unstöchiometrische Zusammensetzung.

Messung von Löslichkeitsprodukten

Hiebei wurden zwei voneinander unabhängige Wege beschritten: Die Bestimmung der Metallkonzentrationen mittels Dithizontitration nach

TABELLE 3

Stöchiometrische Malonate[a]

M^{n+}	Mal	Me	Dime	Diä	Diprop	Dibut	Stöchiometrie
Pb^{2+}	+	—	—	+	+	+	$Pb.Mal.H_2O$
Zn^{2+}	—	—	—	—	+	—	Zn.Mal
Cd^{2+}	—	—	—	—	+	+	$Cd.Mal.2H_2O$
Hg^{2+}	+	—	+	+	+	+	$Hg.Mal.1H_2O$
In^{3+}	—	—	—	+	+	+	In_2Mal_3,In_2Dibut.$2H_2O$
Ga^{3+}	—	—	—	+	+	—	Ga_2Mal_3

[a] + = stöchiometrische Zusammensetzung
— = andere unstöchiometrische Zusammensetzung

Iwantscheff [4] und die Messung auf potentiometrischem Wege mittels Konzentrationsketten der Form $Pb/PbNO_3$ m_1 // KNO_3 ges. // $PbNO_3$ m_2, H_2Mal/Pb
Das L_p ergibt sich aus der Beziehung [5]

$$\log L_p = -\frac{2nF\,\Delta E}{RT} + \log C_{M^{2+}}\,(\text{Std}) + \log C_{Mal^{2-}}\,(\text{Meß})$$

(Std, Standardelektrode. Meß, Meßelektrode.) Der Vergleich beider Methoden bot die Möglichkeit der Kontrolle der Messungen bzw. aus den Differenzen beider Messungen Hinweise auf Unterschiede im Vorliegen der gelösten Verbindungen zu erhalten. Gemessen wurden zwei verschiedene Lösungen:
(1) Gesättigte Lösungen der Salze in Wasser. Zu diesem Zweck wurden die hergestellten Präparate bis zur Gleichgewichtseinstellung mit Wasser geschüttelt. Es wurde eine Ionenstärke von 0,03 durch Zugabe von Kaliumnitrat eingestellt.
(2) Lösungen, in denen die Fällung erst erzeugt wurde, indem zu einer $3 \cdot 10^{-2}$ M Malonsäurelösung verdünnte Metallsalzlösung so lange zugetropft wurde, bis eben eine Spur einer Fällung auftrat. Lösung 1 wurde sowohl durch Dithizontitration als auch auf elektrometrischem Weg vermessen. Die freie $[Mal^{2-}]$ ergibt sich aus dem pH-Wert der Lösung nach der Formel [6] $[Mal^{2-}] = C/(1 + 10^{-(2pH-pK_1-pK_2)})$, worin C die totale Säurekonzentration, pK_1, pK_2 die pK-Werte der Säure und pH der pH-Wert der Mischung (Meßlösung) sind. Die erhaltenen Ergebnisse sind in Tabelle 4 wiedergegeben. Für In, Ga und Zn war keine elektrometrische Bestimmung möglich, weil für die reinen Metallelektroden keine reversibel arbeitenden Halbzellen herstellbar waren.

Diskussion der Ergebnisse

Der Vergleich der sechs verschiedenen Malonate ein und desselben Metalles zeigt, daß der von Feigl [7] beschriebene Gewichtseffekt gering ist. Erst das Dibutylmalonat zeigt gegenüber den anderen ein um 2—3 Zehnerpotenzen kleineres L_p.

TABELLE 4

Löslichkeitsprodukte von Malonaten

Spalte 1: Meßwerte durch Dithizontitration einer gesättigten wässrigen Lösung.
Spalte 2: $3 \cdot 10^{-2}$ M Malonsäure + Metallsalz bis Fällung beginnt. Durch Konzentrationskette vermessen.
Spalte 3: Elektrometrische Vermessung der Lösung 1 (Spalte 1) Ionenstärke $I = 0{,}03$ (KNO_3).

Fällung von	1	2	3
Pb—Mal	$1{,}9 \cdot 10^{-8}$	$2{,}9 \cdot 10^{-8}$	$1{,}0 \cdot 10^{-8}$
Diä	$1{,}2 \cdot 10^{-8}$	$4{,}3 \cdot 10^{-9}$	$1{,}3 \cdot 10^{-9}$
Diprop	$2{,}0 \cdot 10^{-8}$	$3{,}6 \cdot 10^{-10}$	$2{,}5 \cdot 10^{-10}$
Dibut	$5{,}3 \cdot 10^{-10}$	$5{,}4 \cdot 10^{-11}$	$6{,}3 \cdot 10^{-11}$
Zn—Diprop	$3{,}0 \cdot 10^{-4}$	—	—
Cd—Diprop	$5{,}1 \cdot 10^{-7}$	$4{,}3 \cdot 10^{-2}$	$3{,}2 \cdot 10^{-7}$
Dibut	$2{,}1 \cdot 10^{-7}$	$1{,}0 \cdot 10^{-7}$	$1{,}6 \cdot 10^{-7}$
Hg—Mal	$1{,}4 \cdot 10^{-10}$	$3{,}1 \cdot 10^{-11}$	$2{,}5 \cdot 10^{-11}$
Me	$4{,}5 \cdot 10^{-9}$	$4{,}4 \cdot 10^{-8}$	$4{,}3 \cdot 10^{-9}$
Dime	$8{,}3 \cdot 10^{-7}$	$1{,}0 \cdot 10^{-8}$	$4{,}4 \cdot 10^{-8}$
Diä	$3{,}8 \cdot 10^{-8}$	$8{,}0 \cdot 10^{-12}$	$1{,}6 \cdot 10^{-9}$
Diprop	$1{,}5 \cdot 10^{-8}$	$3{,}6 \cdot 10^{-12}$	$1{,}6 \cdot 10^{-11}$
Dibut	$6{,}0 \cdot 10^{-11}$	$2{,}2 \cdot 10^{-11}$	$9{,}5 \cdot 10^{-12}$
In— Diä	$8{,}8 \cdot 10^{-29}$	—	—
Diprop	$5{,}4 \cdot 10^{-30}$	—	—
Dibut	$1{,}9 \cdot 10^{-33}$	—	—
Ga—Diä	$3{,}2 \cdot 10^{-24}$	—	—
Diprop	$4{,}3 \cdot 10^{-23}$	—	—

Bei allen untersuchten Reihen zeigten die Glieder 2 und 3, das sind Me und Dime, Unregelmäßigkeiten. Entweder fielen keine stöchiometrisch reinen Verbindungen aus oder man erhielt stöchiometrisch reine Produkte und diese zeigten eine wesentlich größere Löslichkeit, z.B. Hg-Dime.

Aufgrund des großen Unterschiedes in den Hg-Bestimmungen nach Methode 1 und 2 wurde auf die Bildung undissoziierter Spezies in der Lösung geschlossen. Dies wurde auch polarographisch bestätigt. Bei Pb und Hg zeigt der Vergleich der Spalte 1 mit den Spalten 2 und 3 der Tabelle 4, daß die Werte der beiden letzten Spalten durchwegs kleiner sind. Ursache dafür ist, daß hier nur die freie Metallionenkonzentration gemessen wurde, mit der Dithizonmethode hingegen die gesamte in Lösung befindliche Metallmenge, also auch die undissoziiert vorliegenden gelösten Verbindungen. Die Löslichkeitsverhältnisse beim Hg-Dime werden noch genauer untersucht.

LITERATUR

1 J. Mach, Monatsh. Chem., 100 (1969) 1839.
2 H. L. Riley, J. Chem. Soc., (1929) 1307.
3 G. Schwarzenbach und I. Szilard, Helv. Chim. Acta, 144 (1962) 1223.
4 J. Iwantscheff, Das Dithizon und seine Anwendung in der Mikro- und Spurenanalyse, Verlag Chemie, Weinheim, 1965.

5 G. Kortüm, Lehrbuch der Elektrochemie, Verlag Chemie, Weinheim, 5. Aufl. 1972, S. 313.
6 F. Seel, Grundlagen der analytischen Chemie, Verlag Chemie, Weinheim, 1965, 4. Aufl., S. 119.
7 F. Feigl, Chemistry of Specific, Selective and Sensitive Reactions, Academic Press, New York, 1949, S. 420.

Analytica Chimica Acta, 90 (1977) 355—360

Book Reviews

T. S. West (Ed.), *International Review of Science, Physical Chemistry, Series Two, Vol. 12, Analytical Chemistry, Part 1*, Butterworths, London, 1976, 334 pp., price £13.45.

To both beginner and expert, the publication of review articles covering particular research fields is extremely valuable, if not essential, with the continuing expansion of scientific literature. The two parts of this volume, which are concerned with analytical chemistry, are part of a comprehensive series of publications covering many branches of chemistry and other related subjects. In Part 1 of this volume, the editor has collected together seven topical and useful reviews covering fields which are undergoing, or have recently undergone, rapid development. The standard in most cases is very high and the coverage is of recent developments in each field rather than a complete historical review. The literature is generally reviewed up to early 1974 although some authors have included later references to their own work.

Over half of the book (189 pages) is concerned with Activation Analysis, in three separate chapters. The first of these, by Dams, De Corte, Hertogen, Hoste, Maenhaut and Adams, covers Instrumental Neutron Activation Analysis, i.e. using high-resolution γ-ray spectrometers for multi-element activation analysis, and then applications to the analysis of atmospheric and high-purity samples. The second chapter, by Cornelis, Hoste, Speecke, Vandecasteele, Versieck and Gijbels, is a continuation of the first and deals with applications in geochemistry, forensic science, and biological materials, with smaller sections on errors in 14-MeV neutron activation analysis and charged-particle activation analysis. The third chapter, by Op de Beeck and Hoste, is concerned with the Application of Computer Techniques to Instrumental Neutron Activation Analysis. The subject is ideally suited to a review at this time and the coverage here seems excellent. These three chapters alone make this volume of good value to workers in this field.

The rest of the book consists of four smaller chapters on unrelated topics: Analytical Techniques for Air Pollution Studies, by West (P. W.) and Dharmarajan (38 pages); Developments in Forensic Analysis, by Pearson (32 pages); Developments in Separation Methods using Extraction Chromatography, by Starý (27 pages); and Particle Size Analysis, by Lloyd and Treasure (37 pages). The second and fourth of these maintain the high standard of the first three chapters. The section on air pollution studies is concerned only with inorganic substances, and is generally less adequate than other recent reviews of this subject; the section on particulates is concerned only with analytical techniques and gives very little information on their application in this field. Both this and the chapter on extraction chromato-

graphy seem to encompass only a selected view of their subject. Apart from these deficiencies the book will make a substantial contribution to research and development in the several fields covered and can be recommended as a useful addition to most libraries.

J. M. Ottaway

T. S. Ma and A. S. Ladas, *Organic Functional Group Analysis by Gas Chromatography*, Academic Press, London, 1976, x + 173 pp., price U.S.$14.75 (£6.80).

This short monograph collates the various methods developed by a number of workers over the period 1960—1975 for the determination of organic functional groups.

The book contains seven chapters: a short account of gas chromatography; a discussion of the various techniques used in reaction gas chromatography; chapters devoted to the determination of organic functional groups containing oxygen, nitrogen, sulphur and unsaturated functions, and finally a chapter on miscellaneous functions. The chapters are very well referenced.

It is unfortunate that the introduction to gas chromatography contains errors both in definition and meaning (particularly on page 7). The reader would be advised to consult the texts indicated and ignore this chapter entirely.

The other chapters contain a wealth of practical information, including precise experimental details for the determination of the various functional groups. Clearly most of these details have been taken directly from the original papers and the authors have not modified them in any way. This is perfectly satisfactory for workers familiar with the gas chromatographic technique, but the misleading impression given is that in order to undertake a given estimation it is necessary to work with a particular chromatograph (which is usually obsolete). It would have been preferable to indicate the requirements for the gas chromatograph and allow workers to make their own choice. The techniques described for quantitation cover the entire range of methods which have been developed over the years from "cutting out and weighing" to on-line computers! The impression is also given that, in order to gain maximum benefit from the book, it is necessary to obtain a copy of one of the authors other books. Surely, if this is necessary, these extra details should have been included!

For the chemist without access to modern spectroscopic methods of analysis, particularly g.c.—m.s., this monograph could be very useful, but for those fortunate enough to have access to these techniques, its utility is limited unless routine estimations of a given function are required.

Nevertheless, there is a lot of useful information in this volume, and although it contains more mistakes than one would expect — some trivial, but some inexcusable — it could repay careful reading.

C. F. Simpson

Eugene Sawicki and Carole A. Sawicki, *Aldehydes — Photometric Analysis, Vols. 1 and 2*, Academic Press, London, 1975, xxviii + 283 pp. and + 344 pp., prices £10.50 and £10.80.

Here the authors present the first two volumes of a comprehensive series of seven. These two monographs really form one book; consequently they are reviewed as one book. In 67 chapters, 62 individual aldehydes and 5 different groups of aldehydes (aliphatic, aromatic, α,β-unsaturated, total aldehydes and oxybenzaldehydes) are treated thoroughly in alphabetical order, "Formaldehyde" being the last chapter in volume 1, and "3-Formylacrylic Acid" being the first chapter in volume 2. In most of the chapters the physical and spectral properties of the compound concerned are given, and the reagents and reactions used for its photometric, fluorimetric or phosphorimetric determination are discussed. Extensive information on the determination of the different aldehydes as individuals or in complex mixtures is presented and numerous procedures are described in detail.

It is the enormous wealth of analytical information (more than 2000 literature references) as well as the authors'many years of experience of the analytical chemistry of aldehydes that makes these two monographs unique in the literature at present available for this class of compound. For the user of the book, however, it is sometimes hard to recall the stored information: some data can be found twice within a few pages, but to find other data, one has to read nearly the whole book, In the reviewer's opinion this arises mainly from the separate representation of the aldehydes according to the alphabet. The most useful chapters are those in which closely related aldehydes are treated as one group. Here one can compare directly the chemical, physical and spectral properties of compounds which have the same functional group connected to different organic residues.

Some of the explanations and definitions given on pages xiii to xxv and at some other places in volume 1 are extremely personal, confusing, or different from common analytical usage, but this does not detract from the practical usefulness of the book.

Aldehydes belong to the more important classes of organic substances in biochemistry and environmental chemistry. Therefore the first two volumes of "Aldehydes — Photometric Analysis" can be strongly recommended to all scientists faced with analytical problems in these fields.

D. Klockow

J. Ševčík, *Detectors in Gas Chromatography*, Elsevier, Amsterdam, 1976, 192 pp., price U.S. $23.25, DFl 60.—.

This, the fourth volume in Elsevier's Journal of Chromatography Library, updates and supplements neatly the earlier books on gas chromatography detectors by Jentzsch and Otte (1970) and by D. J. David (1973), which covered the literature up to around 1970. Reference is made to work published up to May, 1974; the author has elected to present a general, concise and critical appraisal of the literature rather than an exhaustive survey. The result is a slim, readable book that can be recommended both to students and to specialists. The standards of production and presentation are excellent; the author has been served well by the translators of his original Czechoslovakian text.

Following a general introduction, chapters are devoted to each of the following types of detector: thermal conductivity, ionization, electron capture, flame ionization, thermionic, photoionization, helium, flame photometric, coulometric and electrolytic conductance detectors. Each chapter explains the detector mechanism involved (with reasonably advanced, but not forbidding, mathematical treatment), discusses the dependence of the detector response on the relevant experimental conditions and their optimization, and concludes with a critical survey of the more recent important and interesting applications; the number of references cited at the end of the chapters ranges from 12 to 105, with a total of 571. This is a good book; the only feature that is slightly substandard is the Index, a short, combined subject and author affair which includes the names of the few authors cited in the text, but does not embrace the references.

D. M. W. Anderson

Alberto Frigerio and Neal Castagnoli (Eds.), *Advances in Mass Spectrometry in Biochemistry and Medicine, Vol. 1*, Spectrum Publications, distributed by Halsted Press (J. Wiley), New York, 1976, xviii + 586 pp., price £27.20, U.S. $46.40.

It is slightly confusing that this, volume 1, is based on the proceedings of the Second International Symposium of Mass Spectrometry in Biochemistry and Medicine, held in Milan in June 1974. Here again, therefore, we have an example of symposium proceedings published two years after the event. This leaves much to be desired; the organisers of Symposia and publishers of similar volumes should study the methods whereby the proceedings of recent Advances in Chromatography Symposia can be published 2—3 months after the event.

Although this is a highly specialized book, and reasonably correctly described by its title, there is a great deal in it for analytical chemists working in specialized areas, particularly in the life sciences. Many of the 51 papers deal with applications of g.c.—m.s., field desorption m.s. and chemical ionization m.s. The topics treated range widely including protein sequencing, drug metabolism, steroid hormones, prostaglandins, pesticides, barbiturates, explosives, diazepines and cannabinoids, and there are several computer-aided studies. The papers come from a large number of authors with international reputations, representing 16 different countries. The standard of the researches reported is high; the standard of the editing and quality of production of the book are both high; the price is high too. There appears to be little hope of the publishers obtaining any sales to private individuals — the diverse range of topics and the outdatedness, added to the cost factor, add up to create a sales resistance barrier that private individuals should not venture to cross.

Analytical chemists will like the Preface, by E. C. Horning. "The rate-limiting step in the scientific development of any field is the state of analytical methodology within that field. This circumstance is not always fully appreciated, and it is not always easy to evaluate new forms of analysis at an early stage." The analytical techniques upon which the contents of this book are largely based originated very early in the sixties but why are analytical chemists always so slow to spot and exploit the real winners?

D. MacDonald

Robert M. Smith and Arthur E. Martell, *Critical Stability Constants, Vol. 4, Inorganic Complexes*, Plenum Press, New York, 1976, pp. xiii + 257, price U.S. $35.40.

This volume has the same philosophy as its companion volumes, namely to provide values of stability constants which, in the opinion of the authors, are the best available. The "ligands" concerned are mostly inorganic anions, and the arrangement is similar to that in the Chemical Society Publication "Stability Constants of Metal Ion Complexes" by Martell and Sillen. A large range of anions is considered, including various polyphosphate ions, and hexacyanoferrate ions, as well as the simpler inorganic ions; and ammonia is also included. The values given, which include protonation constants, are supported by a large reference list (115 pp.), ligand name and formulae indexes, and a list of ligands considered but not included. The information is presented clearly, but, once again, would not have suffered from reproduction on smaller pages, on rather better quality paper.

A. Townshend

Thermal Analysis Vol. 1, 2 and 3, Proceedings of the 4th ICTA Conference, Budapest, 1974, Heyden, London, 1975, each Vol. £25.00, collectively £60.00.

These three volumes collectively report the official proceedings of the 4th Conference of the International Confederation for Thermal Analysis, held in Budapest in 1974. These meetings, held triennially to review progress in thermal analysis, are recognised as the major organ for dissemination of advances in this field. The mass of the present volumes indicates the efforts expended in collecting together the full texts of the 277 papers presented. These contributions are divided as follows: Volume 1 (100 papers) deals with the theory of thermal analysis and developments in its applications to inorganic chemistry. Volume 2 (72 papers) covers organic and macromolecular chemistry and applications to earth sciences. Volume 3 (105 papers) contains reports of developments in applied sciences, methodology and instrumentation.

Printed by an offset photolithographic process from the original manuscripts, these volumes give a true picture of the present state of development of the various thermoanalytical techniques and their diverse applications. Few techniques have shown such a rapid rate of growth in recent years and early publication of these proceedings is essential if workers are to be kept informed of major developments. This has been achieved in the present instance at the cost of excluding all conference discussions of individual papers, but the difficulties in collecting and editing such material at an international meeting where some 600 delegates from 30 countries attended could only have led to unwarranted delays in publication.

Noteworthy in these volumes is the high proportion of papers from Eastern European countries. The fact that all papers are printed in English makes for an easier appreciation of these important contributions. The volumes, which are individually complete, can be purchased separately. There is a reasonable price advantage in purchasing all three volumes.

W. I. Stephen

Analytica Chimica Acta, 90 (1977) 361—364

Announcements

Congrès de Chimie Analytique, 33 ème Congrès du G.A.M.S. Paris, France, 29 novembre—2 décembre 1977

Le Groupement pour l'Avancement des Méthodes Spectroscopiques et Physicochimiques d'Analyse (G.A.M.S.) bénéficie pour son prochain Congrès de la collaboration de la Division de chimie analytique de la Société Chimique de France et du Groupe de chimie analytique de la Société de chimie industrielle, ainsi que du concours de l'Association pour le Salon du Laboratoire. Il aura lieu au Parc des Expositions de la Porte de Versailles (terrasse R) à Paris du 29 novembre au 2 décembre 1977, en même temps que le Salon du Laboratoire.

Ce Congrès aura un caractère national, avec possibilité de participation étrangère. La langue du Congrès sera le français, mais les communications en anglais seront acceptées. Les thèmes du Congrès sont les suivants: la chromatographie sous toutes ses formes, les méthodes spectrométriques tant atomiques que moléculaires, l'automatisation dans l'analyse, les problèmes analytiques de pollution et de toxicologie, l'analyse des matériaux purs, l'analyse et la caractérisation des surfaces, l'électrochimie analytique en solution, la biochimie analytique, l'enseignement de la chimie analytique. Les séances seront précédées de conférences plénières. Certains sujets donneront lieu à des tables rondes. Les problèmes de recyclage et de formation continue feront tout particulièrement l'objet d'un débat. Demandes doivent être adressées au: Secrétariat du G.A.M.S. (Congrès), 88, Boulevard Malesherbes, 75008 Paris, France.

7th European Food Symposium: Product and Process Selection in the Food Industry

The 7th European Food Symposium will take place on 21—23 September, 1977, in Eindhoven (The Netherlands). The symposium will be organized by the Food Working Party of the European Federation of Chemical Engineering in cooperation with the Dutch Society of Nutrition Science and Food Technology and IUFoST* (see below).

There will be 4 themes:

1. Food industry and society
2. Product and process selection: procedures and techniques
3. Examples of product selection based on economic considerations
4. Examples of process selection based on economic considerations.

5th International Symposium on Organosilicon Chemistry

The 5th International Symposium on Organosilicon Chemistry will take place on August 21—25, 1978, at Karlsruhe (Federal Republic of Germany).

The symposium will be organized by Gesellschaft Deutscher Chemiker* (see below).

2nd International Symposium on Inorganic Ring Systems

The 2nd International Symposium on Inorganic Ring Systems will take place on August 28—30, 1978, at Göttingen (Federal Republic of Germany).

The symposium will be organized by the Academy of Sciences, Göttingen, and Gesellschaft Deutscher Chemiker.

*Information on all these meetings can be obtained from:

Gesellschaft Deutscher Chemiker,
P.O. Box 90 04 40
D-6000 Frankfurt/Main 90 (Federal Republic of Germany)

Forthcoming meetings of the Gesellschaft Deutscher Chemiker

1977	
12—16 September	*General Assembly of Gesellschaft Deutscher Chemiker, Munchen.* The following GDCh-Divisions will participate: Analytical Chemistry, Chemical education on the secondary level, Pigments and Dyes, Solid State Chemistry, Independent Chemists, Industrial Juridical Protection, History of Chemistry, Food and Forensic Chemistry, Macromolecular Chemistry, Medicinal Chemistry, Nuclear Chemistry, Water Chemistry.
6—7 October	*Electrolytes — Aqueous, organic, molten, solid electrolytes, ion exchange membranes*, Darmstadt. Meeting of the GDCh Applied Electrochemistry Division.
1978	
1st week of May	*Annual Meeting of the GDCh Water Chemistry Division*, Oberstdorf.
21—25 August	*5th International Symposium on Organosilicon Chemistry*, Karlsruhe.
28—30 August	*2nd International Symposium on Inorganic Ring Systems*, Göttingen. Jointly organised by the Academy of Sciences, Göttingen, and Gesellschaft Deutscher Chemiker.

17—21 September *Chemistry Day of GDCh on the occasion of the 110th Meeting of Gesellschaft Deutscher Naturforscher und Arzte*, Innsbruck (Austria).

25—29 September *12th International Symposium on Chromatography*, Baden-Baden.

Details of the meetings listed above may be obtained from Gesellschaft Deutscher Chemiker, P.O. Box 90 04 40, D-6000 Frankfurt/Main 90 (B.R.D).

New Flame Methods of Analysis
Nova Scotia, Canada — August 24—26, 1977

A conference on new flame methods of analysis, with emphasis on applications of molecular emission cavity analysis, will be organized by the Chemical Institute of Canada (Atlantic Section) on August 24—26, 1977, at Acadia University, Wolfville, Nova Scotia. Further information is available from Mr. James Frazee, Chemistry Department, Acadia University, Wolfville, Nova Scotia, Canada BOP 1XO.

13th International Symposium on Atmospheric Pollution
Paris, France, May 1978

The 13th International Symposium, sponsored by the Institut National de Recherche Chimique Appliquée, will consider topics relevant to urban air pollution: (1) surveys, (2) methods of measurement (gaseous pollutants and suspended matter), (3) health effects, (4) modelling, (5) transport and chemistry. Intending contributors are requested to submit a short abstract (100—200 words) before September 30, 1977.

Oral presentation of the papers at the Symposium will be in French and English. Simultaneous translation will be provided.

We expect to publish the Symposium Proceedings in their entirety in English. The advance registration fee will be FF 800, Further information can be obtained from: M. Benarie, I.R.Ch.A., B.P.N° 1, 91710 Vert-le-Petit (France).

Particle Size Analysis Conference
University of Salford, England, September 13—15, 1977

All aspects of particle characterisation will be covered. These include measurement of particle size distribution (including droplet and aerosol sizing) and surface area; measurement of single particle characteristics such as shape and pore size distribution; associated ancillary techniques; and the

use of particle characterisation methods in the applied sciences such as pharmaceuticals, ceramics, powder metallurgy etc. Plenary lectures will be given by Professor Clyde Orr, Georgia Institute of Technology, Professor Dr. Ing Kurt Leschonski, Technische Universitat Clausthal, and W. Carr, Ciba-Geigy (UK) Ltd. Further information can be obtained from Dr. D. Dollimore, Department of Chemistry, University of Salford, Salford M5 4WT, England.

Prize "Biochemical Analysis" 1978

A prize of DM 10,000 is donated by Boehringer, Mannheim, and is awarded every two years at the "Biochemische Analytik" conference in Munich for outstanding work in the field of biochemical instrumentation and analysis. The award will be made during the 1978 conference (18th—21st April). One or several papers concerning one theme, either published or accepted for publication between October 1st 1975, and September 30th 1977, should be submitted to Prof. Dr. I. Trautschold, Secretary of the prize "Biochemical Analysis", Medizinische Hochschule Hannover, 3000 Hannover 61, Karl-Wiechert-Allee 9, Federal Republic of Germany.

Analytica Chimica Acta, 90 (1977) 365

Erratum

J. Růžička, E. H. Hansen and E. A. Zagatto, Flow Injection Analysis Part VII. Use of Ion-selective Electrodes for Rapid Determination of Soil Extracts and Blood Serum. Determination of Potassium, Sodium and Nitrate, *Anal. Chim. Acta*, 88 (1977) 1—16.

On page 4, Fig. 1(d) was omitted. The complete Fig. 1 is shown below.

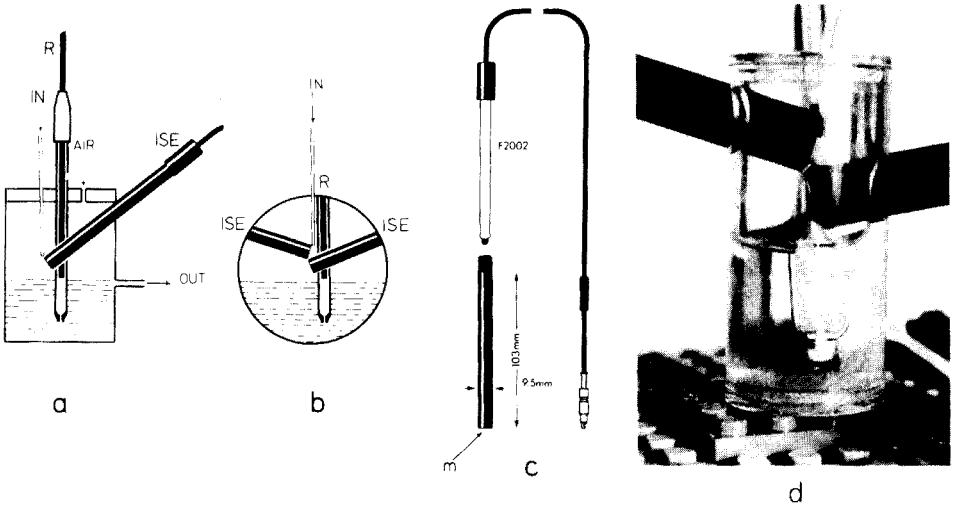

Fig. 1. Flow-through cell accommodating (a) one, and (b) two membrane electrodes. A constant level of liquid is maintained in the reservoir by differential pumping where the rate of the IN-pumping is always 30—50% lower than the OUT-pumping. R, reference electrode; ISE, ion-selective electrode. Fig. 1(c) shows an exploded view of the commercial electrode construction used (Radiometer), where *m* indicates the position of the PVC-membrane. Fig. 1(d) shows a photograph of the two-channel flow cell schematically depicted in (b). Note the flow of carrier solution cascading from indicator electrode 1 to indicator electrode 2 and then to the reservoir in which the ceramic junction of the reference electrode is submerged.

ANALYTICA CHIMICA ACTA, VOL. 90 (1977)

AUTHOR INDEX

ANALYTICA CHIMICA ACTA, VOL. 90 (1977)

SUBJECT INDEX

(continued from page 3 of cover)

ontinued from page 4 of cover)

hort Communications

(continued on page 372)

CONTENTS

(continued on inside page of the cover)